TRANSACTIONS

OF THE

AMERICAN INSTITUTE OF MINING AND METALLURGICAL ENGINEERS

(INCORPORATED)

Volume 135

IRON AND STEEL DIVISION

1939

Notice

This volume is the twelfth of a series containing papers and discussions presented before the Iron and Steel Division of the American Institute of Mining and Metallurgical Engineers since its organization in 1928; one volume each year, as follows:

1928, Iron and Steel Technology in 1928 (later listed as Volume 80 of the TRANSACTIONS); 1929 (vol. 84), 1930 (vol. 90), 1931 (vol. 95), 1932 (vol. 100), 1933, 1934, 1935, 1936, 1937, 1938 and 1939, TRANSACTIONS of the American Institute of Mining and Metallurgical Engineers, Iron and Steel Division.

This volume contains papers and discussions presented at the meetings at Detroit, Oct. 17–19, 1938 and New York, Feb. 13–16, 1939.

Papers on iron and steel subjects published by the Institute prior to 1928 are to be found in many volumes of the TRANSACTIONS of the Institute; in Vols. 37 to 45, inclusive; 47, 50 and 51, 53, 56, 58, 62, 67 to 71, inclusive; 73 and 75. Vol. 67 was devoted exclusively to iron and steel.

Iron and steel papers published in the TRANSACTIONS may be found by consulting the general indexes to Vols. 1 to 35 (1871–1904), Vols. 36 to 55 (1905–1916), Vols. 56 to 72 (1917–1925), and Vols. 73 to 117 (1926–1935), and the indexes in succeeding Year Books.

Reference

FOREWORD

This volume of the TRANSACTIONS of the American Institute of Mining and Metallurgical Engineers, made up as it is of the Howe Memorial Lecture and a selection of the technical papers with their discussions, which were presented before the several meetings of the Iron and Steel Division during the past year, will be of interest to our whole Division membership.

Dr. H. W. Gillett's interesting Howe Memorial Lecture, entitled "Some Things We Don't Know about the Creep of Metals," appears at the beginning of the volume. Its presentation at the February meeting had even greater interest because of the presentation at that time before the Institute of Metals Division of their Annual Lecture entitled "The Creep of Metals," by Prof. Daniel Hanson, of England. Professor Hanson's lecture appears in the current Institute of Metals Division volume (Vol. 133). These two lectures together summarize admirably the status of current knowledge on this important subject.

The two papers in this volume on the Solidification of Rimming-steel Ingots contain a wealth of information on this increasingly interesting and important subject. They will, we believe, be a continuing source of valuable help for steelmakers in improving the quality of soft rimming steel.

Three papers dealing with the properties of iron, two on iron-silicon alloys, two papers referring to the surface characteristics of stainless steel, as well as papers dealing with the heat-treatment of alloy steels, papers of particular interest to physical metallurgists and several papers on general metallurgical subjects, make up the remainder of this volume. Again this year, the Table of Contents of the current Institute of Metals Division volume is printed at the end of this volume.

The Open Hearth Committee and the Blast Furnace and Raw Materials Committee of the Division held a Joint Conference in Cleveland during April of this year—a most successful meeting with an attendance of about 600. The proceedings of this conference are published separately as a 275-page book entitled "1939 Open Hearth Proceedings." These *Proceedings* have become the most authoritative source of information on practical open-hearth operation in this country.

J. H. NEAD, *Chairman,*
Iron and Steel Division.

EAST CHICAGO, INDIANA
August 23, 1939

3

The Howe Memorial Lecture

THE Howe Memorial Lecture was authorized in April, 1923, in memory of Henry Marion Howe, as an annual address to be delivered by invitation under the auspices of the Institute by an individual of recognized and outstanding attainment in the science and practice of iron and steel metallurgy or metallography, chosen by the Board of Directors upon recommendation of the Iron and Steel Division.

So far, only American metallurgists have been invited to deliver the Howe lecture. It is believed that this lecture would gain in importance and significance were it possible to include metallurgists from other countries, but the Institute has not yet been able to do this on account of lack of special funds to support this lectureship.

The titles of the lectures and the lecturers are as follows:

1924 What is Steel? By Albert Sauveur.
1925 Austenite and Austenitic Steels. By John A. Mathews.
1926 Twenty-five Years of Metallography. By William Campbell.
1927 Alloy Steels. By Bradley Stoughton.
1928 Significance of the Simple Steel Analysis. By Henry D. Hibbard.
1929 Studies of Hadfield's Manganese Steel with the High-power Microscope. By John Howe Hall.
1930 The Future of the American Iron and Steel Industry. By Zay Jeffries.
1931 On the Art of Metallography. By Francis F. Lucas.
1932 On the Rates of Reactions in Solid Steel. By Edgar C. Bain.
1933 Steelmaking Processes. By George B. Waterhouse.
1934 The Corrosion Problem with Respect to Iron and Steel. By Frank N. Speller.
1935 Problems of Steel Melting. By Earl C. Smith.
1936 Correlation between Metallography and Mechanical Testing. By H. F. Moore.
1937 Progress in Improvement of Cast Iron and Use of Alloys in Iron. By Paul D. Merica.
1938 On the Allotropy of Stainless Steels. By Frederick Mark Becket.
1939 Some Things We Don't Know about the Creep of Metals. By H. W. Gillett.

CONTENTS

.

BYLAWS OF THE IRON AND STEEL DIVISION

(As approved by the Board of Directors, September 16, 1937; Art. VII, Sec. 7, approved March 17, 1939.)

ARTICLE I

NAME AND OBJECTS

SEC. 1. This Division shall be known as the Iron and Steel Division of the American Institute of Mining and Metallurgical Engineers.

SEC. 2. The objects shall be to furnish a medium of cooperation between those interested in the metallurgy and industry of iron and steel manufacture and use; to represent the A.I.M.E. in so far as ferrous metallurgy is concerned, within the rights given by A.I.M.E. Bylaw XVII, Section 3, and not inconsistent with the Constitution and Bylaws of the A.I.M.E.; to hold meetings for social intercourse and the discussion of ferrous metallurgy; to stimulate the writing, presentation and discussion of papers of high quality on ferrous metallurgy; to reject or accept such papers for presentation before meetings of the Division.

ARTICLE II

MEMBERS

SEC. 1. Any member of the A.I.M.E. of any class and in good standing may become a member of the Division upon registering in writing a desire to do so.

SEC. 2. Any member not in good standing in the A.I.M.E. shall forfeit his privileges in the Division.

ARTICLE III

DUES AND ASSESSMENTS

SEC. 1. Dues or assessments may be fixed by the Executive Committee of the Division, subject to the approval of the Board of Directors of the A.I.M.E.

SEC. 2. The funds received by the Division shall be apportioned by the Executive Committee of the Division.

ARTICLE IV

MEETINGS

SEC. 1. The Division shall meet at the same time and place as the Annual Meeting of the A.I.M.E., and at such other times and places as may be determined by the Executive Committee subject to the approval of the Board of Directors of the A.I.M.E.

SEC. 2. The annual business meeting shall be held within a few days before or after the annual business meeting of the A.I.M.E.

SEC. 3. At any meeting of the Division for which notice has been sent to the members of the Division through the regular mail at least one month in advance, a business meeting may be convened by order of the Executive Committee, and any routine business transacted not inconsistent with these Bylaws or with the Constitution or Bylaws of the A.I.M.E.

SEC. 4. For the transaction of business, the presence of a quorum of not less than 25 members of the Division shall be necessary.

ARTICLE V

OFFICERS AND GOVERNMENT

SEC. 1. The officers of the Division shall consist of a Chairman, three Vice-chairmen, Secretary and Treasurer. The office of Secretary and Treasurer may be combined in one person, if desired by the Executive Committee.

SEC. 2. The government of the affairs of the Division shall rest in an Executive Committee, in so far as is consistent with the Bylaws of the Division and the Constitution and Bylaws of the A.I.M.E.

SEC. 3. The Executive Committee shall consist of the Chairman, three Vice-chairmen, Past Chairman, and nine members, all of whom shall be nominated and elected as provided hereafter in Article VII.

SEC. 4. The Chairman and Vice-chairmen shall serve for one year each, or until their successors are elected. Each member of the Executive Committee shall serve for three years. The Chairman shall remain a voting member of the Executive Committee for one year after his term as Chairman.

SEC. 5. With the exception of the Secretary and Treasurer, no officer or member of the Executive Committee may be immediately re-elected to the same office.

SEC. 6. The Secretary and Treasurer of the Division shall be invited to meet with the Executive Committee, but without ex-officio right to vote. These officers shall be appointed annually by the Executive Committee, from the membership of the Executive Committee or otherwise.

SEC. 7. The annual term of office for officers of the Division shall start at the close of the Annual Meeting of the Institute and shall terminate at the close of the next Annual Meeting.

ARTICLE VI

COMMITTEES

SEC. 1. Standing committees, technical committees and special committees may be established, re-appointed and discharged by the Executive Committee except as provided in Article VI, Section 2.

SEC. 2. After the initial organization any technical committee may, by proper notice to the Executive Committee, elect annually its own officers and members. In the event that any such committee fails to hold annual elections, the right to reappoint or discharge shall revert to the Executive Committee.

SEC. 3. The Committee on Papers and Programs shall consist of the Chairman of the Division and of the Chairmen of the standing technical committees and of such other committees of the Division as the Executive Committee may designate.

SEC. 4. The duties of the technical committees shall be to advance the art of the industry in the field of their assignment and to secure papers within their own fields for presentation at meetings of the Division and of the A.I.M.E., subject to the regulations of the Papers and Programs Committee of the Division.

ARTICLE VII

NOMINATIONS AND ELECTION OF OFFICERS AND COMMITTEES

SEC. 1. Every year the Division shall elect a Chairman, three Vice-chairmen and three members of the Executive Committee.

SEC. 2. A Nominating Committee of five members of the Division shall be appointed by the Executive Committee immediately after the annual meeting.

SEC. 3. The Nominating Committee shall make its report to the Executive Committee not later than June 1.

SEC. 4. Any ten members of the Division may submit nominations for one or more offices to the Executive Committee not later than August 15th, and the persons so nominated shall be included in the official ballot.

SEC. 5. The voting shall be by letter ballot.

SEC. 6. The ballots shall be counted by a committee of tellers appointed by the Executive Committee.

SEC. 7. The Executive Committee shall fill vacancies in any offices of the Division occurring for any reason other than the expiration of term of election.

ARTICLE VIII

AMENDMENTS

SEC. 1. Proposals to amend these Bylaws shall be made in writing to the Executive Committee and signed by at least ten members. They shall be considered by the Executive Committee and announced to the members through the columns of "Mining and Metallurgy," together with any comments or amendments made by the Executive Committee thereon. They shall be voted upon at the annual meeting of the Division in February or by letter ballot, as may be directed by the Executive Committee.

IRON AND STEEL DIVISION

Established as a Division February 22, 1928

Chairman, J. HUNTER NEAD, East Chicago, Ind.
Past Chairman, JAMES T. MACKENZIE, Birmingham, Ala.
Vice-chairman, C. H. HERTY, JR., Bethlehem, Pa.
Vice-chairman, FRANK T. SISCO, New York, N. Y.
Vice-chairman, EARLE C. SMITH, Cleveland, Ohio
Secretary, LOUIS JORDAN, 29 West 39th St., New York N. Y.

Executive Committee

R. H. ABORN,[1] Kearny, N. J.
ERIC R. JETTE,[1] New York, N. Y.
W. J. REAGAN,[1] Pittsburgh, Pa.
WILLIAM A. HAVEN,[2] Cleveland, Ohio
JEROME STRAUSS,[2] Bridgeville, Pa.

KENT R. VAN HORN,[2] Cleveland, Ohio
JOHN CHIPMAN,[3] Cambridge, Mass.
H. J. FRENCH,[3] New York, N. Y.
H. W. GRAHAM,[3] Pittsburgh, Pa.

Mining and Metallurgy
A. B. KINZEL, *Chairman*

R. H. ABORN	F. T. SISCO	KENT R. VAN HORN

Blast Furnace and Raw Materials
RALPH H. SWEETSER, *Chairman*
A. J. BOYNTON, *Vice-chairman*
W. A. HAVEN, *Vice-chairman*
FRANCIS H. CROCKARD, *Secretary*

R. C. ALLEN	P. F. DOLAN	J. A. L. ORTLEPP (S. Afr.)
L. P. BARRETT	P. G. HARRISON	F. G. PERCIVAL (India)
B. M. BIRD	CHARLES HART	F. B. RICHARDS
C. L. BRANSFORD	W. O. HOTCHKISS	C. S. ROBINSON
FRANCOIS L. CLERF	H. W. JOHNSON	F. W. E. SPIES
(France)	F. A. JORDAN	(Netherlands)
T. P. COLCLOUGH	T. L. JOSEPH	H. A. STRAIN
(England)	P. F. KOHLHAAS (India)	CLYDE E. WILLIAMS
T. B. COUNSELMAN	S. M. MARSHALL	CARL ZAPFFE

Wrought Iron
JAMES ASTON, *Chairman*

E. B. STORY	G. B. WATERHOUSE

Open-hearth Steel
L. F. REINARTZ, *Chairman*
E. L. RAMSEY, *Vice-chairman*
CLYDE E. WILLIAMS, *Secretary*

R. L. BOWRON	R. C. GOOD	A. P. MILLER
JOHN T. BREUNICH	C. H. HERTY, JR.	W. J. REAGAN
R. K. CLIFFORD	E. G. HILL	C. E. SIMS
J. F. CONNORS	J. L. HYLAND	GILBERT SOLER
M. J. DEVANEY	J. W. KINNEAR, JR.	DON N. WATKINS
C. R. FONDERSMITH	WILLIAM C. KITTO	F. G. WHITE

Bessemer Steel
H. W. GRAHAM, *Chairman*

G. L. DANFORTH, JR.	G. A. REINHARDT	G. B. WATERHOUSE
E. F. KENNEY		R. J. WYSOR

[1] Until February 1940.   [2] Until February 1941.   [3] Until February 1942.

Membership

W. J. MacKenzie, *Chairman*

J. R. Adams
R. L. Baldwin
R. L. Bowron
W. E. Brewster
C. Y. Clayton
C. R. FonDersmith
H. J. French

F. M. Gillies
O. E. Harder
C. H. Herty, Jr.
E. G. Hill
T. L. Joseph
Charles H. Junge
A. B. Kinzel
J. G. Morrow

Robert M. Parke
H. S. Rawdon
W. J. Reagan
Bradley Stoughton
Ralph H. Sweetser
G. B. Waterhouse
Carl Zapffe

Programs

R. C. Good, *Chairman*

Frank T. Sisco

Clyde E. Williams

Papers

J. Hunter Nead, *Chairman*

James Aston
A. L. Boegehold
John Chipman
Francis B. Foley

H. W. Graham
O. E. Harder
A. B. Kinzel
H. H. Lester

L. F. Reinartz
Jerome Strauss
Ralph H. Sweetser

Nominating

James T. MacKenzie, *Chairman*

F. M. Becket

John Chipman
A. T. Clarage

L. F. Reinartz

H. W. GILLETT

Henry Marion Howe Memorial Lecturer, 1939

Some Things We Don't Know about the Creep of Metals

By H. W. Gillett,[*] Member A.I.M.E.

(Henry Marion Howe Memorial Lecture[†])

. Unlike most previous Howe lecturers, I had not the good fortune to be associated with Henry Marion Howe, nor to be directly one of his students. Yet, through his writings, he has been my teacher, as he has of all American metallurgists.

Instructive as his writings are—I use the present tense because Howe thought so keenly and reasoned so surely, seeing clearly, as if by intuition, what was hazy to lesser minds, that his writings are still vital—it is not those books and papers, nor even the minds he trained in his classes, that were his most outstanding service. It was the spirit of Howe in his approach to the problems of metallurgy, his broad-mindedness and fairness, his recognition of the need for theories and hypotheses to explain metallurgical phenomena, his willingness to use them as servants, as well as his questioning attitude—his refusal to accept them as masters—that comprise his greatest service. This most thoroughly warrants the honor the Institute pays each year to his memory. These traits I so respect and honor in any man that I glory in this opportunity to do reverence to him in whom they were so notably united.

Howe's Discussion of a Creep Problem

I have often wished that Howe were still with us to turn his keen insight upon the problems of the use of metals at high temperatures, a field much studied but still very hazy. Indeed, 53 years ago, in a paper[1] before this Institute, Howe stated a problem closely allied to some that still perplex metallurgists and engineers dealing with the high-temperature field.

Howe was intrigued by a report[2] from another old master, Robert Henry Thurston, on the behavior of annealed vs. cold-drawn iron wire, and in order to broaden the foundation for metallurgical generalization, Howe made experiments of his own on copper and silver. In these tests by Thurston and by Howe, the wires were rapidly loaded to determine the

---

[*] Chief Technical Adviser, Battelle Memorial Institute, Columbus, Ohio.

[†] Presented at the New York Meeting, February, 1939. Sixteenth Annual Lecture. Manuscript received at the office of the Institute Feb. 13, 1939. Issued as T.P. 1087 in Metals Technology, August, 1939.

[1] References are at the end of the paper.

tensile strength, then loads of 90 to 60 per cent of the tensile strength were applied to other wires for long periods, to see whether they broke or, if they did not, how much they stretched.

The tests were made at room temperature, and Howe's phrase for the property he was seeking to measure was the "patience of metals." Today we call it "creep," and we are primarily interested in creep at high temperatures.

Howe's room-temperature creep tests on copper are shown in Fig. 1, from the TRANSACTIONS of the Institute. Perhaps if we turn this around,
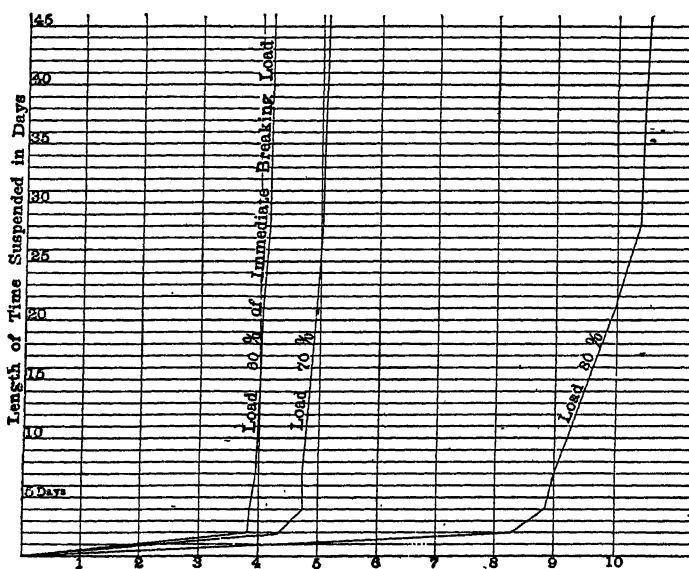
FIG. 1.—HOWE'S CURVES, 1885.[1]

Stretch of annealed copper wire, loaded with 60, 70 and 80 per cent, respectively, of its immediate breaking load.

as in Fig. 2, it will be more evident that Howe's were characteristic creep curves.

After a period of rapid elongation a fairly constant creep rate holds, and in one test it took some 600 hr. for the specimen to settle down to this fairly steady rate. Howe's tests went on for some 6500 hr., though he did not plot them that far, and Thurston's for some 12,000 hr. Howe remarked:

If the curves of stretch for the 60 and 70 per cent loads continued in their present shape, it would probably take some centuries for the amount of stretch under these loads to equal that which had been produced by the 90 per cent load at the moment when the wire parted under it. . . . In view of the extraordinary length of time under which copper stretches under such a small fraction of its immediate breaking load, the interesting question presents itself for our speculation, whether it and similar metals would forever resist any tensile strain, no matter how small, whether even under a

very light stress the metal would not keep on stretching and stretching, very slowly to be sure, but still always stretching, until, after a sufficient number of aeons had rolled by, it would suddenly break.

Interesting questions about creep have been raised, in increasing number, ever since. Some of these have fairly definite answers, thanks to active investigational work, but very many do not.

The high-temperature behavior of metals, and specifically, the creep of metals, appealed to me as a suitable topic for this lecture not because creep is the only, or the most important matter, in the use of metals at high temperatures, but because its consideration needs approach in the questioning attitude of Howe. The rejection of plausible, but untrue, generalizations about creep is, to my mind, necessary before we can have real progress. So my subject is: "Some Things We Don't Know About the Creep of Metals."
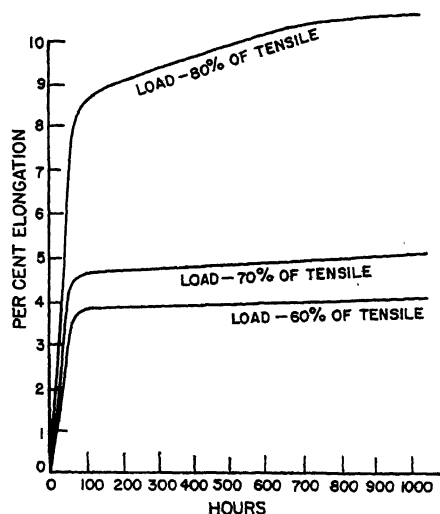
FIG. 2.—HOWE'S CURVES TURNED AROUND.

WHY RELIABLE INFORMATION IS SCANTY

The chief reason we know so little about creep, and that so many of the guiding principles and generalizations put forth prove later to be unsound, is the paucity of reliable experimental data. Good data are scarce because of the time and cost required to get them, and this is because of the extremely tiny deformation with which the student of creep is concerned and the long time over which even very tiny deformation must be postponed in actual engineering service. Experimental difficulties are multiplied, because tests must be made at high temperatures.

In a room-temperature tensile test a permanent deformation of 0.2 per cent is a common criterion of the yield strength, in order that measurement can be reliably made. Turbine engineers demand that turbine disks shall not stretch more than that 0.2 per cent in a life of some 25 years, say 200,000 hr. This permissible rate of creep is one hundredth of one millionth of an inch per inch per hour.

Some high-temperature services, such as heat-resistant alloys in furnaces, tubes in oil cracking, etc., and lead linings for sulphuric acid chambers near room temperature, might stand a total deformation of 5 per cent in their useful life; or, say, a rate of 1 per cent in 10,000 hr. This is about the highest creep rate tolerated in engineering design where

creep is a factor. It corresponds to extension of one millionth of an inch per inch per hour. Engineers dealing with services in which minimum creep and rather liberal amounts of creep are permissible have tended to scoff at each other's ideas of permissible creep and to be intolerant of experiment aimed at the other man's problem. Even the "liberal" creep rate presents difficulties in testing technique. These small rates of creep must be determined on common steels at temperatures of, say, 750° to 1250° F., and on heat-resisting alloys up to 2000° F. The standard test is to apply a fixed load at a fixed temperature for a long time, noting the total deformation and the rate of extension. The creep rate at a given load may increase 10 per cent for an increase of 1° F., though the increase varies with the material and temperature. In other words, a rise of 10° F. may halve the service life. In comparison with the tiny deformations of creep, the thermal expansion of steel is huge. A change of 1° F.will change a 2-in. test length by some 15 to 20 millionths of an inch in pearlitic steels, at the temperatures in question. The experimental difficulties in temperature control are obvious.

Moreover, many steels and other alloys, under the stresses and temperatures of interest in creep, do not settle down to a reasonably definite behavior for hundreds of hours, so that even if we could control the temperature to a hair and accurately measure the rate of deformation in the first stages, we would still fail to evaluate the creep behavior of the sample. Hence, to mean anything, a regulation creep test must go on, under a constant load and at an accurately constant temperature, for at least 1000 hr. Some laboratories are adopting 3000 to 5000 hr. as their standard testing time.

The plastic flow in creep is so tiny that experience with extreme flow, as in hot-rolling or cold-rolling, is not directly applicable. We are dealing with the very onset of plastic flow. Moreover, the creep test is so sensitive that it detects differences in materials not revealed by less sensitive tests. Hence all our conclusions as to creep need to be based on direct tests; collateral evidence is not enough.

RELIABILITY OF DATA

Pioneer data were obtained at such high creep rates, short times, and lax temperature control that they must be discarded either for purposes of engineering or for those of metallurgical generalization. A pertinent question is, then: "Can laboratories today check each other on creep tests?" The Joint Research Committee of the American Society for Testing Materials and the American Society of Mechanical Engineers on Effect of Temperature on the Properties of Metals* studied the testing variables, laid down a test code[3] and had half a dozen laboratories make

---

* Hereafter mentioned as the Joint Committee.

creep tests on a uniform and stable steel. In terms of stress for a rate of deformation of one millionth of an inch per inch per hour at the end of 1000 hr., the laboratories that took the precautions laid down in the Code returned results[4] agreeing within ±3.5 per cent. There is still difficulty in accurate establishment of the creep rates demanded by the turbine engineer, though Norton[5] reports it feasible to determine a creep rate to the nearest 0.1 per cent in 100,000 hr. Accuracy at even the rather high rate of 1 per cent in 10,000 hr. is none too easy at 2000°. It took us three years of struggling at Battelle to work out the technique for such temperatures.

Perhaps a dozen American laboratories and a few foreign ones, like the National Physical Laboratory and Metro Vickers in England, have satisfactorily solved the problem of quantitatively determining creep rates in the ordinary range of temperatures. Little credence can be given to the bulk of the German and Russian work because of the use of "accelerated" methods, and many other laboratories still publish so-called creep data that are meaningless. Houdremont[6] has just gone on record that German methods need to be revised and long-time studies made. Only a small fraction of all the published data may be relied upon, but the situation is rapidly improving.

EXTRAPOLATION

Laboratories ordinarily determine creep in 1000 to 3000-hr. tests. The engineer demands service life of 10,000 to 200,000 hr. Even though we can measure creep reliably throughout the laboratory test, are we justified in such great extrapolation? This is merely a rephrasing of Howe's question as to whether the creep curve continued its course for aeons of time, into terms of extent of deformation in finite time, and with the added complication of the effect of high temperature. It is the vital engineering question about creep. All other problems revolve about this one.

Of almost as great interest is the question: Can we get data equivalent to those shown by creep tests, in shorter time and at less expense?

Before we can appraise what we do and do not know, so as to try to answer such questions, we need to review some of the familiar experimental facts about creep.

THREE STAGES OF DEFORMATION

The creep curve is made up of three stages of deformation, beyond the initial elastic extension. The three stages of creep rate are marked off in Fig. 3. The curve may finally either turn up as *A*; or show a continually decreasing rate as *C*; or go on as *B*, without indicating which will happen. Stage 1 is characterized by rapid initial extension, which *decreases* with time. Stage 2 represents a practically *constant* rate, a

straight line whose slope depends upon conditions. Stage 3 represents an *increasing* rate, which, if allowed to continue, obviously leads to extreme deformation and finally to failure.

How the three stages vary with conditions is shown by an ideal, schematic family of curves, drawn by McVetty,[7] as they might look were very long-time tests available (Fig. 4). From bottom to top the curves represent increasing loads at one temperature, or, equally well, increasing temperatures at one load. The spacing between the curves
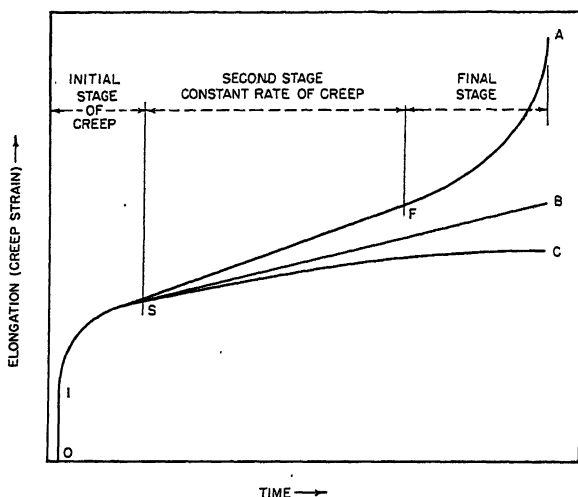
FIG. 3.—TYPES OF CREEP CURVES (NORTON).
(Babcock and Wilcox Tube Co. *Tech. Bull.* 6-C, 1938.)

for given increments of load or temperature cannot be predicted; it is a property of the material.

The vertical line *MN* represents the customary length of time of the ordinary creep test. The middle curve of the family shows decreasing creep at the end of the test, but if the load is kept on the rate of creep will increase. Note the dashed curve drawn through the inflection points of each curve of the family, as we will need to refer to it later.

The phenomena involved in the three stages may not be entirely known, but there are fairly satisfying and rather widely accepted explanations.

Stage 1—Stress Distribution

Stage 1 seems to be a period of stress readjustment. Moore,[8] in the 1936 Howe Lecture, showed "a cartoon of stress distribution," to bring out the fact that on a micro scale stress distribution within a metal is not uniform. On a large scale, stress readjustment among grains is shown by development of Lüder's lines in a tensile test or stretcher strains in deep drawing.

The effect of the abutting of crystals together is obviously to restrict slip. When block slip occurs in a single crystal, the surface becomes roughened. In a polycrystalline metal parts of the crystal may be rigidly held against slip by pressure of its neighbors, so that only a part
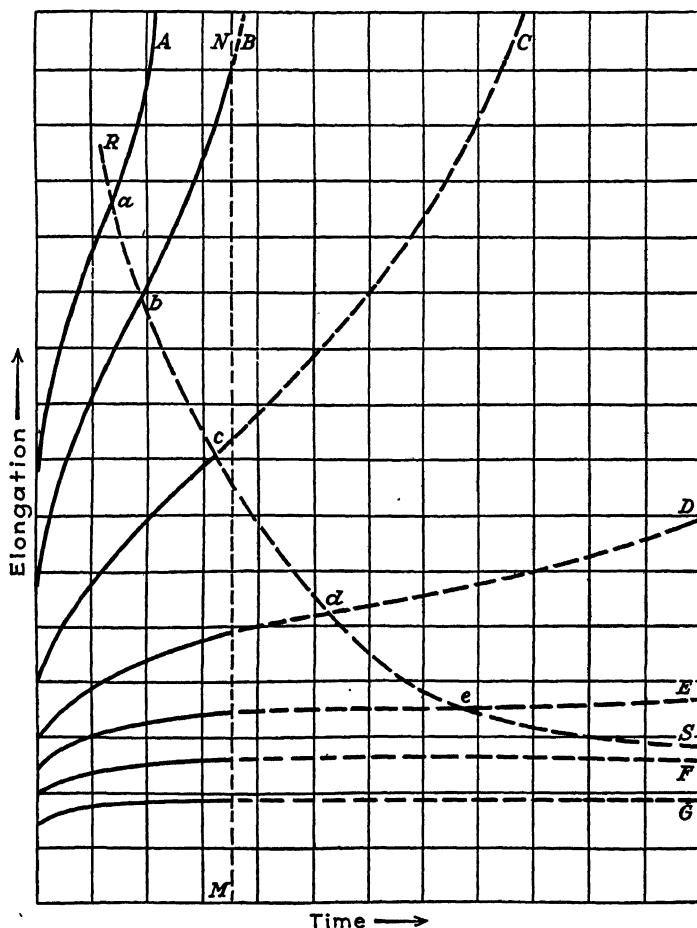
EXTRAPOLATED CREEP CURVES

FIG. 4.—A FAMILY OF CREEP CURVES (McVETTY[7]).

of a crystal may slip, as indicated in Fig. 5 by Burgers.[9] Rhines and Ward,[10] dealing with deformations that are large in relation to creep, note abrupt alterations in direction of plastic flow immediately adjacent to a boundary. They conclude that the nature of the grain boundary itself has less effect upon plastic flow than has the material of the adjacent grains. The stress-distributing action of such partial deformation is quite evident.

Howe[11] reasoned that "the stress must reach any grain through its boundaries, and here the stress is likely to be most sharply localized." He made a statistical study of the location of block slip in relation to grain boundaries at room temperature, with the result shown in Fig. 6.

Crystals have planes of easy slip and when the maximum resolved shear stress coincides with the direction of those planes, the crystal cannot carry as much load as when the stress is applied in some other direction. That creep does not vary with the load alone, but with the maximum resolved shear stress on the planes of easy slip, was nicely shown for single crystals of lead by Baker, Betty and Moore.[12] Chalmers[13,14] presents experimental evidence from room-temperature work on tin, by which he concludes that the boundary between two crystals itself has no effect upon the behavior as to deformation under stress but that, instead, it is the angle at which the lattices of two adjacent crystals are disposed that is the primary variable. This he interprets as evidence that the boundary is a transition zone from one lattice to another; a large angle between the lattice giving a "violent" transition and high resistance to slip; a small angle, a "mild" transition and low resistance to slip—that is, mere geometry seems responsible for at least part of the effect of boundaries.

FIG. 5.—RESTRAINT OF SLIP BY NEIGHBORING CRYSTALS (BURGERS[9]).
Schematic representation of distortion of a crystallite on stretching of a polycrystalline test piece (after W. E. Schmid). The direction of stretching is assumed to be vertical.

No. of Cases	29	14	5 to 10	3 Total 59
	I	II	III	IV
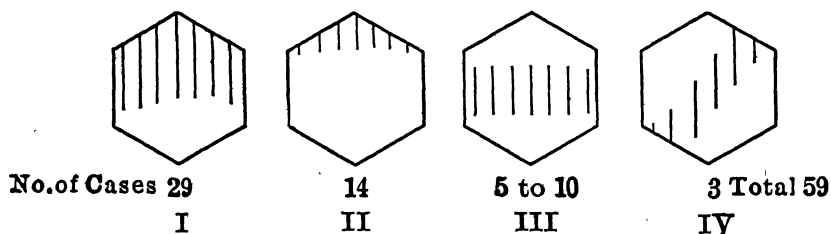
FIG. 6.—LOCATION OF SLIP-BANDS (HOWE[11]).

Thus in a polycrystalline metal the orientation of the crystals to the direction of applied stress will govern the way in which they yield under it. The most unfavorably oriented crystals will slip at once, redistributing the stress, which then affects a larger number of slightly less unfavorably situated crystals, and so on, until the metal has settled down to a con-

dition of rather uniform stress distribution. This accounts nicely for the decreasing rate of creep in stage 1.

The number of unfavorably oriented crystals in a randomly oriented polycrystalline metal is a matter of chance rather than of rule. Hence, the early part of a creep curve may differ materially for sister specimens, and the early creep rate need bear no relation to the creep rate after stress distribution approaches uniformity. Russell and Greenwood[14–23] in respect to lead and Hanson and Sandford[26] in respect to tin, emphasize that the course of the steady stage 2 creep curve is not indicated by its course in stage 1. (See also McKeown[24] and Phillips.[25]) Kanter[27] emphasizes that creep may occur locally rather than generally. Such behavior is often noted in stage 1. The same thing is met with in steels. While it is not possible to predict how long stage 1 will require to settle down, it often takes 500 hr. for it to do so.

Moore, Betty and Dollins[28] note a rotation of the grains in lead in the early stages of creep, which indicates that the mechanism is more complex than slip alone. The stress used in the tests they discuss from this point of view was much higher than would be permissible in service, so the observations do not throw much light on the normal course of early creep. Movement of the grains, however, is a logical concomitant of movement by slip within the grains, for both actions should tend toward the more uniform distribution of stress that seems to characterize stage 1.

Kanter[27,37] suggests that a distinction between short-time deformation and creep deformation resides in the amount of rotation of the grains.

Stage 2—Strain-hardening

The localized slip in stage 1 of course tends to set up strain-hardening by block slip in the crystals or portions of crystals that deform. Slip in stage 2 also tends to strain-harden. Slip is selective, it occurs primarily on certain slip planes, often spaced 1000 atom diameters or more apart, rather than uniformly on every similarly oriented slip plane of the whole lattice. It is as though certain locations in the crystal had imperfections and were weaker than others. The strain-hardening mechanism is variously explained. As satisfying as any is that of Gough[29] (Fig. 7), who postulates that along the slip plane particles are torn out of perfect alignment with the lattice but remain fairly close to that alignment, so that little thermal agitation is needed to restore them to full alignment, thus repairing the crystal and restoring its original, unhardened, properties. Physicists differentiate such a process of crystal repair from that of recrystallization annealing, in which new, randomly oriented crystals are produced from distorted ones. Jeffries and Archer[30] made the distinction long ago and pointed out that repair goes on at very much lower temperatures than does recrystallization.

However, true recrystallization can go on, and it is especially easy after "critical strain," such as is evidenced by Stead's brittleness. Different materials have different degrees of critical strain. Recrystallization is a time-temperature phenomenon. Different temperatures are given as "the" recrystallization temperature. On heavily cold-worked carbon steel, Brandon[32] considers that the "lowest recrystallization temperature" for iron is about 400°, McCarthy[21] gives it at "approximately" 842° F. Sisco[34] gives the recrystallization temperature as 750° F. or above, depending on composition and degree of cold-work. It is true

Slip direction

→

(a)

(b)

(c)
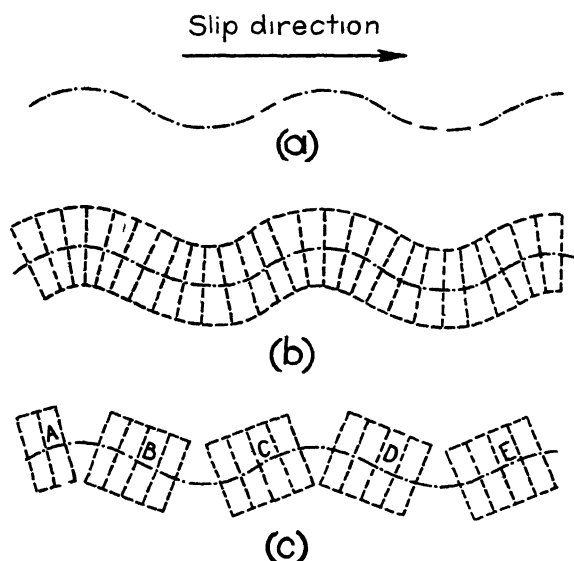
FIG. 7.—POSSIBLE RELATION BETWEEN EFFECTS OF CRYSTAL BREAK-UP AND STRAIN HYSTERESIS AND FRACTURE UNDER STATIC OR FATIGUE STRAINING, AS POSTULATED BY GOUGH.[29]

that ordinarily one does think of a "recrystallization temperature," but this is because ordinary annealing is done in a short time. Under the long times of creep, the time factor as well as the temperature is concerned. Mehl's[31] recent discussion of recovery and recrystallization should aid materially in clarifying the general understanding of these phenomena. That they are complex is evidenced by his statement that to include all the variables would require plotting in five dimensions.

A creep curve that changes direction after critical strain has been reached and recrystallization has taken place is shown in curve A of Fig. 8, from Greenwood and Orr[23] for lead. Here recrystallization could be detected metallographically. However, there need be no visible signs of recrystallization in a specimen that has deformed in creep far beyond the limit we could stand in service, even though there is, in the creep curves, clear evidence of annealing and prevention of, or effacement of, strain-hardening.

Stage 2 seems obviously to represent an approximate balance between the two opposing factors of strain-hardening and the crystal-repair type of annealing. The struggle between the two may go on for a very long period before it becomes evident which will ultimately come out on top. Of course, if deformation goes on for such an extended period that the specimen necks down so that the unit load increases, stage 3 will be entered, unless strain-hardening continually increases the resistance a bit more than incipient necking increases the load. Existence of a condition where strain-hardening clearly predominates is evidenced by a steady
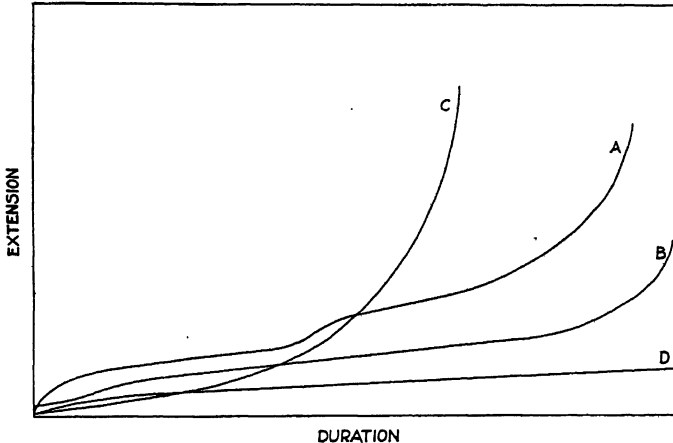
FIG. 8.—VARYING TYPES OF CREEP CURVES FOR LEAD (GREENWOOD AND ORR[23]).

A. Strain-hardening to critical deformation, followed by recrystallization: ductile failure.

B. Annealed lead, no initial strain-hardening, no recrystallization, failure by intercrystalline cracking.

C. No strain-hardening, deformation largely at crystal boundaries, failure by intercrystalline cracking.

D. Recrystallization avoided by addition of a trace of another element in solid solution.

decrease in rate of extension in stage 2. However, we are accustomed, in ordinary tensile testing, to a period of general elongation before necking starts, so that even though the creep rate may not decrease, there may be enough ability for general elongation to make stage 2 very prolonged in creep.

The most important phenomenon in the creep of a stable material is the development or lack of development of strain-hardening under the tiny deformation rate and the temperature obtaining. Creep curves are most sensitive indicators of strain-hardening, and probably the only sufficiently sensitive indicators.

Stage 3—Necking

The ordinary explanation for stage 3 is that the strain-hardening tendency is overcome by the annealing tendency, and necking starts.

However, Kanter[27] says that stage 3 sometimes occurs earlier than would be expected from study of tendencies for general elongation and necking. Moore, Betty and Dollins[28] concur. Thus even the explanations for the mechanism of creep that seem to be the most obvious and simple have still to be classed as tentative and subject to modification when we do know more.

Consideration of the course of the creep curves brings out that we will need to focus attention upon strain-hardening when we come to consider extrapolation.

GRAIN SIZE

A more puzzling matter to explain is the effect of grain size on creep. In the apparently simple cases of certain brasses,[35] tin,[13,14,26] and lead,[15—25] it is found that, at sufficiently high temperatures, coarse-grained material is materially more creep resistant than fine-grained, while at sufficiently low temperatures the fine-grained material is better. The larger the grains, the less the boundary area between them. It has been suggested that the temperature range in which the coarse-grained material is the better is above the temperature of recrystallization. However, Hanff-stengel and Hanemann[36] find that at high enough temperatures or stresses the situation is reversed and fine-grained lead again becomes superior. Greenwood and co-workers[16,20—23] show that leads of 99.99 per cent or better purity, all of the same grain size, vary vastly in creep, depending on the impurity and how it is present, so that while the statement that coarse grain is better in creep is pretty generally valid, there are plenty of exceptions and, at least with lead, plenty of other variables that far overbalance grain size. We do not know enough to make valid generalizations, even about the effect of boundaries in single-phase metals. The case of steel is likewise obscure.

From the early days of creep studies, it has been realized that cast steels with their usual coarser structure tend to be more creep resistant than wrought steels and that, at the higher temperatures at least, coarse-grained steels are inclined to be better in creep than fine-grained steels. Among others, Kanter and Spring[39] and White and Clark[40] noted these generalities. Our understanding of this phase of the problem has been greatly advanced by the work of Cross and Lowther[41] who showed that the true austenitic grain size is a major variable in a variety of killed · steels. They were able to make the same steel very good or very poor in creep by altering the treatment to produce coarse or fine austenite grains, and they demonstrated that in carbon steels the beneficial effect of coarsening held good at temperatures much lower than had been supposed. One set of comparisons is shown in Fig. 9.

Naturally, the virtues of coarse grain for creep resistance must be balanced against the failings of coarse grain in impact resistance, depend-

ing on the type of service. Cross and Lowther have shown that it is sometimes possible to make a compromise, which secures respectable creep without sacrificing too much in impact. In this connection there
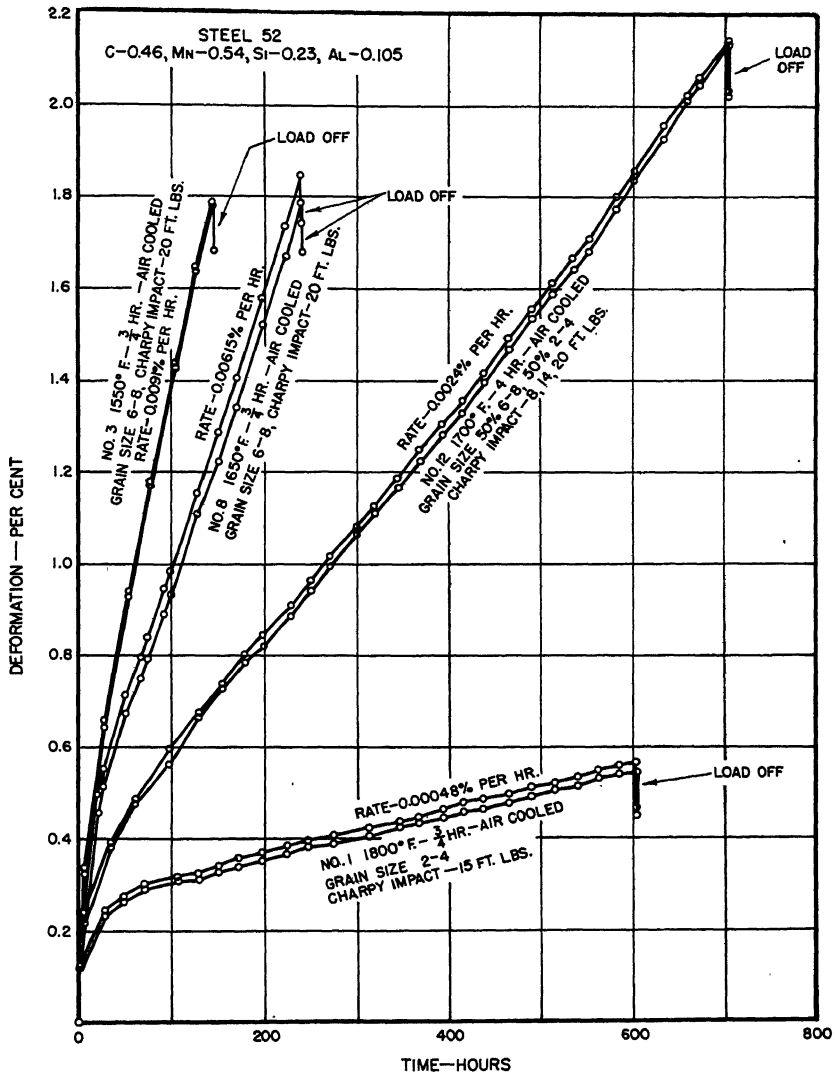
FIG. 9.—CREEP AS AFFECTED BY GRAIN SIZE, FINE, DUPLEX AND COARSE (CROSS, BATTELLE).

arises the question of duplex grain; that is, does a duplex-grained steel show the average of the properties of its grain sizes, or does it have the poor creep properties of its finer-grained fraction and the poor impact properties of its coarser-grained fraction? Mr. Cross has made some

experiments on this; the results are included in Fig. 9. Fig. 10 summarizes the results[41] of several comparisons of coarse and fine grain.

With our present knowledge of the vital effect of grain size, many of the apparent discrepancies in the older data for materials of unknown but different grain sizes would be wiped out. Conversely, it is made evident that all data, even those that were entirely accurate for the particular material tested, but which omit grain-size information, are wiped off the slate as far as their usefulness goes for purposes of generalization, since a major variable was neglected. Obviously, future comparisons must be
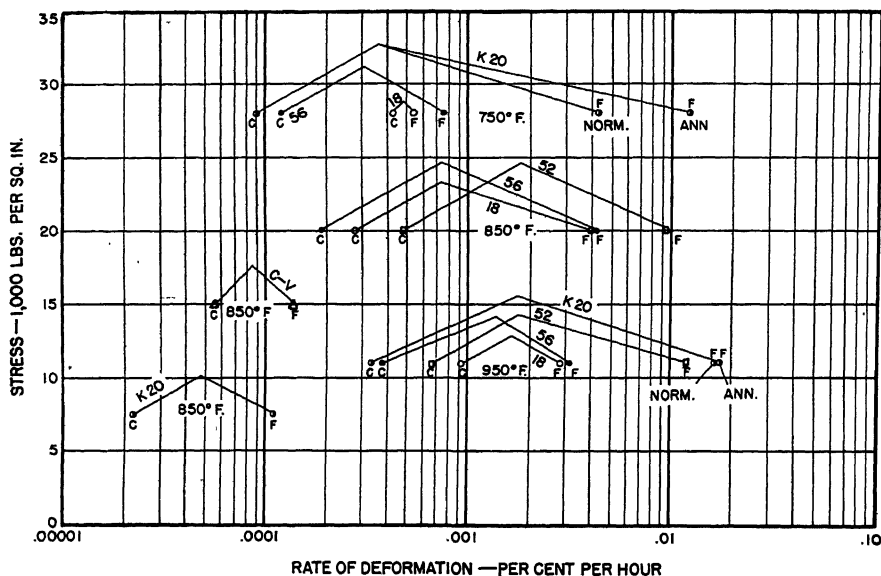
FIG. 10.—SUMMARY OF COMPARISONS OF COARSE (C) AND FINE (F) GRAINED STEELS IN CREEP (CROSS AND LOWTHER[41]).

made on the basis of equal grain size and equal propensities toward coarsening. Even the inclusion of McQuaid-Ehn (often referred to by the bad misnomer of "inherent") grain size, gives no information if the austenitic grain size of the material tested does not happen to be the same as that shown by the particular conditions of the McQuaid-Ehn test.

While the necessity of comparing creep resistance of materials on specimens of equal grain size can hardly be overestimated, we may not jump to the generalization that all we need to make any steel creep resistant is to coarsen its austenitic grain size. Cross[42] found little difference between creep behavior of coarse-grained cast and fine-grained wrought austenitic 18:8, and the widely variable crystal size shown on macroetched heat-resistant alloy castings may have little relation to creep properties.

The prior austenitic grain size of pearlitic steels is not the only factor, for rimming steel, even though coarse grained,[43] is notoriously poor in creep compared with killed steel. Moreover, Jenkins, Tapsell, Mellor,

and Johnson,[44] at the National Physical Laboratory, found one steel of 0.19 per cent C, 0.40 per cent Mn, 0.08 per cent Si classed as a killed steel, which was not improved by coarsening. A single exception is enough to invalidate a generalization. Hence "coarse vs. fine grain" is not the answer in itself, even for killed steels, but must be only an indicator of some other factor that is manifested in grain coarsening of thoroughly killed steels. Just what this more fundamental factor may be is not at all clear. It is within the bounds of possibility that it may be connected with the solution and precipitation of nonmetallics, but this is only one of many possible guesses. We do not yet know just what manufacturing variables in the killing of a steel must be controlled to ensure good creep resistance. The Joint Committee has experimental work in hand, and so has the N. P. L., in England, to throw light on this important question.

The effect of grain size other than austenitic grain size is still a closed book. Weaver[45] attempted to show the effect of what he called "actual grain size," by which he meant the coarseness or fineness of structure of a steel as tested, even in the sorbitic condition, where microscopic evaluation of this "grain size" is only a guess. I do not accept Weaver's quantitative conclusions and believe that all he has shown is an echo of austenitic grain size.

But certainly the effect of ferritic grain size resulting from rates of cooling through the critical as well as that of the prior austenitic grain size demand evaluation. The Joint Committee is studying this too, but so far we know nothing about it.

From the above, one can see that on the basis of creep tests made for sufficiently long times, with sufficiently refined technique and with sufficient attention to grain-size conditions to give data reliable enough for use in generalization, we really know very little. What we do know is only about the effect of factors huge enough to swamp out these variables and still show an effect.

When the grain-size problems have been more thoroughly worked out on the basis of ordinary testing periods, a further question will arise: i.e., is the creep-reducing effect of coarsened grain permanent; does it continue indefinitely?

Theories on Grain Size

There has been no lack of theories aimed at differences between high-temperature and low-temperature behavior. These were evolved not to explain the phenomena of creep at the onset of deformation but rather to explain those that may appear when deformation has advanced to failure. Some metals broken at low temperature break through the grains, the fracture avoids the boundaries; if broken at temperatures near the melting point, fracture may be between the grains; i.e., the fracture may seek the boundaries.

The earliest "explanation" assumed that the boundaries were actually of a different kind of material. Metals were compared to chunks of stone embedded in pitch, the hypothetical pitch phase being an "amorphous cement," and like pitch, being supposed to be strong when cold, so strong that fracture then occurred through the crystals embedded in it, but weak, and the location of fracture, when hot. This idea of a layer between crystals (or on slip planes after slip) made up of atoms that are uninfluenced by the orienting force of the atoms in the crystal lattices, has practically died out, since modern evidence fails to substantiate it. Howe[11] flirted with the amorphous theory, but made it very clear that he was using it as a tool that he was ready to abandon at any time. He remarked, of grain boundaries, that any nonoriented material between the crystals must be very thin indeed.

By electron diffraction methods it can be shown that in the first film of one metal deposited on another by electrolysis, or by condensation of metal vapor in a vacuum, the deposited atoms tend to arrange themselves, not in their own lattice but in that of the metal upon which they are deposited. The strength of the orienting force is made evident. Few people today believe in the existence of an unoriented layer at the boundaries—the amorphous theory appears to be quite wrong and therefore cannot be helpful. (Compare Gough.[29])

Aiming for a convenient shorthand to recall the facts of (usual) transcrystalline failure at low and (occasional) intercrystalline failure at high temperature, Jeffries, and Archer[30] introduced the concept that at some intermediate temperature the propensities just balance, and called this the "equicohesive temperature." This is a concept rather than an experimentally determinable temperature. Metallographic study of fractures seldom succeeds in fixing the "equicohesive" temperature within 100° or more. For carbon steels Jares[46] gives 990°; Wilson,[47] 650° to 750°. This term has been put to use in connection with creep in a way that goes far beyond the original concept of Jeffries and Archer, and one should not hold them responsible.

The basic assumption, made when applying the concept to creep, that the same mechanism of deformation holds in the last stages of failure and at the very onset of deformation, is a treacherous one. Moreover, many metals pulled in tension at very high temperatures draw down to a point with no signs of intercrystalline separation. Wherever intercrystalline separation does appear, in a high-temperature failure, the intrusion of some factor that has changed the structure is either very evident or may be strongly suspected. For example, in 18:8 and austenitic heat-resistant alloys in general, intercrystalline cracking is obviously related to accumulation of carbide at the grain boundaries, and this goes on within the dangerous temperature range if the metal is in unstabilized condition, whether stress is applied or not. Deformation in that temperature range

shows up, by cracking, the changes that have gone on, but shows nothing about any "equicohesive-temperature" effect in relation to the creep mechanism of the material free from boundary carbides.

There is no such sharpness of temperature change from intracrystalline to intercrystalline tensile fractures at high temperature as there often is in the shift from fibrous to granular impact fracture as the temperature of impact testing is reduced. It is often possible to put one's finger on a definite temperature for this impact transition, other conditions being kept constant, and if we must speak of any "equicohesive temperature" the phrase would seem more applicable to the low-temperature than the high-temperature phenomenon.

If there really were a determinable "equicohesive temperature," which could be experimentally established, and if it really did mark out fields in which creep phenomena are definitely different, its determination might be a helpful thing. Since it is not definitely determinable, the phrase tends to muddy our thinking rather than to clarify it. Kanter[27] has been quite explicit on this question. He says that the recrystallization temperature and the "equicohesive temperature" appear to be functions of the straining rate, in accordance with the mechanism of deformation permitted by that straining rate. McKeown, in a recent discussion,[50] uses the equicohesive concept, but is careful to deny that any definite temperature can be set. Houdremont[6] goes so far as to show a schematic solid diagram for stress, time and temperature to produce nonnecking fracture, though he emphasizes that it is only schematic. He compares the stress-time curve to an endurance curve.

All such evidence shows that the equicohesive temperature concept must at least be replaced by one of a stress-temperature relation. I myself question even that and am more inclined to look first for a precipitation-hardening-time factor and then for the effect of stress on precipitation, for I do not see that embrittlement has been proved to be a necessary adjunct of creep in materials in which no precipitation is possible.

Confusion is made worse confounded when "the upper temperature limit for strain-hardening in creep," or "the annealing temperature for crystal repair," "the relaxation temperature," "the recrystallization temperature," and the "equicohesive temperature" are all lumped together under the last phrase and thought of as one and the same, and a definite temperature.

I cannot see that the concept of an "equicohesive temperature" as applied to creep is of the slightest service in the practical solution of creep problems or in clarifying our conceptions of the phenomena involved. Giving a name to something we do not know about does not add to our knowledge. I would prefer to use the terminology "upper-temperature limit for strain-hardening in creep," for so phrasing it tends to keep us from assuming that it is determinable by other means than creep tests.

Definition of the boundary between the two domains of temperature in terms of strain-hardening vs. annealing has been recently given by Clark and co-workers,[51] who have made an attempt to determine the boundary by means other than creep tests. Their method is based on the observation that at low temperatures the tensile strength is not altered by change in rate of loading while at high temperatures it drops as the rate of loading slows down. If a large enough number of tensile tests is made with various rates of loading at each temperature, to overcome the normal scatter among duplicates, that temperature can be found at which rate of loading first cuts a figure. Log-log plotting allows interpolation to a constant time of fracture or rate of loading for the series of steels under study. The tensile strength for this comparable rate of loading is then plotted against temperature, and a break found in the curve. This "critical temperature" (an unfortunate choice of terms) is taken as a criterion of the end of the strain-hardening domain and the beginning of that domain where annealing predominates. For four steels with "critical temperatures" ranging from 640° to 1040°, a semilog plot of critical temperature against creep strength *at* 1000° gives a fairly straight line; so the conclusion is drawn that there may be some relation with creep. But if we plot the author's creep values *at other* temperatures, we get shot-gun curves; so any true relationship must be rather limited.

Since this is the latest published allegation that long-time properties might be determinable by brief tests, and is promulgated by experts with a lively appreciation of the inadequacy of prior allegations by others, it invites our special attention. Clark and co-workers state that they expect a relation only when the creep temperature is near the "critical temperature." While 1040° might be classed as near, 640° seems far away from 1000°. That the steels line up in proper order of creep resistance *only* at 1000° raises considerable question as to the fundamental aspect of the alleged relation.

In discussion of the Hatfield time-yield method, White and Clark[40] previously showed that the plots of time-yield vs. creep cross and that no direct conversion is possible. The same comment seems applicable to the evaluation by "critical temperature."

If we disregard the author's tentative claims for a relationship with creep and merely look at the method to see whether the "critical temperature" evaluates the strain-hardening propensity in creep and shows the upper temperature limit for service, we note that each of the four steels is commercially employed for creep-resistant uses at temperatures above its misnamed "critical." One might suggest that when deformation is smaller and slower, strain-hardening persists usefully to higher temperatures than the test indicates.

One finds it difficult to adopt the assumption underlying this method; that is, that the annealing temperature will be the same whether the deformation is carried to failure in the moderately slow tensile test (say 1 hr. duration) as when the deformation is very small and very slow, as in creep. The method appears to disregard the established fact that annealing is a time-temperature function and that the propensity toward annealing is governed by the amount of prior cold-work. Unless the basic assumptions are proven to be sound, one may well go slow in placing reliance on a short-cut method whose relation, if any, to creep properties holds only at a small temperature range, which seems unpredictable without creep tests to determine it.

So, while it may add another to the various "identity tests" and may help to give some expectation of where the crucial temperature zone may be in creep, from the point of view of telling *creep properties*, the "critical temperature" seems to be in about the same status as the "equicohesive temperature." At least, the applicability of this method cannot yet be classed among the things we know about creep.

FIG. 11.—BURGERS' AND TAYLOR'S CONCEPT OF NOTCHES AT CRYSTAL BOUNDARIES.

The "Notch Effect"

In spite of the failure of available concepts to offer a satisfying explanation of differences in behavior of the grain body and the grain boundary, one still looks for a plausible explanation.

In the discussion of slip, it was noted that block slip occurs chiefly at widely spaced weak planes, where crystal imperfections are postulated. An alternative conception is that these places need not actually be weak, but might rather be considered as locations of stress concentration, of notches within the crystal, if you will. Chalmers[52] suggests that any crystal consists of small blocks of perfect lattice arrangement slightly inclined to one another, the jogs being the imperfections that localize slip. Kochendorfer[53] definitely states that the imperfections may be looked upon as notches.

That notches might also exist at grain boundaries is an old idea. Foley[54] long ago presented a diagram to this Institute, indicating how crystal boundaries might fit together. This concept involves little jogs at the boundaries, which, if they exist as indicated, might well act as

stress raisers. Burgers,[9] citing Taylor (Fig. 11), boldly draws these places like actual wedges, which certainly look like stress raisers. Krivobok[55] mentions concentration of internal stress at grain boundaries in 18:8, as a speculation that might account for the localization of carbide precipitation.

Thus, we have the concept that both within the crystal (on the planes of selective slip), and at the boundaries there are locations of local stress concentration that start movement, either along the "weak" planes of block slip or at the boundaries, as the case may be. In other words, the "defects" within the grains and at the boundaries might differ in degree rather than in kind.

We could go one step further in our thinking. The imperfect lattice within the crystal ought to tend to become more nearly ideal as the
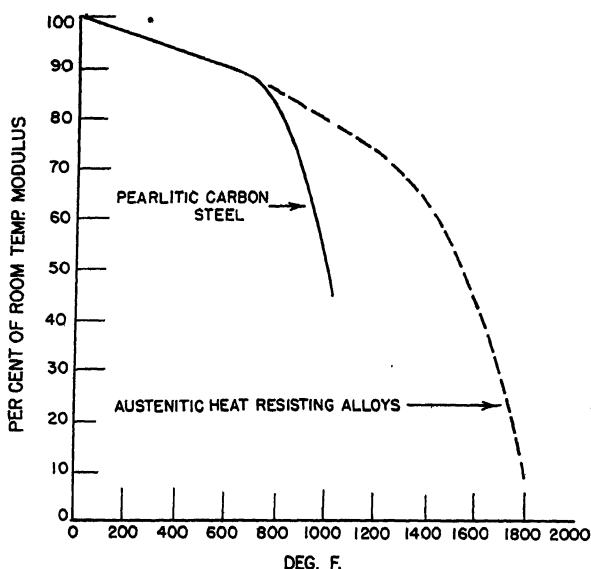
FIG. 12.—SCHEMATIC REPRESENTATION OF CHANGE IN MODULUS OF ELASTICITY WITH TEMPERATURE.

temperature rises and atom mobility increases. How great the increase in atomic mobility and the resultant loss of stiffness may be, can be recalled by Fig. 12, showing how modulus of elasticity changes with temperature. The inside of the crystal should not be far from regularity anyhow, because the orienting forces of all the atoms on all sides are exerted in the directions fixed by their arrangement in the lattice. The boundaries are acted upon by orienting forces of different crystals lying in different directions and hence the boundary notches should not heal so readily as the notches in the interior.

At high temperatures the interior notches may have become smaller and less effective; that is, the crystal interior might be less subject to locally high stress concentration when its notches are pretty well healed. If the boundary notches remained relatively larger (did not heal so readily), and were still effective at high enough temperatures the effective notches would then be almost wholly at the boundaries, and the smaller the boundary area, i.e., the larger the grain, the fewer points of stress concentration would exist.

The concept of healing of internal notches by increase in temperature may not be so far-fetched. In an earlier Howe lecture, Lucas[56] showed cracks in quenched martensite needles. It is believed that such cracks are not formed in "austempering" and that this accounts for the superiority of austempered steel harder than 45 Rockwell C. Tempering to softer than 45 Rockwell is supposed to heal the cracks and the properties of the quenched and tempered and the austempered materials become alike.

Healing of "flakes" by reforging of billets or blooms containing them is well known. Under sufficient deformation at high temperature these large-scale internal notches can be healed, so healing of much smaller notches under creep conditions might be conceived of.

As far as I know, this suggestion of notch-healing as a possible mechanism for boundary behavior in creep has not been made before. If I am responsible for it, and have not picked it up from some unknown source to which it should be credited, I hasten to state that I do not want anybody to believe it. It is merely another way of wording the experimental observations. Whenever a concept that worded the facts in a plausible fashion has been put forth and believed, it has acted as a barrier to experiment and to thinking. Glib phrases like "amorphous cement" and "equicohesive temperature," seeking to summarize, generalize and explain, have not been helpful, and another one will not be beneficial.

The conclusion has to be drawn that we do not know much about the boundary effects that must be the base for the effect of grain size.

Stability

The phenomena of strain-hardening vs. crystal repair and the grain-size factors that have been mentioned as giving a creep curve its course, can affect any metal, no matter how pure or how stable. In actual practice, especially with steel, we often have to deal with a two-phase system and with one that is not stable.

It should be emphasized that at any instant in the course of creep, the rate of deformation at a fixed load and temperature is dependent upon the actual structure of the piece at that instant, whether any difference from the original structure is due to work-hardening or to any other cause.

EFFECT OF COMPOSITION AND STRUCTURE IN PEARLITIC STEELS

The carbon content of pearlitic steels affects the creep resistance, but the strengthening effect of carbon is not as great as would be expected from room-temperature properties. Because of the marked effect of austenitic grain size, truly comparable data on steels of varying carbon content are scarce, and confined to the range 0.15 to 0.60 per cent C. We know practically nothing reliable about creep of carbonless ferrite, since the rimmed vs. killed question comes in to invalidate the older data. The Joint Committee has work in hand on the behavior of carbonless ferrite.
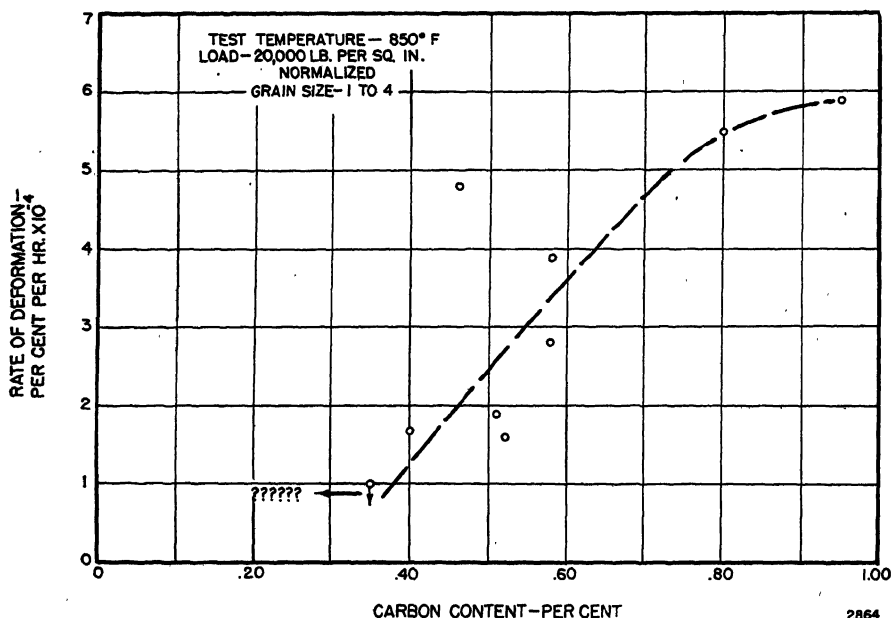
FIG. 13.—RATE OF DEFORMATION AT 500 HR. OF COARSE-GRAINED CARBON STEELS.

0.35 to 0.60 per cent C from Cross and Lowther[41] except 0.40 per cent C from Compilation of Creep Characteristics.[43] 0.80 and 0.95 per cent C, Cross, Battelle. Curve is dashed because its location is still in doubt. The Joint Committee has work in hand to fill out the low-carbon end of the curve. Astonishingly enough, in so far as comparable data are available, the lower the carbon, the better the creep resistance, but this situation is hardly expected to hold down to zero carbon.

On the other end of the scale, data on eutectoid and hypereutectoid steels are missing. Mr. Cross made some special tests so that something could be presented here to fill this gap. His results are shown in Fig. 13. When special experiments are necessary to evaluate so ordinary a thing as the effect of carbon in steel, the state of knowledge is not very far advanced!

Alloying Elements

The effect of alloying elements on creep of steel is in dispute because of the lack of real knowledge about the alloy-free base line. The effect of a few elements, notably molybdenum and to a lesser extent tungsten and vanadium, is so powerful that the benefit of their addition swamps out some of the other variables and makes itself evident. With some others, like chromium and manganese, there is indication that intermediate amounts are better than less or more. It is noteworthy that carbide-forming elements have more effect than do ferrite formers. On the whole, our knowledge in this line is scanty.

Structure

The effect of carbon is most marked when it is present as carbide layers in lamellar pearlite, hinting that the end restraint afforded to the ferrite crystals by the cementite layer is helpful. An analogous observation is that steel with ferritic bands is poor in creep. Rather coarse lamellar pearlite—a normalized structure—is superior to the sorbitic structure obtained by quenching and tempering, though the comparison is marred by the fact that normalizing is ordinarily from a higher temperature than quenching and hence, in steels coarsenable at normalizing temperature, involves larger austenitic grain size. That a given steel, originally of lamellar pearlitic structure, loses creep resistance as cementite divorce and spheroidization progress, is thoroughly established. From the engineering point of view, except for bolt stock, where peculiar service conditions exist that admit quenched and tempered steels, the known facts lead to the use of a killed, normalized steel, stabilized as best we can against spheroidization in service, when a pearlitic steel is chosen.

Stability

The structure of carbon steel is not stable at the higher range of temperatures at which it is commercially used. Not only does the carbide tend to spheroidize, but, as Kinzel and Moore[57] and Wright and Habart[58] have shown, it may even graphitize.

Bailey[59] has paid much attention to the conditions of spheroidization and concludes that in the temperature range in question, below the critical temperature, the rate of spheroidization increases in exponential fashion with temperature. We know it to be a function of time and temperature, to be affected by the initial size and distribution of cementite, and to be affected by the degree of cold-working that has occurred. The effect of stress might also come in.

The tempering and spheroidization effects, by presenting a progressively weaker structure, may destroy the benefit that the strain-hardening

process might have produced had the structure remained as it was at the start. Where structural changes occur, the creep curve is therefore a resultant curve, and one difficult to extrapolate.

The obvious remedies are: (1) start with a structure hard to spheroidize, (2) modify the cementite by addition of a carbide stabilizer (generally molybdenum), and (3) hold the temperature down so that the rate of spheroidization is low.

Precipitation-hardening

Other structural changes, also time-temperature effects, may enter, which can be lumped under the heading of changes of the precipitation-hardening type. Precipitation-hardening effects may be good or bad. In the study of carbon-molybdenum in different conditions of heat-treatment, Miller, Campbell, Aborn, and Wright[60] found indications that precipitation of carbides peppered through the grains had a marked strengthening effect. This may not be as effective in creep at higher temperatures, and Greenwood and co-workers,[16,20-23] in the study of creep of lead at room temperature, report that finely disseminated copper particles induce enhanced creep resistance, while finely distributed particles of lead telluride do not. On the other hand, Hiers and Steers[61] cite service behavior of tellurium-lead that would indicate it to be creep resistant.

While the process of spheroidization is probably but little affected by stress or deformation, we cannot be sure that the stress and deformation in creep do not alter the precipitation propensities.

There is well-founded belief that plastic deformation accelerates precipitation-hardening, and that such hardening, even in the course of the high-temperature short-time tensile test, accounts for the fact that in ordinary steels we get a rise in tensile strength in the range of 350° to 750° F. When such steel is "stabilized," as by addition of sufficient aluminum plus titanium, which should make the carbides, nitrides and oxides to which precipitation-hardening is variously ascribed all insoluble and inert, the hump in the tensile-strength curve is eliminated, as has been shown by Hayes and Griffis.[62]

Since precipitation-hardening is a time-temperature phenomenon, when a precipitation-hardenable alloy is subjected to a temperature that allows separation of the precipitate the first effect may be a keying of slip planes by particles of the correct size, but with passage of time the particles may agglomerate and the material become overaged. The mechanism, and the result upon creep, would be rather analogous to those of spheroidization. Here again, in "keying" of slip planes, we have a phraseology that is helpful in so far as it is accurate, but that may, like other phrases, be dangerous in making us think we understand a mechanism when what we are really doing is characterizing an effect.

Precipitation-hardening or phase changes during a creep test in alloys of the Konel type may be so marked, and accompanied by such a diminution in volume that "negative creep" may occur—the specimen may shorten instead of lengthening! Mochel reports having met negative creep in low nickel-chromium-molybdenum steels (personal communication Jan. 20, 1939).

Embrittlement

Unfortunately, precipitation-hardening is not always beneficial. It may embrittle, and embrittling precipitation of carbides in grain boundaries is far from unknown, particularly in austenitic high-chromium heat-resistant alloys. Especially if oxidation or other chemical attack of the grain boundaries ensues, the bar may show myriads of tiny surface cracks and may fail at low total elongation. Bailey[63] has noted such behavior even in carbon-molybdenum steels, tested at very high loads and high rates of extension, and has suggested that design be limited to such loads as will produce not over 0.5 per cent extension. White, Clark and Wilson[64] reported intercrystalline cracking of carbon-molybdenum steel at 1000°, 12,000 lb. per sq. in., and Thielemann and Parker[65] also reported it at 1100° and 10,000 lb. per sq. in., in "time to fracture" tests. Such loads are excessive in relation to design load. Aborn and Miller[66] pointed out that such behavior was met only under high rates of extension and that these steels were not embrittled until extensions were reached several times that mentioned by Bailey. Bailey[67] once modified his position but more recently[68] reoccupied his first stand. Thielemann and Parker's data seem to indicate that intercrystalline cracks are specific to certain steels (and certainly not related to an "equicohesive temperature"), and Aborn and Miller's indicate that it is a stress (i.e., deformation) problem at least as much as it is a temperature problem. Houdremont[6] brings out the same thing.

The generalization that small deformation avoids intercrystalline brittleness is opposed by Greenwood's[16,20-23] room-temperature work on lead, for he concludes that low stress produces movement at crystal boundaries and that this leads to intercrystalline cracking.

One may take either of two views of these severe overload tests—that they give information about tendencies that might not be suspected without their information, or that since no design ever calls for the extension at which intergranular parting is noted, the information sets up a straw man. A glass water pitcher could be made to appear unserviceable under a sledge-hammer test, but that would not prove glass to be a poor material for a water pitcher. Wright and Habart[58] comment on such tests that "one would scarcely expect such investigations to yield knowledge of value in design" and point out that ferritic tubes in service never fail by intercrystalline cracking at high temperature save in presence of

hydrogen, or, in one case, of highly corrosive high-sulphur oil.   There are no known cases they say, of ferritic tubes designed to operate at stresses high enough to produce intergranular fracture, nor do they actually so fail even in severe cases of overheating.   Room-temperature brittleness, in material *still tough at high temperature*, has been met by Wilten and Dixon[69,70] in certain lots of still tubes containing 5 per cent Cr.   This indicates that some precipitation-hardening effect is involved in that case rather than any mechanism of creep itself.

Wright and Habart discuss brittle behavior of 18:8, pointing out that the effect seems to come from a structural change, intergranular separation of carbides and depletion of chromium content at grain boundaries, followed by oxidation or corrosion of the depleted areas.   That 18:8 does not necessarily become brittle even in a long time, and with greater creep than one would design for, has been shown by Cross.[42]   Embrittlement of cast heat-resisting alloys with relatively high carbon by a mere short heating into the sensitive temperature zone of carbide precipitation is well known, but it can probably be as clearly shown by a room-temperature tensile test after such aging as by behavior in a high-temperature overload test or a creep test.

We must surely differentiate between the result of creep itself and the result of the natural tendency of an unstable material to go, with time and temperature, toward a more stable structure.   Such phenomena are superimposed upon creep phenomena and are not an essential part of it.

The precipitation-hardening phenomena are too specific to the particular composition to make it easy to take them into account in any general method of extrapolation of creep data.   We shall return to the topic of extrapolation a bit later.   The embrittlement problem raises an unanswered fundamental question—will the mode of failure of carbon-molybdenum or other steels be the same if a low creep rate is continued till the total deformation is reached, that is produced in the tests at higher loads, and more rapid rates?   In seeking an answer it will be necessary to untangle the precipitation phenomena from those that occur in materials not subject to precipitation.

Is Creep Testing Essential?

Having enumerated some of the matters, strain-hardening vs. crystal repair, grain size, and structural stability, that come as legitimate parts of, or a concomitant occurrence with, the creep resistance of metal, we may turn to the question whether shorter and cheaper methods will give information that can be exactly correlated with creep and thus render creep testing unnecessary.

The answer can be quite definite.   Strain-hardening in stage 2 of creep is so sensitive to conditions that no way is known to detect it other than the creep test.

There is no certain correlation between creep and short-time high-temperature tensile tests, longer ones of the "stress to fracture" type, rapid high-temperature proportional-limit tests, or the somewhat slower ones termed by Hatfield "time yield" tests. The lack of correlation has been summarized in several publications.[71-73] Very recent statements reiterating the lack of correlation between short-time tests and creep have been made by Moore, Betty and Dollins[28] by McKeown[50] and by Lea.[74] Some of the tests have value in showing behavior under high overload, but if one wants to appraise creep properties, the accelerated tests have not yet been proved to mean anything.

ALTERNATIVE TESTS

The next question is: Are there alternative, simpler and cheaper creep tests? There is a possibility that torsion creep tests, testing directly in shear, might have an advantage over tensile creep determinations, but the technique is not yet as well perfected, and the indications are that they will be no less expensive.

To use the same specimen at different loads, either starting with a low load and increasing it, or with a high load and decreasing it—i.e., "up-step" and "down-step" testing—introduces uncertainties as to the effect of prior deformation. The greatest difficulty is in setting up a standard loading schedule so that different materials can be compared. A variant of down-step testing is the "relaxation test," in which the specimen is stressed in such fashion that as creep progresses the stress is automatically decreased along whatever time-stress curve the specimen's own properties may set. This is directly applicable to the case of flange-connection bolts in rigid flanges. Carried out so that it duplicates service conditions, it is a good straightforward engineering test. In the temperature range where strain-hardening is active, it gives information of direct value on bolting stock. Some people claim to be able to extract true creep information, applicable to other service conditions, from such tests, but the processes of reasoning by which they do so seem clear only to the few that make the claim. Soderberg[75] points out that relaxation data cannot be obtained from creep tests, and the reverse should be equally true. I do not see how one may translate into comparable figures the results of tests made under different programs of stress application. Nadai and Boyd[76] offer hope of a method based on a new automatic relaxation outfit in which it would appear that the specimen does not creep but the load decreases according to the amount that the specimen would stand if it did creep. This is a bit confusing, but these investigators may be opening a path toward determination of a fundamental property of metal, uncontaminated by nonreproducible testing technique, and they hold out some hope for a rapid test, provided, they say, aging phenomena are not involved. It is a bit difficult to see how strain-hardening tendencies can

be appraised without having deformation, and one might guess that when the method is perfected it will be used to get information that will be used together with, but not supplant, creep data.

IDENTITY TESTS

Experienced workers in creep recognize that the creep properties of an unknown steel cannot yet be appraised by anything short of actual creep tests, but there is still the possibility that rapid tests may serve when we have once produced a steel of definite creep resistance, as shown by experience or extensive laboratory creep tests, and want to know whether another lot of steel, whose chemistry, treatment, and structure are held as closely as possible the same, has the same creep resistance.

This question has arisen because of highly disconcerting differences in creep behavior of steels practically identical as to ordinary chemical analysis, room-temperature properties, and microscopic structure in the condition of test. Since the creep differences appear in elevated-temperature tests, possibly other high-temperature tests will show the differences or prove the identity. Short-time high-temperature tensile tests are not particularly sensitive to these differences. Load-to-fracture tests, i.e., a series of slow tensile tests taking 10, 100, or a few hundred hours for complete failure, are being used considerably for this purpose just now and are said to sort materials into the same order as they are sorted by creep tests. I cannot see how a test under a terrific overload can be expected to tell anything about the onset of the tiniest plastic deformation and would consider such tests the type least likely to bear an accurate relation to creep properties, whatever they may tell about resistance to overload.

The advocates of accelerated creep tests are, either admittedly or tacitly, actually working on the basis of comparison with a known "prototype" steel and examining other lots to see whether the early course of the creep curve is the same as that of the prototype.

Jasper[77] has recently reiterated his belief that design can be based on what he calls the "long-time limit of proportionality," determined by a series of tests up to 48 hr. As Thum pertinently points out in a footnote, deformation does go on at loads lower than this so-called limit, and the only thing that saves such design is the use of a factor of safety. It seems to me that Jasper's success in design, using what appears to me to be an unsound basis, is that in truth he is probably not really designing on the basis of his test figures at all, but on engineering experience with a certain class of steel, his test merely giving him some assurance of the identity of the lot being tested with that general class, i.e., with a prototype, in a given type of service. This rough and ready method presupposes a large acquaintanceship with the prototype. Anyone using a

new and different class of steel or a more exacting type of service and trying to design on the "long-time limit of proportionality," using only the pound-per-square-inch figure without certainty as to the applicability of the same old factor of safety, may have a rude awakening, because the behavior up to 48 hr., and even to much longer periods, does not necessarily tell what the behavior is going to be for thousands of hours.

One who has made many duplicate creep tests of the same material is impressed with the variety of behavior that may be shown in the early part of the creep curves on samples that, after that, settle down to similar behavior. What course a piece of metal will take while it is settling down to uniform creep behavior seems quite unpredictable, and as long as it does ultimately settle down this early behavior is relatively unimportant from the engineering point of view. One might easily throw out good material by demanding identity from the very start of a creep test.

The identity tests are on trial, with the chances very slim that any of them will prove really valuable in the long run. Creep is extremely sensitive to what we would normally consider minor variables. The identity tests seem unlikely to show equal sensitivity. At any rate we cannot yet claim real knowledge of their utility.

The nub of the whole matter seems to be that the short-cut tests are usually related to large deformation while creep is a matter of tiny deformation. Unless the mechanisms of deformation are the same, irrespective of the amount of deformation, the phenomena we wish to evaluate may be thoroughly swamped out by those that are not pertinent.

Gough[29] has reviewed these matters, in special reference to fatigue, and his ideas seem equally applicable to creep. He points out that deformation proceeds in four steps: (1) crystal fragmentation (strain-hardening by slip), (2) disturbance of electronic arrangement, (3) lattice distortion, (4) preferred orientation. Tests to failure carry the deformation clear through the gamut, while deformation in creep, of any permissible degree, certainly falls far short of producing preferred orientation.

It is much the same old story that crops up so often in corrosion and wear testing—if we exaggerate and intensify the conditions of attack until we produce a different type of attack, the answers we get from the tests are those that relate to other than service conditions and may be highly misleading when we attempt to apply them to true service conditions. If we need to trace a baby's growth on a milk diet, we do not try to speed up the experiment by feeding him whiskey, but when we deal with metals we are all too prone to make ourselves just as ridiculous in the way we frame our test methods.

Moore, Betty and Dollins[28] note a difference in creep behavior of lead at low load, i.e., decent design loads, compared to that at high loads. Log-log plots stubbornly refuse to be straight lines at the low stress end.

EXTRAPOLATION

Thus it appears that if we want information on creep we can, so far, obtain it only by creep tests, and we come back to the question of extrapolation. To look first at the dark side of the picture, recall that stage 2 may extend for thousands of hours, indicating satisfactory balance between strain-hardening and crystal repair, yet at a later period stage 3 may show up. Consider Fig. 14 from Clark and White.[35] The higher
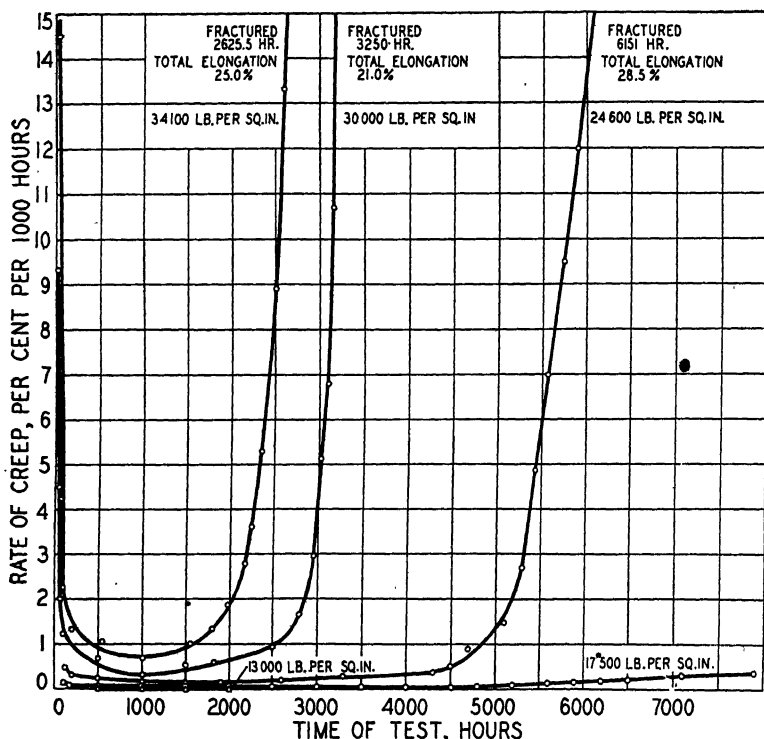
FIG. 14.—STAGE 3 DEFORMATION UNDER EXCESSIVE LOADS (CLARK AND WHITE[35]).

loads used were intentionally chosen to produce large deformations; only the lower two are anywhere near the 1 per cent in 10,000 hr. that experience has shown is somewhere within gunshot of the deformation resulting from the limit of useful loading. However, even here the 17,500 lb. per sq. in. curve showed a fairly constant rate from 1000 to 3000 hr., but from 3000 to 8000 hr. the rate increased.

Clark and Robinson[78] gave a similar family of curves. Foley showed the curves of Fig. 15 and remarked[79] that it is useless to test at a creep rate much above 0.1 per cent in 1000 hr. Foley's comment hits the nail on the head, for when the deformation is held down to such a figure, comparable with present design values, stage 2 is extremely long, in a

stable material. Under such conditions, we may have an extremely long period of constant creep. Figs. 16 and 17, from Cross and Lowther[80],[81] show results for 18:8 and an annealed carbon steel, respectively, under the conditions shown. Fig. 17 records diminishing creep for 4000 hr., and a very constant rate thereafter for the remainder of the 20,000-hr. test.

Subsequent to this 20,000-hr. test, this specimen was run 4000 hr. more at lower and higher temperatures, to a total deformation of 2.16 per cent. Metallographic study and tensile and impact testing after
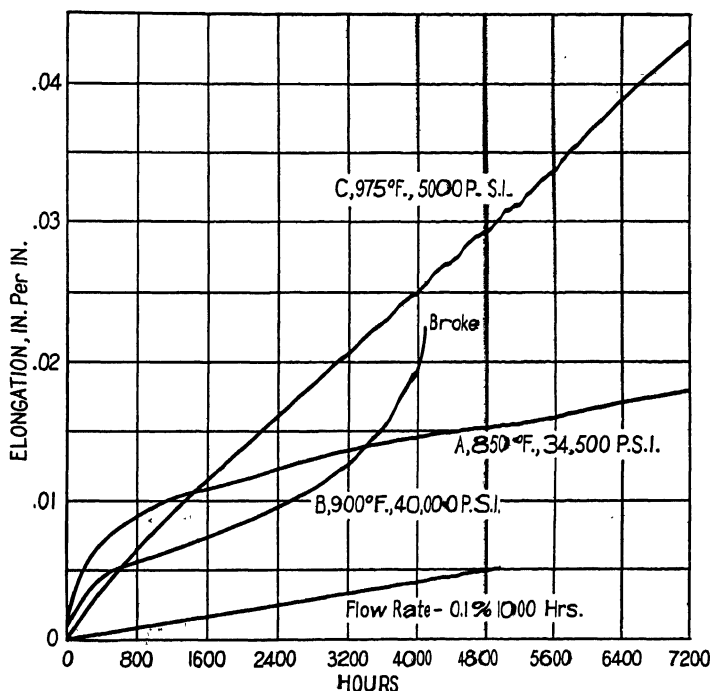
FIG. 15.—CREEP CURVES FROM FOLEY.[79] PEARLITIC ALLOY STEELS UNDER VARIOUS LOADS AND TEMPERATURES.

creep showed no deterioration of the bar. After the intitial 4000 hr., the bar showed good constancy of creep rate and no tendency to enter stage 3. This steel was exceptionally uniform, and the bar was initially in a very stable state.

The best we can do is to extrapolate on the basis of a constant stage 2 rate of deformation and make the best possible effort to ensure that the material is so stable that such an extrapolation will hold.

Graphic Extrapolation

With the definite understanding that we are using the assumption that stage 3 will *not* be entered, an approximate extrapolation is possible. The relation between stress and rate of stage 2 deformation is a function
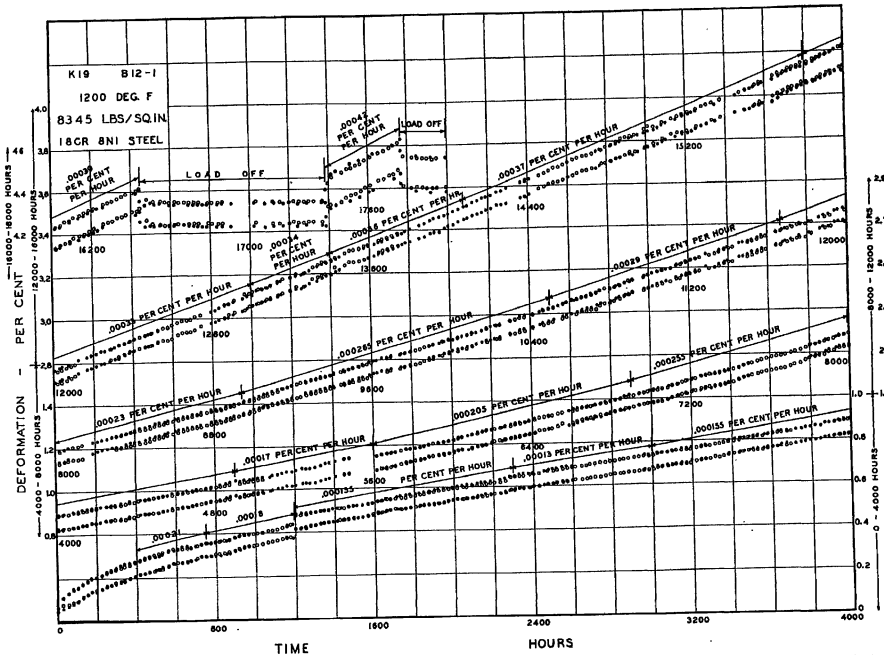
FIG. 16.—CREEP TEST ON 18-8 FOR 17,000 HOURS AT HIGHER THAN DESIGN LOADS, SHOWING LONG MAINTENANCE OF STAGE 2 (CROSS AND LOWTHER[80]).
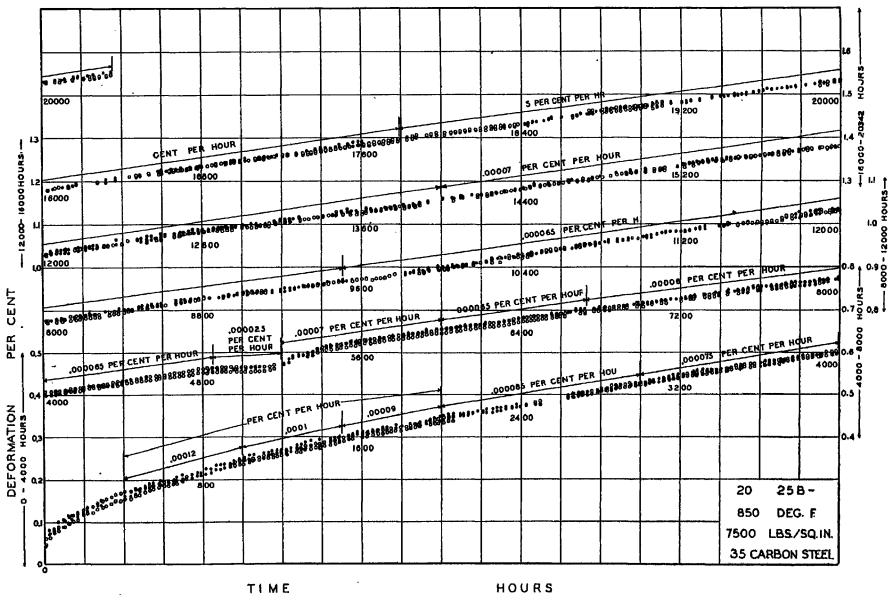
FIG. 17.—CREEP TEST ON 0.35 PER CENT C STEEL FOR 20,000 HOURS, STILL IN STAGE 2 (CROSS AND LOWTHER[81]).

of approximately exponential form, so, by log-log plotting, we approach a straight line. This method of reporting creep data is universally used, and gives some approximation to a means of extrapolation. However, the slope of the line varies greatly. You must have more than one point to plot before you can draw the line.

I have been careful to use the word "approximate" because the log-log plots are not necessarily straight. Kanter[27] states, and Norton agrees, that the log-log plot is not exact enough to use with complete assurance
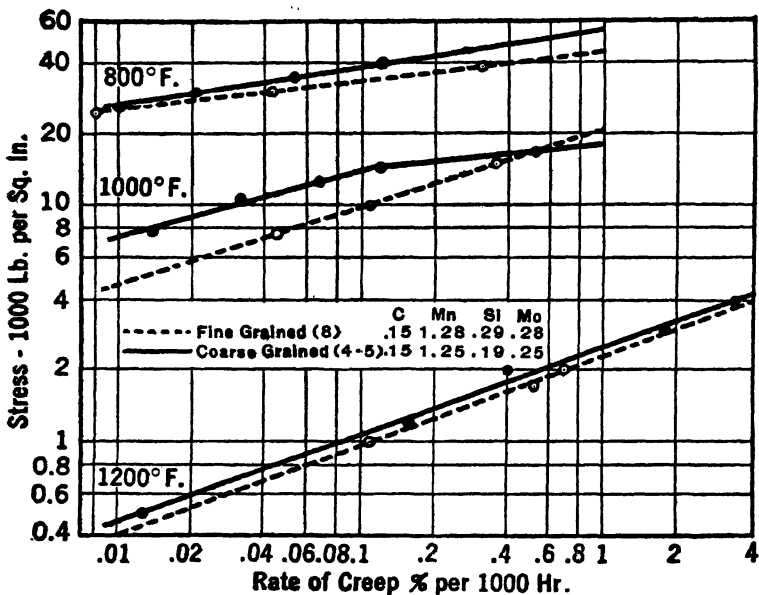
FIG. 18.—LOG-LOG PLOTS (WHITE AND CLARK[40]).

for large extrapolation. Nadai[82] finds that a hyperbolic sine function fits experimental data better than an exponential function. The fit, however, is none too good. That the log-log plots are not necessarily straight and that the slopes vary is nicely shown in Fig. 18, from White and Clark.[40] Further comment to similar effect is made by Boyd,[83] and Moore, Betty and Dollins[28] show Fig. 19.

Mathematical Extrapolation

There have been many attempts to develop mathematical formulas that will take in more factors than does graphical extrapolation. Fig. 20, from Marin,[84] indicates that two of the most thoroughly thought-out mathematical systems of extrapolation appraise the same data differently. It is interesting to follow successive publications of some of the exponents of mathematical attack. The early hopes grow dim as they think and experiment further upon the possibility of establishing mathematical

Tensile Stress in lb. per sq. in.

Creep Rate in Per Cent in 10 000 Hours
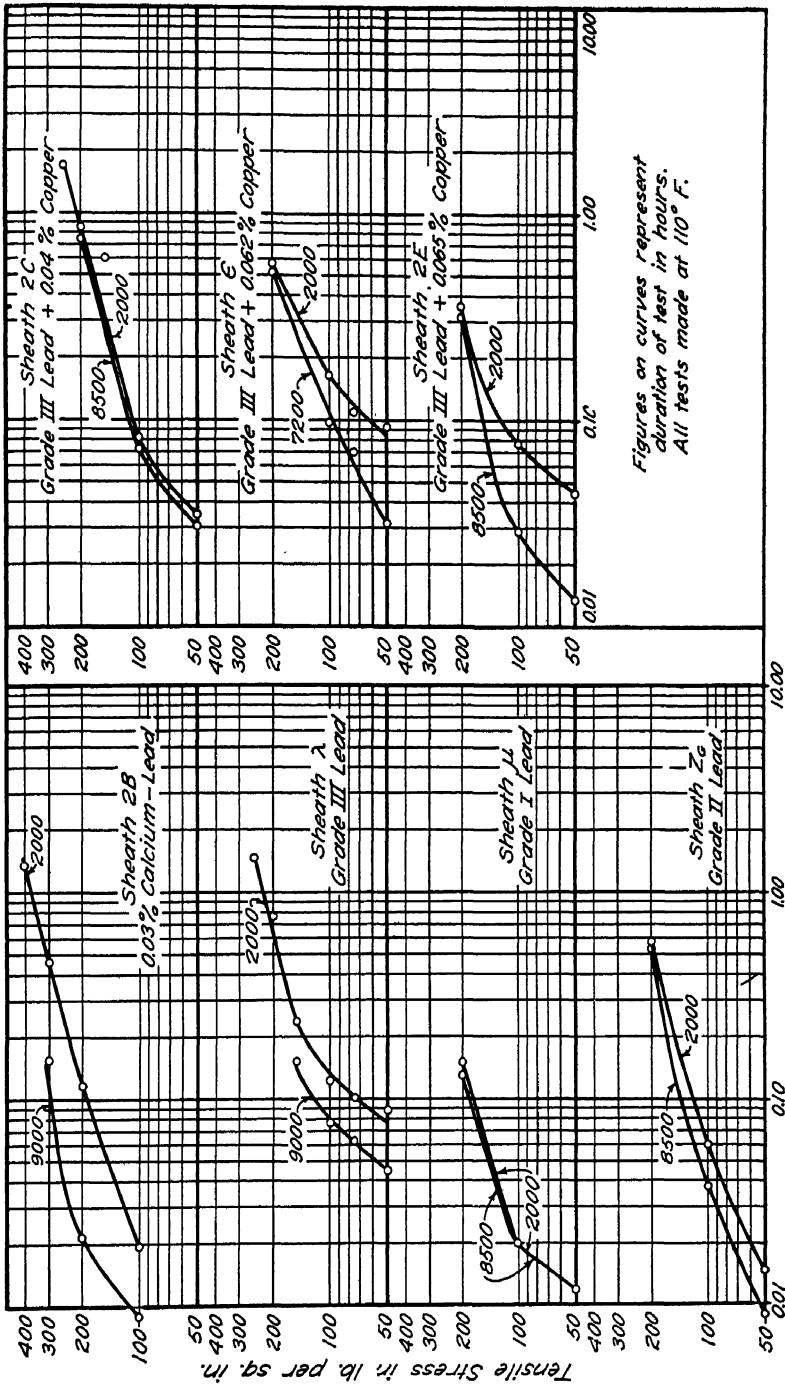
FIG. 19.—LOG-LOG PLOTS (MOORE, BETTY AND DOLLINS[28]).

functions for strain-hardening, annealing, spheroidization and precipi-
tation-hardening effects, and combining them all into a formula that will
express the future course of a creep curve for 10 or 20 years. They are
beginning to admit[85] that the situation is still too complex for accurate
mathematical analysis, to say nothing about mathematical prediction.
It is possible to draw up a formula to fit a given family of creep curves
and fix the exponents for each separate function, but that is only a post
mortem. All the exponents for the next materials must be known, and
they can be found only by experiment.
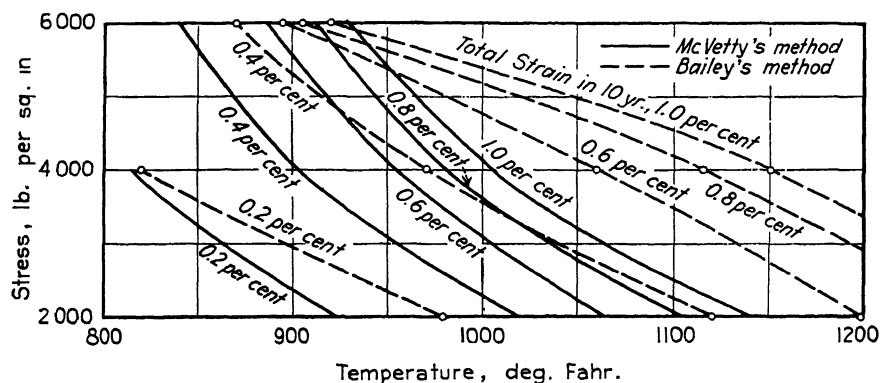
FIG. 20.—TWO MATHEMATICAL SYSTEMS OF EXTRAPOLATION APPLIED TO THE SAME
DATA (MARIN[84]).

From the cold-blooded point of view of reporting on what we actually
know, I cannot see that the mathematical attack has brought us far
beyond what we would know by simple inspection of the scanty reliable
data at hand; for example, by the dashed curve of Fig. 4. Putting the
data in the form of a family of curves like that and sketching in the dashed
curve free hand prevent us from fooling ourselves in the belief that we are
extrapolating on a mathematically exact basis, because it shows just how
much or how little primary information we have. I would rather see
man-hours spent in collecting primary data than in figuring formulas,
for a while yet.

To one with this point of view there is a degree of amusement in
publications that came to hand about the middle of January 1939.
Robinson[86] had adduced certain empirical formulas by which to "correct"
creep data to other loads or temperatures than those of the test. Kanter
had previously[27] presented some mathematical concepts of creep behavior,
and in discussion[87,88] of Robinson's paper again states them with log creep
rate vs. reciprocal absolute temperature straight-line plots as parallel
lines. In the course of his discussion he shows that some of Robinson's
formulas do not correctly represent actual data. Robinson[89] comes back
with a table to show that Kanter's "constant" Q is 29,000 and 140,000
and 84,000 at 800° and 900° and 1000° F. for one steel.

The same day the journal containing this discussion came in, there came also the bulletin by Moore, Betty and Dollins,[28] who state that they have plotted their data for lead in the same fashion that Kanter plotted his data for steel and brass, but they cannot make them fall on the parallel straight lines called for by Kanter's equations.

Were I a mathematician, I should be very chary of printing a formula alleged to represent the fundamentals of creep in such shape that anyone could use it for extrapolation, for I should fear that some rude experimenter would pick some new alloy blindfold and by his actual tests show that my formula was inadequate to express its behavior.

In fact, I have come to expect each alloy, even one that may seem to differ but little in analysis and structure from another one of known behavior, to show a decided individuality in creep until the contrary is proved. I want test points to plot before I draw a curve! Moore, in an earlier Howe lecture,[8] expressed his opinion of "formula worship," and his comments may well be applied to the case under discussion.

THE ENGINEERING ASPECT

If we cannot extrapolate with mathematical accuracy, where do we stand from the engineering point of view? Well, we can still use common sense, apply proven metallurgical principles and come out with a reasonable guess, which is often pretty good engineering.

Most of us can remember when fatigue testing and the engineering application of fatigue data were as hazy as the creep problem is today. Many "accelerated tests" were flirted with, to no avail. Finally, we came to understand that the endurance limit, determined on a polished specimen, merely establishes the stress level that can be withstood, and that any type of stress raiser—poor fillets, rough surface, notches and the like—introduces stress concentration that can seldom be quantitatively evaluated except by fatigue testing itself. We recognize, too, that corrosion-fatigue introduces a different set of conditions in which design must take the time element, and the rate of stressing, into consideration. The effects of overstressing and understressing are differentiated from the behavior of virgin specimens. A general, purely qualitative, but usable, understanding of the properties of different alloys under repeated stress has been built up, based primarily on the continued attempts to get reproducible, quantitative results in the laboratory. Even though the endurance limit, or the corrosion-fatigue limit determined under definitely recorded conditions, serve only as points of departure, the present acquaintanceship with the factors affecting endurance is of inestimable engineering value.

Similarly, I think, we shall reach the point where the single load and temperature creep test, continued long enough to show a clear-cut stage 2 creep rate, and give an inkling of the strain-hardening behavior, will

become a similar point of departure. The grain-size variables, the effect of changes in stress or temperature, the metallurgical stability, the propensities toward general or intergranular oxidation or corrosion from
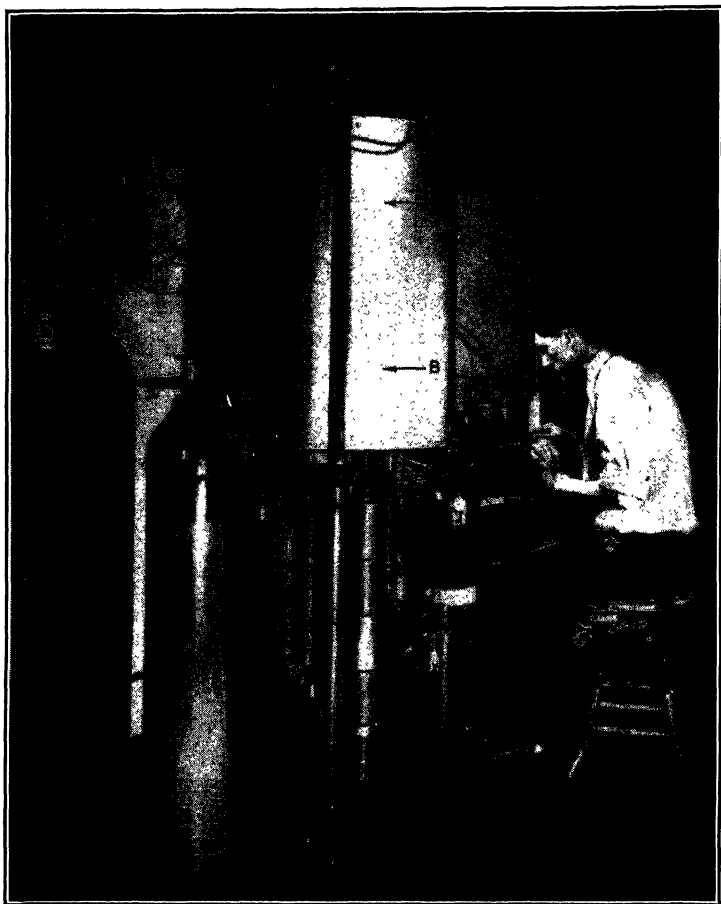
FIG. 21.—GRADIENT FURNACE FOR PRELIMINARY EXPLORATION OF CREEP BEHAVIOR, PREPARATORY TO REGULAR CREEP TESTS (BATTELLE).
A, top heater plate maintained at 800° F.; *B*, bottom heater plate maintained at 1085° F.
Test specimens were ⅛-in. diameter cold-drawn nickel-manganese steel rods with center 20 inches of length between *A* and *B* divided into 2-in. gauge lengths by spot-welded platinum beads. Rods were run through Pyrex tubes and an atmosphere of nitrogen was maintained to reduce oxidation.

the outside or accumulation of intergranular material from the inside, as well as the effect upon creep of vibration, of impact, and of intermittent or cyclic heating, will all be taken into consideration, and as many of these factors as apply in a particular case will be superimposed on the base line of creep behavior under test conditions.

Our great engineering need is for a thorough, even though qualitative, metallurgical insight into the idiosyncrasies of the individual materials we want to use at high temperatures. We can study stability, tempering and spheroidization propensities, precipitation-hardening and embrittlement tendencies, by rather inexpensive methods. It is not difficult to evaluate the grain-coarsening propensities. Unfortunately, evaluation of strain-
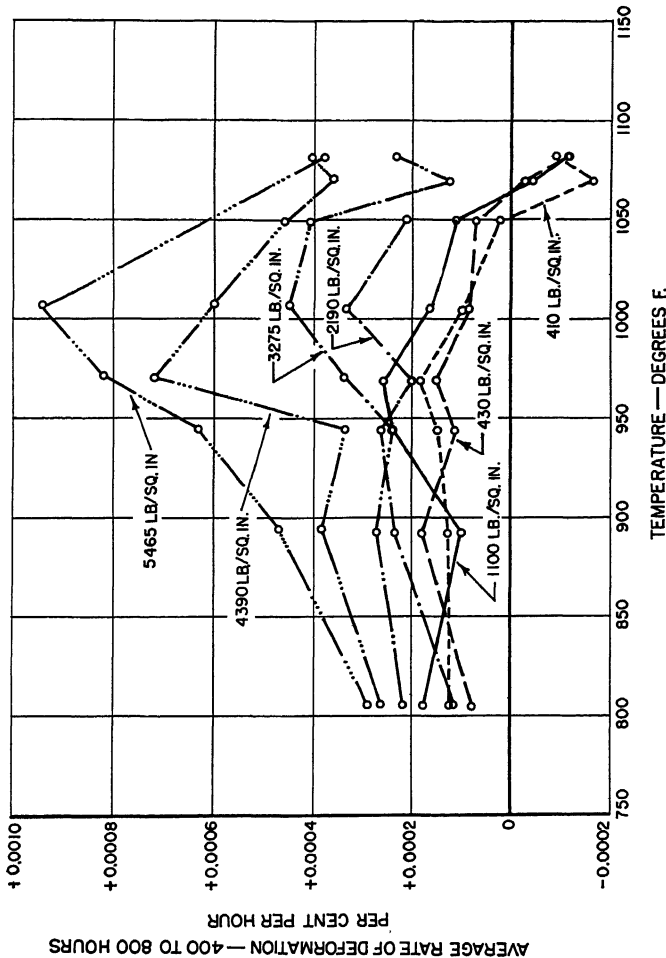
FIG. 22.—GRADIENT TEST DATA FOR AUSTENITIC MANGANESE-NICKEL STEEL, The test was carried out in a nitrogen atmosphere to avoid oxidation, to which this steel is prone. Tested as ⅛-in. diameter rods (C, 0.81; Mn, 13.8; Si, 1.1; Ni, 3.86).

hardening proclivities under creep conditions does call for the application of creep conditions.

To get qualitative strain-hardening information of this type, and to produce a rough family of curves from which one might select a very few loads and temperatures for true quantitative creep tests, a "gradient furnace" has been designed at Battelle, and Mr. Cross made a run with it for inclusion in this lecture. The furnace is shown in Fig. 21. In this

method test lengths of wires made of the steel to be studied are marked off (upon welded-on platinum beads) and the wires dead-loaded, very much as Howe did so long ago. The furnace is so heated that the specimens have a uniform temperature gradient over the gauge length. At suitable intervals, say 500 hr., the wires are removed and the total creep is measured. Data obtained for me by Mr. Cross, upon austenitic nickel-manganese steel supplied by Mr. Earnshaw Cook, are plotted in Fig. 22.

There are obvious limitations in the test, particularly in making sure that the wire has been put into exactly the same condition as the more massive shapes that would be used in industry, but it seems to have possibilities as a pilot test.

Incidentally, the steel used was not chosen with the idea that it would be useful in high-temperature service, but rather to get data into the literature to prevent the generalization that because 18:8 and the austenitic nickel-chromium heat-resistant alloys are creep resistant that property is inherent in the austenitic state!

The more I think about creep, the more convinced I am that the creep properties of metals and alloys are so extremely varied, complex, and characteristic of particular compositions, structures and grain sizes that generalizations on creep are likely to be premature. Our energies might better be concentrated on the accumulation of more facts to fill the yawning gaps of the things we don't know, which become evident in every attempt to summarize on creep.[43,90,91,92] With plenty of facts about individual alloys and conditions of actual service, plain horse sense can do an excellent engineering job.

Whitney[93] commented, in reference to electricity, "The more we learn about our ignorance, the larger and more useful it becomes." He defines *useful* ignorance as that which leads us to experiment. We have plenty of ignorance about creep, let us hope it will lead in the direction of experiment.

From the vantage point of his 90 years, the only living one of the founders of the Physical Society in England remarks:

> When we come to look back on the work of physicists during the 1870s' we find that their inventions, discoveries of fact and ascertained principles remain with us today, of permanent value, forming part of our useful knowledge. But their theories and speculations as to underlying causes and nature have nearly all passed away. Perhaps it will also be the same with our present-day work. If some 60 years hence, a fellow of the Physical Society gives a talk on the physics of the 1930s', he will have to record great additions to knowledge of physical facts. But he may also have to say that our explanations and theories concerning them have all vanished, or at least been replaced by others also destined in turn to pass away.[94]

Howe[1] ended his paper of 53 years ago with the remark that he had made a certain inference about creep, or as he called it, "patience," but that "further tests are required before this inference can be regarded as an

established fact." We certainly need further tests even now. An equal need is that the minds that plan and interpret the tests should combine the insight and the impartiality of Henry Marion Howe. God gave him that insight, but I think Howe himself was responsible for his impartiality. Few will attain his insight, but we can all emulate his impartiality.

We students of creep may well do as Howe always did, draw inferences, but state them tentatively and hold them tentative, always being ready to abandon them when they fail to check with new facts. So far creep has had a plethora of inferences, and inferences far too tenaciously held. I plead for more facts.

REFERENCES

1. H. M. Howe: The Patience of Copper and Silver as Affected by Annealing. *Trans.* A.I.M.E. (1885) **13**, 646–656.
2. R. H. Thurston: Notes Relating to a Peculiarity Distinguishing Annealed from Unannealed Iron. *Science* (1883) **1**, 418–419.
3. Tentative Method of Test for Long-Time (Creep) High-Temperature Tension Tests of Metallic Materials, E22–33T. *Proc. Amer. Soc. Test. Mat.* (1933) **33**, pt. 1, 1004–1012; E22–38T, *Idem* (1938) **38**, pt. 1, 1301–1306.
4. C. L. Clark: Appendix III, Joint Research Committee Report. *Proc. Amer. Soc. Test Mat.* (1938) **38**, pt. 1, 130–141.
5. F. H. Norton: Babcock and Wilcox Tube Co. *Tech. Bull.* 6C (1938).
6. E. Houdremont: Linien in der Entwicklung legierter Stähle. *Stahl und Eisen* (Jan. 5, 1939) **59**, 1–8.
7. P. G. McVetty: The Interpretation of Creep Tests. *Proc. Amer. Soc. Test. Mat.* (1934) **34**, pt. 2, 105–122.
8. H. F. Moore: Correlation between Metallography and Mechanical Testing. *Trans.* A.I.M.E. (1936) **120**, 13–35.
9. W. G. Burgers: Chapter 5 in R. Houwink's Elasticity, Plasticity and Structure of Matter. 1937. 376 pages.
10. F. H. Rhines and R. Ward: The Microgrid, a Method for the Observation of Plastic Deformation on a Microscopic Scale. To be published in *Metals and Alloys* (1939).
11. H. M. Howe: Metallography of Steel and Cast Iron. 1916. 641 pages.
12. J. B. Baker, B. B. Betty and H. F. Moore: Creep and Fracture Tests on Single Crystals of Lead. *Trans.* A.I.M.E. (1938) **128**, 118–136.
13. B. Chalmers: Microplasticity in Crystals of Tin. *Proc. Roy. Soc.* (1936) **156-A**, 427–443.
14. B. Chalmers: Influence of the Difference of Orientation of Two Crystals on the Mechanical Effect of Their Boundary. *Proc. Roy. Soc.* (1937) **162-A**, 120–127.
15. R. S. Russell: Influence of Impurities on the Properties of Lead, I. *Proc. Australian Inst. Min. and Met.* (1932) 135–166.
16. J. N. Greenwood: Influence of Impurities on the Properties of Lead, II. *Ibid.* (1934) 79–124.
17. R. S. Russell: Influence of Impurities on the Properties of Lead, III. *Ibid.* (1934) 125–159.
18. R. S. Russell: Influence of Impurities on the Properties of Lead, IV. *Ibid.* (1936) 23–32.
19. R. S. Russell: Influence of Impurities on the Properties of Lead, V. *Ibid.* (1936) 33–56.

20. J. N. Greenwood: Influence of Impurities on the Properties of Lead, VI. *Ibid.* (1936) 57–87.
21. J. N. Greenwood and H. L. Wormser: Influence of Impurities on the Properties of Lead, VII. *Ibid.* (1936) 385–419.
22. J. N. Greenwood: The Failure of Lead by Creep. *Ibid.* (1935) 477–498.
23. J. N. Greenwood and C. W. Orr: Influence of Composition on the Properties of Lead. *Ibid.* (1938) 1–24.
24. J. McKeown: Creep of Lead and Lead Alloys. *Jnl.* Inst. Metals (1937) **60**, 201–222.
25. A. J. Phillips: Some Creep Tests on Lead and Lead Alloys. *Proc.* Amer. Soc. Test. Mat. (1936) **36**, pt. 2, 170–193.
26. D. Hanson and E. J. Sandford: Creep of Tin and Tin Alloys. *Jnl.* Inst. Metals, (1936) **59**, 159; (1938) **62**.
27. J. J. Kanter: Interpretation and Use of Creep Results. *Trans.* Amer. Soc. Metals (1936) **24**, 870–912. Discussion F. H. Norton 913–915; A. Nadai, 916–917.
28. H. F. Moore, B. B. Betty and C. W. Dollins: Investigation of Creep and Fracture of Lead and Lead Alloys for Cable Sheathing. Univ. Illinois *Bull.* (1938) **35**; *Bull.* 306, Univ. Illinois Eng. Exp. Sta. 90 pages.
29. H. J. Gough: Crystalline Structure in Relation to Failure of Metals, Especially by Fatigue (Marburg Lecture). *Trans.* Amer. Soc. Test. Mat. (1933) **33**, pt. 2, 3–114.
30. Z. Jeffries and R. L. Archer: Science of Metals. 1924. 460 pages.
31. R. F. Mehl: Recrystallization. *Metal Progress* (Feb. 1939) 156–159, 192–196.
32. F. C. Brandon: Effect of Under-critical Annealing Treatment on Cold Drawn Carbon and Alloy Steels. *Wire and Wire Products* (Oct. 1938) 531–543.
33. B. L. McCarthy: Fundamental Principles of Steel Metallurgy. *Wire and Wire Products* (Nov. 1938) 655.
34. F. T. Sisco: Alloys of Iron and Carbon, II, 151. 1937.
35. C. L. Clark and A. E. White: Properties of Metals at Elevated Temperatures. Univ. Mich. Eng. Res. *Bull.* 27 (1936). 100 pages.
36. K. Hanffstengel and H. Hanemann: Der Kriechvorgang in belastetem Blei. *Ztsch. Metallkunde* (Feb. 1938) **30**, 41–46.
37. O. Bernhardt and H. Hanemann: Über den Kriechvorgang bei dynamischer Belastung und den Begriff der dynamischen Kriechfestigkeit. *Ztsch. Metallkunde* (Dec. 1938) **30**, 401–409.
38. O. Heckler, W. Hofmann and H. Hanemann: Beobachtungen über die Aushärtung und Dauerstandfestigkeit von Blei-Kalzium Legierungen. *Ztsch. Metallkunde* (Dec. 1938) **30**, 419–422.
39. J. J. Kanter and L. W. Spring: Some Long-Time Tension Tests of Steels at Elevated Temperatures. *Proc.* Amer. Soc. Test. Mat. (1930) **30**, pt. 1, 110–132.
40. A. E. White and C. L. Clark: Influence of Grain Size on the High Temperature Characteristics of Ferrous and Non-Ferrous Alloys. *Trans.* Amer. Soc. Metals (1934) **22**, 1069–1098.
41. H. C. Cross and J. G. Lowther: Progress Report on Study of Effects of Manufacturing Variables on the Creep Resistance of Steels. Appendix V to Joint Research Comm. Report, Amer. Soc. Test. Mat. (1938) **38**, pt. 1, 149–171.
42. H. C. Cross: High-Temperature Tensile, Creep and Fatigue of Cast and Wrought High and Low-Carbon 18 Cr, 8 Ni Steel from Split Heats. Progress Report, Joint Res. Comm., *Trans.* Amer. Soc. Mech. Engrs. (1934) **56**, 533–553.
43. Compilation of Available High-temperature Creep Characteristics of Metals and Alloys. Joint Res. Comm., Steel 8b, 4. A.S.T.M.-A.S.M.E. (1938).

44. C. H. M. Jenkins, H. J. Tapsell, G. A. Mellor and A. E. Johnson: Some Aspects of the Behavior of C and Mo Steels at High Temperatures. *Trans*. Chem. Eng. Congress of the World Power Conference, London (1936) **1**, 122–162.

45. S. H. Weaver: Actual Grain Size Related to Creep Strength of Steel at Elevated Temperatures. *Proc*. Amer. Soc. Test. Mat. (1938) **38**, pt. 1, 176–181. Note discussion, 182–196.

46. V. Jares: Discussion, Int. Assn. Test. Mat., London Congress (April 1937) 182.

47. R. L. Wilson: High Temperature Strength of Steels. *Metal Progress* (May 1938) 499–505.

48. A. E. White, C. L. Clark and R. L. Wilson: Qualifications of Steels for High-Temperature Service in Petroleum Refinery Equipment. *Oil and Gas Jnl.* (Aug. 2, 1934) **33**, 18–19. See also reference 49.

49. A. E. White, C. L. Clark and R. L. Wilson: *Ibid.* (Aug. 9, 1934) 16, 33–36.

50. J. McKeown: Creep in Non-Ferrous Metals. Advance Copy, Soc. of Chem. Ind., meeting of January 9, 1939. 8 pages.

51. C. L. Clark, A. E. White and G. J. Guarnieri: A New Application for the Short-Time High Temperature Tensile Test. *Trans.* Amer. Soc. Metals (Dec. 1938) **26**, 1035–1049.

52. B. Chalmers: Metal Crystals—An Examination of their Physical Characteristics. *Metal Ind.*, London, **53**, 243–246, 295–298, 323–325.

53. H. Kochendorfer: Plastizität und Mosaik struktur der Kristalle. *Ztsch. Metall-kunde* (Sept. 1938) **30**, 299–305.

54. F. B. Foley: Amorphous Cement and the Formation of Ferrite. *Trans.* A.I.M.E. (1926) **73**, 850–858.

55. V. Krivobok: Discussion. *Trans.* Amer. Soc. Steel Treat. (1930) **18**, 880.

56. F. F. Lucas: On the Art of Metallography. *Trans.* A.I.M.E. (1931) **95**, 11–44.

57. A. B. Kinzel and R. W. Moore: Graphite in Low-carbon Steel. *Trans.* A.I.M.E. (1934) **116**, 318.

58. E. C. Wright and H. Habart: Typical Failures of Still Tubes in Refineries, A—Carbon Steel Tubes. *Metal Progress* (Nov. 1938) 573–578; B—Alloy Steel Tubes. *Ibid.* (Dec. 1938) 685–688.

59. R. W. Bailey: Creep of Steel under Simple and Compound Stresses. *Engineering* (1930) **129**, 265–267, 327–329.

60. R. F. Miller, R. F. Campbell, R. H. Aborn and E. C. Wright: Influence of Heat Treatment on Creep of C–Mo and Cr–Mo–Si Steel. *Trans.* Amer. Soc. Metals (Oct. 1937) **26**, 81–105.

61. G. O. Hiers and G. A. Steers: Tellurium Lead for Plating and Pickling Equipment. *Metal Ind.* (N. Y.) (Dec. 1938) **36**, 563–566.

62. A. Hayes and R. O. Griffis: Non-aging Iron and Steel for Deep Drawing. *Metals and Alloys* (1934) **5**, 110–112.

63. R. W. Bailey: Creep and Engineering Design. Int. Assn. Test. Mat., London (April 1937) 15–17.

64. A. E. White, C. L. Clark and R. L. Wilson: The Rupture Strength of Steels at Elevated Temperatures. *Trans.* Amer. Soc. Metals (1938) **26**, 52–80.

65. R. H. Thielemann and E. R. Parker: Fracture of Steels at Elevated Temperatures after Prolonged Loading. This volume, page 559.

66. R. H. Aborn and R. F. Miller: Ductility of Creep-Resistant Steel at Elevated Temperatures. *Metals and Alloys* (1938) **9**, 104.

67. R. W. Bailey: Steel at Elevated Temperatures. *Jnl.* West Scotland Iron and Steel Inst. (1937–38) **45**, 11–22.

68. R. W. Bailey: Failure of Still Tubes. *Metal Progress* (Jan. 1939) 71. (Letter to Editor.)

69. H. M. Wilten and E. S. Dixon: Aging Embrittlement of 4 to 6 Per Cent Cr Steel. *Proc.* Amer. Soc. Test. Mat. (1934) **34**, pt. 2, 59–78.
70. H. M. Wilten: *Trans.* Amer. Soc. Metals (1935) **23**, 915–967.
71. F. T. Sisco: Alloys of Iron and Carbon, 2, 500–504. 1937.
72. D. K. Bullens and Battelle Mem. Inst.: Steel and Its Heat Treatment, 2, 340–343. 1939.
73. A. Krisch: Bestimmung der Dauerstandfestigkeit nach verschiedenen Verfahren. *Archiv Eisenhüttenwesen* (Oct. 1938) **12**, 199–206.
74. F. C. Lea: The Creep of Metals under Static and Repeated Stresses. *Foundry Trade Jnl.* (Oct. 6, 1938) **59**, 251–252.
75. C. R. Soderberg: Plasticity and Creep in Machine Design. In Stephen Timoshenko Sixtieth Anniversary Volume, 197–210. 1938.
76. A. Nadai and J. A. Boyd: Relaxation of Steels at Elevated Temperature. Abst., *Jnl. App. Mech.* (Sept. 1938) A-118.
77. J. M. Jasper: Application of Steel to Operations at High Temperature. *Metal Progress* (Feb. 1939) 160–163.
78. P. H. Clark and E. L. Robinson: An Automatic Creep Test Furnace Guide. *Metals and Alloys* (1935) **6**, 46–51.
79. F. B. Foley: Discussion. *Metals and Alloys* (1935) **6**, 50–51; *Trans.* Amer. Soc. Metals (1934) **22**, 1095.
80. H. C. Cross and J. G. Lowther: Report on Long-Time Creep Tests of 18% Cr 8% Ni Steel K19 and 0.35% C Steel K20. Appendix III to Joint Res. Comm. Rept. *Proc.* Amer. Soc. Test. Mat. (1937) **37**, pt. 1, 178–186.
81. H. C. Cross and J. G. Lowther: Report on Long-Time Creep Test of 0.35% C Steel K20. Appendix II to Joint Res. Comm. Rept., Amer. Soc. Test. Mat. (1938) Preprint 29.
82. A. Nadai: The Influence of Time Upon Creep, the Hyperbolic Sine Creep Law. In Stephen Timoshenko Sixtieth Anniversary Volume (1938) 155–170.
83. J. Boyd: Discussion. *Trans.* Amer. Soc. Test. Mat. (1937) **37**, pt. 2, 265–267.
84. J. Marin: Comparison of Methods Used in Comparing Creep Test Data. *Trans.* Amer. Soc. Test. Mat. (1937) **37**, pt. 2, 258. Compare with ref. 85.
85. C. R. Soderberg: Plastic Flow and Creep in Polycrystalline Metals. Abst., *Jnl. App. Mech.* (Sept. 1938) **5**, A-13; also references 75 and 82.
86. E. L. Robinson: Effect of Temperature Variation on the Creep Strength of Steel. *Trans.* Amer. Soc. Mech. Engrs. (1938) R.P. 60-5, 253–259.
87. J. J. Kanter: The Problem of the Temperature Coefficient of Tensile Creep Rate. *Trans.* A.I.M.E. (1938) **131**, 413.
88. J. J. Kanter: Discussion. *Trans.* Amer. Soc. Mech. Engrs. (1939) 49–52.
89. E. L. Robinson: Discussion. *Trans.* Amer. Soc. Mech. Engrs. (1939) 52–53.
90. H. J. Tapsell: Creep of Metals. 285 pages. Oxford Univ. Press (General Discussion), 1931.
91. Symposium on Effect of Temperature on the Properties of Metals, 1931. 829 pages. A.S.T.M. and A.S.M.E. (Engineering requirements and properties of available metals.)
92. W. H. Hatfield: Heat-resisting Steels. *Jnl.* Inst. Fuel. (1938) **11**, 245–304, 440–450. Contains a notable bibliography.
93. W. R. Whitney: It's Called Electricity. *Genl. Elec. Rev.* (June 1938) **41**, 260–264.
94. A. Fleming: Physics and the Physicists of the 1870's. *Nature* (Jan. 21, 1939) **143**, 99–102.

Reduction of Iron Ores under Pressure by Hydrogen

By Michael Tenenbaum* and T. L. Joseph,† Member A.I.M.E.

Recent researches on the reduction of iron ores have stimulated interest in the effect of increased pressures within the iron blast furnace. From a physicochemical viewpoint, it seems logical to suppose that the increased pressure would increase the rate of reduction of the iron ore within the furnace. This increased reaction velocity would in turn be reflected in an increase in the output of the blast furnace. Any substantial effect of elevated blast-furnace pressures should accordingly be of both technical and economic interest to the operator.

It is doubtful whether it is possible to increase the pressure in the stack of the blast furnace beyond two or three atmospheres without incurring severe mechanical difficulties. The benefits to be procured by elevations in pressure must therefore be restricted to pressures below two, or at the most, three atmospheres. Within this range it would seem both economically and mechanically feasible to modify the present design of the upper portion of the blast furnace to accommodate these more stringent operating conditions.

This investigation was undertaken to study the effect of moderate pressures on the rate of reduction of iron ore with hydrogen. The use of carbon monoxide is contemplated for later work. Although any results that are obtained in the laboratory cannot be interpreted directly in terms of large-scale commercial operations, it is possible, through such an investigation, to ascertain the order of magnitude of the effects of higher pressure. A more quantitative conception of the effects that would result from the use of increased pressures in the modern blast furnace is needed.

In some recent work, Diepschlag[1] found that, all other factors remaining constant, the degree of reduction of iron ores was much greater when carried out under pressure. Pressures as high as seven atmospheres were used. The degree of reduction was determined from the ferrous and ferric iron in the sponge iron. Results were obtained using both carbon monoxide and hydrogen at temperatures of 400°, 600° and

800° C. Diepschlag points out that, owing to carbon deposition, reduction with carbon monoxide went further than with hydrogen. His work shows clearly that the elevation of pressures up to three atmospheres was far more effective than further increases in pressure.

In a recent discussion of the factors that would be involved in increasing the pressures in the pig-iron blast furnace, Avery[2] enumerates several of the more direct effects as follows:

1. Iron ore would be reduced more rapidly and at a higher level in the furnace.

2. The amount of solution loss would then be decreased since the amount of carbon dioxide formed in the high-temperature zones would be reduced.

3. The amount of coke required per ton of pig would be decreased.

4. For a given rate of production, the blast rate would be less. From experience, it seems that this would result in changes as follows: (a) less channeling, (b) less dusting, (c) decreased pressure drop, (d) better gas solid contact. Each of these effects indicates the importance of any such modification of present practice. Although the net benefits of such a procedure are not immediately apparent, it seems clear that pressure operation of the iron blast furnace represents a fertile field for investigation.

GAS-SOLID REACTIONS

Some theoretical aspects of reduction will be presented to indicate the manner in which pressure may affect the process. The discussion is offered to give an approximation of the extent to which pressure may be expected to change the time required for reduction at various temperatures. Although the data obtained are not extensive, some consideration of the underlying principles of the reduction process is necessary for their interpretation.

The reduction of solid Fe_2O_3 by hydrogen is probably carried out in several stages, as follows:

$$3Fe_2O_3 + H_2 \rightarrow H_2O + 2Fe_3O_4$$
$$Fe_3O_4 + H_2 \rightarrow H_2O + 3FeO$$
$$FeO + H_2 \rightarrow H_2O + Fe$$
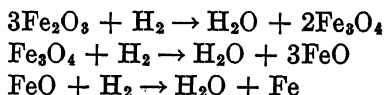
It is generally known that the reduction of FeO is much slower than either of the preceding stages and therefore determines the over-all rate of reduction.

In reactions in which a solid substance is reacted upon by a gas, two interrelated factors determine the rate at which the process proceeds: (1) the rate at which the reaction progresses in the region of the change, (2) the rate of diffusion of gases to and from reacting interfaces. Considering the first factor, Langmuir[3] suggested that in reduction the

reactions proceed along interfacial surfaces between the oxide and the reduced metal. Films of the reacting gas, in this case hydrogen, are adsorbed on the surface of the oxide at the reacting interface. The reaction between this adsorbed film and the oxide is the basis of reduction. The rate of adsorption of the gas on the surface would be proportional to the available surface and the pressure. The freshly reduced metal at the interface acts as an autocatalyst for the reaction. Benton and Emmet,[4] from their work on the reduction of the oxides of nickel and iron, point out that the rate of reduction is proportional to the interfacial area, which is, in turn, dependent upon the extent to which the reactions has proceeded.

Role of Pressure in Reduction

The rate of reaction between hydrogen and solid iron oxide at the reacting interface would primarily be dependent on the concentration of hydrogen in the adsorbed film. This in turn depends upon the number of molecules of reducing gas striking the available surface during any interval. Langmuir's studies of the behavior of tungsten filaments in contact with gases at low pressures indicate the probable mechanism of gas-solid reactions. At low pressures, the number of gram molecules u of any gas of molecular weight M striking a unit surface per second may be expressed as follows:

$$u = 43.74 \times 10^{-6} \frac{P}{\sqrt{MT}} \qquad [1]$$

The rate of oxidation of tungsten filaments at low pressures was proportional to the pressure of oxygen in agreement with the equation above for the rate at which oxygen reaches the surface. Neglecting the effect of diffusion it appears that the rate of reduction of solid iron oxides with hydrogen would increase approximately with pressure.

A portion of the hydrogen molecules striking the surface are adsorbed and react to form a second gaseous component, water vapor, which occupies a portion of the surface previously available to the hydrogen. As the partial pressure of the water vapor increases the fraction of the total surface available for hydrogen adsorption decreases, thus reducing the rate of reduction.

Role of Diffusion in Reduction

The transfer of gas to and from reacting interfaces is a process of diffusion. In this respect, we accept Graham's law, which states that the rate of diffusion is inversely proportional to the square root of the molecular weights of the gases. It is also accepted that the rate of diffusion is proportional to the concentration gradient of the gas. For the

same gradient, however, the ratio of the rates of diffusion of hydrogen and water vapor may be expressed by the equation

$$\frac{R_{H_2}}{R_{H_2O}} = \frac{\sqrt{18}}{\sqrt{2}} \qquad [2]$$

It is evident, therefore, that the rate of diffusion of hydrogen would be three times that of water vapor.

Pease and Taylor[5] found that in the reduction of copper oxide with hydrogen, the introduction of water vapor into the gas retarded only the initial or the incubation period of the reaction, but had no appreciable effect beyond this point when compared to reduction by the pure gas. Jones and Taylor[6] obtained similar results using carbon monoxide for a reducing agent and adding carbon dioxide. In either case, this phenomenon could be attributed to the fact that the water vapor or the carbon dioxide was adsorbed over a portion of the reacting surface, thus reducing the active area. When the pure gas was used, it was not long after the reaction began that the pressure of the products of the reaction (H_2O or CO_2) built up; so that after the reaction had proceeded to any extent, the conditions in both instances were very similar.

It appears that the pressure of the water vapor formed as a result of hydrogen reduction has a considerable effect in retarding the rate of the reaction. An important factor, therefore, in determining the velocity of reduction at varied pressure would be the rate of diffusion of this water vapor through the ore into the surrounding atmosphere.

In a discussion of diffusion, Kuenen[7] points out that the rate of diffusion varies inversely with the pressure of the surrounding atmosphere, or

$$D = D_{760} \times \frac{760}{p} \qquad [3]$$

where D_{760} and D represent the rates of diffusion at atmospheric and observed pressures, respectively.

PRESSURE AND RATES OF REDUCTION

The obvious effects of an increase in pressure, then, can be listed as:

1. An increase in the initial rate of reduction. Whether this increased rate persists throughout the reduction depends on the succeeding two factors.

2. An increase in the amount of water vapor present due to this increased rate of reduction.

3. A decrease in the rate of diffusion of the water vapor. Any increase in the net rate of reduction of the entire piece would represent the difference between the first and the last two factors mentioned.

If we consider the ideal case, in which the pressure remains constant and the products of the reaction are removed immediately, we have

$$\frac{d(H_2O)}{dt} = kp(FeO) \qquad [4]$$

where p is the pressure of the H_2 gas, $\dfrac{d(H_2O)}{dt}$ represents the rate at which H_2O is formed and FeO is the ferrous oxide available for the reaction. By using pieces of ore of the same shape and size, the available FeO can be made comparable in each reduction.

It is desirable to obtain the relation between the time for 90 per cent reduction and pressure, as the time to attain this degree of reduction is used later in comparing rates. Equation 4 can also be written:

$$\frac{-d(FeO)}{dt} = kp(FeO)$$

integrating

$$-\frac{1}{kp}\int_{t_0}^{t_1}\frac{d(FeO)}{FeO} = \int_{t_0}^{t_1}dt$$

we obtain

$$\frac{1}{kp}\log_e\frac{(FeO)_0}{(FeO)_1} = t_1 - t_0$$

The time required for 90 per cent reduction can now be expressed as

$$t_{90\%} = \frac{2.303}{kp} \qquad [5]$$

Neglecting diffusion, we see from this expression that a twofold increase in the pressure of the reacting gas would reduce the time required for 90 per cent reduction by one-half.

In the actual reduction, however, the products of the reaction are not removed immediately, but must diffuse through the piece of ore being reduced. At the instant when the reaction begins, the preceding considerations would apply. It has been shown that the hydrogen will diffuse at a much faster rate than water vapor. Except for the initial stage, the hydrogen pressure at the reacting surface would be less than that of the surroundings by an amount equal to the partial pressure of the water vapor present. Under such conditions the equation for the velocity of the reaction can be written:

$$\frac{-d(FeO)}{dt} = k(P_{H_2} - P_{H_2O})(FeO) \qquad [6]$$

where P_{H_2} represents the constant hydrogen pressure maintained in the system, and P_{H_2O} is the partial pressure of the water vapor present at

the reacting interface at any instant. It is evident that the partial pressure of the hydrogen at the reacting interface is equal to $P_{H_2} - P_{H_2O}$. We can now express the time required for 90 per cent reduction by the following equation:

$$t_{90\%} = \frac{2.303}{kp_{H_2}} + \frac{1}{P_{H_2}} \int^{t_{90\%}} P_{H_2O}dt \qquad [7]$$

For each set of conditions the integral term would assume a different set of values. It would accordingly be difficult to obtain an exact expression for the effect of the water vapor present. However, if we use an average value, $\bar{P}_{H_2O}$, for the pressure of the water vapor we can rewrite the preceding expression in the form

$$t_{90\%} = \frac{2.303}{k(P_{H_2} - \bar{P}_{H_2O})} \qquad [8]$$

In this case, the time required for reduction is a function of both the pressures of the hydrogen and the water vapor at the reacting interface. It is evident that the presence of the water vapor has a retarding effect on the rate of reduction.

If we compare the time t_{H_2O} required for reduction when the water vapor interferes with the reaction against t_I required under ideal conditions, we obtain the following expression:

$$t_{H_2O} = \frac{P_{H_2}}{P_{H_2} - \bar{P}_{H_2O}} \times t_I \qquad [9]$$

From this equation, we see that in the presence of water vapor to retard the reaction, the time required for reduction is increased in the ratio of P_{H_2}, the hydrogen pressure in the surrounding atmosphere, to $P_{H_2} - \bar{P}_{H_2O}$, the actual effective hydrogen pressure at the reacting interface. Although these equations by no means exactly represent the rate of reduction of any piece of ore, they do give a quantitative conception of the relative effect of pressure and diffusion.

TEMPERATURE AND DIFFUSION

Taylor[3] has pointed out that the influence of temperature on the diffusion of gases is generally expressed by an equation of the form

$$D \alpha T^x \qquad [10]$$

While the exponent x varies considerably, it assumes values closely approaching 2 when vapors are being considered. A decrease in temperature, therefore, would result in a greatly reduced rate of diffusion; consequently higher pressures would be built up. From equation 8, then, it would seem that the effect of pressures on the rate of reduction would be less marked at lower temperatures.

REDUCTION TESTS AT VARIOUS PRESSURES

The reductions in this investigation were carried out on several series of $\frac{9}{16}$-in. cubes, each series being prepared from the same lump of limonitic iron ore. All cubes were prepared in a similar manner to present comparable surfaces to the reducing gases. Prior to reduction,

TABLE 1.—*Physical Properties of Cubes Used in Reduction*

Series	Specimen No.	Weight, Grams	Density		Porosity, Per Cent	Remarks
			Apparent	True		
1	1	5.7426	2.24	3.83	41.5	Discarded
	3	6.3393	2.38	3.83	37.9	
	4	6.2739	2.39	3.83	37.5	
	5	6.5647	2.68	3.83	36.0	
	6	5.5650	2.20	3.83	42.5	Discarded
	9	6.3870	2.36	3.83	38.4	
	10	6.1715	2.45	3.83	36.1	
	11	6.2772	2.42	3.83	36.8	Broke during reduction
	12	6.2082	2.40	3.83	37.1	
2	13	8.0670	2.56	3.15	18.4	
	14	8.1452	2.46	3.15	21.7	
	15	8.4940	2.56	3.15	18.4	
	16	8.4335	2.57	3.15	18.3	
	17	8.1415	2.49	3.15	20.9	
	18	8.5931	2.57	3.15	18.2	
3	19	6.8618	2.39	3.69	35.4	
	20	7.6244	2.61	3.69	29.4	
	21	6.6868	2.41	3.69	34.8	
	22	7.6970	2.63	3.69	28.9	
4	23	8.5640	2.79	3.92	28.8	
	24	8.6195	2.72	3.92	30.6	
	25	8.2750	2.76	3.92	29.7	
	26	9.0355	3.02	3.92	23.1	Discarded
	27	8.5830	2.83	3.92	27.9	

the cubes were dehydrated at 500° C. Determinations were then made of the apparent and true densities of the dried cubes. The method used in these determinations was the same as that outlined by Joseph[9] in his paper on the reduction of iron ores.

POROSITY OF ORE CONTROLLED

One of the authors has shown conclusively that the porosity of a piece of iron ore has a marked effect on its rate of reduction. Therefore,

in this work, only pieces of similar porosities are compared in each series of tests.   It can be seen from Table 1 that only one value for the true density is given for each series.   This value represents an average of three determinations on pulverized samples of the pieces of ore that remained after the cubes had been cut from the original lump.   Although the values for the porosity in the third series seem to be widely spread, it can be seen that of the four values shown two pairs can be selected having similar porosities.   In reducing these cubes, one of each pair was reduced at each pressure in order to give comparable data.

These porosities are given in order to show that, within practical limits, the physical properties of the cubes were sufficiently alike to allow comparisons of the rates at which they would reduce under various pressures.   Any cubes that exceeded these limits were discarded prior to reduction.
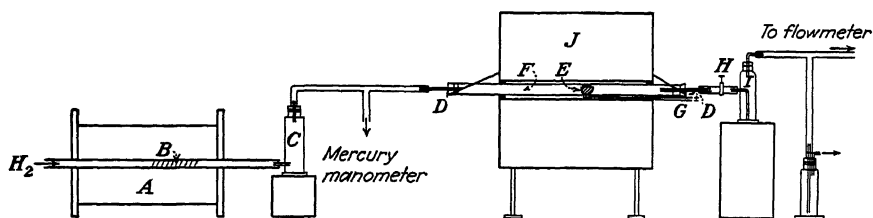

FIG. 1.—DIAGRAMMATIC SKETCH OF REDUCTION APPARATUS.

A, electric furnace for removing oxygen. F, Vitreosil tube.
B, platinized asbestos. G, thermocouple.
C, drying bottle. H, clamp for regulating pressure.
D, braces for rubber stoppers. I, absorption tower.
E, Nichrome wire screen boat. J, electric reduction furnace.

The cubes of ore used in the porosity determinations were reduced in an atmosphere of hydrogen at 600°, 700° and 800° C. in the apparatus shown in Fig. 1.   Rubber stoppers used at both ends of the quartz tube in the reduction furnace were backed up by metal plates bolted to the furnace itself to prevent the corks from blowing out.

EXPERIMENTAL PROCEDURE

Nitrogen was run through the tubes while the entire system was brought up to temperature.   The desired pressures and rates of flow were adjusted while the nitrogen was passing through the system.   After the cube had been up to temperature for about 20 min., the nitrogen valve was closed.   The pressure was then allowed to decrease to about 5 in. of mercury and hydrogen was introduced.   The rate of flow was maintained at 600 c.c. per minute.   Zero time in the reduction tests was taken from this instant.   A period of about 15 sec. was required to establish a constant pressure in the system.   During the first part of the reduction it was necessary to adjust the pressure controls frequently, as the water

formed during the reaction restricted the gas flow in the tube leading from the furnace.

The water formed during the reduction was collected in alternate drying towers filled with dehydrite. These towers were refilled at intervals to insure complete absorption. For the first 40 min. the water formed was weighed at 5-min. intervals and later at 10-min. periods.

The cubes of each series were reduced at the same temperature but at different pressures. The results of these reductions have been plotted cumulatively against time and are shown in Figs. 2, 3, 4 and 5. In each series of cubes, a distinct increase in the rate of reduction can be noted wherever pressures of 20 in. of mercury or more were employed. It is also apparent that the relative increase was more marked at 800° C. than at 700° or 600° C.
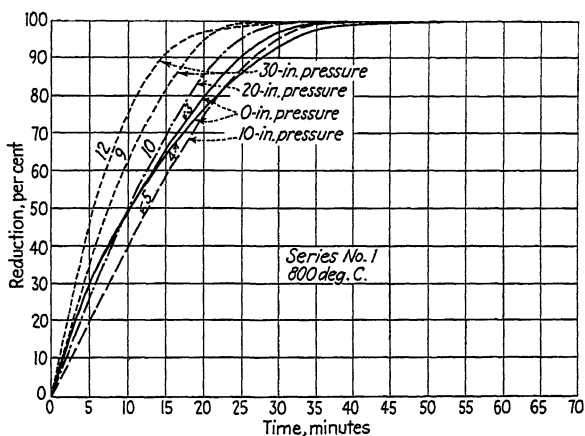

FIG. 2.—EFFECT OF PRESSURE ON TIME OF REDUCTION.

Fig. 2 shows the reduction curves of the first series. Two cubes, reduced at atmospheric pressure, are represented by the solid lines on the graph. The curve for a pressure of 10 in. of mercury fell between the preceding two. This reduction lagged slightly because of the condensation of some of the water in the tube leading to the absorption towers. At a pressure of 20 in. of mercury an appreciable increase in the rate of reduction is apparent. The two curves at 30 in. show a definite increase in the rate of reduction. The porosity of the cubes reported in this series of tests ranged from 36.1 to 38.4 per cent.

The cubes reported in Fig. 3 were reduced at pressures of approximately one or two atmospheres and at 800° C. The curves segregate themselves into two groups and clearly show the effect of pressure. The porosity of this group of cubes ranged from 18.2 to 21.7 per cent.

The rates of reduction at 600° C. shown in Fig. 4 were much slower than at 800° C. The pressures used at 600° C. were the same as those

used at 800° C. in Fig. 3.   The increase in the rate of reduction at higher pressure was, however, not as great at the lower temperature.   The effect of the higher pressures at 700° C. shown in Fig. 5 is less marked than at the other two temperatures.

One of the authors[9] has selected as an index of reducibility the time required for 90 per cent reduction.   This same means is used in this paper for comparing the reducibility at varied pressures.   The time
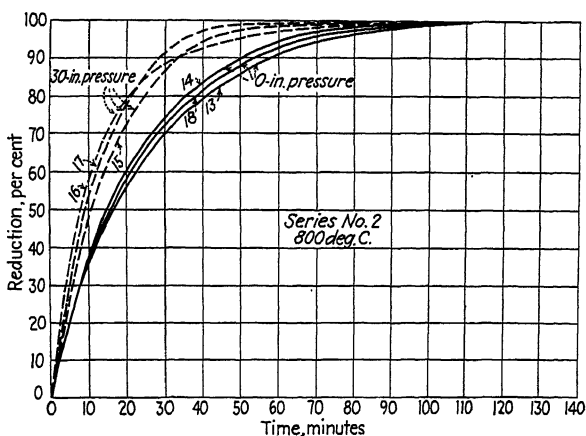

FIG. 3.—EFFECT OF PRESSURE ON TIME OF REDUCTION.

required for 90 per cent reduction at one atmosphere and at a pressure of 30 in. of mercury or two atmospheres is given in Table 2.

TABLE 2.—*Effect of Doubling Pressure on Time of Reduction*

Series	Temperature, Deg. C.	Minutes Required for 90 Per Cent Reduction			
		One Atmosphere	Two Atmospheres	Decrease	Percentage of Decrease
1	800	26	16	10	39
2	800	51.8	30.5	21.3	41
3	600	111.0	82.5	28.5	26
4	700	42.5	34.5	8.0	19

Table 2 demonstrates clearly that the use of pressure increased the rate of reduction with hydrogen.   In series 1, 2 and 3 the values shown are the averages of several reductions.   Series 4 represents single values. The reducibility of various cubes did not increase regularly with the pressure.   Variations in the physical structure between single cubes tended to mask the effect of pressure.   The data reported in Figs. 2 and 5 show, however, that the rate of reduction at pressures of 10 and 20 in. of mercury was definitely more rapid than at barometric pressure.

Table 2 indicates that the increase in the rate of reduction at 600° and at 700° C. was not as marked as at 800° C. Doubling the pressure at 800° C. decreased the time required for reduction by about 40 per cent. At the lower temperatures this decrease was appreciably less. Neglecting
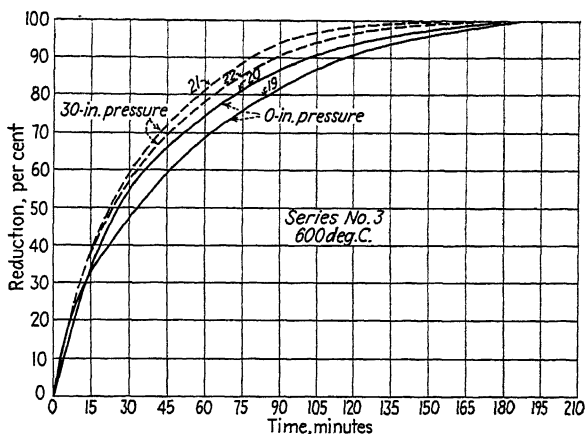

FIG. 4.—EFFECT OF PRESSURE ON TIME OF REDUCTION.

diffusion, the time should be reduced 50 per cent. The somewhat longer time actually observed at 800° C. is attributed to the effect of diffusion as expressed in the second term of equation 7. The reduced effect of the doubled pressure at lower temperatures may be attributed to the decrease in the rate of diffusion as was pointed out in equation 10.
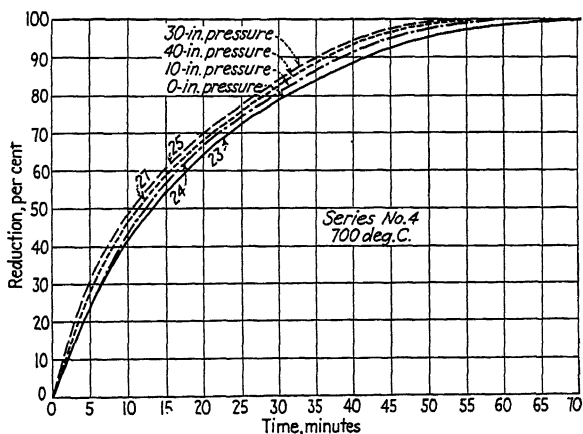

FIG. 5.—EFFECT OF PRESSURE ON TIME OF REDUCTION.

It is interesting to note again the results obtained by Diepschlag in his investigation. He found that the degree of reduction by hydrogen during a given period of time was materially increased by elevating the pressure from one to as high as seven atmospheres. His work shows also

that the increase in the degree of reduction at 600° C. was greater than at 800° C.

Superficially this would seem to contradict the results of this investigation. However, in Diepschlag's work the degree of reduction with hydrogen ranged from as low as 5 per cent at one atmosphere and 400° C. at a maximum of about 85 per cent at 800° C. and seven atmospheres. At lower temperatures, his data show only the effect of pressure in the early stages of reduction, whereas the present data show the effect of pressure on the time required for complete reduction. For example, at 400° C. no metallic iron was formed in his hydrogen reduction tests. His data, accordingly, show the effect of increased pressure on the conversion of ferric oxide to ferrous oxide.

On the other hand, at 800° C. and one atmosphere pressure, practically all the ferric oxide was reduced; and the effect of increased pressure was observed on the ferrous iron, which is more difficult to reduce. Consequently, Diepschlag's results on the effect of pressure at low temperatures are not strictly comparable with the present data. Since, in practice, we are interested chiefly in the time required for complete reduction, the entire significance of Diepschlag's data is not immediately apparent.

Another point of interest is a comparison of the influence of pressure and porosity with the effect of changes in the porosity on the rate of reduction. One of the authors[9] has developed a relation between the time for 90 per cent reduction and the porosity. Differences in porosity changed the rate of reduction as much as sixfold. However, the range of porosities for such a change varied from practically zero to over 65 per cent. When we consider ores having porosities in the range of the ore used in this research, a decrease of 40 per cent in the time of reduction, such as was obtained by doubling the pressure at 800° C., would be equivalent to practically doubling the porosity of the ore.

Although care was taken throughout this work to minimize differences in porosities, it was impossible to eliminate this variable entirely. It is, therefore, possible that the small irregularities in the results obtained can be attributed largely to the effect of porosity. Other factors, such as the chemical and the mineral composition of the individual cubes of ore may also have influenced reduction somewhat. However, the general trend of the effect of increased pressures is consistently and clearly indicated throughout the experimental work. The apparent general agreement of these results with the initial theoretical predictions would indicate that the effect of all variables except temperature and pressure had been largely eliminated.

SUMMARY

A number of cubes of iron ore were reduced by hydrogen under comparable conditions at several pressures. It was noted that pressures

greater than 10 in. of mercury materially increased the rate of reduction of the ore cubes. This increased reaction velocity was not as great at 600° or 700° C. as it was at 800° C. Both of these results are in agreement with the theoretical discussion given in the first part of the paper.

ACKNOWLEDGMENT

The writers wish to acknowledge the assistance of the Works Progress Administration, O.P. 665–71–3–69, in the preparation of the cubical specimens of iron ore used in reduction tests.

REFERENCES

1. E. Diepschlag: Die Reduktion von Eisenerz unter Andwendung Hoherer Drucke. *Archiv Eisenhuttenwesen* (Nov. 1936) 179–181.
2. J. M. Avery: Pressure Operation of the Pig-iron Blast Furnace and the Problem of Solution Loss. *Trans.* A.I.M.E. (1938) **131,** 102.
3. I. Langmuir: The Constitution and Fundamental Properties of Solids and Liquids. *Jnl.* Amer. Chem. Soc. (1916) **38,** 2263.
4. A. F. Benton and P. H. Emmet: Reduction of Nickelous and Ferric Oxides by Hydrogen. *Jnl.* Amer. Chem. Soc. (1924) **46,** 2728.
5. R. N. Pease and H. S. Taylor: Reduction of Copper Oxide by Hydrogen. *Jnl.* Amer. Chem. Soc. (1921) **43,** 2179.
6. H. A. Jones and H. S. Taylor: Reduction of Copper Oxide by Carbon Monoxide. *Jnl.* Phys. Chem. (1923) **27,** 623.
7. C. D. Kuenen: *Handbuch allgem. Chem.,* III (1919) 1–139.
8. H. S. Taylor: Treatise on Physical Chemistry, **2,** 1021.
9. T. L. Joseph: Porosity, Reducibility, and Size Preparation of Iron Ores. *Trans.* A.I.M.E. (1936) **120,** 72–98.

DISCUSSION

(C. D. King presiding)

H. COPE,* Donora, Pa.—I have been keenly interested in this subject ever since its first presentation by Mr. Avery and the treatment of it by Messrs. Tenenbaum and Joseph has given me a large measure of satisfaction and encouragement. If we can obtain in the blast furnace only 50 per cent of the results that have been indicated in the use of hydrogen as a reducing agent, we are certainly on the way to greater economies in blast-furnace operation. I wonder if it would be possible to break down the indicated total economy into two divisions; namely, the economies effected by more intimate gas-solid contact caused by increased gas pressure operation and those caused by the hastening of the chemical reaction after the increased gas-solid contact has been effected. I realize that this is a difficult problem but I believe we should not lose sight of the fact that there are these two definite interlocking phases.

J. M. AVERY,† New York, N. Y.—My interest in this paper has to do with pressure reduction as applied to the very practical operation of smelting pig iron in blast furnaces. I am sure that Professor Joseph would be the first to agree with me that for many reasons it is probably impossible to simulate in a laboratory conditions closely paralleling those in a blast furnace, with respect to ore reduction, and

---

for that reason great caution must be exercised in attempting to interpret laboratory results on reaction rates in a quantitative sense in terms of blast-furnace operation. Nevertheless, since tests on an actual blast furnace are necessarily costly, any information that can be obtained in the laboratory regarding the effect of pressure on the rate of reduction of iron ore by gases is helpful in setting at rest any question as to whether pressure *does* increase the rate of reduction. It is also helpful in arriving at a first approximation as to the probable order of magnitude of the effect of a given increase in pressure under given conditions. I am, therefore, grateful for the support this paper gives to the general theory of pressure operation of the blast furnace.

In interpreting the data, however, it is important to observe that the various groups of samples, each of which was reduced under a different combination of temperature and pressure conditions, differed rather widely in porosity. As Professor Joseph has shown in earlier work, the apparent porosity of ore has a direct effect on the rate of reduction. Another factor that indicates need for caution in interpreting the data is the fact that the same mass rate of flow of gas was used in all tests, and, as the rates of reduction differ, it is obvious that the composition of the gas resulting from the reaction also differed. This, of course, results in a tendency to decrease the apparent effect of pressure, though probably not to an important degree. The influence of the countercurrent flow of ore and gases, in a mass reaction relationship with fresh ore constantly available in the blast furnace, should also not be overlooked.

The heterogeneous reaction of reducing solid ore by gases is so complex in its mechanism, involving as it does the phenomena of actual and relative diffusion rates, adsorption and desorption effects, specific surface reaction rates, temperature effects and the like, that one must be cautious in setting up quantitative formulas for the effect of pressure, beyond the broad statement that pressure must, in general, increase the rate of reduction.

Two encouraging factors should perhaps be mentioned here:

1. In most blast furnaces, the ore quickly reaches temperatures greater than 700° C., and probably in regard to a blast furnace we are, therefore, most concerned with rates of reduction at higher temperatures, rather than lower, since such temperatures prevail throughout most of the stack. Tenenbaum and Joseph's results show a gratifying effect of pressure at 800° C.

2. Whatever results are obtained in the laboratory, it may be expected that the effect of pressure will be considerably greater in an actual blast furnace, because of the indirect effect of pressure on gas-solid contact through decreased channeling, decreased segregation of dust, and the like.

The use of pure hydrogen in the tests by Tenenbaum and Joseph leaves much room for speculation as to what the effect of pressure would be with blast-furnace gases containing perhaps 20 to 30 per cent of carbon monoxide. Diepschlag's data show that pressure was much more effective with carbon monoxide than with hydrogen, at least under his conditions. Further, an over-all pressure of two atmospheres absolute with pure hydrogen corresponds to a blast-furnace pressure, assuming 20 per cent reducing gas, of 10 atmospheres absolute, or about 130 lb. gauge, which is much higher than is contemplated for blast-furnace operation. Since Diepschlag reports, as might be expected, that the effect of pressure with both hydrogen and carbon monoxide falls off as the pressure increases, it may well be that the true chemical effect of pressure would be much greater under actual blast-furnace conditions than was indicated by the present experiments.

In short, Tenenbaum and Joseph's data, together with Diepschlag's published results, prove conclusively that pressure does substantially increase the rate of reduction of iron ore, and there are good grounds for believing that in an actual blast furnace the effect of pressure will be much greater than has yet been indicated by laboratory experiments.

Induction Furnaces for Rotating Liquid Crucibles

By E. P. Barrett,* W. F. Holbrook,† and C. E. Wood,‡ Member A.I.M.E.

The high-frequency laboratory induction furnace with a rotating liquid crucible enables research workers to conduct certain investigations heretofore very difficult or impossible to realize because vessels are not obtainable that are capable of resisting the physical conditions or the chemical actions to which they are subjected. Applications for patents covering commercial uses of centrifugal liquid crucibles were filed in the United States in 1919,[1] in France in 1925, in the United States and Germany in 1926,[2] and in France in 1927.[3] In 1928, Schuette and Maier,[4] of the Bureau of Mines, reported the construction of a whirling table beneath a high-frequency induction furnace.

Shape and Size of Centrifugal Liquid Crucibles

When a vessel containing a liquid is rotated, the inner surface of the liquid takes the shape of a paraboloid under the simultaneous action of centrifugal force and gravity. The internal dimensions of the paraboloid rotating liquid crucible are governed by the diameter of the container and its speed of rotation. Melted Wood's metal was poured into cylinders 2½ in. in diameter, which were rotated at 180, 300, and 468 r.p.m. When the metal was solid, a slurry of plaster of Paris was added, and rotation continued until the plaster had set. Fig. 1, a photograph of sections of the cylinders, shows the effect of speed of rotation of the containers upon the shape of the inner surface of the rotating liquid crucibles.

Types of Furnaces

Three types of high-frequency induction laboratory furnaces using liquid-metal crucibles were designed and constructed by the Blast

Furnace Studies Section of the Metallurgical Division of the Bureau of Mines:

1. A furnace in which a graphite crucible packed in lampblack in a refractory tube was rotated concentrically within the coil.

2. A furnace in which a super-refractory crucible containing molten metal was rotated within a graphite-lined stationary cylindrical furnace.

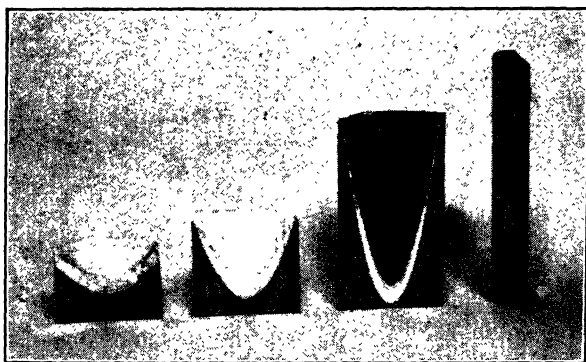3. A cylindrical furnace that was rotated as a unit.

FIG. 1.—EFFECT OF SPEED OF ROTATION ON SHAPE AND SIZE OF ROTATING LIQUID CRUCIBLES.

Type 1 Furnace

The inductor coil (5½ in. outside diameter, 4⅝ in. inside diameter and 6½ in. high), consisting of 35 turns of flattened copper tubing, was mounted in a transite-board box. A ¹⁄₁₆-in. layer of sheet mica was placed inside the coil for electrical insulation. The die in which the ⅜-in. copper tubing was flattened and the mandrel on which it was wound are shown in Fig. 2. The coil and the transite-board box with coil are shown in Fig. 3.

A table 12 in. square by 18 in. high, for mounting the coil, was constructed from 1½ by ⅛-in. angle iron, with a transite-board top ½ in. thick having a central opening 8 in. in diameter. A vertical shaft ¾-in. dia. by 15 in. long, was installed at the center of the table. A disk 7½ in. in diameter and four rings, each 7½-in. outside diameter by 4¾-in. inside diameter, of ½-in. transite board, were bolted to a circular steel plate attached to the upper end of this shaft. The weight of the rotating unit was supported by a ball thrust-bearing. A refractory tube, 4¼-in. outside diameter and 12 in. long, was centered in the opening in the transite-board rings, and the space between the tube and the rings was filled with a slurry of RA-162 Alundum cement.

The most serviceable refractory tube (4¼-in. outside diameter, 3½-in. inside diameter and 12 in. long) was made in the laboratory from a mixture of equal parts of Thermolith and RA-162 Alundum cements

moistened with a 10 per cent solution of sodium silicate.   After air-drying for 24 hr. the tube was fired to 1250° to 1300° C. in about 2 hr. and cooled
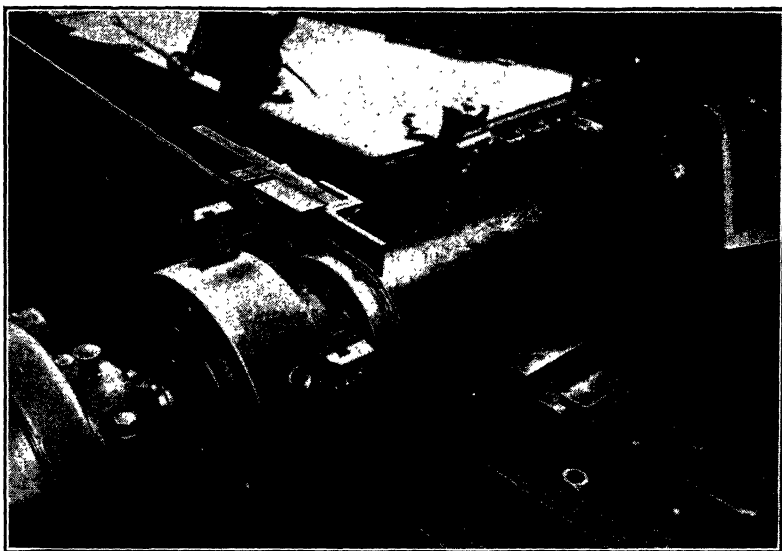

FIG. 2.—FORMING AND WINDING FLATTENED COPPER TUBING ON A 4½-INCH MANDREL.

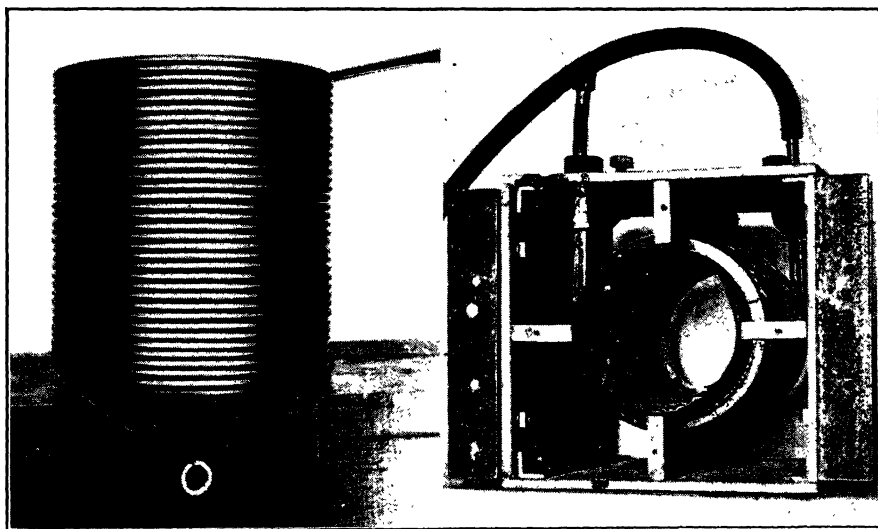a   b

FIG. 3.—COIL A AND BOX ASSEMBLY B FOR ROTATING CRUCIBLE FURNACES, TYPES 1 AND 2.

in the furnace.   The refractory tube, mounted in the rotating mechanism, and the completed furnace are shown in Fig. 4.

A jig was used to center a graphite sleeve in the refractory tube with respect to the axis of rotation, and lampblack was packed between the sleeve and the tube for heat insulation. The containers for the rotating liquid crucibles were machined from graphite electrodes, the outside diameter of the container being $\frac{1}{16}$ in. less than the inside diameter of the graphite sleeve. A section of the furnace is shown in Fig. 5 and the relative position of the liquid crucibles and slags in Fig. 6.
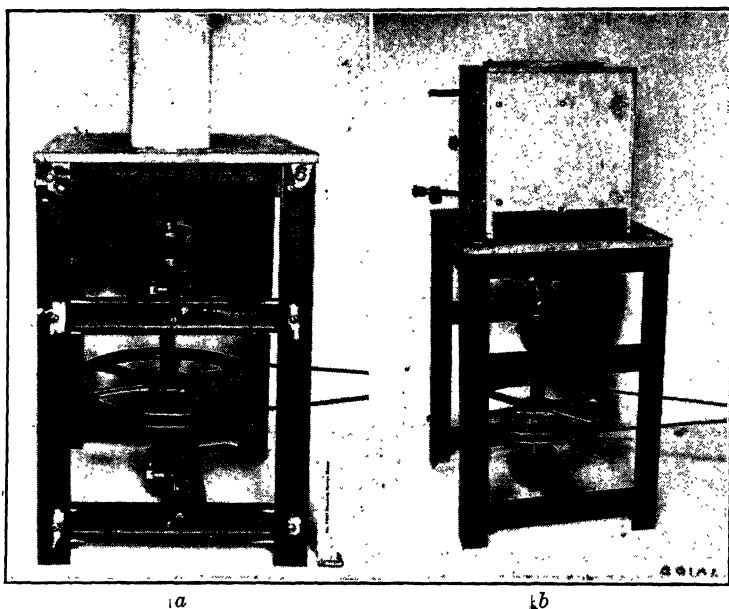
$_ia$ $_{k}b$
FIG. 4.—HIGH-FREQUENCY ROTATING INDUCTION FURNACE, TYPE 1.
a, refractory tube and rotating mechanism; b, completed furnace.'

Type 2 Furnace

Type 2 furnace was designed to eliminate the use of graphite containers for rotating liquid crucibles. The mounted inductor coil used in type 1 furnace was lined with bonded mica sheet $\frac{1}{16}$ in. thick. A graphite cylinder $7\frac{1}{2}$ in. long, $2\frac{3}{4}$ in. inside diameter and $3\frac{1}{4}$ in. outside diameter, was centered within the coil and lampblack packed between the graphite and the mica insulation. The graphite cylinder or heating unit did not rotate in this furnace.

The refractory tube and transite-board rings attached to the rotating shaft used with type 1 furnace were replaced by a refractory ring $7\frac{1}{2}$ in. in diameter by 2 in. thick with a 3-in. opening at the center. A graphite spindle of $2\frac{1}{2}$-in. dia. and 6 in. long was centered in the opening in the refractory ring and held in place with Alundum cement. The rotating mechanism, refractory crucible, and completed furnace are shown in Fig. 7, and a section of the furnace in Fig. 8.

Controlled Atmosphere.—The upper end of the rotating shaft and the furnace were enclosed in a transite-board box having a detachable cover.
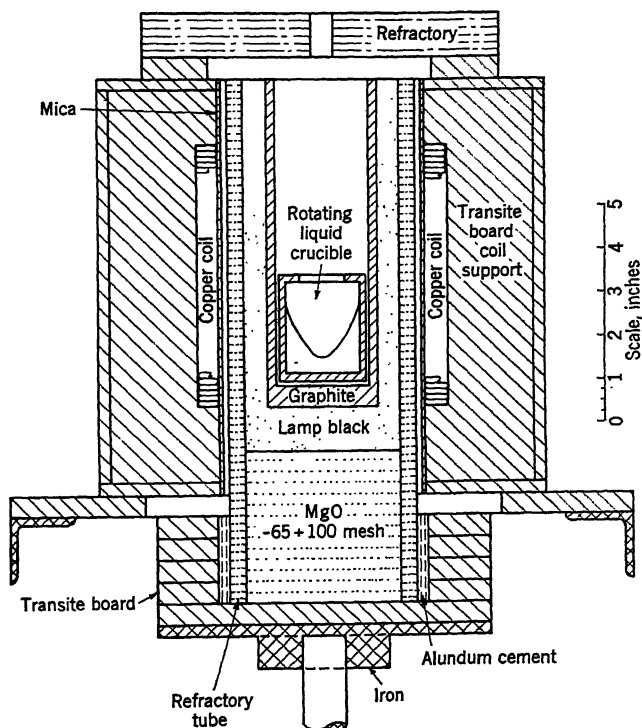
FIG. 5.—SECTION OF HIGH-FREQUENCY INDUCTION LABORATORY FURNACE, TYPE 1, USING ROTATING LIQUID CRUCIBLES.
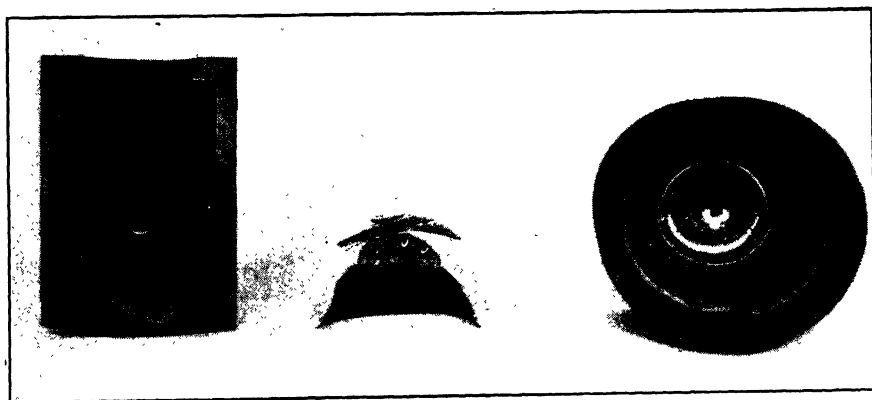
FIG. 6.—RELATIVE POSITION OF LIQUID CRUCIBLES AND SLAGS COOLED WHILE ROTATING. *a*, section of ferrous sulphide and slag in a graphite crucible; *b*, inverted section of iron and slag; *c*, top view of iron and slag in a refractory crucible.

To prevent damage should there be an explosion, a 3-in. dia. opening in the lower portion of one side of the box was covered with a piece of

$\frac{1}{16}$-in. asbestos paper painted with sodium silicate solution. An atmosphere of nitrogen under slight pressure was maintained in the box to prevent the entrance of air and subsequent formation of carbon monoxide due to contact with incandescent carbon. A 1-in. pipe attached to the cover was fitted with a window through which the charge was observed, and the temperature was determined by sighting with an optical pyrometer. Briquets of slag or other material were introduced into the rotating liquid crucible through a tee and plug without changing the atmosphere within the furnace.

Refractory Crucibles in Which Rotating Liquid Crucibles Were Formed.— The experiments for which type 2 furnace was designed could not be
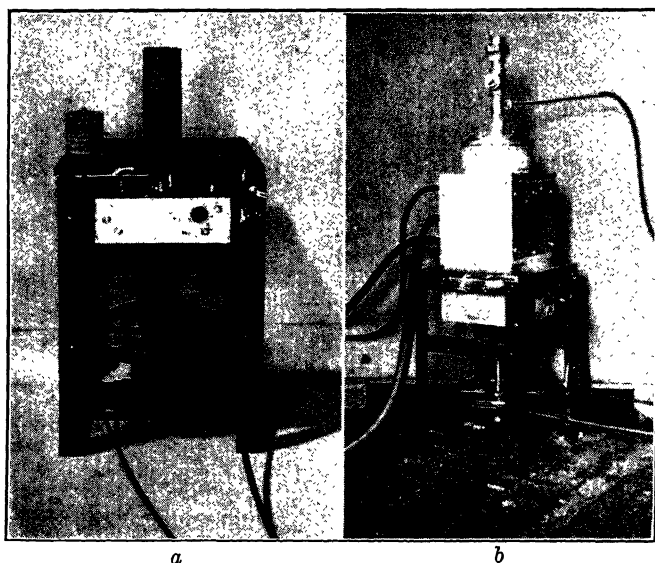
a   b
FIG. 7.—HIGH-FREQUENCY INDUCTION LABORATORY FURNACE, TYPE 2, USING ROTATING CRUCIBLES.
a, rotating mechanism, spindle and crucible; *b*, completed furnace.

performed in liquid crucibles in graphite containers. The low-carbon iron that formed the rotating liquid crucibles was held in fused-magnesia or fused-alumina crucibles, $2\frac{1}{2}$ in. high by $2\frac{1}{2}$-in. dia., formed by the vibrator method developed by Barrett and Holbrook.[5] To facilitate centering on the spindle, the refractory crucibles were formed with a projection at the center of the bottom, which fitted into a hole at the center of the top of the graphite spindle. The diameter of the hole in the spindle was $\frac{1}{16}$ in. greater than that of the projection on the bottom of the refractory crucible.

Type 3 Furnace

This furnace was designed to eliminate graphite parts, lampblack heat insulation, and preformed refractory crucibles. The heat was generated

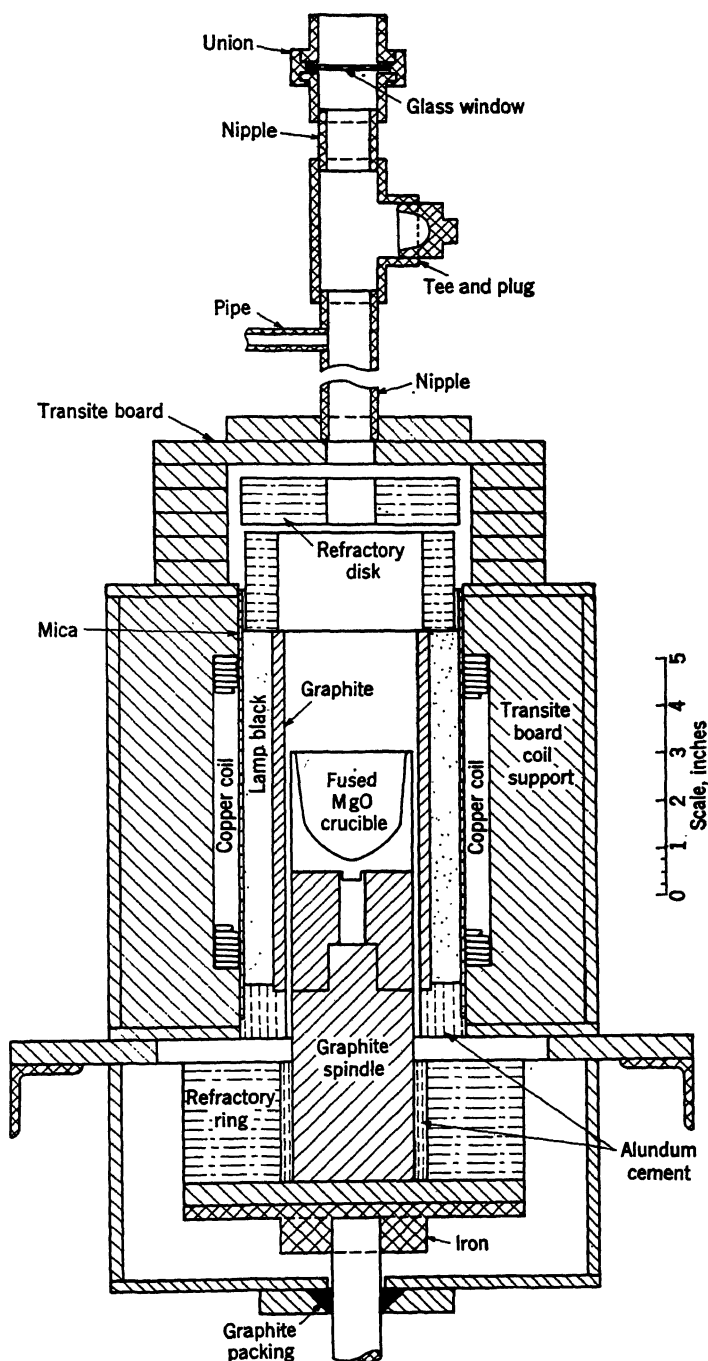FIG. 8.—SECTION OF HIGH-FREQUENCY INDUCTION LABORATORY FURNACE, TYPE 2, USING ROTATING LIQUID CRUCIBLES.

in the charge by direct induction.   An inductor coil identical with that used in types 1 and 2 was mounted in a transite-board frame attached to a steel plate welded to the upper end of a vertical hollow shaft.   The shaft was made from a piece of 1-in. seamless tubing 25 in. long, turned to $1\frac{9}{32}$-in. outside diameter and mounted in the center of an angle-iron frame 18 in. square by 28 in. high, constructed in a manner similar to that used on the shaft for types 1 and 2.   The weight of the rotating parts rested on a ball thrust-bearing.   The coil in the transite-board frame is shown in Fig. 9.

Water Connections.—Inasmuch as the coil rotated in type 3 furnace, it was necessary that both inlet and outlet connections for the cooling water be installed in the hollow shaft.   The details of construction of the hollow shaft are shown in Fig. 10.   The coil was insulated electrically from the shaft by two pieces (each about 40 in. long) of $\frac{3}{8}$-in. reinforced hose between the ends of the coil and the copper tubes extending from the top of the hollow shaft, as shown in Fig. 11.

Slip Rings and Brushes.—The electrical energy was transmitted to the inductor coil through two pairs of carbon brushes, each pair connected in parallel in contact with slip rings $8\frac{3}{8}$ in. outside diameter made from 1 by $\frac{1}{8}$-in. brass and installed concentrically at the ends of the coil.   One of each pair of brushes and the slip rings are pictured in Fig. 11.

FIG. 9.—COIL AND TRANSITE-BOARD FRAME FOR ROTATING INDUCTION FURNACE, TYPE 3.

Method of Lining.—A layer of bonded mica sheet $\frac{1}{16}$ in. thick was placed inside of the coil.   By the use of a jig a piece of graphite electrode $8\frac{1}{4}$ in. long, $2\frac{3}{4}$-in. dia. at the bottom and $2^{15}\!/_{16}$-in. diameter at the top was centered in the coil.   Dry fused magnesia, of mixed grain sizes to provide a dense mix, was rammed between the graphite form and the mica to within 3 in. of the top.   A dry mixture of fused magnesia and 3 per cent boric acid was used to form the next $1\frac{1}{2}$ in. of lining.   The space remaining was filled with a stiff mix of RA-162 Alundum cement and water.   When the cement had set, a piece of firebrick was placed on
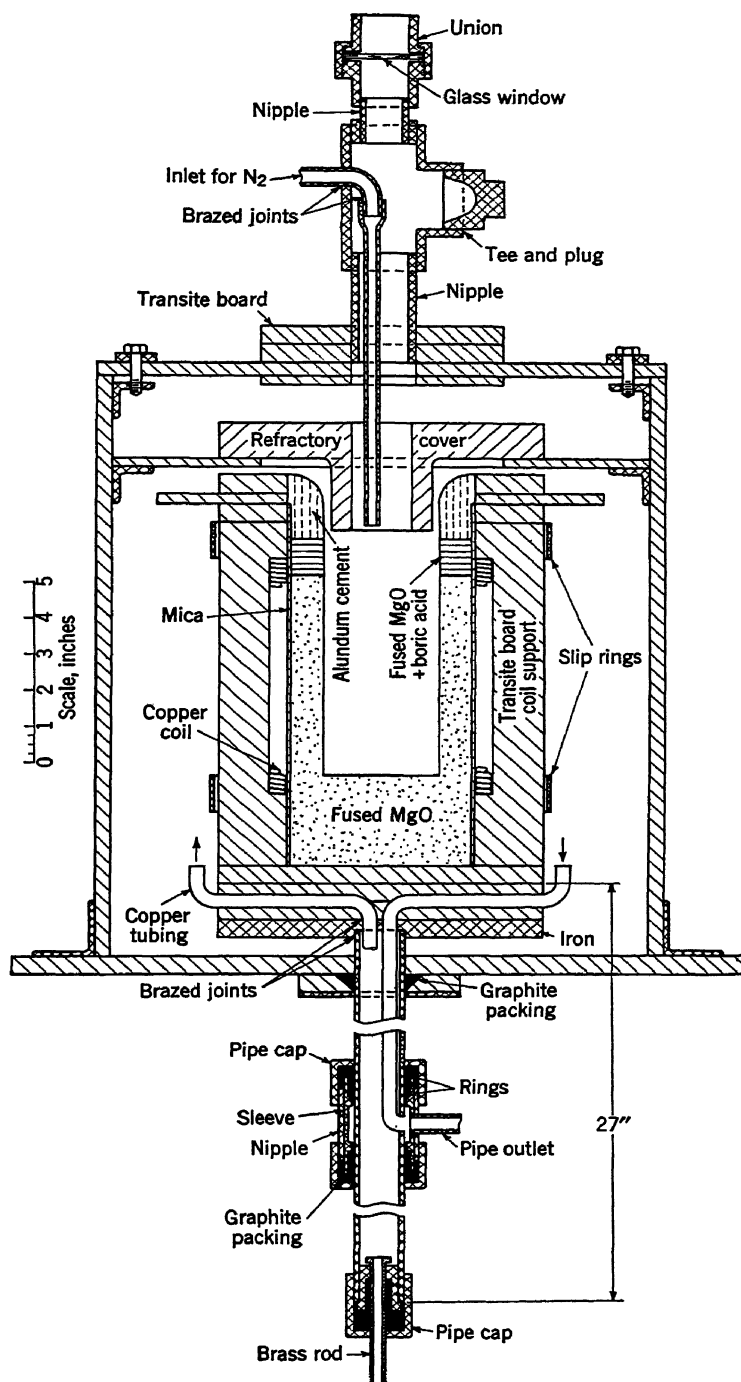
FIG. 10.—SECTION OF ROTATING INDUCTION FURNACE, TYPE 3.

top of the graphite form and the graphite heated to about 1550° C., at which temperature a thin layer of the fused magnesia next to the graphite was sintered to form a crucible in the furnace. The graphite form was removed immediately after the power was turned off.
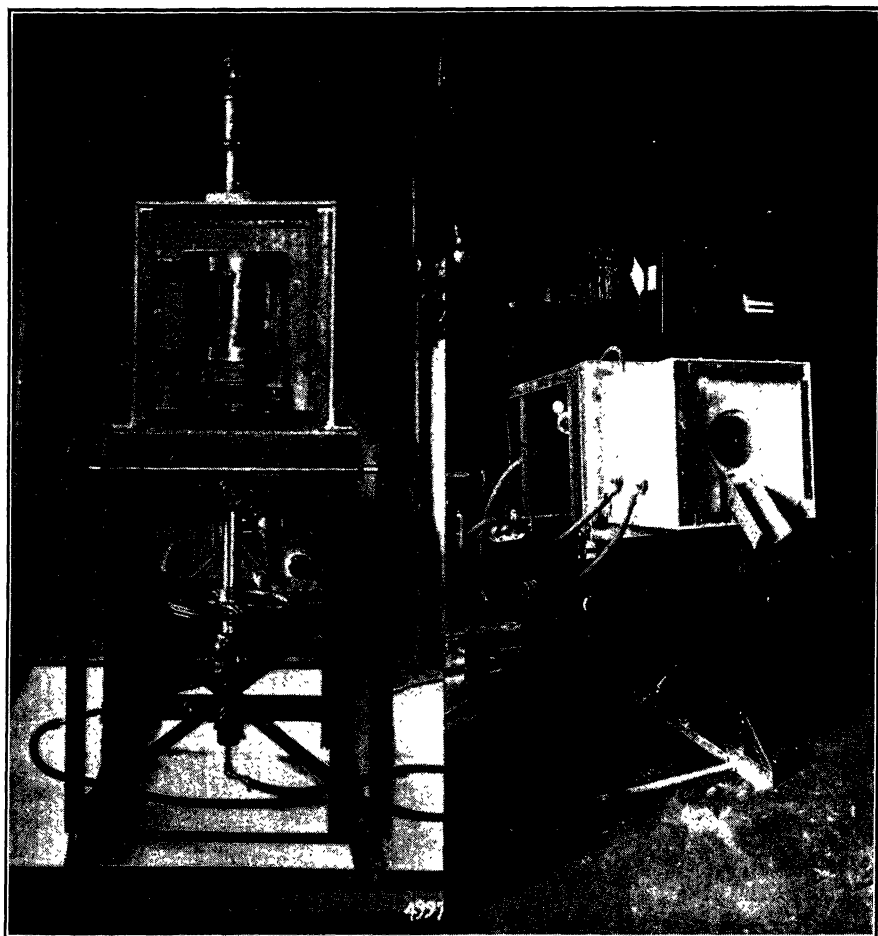
FIG. 11.   FIG. 12.

FIG. 11.—ROTATING INDUCTION FURNACE, TYPE 3, WITH FRONT OF BOX REMOVED.

FIG. 12.—ROTATING INDUCTION FURNACE, TYPE 3, IN POURING POSITION.

To facilitate removal of the graphite form, a hole 1½ in. in diameter by about 2 in. deep was turned in the upper end. A groove about ½ in. square was turned at the bottom end of the 1½ by 2-in. hole to provide a grip for the tongs used to remove the graphite form.

The top of the furnace was covered with a refractory lid made from a mixture of equal parts of RA-162 Alundum cement and Carbofrax cement No. 3, moistened with a 10 per cent solution of sodium silicate.

Reinforcements of Nichrome wire were placed inside the lid. After air-drying overnight it was fired to 1250° C.

The transite-board box was fitted with a removable cover to which was attached a piece of 1½-in. pipe with a glass window through which the charge was observed and the temperature determined by sighting with an optical pyrometer. Briquets of slag or other material were introduced into the rotating liquid crucible through a tee and plug without removing the top of the furnace.

To prevent oxidation of the molten metal, an atmosphere of nitrogen under slight pressure was maintained in the box. The nitrogen was introduced into the upper portion of the crucible through a piece of flattened ⅛-in. Allegheny 55 seamless tubing inside of the 1½-in. pipe and extending through the refractory cover. The observation tube, nitrogen inlet and refractory cover are shown in Fig. 10.

WEIGHT OF METAL AND SIZE OF ROTATING LIQUID CRUCIBLE

About 4½ lb. of molten Armco iron, when rotated at 280 r.p.m., formed a liquid crucible approximately 2¾ in. in internal diameter at the top by 2¼ in. deep.

TILTING FURNACE

To preserve the lining it was necessary to remove the molten metal at the end of each melt. This was readily accomplished by attaching a refractory-lined spout and by tilting the furnace so that the metal was poured into a split-type mold of 2⅝-in. diameter. The small ingots were remelted in the furnace. Fig. 12 shows the furnace in the tilted position.

SUMMARY

1. High-frequency induction furnaces using rotating liquid-metal crucibles are especially adapted to a study of slag-metal reactions.

2. Rotating liquid-metal crucibles are slag proof and eliminate contamination of the slag by the refractory.

3. Type 2 induction furnace for rotating crucibles was the simplest to construct and most flexible to operate, and provided the smallest temperature gradient in the hot zone.

4. Rotating induction furnace, type 3, was the most difficult to construct. Graphite parts and preformed refractory crucibles were eliminated. The iron used for the rotating liquid crucibles was heated direct by induction from electrical energy transmitted through slip rings.

5. The high-frequency induction laboratory furnace using rotating liquid-metal crucibles is a useful tool for research workers.

REFERENCES

1. E. F. Northrup: Method and Apparatus for Melting Oxides, etc., without Contamination.   U. S. Patent 1378189 (May 17, 1921).
2. J. Maximoff and M. Steela de Costa (née Vincent): Vorrichtung zur Ausfuhrung physikalischer oder chemischer Vorgänge.   German Patent 470748 (Jan. 10, 1929); Centrifugal Liquid Crucible.   U. S. Patent 1684800 (Sept. 18, 1928).
3. M. Ribaud: Procédé et dispositifs pour effectuer des traitements thermiques de matières, plus particulierement au four électrique.   French Patent 632343 (Jan. 7, 1928).
4. C. N. Schuette and C. G. Maier: High-frequency Induction Furnace for Chemical Preparations above 1000° C.   Amer. Electrochem. Soc.   Preprint No. 18 (Sept. 1928).
5. E. P. Barrett and W. F. Holbrook: An Improved Method for Forming Fused Magnesia Crucibles.   *Ind. and Eng. Chem.* (1938) **10**, 91–93.

DISCUSSION

(C. D. King presiding)

J. H. SCAFF,* New York, N. Y.—Barrett, Holbrook and Wood have described a furnace design that will be very useful for slag-metal studies because it eliminates reaction between the slag and refractory lining.   Heretofore this has been one of the main sources of difficulty in studies of this sort.

It would be interesting to know, however, whether the same relative stirring action is obtained between the slag and the metal in the rotating furnace heated by direct induction as is obtained with stationary furnaces.   It has been known for some time that rapid refining can be obtained by slags in the induction furnace because of this stirring action, but that one of the main difficulties in refining in the induction furnace is the rapid erosion of the lining at the slag-metal interface.   One naturally wonders therefore whether this principle might not be applied to furnaces of larger size as a means of eliminating or reducing this difficulty.

E. P. BARRETT (author's reply).—I believe that the stirring action is present in the rotating liquid-metal crucibles.   The charges we used in our furnaces were small, therefore the stirring action was not observed.   Our furnaces are merely laboratory tools, which could be constructed in larger sizes.   I would wish to see a 50-lb. furnace in operation before I would consider building a larger one.

---

* Bell Telephone Laboratories.

Mechanism of Solidification and Segregation in a Low-carbon Rimming-steel Ingot

By Anson Hayes[*] and John Chipman,[†] Members A.I.M.E.

The quality of sheet and strip products made of rimming steel is closely related to the structure and chemistry of the ingots. The variation in composition throughout the ingot, as affected by segregation, is of great importance, as are also the form and distribution of the voids that result from the gases evolved. It is because of this importance that the considerable literature in this field has accumulated. No attempt is made in the present paper to compile a bibliography of the excellent work that has already been done, as this has been adequately covered in the many excellent reports on the heterogeneity of steel ingots prepared by a joint committee and published by the Iron and Steel Institute.[1]

From time to time, in any field of investigation new tools and new technique are developed, which make further progress possible. In the field with which this paper is concerned, this is true. The development of the vacuum-fusion method as a means of following oxygen segregation, and a technique for obtaining the volume and composition of the gases evolved during solidification, have opened the way to obtaining data by means of which some considerable progress has been realized in developing more of the detailed mechanisms of solidification and segregation in rimming-steel ingots.

General Theory of Segregation

The basic cause of segregation lies in the fact that the impurities are less soluble in solid than in liquid iron. The solid that forms from the impure liquid is more nearly pure than the liquid itself. If solidification proceeds slowly enough, or if the liquid and solid phases are maintained in contact with one another for a sufficient time, a condition of equilibrium is set up, which may be represented by a phase diagram. Portions of the

diagrams for the systems iron-carbon and iron-copper in the delta iron region are shown in Fig. 1. When a liquid whose composition is represented by a point on the line AB begins slowly to solidify, the solid has a composition represented by a point on the line AH at the same temperature. In general, the ratio of the concentration in the solid phase to that in the equilibrium liquid phase is approximately constant, and this ratio may be called the distribution constant. For carbon, the point H is 0.075 per cent, and B is 0.59 per cent. The ratio, which we will call k, is
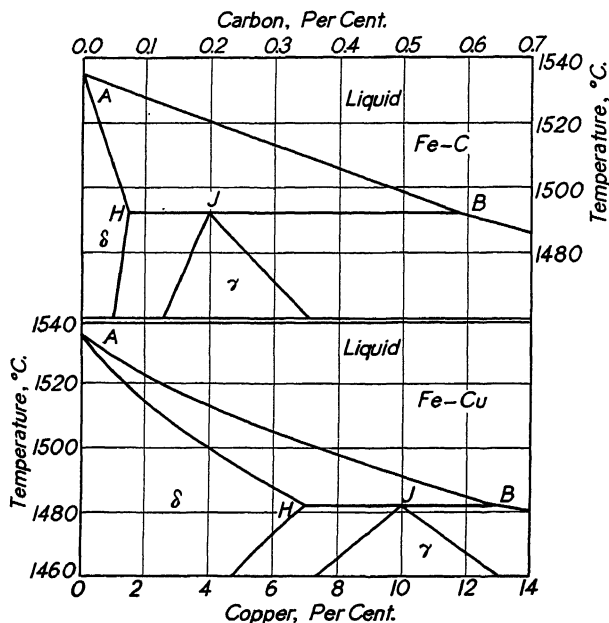
FIG. 1.—DELTA REGIONS OF SYSTEMS IRON-COPPER AND IRON-CARBON.

0.13. For copper k is 0.56. In general, the smaller the value of k, the greater is the tendency to segregate. The quantity $1 - k$ may be used as a measure of the tendency to segregate, and will be called the "segregation coefficient."

While solid is forming from liquid, the excess of dissolved substance above that which is dissolved in the solid is thrown back into the liquid adjacent to the solid. This normally results in the accumulation of impurities near the solidifying interface. If solidification is proceeding very slowly, or if the liquid is stirred, there will be a tendency for the excess impurities to mix with the bulk of the liquid, causing a gradual rise in its concentration. If, however, there is no stirring, and if solidification occurs at a finite rate, the next succeeding layer of solid will be formed from a liquid whose concentration is higher than that of the bulk of the system. For this reason, the concentration of the solid will be greater than its equilibrium value. Part of the excess impurity that was

thrown out of the solid thus becomes chemically entrapped in the succeeding growth of the crystal.

When crystal growth is dendritic, and interlocking branches are formed, there is inevitably a considerable amount of the liquid entrapped physically between the crystals with no opportunity for its excess impurities to be mixed with the bulk of the liquid. Entrapment is a factor that tends to diminish segregation, and may in certain cases almost entirely eliminate it. In general, the entrapment will be greater the greater the rate of crystal growth and the smaller the amount of stirring. In the solidification of rimming steel, the violent stirring action set up by the escaping gases diminishes the amount of entrapment, and leads to a much more pronounced segregation than occurs in killed steel.

Segregation in rimming ingots is further affected by the loss of substantial amounts of carbon and oxygen in the evolved gases. The loss of material from the liquid by gas evolution or by precipitation and floating out of a nonmetallic phase tends to offset in some degree the accumulation of impurities in the liquid metal remaining in the center of the ingot.

Theoretical Treatment of Maximum Segregation

In the preceding description of some of the factors affecting the actual results of the solidification of rimming steel, two of rather major importance have been mentioned: one, that of the equilibrium distribution of dissolved elements between solid and liquid, can be shown to be primarily responsible for the segregation effects for a given impurity; the other, that of entrapment, tends to diminish segregation.

It is thought desirable, therefore, to present the theoretical treatment of segregation resulting from the limiting condition of equilibrium distribution. By means of this hypothetical solidification, it is then possible to present the manner in which a number of modifying factors influence this behavior so as to result in the actual segregations obtained in the commercially produced ingot.

The following treatment of segregation of elements that are not involved with gas-forming reactions during the solidification of rimming ingots is based on the assumption that during solidification of the rim zone there is instantaneous equilibrium between the dissolved constituent in the solid that is forming and the liquid from which it formed; and, further, there is complete mixing at all times in the liquid that remains.

Let W_0 = weight of ingot in question,
$\quad W_l$ = weight of remaining liquid at any instant,
$\quad W_s$ = weight of solid remaining at any instant during solidification,
$\quad C_0$ = concentration of the element in the liquid at zero time,
$\quad C_s$ = concentration of the element in the solid forming at any instant,
$\quad C_l$ = concentration of the element in the liquid remaining at any instant.

Assume, further, that there is no appreciable diffusion of the element in the solid phase during the period of rim-zone solidification. Then the following relations should hold:

$$\frac{C_s}{C_l} = k \tag{1}$$

$$W_0 - W_s = W_l \tag{2}$$

$\int_0^{W_s} C_s dW_s$ = total weight of the element in question in the portion solidified at any instant

$W_0 C_0 - \int_0^{W_s} C_s dW_s$ = weight of element in question in the liquid phase at any instant

Then

$$C_l = \frac{W_0 C_0 - \int_0^{W_s} C_s dW_s}{W_l} \tag{3}$$

And

$$\frac{C_s W_l}{W_0 C_0 - \int_0^{W_s} C_s dW_s} = k \tag{4}$$

which, when combined with eq. 2 becomes:

$$k W_0 C_0 - k\int_0^{W_s} C_s dW_s = C_s W_0 - C_s W_s \tag{5}$$

Differentiating eq. 5,

$$-k C_s dW_s = W_0 dC_s - W_s dC_s - C_s dW_s$$

Or:

$$C_s dW_s - k C_s dW_s = (W_0 - W_s) dC_s \tag{6}$$

This may be written:

$$\frac{dC_s}{C_s(1 - k)} = \frac{dW_s}{W_0 - W_s} \tag{7}$$

Integrating eq. 7 gives:

$$\frac{1}{1 - k} \ln C_s = -\ln (W_0 - W_s) + M \tag{8}$$

where M is an integration constant, which may be evaluated when $W_s = 0$, and $C_s = kC_0$

$$\frac{1}{1 - k} \ln kC_0 = -\ln W_0 + M \tag{9}$$

Solving eq. 9 for M and substituting its value in eq. 8 gives:

$$\frac{1}{1-k} \ln C_s = -\ln (W_0 - W_s) + \frac{1}{1-k} \ln kC_0 + \ln W_0$$

Or:

$$\ln \frac{kC_0}{C_s} = (1-k) \ln \left[\frac{W_0 - W_s}{W_0} \right] \qquad [10]$$

It will be noticed that $\frac{W_0 - W_s}{W_0}$ is the fraction of the ingot which remains liquid at any given time. Also, it will be noticed that the fraction kC_0/C_s represents the ratio of the concentration of the element in the portion earliest solidified to that in the solid forming at any later time during the
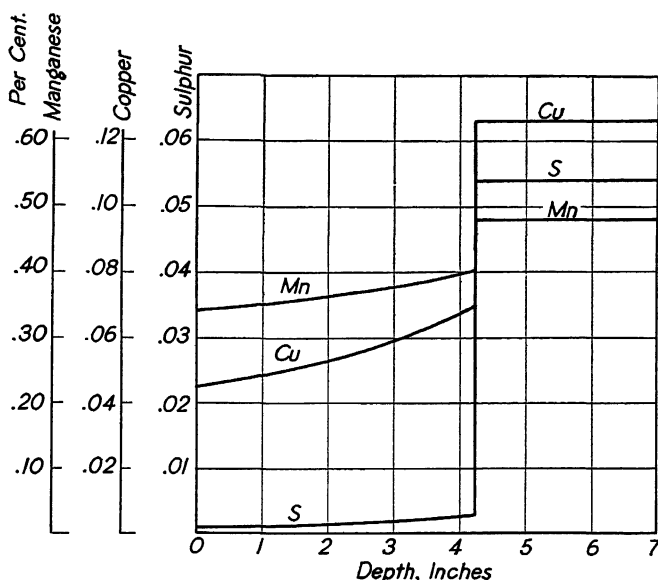
FIG. 2.—MAXIMUM SEGREGATION CURVES COMPUTED FROM LIMITING DISTRIBUTION MECHANISM.

rimming period. If k is known for a given element involved in the segregating action, it is possible to calculate the form of the curve representing the variation in concentration of the element in question in the rim zone and its concentration in the residual liquid metal at the end of the rimming period.

The results of the calculation for an ingot of ladle analysis Mn 0.41 per cent, S 0.020 and Cu 0.081 are shown in Fig. 2. The curves show the following noteworthy points:

1. That the limiting distribution mechanism produces more pronounced segregation for the constituents having smaller values of k.

Sulphur with a value of $k = 0.05$ segregates much more than does copper, $k = 0.56$, and manganese $k = 0.84$.

2. Comparison of this figure with Figs. 8 to 13, for actual segregation, shows that for all segregating impurities the limiting mechanism produces much lower concentrations of the impurities in the solid phase than does the actual process of solidification.

3. The greater the percentage of the ingot formed by the limiting solidification mechanism, the greater is the concentration of any given element in the core of the ingot.

4. The limiting mechanism would be accompanied by a much greater degree of segregation than is obtained in practice.

Factors Influencing Actual Solidification

The development of a quantitative treatment of the actual mechanism of segregation based upon the foregoing limiting mechanism requires a knowledge of the following experimentally determinable factors:

1. Distribution of elements between solid and liquid iron.
2. Rate of solidification of the ingot.
3. Rate of gas evolution and composition of gas.
4. Distribution of elements in the solid ingot.
5. The fraction of the ingot contained in the rim zone.
6. The approach of the liquid temperature to the freezing point.

In addition to these, the first five of which are now available, it will be necessary to compute certain related quantities and to assume or infer a certain amount of information regarding other factors, including:

7. The composition of the liquid metal and the concentration of impurities near the solidifying interface.
8. The entrapment of these impurities in the rapidly growing crystals.
9. Intermixing of the concentrated layer with the bulk of the liquid.
10. Mechanism of the formation of gas and of the precipitation of nonmetallic matter.

Distribution of a Dissolved Element between Solid and Liquid Iron

The general relationship between the composition of a liquid solution and that of a solid solution with which it is in equilibrium is given by the following formula, which is strictly valid only when both phases conform to the laws of the perfect solution:

$$\log N_1(\text{liq.}) - \log N_1(\text{solid}) = \frac{\Delta H}{2.3R}\left(\frac{1}{T_m} - \frac{1}{T}\right) \qquad [11]$$

where N_1 is the mol fraction of the solvent in the respective phases at the absolute temperature T, ΔH is the heat absorbed in transferring one mol of solvent from the solid solution to the liquid, and T_m is the melting point of the pure solvent.

This expression may be greatly simplified for systems in which the amount of dissolved substance is relatively small; let us say, not more than a few per cent. In such a case, if we designate by $N_2(s)$ and N_2(liq.) the mol fractions of the dissolved substance in the two phases, their ratio will be constant for a restricted range of composition and temperature near the melting point of the pure solvent. This we will call the distribution constant k, defined by the equation

$$\frac{N_2(s)}{N_2(\text{liq.})} = k \qquad [12]$$

The equation connecting composition and melting point in the dilute solution[2] may now be written,

$$N_2(\text{liq.}) = \frac{\Delta H \cdot \Delta T}{RT^2(1 - k)} \qquad [13]$$

where ΔT is the lowering of the melting point. For iron, of which the melting point is 1535° C. or 1808° K., and the heat of fusion is 3630 cal. per gram atom, the equation becomes:

$$N_2(\text{liq.}) = 0.00056 \frac{(\Delta T)}{(1 - k)} \qquad [14]$$

For a substance of molecular weight M dissolved in iron the mol fraction and per cent by weight in a dilute solution are related by

$$N_2 = \frac{\%}{1.79M} \qquad [15]$$

Hence, the equation may be rewritten

$$\%(\text{liq.}) = 0.001M \frac{(\Delta T)}{(1 - k)} \qquad [16]$$

In this equation "$\%$(liq.)" represents the percentage of the dissolved substance in the liquid phase and k is simply the ratio $\%(s)/\%$(liq.). We may write also the alternative form

$$\%(\text{liq.}) - \%(s) = 0.001M\Delta T \qquad [17]$$

Equation 17 will be applied first to the iron-carbon system to determine the value of k in the delta region. The peritectic[3] occurs at 1492°; the delta iron contains 0.075 per cent C, while the composition of the liquid has been variously reported from 0.36 to 0.71 per cent. According to the equation, the liquid should contain 0.59 per cent and the value of k is approximately 0.13.

The solidus of the iron-silicon system is not precisely known, but Ruer and Klesper[4] and Haughton and Becker[5] are in agreement on the liquidus, which at 1 per cent Si is 12° below the melting point of pure iron. Our equations show that the solidus at this temperature is 0.66 per cent and

$k = 0.66$. According to Ruer and Klesper[4] the melting point of iron is lowered 7° by 1 per cent Cu. The value of k is accordingly about 0.56.

The liquidus of the iron-manganese system is flat near the melting point of iron.[6] At the peritectic, 8 per cent Mn, the liquidus is 23° below that of pure iron. Hence, $k = 0.84$. This does not agree with Gayler's data on the solubility of manganese in delta iron, but is more consistent than her value with the segregation behavior of this element.

Tritton and Hanson[7] report for the solubility of oxygen in liquid and solid iron, respectively, 0.21 and 0.05 per cent, the latter being a rough estimate. From these data, $k = 0.24$, a value that will be shown later to be incompatible with the result of the present investigation. It will be shown that k is certainly less than 0.14, and we will use tentatively $k = 0.10$.

According to Friedrich,[8] 3 per cent FeS lowers the melting point 31°, while 5 per cent lowers it 57°. The first point corresponds to a solid solubility of 0.3 per cent FeS, the second to complete insolubility in the solid. The value of k is certainly very small; for purposes of the present discussion, the average of the two results, 0.05, will be used.

Haughton's[9] study of the iron-phosphorus system showed that the ratio of phosphorus in delta iron to that in the equilibrium liquid was about 0.13 in the alloys he employed. This value of k is consistent with a melting point lowering of 27° for 1 per cent P, which agrees well with 25° read from Haughton's curve.

The calculated values of k that are of interest in the study of segregation, as well as the "segregation coefficient," $1 - k$, are summarized in Table 1.

TABLE 1.—*Distribution of Substances between Delta and Liquid Iron*

Substance	k	$1 - k$
Carbon	0.13	0.87
Oxygen	0.10	0.90
Sulphur	0.05	0.95
Copper	0.56	0.44
Manganese	0.84	0.16
Silicon	0.66	0.34
Phosphorus	0.13	0.87

EXPERIMENTAL STUDY OF SEGREGATION

Rate of Solidification of Rimming Ingots

The rate of solidification of ingots of the same size as that used in the present study has been previously reported.[10] The curve showing thickness of the solidified shell of the ingot as a function of time is reproduced in Fig. 3. A second curve is included to show the percentage of the

cross section solidified at any given time after the ingot is filled. In this investigation it was possible to follow the course of segregation during the first 30 min., which corresponds to a depth of 4.8 in. The curves must not be extrapolated beyond this point, as it appears that the manner of solidification is very different in the interior of the ingot. The rate of increase in thickness was expressed by the following equation, in which D is the thickness in inches and t the time in minutes,

$$D = -0.12 + 0.9\sqrt{t}$$
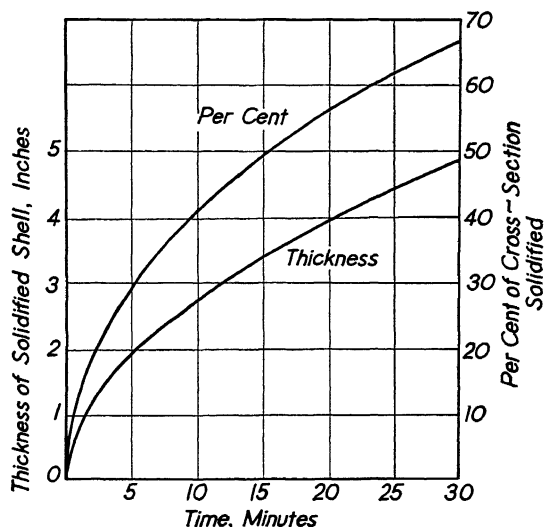
FIG. 3.—RATE OF SOLIDIFICATION OF 18 BY 39-INCH RIMMING INGOTS.

Gas Evolution

The ingot used in this investigation was taken from one of the heats employed in the study of evolution of gases from rimming ingots recently reported by McCutcheon and Chipman.[11] In heat No. 7 of that paper, the fourteenth ingot was set aside for the segregation study and the thirteenth was covered for the collection of gases. The volume of gas evolved is shown graphically in Fig. 4. In this figure, the amount of gas evolved during the filling of the mold was estimated from the carbon drop by a method that will be described later. The volume evolved after pouring, but before the meter was connected, was estimated by extrapolation by a method illustrated in Fig. 5. In this figure the volume of gas measured by the meter is plotted against the percentage of the ingot cross section that has solidified. Heats 7 and 8 gave straight lines during the active rimming period, which may be extrapolated back to show the amount evolved from the time the ingot began to solidify (i.e., from the time it was poured). Thus, for heat No. 7, it is found that 15 cu. ft. must be added to the measured volume. By way of explanation, it may be

pointed out that the break in the evolution curve for heat 9 was occasioned by the addition of a large excess of aluminum in the mold. The initial rate of evolution was greatly retarded, but a normal rate was
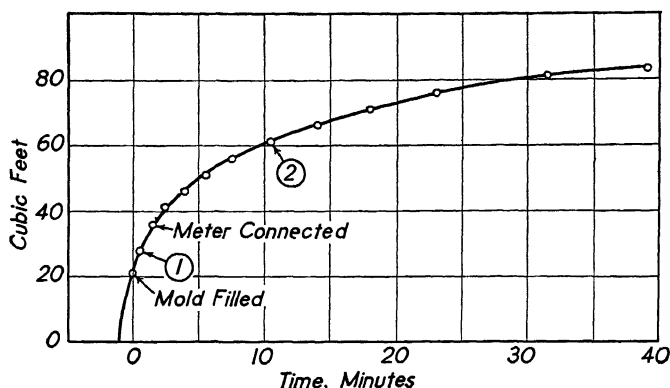
FIG. 4.—VOLUME OF GAS EVOLVED FROM INGOT OF HEAT 7 DURING POURING AND SOLIDIFICATION.

FIG. 5.—VOLUME OF GAS EVOLVED AS COMPARED WITH PERCENTAGE OF CROSS SECTION SOLIDIFIED.

obtained after about 25 per cent of the metal had solidified; that is to say, about 3 min. after the mold was filled.

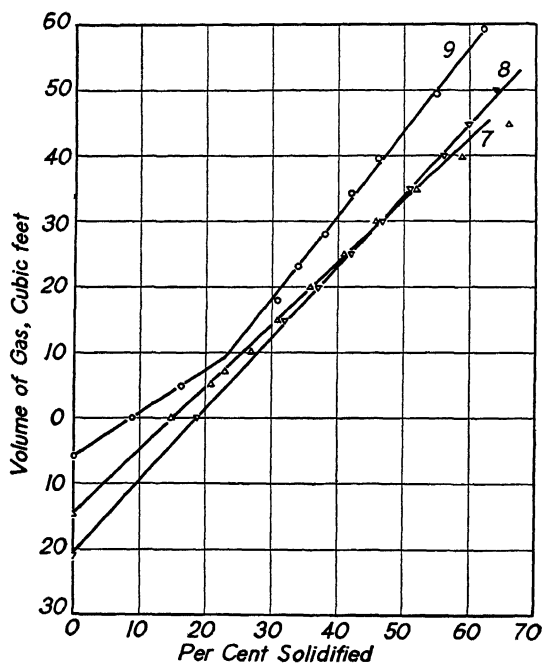Fig. 5 is also of interest in that it establishes a very direct relationship between the amount of gas evolved and the amount of metal solidified.

It is believed that this establishes definitely the fact that the gas is evolved at the surface of the solidifying metal.

The composition of the gases evolved from the ingot of heat 7 is shown in Table 2. From the gas analysis and temperature (38° C.), it is computed that on the average each cubic foot contained 0.028 lb. carbon and 0.038 lb. oxygen.

TABLE 2.—*Gases Evolved from Ingot*

Sample No.	Time after Filling Mold, Min.	Gases, Per Cent					
		CO$_2$	O$_2$	CO	H$_2$	CH$_4$	N$_2$
1	4.0	6.40	0.05	88.65	3.30	0.40	1.20
2	6.8	2.85	0.05	91.05	3.60	0.25	2.05
3	13.1	2.45	0.10	92.35	3.85	0.40	0.85
4	14.6	2.35	0.05	92.40	4.15	0.15	0.90
5	17.5	2.30	0.10	92.40	4.00	0.30	0.90
6	21.6	2.30	0.10	92.20	3.95	0.45	1.00
7	26.2	1.80	0.10	91.95	4.85	0.25	1.05
8	29.8	1.80	0.15	91.75	5.00	0.25	1.05

History of the Ingot

The heat from which the ingot was secured was considered a normal heat, and exhibited normal action during its solidification. The composition of the bath before tapping is given in the first line of Table 3. In the ladle, 1300 lb. of ferromanganese and 20 lb. of aluminum were added. The ladle analysis is shown in Table 3. The heat was poured into twenty-six 18 by 39-in. ingots each weighing about 11,500 lb. An aluminum addition of 0.15 lb. per ingot was made in the molds. Pouring time was 60 sec. per ingot, including topping. The metal worked down about 3 in., came up 1 in. and rimmed flat. Temperature was normal, as shown by a very small ladle skull. Samples were dipped from the liquid metal in an

TABLE 3.—*Samples from Furnace, Ladle and Molds*

Sample	Composition, Per Cent					
	C	Mn	S	P	Cu	O
Furnace at tap.................	0.08	0.147	0.018			0.047
Ladle........................	0.087	0.41	0.019	0.008	0.081	
Ingot: sample 1, ¼ min.........	0.081	0.40	0.019			0.035
Sample 2, 10 min...........	0.078	0.38	0.023			0.024

adjacent ingot at ¼ min. and 10 min. after filling the mold. Their analyses are included in Table 3. A sample of the nonmetallic matter, or "scum," which accumulates on top of rimming ingots was also obtained.

For this purpose another ingot was covered with sheet to protect the surface from oxidation. Fourteen minutes after this ingot was poured, the nonmetallic sample was obtained and allowed to solidify in the sampling spoon; its analysis was as follows: FeO, 28.36 per cent; Fe_2O_3, 4.42; CaO, 1.57; SiO_2, 3.16; MnO, 55.86; Al_2O_3, 7.32; S, 0.17 (grav.).

Method of Sampling

Since the purpose of the investigation was to study the mechanism of solidification, rather than to locate points of highest segregation, the abnormal portion of the ingot in the extreme top center and the extreme bottom were omitted. The locations selected were at $\frac{1}{6}$, $\frac{1}{2}$ and $\frac{4}{5}$ the height of the ingot. The ingot was first split vertically into halves, using dynamite. An oxygen torch was then used to cut out solid pieces extend-

FIG. 6.—INGOT AFTER REMOVAL OF SAMPLES FOR ANALYSIS.

ing from the skin to beyond the center of the ingot. A photograph of the ingot after sampling is shown in Fig. 6. The pieces were shaped up by milling to remove all of the torch-cut surface, and were then sawed into a number of slices parallel to the surface of the ingot, so that each slice represented a uniform depth beneath the skin. The pieces were designated A, B, C, from bottom to top of the ingot, and the slices were numbered consecutively from the skin to the center. The number and location of each slice are shown in the first two columns of Table 4.

Each slice was accurately measured and weighed, and its density computed. This is shown in the third column of the same table. Each slice may be considered as representative of a shell of uniform depth extending all around the ingot, each of the three cuts, A, B and C, being considered representative of one-third of the ingot. The cross-sectional area of each shell was computed from the dimensions of the ingot. This area multiplied by the density and by one-third of the height of the ingot gives the weight of the shell within that third. Now, if the sampling and weighing have been accurately performed, the total weight should check the known weight of the ingot. The totals for each cut are shown in the fifth column of Table 4. The total weight is computed on an

TABLE 4.—*Location, Density, and Weight of Samples*

Slice No.	Depth of Inner Edge, In.	Density, Lb. per Cu. In.	Area of Shell, Sq. In.	Weight of Shell, Lb.
CUT A, BOTTOM (18 BY 39 IN.)				
1	0.38	0.275	41.8	265
2	0.75	0.184	40.5	171
3	1.13	0.181	39.4	164
4a	1.75	0.190	63.4	277
4b	2.38	0.217	60.4	301
4c	3.0	0.240	57.3	317
5	3.38	0.229	32.9	172
6	4.0	0.217	52.0	260
7	4.63	0.245	49.3	278
8–11	Center	0.283	258.0	1,675
Cut A........	Total		695.0	3,880
CUT B, MIDDLE (17¼ BY 38½ IN.)				
1	0.38	0.274	40.8	257
2	0.75	0.264	39.7	240
3	1.13	0.230	38.5	203
4	3.0	0.245	176.0	990
5	3.38	0.267	31.9	195
6	4.0	0.262	50.5	303
7	4.63	0.237	47.6	270
8–11	Center	0.277	233.0	1,482
Cut B........	Total		658.0	3,940
CUT C, TOP (16½ BY 38 IN.)				
1	0.50	0.275	53.0	336
2	1.0	0.272	51.0	320
3	1.5	0.253	49.0	285
4	2.0	0.273	47.0	294
5	2.5	0.272	45.1	280
6	3.0	0.253	43.1	251
7	3.5	0.270	41.1	255
8	4.0	0.275	39.1	248
9	4.5	0.227	37.1	193
10–18	Center	0.271	216.5	1,348
Cut C........	Total		622.0	3,810
Total weight of ingot....				11,630

effective height of 69 in. divided into equal parts of 23 in. each.   In computing each cross section, an allowance of 1 per cent has been subtracted for rounded corners.   The total weight, 11,630 lb., is about average for ingots of this size and type.

Location of Blowholes

The general structure of the ingot was normal for the grade represented.   It contained a well developed honeycomb of rim blowholes in its lower half, extending from about ½ in. beneath the surface to about 2½-in. depth.   The deep-seated blowholes averaged 4¼ in. from the surface in the top and middle, and were slightly closer to the surface in
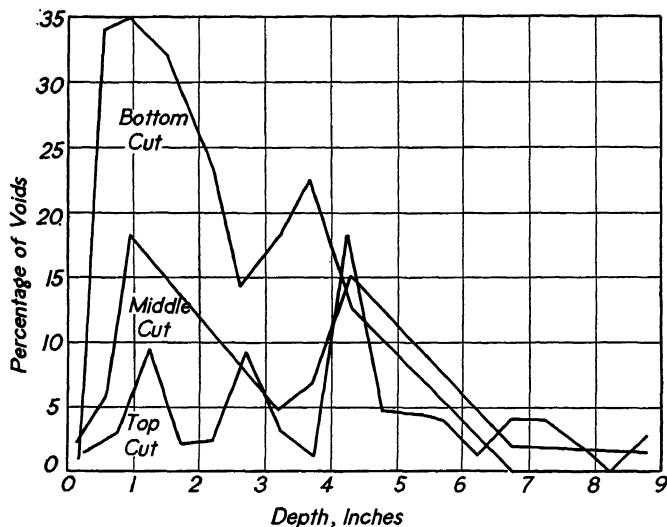
FIG. 7.—POROSITY IN RIMMED-STEEL INGOT.

the bottom part.   The ingot contained a very porous central zone in the extreme top, above the highest point of sampling.   Ingot structures of the same kind were reported by Washburn and Nead.[12]   The thick-skinned rimmed ingot found in their experiment E was very similar although slightly larger.

From density measurements, the percentage of voids at each level in the ingot has been computed.   The results are shown graphically in Fig. 7.

Analyses

Each slice was analyzed for oxygen and nitrogen by the vacuum-fusion method, and for the common elements by the usual chemical methods.   The results are presented graphically in Figs. 8 to 13.   Each point on the plots represents the analysis of a slice, the thicknesses varying

between ⅜ and ⅝ in., plotted at a depth corresponding to the midthickness of the piece.   Practically all of the results are fitted by the smooth curves within the usual analytical tolerance.   The shape of these segrega-
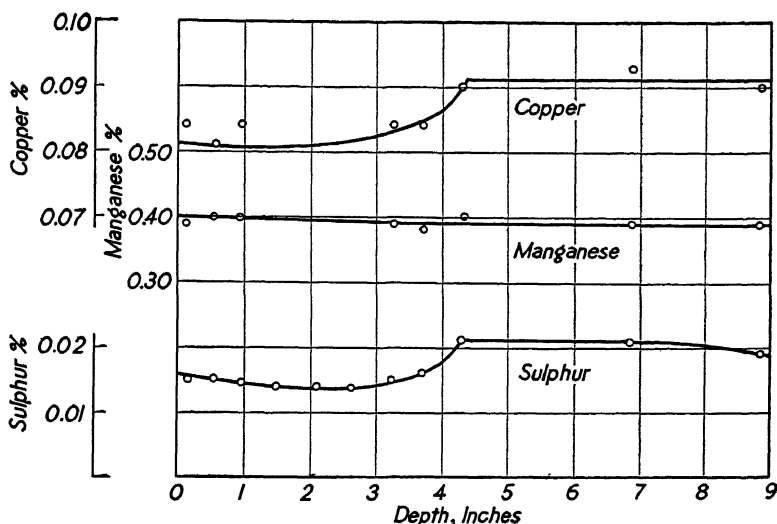
FIG. 8.—SEGREGATION OF COPPER, MANGANESE AND SULPHUR IN BOTTOM CUT.

tion curves is of great interest and will be the subject of a later section of this paper.   It will be noted that the percentage of each element decreases
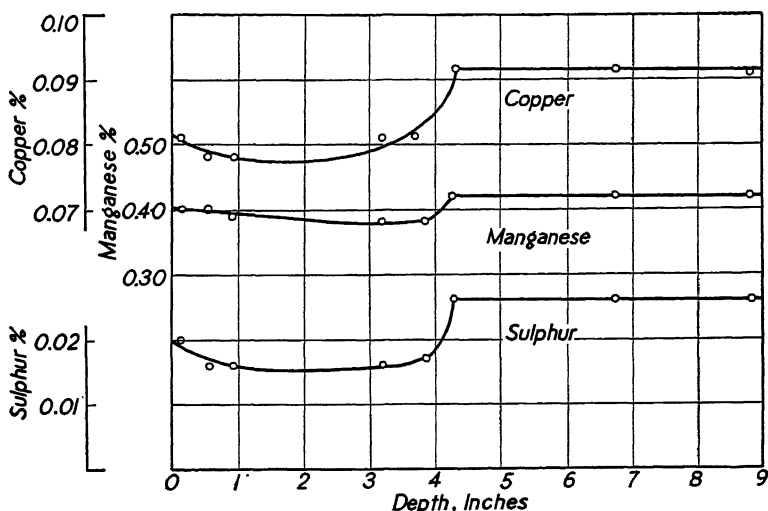
FIG. 9.—SEGREGATION OF COPPER, MANGANESE AND SULPHUR IN MIDDLE CUT.

to a minimum at a depth of 2 to 3½ in., then rises to a maximum at about the locus of the deep-seated blowholes, and is roughly constant throughout the central portion at any given height.

Integrated Composition of Ingot

If each of the three cuts is representative of the average composition of one-third of the ingot, the total weight of each element in each shell can be computed and by summation the total weight of each in the whole
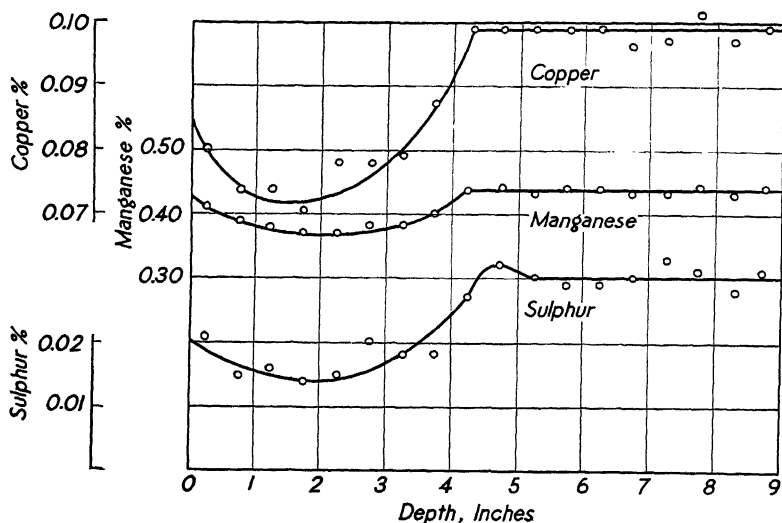
FIG. 10.—SEGREGATION OF COPPER, MANGANESE AND SULPHUR IN TOP CUT.
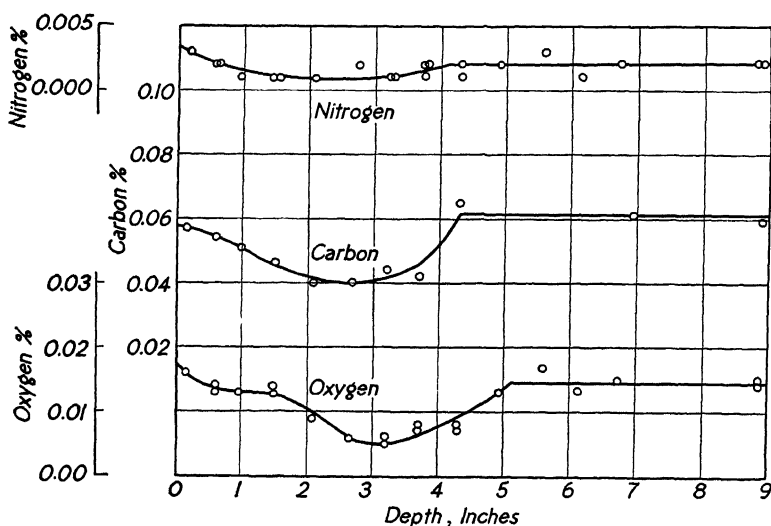
FIG. 11.—SEGREGATION OF CARBON, OXYGEN AND NITROGEN IN BOTTOM CUT.

ingot can be obtained. The average composition of the ingot reconstructed in this way ought to check the ladle analysis for the elements whose total amount does not change during solidification. For carbon and oxygen, which are evolved from the ingot, the discrepancy should

indicate the amount of each evolved, as gas, during the solidification. The amount of each element in each shell is shown in Table 5. At the foot of each column will be found the total weight in the ingot and the average percentage. The results for copper, manganese, and sulphur agree with the ladle analysis within usual analytical limits.

FIG. 12.—SEGREGATION OF CARBON, OXYGEN AND NITROGEN IN MIDDLE CUT.

FIG. 13.—SEGREGATION OF CARBON, OXYGEN AND NITROGEN IN TOP CUT.

Carbon and Oxygen in Evolved Gas

Analysis of the killed ladle test gives us the total amount of carbon and oxygen contained in the liquid metal poured into the mold. Two

TABLE 5.—*Weight of Each Element in Each Third of the Ingot*

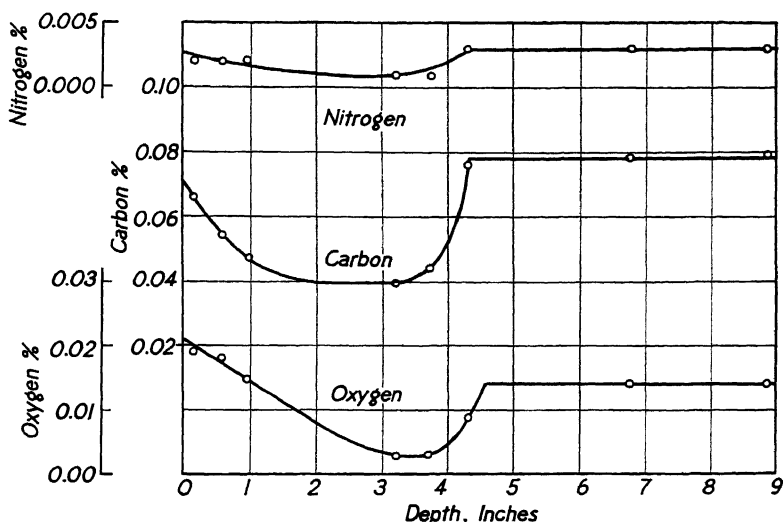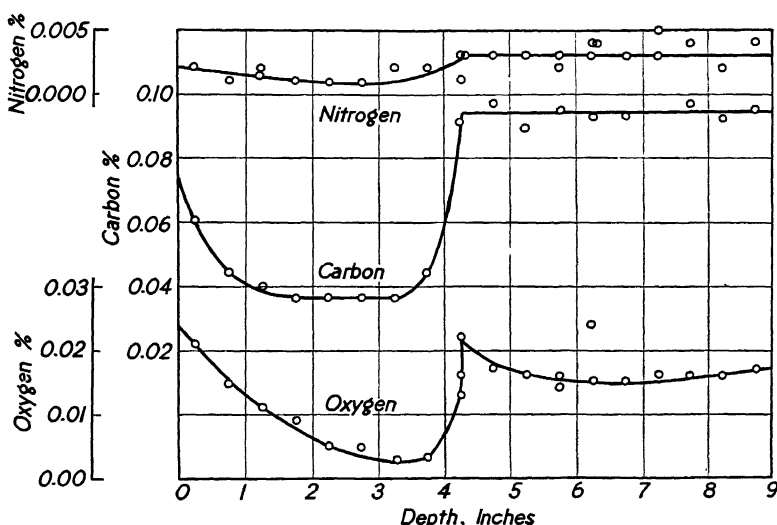| Slice No.	Weight of Shell, Lb.	Weight of Element, Lb.				
		Cu	Mn	S	C	O
BOTTOM THIRD						
1	265	0.213	1.06	0.042	0.153	0.042
2	171	0.137	0.68	0.026	0.092	0.024
3	164	0.133	0.65	0.025	0.084	0.021
4a	277			0.039		
4b	301	0.730	3.50	0.042	0.376	0.089
4c	317			0.044		
5	172	0.144	0.67	0.025	0.072	0.009
6	260	0.220	1.01	0.041	0.120	0.017
7	278	0.250	1.08	0.058	0.170	0.025
8–11	1,675	1.525	6.53	0.350	1.022	0.242
Cut A.......	3,880	3.353	15.18	0.692	2.089	0.469
Average.....		0.086	0.39	0.018	0.054	0.012
MIDDLE THIRD						
1	257	0.208	1.03	0.049	0.170	0.050
2	240	0.188	0.96	0.040	0.125	0.041
3	203	0.160	0.79	0.032	0.095	0.030
4	990	0.780	3.77	0.154	0.405	0.080
5	195	0.157	0.74	0.031	0.055	0.006
6	303	0.250	1.15	0.051	0.133	0.009
7	270	0.243	1.14	0.070	0.205	0.024
8–11	1,482	1.364	6.22	0.385	1.175	0.207
Cut B......	3,940	3.350	15.80	0.812	2.363	0.447
Average.....		0.085	0.40	0.020	0.060	0.011
TOP THIRD						
1	336	0.268	1.38	0.070	0.205	0.070
2	320	0.240	1.25	0.054	0.147	0.051
3	285	0.208	1.08	0.043	0.114	0.032
4	294	0.212	1.08	0.041	0.104	0.024
5	280	0.205	1.03	0.039	0.100	0.014
6	251	0.190	0.93	0.038	0.090	0.009
7	255	0.204	0.97	0.046	0.092	0.008
8	248	0.216	1.00	0.054	0.104	0.008
9	193	0.190	0.83	0.052	0.175	0.032
10–18	1,348	1.334	5.86	0.405	1.270	0.216
Cut C.......	3,810	3.267	15.41	0.842	2.401	0.464
Average.....		0.086	0.41	0.022	0.063	0.012
Total.......	11,630	9.970	46.39	2.346	6.853	1.380
Percentage in ingot.....		0.085	0.40	0.020	0.059	0.012
Ladle analysis........		0.081	0.41	0.019	0.087	

killed samples were taken during solidification and these give the amount of carbon and oxygen in the liquid metal at the time of sampling. Since the rate of solidification is known, the amount of solid metal that had been formed when each of these samples was obtained is also known, and from its analysis the actual weight of these elements in the solidified part can be computed. Thus, we know the amount of each element in the ingot at the time each sample was obtained. Also, from the gas analysis and the volume of gas evolved, the weight of carbon and oxygen in the gases may be accounted for.

A killed sample dipped from the mold 0.3 min. after filling contained 0.081 per cent C. At this moment the 800 lb. that had solidified contained 0.5 lb. C, and the 10,830 lb. of remaining liquid contained 8.8 lb., or a total of 9.3 lb. The ladle analysis was 0.087 per cent, which corresponds to 10.1 lb. C. From these figures, it is estimated that 0.8 lb. C, or 28 cu. ft. of gas, was evolved before this sample was taken. The approximate nature of this computation will be fully appreciated when it is realized that 0.001 per cent in the carbon analysis corresponds to about 4 cu. ft. of gas. By extrapolating the rate of gas evolution, it is estimated that 15 cu. ft. was evolved between filling and covering, which would mean that approximately 8 cu. ft. was evolved after sample No. 1 was taken, but before the meter was connected. The total gas measured was 47 cu. ft., and it is accordingly estimated that a total of 83 cu. ft. was evolved during the pouring and solidification.

A second killed sample was dipped from the liquid 10 min. after the mold was filled. It is possible to account for the carbon and oxygen present

TABLE 6.—*Distribution of Carbon and Oxygen during Solidification*

		Sample		
	Ladle	1	2	Ingot
Time after filling mold, min.........		0.3	10.0	
Average thickness, solidified, in......	0	0.5	2.8	
Weight of solid, lb................	0	800	4,880	11,630
Weight of liquid, lb...............	11,630	10,830	6,750	
Volume of gas evolved, cu. ft.......	0	28	60	83
Carbon, lb.:				
In solid....:..............	0.0	0.5	2.2	6.9
In liquid...................	10.1	8.8	5.3	
In gas.....................	0.0	0.8	1.7	2.3
Total carbon....................	10.1	10.1	9.2	9.2
Oxygen, lb.:				
In solid...................	0	0.1	0.6	1.4
In liquid..................		3.8	1.6	
In gas....................	0	1.1	2.3	3.2
Total oxygen...................		5.0	4.5	4.6

in the solid, liquid, and gaseous phases at the time each sample was dipped, in the final solid ingot, and with respect to carbon in the ladle. The data are shown in Table 6. The total amount of carbon and oxygen accounted for in the three phases is substantially constant, the slight decrease being accounted for by loss of oxides to the "scum," and by accumulation of carbon above the highest point of sampling.

Nonmetallic Inclusions

A microscopic study of the inclusions occurring in the top, middle, and bottom portion of the ingot was made. The selection of pieces for this study was based upon the oxygen and sulphur distribution and included the following points:

1. The outside cut, or skin: A-1, B-1, C-1.
2. The minimum on the oxygen curve: A-6, B-6, C-7.
3. The outermost part of the internal segregate containing the deep-seated blowholes: B-7, C-9.
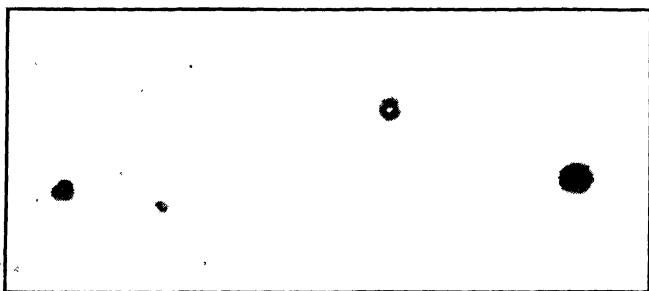4. The center of the ingot: A-11, B-11, C-18.

FIG. 14.—TYPICAL NONMETALLIC INCLUSIONS IN SKIN OF INGOT.   UNETCHED.   × 1000.
    Manganese oxide dark; manganese sulphide gray.   Center glassy silicate.   Sample from C-1.

Throughout this study, polarized light played an important part in classifying the types of inclusions, and often facilitated the subsequent identifications through etching methods.

In general, the inclusions found in the skin and the 4-in. cuts were very small; their exact identification was, therefore, difficult. On the other hand, the inclusions in the central areas of the ingot, although complex in nature, were of sufficient size to be capable of identification. Typical inclusions in the top and middle cut, edge position, are shown by Fig. 14. The large inclusion consists of manganese oxide (dark) and sulphide (light), while the smaller, spherical one is a glassy silicate. Most of the inclusions found in the bottom cut, edge portion, are of the same types.

Specimens taken 3½ to 4 in. from the skin, top, middle and bottom cuts, represent portions of the ingot having lowest oxygen content. Since

the sulphur in these areas is approximately four times the oxygen, we would expect largely sulphide inclusions; however, most of the sulphides observed appear to contain some oxides. Fig. 15 is typical of the few inclusions of any size found in the top cut, and is representative of each
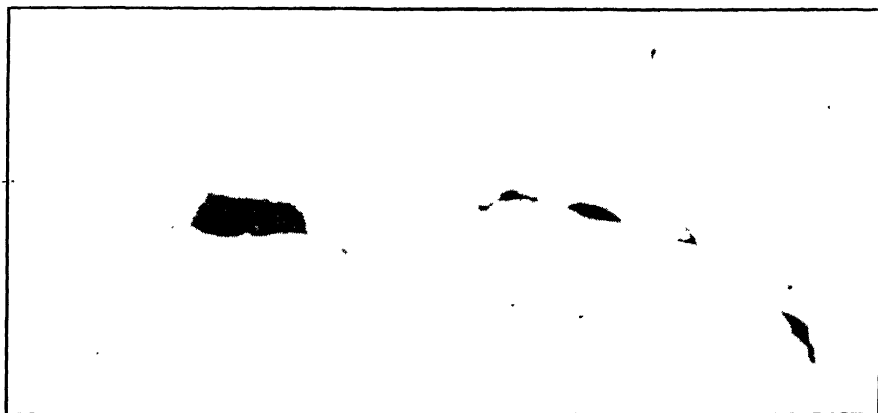
FIG. 15.—INCLUSIONS FOUND IN LOW-OXYGEN PORTION OF INGOT. × 1000.
Sulphides of iron and manganese containing some oxides. Sample from C-7.
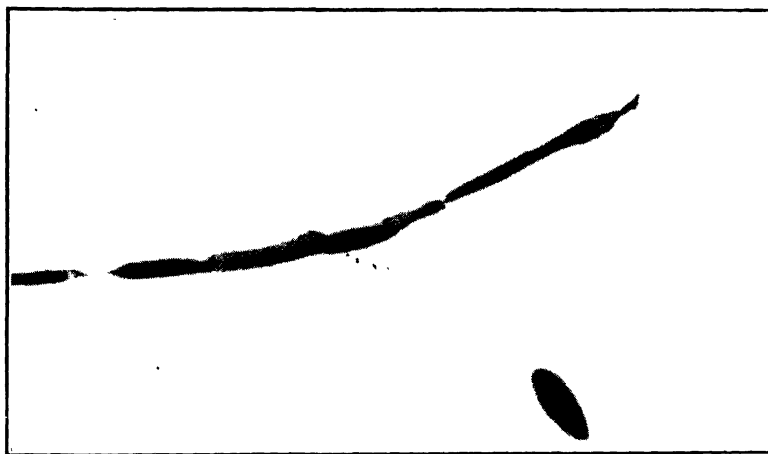
FIG. 16.—STRINGER INCLUSIONS. × 1000.
Oxide, dark; and sulphide, gray; found in vicinity of voids at center of ingot.
Sample from C-18.

of the three cuts, showing oxide-sulphide inclusions of eutectic appearance associated with grain-boundary material, mainly ferrous sulphide.

As would be expected, the central portion of the ingot proved to be the most fruitful from an inclusion standpoint. The inclusions were generally fairly large and easily identified. Chemical analysis showed a considerable segregation of sulphur in this portion of the ingot, a fact that was borne out by the large proportion of sulphide present in the inclusions.

In the top cut many void spaces were found, which were associated with long stringer inclusions of the type shown by Fig. 16, consisting of oxide (dark) and sulphide (gray). Another inclusion of the same con-
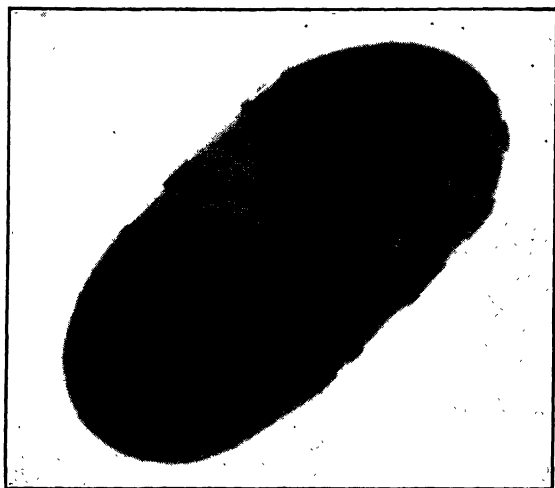
FIG. 17.—STRINGER INCLUSION.   × 1000.
Manganese oxide, dark; and sulphides, gray; from center of ingot.   Sample from C-18.
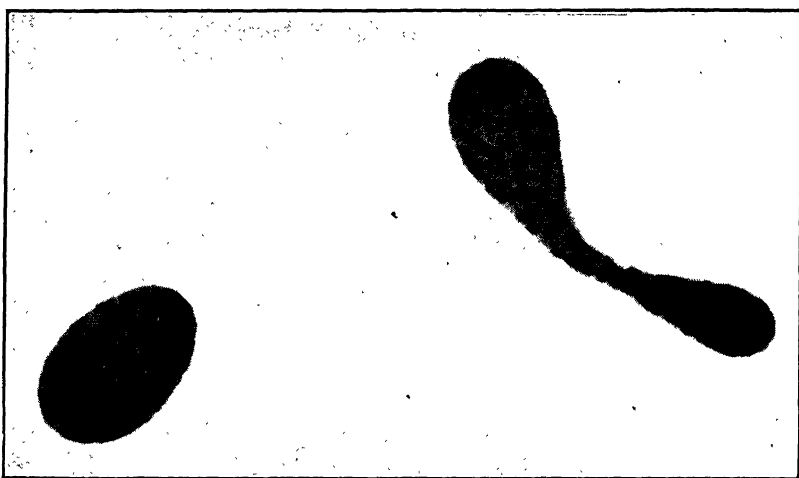
FIG. 18.—TYPICAL OXIDE-SULPHIDE INCLUSIONS FOUND IN CENTER OF INGOT.   SAMPLE FROM B-11.

stituents, but of different form, found in this cut is shown in Fig. 17. Inclusions found in the center of the middle cut are shown in Figs. 18 and 19. Fig. 18 is typical of many oxide-sulphide inclusions in the central portion of the ingot; a portion of a very large one is shown in Fig. 19. The

FIG. 19.—PART OF LARGE INCLUSION FOUND IN CENTER OF INGOT.   × 1000.
Manganese oxide, dark; iron sulphide, light; manganese sulphide, intermediate
Sample from B-11.

FIG. 20.—GROUP OF INCLUSIONS FOUND IN DEEP-SEATED BLOWHOLE PORTION OF TOP
CUT.   × 1000.
This group includes oxides, sulphides, and silicates.   Sample from C-9.

lighter parts of this inclusion are iron-manganese sulphide, with varying percentages of the two constituents, while the darker portions are oxide of manganese and iron.

The bottom portions of the ingot, central area, contained fewer and generally smaller inclusions than those described for the top and middle; however, they were of the same types and need no further description.

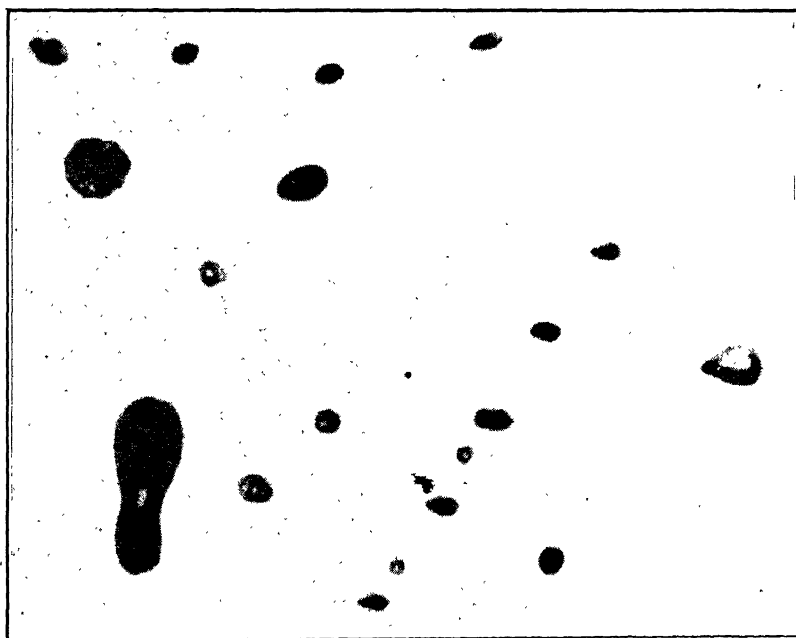The outer portion of the central segregate in the top cut containing the deep-seated blowholes contained inclusions similar to those shown in Fig. 18. In addition to these, some large groups of very small inclusions were found, many of which were identified as silicates. A portion of such a group is shown in Fig. 20. The outer portion of the central segregate, middle, and bottom cuts, also containing the deep-seated blowholes, contained inclusions similar to the smaller ones of Fig. 18 and the larger one of Fig. 15. The large groups of numerous small inclusions, typical of the top cut, were not present in the middle to bottom cuts.

Discussion of Results

The general shapes of the segregation curves are similar to those reported by Swinden[13] for a rimmed Bessemer ingot. In all cases the composition passes through a minimum at a depth of 2 to $3\frac{1}{2}$ in. and reaches a maximum in the vicinity of the deep-seated blowholes. The noticeable hump in Swinden's curves at this point was found only in our top cut. Failure to encounter this peak in the other cuts may have been due to the fact that samples were not taken sufficiently close together. In general the analyses from the deep-seated blowholes to the center were sufficiently constant to be represented by horizontal lines. Spot segregates cause some irregularity in this region but no differences of sufficient magnitude to be regarded as secondary maxima or minima were found.

There is no evidence from the shapes of the curves that the segregation of any one element depends upon that of any other. It would appear, on the contrary, that each element is behaving independently, although they are all following the same general scheme. The segregation of carbon and oxygen are affected by gas evolution but the full explanation of this effect must await the development of a satisfactory mathematical treatment of the simpler curves. The curves give no obvious evidence for or against the existence of stable oxides or sulphides of copper or manganese in the liquid metal. However, it will be found possible in later sections to account for the behavior of these metals without postulating the existence of such compounds in solution in the liquid metal.

Our curves differ from those recently published by Halley and Washburn[14] in one respect. These authors showed a very abrupt rise in concentration of all elements at the secondary blowholes, whereas our results indicate a much more gradual rise. The two investigations are in good agreement regarding longitudinal segregation up to the highest point that

we examined. However, there is a marked difference between our top cut at 80 per cent of the height of the ingot and their cross-sectional curve at 85 per cent. The latter showed a very marked peak at the extreme center of the ingot, which was entirely absent in our top cut.

The results for oxygen and nitrogen deserve special comment, as these are the first results that have been published for segregation of these elements in a rimming ingot. The analyses were made by the vacuum-fusion method, using a graphite crucible heated by high-frequency induction. The crucible was prepared by evacuation at 2100° C. and the analysis was conducted at about 1620° C. The base pressure in the furnace was of the order of 10⁻⁴ mm. and the blank was small compared to the lowest oxygen reported. Oxygen undergoes the greatest segregation of any element investigated. The extreme minima in the curves at 0.003 per cent oxygen were verified by check analyses. These extremely low concentrations are brought about by the combined influence of ordinary segregation, gas evolution, and the precipitation and flotation of oxides. The percentage of nitrogen is so small that no great certainty can be attached to the shape of the curves. They have been drawn to imitate the shapes of the curves found for the other elements.

FURTHER DEVELOPMENT OF THE THEORY OF SEGREGATION

The data reported in the foregoing sections enable us to take a number of steps toward a more complete understanding of the mechanism of solidification and segregation. The shapes of the segregation curves are directly related to the several stages of solidification, and the following qualitative discussion of their relationships will serve as an introduction to the more quantitative discussion that will follow.

When steel is poured into the mold, the first metal to solidify, as represented by the outer ⅜-in. slice, has a composition approximately equal to that of a "live" ladle test, cast without addition of aluminum. The sulphur, manganese and copper of this layer are practically equal to their percentages in the liquid metal while carbon and oxygen are each about 0.020 to 0.025 per cent lower.

As solidification proceeds, and as the rate of growth of the crystals decreases, the concentration of impurities in the solid also decreases. This occurs in spite of the fact that the concentration in the liquid is increasing. During this stage of crystallization there is a temperature gradient between solid and liquid metal and the growth of crystals occurs mainly in the direction of this gradient, occasionally being influenced slightly by upward currents in the liquid metal. During the formation of this rim zone the upward currents and rising gases in the middle and upper portion are sufficient to sweep off the gas bubbles as fast as they are formed at the interface. In the lower part of the ingot the formation of gas is opposed by the great ferrostatic pressure of molten

metal. Here also the upward currents are weaker and the interface is not swept as clean as in the upper parts. Once a gas bubble is permitted to remain on the surface even for a few moments, that part of the surface lags behind in crystal growth while near-by areas of contact are growing rapidly. When a blowhole is once begun, it is practically impossible for it to heal over by solidification because the void itself acts as an insulator to prevent the transfer of heat from the point of solidification to the exterior. The latent heat can be dissipated only through the solidified metal, and once a blowhole is started it continues to grow as long as the rapid growth of crystals continues all around it. The result is a honey-comb of pencil-like blowholes.

From the secondary blowholes inward the whole mode of crystalliza-tion is different. There appears to be no uniformity in the direction of growth of the crystals. The liquid and solid are probably at exactly the same temperature and crystal growth can occur in any direction. In order that a given crystal may grow it is no longer necessary that its neighbor grow along with it; it becomes possible for single crystals to extend far out into the liquid. This results in an interlocking mesh of crystals throughout the center of the ingot, which virtually prevents any further changes in gross composition. Localized segregation can occur and the further formation of scattered blowholes does occur at the most highly segregated spots.

As the fraction of solid metal in the now "mushy" center of the ingot increases, there is a gradual contraction, which is accompanied by the further development of voids, particularly in the extreme top portion. The settling that accompanies contraction may occur irregularly along rough planes of slippage, giving rise to the "streamer" segregates that are quite noticeable in sulphur prints. Gradual settling of crystallites may contribute to the greater purity of the bottom portion of the central segregate. It also leads to the accumulation of the last remaining liquid at the top, thus accounting for the extreme segregation at the extreme top of the central portion.

Composition of Liquid Metal during Solidification

During the active rimming period of a number of heats, several sam-ples of liquid metal were dipped from the interior of the ingot. These samples were taken in small iron spoons containing a coil of aluminum wire, by means of which it was possible to determine the oxygen content as Al_2O_3 in the solid sample. The composition of the samples from heat No. 7 and the ladle analysis of the heat are recorded in Table 3.

In general, it was found that the oxygen content of these samples depended primarily upon the carbon content. The sulphur appeared to be independent of carbon, oxygen and manganese, and was related only to ladle sulphur and time. In all cases there was a rapid increase in the

sulphur content of the residual liquid metal. Fig. 21 shows the percentage increase in sulphur above the ladle analysis as a function of time after filling the mold. As nearly as can be determined from the analyses, the rate of increase is linear with time. The straight line representing ingot F may be taken as the average for the entire group; the amount of departure from this average line does not exceed 0.002 per cent S. The average can, therefore, be used in computing the sulphur content of the liquid metal at any time up to 25 min., or during the solidification of 60 per cent of the ingot. It must be borne in mind that this represents
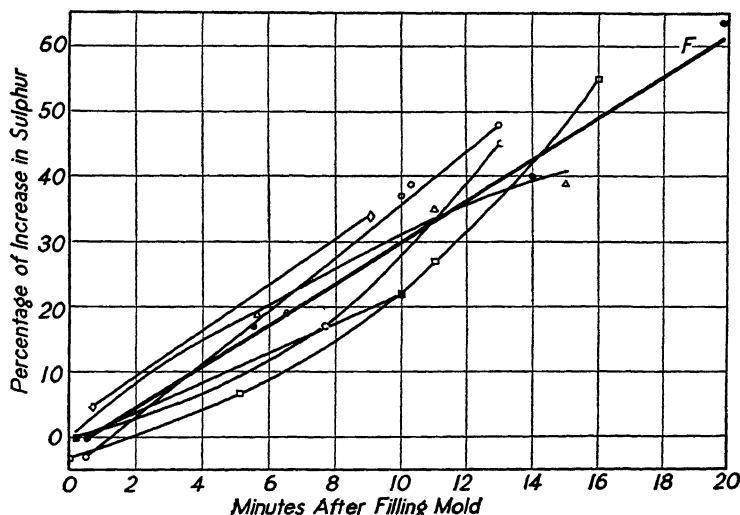

FIG. 21.—RATE OF ACCUMULATION OF SULPHUR IN LIQUID INTERIOR OF INGOT.

the sulphur content of the liquid only in the extreme top portion of the ingot.

In computing the average composition of the ingot from the segregation data, it was noted (Table 5) that the average sulphur contents at the three levels represented by cuts A, B and C were, respectively, 0.018, 0.020 and 0.022 per cent. It is improbable that this difference could have arisen after the ingot had frozen over. Nor is the difference attributable to analytical errors. A real difference exists, and it must have been built up during the rimming period.

In the early stages of solidification, gas evolution probably is occurring all over the solidifying interface. General stirring is therefore prevalent throughout the liquid, and the bulk of the liquid has a uniform composition from top to bottom. On account of the ferrostatic pressure, active evolution will cease first in the bottom of the ingot, and, consequently, there will be a cessation of mixing in this portion of the ingot. Later, as the carbon and oxygen contents decrease, mixing will cease in the middle and upper portions.

It has been pointed out that a major factor in segregation is found in the formation of an enriched film in the liquid adjacent to the solidifying interface. Let us now examine more closely the nature and effects of this film, which may be represented schematically as in Fig. 22. Here C_0 represents the initial concentration of a given element, C_l its concentration in the liquid and C_m in the solid metal at time t. The liquid immediately adjacent to the solidifying interface contains the excess solute rejected during the formation of the purer solid, and the enriched film results. The composition within the film itself is represented by the curve A-C_l and the shaded area is the total excess solute within the
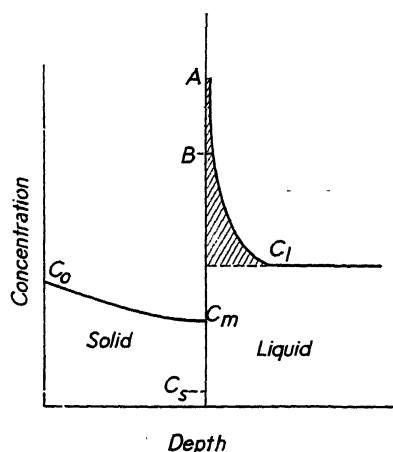

FIG. 22.
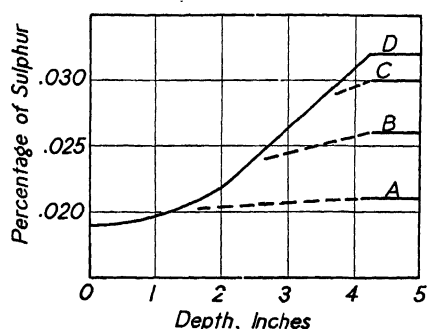
FIG. 23.

FIG. 22.—COMPOSITION OF SOLID AND LIQUID METAL NEAR INTERFACE (SCHEMATIC).
FIG. 23.—ESTIMATED SULPHUR CONTENT OF LIQUID METAL AT TIME OF SOLIDIFICATION AT INDICATED DEPTH.

film. The shape of the curve varies from one impurity to another and the maximum concentration that may be reached by the point A depends upon the distribution coefficient. The concentration of carbon and oxygen in the film may exceed greatly their equilibrium values and the escaping tendency of the carbon oxides may therefore become much greater than the ferrostatic pressure, with the result that gas bubbles are formed within the film itself.

The formation of gas bubbles at the interface dislodges part of the film, which is then carried upward by the rising stream of gas bubbles and by the general upward motion of the liquid metal near the interface. When the rate of evolution is not sufficiently violent to cause complete mixing in the liquid, the result will be the concentration of impurities toward the top of the ingot. This mechanism is suggested as the explanation of the longitudinal segregation that is always observed in rimmed ingots.

If the concentration of any substance in the enriched film tends to exceed its solubility in liquid iron, a new phase will appear. For example, if B represents the limiting solubility of a nonmetallic element, the excess portion BA separates out as a nonmetallic inclusion. This may adhere to the wall and be frozen in or may be carried upward with the gas stream. If carried with the gas, it may join the "scum" on top of the ingot or it may partially redissolve as it rises through the liquid metal, thus contributing to longitudinal segregation.

The solubility of oxygen in liquid steel is decreased by addition of manganese. The position of the point B is therefore higher in the absence of manganese and progressively lower as the manganese content increases. Herein lies the basis for a complete explanation of the effect of manganese on the rimming characteristics of ingots. Similarly, the presence of sulphides in the film may extract a part of the oxygen, thus exerting an
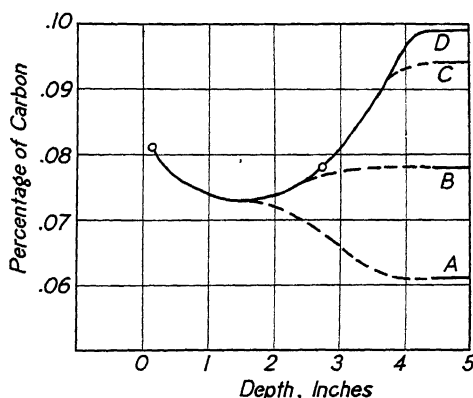
Fig. 24.—Estimated carbon content of liquid metal at time of solidification at indicated depth.

effect upon the rimming action. A full discussion of these factors is beyond the scope of this paper.

When gas evolution ceases, the remainder of the liquid metal solidifies without further change in concentration, as evidenced by the constancy of the analytical results from the deep-seated blowholes inward. This portion of the segregation curves may be used to establish the composition of the liquid metal at this stage of solidification at the three positions investigated.

In Fig. 23 the solid curve shows the percentage of sulphur in the top part of the ingot as established by the dipped samples previously discussed. The horizontal portions of the three curves, A, B and C, represent the composition in the central portion of the ingot at the three levels, and D the estimated final sulphur content of the liquid at the extreme top. The manner in which the curves A, B and C are drawn from curve D to the horizontal portions is based upon the theory of longitudinal

segregation outlined above, the dotted portion of curve B being drawn to represent the average composition of the residual liquid metal as computed from the segregation data of Table 5.

A similar set of curves for the carbon content of the liquid metal is shown in Fig. 24. Here there are only two experimental points to establish the location of curve D, and for the other three curves only the initial and final values are known. Curve B, representing the middle cut of the ingot, is drawn approximately according to the estimated average percentage of carbon in the entire amount of liquid remaining in the ingot, the calculation being based upon the segregation data and the volume of gas evolved. Curves A and C are drawn so as to depart from curves B and D, in somewhat the same manner as the sulphur curves were drawn.

With respect to copper, no intermediate points are available, and the shapes of the lines shown in Fig. 25 are largely hypothetical.
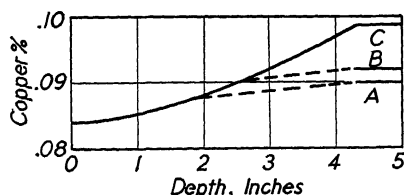
FIG. 25.

FIG. 26.

FIG. 25.—ESTIMATED COPPER CONTENT OF LIQUID METAL AT TIME OF SOLIDIFICATION AT INDICATED DEPTH.
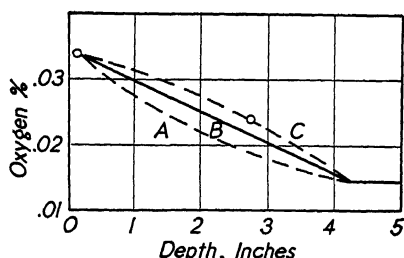
FIG. 26.—ESTIMATED OXYGEN CONTENT OF LIQUID METAL AT TIME OF SOLIDIFICATION AT INDICATED DEPTH.

The oxygen content is remarkably constant from top to bottom of the ingot. In Fig. 26 the oxygen at the middle level is represented by a straight line connecting the first sample with the central composition. The other two curves are sketched in so that the upper one includes the second experimental point.

Obviously, there is a large element of uncertainty regarding the shapes of all of these curves. They have been drawn on the basis of our current hypotheses regarding changes in liquid composition during solidification, but it should be expected that actual sampling of the liquid at different levels would modify the position and shape of the curves.

Entrapment as a Factor in Segregation

In the development of a general theory of segregation it was pointed out that the basic cause of the phenomenon lies in the fact that the impurities are less soluble in solid than in liquid iron. It was shown further that if this were the only factor to be considered, and if equilibrium existed between solid and liquid phases, the amount of segregation would

be greater than that which is actually observed. The major modifying influence is the entrapment of excess impurities or of a part of the liquid metal in the growing crystals at the solidifying interface.

The nature and amount of this entrapment may be visualized with the aid of Fig. 22 and the following example. Liquid metal containing 0.020 per cent S (C_l) would produce, under equilibrium conditions, a solid containing 0.001 per cent (C_s). The remaining 0.019 per cent would remain in the adjacent liquid and would increase greatly its sulphur concentration. If there is no stirring, and if solidification is much more rapid than diffusion, the concentration of sulphur in the adjacent liquid will continue to build up until the solid that is forming has the same composition as the bulk of the liquid from which it is formed, after which the con-
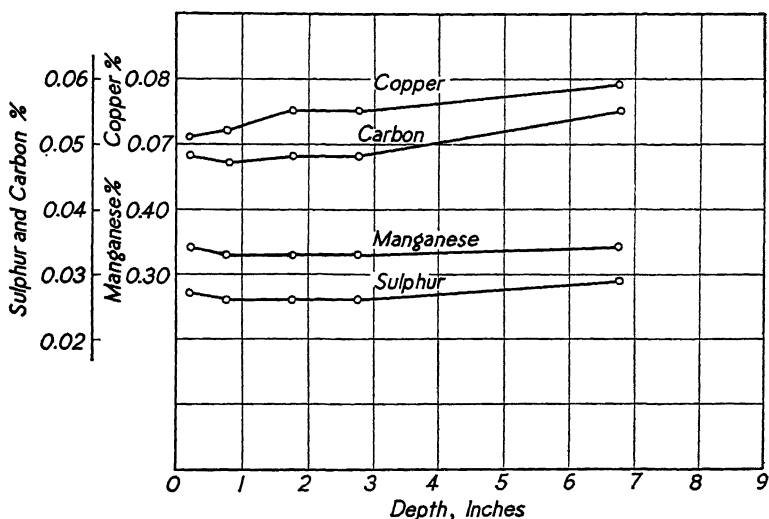
FIG. 27.—SEGREGATION IN LOW-CARBON KILLED INGOT, TOP CUT.

centration within the film of liquid in contact with the solid will remain constant. The maximum concentration of the enriched film (A) will be C_l/k, in this case 0.40 per cent S, and the composition of the solid may be expressed by stating that 100 per cent of the excess sulphur is entrapped.

In the early stages of solidification of a fully killed ingot, when rate of solidification is rapid and there is very little stirring, this condition is closely approached. Fig. 27 shows the segregation of carbon, manganese, sulphur and copper in a killed ingot of approximately the same composition as the rimmed ingot investigated. The killed ingot was sampled in the same manner and the curves of Fig. 27 represent its composition at four-fifths of its height. The flatness of the curves during the first few inches of solidification is in marked contrast to the sharp curvature encountered in the rimmed ingot. The difference occurs because in the killed ingot there is a nearly complete entrapment of the excess impurities

whereas in the rimmed ingot the entrapment has been decreased by the rapid stirring occasioned by the evolution of gases.   If the stirring were sufficiently violent to cause complete mixing of the excess impurities with the bulk of the liquid, the extreme segregation represented by the calculated curves of Fig. 2 would occur.   The segregation actually observed in a rimmed ingot is intermediate between these two extremes and depends upon the fraction of the excess impurities entrapped, which in turn is a function of rate of solidification and rate of stirring.

In addition to the mechanism outlined above, by which excess impurities in the enriched film are entrapped by the solid, a second cause of enrichment of the solid is found in the actual physical entrapment of part of the liquid between the growing crystals, when crystal growth is dendritic or when enough solid is present to produce a "mush."   This type of entrapment is found in the central portion of rimming ingots and the flatness of the segregation curves in the central section at all three levels indicates complete entrapment of all remaining impurities.

Probably both of these mechanisms of entrapment are effective in greater or less degree during the rimming period and in the present state of our knowledge it does not seem possible to distinguish clearly between them.   The following mathematical treatment will be understood to include both types of entrapment.

Mathematical Treatment of Entrapment

Let C_s represent the concentration of a given element in the solid that is in equilibrium with the bulk of the liquid, the concentration of which is C_l.   Let C_m represent the concentration in the final solid metal as determined by analysis.   If unit mass of liquid solidifies to form the equilibrium solid, the amount of excess solute will be $C_l - C_s$.   Let f be the fraction of this excess that is entrapped.   The over-all concentration of the solid will then be $C_s + f(C_l - C_s)$, or, since $C_s = kC_l$,

$$C_m = kC_l + f(1 - k)C_l \qquad [18]$$

Or, for the fraction entrapped,

$$f = \frac{C_m - kC_l}{C_l - kC_l} \qquad [19]$$

All data necessary for the calculation of the fraction entrapped are now available.   Values of C_m are taken from Figs. 8 to 13, while approximate values of C_l are available in Figs. 22 to 25.   Table 1 contains values of k. The results of the calculation are shown in Table 7.   The calculated values of f are very sensitive to minor analytical errors, especially for elements for which k is large.   For this reason the values calculated for sulphur are more dependable than those for copper, and it was not considered worth while to go through the calculation for manganese.   The

results for copper and sulphur in the top and middle cuts are in very fair agreement.   In the bottom cut the chances for error are much greater on account of the smaller degree of segregation and the greater uncertainty regarding the composition of the liquid.   The results for carbon and oxygen are expected to be lower than for sulphur and copper because a part of the excess of these elements which otherwise would have been entrapped is instead evolved as gas.   For oxygen the result involves the very large uncertainty in the value of k, which has been pointed out in an earlier section.   At the low point of the oxygen curve, if k were taken as 0.14, the value of f would be zero while larger values of k would lead to negative values of f.   Similarly, if k were zero, f would still be only 0.14.

TABLE 7.—*Fraction of Excess Constituent Entrapped in Solid*

Elements	Depth, In.								
	0.5	1.0	1.5	2.0	2.5	3.0	3.5	4.0	4.3
	Percentages								
Top cut:									
Sulphur......	0.89	0.74	0.65	0.62	0.56	0.60	0.67	0.83	1.00
Copper......	0.81	0.71	0.60	0.59	0.60	0.66	0.74	0.91	1.00
Carbon......	0.62	0.48	0.44	0.40	0.39	0.37	0.35	0.57	1.00
Oxygen......	0.53	0.40	0.27	0.17	0.07	0.03	0.05	0.34	1.00
Middle cut:									
Sulphur......	0.89	0.79	0.70	0.67	0.61	0.63	0.63	0.68	1.00
Copper......	0.88	0.83	0.77	0.75	0.74	0.75	0.78	0.84	1.00
Carbon......	0.71	0.58	0.51	0.47	0.46	0.45	0.47	0.62	1.00
Oxygen......	0.52	0.41	0.32	0.25	0.13	0.05	0.06	0.23	1.00
Bottom cut:									
Sulphur......	0.78	0.74	0.68	0.68	0.65	0.65	0.70	0.85	1.00
Copper......	0.92	0.90	0.86	0.84	0.86	0.86	0.88	0.91	1.00
Carbon......	0.69	0.63	0.57	0.53	0.51	0.56	0.65	0.83	1.00
Oxygen......	0.41	0.40	0.46	0.45	0.27	0.19	0.30	0.49	1.00

The two major factors that determine the amount of entrapment of impurities are believed to be rate of solidification and rate of stirring. Since the latter is largely dependent upon gas evolution, which in turn is related to the rate of solidification (Fig. 5), it may be inferred that entrapment bears a definite relationship to solidification rate during the rimming period.   In Fig. 28 the entrapment of sulphur and copper in the top cut is plotted against the rate of solidification in inches per minute. The data may be represented by two lines intersecting at the point of minimum entrapment, the first line a nearly linear function of rate, and the second apparently dependent upon a higher power of rate and sloping in the opposite direction.   This is exactly what might be expected if entrapment is a product of two forces.   It is evident that along the first branch of the curve the rate of solidification is the controlling factor, the

specific effects of gas evolution and stirring being hidden by the fact that they are also proportional to rate of solidification. Along the second branch the rate of stirring is rapidly approaching zero and entrapment is approaching unity. It is quite possible that the two branches represent the two different types of entrapment that have been mentioned, the first
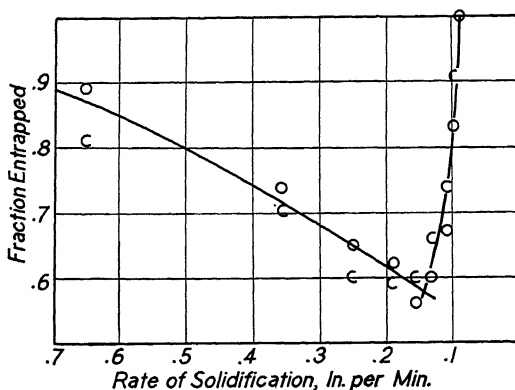

FIG. 28.—RELATION BETWEEN ENTRAPMENT AND RATE OF SOLIDIFICATION.
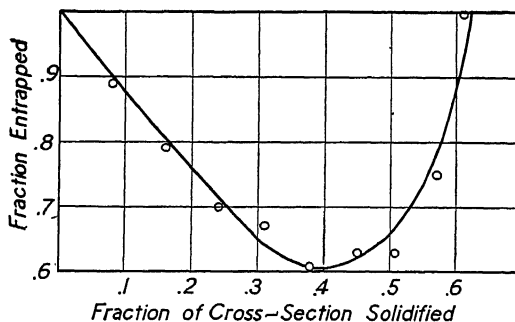
FIG. 29.—ENTRAPMENT IN MIDDLE CUT AS A FUNCTION OF FRACTION SOLIDIFIED.

branch being due to enrichment of the solid through an enriched liquid film and the second to physical entrapment of the residual liquid in the spaces between the growing crystals. A mathematical expression for entrapment is needed for use with the equations that have been developed for segregation (eqs. 1 to 10). For this purpose it will be convenient to express the fraction entrapped as a function of the fraction of the ingot that has solidified, or, more accurately, the fraction of the cross section that has solidified. The entrapment of sulphur in the middle cut of the ingot is represented in Fig. 29. The smooth curve, which is a fair approximation to the points, is fitted by the following equation in which X is the fraction of the cross section solidified:

$$f = 1 - 1.3X + 5X^4 \qquad [20]$$

Calculation of Segregation Curves

It should now be possible, by combining equation 20 with the equations developed earlier in this paper, to obtain a mathematical expression representing the form of the observed segregation curves. No attempt will be made at the present time to express longitudinal segregation in mathematical form. The equations that will be derived must therefore be restricted to the middle cut of the ingot where this effect is least noticeable.

Using the same nomenclature that was employed in equations 1 to 10 and 18 and 19, eq. 5 now becomes:

$$kW_0C_0 - k\int_0^{W_s}C_m dW_s = C_s W_0 - C_s W_s \qquad [21]$$

Now if we let X be the fraction of the cross section that has solidified up to any given time, then for practical calculations we may write $W_s/W_0 = X$. Dividing eq. 21 by W_0 we find

$$kC_0 - k\int_0^X C_m dX = C_s - XC_s \qquad [22]$$

or, since $C_s = kC_l$

$$\int_0^X C_m dX = C_0 - (1 - X)C_l \qquad [23]$$

Which on differentiation and rearrangement yields the general expression:

$$\frac{dC_l}{dX} = \frac{C_l - C_m}{1 - X} \qquad [24]$$

When the value of C_m is substituted from eq. 18, we obtain:

$$\frac{dC_l}{C_l dX} = \frac{(1 - k)(1 - f)}{1 - X} \qquad [25]$$

This expression may be integrated when f is known as a function of X. Thus, for sulphur at the midlevel of the ingot the value of f may be substituted from equation 20:

$$\frac{dC_l}{C_l dX} = \frac{(1 - k)(1.3X - 5X^4)}{1 - X} \qquad [26]$$

The integration of which between 0 and X yields:

$$2.3 \log \frac{C_l}{C_0} = (1 - k)\left[3.7X + 5\left(\frac{X^2}{2} + \frac{X^3}{3} + \frac{X^4}{4}\right) + 3.7 \ln (1 - X)\right] \qquad [27]$$

It is possible, from eq. 27, to compute the average composition of the liquid metal with respect to any constituent that has the same entrapment factor as sulphur. This should apply, at least approximately, to copper and manganese but not to carbon and oxygen. The results of the calculation are shown in Table 8. The values of C_0 for sulphur, manganese and copper in the ingot examined were taken as 0.020, 0.40 and 0.085, respectively, the average composition at the middle level being used in preference to the ladle analysis. The calculated values agree fairly well with the curves for position B shown in Figs. 23 and 25. The
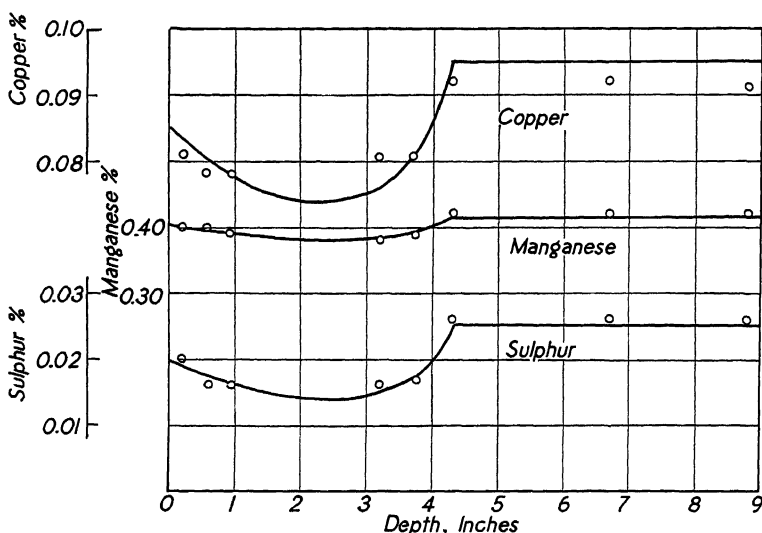

FIG. 30.—CALCULATED SEGREGATION IN MIDDLE CUT COMPARED WITH EXPERIMENTAL POINTS

agreement is not to be regarded as a confirmation of any of the assumptions that have been made in deducing either the curves or the equations. Rather, the results shown in Table 8 may be considered a second approximation toward the composition of the liquid metal during solidification.

An equation for the composition of the solid metal could be obtained by combining equations 27, 18 and 20. It proves simpler, however, to compute the solid composition by applying eq. 18 directly to the liquid compositions of Table 8, using the values of f given by eq. 20. The results of this calculation are shown in the last three lines of Table 8 and are reproduced in the smooth curves of Fig. 30. The observed analytical data are shown as circles. Since the calculations were based upon sulphur, the curve for this element must necessarily fit the data. The agreement in the other curves is considered satisfactory. The slight divergence of copper indicates that its true value of k is probably slightly larger than that used in the calculations.

TABLE 8.—*Calculated Composition of Liquid and Solid Metal at the Middle Cut during Solidification*

Depth Solidified, In.	0.5	1.0	1.5	2.0	2.5	3.0	3.5	4.0	4.3
Fraction solidified, X	0.08	0.16	0.24	0.31	0.38	0.45	0.51	0.57	0.61
Composition, Per Cent									
Liquid:									
Sulphur	0.020	0.020	0.021	0.021	0.022	0.023	0.024	0.025	0.025
Manganese	0.40	0.40	0.40	0.405	0.41	0.41	0.41	0.415	0.415
Copper	0.085	0.085	0.086	0.088	0.089	0.091	0.093	0.094	0.095
Solid:									
Sulphur	0.018	0.016	0.015	0.014	0.014	0.015	0.016	0.020	0.025
Manganese	0.395	0.39	0.385	0.385	0.385	0.385	0.39	0.40	0.415
Copper	0.081	0.077	0.075	0.074	0.074	0.075	0.078	0.085	0.095

Evolution and Segregation of Carbon and Oxygen

In order to apply similar methods to the study of segregation of carbon and oxygen, it is necessary to take into account the amounts of these two elements evolved as gases. It has been assumed that gas is evolved from the enriched film adjacent to the solidifying crystals. This need not imply that all the gas is evolved from this film or that all of the excess gaseous elements in the film are evolved. On the contrary, it was shown in Table 7 that substantial amounts of the carbon and oxygen of the enriched film are entrapped in the growing crystals, and the following calculations indicate that the oxygen content of the film is insufficient to account for all of the gas evolved.

Let g be the fraction of the excess solute in the enriched film that is evolved as gas. Of that which remains let f' be the fraction entrapped in the solid. The value of f' should be numerically the same as f for a nonvolatile element, such as sulphur in Table 7. Following the same method that was used in obtaining eq. 18, we find:

$$C_m = kC_l + f'(1-k)(1-g)C_l \qquad [28]$$

If we assume that f' has the same value as f for a nonvolatile element as shown in eq. 20, it is possible to compute the magnitude of g from the known values of C_m and k and the approximate values of C_l in Figs. 24 and 26.

The results for the middle cut of the ingot are given in Table 9. It is not expected that the fractions of carbon and oxygen evolved should be the same, since the two elements are not present in stoichiometric proportions.

The actual amounts of each element evolved from the enriched film, expressed in pounds per hundred pounds of metal solidified, may be given the symbol C'_g and computed from the formula

$$C'_g = gC_l(1 - k) \qquad [29]$$

Values of C'_g are shown in Table 10. Here one might expect, on the basis of the gas composition, that the oxygen evolved would be about 35 per cent greater than the carbon. That the results for oxygen are actually 30 per cent lower than for carbon may be owing to the accumulation of errors involved in uncertain values of k and of C_l. On the other hand, if the observed difference is real, it would indicate that some gas is formed by reaction of carbon of the enriched film with oxygen of the bulk of the

TABLE 9.—*Fractions of Carbon and Oxygen of Enriched Film Which Are Evolved as Gas (Middle Cut)*

Depth, in..............	0.5	1.0	1.5	2.0	2.5	3.0	3.5	4.0
g for carbon..............	0.25	0.28	0.30	0.29	0.30	0.33	0.29	0.17
g for oxygen............	0.43	0.45	0.55	0.60	0.68	0.84	0.80	0.69

TABLE 10.—*Weight of Carbon and Oxygen Evolved from Enriched Film in Pounds per 100 Pounds of Metal Solidified (Middle Cut)*

Depth, in..............	0.5	1.0	1.5	2.0	2.5	3.0	3.5	4.0
C'_g for carbon...........	0.017	0.018	0.020	0.019	0.020	0.022	0.020	0.012
C'_g for oxygen..........	0.012	0.012	0.014	0.013	0.014	0.015	0.013	0.010

liquid. The fact that only a small fraction of the carbon in the enriched film is used up means that a relatively large amount of this element remains to take part in the same sort of longitudinal segregation that was discussed in connection with sulphur. On the other hand, the greater part of the oxygen content of the film is evolved as gas, so that very little longitudinal segregation of this element can occur.

Now, from the measured rate of gas evolution, may be found the total weight of carbon and oxygen evolved per 100 lb. of metal solidified. In Fig. 5 it was shown that during the solidification of the first 60 per cent of the ingot a total of 57 cu. ft. of gas was evolved, and that the volume evolved was proportional to the weight solidified. This means that gas evolution occurred at a constant rate of 0.82 cu. ft. per 100 lb. of metal solidified. The temperature and composition were such that the gas contained 0.028 lb. carbon and 0.038 lb. oxygen per cubic foot. The total evolution, therefore, was occurring at a rate of 0.023 lb. carbon and 0.031 lb. oxygen per 100 lb. of metal solidified. These quantities may be called C_g for the two elements and are to be compared with the figures for C'_g given in Table 10, which represented gas evolution from the active film. The comparison indicates that practically all of the carbon loss occurs in the

enriched film. For oxygen the observed evolution is more than twice the amount evolved by the enriched film. It is, in fact, greater than could be accounted for by the film alone if it were completely evolved as gas. Approximately half of the oxygen of the evolved gas comes from the bulk of the liquid metal, a conclusion that is substantiated by the observed decrease in oxygen content of the residual liquid shown in Fig. 26.

SUMMARY

This paper describes a detailed experimental and theoretical study of the mechanism of the processes by which segregation occurs in a low-carbon rimming-steel ingot. A general theory of segregation is developed in which the primary cause of segregation is shown to be the distribution of impurities between solid and liquid iron. A second major factor is the formation of an enriched film in the liquid adjacent to the solidifying interface and the entrapment of part of this film in the growing crystals. This entrapment is in turn greatly affected by rate of solidification, and rate of stirring, the latter being almost entirely dependent upon gas evolution. A further contributing factor is the loss of carbon and oxygen by gas evolution and of the latter by precipitation of nonmetallics.

A mathematical treatment is presented which applies to a simplified hypothetical type of segregation in which equilibrium exists between solid and liquid phases, and the enriched film is completely mixed with the bulk of the solution. Such a process would yield the maximum segregation.

The literature on the distribution of impurities between solid (delta) and liquid iron is critically reviewed in the light of thermodynamics, and a table of distribution ratios and segregation coefficients is presented.

The ingot selected for experimental study was from a heat of mild steel, which had been used in the previously reported study of evolution of gases. The ingot was sampled from surface to center at points corresponding to $\frac{1}{6}$, $\frac{1}{2}$ and $\frac{5}{6}$ of its height. The analytical study included determination of oxygen and nitrogen by the vacuum-fusion method.

As solidification proceeds the concentration of impurities in the solid metal decreases to a minimum at a depth of 2 to $3\frac{1}{2}$ in., then increases to a maximum at a depth of 4 to $4\frac{1}{2}$ in. where the secondary blowholes occur. From this depth to the center the composition is practically constant. Longitudinal segregation of impurities toward the top of the ingot is particularly noticeable in connection with sulphur and carbon.

The average composition of the ingot, found by integrating the analytical results, is in agreement with the ladle analysis, except for carbon, where it is 0.028 per cent lower, and oxygen, which was not included in the ladle analysis. From the ladle and ingot analyses, the gas-evolution data, and from samples taken from the residual liquid during solidification, it is shown that the total amounts of both carbon

and oxygen in solid, liquid and gas phases during solidification are essentially constant.

A study of the distribution of nonmetallic inclusions in the ingot was made and illustrated by photomicrographs.

In the further development of the theory of segregation, based upon results of the experimental study, the first step is a careful estimate of the composition of the liquid metal during solidification. It is shown that a vertical concentration gradient builds up during the rimming period, giving rise to longitudinal segregation. The cause lies in the elevation of part of the enriched film by upward currents near the solid interface.

The entrapment of a fraction of the excess impurities in the enriched film is studied mathematically and the fraction entrapped is calculated from the simultaneous compositions of solid and liquid metal. Sulphur and copper show essentially the same entrapment while a much smaller fraction of carbon and oxygen is entrapped.

The entrapment figures for sulphur are considered more dependable than those for the other elements. Assuming that the fractions entrapped are the same for manganese and copper as for sulphur, it is now possible to compute the segregation curves for these elements in the middle cut of the ingot. The calculated curves are in good agreement with the analytical data.

Similar methods are applied to the entrapment of carbon and oxygen on the basis of the simple assumptions that a part of the enriched film is evolved as gas and that the fraction of the remainder entrapped in the solid is the same as for the nonvolatile elements. On this basis the fraction of the film evolved as gas is computed, as well as the total weight of carbon and oxygen evolved from the film. It is found that the film loses about three tenths of its carbon content and more than half of its oxygen.

The total carbon and oxygen losses are known from the rate of gas evolution. It is found that the greater part of the carbon and less than half of the oxygen evolved have their origin in the enriched film itself, the remainder coming from the adjacent liquid.

REFERENCES

1. First to Seventh Reports, inclusive, on the Heterogeneity of Steel Ingots. Iron and Steel Institute, London.
2. G. N. Lewis and M. Randall; Thermodynamics, 238.
3. S. Epstein: Alloys of Iron and Carbon, 1.

4. R. Ruer and R. Klesper: *Ferrum* (1914) **11**, 257.
5. J. L. Haughton and M. L. Becker: *Jnl.* Iron and Steel Inst. (1930) **121**, 315.
6. M. L. V. Gayler: *Jnl.* Iron and Steel Inst. (1933) **128**, 293.
7. Tritton and Hanson: *Jnl.* Iron and Steel Inst. (1924) **110**, 96.
8. K. Friedrich: *Metallurgie* (1910) **7**, 257.
9. J. L. Haughton: *Jnl.* Iron and Steel Inst. (1927) **115**, 417.
10. J. Chipman and C. R. Fon Dersmith: *Trans.* A.I.M.E. (1937) **125**, 370.
11. K. C. McCutcheon and J. Chipman: *Trans.* A.I.M.E. (1938) **131**, 206.
12. T. S. Washburn and J. H. Nead: *Trans.* A.I.M.E. (1937) **125**, 378.
13. T. Swinden: Seventh Report on Heterogeneity of Steel Ingots. Iron and Steel Inst. (1937) 15.
14. J. W. Halley and T. S. Washburn: *Trans.* A.I.M.E. (1938) **131**, 195.

DISCUSSION

(*C. H. Herty, Jr., presiding*)

A. HULTGREN* AND G. PHRAGMÉN,† Stockholm, Sweden.—The mode of solidification and the pattern of segregation of rimming-steel ingots, compared with those of the better understood killed-steel ingots, present several peculiarities for which the correct explanations are not obvious or agreed upon. Having made an attempt to elucidate this subject ourselves,[15] we welcome the authors' interesting paper. One of us would also like to acknowledge the pleasant discussion he has had with them.

In our study of the primary structure and segregation of rimming-steel ingots of a range of compositions we have arrived at conclusions of which part agree with and part differ from those reached by Hayes and Chipman. The latter will form the main subject of this discussion.

Hayes and Chipman rightly stress the importance of stirring and of entrapment of mother liquor for the distribution of alloy elements in the solid and liquid during rimming. Their mathematical treatment of the limiting case of perfect mixing in the liquid and absence of diffusion in the solid is very interesting. The difference between the distribution in the rim zone thus calculated and the actual one gives the amount of entrapment. In our study we have treated the same problem qualitatively, using a tentative ternary equilibrium diagram Fe-C-O.

The authors assume two possible mechanisms of entrapment. According to the first one, under condition of quiet freezing and solidification much more rapid than diffusion, as in a killed-steel ingot, the concentration of an element in the liquid film adjacent to the advancing interface is thought to "continue to build up until the solid that is forming has the same composition as the bulk of the liquid from which it is formed" (p. 115). In the example chosen, the sulphur content of the solid would become 0.020 per cent, that of the liquid film 0.40 per cent. We find it difficult to visualize such a mechanism of solidification, for the following reasons: The temperature at the interface, as a result of the high alloy content, would be considerably lower than the liquidus temperature of the unchanged liquid. In consequence, the liquid layer immediately beyond the enriched film would rather start to form a new growth of crystals, unless the temperature gradient across the thin film were very steep. By the way, that mechanism, applied to dendritic growth, has been assumed to account for the formation of free crystals in a killed-steel ingot at a depth where solidification

---

* Professor of Metallography, K. Tekniska Hogskolan.

† Metallografiska Institutet.

[15] *Jernkontorets Ann.* (1938) **122**, 377. A revised translation appears in this volume, beginning on page 133.

is overtaken by diffusion in the liquid.[16]   On the other hand, as far as we know, all killed-steel ingots investigated have had a dendritic structure (except for the cases of globular structure in the interior).   The authors' second mechanism of entrapment (residual liquid being caught in the spaces between the growing crystals) would therefore apply.

In rimming-steel ingots a dendritic structure is sometimes visible near the surface, extending to varying depth, but often lines originating from temporary blowhole seats, sometimes with attached small segregate lines, are the only structure visible in the main part of the rim zone.   Nevertheless, there is, in our opinion, no reason to doubt the dendritic growth, but the dendrites are probably disturbed in their growth by the passing liquid and therefore shorter.[17]   In the inner region of the rim zone, we have often found indications of small free crystals formed in the liquid and caught by the growing rim zone.   We have also found deformation segregate lines even in the outer half of the rim zone, which, we believe, prove that small pools of mother liquor were still present in this portion when the top had closed and the interior pressure had risen considerably.   Of course, these conditions are largely governed by the composition of the steel; i.e., its freezing range.

In the discussion of Fig. 28, it is suggested that the two branches of the entrapment curve in the rim zone might represent the two different types of entrapment mentioned. For the reasons given above we question the validity of this tentative conclusion and would rather suggest the possibility that during the solidification of the inner portion of the rim zone the proportion of suspended crystals being attached to the growing wall is gradually increasing, the entrapment of the liquid between those crystals being thus facilitated.

Like the authors, we believe that during freezing the solid just crystallized is very nearly in equilibrium with the adjacent liquid layer.   Therefore their statement (p. 86) that the concentration of the solid will be greater than its equilibrium value seems to require explanation.

The authors suggest (p. 112) that the longitudinal segregation always found in rimming-steel ingots occurs because part of the enriched liquid film near the interface is carried upward at a rate not rapid enough to cause complete mixing in the liquid. This is probably true when the alloy contents in the rim zone increase toward the top, but it is not invariably so.   As Figs. 8 to 10 show, the minimum value for copper in the rim zone decreases toward the top.   For manganese, the minimum value also decreases; for sulphur, it remains constant.   The opposing factor probably is the increasing velocity of the current as it rises from bottom to top and its consequent increasing efficiency in removing the enriched film.

It is assumed (p. 111) that as rimming goes on the carbon and oxygen contents of the liquid decrease and therefore gas evolution will finally cease.   The crystallization of solid, by itself, will cause an increase in the carbon and oxygen contents of the liquid, thus continually making it oversaturated with respect to the gas equilibrium. Therefore gas will be evolved along with the crystallization, the composition of the liquid as a result changing gradually along the line on the liquidus surface where the gas equilibrium surface at the prevailing pressure intersects the former.   Thus, a liquid of higher carbon content will change toward higher carbon and lower oxygen, a liquid of lower carbon content toward lower carbon and higher oxygen.   For an intermediate "balanced" composition there will be no change in carbon and oxygen during rimming.   These conclusions apply to liquid steel from the beginning in equilibrium with gas.   If it is oversaturated the gas evolution during the early stage of freezing will probably bring the composition to the equilibrium line where it should

---

[16] *Jnl.* Iron and Steel Inst. (1916) **94**, 181; (1929) **120**, 96.
[17] Compare *Jnl.* Iron and Steel Inst. (1929) **120**, 106.

stay during rimming. For one atmosphere this line represents a constant product of percentage of carbon and oxygen in solution in the liquid, approximately 0.0025. We venture to suggest, therefore, that the mother liquor will not lose its gas-evolving power anywhere at the interface as long as the pressure remains unchanged; i.e., until the pressure rises after the top is closed.

A rim hole, according to our belief, continues to grow as long as gas is evolved, and the stirring action of the passing current is not strong enough to completely remove the bubble protruding from it. When rim holes cease to grow before the top is closed, it is probably not due to discontinuance of gas evolution, but rather to an increased "scrubbing" action by the liquid, possibly owing to the free crystals swept along with it. In fact, we have observed structures that indicate that the inner end of a rim hole, the bubble, has been dislodged. If the authors have evidence to prove that gas evolution ceases before the top of the ingot is closed, we should appreciate having their theoretical explanation of such a phenomenon.

From the contents of carbon and oxygen given in Table 3 their product at various stages may be calculated. Taking account of the oxygen removed out of solution by the aluminum added, it is seen that the steel, on casting, was somewhat oversaturated with respect to the gas reaction at a pressure of one atmosphere. After $\frac{1}{4}$ min., it was practically saturated; after 10 min., the product was as low as 0.0017. The deficit probably is due to the presence in the sample of free crystals low in carbon and oxygen.

As to the carbon and oxygen distribution in the rim zone (Figs. 11 to 13) the low values near the surface in the bottom cut are peculiar, and perhaps connected with the turbulence in casting this part of the ingot. The minimum values for both elements and of the product carbon by oxygen decrease somewhat toward the top. This may be due both to the decreasing hydrostatic pressure and to the increasing stirring action toward the top.

In the distribution curves for the central region, both copper, manganese, sulphur and carbon increase toward the top. Although the rising liquid film during the later part of rimming, as suggested by the authors, may have caused some accumulation of the elements in the top portion of the interior, we believe that sedimentation of suspended crystals after circulation has slowed down owing to suppressed gas evolution is largely responsible for this longitudinal segregation. Otherwise, it is difficult to see how carbon could take part in it. This phenomenon is also well known in killed-steel ingots. The fact that oxygen does not change from bottom to top may be explained as the result of two opposing tendencies: sedimentation of crystals and oxide inclusions being carried down with them.

It follows that we do not believe that the curves A, B, C and D (Figs. 23 to 25) represent the composition during rimming of the liquid metal in the interior at different levels. Particularly the carbon diagram (Fig. 24) seems impossible. There might rather be a decrease of carbon toward the top on account of the hydrostatic pressure. The product of carbon and oxygen in the interior as indicated at A (Figs. 24 and 26) is 0.0008; i.e., a fraction of the equilibrium value for liquid steel at the total pressure of this point. If it is assumed that the carbon content of the interior on closing of the top is represented on an average by the value for B, the product becomes 0.0011, which is also much less than the equilibrium value. The conclusion, it seems to us, must be that a considerable number of crystals were present in the interior mass when gas evolution ceased.

R. S. ARCHER,* Chicago, Ill.—In a paper by McCutcheon and Chipman (ref. 11) the following statement was made: "The calculated pressures are sufficient to evolve
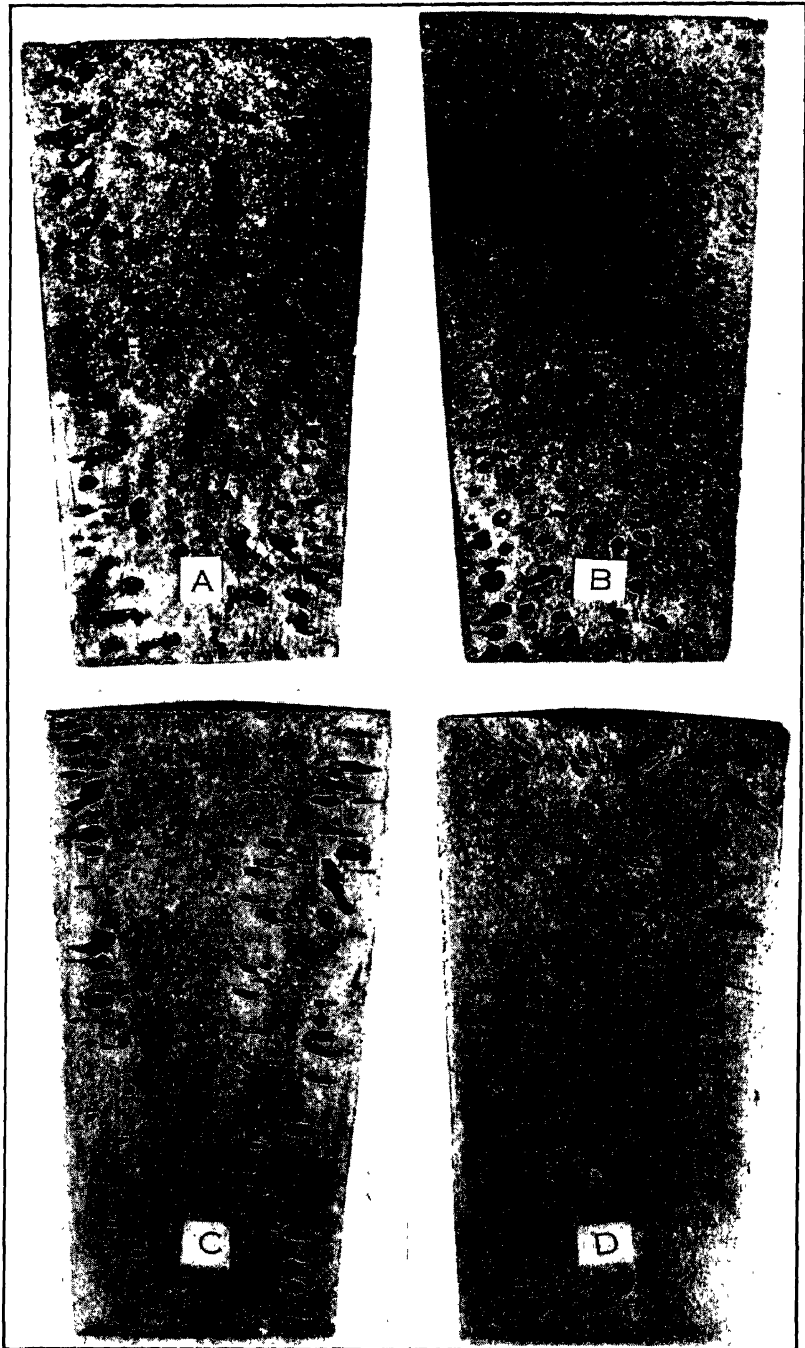

FIG. 31.—For caption see opposite page.

gas under a considerable ferrostatic head. A pressure of 1.4 atmospheres total would correspond to a depth of about 24 in. below the surface of the ingot. This does not mean that no gas can be evolved at a greater depth or that evolution could be suppressed by applying a pressure of 1.4 atmospheres. If evolution were momentarily stopped the carbon and oxygen content of the liquid metal would rapidly increase on account of segregation, so that the gas pressure would soon overcome the external pressure. This is doubtless exactly what happens in the lower half of the ingot; the gas cannot evolve until the carbon and oxygen percentages have been built up to such amounts that the gas pressure exceeds the sum of the atmospheric and ferrostatic pressures. This occurs only in highly localized positions between the rapidly growing crystals of the solidifying wall, and the result is a honeycomb of long, narrow blowholes. In the upper portion of the ingot, where the gas pressure exceeds the sum of atmospheric and ferrostatic pressure, free evolution of gas occurs and no blowholes are formed, the gas evolution being fast enough to sweep off any bubbles adhering to the solid wall." (Ref. 11, p. 223.)

This statement seems to imply that the honeycomb blowholes in the lower part of the ingot will be farther from the surface of the ingot, the lower the carbon-oxygen product. The authors suggest that gas begins to form when the carbon-oxygen product has been built up by local segregation to such a value that the ferrostatic pressure is exceeded. From this it might be concluded that the honeycomb blowholes in the lower part of the ingot could be caused to form at a greater depth by increasing the deoxidation in the lower part of the ingot, thereby causing a greater time to be required for local segregation to raise the carbon-oxygen product to a value that would permit the evolution of gas. This conclusion seems to be at variance with some practical experience, so I should like to ask Dr. Chipman whether I have correctly interpreted the views that were expressed in his previous paper.

A. J. DORNBLATT,* Washington, D. C.—Some results obtained by C. W. Briggs† and H. F. Taylor,‡ who, at the writer's suggestion, have been studying the effects of adding silver to iron, are worthy of note because of their possible bearing on the solidification and segregation characteristics of low-carbon rimming steel as well as for the unexpected and as yet unexplained effect of small silver additions.

Briggs and Taylor made two series of melts, using a small induction furnace. In the first series, 0.05 and 0.50 per cent of silver were added to Armco iron. In view of an indication that silver had reduced the tendency of the ingots to exhibit "rimming" and had reduced the blowhole porosity of the metal in some manner, a second series was made up from 64 lb. of metal, and duplicate 8-lb. ingots were then cast successively, with no silver addition and with additions of 0.025 per cent, 0.050 and 0.25 per cent of silver. The silver was added as a silver-manganese alloy containing 17.9 per cent manganese.

* American Silver Producers' Research Project.
† C. W. Briggs, Steel Founders' Society of America, Cleveland, Ohio.
‡ H. F. Taylor, Division of Physical Metallurgy, Naval Research Laboratory, Washington, D. C.

FIG. 31.—INGOTS OF ARMCO IRON, SHOWING INFLUENCE OF SILVER ADDITIONS.

Ingot	Silver Added, Per Cent	Silver Retained, Per Cent	Ingot	Silver Added, Per Cent	Silver Retained, Per Cent
A	None		C	0.050	0.004
B	0.025	0.007	D	0.250	0.061

On the first series metallic silver was used, and the silver retained in each ingot was 0.002 per cent. Fig. 31 shows the apparent effect of silver additions in the second series of ingots. Each ingot has been sectioned through its middle in the vertical plane, and the reduced blowhole porosity in the ingots representing portions of the melt with the larger silver additions is quite evident. The ingots are identified as follows:

The analyses for silver were obtained through the courtesy of the U. S. Metals Refining Co. It is considered unlikely that if mechanically entrapped silver were excluded silver by analysis would have exceeded 0.01 per cent in ingot D.

While additional work along these lines has been planned, at the moment no satisfactory explanation can be offered for the apparent effect of very small silver additions to reduce blowholes and for the "rimming" tendency in the low-carbon steel (Armco iron) in question.

T. S. WASHBURN,* Indiana Harbor, Ind.—Because of the difficulty in determining the distribution of oxygen between manganese and iron, it was not possible for the authors to consider the effect of this factor on rimming action and ingot structure. There are indications, however, that this relation is important and accounts for some of the variations observed in the rimming action and ingot structure of different types of steel; i.e.:

On ingot iron with low manganese, most of the oxygen is in the form of FeO, which is more reactive than MnO. There is also more total oxygen present, therefore the concentration of FeO builds up rapidly at the liquid-solid interface and the reaction between FeO and C starts immediately and results in a vigorous gas evolution throughout the rimming period. This type of gas evolution apparently results in a condition where the gas is freed readily at the surface of the solidifying metal and is not entrapped to form blowholes. At the other extreme of the rimming series is the high-carbon high-manganese type. In this grade there is less total oxygen present and more of it is present in the form of MnO. Under these conditions, a sufficient concentration of FeO (or the still higher concentration of MnO necessary to develop a reaction with C) is not formed as soon or as rapidly at the interface, and the delayed and more sluggish gas evolution is associated with entrapment of some of the gas in the form of blowholes.

The type of distribution curve in the rim zone shown by Hayes and Chipman differs from those previously reported by Halley and Washburn.[18] This may be because the former covered a longer period, the ingots being allowed to rim past their normal capping time with a consequent entrapment (?) of impurities at the interface—resulting in increasing the concentration in the solidifying metal in the earlier stages of forming the rim zone.

We believe that the uniform distribution shown in the core zone at the top is not representative—there will normally be an increase at the center.

A. HAYES AND J. CHIPMAN (authors' reply).—We accept gladly a number of the suggestions made by Professor Hultgren and Professor Phragmén, and will attempt to present here our answers to the objections they have raised to several of our hypotheses. We have the greatest admiration for their work on the same subject, and feel that an acceptable theory of segregation will result from the two methods of attack.

Messrs. Hultgren and Phragmén find it difficult to visualize a mechanism of entrapment of impurities by solidification from an enriched film, for the reason that the purer liquid beyond the film "would rather start to form a new growth of crystals unless the temperature gradient across the thin film were very steep." During the

* Metallurgist, Inland Steel Co.
[18] *Trans.* A.I.M.E. (1938) **131**, 195.

early stages of solidification there is an enormous flow of heat across this interface, which could not occur in the absence of a steep temperature gradient. In later stages of rimming, when solidification is slower, it becomes possible for individual crystals to form within the liquid by transferring their heat of crystallization through the film by virtue of this gradient. Indeed, the existence of the enriched film seems a necessary part of the mechanism for the formation of free crystals. It may be added that the computed film composition in the case cited is a limiting value probably not approached in a rimming ingot.

A clearer statement than the one referred to on page 86 would be: "For this reason, the concentration of the solid will be greater than that corresponding to equilibrium with the bulk of the liquid."

The decrease in alloy content at the minimum point of the rim zone toward the top of the ingot must certainly be ascribed to the more rapid stirring at the top. The fact that this decrease is less pronounced with sulphur, which has a higher segregating tendency than copper or manganese, could be interpreted as substantial evidence for the proposed explanation of longitudinal segregation. Since sulphur increases in the enriched film to a much greater extent than either copper or manganese, a greater increase in the liquid portion is likewise to be expected toward the top of the ingot. The effect of this upon the minimum concentration of sulphur in the solid apparently offsets the effect of increased stirring.

No one who has watched the solidification of a rimming ingot would suggest that gas evolution ceases before the top of the ingot is closed. The invitation to present a theoretical explanation of such a nonexistent phenomenon must, therefore, be declined. It should be pointed out that limited amounts of gas may be formed from a liquid whose over-all composition is less than that corresponding to equilibrium provided that solidification is occurring at such a rate that an enriched film is produced. Such gas formation is very different in its stirring effect from the free evolution of large volumes of gas during the earlier stages of rim formation.

The changes in composition of the liquid interior portion of eight ingots during the rimming period were reported by McCutcheon and Chipman (ref. 11). In agreement with theoretical considerations presented by Hultgren and Phragmén (ref. 15), ingots that were low in carbon showed a decrease in this element and an increase in oxygen. A liquid of high carbon content (above about 0.06 per cent) tended toward higher carbon and lower oxygen. The carbon-oxygen product was about 0.0028 when the mold was filled, and decreased to an average of 0.0022 during 10 min. The ingot used in this study of segregation decreased to 0.0019 (not 0.0017), which was considered acceptable agreement with the average of the group. The value 0.0022 corresponds to equilibrium at a *total* pressure of one atmosphere. It is thus unnecessary to postulate the existence of free crystals in the liquid 10 min. after the ingot is teemed.

We accept, however, the conclusion that a considerable number of crystals were present in the interior mass when gas evolution ceased. The curves of Figs. 23 to 26 must be interpreted as the average composition of the liquid and the free crystals and not as that of the liquid phase itself. Although this admission will probably not increase the critics' belief in the shapes of the curves, it must be pointed out that these are not so fanciful as might have been supposed. Consider the curves for sulphur (Fig. 23) after the lapse of 12 min., when the solidified rim is 3 in. thick. According to Fig. 21, curve F (average of seven ingots), the sulphur content in the top portion has increased 35 per cent; i.e., it is now 0.025 per cent. The total weight of sulphur in the solidified portion is, according to Table 5, 0.8 lb. The total sulphur in the entire ingot by the ladle analysis is 2.2 lb. Accordingly, 1.4 lb. of sulphur remains in the 6680 lb. of unsolidified interior, or an average of 0.021 per cent. Even allowing for some uncertainties in the calculation, it is clear that the average composition of the interior is definitely lower than that at the surface.

It would be futile at this time to attempt to decide which of the two now recognized causes of longitudinal segregation is the more important.   It seems to us that there is convincing evidence that crystal sedimentation and enriched film flotation both occur during the later stages of the rimming period, and that when gas evolution ceases the distribution of impurities throughout the mass of metal is substantially that found by dissecting the finished ingot.

The section of a former paper to which Mr. Archer refers is an attempt to explain the formation of rim holes in only the lower portion of the ingot.   That this attempt falls far short of completeness must be freely admitted.   The formation of a sound skin appears to be associated with rapid evolution of gas, and the honeycomb blowholes should be farther from the surface when the carbon-oxygen product is higher.   Rim holes form when the rate of gas evolution falls below the rate that is favorable to the formation of sound metal, and this decrease in rate occurs first in the lower part of the ingot.   That it is only a decrease in rate, and not a cessation of evolution, is ascribed to the presence of excess carbon and oxygen at the interface, as mentioned in the paragraph quoted.   We regret that the wording of this paragraph seemed to imply that gas evolution ceased, even momentarily, during the early stages of rimming, and we thank Mr. Archer for bringing this to our attention.   More recently, the mechanism of rim-hole formation has been greatly clarified by Hultgren and Phragmén, who have shown that under some conditions blowholes begin to form even in the soundest parts of the ingot, and are subsequently refilled with metal.

We concur with Mr. Washburn's remarks, except in one point.   It is difficult to see why their earlier capping of the ingot would have affected the concentration of the solidifying metal in the earlier stages of forming the rim zone.   The difference in capping time, however, explains the more abrupt rise in concentration which Halley and Washburn found between the rim and core zones.

We wish to emphasize one viewpoint that may not have received sufficient emphasis in the paper: i.e., that our experimental work was confined to one ingot size and to a relatively small number of types of rimming steel; segregation studies were based on a single rimmed ingot.   It would be unwise to generalize too broadly on this basis. There is much work yet to be done on the mechanism of segregation.   Refinements in experimental technic are needed.   Methods for sampling liquid metal in the bottom part of the solidifying ingot and for measuring temperature at various points during solidification would contribute valuable information.   Further studies along these lines, coupled with the application of the extremely valuable metallographic methods of Hultgren and Phragmén, can be depended upon to remove a few more of the mysteries that are still associated with the production of high-quality rimmed ingots.

.

Solidification of Rimming-steel Ingots

BY A. HULTGREN,* MEMBER A.I.M.E., AND G. PHRAGMÉN†

CONTENTS

IN 1934, Jernkontoret (The Swedish Ironmasters' Association) appointed a committee for the study of the structure of rimming-steel ingots and the various phenomena associated with their solidification. The members of the committee, including those who have joined it later, have been: I. Bohm, B. D. Enlund, B. Kalling, M. Tigerschiöld, S. Wohlfahrt and the authors. The present paper‡ is a somewhat

---

* Professor of Metallography, K. Tekniska Hogskolan, Stockholm, Sweden.

† Metallografiska Institutet, Stockholm, Sweden.

revised translation of a report that appeared in Swedish in *Jernkontorets Annaler*, Vol. 122 (1938), pages 377–465. The paper is based on the experience and observations of the whole committee.

OUTLINE OF PROGRESS OF KNOWLEDGE AND THEORIES ABOUT GAS EVOLUTION IN STEEL INGOTS, AND ITS INFLUENCE ON CRYSTALLIZATION AND SEGREGATION

In spite of the rather large space that is necessary, the authors have thought it advisable to extend the review of previous research far into the past. Some of the old publications contain ideas that have not received the attention they really deserved. Other publications have influenced general opinion in a decisive way up to the present time, more attention having been paid to the conclusions than to their uncertain experimental foundation.

The gas evolution causing blowholes in steel ingots and castings has been known as long as crucible steelmaking. When the Bessemer process came into common use the trouble caused by gas evolution during solidification was more apparent, as the major part of Bessemer steel was of low carbon content and there was no possibility of "dead-melting." One of the first methods tried for the elimination of blowholes was solidification under a high pressure. Bessemer patented hydraulic compression of incompletely solidified ingots as early as 1856. Gaseous pressure on the still liquid ingot top has also been tried (ref. 7;* 27, p. 157, compare also ref. 137).

In 1862 Bessemer exhibited perfectly sound steel ingots and castings obtained by the addition of liquid pig iron with high silicon content just before casting.[1,2] Bessemer[4] stated in 1877 that he had arrived at this conclusion by analyzing "well-melted" crucible steel that was known to form sound ingots. Gauthier,[3] in 1877, explained the effect of silicon by the assumption that silicon was oxidized preferentially to carbon, as was known from the Bessemer process, thereby preventing the formation of carbon monoxide.

In 1878 F. C. G. Müller[5] published a paper on the chemistry of the Bessemer process. He had made the very important discovery that more silicon would be left in the liquid metal at a certain stage of carbon removal if the temperature were high. The chemical affinity was assumed to be a function of temperature and the ferrous oxide to be dissolved in the liquid steel, just as carbon, manganese and silicon.

In 1879 Müller[6] published a paper on gas present in solid steel. Holes were drilled in small ingots under water. Large quantities of gas were collected, containing 65 to 90 per cent hydrogen, 10 to 30 per cent nitrogen and 0 to 2.5 per cent carbon monoxide. Müller was astonished

---

* References are at the end of the paper.

at first and thought that the hydrogen must originate in the water. When the drilling was repeated under rape oil, however, he obtained the same result and became convinced that the gas had been present in the steel. Gas was obtained in large amounts not only from honeycombed steel but also from sound steel and from cast iron.

In a following paper Müller pointed out the analogy between the evolution of gas on solidification of steel and the well-known expulsion of oxygen when silver was solidifying. That the cause of the gas evolution was a lower solubility in the solid than in the liquid was particularly evident when water saturated with air was freezing and ice "ingots" might contain elongated blowholes very similar to those present in many steel ingots. The influence of silicon was denied, being "an absurdity from a scientific point of view." The soundness of specimens cast before the end of the eruption period of the Bessemer blow was explained by the assumption that the carbon monoxide (and the nitrogen) promoted the escape of hydrogen in the same way that a current of air would remove bromine or ammonia from a water solution.

Müller's hydrogen theory was not accepted without opposition. Bessemer[10] reported an experiment he had made many years earlier. Pig iron was melted and decarburized in a crucible. The hot crucible was put into a vessel that could be evacuated. When the pressure was lowered gas was given off, and when it was increased the gas evolution stopped again. The gas was shown by analysis to be carbon monoxide.

Walrand[12] made the important observation that a crust without blowholes would solidify when the gas evolution was rapid, if only the gas bubbles were swept away by the boiling motion in the liquid steel. When the top of the ingot solidified, gas evolution was prevented by increasing pressure and the motion in the liquid came to an end. The gas bubbles next to the solid steel would now adhere, forming a zone of blowholes. Gas bubbles further inside the ingot might rise in the still fluid steel, joining and forming a cavity under the solid top crust.

Walrand assumed the mold gas to be carbon monoxide, forming by reaction between carbon and ferrous oxide dissolved in the molten steel. He supposed the oxygen content to increase when the carbon content decreased, thus explaining the observation that the thickness of the sound crust also increased in this case. The disappearance of the blowholes after sufficient additions of silicon was verified (additions of manganese only had no effect), and could easily be explained by the assumption that the silicon combined with the oxygen, thereby preventing the formation of carbon monoxide. In his opinion, an influence of silicon on hydrogen was not conceivable. Moreover, Walrand had repeated Müller's drilling experiments, using mercury to exclude the air, but he had not been able to find any gas. Similar views were expressed by Pourcel.[13] Richards,[14] repeating the drilling experiments again under mercury, found

very small amounts of gas, compared with those obtained with the same metal under water.

Müller[15] did not, however, give up the hydrogen theory. The blow-hole-preventing action of silicon was accepted, and was explained by the assumption that silicon increased the solvent power of solid steel for gases, especially hydrogen. The hydrogen was supposed to be thrown out within the steel already solidified, penetrating to the boundary between solid and liquid and forming round bubbles adhering to the solid wall. The solidification would proceed between the bubbles and at the same time more hydrogen would accumulate in the bubbles, causing them to expand in the only possible direction—into the liquid—thus becoming elongated or tubular. Similar blowholes had been observed on freezing of water, which also had the power of dissolving gases.

At the same time C. A. Caspersson[16,17] published a paper on the influence of heat in the Bessemer blow on the nature of the ingots. The soundness of the ingots was found to increase with increasing temperature and carbon content. Steel with medium carbon content blown at a very high temperature would solidify into ingots without blowholes. If the temperature was somewhat lower, the ingots would be honeycombed externally, and the steel would rise in the mold during solidification. If the temperature was still some steps lower, the ingots would have, however, a sound crust and blowholes in the center. Hard steel should be blown at a high temperature, as blowholes in the ingots might not weld up completely. Mild steel ingots could not be made completely sound and the type with solid crust and internal blowholes should be aimed at, the external blowholes causing "roaks" in the end product. The paper by Caspersson is probably the first one in which it is clearly indicated that good steel ingots may be divided into two classes: sound ingots and ingots with sound crust and blowholes in the center; that is, what are now called rimming-steel ingots.

It should be mentioned that Müller[3] calculated the gas pressure in the blowholes at the solidification temperature, obtaining values up to 40 atmospheres. He did not extend the calculation to steel without blowholes, from which similar gas quantities had been obtained. Ledebur,[18,36] accepting Müller's pressure values, concluded that hydrogen must have accumulated in the blowholes after the complete solidification, and during the cooling of the ingot. This conclusion obviously followed from the conviction that the molten steel could not resist such a high pressure.

In a paper published in 1883, Müller[22] modified the hydrogen theory once more. He had a large number of analyses made on mold gas, and was forced to acknowledge that the major constituent of gas from low-carbon steels was carbon monoxide. He then divided the gas evolution into two types: the gas evolution in the completely liquid steel on cooling, causing "spattering" (*Spratzen*) and the gas evolution when the steel

is "rising," caused by the formation of the external elongated blowholes. The spattering was assumed to be caused by carbon monoxide escaping without the formation of blowholes, whereas the rising was assumed to be caused by hydrogen. The addition of silicon would end the formation of carbon monoxide, thus quieting the molten steel. Müller had observed that the addition of silicon could change the solidification from the "spattering" to the "rising" condition. This observation was taken as a confirmation of the hydrogen theory, the quantity of hydrogen left in solution being larger when the quantity of carbon monoxide evolved was smaller. The formation of hydrogen bubbles with very low carbon monoxide content was made conceivable by the assumption, already mentioned, that the hydrogen was thrown out of the solid but still hot steel. At the end of the paper Müller came to the conclusion that the hydrogen blowholes formed entirely within the almost solid steel, the high gas pressure calculated being thus conceivable. He paid no attention to an observation, recorded in the first part of his paper, that when the molten interior of partly solidified ingots of rising steel was poured out, the tubular blowholes were visible as perforations in the solid wall.

Müller's work had a great influence on the current opinion. The hydrogen theory is to be found in many textbooks, and, as will be seen from the following, this theory, up to the present time, is founded largely on the work of Müller.

Müller assumed the carbon monoxide to be evolved from the boundary between solid and liquid, being insoluble in the solid steel. This is really a case of segregation caused by selective solidification. The fact that segregation of dissolved substances should occur in solidifying steel ingots was pointed out by Parry[9] and verified experimentally by Stubbs[11] in 1881. In 1884, Guthrie[25] introduced the term "eutectic" and observed the continuous transition from dissolving to melting, the solubility curve of a solid substance in a liquid being extended to the melting point of the former; that is, the solubility curve was changed into what is now called a "liquidus curve."

The influence of temperature on the gas evolution from open-hearth steel was discussed by Odelstjerna[24] in 1883. He stated that hot steel would at first be quiet in the mold and then "rise," whereas cold steel would boil vigorously during casting, forming "boot-leg" ingots (Walrand used the term *tige de botte*). At intermediate casting temperatures the ingots were found to be comparatively sound. The temperature was estimated from the melting off at the end of iron rods dipped into the steel bath. The use of wet sand on the top crust and a firmly attached cover plate on the mold was stated to be generally used for the prevention of "rising," and molds for bottom-casting with only a small opening in the top were described as being used for the same purpose in England.

The theory that the carbon monoxide evolved from solidifying steel was formed by reaction between carbon and ferrous oxide in solution was rejected by Müller, in spite of the fact that he had previously assumed carbon and ferrous oxide to be dissolved simultaneously in the liquid steel.[5]   Howe (ref 27, p. 139), in 1890, wrote: "It is conceivable that the very act of solidification might cause previously uncombined carbon and oxygen to unite in such a manner that their escape would closely simulate that of a previously dissolved gas.   But it is certainly far more natural to refer the phenomena to an escape from solution." He assumed that hydrogen was the chief component of the gas forming the blowholes (ref. 27, p. 41), carbon monoxide being, however, present in the gas evolved.   The absence of carbon monoxide in the blowholes after cooling down, as observed by Müller, was supposed to be caused by re-absorption.   Howe also discussed rather extensively the segregating on solidification.

In 1892, Styffe[28] described the influence of aluminum additions.   In ingots without additions, from a particular heat of steel containing 0.15 per cent carbon, blowholes were located in a zone about 50 mm. from the surface.   Ingots from the same heat, to which 0.02 per cent aluminum had been added in the mold, were honeycombed externally so as to be completely useless.   Ingots with an addition of 0.04 per cent aluminum were free from blowholes.   Styffe realized that the influence of small aluminum additions was not consistent with the accepted theory that aluminum increases the solvent power of solid steel for hydrogen, but he did not propose any explanation.   The ideas of Walrand[12] about the effect of the boiling motion in the liquid steel were evidently forgotten, in spite of the fact that they had been reprinted in *Jernkontorets Annaler* at a time when Styffe was one of the editors.

In 1893, Pourcel[29] mentioned that segregation in steel ingots could be eliminated by a sufficient addition of aluminum.

In 1896, von Dormus[30] described some observations on the structure of steel rails.   If a cross section was etched, the core was much more attacked than the outer part.   The boundary between the core and the outer part was distinct and often contained traces of blowholes, not completely welded up.   The difference between core and case had been observed earlier, and explained as a result of "compression" of the latter on forging or rolling.[26]   The difference, however, was observed also in axial and transverse sections of ingots and von Dormus concluded that it was due to segregation during the solidification.   Tetmajer[31] verified these observations and found further that the difference was reduced or disappeared if a sufficient quantity of silicon was added to the steel; in this case no blowholes were present.   In the same year Wedding,[32] although one of the early followers of the carbon monoxide theory, published a large textbook, in which only the hydrogen theory was

mentioned. Ruhfus,[33] in 1897, collected mold gas from low-carbon steel, and found that it contained much more carbon monoxide than hydrogen. He also investigated transverse sections from top end blooms, observing an outer zone which was etched more slowly than the core. The contrast was great when the casting temperature was high, and the quantity of gas evolved large. If 0.05 per cent aluminum or 0.2 per cent silicon was added the ingots were quite sound and no segregation was observed. The influence of rising gas bubbles on the movement of segregating substances (supposed to be oxygen compounds only) was discussed.

The influence that small additions of silicon or aluminum might have, causing external honeycombing, was observed again by Brinell and Wahlberg.[34,35] They explained the influence of temperature and carbon content, observed by Caspersson,[16,17] as a secondary effect, the primary effect being the influence on the manganese and silicon content. It was also observed that gas might be evolved during the solidification of a shell free from blowholes, but the influence of motion in the liquid steel was not taken into consideration. The zone of deep-seated blowholes was assumed to form at the moment when the top of the ingot had solidified, and the gas was thus prevented from escaping. The influence of the size of the ingot was noted, a large ingot requiring a higher percentage of manganese and silicon or aluminum in order to have a similar arrangement of blowholes to that of a small ingot under similar conditions. Silicon and aluminum were supposed to act by increasing the solvent power of steel for gases, particularly hydrogen.

A very important contribution was made by Stead[37] in 1905. He had observed the motion in steel without aluminum or other killing additions, continuing a considerable time after the mold had been filled and keeping the top surface molten a longer time than if the steel had been quiescent. It was stated that "the segregate . . . always being thrown off would have a good chance of flowing up the sides to the top, firstly, because the branches of the crystallites would be small, and, secondly, on account of the moving liquid sweeping the rejected segregates from the thickening walls of the ingot."

Howe,[39] in 1906, accepted Stead's views, writing about "the evolution of gas and the violent upward convection currents" and its influence on the "long pine-tree crystals." With reference to the blowholes, it may be mentioned that Howe had observed that the surface tension should have some influence, the gas pressure in a very small bubble being larger than in a larger one. The general shape of an elongated blowhole "of the outer ring" was supposed to be influenced by surface tension and gravity and by "the columnar crystals between which it forms."

In 1907, von Maltitz[40] assumed the formation of carbon monoxide on solidification of steel to be caused by selective solidification. Carbon

and ferrous oxide would accumulate in the still liquid steel, the layers first solidified being purer than the original liquid. When the concentration was sufficient the mutual reaction would start. Hydrogen was assumed to be the major constituent of blowhole gas, and carbon monoxide to have a decided influence on its liberation. It was observed that ingots stripped red hot were often darker in the lower part than in the upper. When such ingots were cut blowholes close to the surface were found in the lower part only.

An investigation of rail-steel ingots and blooms, made at the Watertown Arsenal, was reported by Wheeler[41] in 1910. The ingots and blooms were sectioned axially or transversely, and the sections were polished and etched with iodine, making the primary structure visible. A large number of photographs, showing many interesting details, are reproduced. The steels were of the "semikilled" type, the lower part of the ingots being quite free from blowholes. In the upper part of these ingots an external zone, containing numerous blowholes, was present. No discussion of the primary structure or the blowhole formation was included, but some of the photographs clearly show refilled blowholes and traces of periodical formation and removal of gas bubbles. The investigation of the blooms brought evidence that the blowholes in rail steel would weld up in a rather late stage of rolling.

Wüst and Felser,[42] in 1910, investigated ingots of what is now called rimming steel. The ingots were sectioned axially and transversely. The report contains photographs of polished and etched sections and of sulphur prints according to the method proposed by Baumann[38] in 1906. The existence of an outer case and a less pure core, separated by a row of round or irregular blowholes, was very clearly shown by the sulphur prints. Tubular blowholes were present in the lower part of the outer zone, but not in the upper part. This fact was assumed to be due to slow solidification in the upper part, the mold walls being preheated from the molten steel below. In the part of the outer zone where there were no blowholes, long thin segregate streaks at right angle to the mold wall were shown in the sulphur prints. These segregates were assumed to mark the interstices between the steel crystals, which had grown inward from the surface.

"Blowhole segregation" was observed by Stead[44] who suggested the following explanation. The pressure in the interior of the ingot was supposed to increase successively after the solidification of the top crust. Thereby residual liquid steel with a high content of segregating substances was forced into blowholes that had formed at a lower pressure.

The question whether carbon monoxide is present "as such" when dissolved in liquid steel was discussed, as mentioned, at a rather early time. Walrand[12] and Ledebur[23] had realized that the oxygen content of liquid steel increased when the carbon content decreased. Ledebur,

however, clearly expressed the opinion that, if only the steel were kept fluid for sufficient time, one of the two substances would disappear completely from the solution. The famous paper by Guldberg and Waage on the law of mass action was published in 1867, and printed again in 1879. The influence of temperature on chemical equilibrium was cleared up by van't Hoff in the years 1884 to 1886. The first number of the *Zeitschrift für physikalische Chemie* was published in 1887.

Many years appear to have passed before the theory of equilibria in solutions was applied to the metallurgy of steel. Héroult,[43] in 1910, assumed that carbon and ferrous oxide might be in equilibrium in the liquid steel. If the temperature was increased, the reducing action of carbon was assumed to increase and carbon monoxide to be evolved. If the temperature was lowered nothing would happen until the steel partly solidified, when carbon and oxygen concentrated in the mother liquor would react. He also stated his view that hydrogen and nitrogen were not the cause of blowholes, but accumulated in them during the cooling of the ingot.

A fundamental contribution was made by Le Chatelier[45] in 1912. He indicated how the reaction theory implied that the product of the carbon content and the oxygen content should be proportional to the equilibrium pressure of carbon monoxide, the proportionality coefficient being a function of temperature. The influence of the temperature might be calculated from the heat of reaction and the change of solubility of carbon and oxygen with the temperature. Le Chatelier supposed the change of solubility to have the greater influence, causing the carbon-oxygen product to increase with the temperature. He never mentioned the possibility that some part of the carbon monoxide might be present in solution without being dissociated.

Heyn[48] held the opinion that the gas forming on solidification might pass away if the gas evolution were feeble, but if it were strong blowholes would form in the outer layer of the ingot.

In textbooks by Edwards[49] and Mathesius,[50] published in 1916, only the hydrogen theory is mentioned in the account of the formation of blowholes.

The idea about the effect of motion in the liquid steel on the bubbles adhering to the already solidified wall was revived by Hibbard[51] in 1919. He divided all steels into two classes: noneffervescing or killed, and effervescing. In Hibbard's description of the solidification of an effervescing-steel ingot the term "rim" was used, perhaps for the first time in print. The ingot was said to "rim in" if the top crust grew progressively inward from the mold walls, forming a frame or rim around the still open center of the top surface, from which large quantities of gas were evolved.

Hibbard noted that if the effervescence was too mild, the liquid steel would "rise" in the mold after teeming was finished, the rising being

caused by the formation of blowholes in the solidifying wall. If the volume of gas bubbles in the liquid steel was larger than the volume of the blowholes in the solid steel, the steel would settle in the mold, forming a "boot leg." The ideal case was assumed to be when the top surface was "rimming in" horizontally, neither rising nor settling.

Hibbard, still under the influence of Müller's ideas (but presenting his views as a matter for speculation), assumed the blowholes in the wall solidified during rimming to be caused by hydrogen. If the evolution of carbon monoxide was sufficiently brisk, the hydrogen bubbles would be washed off mechanically by the rising carbon monoxide bubbles, escaping from the open surface of liquid steel. The presence of "skin holes" in the lower part of the ingot only was often observed in axial sections of ingots and might also be seen on an ingot when stripped red hot, as mentioned by von Maltitz earlier, areas with external blowholes becoming black more quickly than the remainder of the ingot. The absence of external blowholes in the upper part of the ingot when such holes were present in the lower part was taken to support the theory of the "washing action" of the carbon monoxide, which should be weaker near the bottom of the ingot.

Deep-seated blowholes, called "intermediate holes," were found in a zone inside the elongated blowholes. Hibbard thought the existence of two separate zones of blowholes in the same ingot to be a fair evidence that they were formed by different gases. The intermediate blowholes were assumed to be caused by carbon monoxide. The blowholes that were distributed irregularly in the core of the ingot were assumed to be caused by nitrogen or ammonia.

A. Johansson, [52] in 1920, recorded the influence of early closing of the ingot. By this procedure the circulation in the still liquid steel was arrested and "the blowhole zone" formed nearer to the ingot surface. The larger core would have a relatively lower content of segregating substances. Blowhole segregation was observed and explained on the assumption of an increasing internal pressure (compare ref. 44). Oberhoffer[53] attributed the blowhole segregation to the lowering of the gas pressure in the blowholes by the decrease in temperature.

The blowhole segregation was found by von Keil and Wimmer[55] to be particularly considerable in the zone of intermediate blowholes.

Hibbard,[54] in 1925, discussed the influence of the temperature of open-hearth steel on the gas evolution on solidification. A rimming steel of ordinary composition would give off less gas when hot than when the temperature was normal; an excessively hot steel would have an "oily appearance" in the mold, and would "rise" because of blowhole formation in the outer zone. Klinger[56] found that mold gas from steel without silicon or aluminum addition (*unberuhigter Stahl*) contained much carbon monoxide, some nitrogen and, at the beginning of solidification,

less than 10 per cent of hydrogen, the hydrogen content increasing at the end of solidification. Peirce,[57] in 1926, accepted the opinions of Hibbard; he used the designation "rimming steel" or "rimmed steel." Reinartz,[58] in the discussion of Peirce's paper, stated as his belief that carbon monoxide caused most of the blowholes, and mentioned overdosing with aluminum as a cause of external blowholes, as exemplified by photographs of split ingots. Feild[59] pointed out that more reliable methods of analysis lead to the conclusion that the hydrogen content of solid steel was very low. He also objected to Hibbard's assumption that ammonia caused the central blowholes, as ammonia was known to decompose at a rather low temperature in the presence of iron. In the same year a new edition of a well-known textbook by Osann[62] was published, in which it was stated that the correct explanation of the formation of blowholes in ingots had been proposed by Müller.

Améen and Willners,[64] in 1928, presented some more evidence on the low hydrogen content in mold gas from steel without quieting additions, particularly during the first stage of the solidification.

A Committee on the Heterogeneity of Steel Ingots, appointed by the British Iron and Steel Institute, presented a report[65] in which, among other things, some ingots of "steels other than killed" were described. The influence of gas evolution on the segregation was discussed. The conclusions were very similar to those expressed by Stead[37] 23 years earlier. The elongated blowholes were assumed to form between columnar crystals. The quieting or even killing action of sulphur in free-cutting steels was stated to be a well-known fact. One example mentioned was that a steel with 0.12 per cent carbon, 0.03 per cent silicon, 0.11 per cent sulphur and 0.10 per cent phosphorus formed completely sound ingots without any aluminum addition.

In an A.I.M.E. round table discussion in 1929, McKune[66] confirmed the low hydrogen content in mold gas from rimming steel. Feild[67] characterized Müller's results as "ill-advised conclusions, which practically killed Bessemer's original idea." Carlin[68] stated that "even at that time it was a question whether or not a heat would rim properly." Hultgren,[69] by subjecting an ingot of killed steel to repeated oscillations around its vertical axis during solidification, produced general segregation effects not unlike those observed in rimming-steel ingots, including a minimum in the carbon content within the outer layer. He concluded that the analogous segregation in rimming-steel ingots was a result of the rapid movement of the liquid metal, caused by rising gas bubbles.

Stadeler and Thiele,[73] in 1931, assumed that the elongated blowholes formed between dendritic crystals growing from the surface inward, thus determining the general shape and position of the blowholes. The caterpillar-like shape (called "lenticular" or "scalloped" by Feild[67]) was supposed to be due to an increase by jerks, caused by the surface tension.

The gas forming these blowholes was believed to be hydrogen.   In the upper part of the ingots, the outer zone contained no blowholes but did contain streaks of segregate (*Seigerungsrinnen*), as found earlier by Wüst and Felser.[42]   The segregate streaks were assumed to be caused by the increase in gas pressure in the ingot when the top crust had solidi-fied, liquid steel having been pressed into previously existing elon-gated blowholes.

Herzog,[79] discussing the paper by Stadeler and Thiele, directed atten-tion to the motion in the still liquid steel in the mold.   The rising gas bubbles, forming at the boundary between solid and liquid, would cause a current in the liquid steel, rising at the wall and descending in the center, as could be observed at the open top surface.   In the upper part of the ingot the current would wash the gas bubbles away from the wall. The segregation streaks in this region would form during solidification, being centers of gas evolution.   It was assumed that the gas evolved from the beginning was carbon monoxide, containing some hydrogen and nitrogen.   Oertel and Schepers[80] assumed a columnar (*transkristalline*) zone in rimming-steel ingots.   They stated that intermediate blowholes (*innerer Blasenkranz*) would disappear after an addition of some hundredths of one per cent of silicon.

Hibbard,[84] in 1932, adhered to his theory of three different gases caus-ing the three different kinds of blowholes.   Eichholz and Mehovar[85] accepted Herzog's view on the formation of blowholes, characterizing the hydrogen theory as improbable.   They also pointed out the influence of slow casting on the outer blowholes, the gas evolution starting under a lower liquid pressure.   The absence of outer blowholes in short ingots, being stated as a well-known fact, was also taken as an evidence in favor of the theory of washing action.   Eichholz and Mehovar held the opinion that the segregate streaks formed between columnar crystals.   The British Ingot Committee[88] assumed that the skin outside the elongated blowholes formed before the beginning of the gas evolution.   Nothing was said about a circulation current in the still liquid metal.   The impuri-ties expelled from the crystallizing steel were supposed to attach them-selves to the surface of the bubbles and thus to be carried upward, in the same manner as in the process of mineral flotation.   It was questioned whether or not ferrous oxide segregates.   No satisfying explanation of the phenomena associated with rimming-steel ingots was regarded as estab-lished.   The term "rim" was used to designate the outer case or crust, and this changed meaning is met with in a number of later publications.

S. Caspersson and K. Johansson[91] investigated the structure of an ingot of steel with 0.05 per cent carbon.   In the outer zone blowholes were present in the lower part only.   In etched axial sections they observed streaks or rows of small pits in parts of the outer zone where no blowholes were present.   The streaks extended from the ingot surface

to the intermediate blowholes. As they were not observed on the unetched sections (which were, however, not polished) it might have been supposed that they were caused by dissolution of segregation streaks. From X-ray shadow pictures it was evident, however, that they were real streaks of porosity. It was suggested that the pores might be remnants of blowholes.

In 1933, the Ingot Committee[94] presented a general description of different types of steel ingots. *Rimming-steel ingots* might be of three types: *box-hat ingots, true rimming-steel ingots* and *rising-steel ingots.* Next to the rising-steel ingots came the *semikilled steel ingots,* made of steel of the rimming type by addition of aluminum or some aluminum alloy when the teeming was almost completed. *Balanced-steel ingots* were defined as ingots with superficial blowholes in the upper part only, and widely distributed blowholes in the head (the schematic section of this type was in discordance with the description, having elongated outer blowholes in the lower part of the ingot only).

This committee report also contained a paper by Edwards and Jones,[95] on the influence of aluminum additions to steel with high oxygen content. Five laboratory melts of Armco iron were made in clay crucibles. To each melt was added 0.2 per cent oxygen as iron oxide, and after that some quantity of cast iron to obtain the carbon content desired. From each melt a number of small ingots were cast, to which successively increasing amounts of aluminum were added. These laboratory ingots showed several features characteristic of ordinary ingots of rimming steels. With no additions of aluminum, or very low additions, box-hat ingots were obtained if the carbon content was not too low or too high. These ingots had a sound outer case or "rim." When the aluminum addition was increased the ingot type changed, successively, into a type with sound rim zone and little or no settling in the mold, a type with blowholes in the rim and rising of the liquid steel in the mold, and finally sound piped ingots.

In the discussion of the Committee report Benedicks[96] put forth the theory of different gases causing the outer and inner zone of blowholes by a "double evolution of gas."

The explanation of the limited thickness of the rim zone is simple from the "washing action" point of view: the rimming action is checked after some time. The cause of this was thought to be that the interior of the ingot became "semipasty"[51] or "mushy" (ref. 65, p. 484). It had been suggested by Walrand[12] that the gas evolution and motion in the liquid interior of an ingot would come to an end when the top crust was completely closed and that a zone of blowholes would mark this moment (compare refs. 34 and 35). The same idea had been presented by Johansson,[52] who also had described the use of early closing in practical steelmaking and its influence on segregation.

These ideas seem, however, not to have attracted much attention until they were set forth again by Nead and Washburn,[98] who clearly explained the influence of the closing of the ingot top. They also observed that not only the rim zone but also the core might contain considerably less carbon than the liquid steel before casting. In one heat the carbon content was 0.097 per cent; the average carbon content in the rim zone was 0.040 per cent, and in the core 0.064 per cent. It was further observed that in "thick-skinned" ingots the "skin" outside the elongated blowholes increased in thickness from the bottom end upward.

Egler and Tatman[99] described the method of shaking or jarring the molds in the vertical direction during the rimming period. This method had been used in regular production and was stated to promote the removal of blowholes in the rim zone. Herzog[100] made some experiments with a similar method but was not able to begin the jarring before the solidification of a top crust; otherwise liquid steel would splash over. He observed marked zones of segregation in rimming-steel ingots as well as in killed-steel ingots, treated in that way.

Kalling[101] found by calculation that the carbon-oxygen reaction product should increase a little with increasing temperature. Fleming[102] put forth some observations on the manufacture of rimming steel. The influence of Müller's ideas is evident in Fleming's statement that aluminum "in some mysterious way increases the solubility of entrapped gases in the steel." Geiger[103] directed attention to the simultaneous loss of carbon and oxygen during solidification. One heat contained 0.07 per cent carbon, 0.048 per cent oxygen and 0.37 per cent manganese. The rim of a billet held 0.04 to 0.05 per cent carbon and 0.015–0.020 per cent oxygen; the core 0.07 per cent carbon and 0.04 to 0.05 per cent oxygen. The average for the billet would be 0.055 per cent carbon and about 0.03 per cent oxygen. It was not mentioned at what height in the ingot the billet was taken.

Meyer[104] investigated the segregation in some rimming-steel ingots. The variation in composition was represented by a three-dimensional diagram, the base plane of which was the axial section of the ingot. In a transverse section the composition was taken as constant within the rim zone, changing discontinuously at the boundary toward the core and then remaining constant within the core. Thus, the average composition of the rim zone and that of the core were represented as functions of the height in the ingot.

The influence of slow casting on the thickness of the skin outside the outer blowholes was discussed by H. Schenck (ref. 106, p. 257) on the basis of the observations by Eichholz and Mehovar.[85] The skin was supposed to solidify under gas evolution, like the upper part of the rim zone in normal ingots. Schenck presented, however, also a contrary theory (ref. 106, p. 244), according to which a high oxygen content in

the liquid steel would cause an early evolution of gas and a thin skin. He further discussed the influence of manganese (ref. 106, p. 242) on the evolution of carbon monoxide. His explanation will be illustrated here through one of his examples. The liquid steel was assumed to contain 0.1 per cent carbon and 0.7 per cent manganese. When solidification began, carbon, oxygen and manganese would accumulate in the still liquid steel. This would cause evolution of carbon monoxide, lowering the carbon content and, relatively much more, the oxygen content. The manganese content in the liquid was assumed to increase so much that manganese oxide would crystallize at some later stage, causing the oxygen content of the liquid to decrease so rapidly that the formation of carbon monoxide was arrested. At the manganese content mentioned, 0.7 per cent, the core of the ingot was assumed to solidify without gas evolution, even if the pressure was only one atmosphere.

In 1935, Edwards[108] accepted the theory of the sweeping action of "the rising stream of small bubbles." He also held the view that "rimming is caused by chilling or supercooling effects disturbing the conditions of equilibrium and causing abnormal segregation, thus forcing the reaction of oxide and carbon to take place."

Swinden and Stevenson[109] expressed the view that the "skin holes" in rimming steel were due essentially to a gas coming out of solution (either hydrogen or carbon monoxide), while the "interior holes" were a result of the FeO + C reaction. Andrew and Trent[110] observed "V-shaped markings," which were thought "to be due to blowholes refilled by molten metal." Edwards, Higgins, Alexander and Davis[111] concluded from laboratory experiments that "the gaseous products were evolved in at least two stages—a 'primary' and a 'secondary' evolution." The rimming phenomenon was supposed "practically to terminate when dendritic crystallization ends."

Hatfield[113] held the opinion that "rimming steel would be found definitely to be explained by a consideration of the allotropic modifications of iron which are deposited from the liquid solutions." He assumed one case of marked segregation observed in low-carbon steel to be caused by the coexistence of two concentrations of solution in the liquid steel.

In 1936, Jackson[115] suggested the method of killing the core of a rimming-steel ingot after the solidification of the rim zone. Danforth[117] proposed the addition of sodium fluoride in the mold, stating that it improved the rimming action of the steel and therefore the structure of the ingot.

The gas evolution from liquid steel was discussed by Chipman and Samarin[120] in 1937. From the viewpoint of physical chemistry they concluded that the evolution of hydrogen and carbon monoxide separately was impossible. The hydrogen content of an ordinary heat was

known by analysis to be only about 0.15 of the saturating value at one atmosphere. The partial pressure of hydrogen, being proportional to the square of its concentration, would be only 0.02 atmospheres. The accumulation in the interfacial film would increase the hydrogen content in the gas evolved somewhat, perhaps to 5 per cent. A similar result was obtained for nitrogen. It was found theoretically that the carbon-oxygen product should increase somewhat with rising temperature.

Washburn and Nead[122] presented some new experimental results, supporting the conclusion that the secondary blowholes formed at the moment when the ingot top was closed. Carbon monoxide was supposed to be the cause of the outer blowholes as well as of the intermediate and the core holes. In the discussion Herty[123] said that the presence of a sound layer between the outer and the intermediate blowholes was difficult to explain. Reinartz[124] mentioned the series of lines across the primary blowholes, which might be explained by the assumption that the gas "came off in surges." Hibbard[126] adhered to the hydrogen theory and also objected to the use of the term "rim" for the whole of the solid outer shell, as it had originally been used only for the top of this shell.

Swinden[127] studied the variation of composition from the outside to the center at the half height of a 4.5-ton ingot of low-carbon steel. This investigation was carried out with great precision, the number of samples analyzed being large. Thus, it was found that the content of carbon, sulphur, phosphorus and manganese varied considerably in the rim zone. The curve representing the carbon content began at 0.065 per cent at the surface, passed a minimum at 0.04 per cent, rose to a peak at 0.08 per cent in the zone of intermediate blowholes, and wavered a little around 0.07 per cent in the core. The sulphur and phosphorus curves were similar, the distances from the surface to the minimum points differing somewhat from that for the carbon curve.

Halley and Washburn,[133] in 1938, described the distribution of carbon, manganese and sulphur in a "normal ingot," using perspective diagrams similar to those used by Meyer.[104] Halley and Washburn took account of the change in composition from surface to center, the diagrams being, however, rather schematic.

The review of more recent publications has been condensed very much, as they are easily accessible, and of course, this prevents full justice to the authors of these publications. The review has been restricted to ideas or statements of general importance for understanding the process of solidification, gas evolution and segregation.

OBJECT OF PRESENT INVESTIGATION

Although, as seen from the preceding review, the main features of the solidification process of rimming steel were known, certain phe-

nomena associated with it were little understood, such as the freedom from blowholes in the surface layer outside the elongated blowholes, the similar conditions in the zone between the blowholes mentioned and the intermediate holes, and the relation between the elongated blowholes and the so-called columnar crystals. In discussing the gas evolution and the effect of various alloying elements on solidification, the laws of physical chemistry had not always been considered.

In earlier investigations the solidification structure of the rim zone had not been studied in sufficient detail, obviously owing to etching difficulties. By a special preparation and etching process, it has been possible to bring out the detail of this structure fairly well in most of the ingots examined. The information thus obtained has served as a basis for an explanation of the solidification process of the rim zone and the gas evolution in that zone. Under intentionally changed conditions the effects of special variables has been studied. General segregation, blowhole segregates, irregular cavities near the axis of the ingot and certain deformation phenomena have also been discussed.

To facilitate the theoretical discussion, we have put together a partial equilibrium diagram for the system Fe-C-O, in which liquid steel in equilibrium with a gas phase containing CO and CO_2 is represented by a surface, just as equilibrium with a condensed phase is represented. On the basis of this diagram the solidification of pure Fe-C-O alloys has been discussed, and then the influence of manganese, sulphur and phosphorus. For the construction of the equilibrium diagram and the deductions made from it a number of assumptions have been made that we believe to be correct in principle but necessarily are qualitative only. But even a merely hypothetical diagram may be useful as a guide in discovering the essential variables.

After a section dealing with theory in a schematic way, follows a section giving the experimental results and observations. Finally a general discussion of the solidification process combining theory and observations is presented.

Because of the small size of the ingots studied (maximum 700 kg.), and their limited number, some caution should be exercised in trying to apply our conclusions to actual conditions that may differ from those of the present investigation.

THEORETICAL DISCUSSION OF PROCESS OF SOLIDIFICATION

GAS GIVEN OFF FROM RIMMING STEEL DURING SOLIDIFICATION

The peculiarities of rimming steel, as compared with killed steel, are due to the fact that a large quantity of gas is evolved during solidification. The major constituent of this gas is carbon monoxide, as has been well known for more than half a century.[10,22,33,56,64,103] Hydrogen,

nitrogen and carbon dioxide are present in varying amounts. The quantity of carbon dioxide depends on the carbon (and oxygen) content of the steel. Hydrogen and nitrogen diffuse into the liquid steel from the furnace gases or the converter blast, and it is thus obvious that their concentrations must be lower than if the steel were saturated with one of these gases at atmospheric pressure. The evolution of carbon monoxide during the working of the heat causes other gases to be washed out.[8,120] The decrease of the temperature of the liquid steel from working temperature to solidification temperature, perhaps 150° C., will cause an increase in the relative hydrogen saturation of only about 10 per cent. It will be shown later that this drop in temperature does not cause any great change in the carbon monoxide "saturation." In full agreement with these conclusions are some experimental results recently published[135] as well as some results obtained in connection with the present investigation, according to which the hydrogen content of the mold gas from a number of normal rimming-steel heats was less than 10 per cent.

If somehow a hydrogen-gas bubble were introduced into liquid steel giving off a mold gas with such a low hydrogen content, this bubble would rapidly take up carbon monoxide (ref. 27, p. 137) and approach the equilibrium composition.[120] Thus, it appears as though the only course left to maintain the old theory of hydrogen as the cause of the elongated blowholes in the outer zone of rimming-steel ingots[6,8,9,15,27,32,49,50,51,62,77,78,82,84,88,96,126,140] is to assume the hydrogen to separate under such conditions that it is not in contact with the large mass of circulating liquid steel in the interior of the ingot. Müller may have been aware of this; anyhow, in a later paper[22] he assumed the elongated blowholes to form within the solid or almost solid outer crust (compare ref. 27, p. 126). The assumption that these blowholes are due to gas trapped between growing dendrites (for instance ref. 125) also suggests the evolution of this gas at a late stage of solidification. The evolution, at this stage, of gas rich in hydrogen might be possible if the solubility of hydrogen in the liquid steel were much larger than the "solubility" of carbon monoxide. A low-carbon steel saturated with hydrogen will, however, give off only about one cubic centimeter S.T.P. of hydrogen per cubic centimeter steel, when solidifying under equilibrium conditions. A steel with, for instance, 0.1 per cent carbon will contain about 0.025 per cent oxygen, as will be discussed later, and this oxygen quantity corresponds to about 2 c.c. S.T.P. of carbon monoxide.

Hence, it does not appear probable that the gas evolved when the last parts of the residual liquid between the dendrite branches solidify should have a high hydrogen content. It is true that the evolution of carbon monoxide may be suppressed to a relatively high degree (p. 218); but probably the hydrogen evolution is affected in a similar way. Further, and this is more important, it may be concluded from the structure

of the rim zone that the elongated blowholes form from bubbles having a comparatively large surface in contact with the circulating liquid steel.

The presence of a "secondary skin"[140] between the rim holes and the intermediate holes (see, for example, Fig. 18) has been taken as evidence that these two kinds of blowholes are caused by different gases[51] or a "double evolution of gas"[96,111] (compare ref. 123). It has also been assumed[109] that the rim holes were due to "gas coming out of solution," while the interior holes were "a result of the iron-oxide carbon reaction." This assumption is very improbable; it is known that the chemical reactions in liquid steel proceed very rapidly,[93] and also that the quantity of carbon monoxide dissolved "as such" is small compared with the total oxygen or carbon content. It has further been assumed that hydrogen and oxygen would react, the water vapor formed causing blowholes.[88] It has been shown experimentally, however, that the H_2O pressure is much lower than the H_2 pressure, even if the steel is saturated with FeO.[120]

The following observations are not compatible with the theory of a "double gas evolution." In the "secondary skin" traces of refilled blowholes have been observed (Figs. 41, 43). The rim holes may extend to the boundary between rim zone and core in the bottom part of the ingot, particularly if the steel has a tendency to rise; at the same time the rim holes may be separate from actual intermediate holes at a higher level (Figs. 19, 40, 42). After early closing of the ingot top the rim holes also extend through the rim zone, and the intermediate holes in the upper part of the ingot have obviously formed simultaneously with the inner ends of the rimholes (Fig. 35).

Thus, there seems to be no reason for accepting hydrogen as the cause of rim holes. Of course, hydrogen blowholes may be present in *killed* steels (compare ref. 109). In this connection an old theory of Ledebur[18,36] should be remembered, according to which hydrogen, diffusing rather rapidly in the solid but still hot steel, may accumulate in blowholes already formed. It is now known that the hydrogen solubility in solid steel is rather high at high temperatures and decreases rapidly when the temperature is lowered. That is, the relative saturation increases and also the equilibrium pressure.

### EQUILIBRIUM DIAGRAM OF THE IRON-CARBON-OXYGEN ALLOYS

According to the views just presented, the process of solidification of rimming-steel ingots is influenced in a decisive way by the evolution of gas, the major constituent of which is carbon monoxide. The understanding of this solidification process will be facilitated by the construction of an equilibrium diagram which, of course, is directly applicable only to a ternary alloy system. Thus, the discussion will at first be limited to pure iron-carbon-oxygen alloys.

The carbon content of rimming steels is comparatively low.   In this range of composition the one-phase space. of liquid steel is limited by four surfaces, representing equilibria with a gas phase, a liquid oxide phase, δ iron, and γ iron.   From the shape of these surfaces and their intersection curves the solidification process in the ideal case of equilibrium may be deduced.

Is the carbon monoxide dissolved "as such" in liquid steel or is it formed by reaction between carbon (or some carbide) and oxygen (or some oxide) when the steel is solidifying?   As mentioned before, this question was discussed by Howe (ref. 27, p. 122), who was not able to arrive at a final conclusion (compare also ref. 119).   Le Chatelier[45] accepted the reaction theory, without any experimental evidence.   As a consequence of this theory he found that the product of the carbon and the oxygen content should be independent of the composition and proportional to the carbon monoxide pressure.   Herty[73] as well as Vacher and Hamilton[76] confirmed this conclusion by different experimental methods, the carbon-oxygen product being 0.0025 at 1600° C. if the contents were expressed in weight per cent.

Thus it is evident that the content of carbon monoxide dissolved as such in liquid steel is small against the total content of oxygen or carbon (ref. 83, p. 129).   Experiments have also been made with the purpose of solving this question in a different way, the steel being dissolved in water solutions; for instance, a solution of mercury chloride.   Even if the solidification of the steel did not change the equilibrium conditions entirely, the possibility of secondary reactions on dissolving makes such experiments inconclusive (compare ref. 111, p. 209).

The influence of temperature on this equilibrium has often been discussed.   The question may be put thus: If a quantity of liquid steel is in equilibrium with carbon monoxide of a certain pressure at a certain temperature, and the temperature of the steel is then increased, the pressure being constant, will carbon monoxide now be given off from the liquid steel?   This question has generally been answered in the affirmative;[43,74,77,103,111,119,136] it has been felt as paradoxical that carbon monoxide is evolved during solidification.[68,88,112]   The reaction

$$C + FeO \rightarrow Fe + CO; \quad \Delta H = 35,000 \text{ gcal.}$$
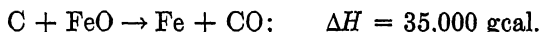
is endothermic, that is, heat is being absorbed and such a reaction is, as well known, promoted by an increase in temperature.
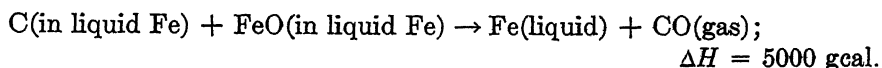
This conclusion is in itself correct.   The equilibrium pressure over a mixture of solid carbon and free ferrous oxide increases rapidly with temperature.   We wish, however, to calculate the change in the carbon monoxide pressure of liquid steel of *constant* composition.   The solubility of carbon and oxygen increases with the temperature; that is, the relative saturation decreases.[45]   The oxygen content at equilibrium

with ferrous oxide increases very rapidly[63,92] and the result of a calculation is that the change of the carbon monoxide pressure with temperature is small (ref. 83, p. 129).

This result may be formulated in another way. From the great increase in the iron oxide solubility may be concluded that the heat of solubility is great (ref. 83, p. 123):

FeO (in oxide phase) → FeO (in liquid Fe); ΔH = 30,000 gcal.
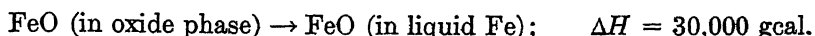
and thus, by subtraction from the reaction formula mentioned before, we obtain:

C(in liquid Fe) + FeO(in liquid Fe) → Fe(liquid) + CO(gas);
$$\Delta H = 5000 \text{ gcal.}$$

In this calculation we have left out the heat of solution of graphite, the correct value of which cannot be calculated from the iron-carbon equilibrium diagram because the liquid steel saturated with graphite is not a dilute solution (ref. 83, p. 125). The oxide phase is liquid at this temperature and its composition is variable and only approximately corresponding to the formula FeO, and the effect of this has not been taken into consideration. Further, the ΔH of the last reaction formula has been obtained as a difference between two comparatively large quantities not accurately known. To sum up, the value given is not very reliable, and the only statement that may be made with safety is that the numerical value of ΔH is much less than 35,000 gcal. It is even uncertain whether ΔH is positive or negative.

An experimental investigation of the carbon-oxygen equilibrium in liquid steel by Kalling and Phragmén (not yet published) was not sufficiently accurate to decide the direction of change when the temperature is increased from 1550° to 1700° C. Thus, for the construction of the ternary equilibrium diagram it has been assumed that the carbon-oxygen product at constant carbon monoxide pressure does not change with the temperature.

The gas phase also contains some carbon dioxide. When the liquid steel is saturated with FeO the gas will contain about 20 per cent CO_2; when the oxygen content of the steel is 0.05 per cent the CO_2 content is about 5 per cent, and decreases when the temperature increases. That is, the gas-equilibrium surface limiting the one-phase space of liquid steel is almost parallel to the temperature axis; the isothermal sections of the surface approach hyperbolas.

Liquid steel with low carbon content may be assumed to be a "dilute solution." As carbon and oxygen are not mutually combined, the actual melting-point lowering is approximately equal to the sum of the lowerings caused by the carbon and oxygen contents separately; that is, the liquidus

surfaces of δ iron and γ iron are approximately plane. It may further be assumed that the oxygen content of liquid steel in equilibrium with the ferrous oxide phase will not be influenced very much by carbon in solution, as long as the solution may be taken as "dilute."

The relative positions of the surfaces limiting the one-phase space of liquid steel are schematically indicated in Fig. 1. Such a diagram is strictly valid only for a certain pressure. The surfaces representing equilibria without a gas phase are, however, only slightly displaced even by a rather great change in pressure. The gas-equilibrium surface, on the other hand, is displaced very much, the carbon-oxygen product being proportional to the partial pressure of carbon monoxide. Thus, in order to represent approximately the conditions at higher pressures, the surfaces 1 and 2 in Fig. 1 may be extended toward higher carbon content as shown, and the gas-equilibrium surface moved into different positions as the pressure is varied.
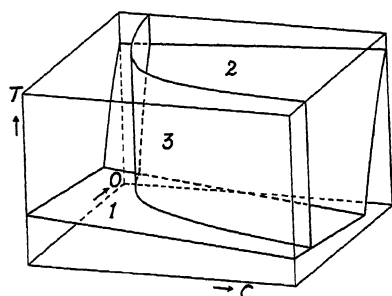
FIG. 1.—PERSPECTIVE SKETCH OF BOUNDARY SURFACES OF LIQUID METAL PHASE.

(1) δ-liquidus, (2) oxide saturation and (3) CO + CO_2-equilibrium surface.

An attempt to represent the quantitative relations in the ternary diagram is given in Fig. 2. To begin with, the binary diagrams Fe-C and Fe-O will be considered. The former may be taken as known, the latter is more uncertain. At temperatures above 1400° C. the oxide phase is liquid; when in equilibrium with steel in the range of temperature discussed here it is, as mentioned, approximately represented by the formula FeO. The oxygen content of liquid steel saturated with FeO is, according to theory, an exponential function of the temperature. If this fact is considered in evaluating the experimental results, a monotectic point at 0.24 per cent oxygen seems to be more probable than at the generally accepted value 0.21 per cent.

For the solubility of oxygen in solid iron, some rather high values, about 0.1 per cent at 1000° C., have been published.[90] From other experiments[81,87] it appears probable that the actual solubility at this temperature is lower than 0.01 per cent. If the heat of solution of FeO in solid iron has as high a value as in liquid iron, the solubility will be some 10 times larger at 1520° than at 1000° C. We have chosen the value of 0.03 per cent for the oxygen content of δ iron at the monotectic temperature but wish to point out that it is *purely hypothetic*.

In Fig. 2 *ABIF* is the liquidus surface of δ iron and *AELH* the corresponding solidus surface. *FIK* is the liquidus surface of γ iron with a corresponding solidus surface *GMN*. The FeO saturation surface of the liquid steel extends from the curve *DB* toward higher carbon content and
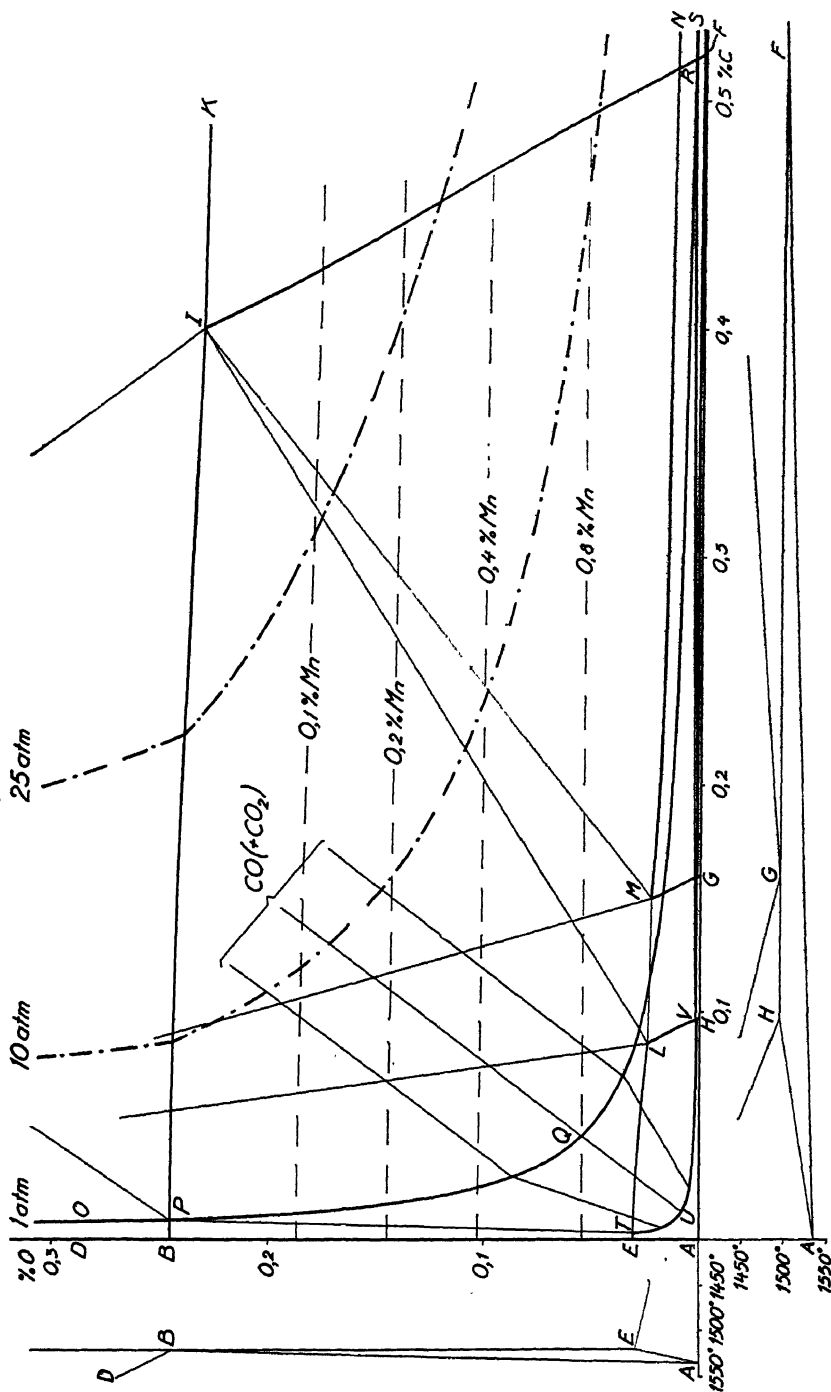
FIG. 2.—TENTATIVE FE-C-O EQUILIBRIUM DIAGRAM, ALSO INDICATING INFLUENCE OF MANGANESE AND PRESSURE.

intersects with the liquidus surfaces along BI and IK. Corresponding FeO saturation surfaces for δ and γ iron extend from the curves EL and MN toward lower temperatures.

The $CO + CO_2$ equilibrium surface for atmospheric pressure and the other boundary surfaces of the one-phase space of liquid steel intersect in the curves OP, PQR and RS. The curve PQR has a temperature maximum in Q. On the solidus surface there is a corresponding curve TUV; the points P and T represent phases in mutual equilibrium, as well as Q and U, R and V.
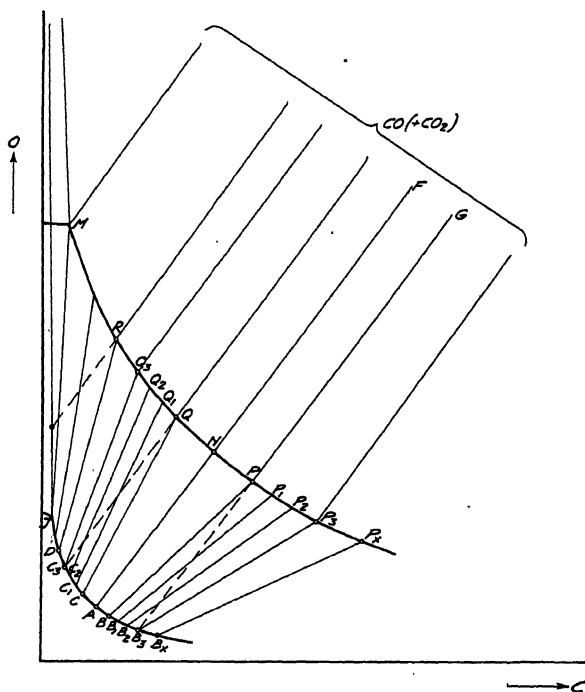
FIG. 3.—SCHEMATIC FREEZING DIAGRAM FOR FREE GAS EVOLUTION.

From the curve TUV a surface extends downward, representing δ iron in equilibrium with $CO + CO_2$ at atmospheric pressure. According to the assumptions made this surface is approximately parallel to the temperature axis. The surfaces extending from the curves EL, MN and TUV toward lower temperatures are useful for the discussion of reactions occurring on cooling between gas enclosed in a blowhole and the surrounding steel; their positions are indicated in Fig. 60 (p. 236).

Fig. 2 also contains two curves, showing the gas equilibrium at 10 and 25 atmospheres. The corresponding curves on the solidus surfaces have been left out, in order to avoid complication.

SOLIDIFICATION OF PURE IRON-CARBON-OXYGEN ALLOYS

In the following examples it is assumed that the liquid metal before solidification is in equilibrium with $CO + CO_2$ gas at atmospheric pressure.

Solidification When Carbon Monoxide Is Given Off at Constant Pressure

Complete Diffusion.—As a first example we assume the liquid to have a composition corresponding to the maximum temperature on the curve *PQR* of Fig. 2. This part of the diagram is seen on a larger scale in Fig. 3. Such a steel will solidify without the liquid phase changing its composition; that is, the point *N* is situated on a straight line between the corresponding point *A* on the solidus surface and the point representing the gas composition in the direction *F*. The temperature is constant during solidification.

As a second example we assume the liquid steel to have the composition, represented by point *P*, at a higher carbon content than point *N*. The solid steel that separates at first will have a composition represented by *B*. There is an angle between the lines *PG* and *PB*, and the composition of the liquid will change toward higher carbon and lower oxygen content along the curve $PP_1P_2P_3$, the composition of the δ iron meanwhile changing from *B* to B_3, which is situated on the extension of the line *GP*. If the change of the gas phase can be neglected, there will be nothing left of the liquid, that is, the solidification range is PP_3.

As a third example, we assume the liquid to have the composition *Q*, at a lower carbon content than point *N*. During solidification the carbon content of the liquid phase decreases and the oxygen content increases and at the end of solidification the solid steel has the composition represented by C_3.

As a last example, we assume the liquid steel to have a very low carbon content, *R* in Fig. 3. The composition of the liquid phase changes until the point *M* is reached. At this point separation of δ iron, gas and FeO-phase will take place at constant temperature, and the solidified steel will contain a quantity of liquid oxide.

These examples show that liquid steel of the composition represented by *N* is distinguished by the property that its composition does not change during solidification at a pressure of one atmosphere. We will designate this composition as the "balanced composition," remarking that it should not be confused with the composition of "balanced-steel ingots." Liquid steel with higher carbon content will have its carbon content increased during solidification, whereas liquid steel with lower carbon content will have it decreased.

Incomplete Diffusion in Solid Phase.—At other compositions than the balanced one the change in composition of the liquid during solidification

will be greater than if equalizing by diffusion is complete. For instance, the liquid P of the preceding example will not stop at P_3 but proceed to P_z of Fig. 3.

Solidification When Gas Evolution Is Suppressed

We assume that the pressure is high enough to prevent the evolution of carbon monoxide. From a liquid steel corresponding to Q in Fig. 4, δ iron corresponding to C will solidify. While the temperature falls the composition of the liquid phase changes along QQ_1, and that of the δ iron along CC_1. In the figure it is assumed that C_1 and Q_1 are situated on the straight line CQ and its extension, but this is no essential assumption. When the points Q_1 and C_1 are reached, δ iron and oxide phase will

FIG. 4.—SCHEMATIC FREEZING DIAGRAM FOR SUPPRESSED GAS EVOLUTION.

separate at the same time. The composition of the liquid is then represented by some point on the line Q_1Q_2, that of the δ iron by C_1C_2. If the composition within each phase is equalized by diffusion, the solidification will be complete when the δ iron reaches the point C_2 on the extension of a straight line from the oxide-phase composition point to point Q. The composition of the last liquid is represented by Q_2. If the composition is not completely equalized the composition of the last liquid present and the last δ iron crystallizing will be represented, for instance, by Q_3 and C_3. If the carbon content of the mother liquor is high enough, say as a result of incomplete equalizing by diffusion, the liquid steel may reach the composition I in Fig. 2, where γ iron will form.

The lowest pressure that is sufficient to prevent gas evolution depends on the composition of the liquid, and may be seen at once if a sufficient number of isobaric curves are constructed in the diagram. The pressure increases all the time during solidification.

It seems probable that the gas evolution can be suppressed by very rapid solidification, through some kind of undercooling. It may be

supposed that the conditions of rapid solidification are similar to those prevailing at a high pressure.

Schematic Application on the Solidification of Rimming-steel Ingots

If, as a first approximation, the rim zone of a rimming-steel ingot is assumed to solidify under free gas evolution, and the core without any

FIG. 5.—SCHEMATIC DIAGRAM: FREEZING OF RIM ZONE AND CORE, HIGHER CARBON CONTENT.

gas evolution, the diagrams shown in Figs. 5 and 6 will illustrate the solidification process. Two typical compositions, one with higher and one with lower carbon content than the balanced composition, are con-
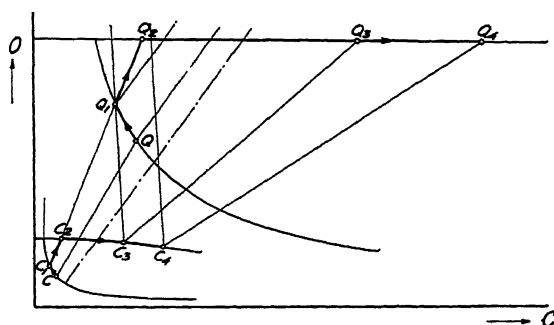
FIG. 6.—SCHEMATIC DIAGRAM: FREEZING OF RIM ZONE AND CORE, LOWER CARBON CONTENT.

sidered. The diagrams are self-explanatory. It is assumed that there is no reaction between rim zone and core, while the latter is solidifying. P_3 and Q_3 represent the composition of the liquid at the end of solidification under the assumption that the composition of the core is completely equalized, P_4 and Q_4 indicate imperfect equalizing.

In an actual ingot the gradual shrinking during the freezing of the core will allow the evolution of a correspondingly increasing volume of gas. This gas evolution, however, will change the composition of the liquid steel relatively little. If the blowhole volume is assumed to be 10 per cent of the steel volume and the gas pressure is assumed to be 10

atmospheres, the sum of the changes in carbon and oxygen contents will be only 0.003 per cent. Thus, the influence of the gas accumulation in blowholes on the gas pressure will be small.

The quantity of gas evolved during the rimming period will have a strong influence on the solidification process and the resulting structure. The gas quantity depends on the composition of the steel and for the idealized solidification process discussed here it may be estimated by means of the diagram. A liquid steel P (Fig. 3) solidifies with a composition B_3. The weight ratio of gas evolved to steel solidified is equal to the length ratio of PB_3 and PG, the latter being extended to the representative point of the gas phase. This extended line is long as compared with PB_3; that is, the relative variation of its length may be neglected. Thus the gas quantity is proportional to the intercept between the two curves on a line approximately parallel to NA, and it will have its greatest value for a composition not very far from N. Indeed, it is obvious that the evolution of carbon monoxide must be small at very low oxygen content as well as at very low carbon content.

INFLUENCE OF MANGANESE, SULPHUR AND PHOSPHORUS

Manganese is usually present in considerable amounts in rimming steel. It has an important influence on the solidification process because of its relatively large affinity for oxygen. The equilibrium between iron-manganese alloys and mixtures of FeO and MnO has been investigated by Körber and Oelsen.[92] The oxygen content of the liquid metal, when in equilibrium with the slag phase mentioned, is a function of the manganese content, just as it is a function of the carbon content when the metal is in equilibrium with carbon monoxide. One difference is that the composition of the oxide phase changes rather rapidly, and thus the product of the manganese and oxygen contents is far from constant. When the manganese content is higher than 0.34 per cent, the oxide phase that is in equilibrium at the same time with solid and liquid metal is solid. The equilibria observed are in full accordance with the assumption that manganese is not combined with oxygen in the liquid steel; that is, manganous oxide may be stated to be "insoluble as such" in liquid steel.

We must then consider the possibility of the formation of chemical compounds of manganese, carbon and oxygen when they coexist in solution in liquid steel. It was found by Körber and Oelsen[114] that addition of carbon, in amounts up to 0.5 per cent, to liquid iron, containing manganese and silicon in solution, did not change the equilibrium between the manganese and the silicon and a silicate slag phase. Of course, a high content of carbon will change the equilibrium conditions very much, the liquid metal being in this case no "dilute solution." The manganese-silicon equilibrium in dilute solution was also found to be in accordance with the assumption that no compound of silicon and

manganese formed and that the solubility of "silica as such" was extremely low.[97] When the manganese content was increased the conditions became more complicated.[118]

It may be mentioned here that it has been found that the solubility of manganous sulphide "as such" is also very small.[131] Thus, it seems to be a general rule that chemical compounds dissociate almost completely when they dissolve in liquid steel. It has been suggested, as a hypothesis, that this rule might be extended so far that even iron compounds, such as FeO or FeS, are assumed to dissociate when dissolved.[132]

If it is assumed that manganese does not enter into combination with any of the other constituents, when present in dilute solution in liquid steel, a consequence is that in the iron-carbon-oxygen equilibrium diagram only one surface will be changed in a considerable degree. The oxygen solubility surface will move toward lower oxygen contents, and we assume the change practically not to be affected by a low carbon content. When the manganese content increases above 0.34 per cent, the monotectic line corresponding to BI changes into a eutectic one. The approximate positions of this line for some different manganese contents are indicated in Fig. 2.

The liquidus and solidus surfaces of δ iron are lowered by the addition of manganese, but not very much, as the difference between corresponding manganese contents in the liquid and the solid phase is rather small; manganese is known to segregate less than, for instance, carbon. The peritectic intersection line FI of the liquidus surfaces of δ and γ iron may be displaced considerably, as the angle between these surfaces is small.

The influence of manganese on the $CO + CO_2$ equilibrium should also be negligible as long as the liquid steel behaves as a dilute solution.

It should be remembered, when the diagram Fig. 2 is used for the discussion of the solidification of alloys containing manganese, that the manganese content of the liquid will increase a little owing to selective solidification and, when the oxygen solubility surface is reached, it will decrease again on account of the relatively high manganese content of the oxide phase separating from the liquid.

With these precautions, which apply whenever a three-dimensional diagram is to be used for a quaternary alloy, the diagram may be used for an approximate discussion of the influence of manganese on the solidification and particularly on the gas evolution.

In most cases a manganese addition will have no immediate influence on the oxygen content of the liquid steel. The gas evolution during solidification under equilibrium conditions at atmospheric pressure will probably be influenced by ordinary manganese additions only if the carbon content is lower than at the "balanced" composition. Thus, the "rimming action" in ordinary rimming steels, the carbon content of

which is higher than that of the balanced composition, will presumably be affected only in so far that the suppression of the gas evolution because of rapid cooling (p. 218) may be facilitated.

It will, however, have an important effect on the final pressure after the top surface of the ingot has solidified. The discussion of the various cases will be similar to that of pure iron-carbon-oxygen alloys, except that the maximum oxygen content of the liquid phase is lower, and thus the final $CO + CO_2$ pressure lower.

It has been stated as a well-known fact that *sulphur*, in amounts used in free-cutting steels, has a strong killing action.[65,77,110,117]   It has also been stated, as an experience from practical steelmaking, that steel with more than 0.1 per cent sulphur may rim in quite normally.[130]   No ingots with high sulphur content being included in the present investigation, the authors desist from a discussion of this controversial question.   They feel justified in assuming that the low sulphur content of ordinary rimming steel has little influence on the ternary equilibrium diagram, sulphur dissolved in the liquid steel forming no compounds with other solutes.[129,132] There is evidence that a sulphide phase will not separate until at a rather late stage of solidification.[86]   The content of sulphur dioxide in the gas phase will also be negligible; it is possible to melt FeO and FeS together under atmospheric pressure.

Phosphorus has also been supposed to have a quieting effect on rimming steel.   The affinity between phosphorus and oxygen is rather small, as is well known from the Bessemer and the acid open-hearth processes. It is evident that phosphorus will not act as a real deoxidizer in steel. In some experiments made in connection with other research, a deoxidizing effect of phosphorus additions was found to be caused by a considerable content of aluminum and silicon in the phosphorus alloy.

EXPERIMENTAL WORK

LIQUID STEEL AND THE MOLD GAS

The oxygen content of the liquid steel is important for the solidification process.   Indeed, it should be determined before the casting of ingots for investigation.   The sampling for oxygen determination implies, however, difficulties.   When the sample is taken in a slagged test spoon and killed with aluminum, as proposed by Herty et al.,[72] there is risk of absorption of oxygen from the air and from the oxidizing slag in the test spoon.   Schenck et al.[89] used a tubelike test spoon of heat-resisting steel, the opening of which was closed with a thin steel strip, which melted when the test spoon was put down in the liquid steel.   In the tube was placed a piece of aluminum wire.   It is, however, difficult or impossible to prevent some slag from sticking to the thin steel cover, and this slag will be mixed into the sample.

Kalling and Rudberg[116] have proposed the use of a similar apparatus, the opening of which was kept open during immersion by passing nitrogen gas through it. The walls of this "test mold" were made rather thick, in order to make the sample solidify rapidly. Even with this apparatus there is some risk of furnace slag accompanying the steel, and even a small quantity of the oxidizing basic open-hearth slag may cause a considerable positive error in the oxygen value. Some Al_2O_3 might rise to the surface of the sample, particularly if the solidification were slow, thereby causing negative errors.

Oxygen samples from the liquid steel were taken only from one of the heats here discussed (heat F) but, unfortunately, without success. Some similar heats were investigated by students at the Tekniska Högskolan, Stockholm, under the direction of Professor B. Kalling; the details of this investigation will be published later. Samples were taken according to Schenck as well as according to Kalling and Rudberg, and analyzed by vacuum fusion. In view of the aluminum content of 0.3 to 0.5 per cent, a temperature about 1700° C. was used for gas extraction.

It was found that the carbon-oxygen product of steel in the furnace or the ladle was 0.003 to 0.008, the contents being expressed in per cent. Samples were also taken in the mold during the rimming period, at a small depth below the liquid-steel surface. In these samples the carbon-oxygen product was found only slightly to exceed the equilibrium value 0.0025.

The change in composition in the liquid interior part of ingots during rimming was also investigated. It has been pointed out (p. 157) that this change depends on the relation between the actual and the "balanced" composition. From the assumption that the liquidus surface is plane, the value 0.05 per cent is obtained as an approximation of the balanced carbon content at atmospheric pressure. According to the experimental results, the carbon content decreases during rimming if below 0.07 per cent and increases if above 0.09 per cent, indicating a balanced carbon content between these limits. The experimental results are not, however, thought to be sufficient for deciding this question.

In some cases the gas given off from the steel in the mold was collected and analyzed, 80 to 90 per cent being carbon monoxide and the rest hydrogen, nitrogen and carbon dioxide. Of course, the molds were not "washed." As will be shown later (p. 221) it may be concluded from the structure observed in the rim zone that the rate of gas evolution immediately after casting should be greater at low than at high carbon contents. The measuring of the gas evolution in the first part of the rimming period was found, however, to be rather difficult, presumably because of leakage and cooling of the gas in the "dead space" between the liquid steel and the cold cover, and the results obtained do not seem to be reliable.
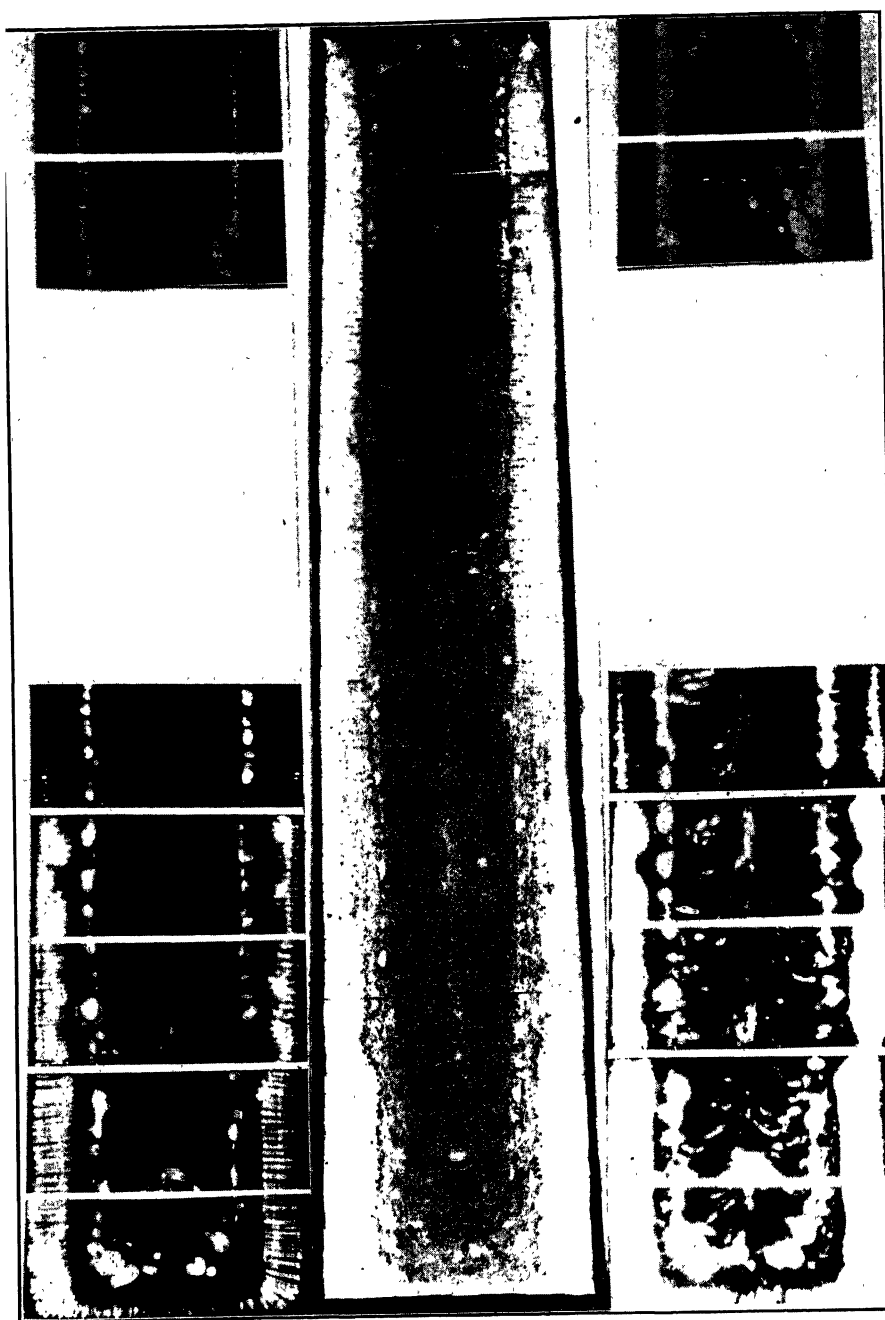
FIG. 7.—INGOT A. C, 0.08; MN, 0.40 PER CENT. × 0.18.
Sulphur print and radiograms. Rim holes terminate on irregular surface. Rim channels in upper part. Symmetrical deformation lines, two sets. Low freezing center.

The influence of the working temperature in the furnace, and that of the casting temperature, are probably very important, as will be discussed later (p. 197).   In the experiments described here the temperature was observed with an optical pyrometer on tapping and casting.   The
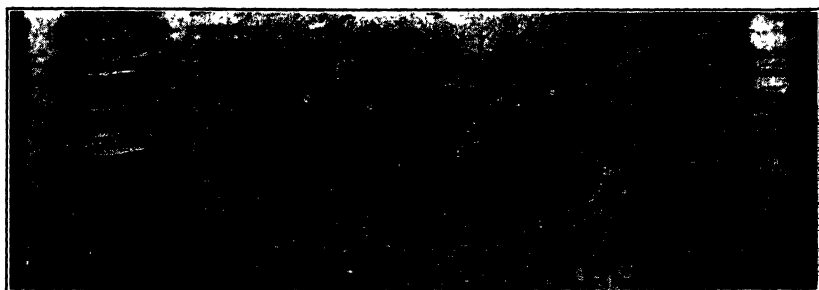
FIG. 8.—INGOT A.   AXIAL SECTION, BOTTOM END.   × 0.5.
Synchronized contractions and expansions in rim holes.   Deformed core holes and hole segregates.   Upset structure in intermediate zone.

results, however, were inconsistent, indicating that the emissivity under those conditions was variable, and they are not included in Table 1.

An investigation of the temperature influence, by the use of other methods for measuring the temperature, is planned in continuation of the present work.

FIG. 9.—INGOT A.   AXIAL SECTION, HALF HEIGHT.   × 0.5.

INGOTS INVESTIGATED AND METHODS USED

The ingots that were investigated were made at the Kallinge and the Nykroppa steelworks.   The main data for the ingots are collected in Table 1.   The very small, bottom-cast ingots A to D contain about 0.08 per cent carbon and 0.4 per cent manganese, whereas the somewhat larger top-cast ingots represent three types of steel: G, about 0.05 per cent carbon and 0.1 per cent manganese; F, H, I, L and M about 0.15 per cent carbon and 0.5 per cent manganese, and K 0.21 per cent carbon and 0.65 per cent manganese.   The analyses given in the table are made on ladle samples, to which some aluminum had been added to quiet the

TABLE 1.—*Data on Ingots*

Ingot	A	B	C	D	F1	F2	F3	G	H	I	K1	K2	K3	K4	K5	N
Ladle sample:																
Per cent C	0.08	0.09	0.08	0.08		0.14		0.046	0.15	0.17			0.21			0.08
Per cent Si						0.009		0.007	0.01	0.01			0.01			
Per cent Mn	0.40	0.53	0.40	0.43		0.47		0.09	0.50	0.60			0.65			0.27
Per cent P	0.011	0.013	0.012	0.014		0.026		0.007	0.027	0.028			0.025			0.015
Per cent S	0.031	0.029	0.035	0.029		0.035		0.025	0.028	0.038			0.022			0.050
Ladle addition, per cent Al						0.0009		0.025					0.0009			
Method of casting		Bottom-cast				Top-cast										Bottom-cast
Time of casting, sec					33	32	37	40					about 30			
Mold addition, per cent Al	0.0065		0.0015		0.0000	0.0015	0.0037	0.003	a		0	0	0	0	c	
Ingot height, cm	92	90	90	88	124	123	133	119	80b	125	129	127	128	131		138
Top width, cm	16	16	16	16	30	30	32	31	30	32	30	30	30	30	30	26
Bottom width, cm	20	20	20	20	25	24	24	25	26	25	25	25	25	25	25	30

a Ore addition during casting.
b Boot leg not included.
c Sulphur addition in the mold, 6 × 0.02 per cent.

steel. There are indications that the aluminum addition was not sufficient to kill some of the samples completely.

The three ingots of heat F constitute a series of increasing aluminum
addition in the mold, F1 being cast without addition, F2 with 0.0015 per
cent and F3 with 0.0037 per cent aluminum added. The last aluminum
addition would combine with 0.0033 per cent oxygen. The oxygen
content of the liquid metal was not determined but is supposed to have
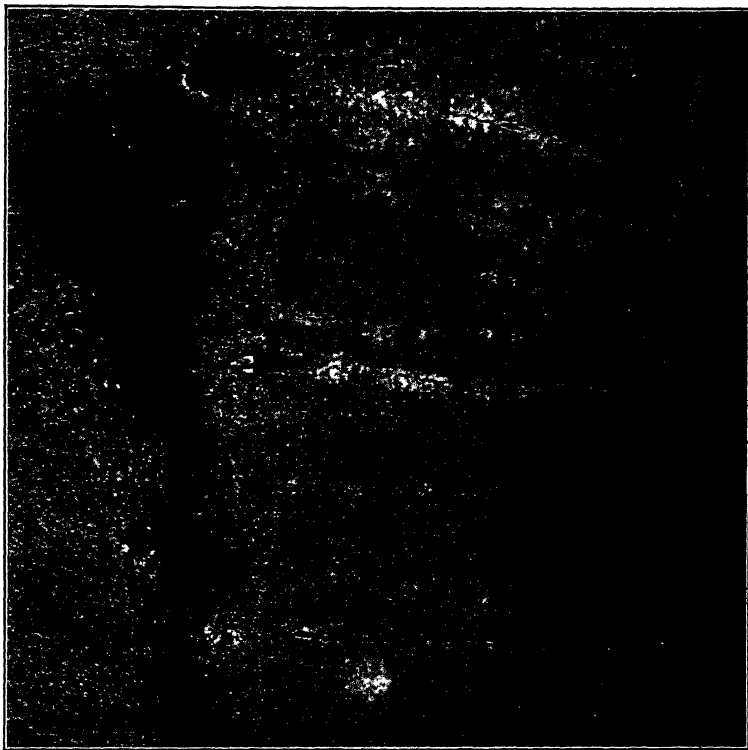
FIG. 10.—INGOT A. RIM ZONE AND PART OF CORE, NEAR TOP. X 2.
Rim channels with arrow segregates and pores. Some channels end visibly in
intermediate holes. Intermediate hole segregate. Primary structure: rim zone fine,
indistinct, core globular.

been something like 0.02 per cent (compare Table 2, p. 192). The great
influence of this relatively small aluminum addition on the formation of
rim holes (Figs. 17, 18, 19) is interesting.

For ingots H, I and four ingots of heat K the conditions of solidification were intentionally varied as follows:

Ingot H. After the mold was half filled, 450 grams (1 lb.) powdered
ore was gradually added. As expected, a "box-hat" or "boot-leg"
ingot was obtained.

Ingot I, during freezing was subjected to repeated oscillations about
its axis, through an angle of 32° 29 times in one minute, the movement
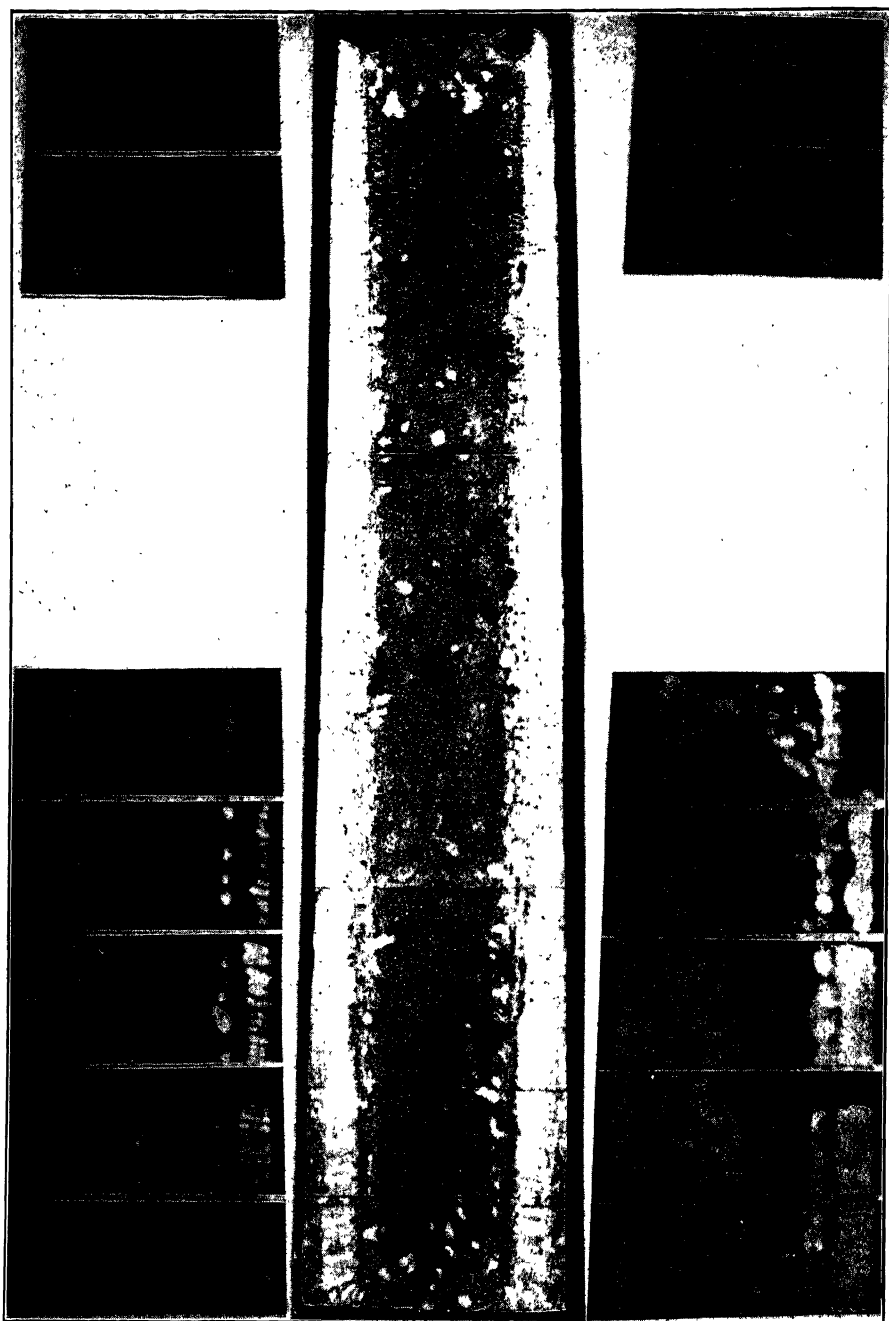
FIG. 11.—INGOT B.   C, 0.09; MN, 0.53 PER CENT.   × 0.18.
Sulphur print and radiograms.   Similar to Fig. 7, but less pronounced deformation lines.

in one direction being stopped by impact. The oscillations began 13 sec. after casting and were discontinued 8 min. later.

FIG. 12.—INGOT B. AXIAL SECTION, BOTTOM END. × 0.5.
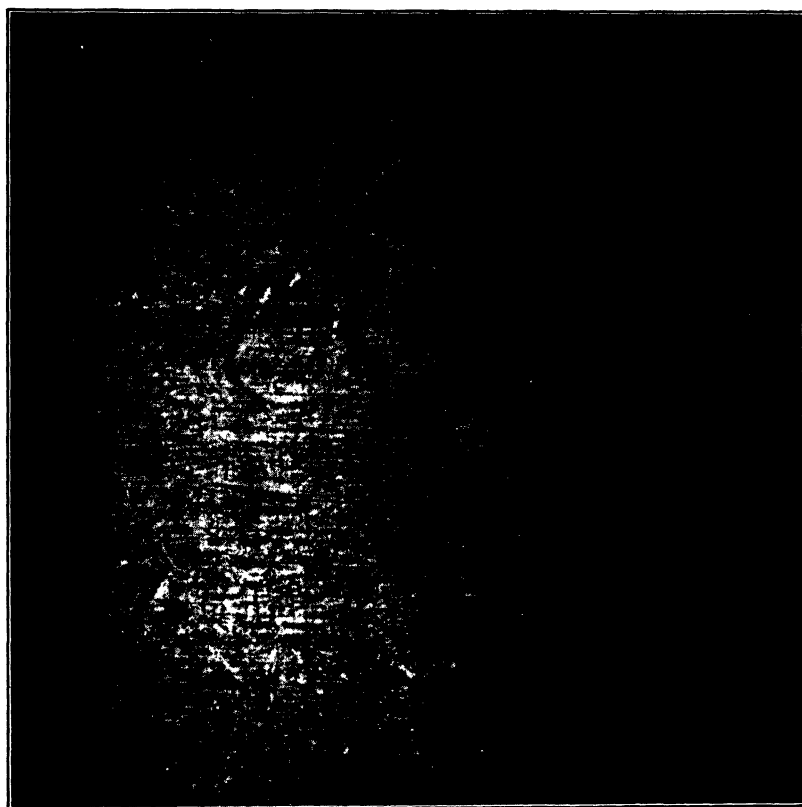
FIG. 13.—INGOT B. SKIN AND RIM HOLES, BOTTOM END. × 4.
Faint dendritic structure and series of hole-contour lines in skin.

*Ingot K*1 was cast into a mold having a special closing device consisting of a fixed cover with a central casting hole into which a plug

was inserted and fastened immediately after casting.   The mold was filled to 20 mm. below the cap but the steel soon rose to the cap and early closing of the top was achieved, although not as early as had been planned.

Ingot K2 was allowed to freeze normally, a cooler plate being laid on the top after the rimming was well advanced.

Ingot K3 was cast into a mold, on which immediately after casting was applied a gastight cover, having a water-cooled outlet pipe for collecting the gases given off during freezing.   These were measured and analyzed from time to time.
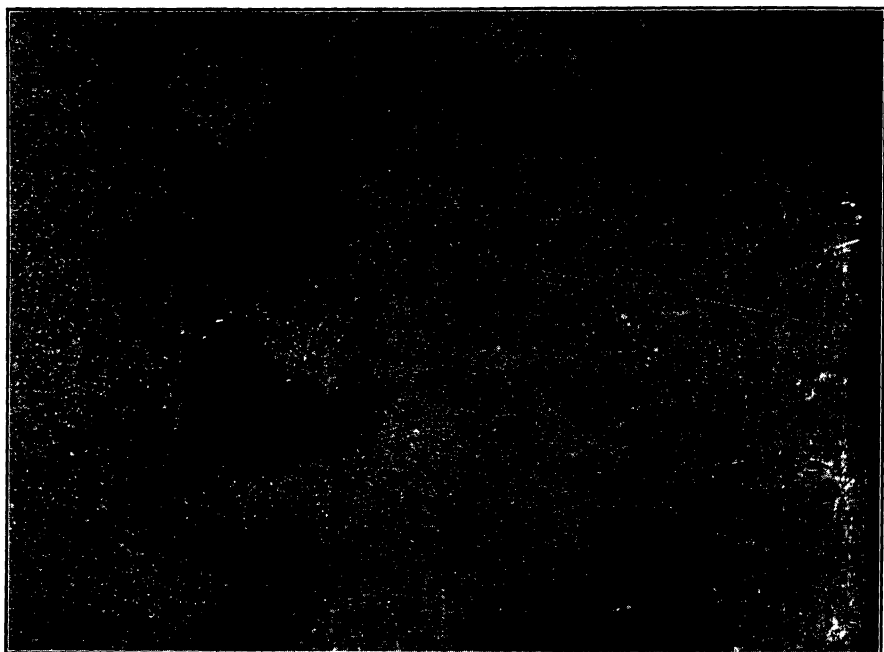
Fig. 14.—Ingot B.   Rim zone and part of core, half height.   × 2.
Transition between rim hole and rim channel regions.   Indications of fine globular structure in inner part of rim zone.   Flattened intermediate holes.

Ingot K4.   The mold, immediately after casting, was covered with a plate, the lower side of which was heat-insulated with asbestos board, and which had a narrow outlet for the gases.

Into two ingots, K5 and M, sulphur was added repeatedly in order to determine the rate of solidification.

The ingots were heat-treated to eliminate the secondary structure (see Appendix) and sectioned axially (the ingots with sulphur additions only transversely).   Sulphur prints were taken and the sections were then cut into smaller pieces for polishing and macroetching (see Appendix). Finally, some samples were taken for chemical analysis.   Oxygen determinations were made on some billets and rods.
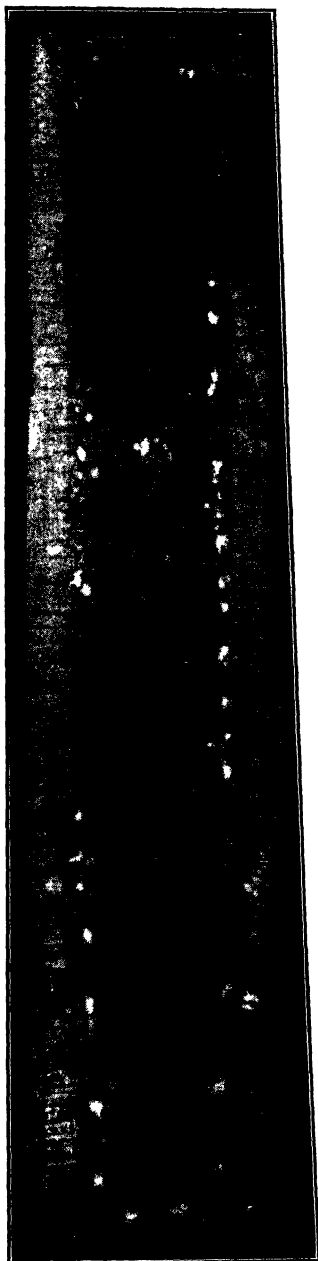
FIG. 15.   FIG. 16.
FIG. 15.—INGOT C.   C, 0.08; MN, 0.40 PER CENT.   × 0.18.
Sulphur print.   Deformation lines, two sets; low freezing center.
FIG. 16.—INGOT D.   C, 0.08; MN, 0.43 PER CENT.   × 0.18.
Sulphur print.   Deformation lines, two sets; low and extended freezing center
with irregular blowholes.
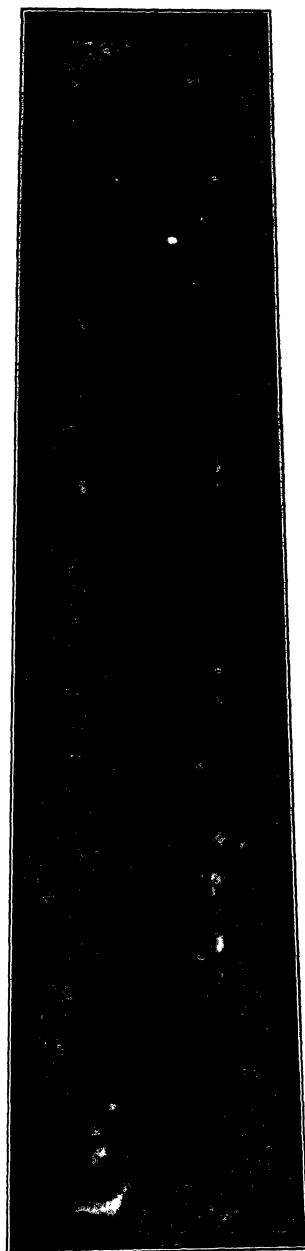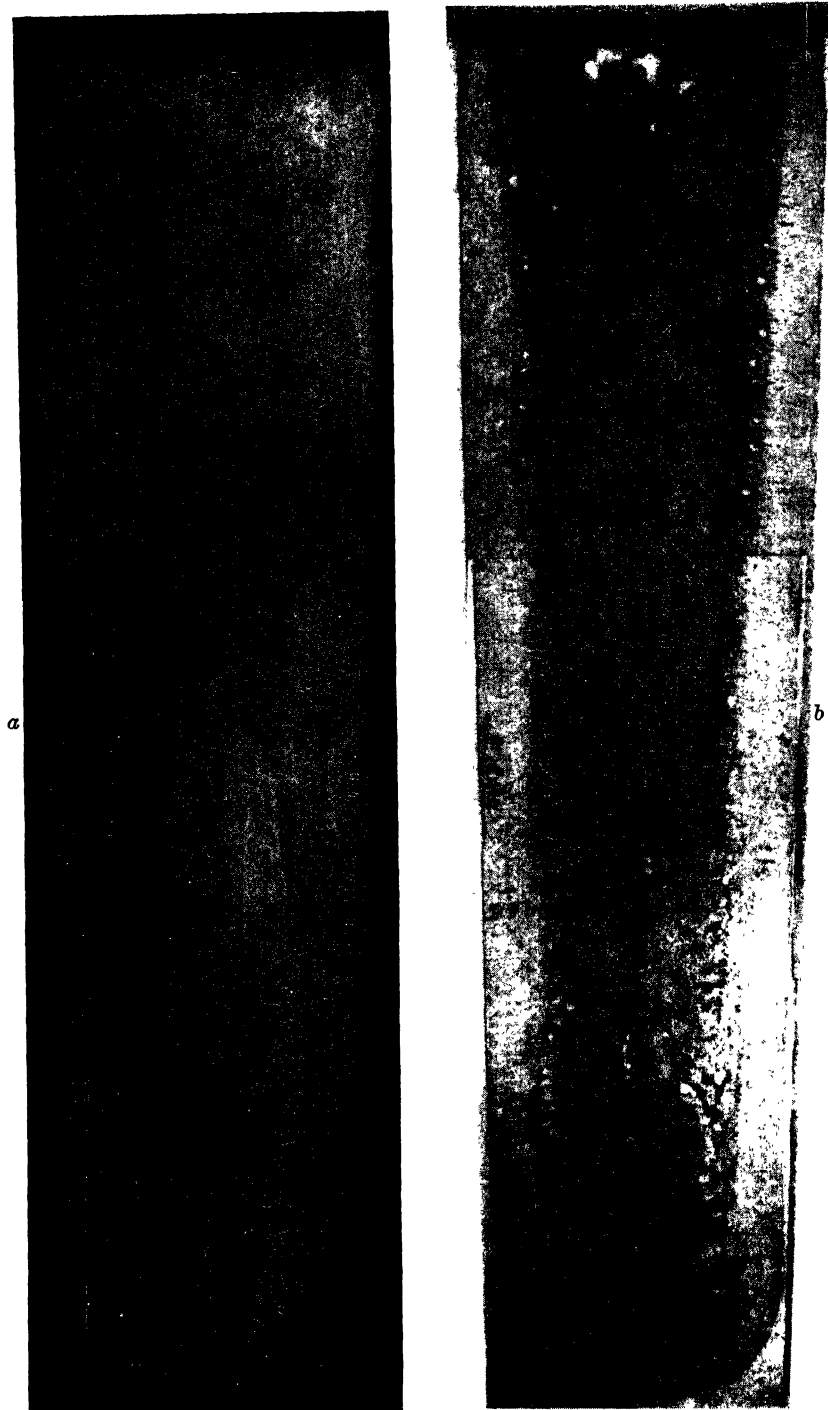
FIG. 17.—INGOT F1.   C, 0.14; MN, 0.47 PER CENT.   NO AL ADDITION IN MOLD.
× 0.15.
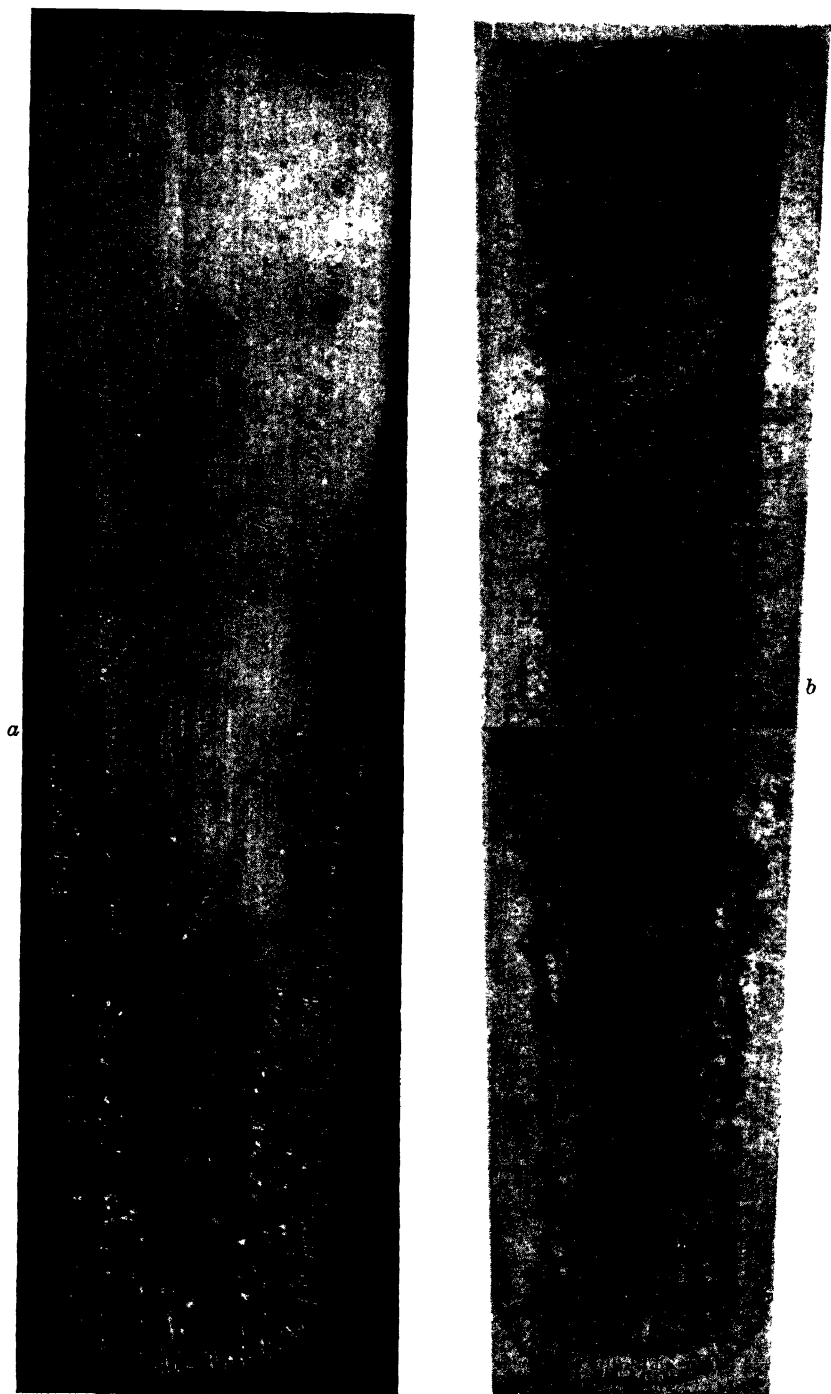
FIG. 18.—INGOT F2.   C, 0.14; MN, 0.47 PER CENT; 15 GRAMS AL PER TON ADDED
IN MOLD.   × 0.15.
Three sets of deformation lines at half height, otherwise similar to Fig. 17.

INGOT STRUCTURE

The observations on the ingot structure are grouped around various phenomena of the solidification process. It is believed that this manner of presenting the results will give more prominence to the general features of solidification than describing each ingot separately with all observations. Reference will be made repeatedly to particular ingots, however. The following terminology will be used:

Rim—solid edge growing progressively from the mold wall inward, at the ingot top, the central part of the top surface still being fluid.

Rim Zone—outer layer or shell of steel with relatively low content of segregating substances.

Core, or *Central Region*—part of ingot inside of rim zone, with relatively high content of segregating substances.

Rim Holes—elongated blowholes in rim zone.

Skin—layer separating rim holes from ingot surface.

Skin Holes—small blowholes in skin, just inside of surface.

Rim Channels—streaks of small blowholes or pores in rim zone.

Intermediate Holes—blowholes, generally irregularly shaped, in the boundary between rim zone and core.

Core Holes—scattered blowholes in core, in some cases with no sharp differentiation from intermediate holes.

Hole-contour Lines—lines showing contours of bubble seats or blowholes which were later filled with liquid steel.

Blowhole Segregate—segregate in partly or wholly refilled blowholes.

Rim-hole Point Segregate—segregate at inner end of rim hole.

Rim-hole Sweat, Blowhole Sweat—droplets of mother liquor squeezed from surrounding aggregate and lining hole surface.

Arrow Segregate—small segregate streaks at rim channels or rim-hole contour lines, inclined to axis of rim hole or channel.

Upset Structure—structure resulting from aggregate of solid with some liquid being deformed by pressure in one direction, whereby segregate lines are formed vertical to this direction.

Freezing Center—point or region in central portion toward which freezing finally converges.

Structure of Rim Zone

Before describing the structure of the rim zone, it is necessary to point out that the term "columnar crystals" for the primary structure of rimming-steel ingots of low carbon content may be erroneously applied, since the columnar structure sometimes revealed in such ingots is a secondary one, formed by transformation from δ to γ iron during cooling (see Appendix).

It might be expected that the evolution of gas during rimming would leave traces in the structure of the rim zone, besides blowholes; and this,

---

FIG. 19.—INGOT F3.   C, 0.14; MN, 0.47 PER CENT; 37 GRAMS AL PER TON ADDED IN MOLD.   × 0.135.

Steel rose in mold. Rim-hole region extends almost to top. Rim holes reach intermediate holes in lower half. Few core holes and marked deformation lines in lower half.

Fig. 19.—For descriptive legend see opposite page.

in fact, does occur. Such traces take the form of curved lines, obviously outlining the temporary contour of a blowhole, the gas contents of which were suddenly replaced by liquid metal (compare refs. 41 and 110). Such "hole-contour lines" may be seen in the outer (Figs. 13, 14, 20, 25, 30, 32, 37, 38, 41) and in the inner part of the rim zone (Figs. 41, 42, 43). Sometimes they are arranged in succession along the axis of a rim hole. When such contour lines are present in sufficient numbers, no further macrostructure is revealed by etching. When the outer part of the rim zone shows the characteristic elongated dendritic structure, it may be
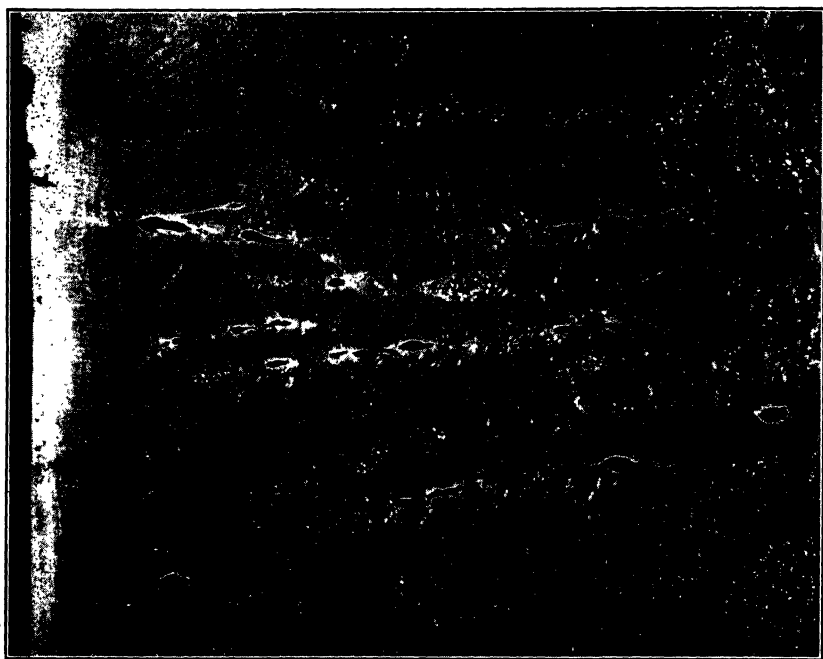
FIG. 20.—INGOT F1. RIM ZONE. × 2.
Dendritic structure in skin, globular in inner portion of rim zone. Series of hole-contour lines and arrow segregates in line with rim channels.

concluded that no gas bubbles were formed during the freezing of that portion.

The primary structure of the skin varies with the composition, roughly with the carbon content of the steel, and with the height in the ingot, in the following manner:

In ordinary rimming-steel ingots of *higher carbon contents*, heat K (0.21 per cent C, Figs. 35, 40, 42, 46) and F (0.14 per cent C, Figs. 17, 18), beginning at the surface (all these ingots were top-cast):

1. Near the surface is a perfectly sound skin with elongated dendritic structure (Figs. 20, 36, 37) the thickness of which tapers out upwards and disappears not far from the top.
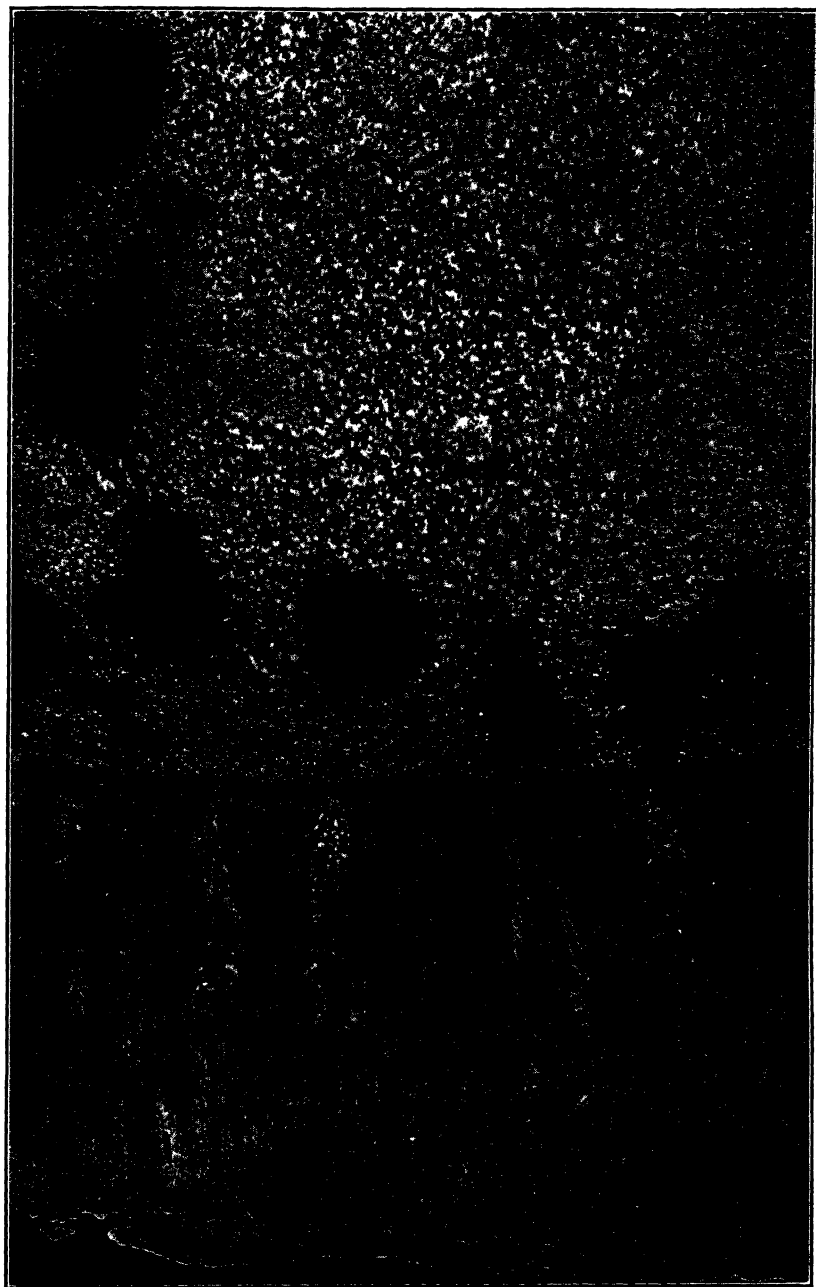
FIG. 21.—INGOT F1. RIM ZONE AND CORE, NEAR TOP. × 2.

Similar to Fig. 20. Compressed intermediate holes with segregates. Core-hole segregates with dendritic structure, no core holes visible. Otherwise globular structure in core.

2. At a certain depth beneath the surface appear:

    a. Near the bottom; rim holes, the sound steel portion between them still showing an elongated dendritic structure (Fig. 36).

    b. Further upward, hole-contour lines, often centered by rim channels, further inward succeeded by rim holes (Fig. 37).

    c. Still higher in the ingot, hole-contour lines, often centered by rim channels, which further in lose their escort of hole contours (Figs. 20, 21).

The mechanism by which this sequence of structures was formed is probably as follows: The sound skin froze without gas evolution. At a certain depth—less, the higher up in the ingot—gas bubbles were set free, which adhered to the freezing wall. In the lower part of the ingot these bubbles grew inward, at a rate similar to that of the freezing wall and developed into the elongated rim holes. At a certain height this process was disturbed in its beginning by the adhering bubbles, partly embraced by solid steel, being wholly or partly dislodged, often repeatedly, and replaced by the liquid metal. The portions of the latter freezing within the cavities thus left after the bubbles developed narrow channels, which later grew into ordinary rim holes (Fig. 37). The mechanism of this will be discussed later. At still higher levels rim holes never formed but rim channels grew all through the rim zone, sometimes ending in *intermediate holes* (Figs. 20, 21).

By adding 37 grams aluminum per ton in the mold, causing the metal to rise (ingot F3, Fig. 19) the same sequence was obtained but modified as follows:

1. The thickness of the sound skin for a given level increased somewhat.

2. The row of rim holes extended almost to the top, both features indicating, as a result of the aluminum addition, lessened gas evolution and slower movement of the metal during the rimming period (Figs. 23, 24, 25).

Ingots A to D (Figs. 7, 11, 15, 16) represent a *medium carbon* content (0.08 to 0.09 per cent). They are smaller than the former, and were bottom-cast.

The apparently sound skin is fairly thick near the bottom but becomes gradually thinner up to about half the ingot height, where the rim holes disappear (Figs. 8, 9, 13, 14). The skin is not, however, perfectly sound. It shows in the lower portion an elongated dendritic structure in places, greatly interfered with by contour lines—more so, the higher the level (Figs. 13, 14). It contains scattered rim channels, and may therefore be called *porous.* In the upper portion the rim zone is traversed by rim channels from the surface to the intermediate holes.

Ingot G was top-cast and had *low carbon content* (0.046 per cent. Fig. 27). The rim zone contains no rim holes, except at the very bottom

end, but numerous rim channels reaching from the surface to the intermediate holes (Figs. 28, 29). This ingot proved, unfortunately, not to respond to any kind of primary etching solution tried. Judging from the presence of rim channels, it is fairly certain, however, that no undisturbed dendritic structure could exist in the rim zone.

Comparing the series of ingots thus described, it is obvious that as the carbon content decreases the gas evolution sets in sooner after casting and proceeds with greater force.

Before leaving the outer portion of the rim zone, attention is called to a peculiar form of segregation, here called *arrow segregates*, associated with outer hole-contour lines, and rim channels (Figs. 10, 13, 14, 20, 21, 36). They consist of short lines perpendicular to the contour lines and inclined to the axes of the rim channels. Similarly situated arrow pores also occur (Fig. 10). It may also be pointed out that in an axial section of the ingot the rim channels appear as disconnected narrow holes.

FIG. 22.—INGOT F2, HALF HEIGHT. Sketch showing three sets of symmetrical deformation lines.

Other structural features of the rim zone as they occur on increasing depth beneath the surface. The rim holes usually slope somewhat upward; the more so, the higher they are situated in the ingot (Figs. 24, 41). The rim channels, however, appear to grow perpendicularly to the freezing wall (Figs. 10, 14), although great variations in direction are found (Figs. 11, 21, 57).

Adjacent rim holes in the lower part often show contractions recurring simultaneously (Figs. 7, 8, 11, 19, 58). By joining a set of such contractions, the temporary position of the freezing interface may be reconstructed. It is often found to be irregular (Fig. 58). Toward the upper part of the ingot, the rim holes become smoother and their mean diameter increases (Fig. 19). The rim holes usually end before they reach the intermediate holes and often on an irregular surface (Figs. 7, 11, 17, 18). Sometimes, however, they may be continuous with the intermediate holes in the lower part of the ingot (Fig. 42). The inner end of a rim hole generally contracts to a rounded point.

If the ingot is closed early the growth of the rim holes is stopped, and their inner ends are usually blunt in a characteristic manner. This is caused by mother liquor being later forced into the holes through their open ends, forming so-called *rim-hole point segregate* (Figs. 19b, 35, 36, 37). Such segregates may also be found in other cases (Figs. 42, 43, 44).

The outer, and generally greater part of the rim zone shows a fine primary structure, whether its details be distinct or confused. The inner part, however, often has a coarser, globular structure (Figs. 14, 20, 23, 25, 41) and, as stated already, is generally free from rim holes. This structure is probably due to the presence of crystal nuclei in the liquid metal at that stage of freezing.

Usually the inner part of the rim zone, when rim holes are present, shows a kind of laminated structure, with thin segregate lines running
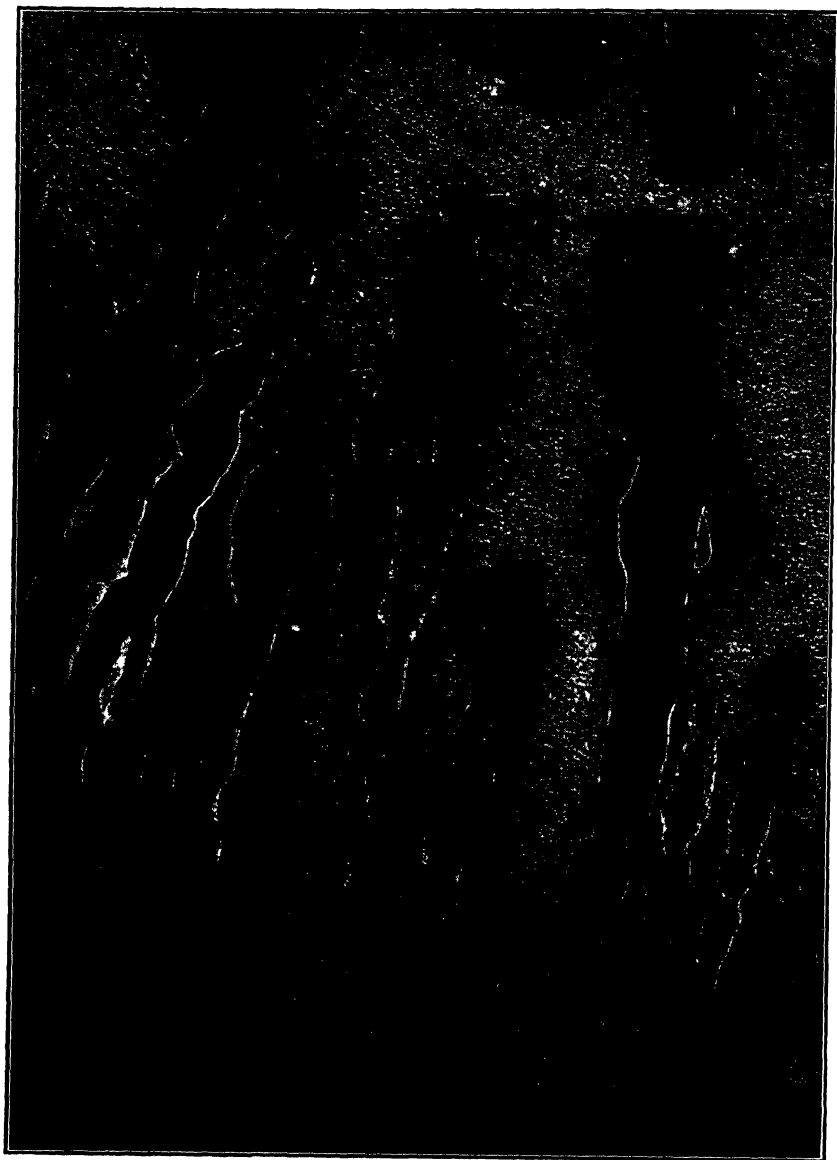
FIG. 23.—INGOT F3.   RIM ZONE AND CORE, BOTTOM END.   × 2.
Dendritic structure in skin, globular and upset structure in inner portion of rim zone.   Inner ends of rim holes compressed and distorted.

parallel to the surface of the ingot.   The corresponding parts of the rim holes are then deformed by transverse compression and appear to have been subjected to a certain distortion.   The structure in question is

called *upset structure*, indicating an upsetting action from an increased pressure having developed in the interior of the ingot after the formation of the rim holes (Figs. 23, 24, 43, 44, 45). This structure is particularly marked after early closing (Figs. 36, 37, 58). On the hole walls are often seen longitudinal, disconnected ridges, which are believed to have been formed by droplets of mother liquor in the surrounding aggregate that were squeezed into the hole (Fig. 58). This phenomenon may be called

FIG. 24.—INGOT F3. RIM ZONE ONE-FOURTH FROM TOP. × 2.
Dendritic structure in skin. Sloping rim holes with smooth contour.

blowhole sweat, since it may be observed in blowholes generally. The presence of long segregate lines in the upset structure, and of rim-hole sweat, points to the fact that that portion of the rim zone had not become completely solid when a high pressure developed in the interior.

Structure of Core

At the junction between rim zone and core lie the intermediate blowholes. Sometimes their connection with rim holes or rim channels is obvious; sometimes it is not. In the former case they are usually pear-shaped, i.e., flattened at the inner end (Figs. 10, 14, 21, 43); in the latter irregular, often also flattened (Figs. 10, 14, 21) or with their inner ends compressed sideways so as to form a narrow extension of the main hole (Figs. 21, 25, 43). The narrow portions are probably more frequent

than they appear to be because they do not always happen to be sectioned. The intermediate blowholes are usually accompanied by segregate, either local (Figs. 10, 21, 41, 43) or more or less continuous (Figs. 41, 44). The surrounding mass, which has a globular primary structure, nearly always shows signs of deformation—upset structure. Obviously, the holes were larger when newly formed, and afterward became compressed.

The structure of the main central region is generally characterized by the following features:

1. Globular primary structure.

2. Scattered, irregular blowholes, so-called *core holes*, usually accompanied by segregate; often segregates without visible connection with blowholes (Figs. 21, 40b, 46).

3. Somewhere on the axis one or more larger, sometimes elongated blowholes with marked irregular outline and accompanied by larger segregate (Figs. 17, 18, 26, 27, 40).

4. Often sloping deformation lines, situated symmetrically to the axis, of upward or downward slope (Figs. 7a, 7c, 10, 11, 13b, 20b, 36b, 43). Sometimes two or three successive systems of deformation lines in alternate directions may be seen (Fig. 18b; half height, Fig. 22).

This structure in its entirety suggests that in the central region the freezing proceeds inward under gradually increasing pressure, whereby outer zones that have developed blowholes and are not yet rigid enough— i.e., usually still contain mother liquor—are successively compressed from within by the increased pressure in an inner zone that is forming blowholes. This process, the formation and subsequent compression of blowholes, goes on continuously until the whole central region is frozen. The symmetrical deformation lines suggest a pressure gradient in the axial direction at a stage when the solid-liquid aggregate has acquired some cohesion.

Structures Obtained under Special Conditions of Freezing

The effect of certain intentional variations in freezing conditions have been studied:

Early Closing of the Ingot Top.—Ingot K1 (0.21 per cent C, Fig. 35, cf. pp. 169 and 196). The effect on the structure of the rim zone has already been described. In line with the inner end of the rim holes in the lower part of the ingot is a set of intermediate holes in the upper part. From several of those holes emanate sloping lines of segregate, which disappear at a certain depth (Figs. 35b, 38, 39). These are probably formed by bubbles rising from the blowholes and pushing their way through the aggregate, which was fairly mobile owing to the early closing. The crystals pushed aside would stay while the mother liquor would flow in behind (ref. 69, p. 107; ref. 105). The escaping bubbles probably joined the blowholes at the top.
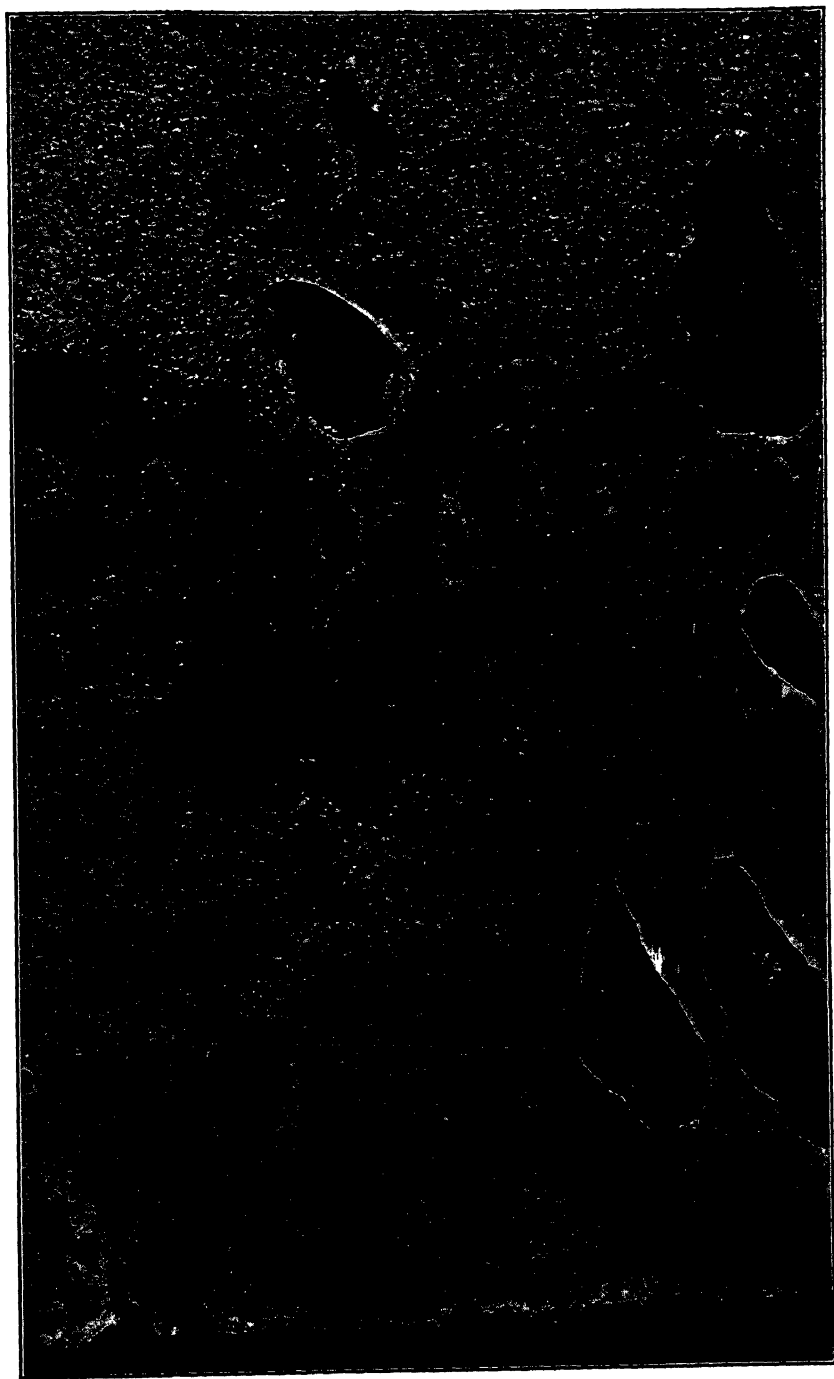
FIG. 25.—INGOT F3.   RIM ZONE AND CORE, NEAR TOP.   × 2.
End of rim-hole region.   Hole-contour lines.   Upset structure in inner portion of rim zone.
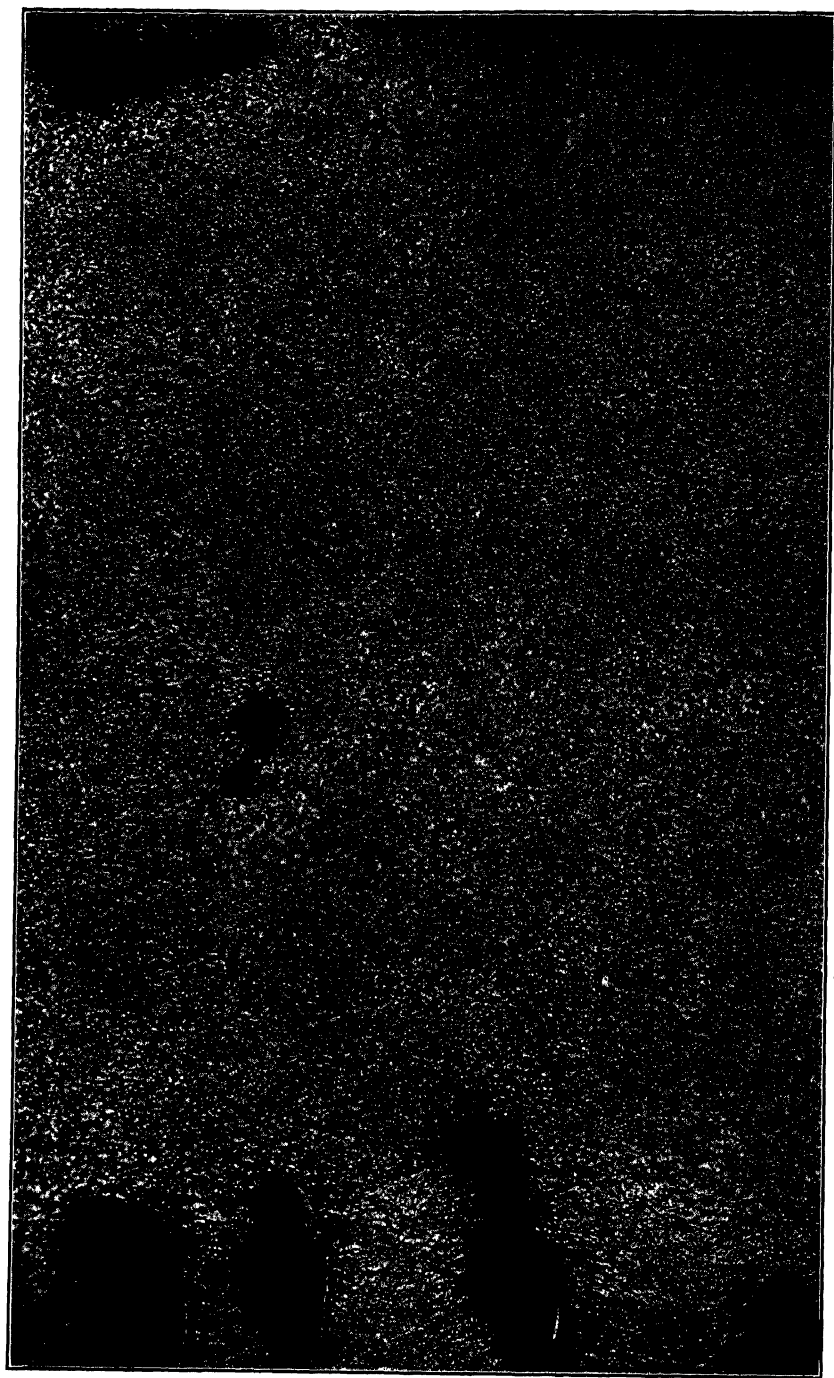
FIG. 26.—INGOT F3. CORE, HALF HEIGHT. × 2. Axial core hole with irregular contour and segregate, indicating lower end of freezing center. Intermediate holes with segregate.

The main part of the central region of this ingot shows no sign of blowholes or blowhole segregate, but symmetrical deformation lines of the type called V-segregate in killed-steel ingots (Figs. 35b, 39). This will be discussed later.

Delayed Closing of the Top.—Ingot K4 (0.21 per cent C, Fig. 46, cf. pp. 170 and 207). The mold was covered by a heat-insulating plate and no cooler plate was applied. Both circumstances would tend to delay the freezing of the top crust. The metal rose at a late stage, breaking through the weak top crust, probably more than once. By the relief of internal pressure thus obtained, the intermediate and core holes grew to large size. Significantly enough, there is no sharp distinction between intermediate and core holes. The holes around the axial portion show large segregates formed by compression after the final closing of the top.

Exclusion of Air during Rimming.—Ingot K3 (0.21 per cent C, Fig. 42, cf. pp. 170 and 203) may serve to exemplify this condition, together with ingots K1 and K4. The gas outlet was water-cooled. It may be assumed that this has little affected the freezing while the gases were given off, but that some cooling effect was felt by the ingot top after it had frozen over. Ingot K2 (Fig. 40) represents normal freezing conditions; that is, without cover during rimming, a cooler plate being applied after a good rim had developed. On comparing the two, it is seen that the main central portion of ingot K3 has frozen with little gas evolution, somewhat like ingot K1. A few large segregates have formed, however.

Addition of Powdered Ore during Casting.—Ingot H (0.15 per cent C, Fig. 29, cf. pp. 167 and 188). As expected, the metal frothed and sank, producing a box hat in the upper third of the ingot. The ore addition also cooled the metal considerably. As seen from Fig. 30, there is a sound skin followed by marked hole-contour lines, and wide rim holes at the bottom. Globular structure—a result of the cooling referred to—upset structure, and contraction of blowholes are in evidence in the rim zone.

Oscillations of Mold around Its Axis during Rimming.—Ingot I (0.17 per cent C, Fig. 31 and cf. p. 167). Short rim holes occur up to one-fourth of the ingot height. A second set of intermediate holes is seen 30 mm. inside the first. The sound rim zone contains numerous hole-contour lines and few rim channels, a result of the additional agitation produced by the oscillation. The inner part of the rim zone has a globular structure, and shows an increasing segregation of sulphur. The lower part of the central region is perfectly sound and very uniform. Above this part signs of axial deformation appear up to half the ingot height.

The double set of intermediate holes may be explained as follows: The turbulence caused by the oscillations, assisted by the square shape of the freezing wall, has served to mix the enriched liquid in front of the latter efficiently with the main liquid until the wall assumed a more rounded shape, when the oscillations have only caused a highly segregated layer of liquid to accumulate near the wall, thus retarding its growth.
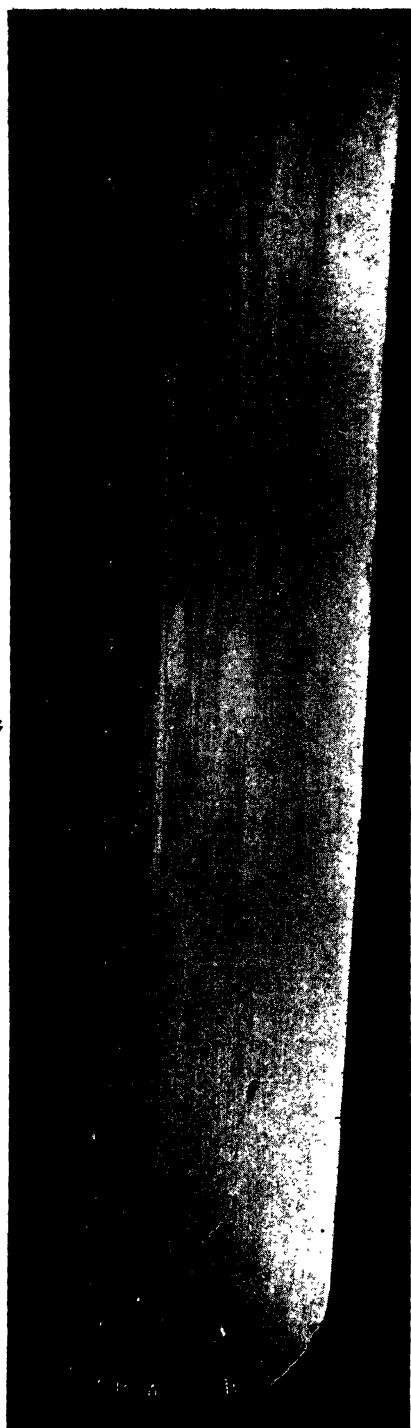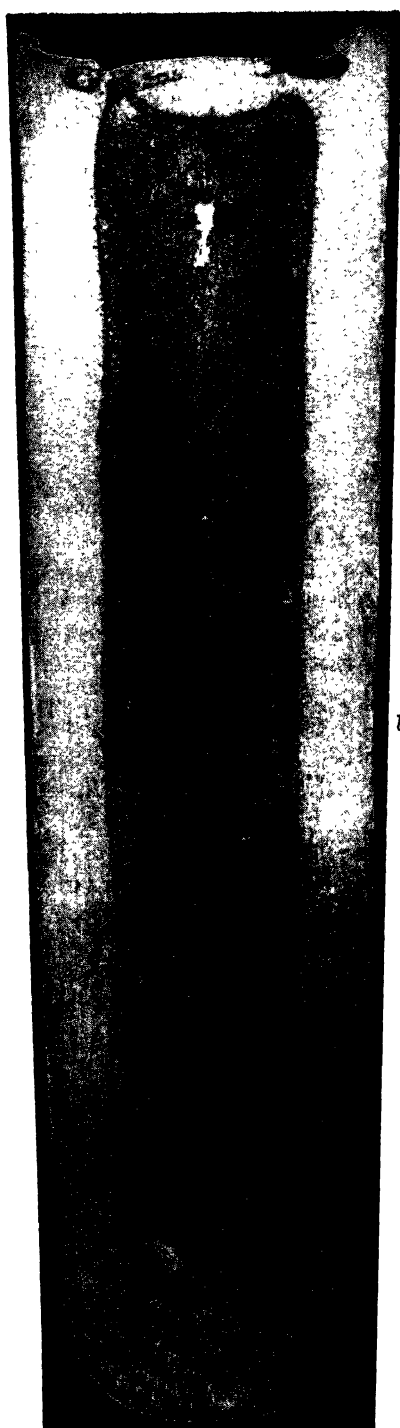
Fig. 27.—For descriptive legend see opposite page.

Crystal nuclei have then formed in the hotter but purer metal further in, the crystals growing into a more or less solid mass, divided by the impure liquid from the outer wall. The inner wall thus separated two freezing and gas-evolving zones from each other at the stage when the closing of the top prevented the gas from rising. Thus, the two sets of intermediate holes were formed.

From the same heat an ordinary ingot was examined by taking a sulphur print of a cross section 200 mm. from the top (Fig. 33). The structure and distribution of blowholes are normal. It is interesting
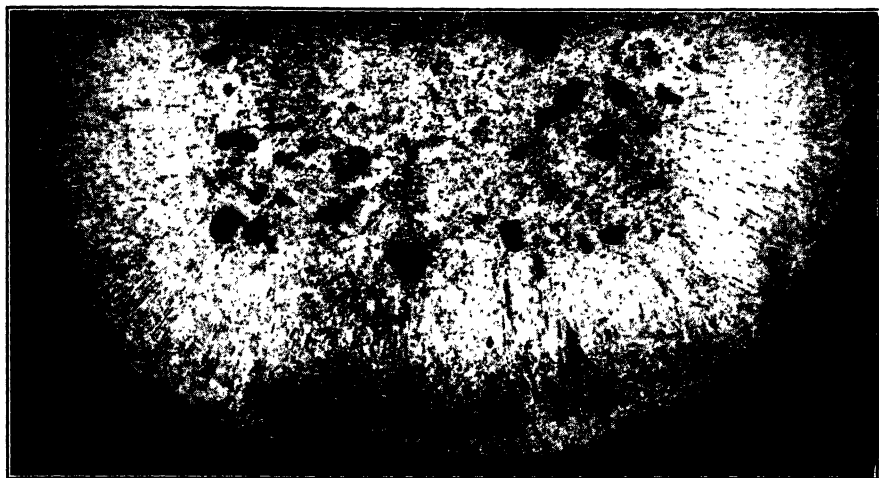
FIG. 28.—INGOT G. AXIAL SECTION, BOTTOM END (HEYN ETCHING). ✕ 0.4.

that the rim zone is 50 per cent thicker on the sides than at the corners, where a certain tendency to form rim holes is in evidence. Possibly differences in heat dissipation to the mold are responsible for this.

For comparison, Fig. 34 shows a fractured section of another somewhat larger ingot. Here the rim holes are shorter in the corner portions while the rim zone is thicker there (compare ref. 42, plate II). These effects would be expected from faster freezing, consequently more copious gas evolution and more rapid movement at the corners. It should be mentioned, however, that the rim holes may be longer in the corners (ref. 44, Fig. 1).

DISTRIBUTION OF METALLOIDS

A picture of the freezing process would not be complete without giving the distribution of the various elements in the ingot. A theory for freezing not accounting for the actual distribution would be inadequate.

FIG. 27.—INGOT G. C, 0.046; MN, 0.09 PER CENT. UNETCHED AXIAL SECTION AND SULPHUR PRINT. ✕ 0.15.

Wide rim zone, with rim holes only at bottom, otherwise rim channels. Freezing center, indicated by irregular holes and segregate, extends through greater part of ingot.

Carbon, phosphorus and *sulphur* were determined from drilled samples taken in a continuous row from surface to center at a certain level of the ingot. From the skin no sample was taken. Ingot F1 was analyzed at two levels: 0.1 and 0.6 of the ingot height; ingots F3 and G at 0.6 of the height. The results are plotted in Figs. 47 to 50 (the ladle analyses being indicated to the right) and may be summed up as follows:

FIG. 29.—INGOT H. C, 0.15; MN, 0.50 PER CENT. ORE ADDITION DURING CASTING. × 0.18.
Sulphur print. "Solid" part of boot-leg ingot. Short rim holes in lower part, otherwise rim channels.

Ingot F1; no aluminum, ladle analysis 0.14 per cent C, 0.026 per cent P and 0.035 per cent S (Figs. 47 and 48):

1. The rim zone, which is about 60 mm. thick, is lower in carbon, phosphorus and sulphur than the core and lower than the ladle sample.

2. Within the rim zone, from the surface inward, phosphorus and sulphur fall to a minimum, 15 to 40 mm. beneath the surface, and then rise steeply to a maximum, somewhat beyond the intermediate blowholes. The carbon concentration is fairly uniform, 0.02 to 0.04 per cent below the ladle analysis for about 40 mm., but rises from this point to a maximum at the same point as do the concentrations of the other elements. The upper level is higher in the three elements than the lower one. Judging from the dendritic structure of the skin, the steel near the surface probably solidified without gas evolution; i.e., practically without change of composition. That would mean a fall in all the elements from the surface to where the curves begin.

3. In the core from the maximum inward the curves for all three elements fall toward the axis, but on the lower level they turn upward
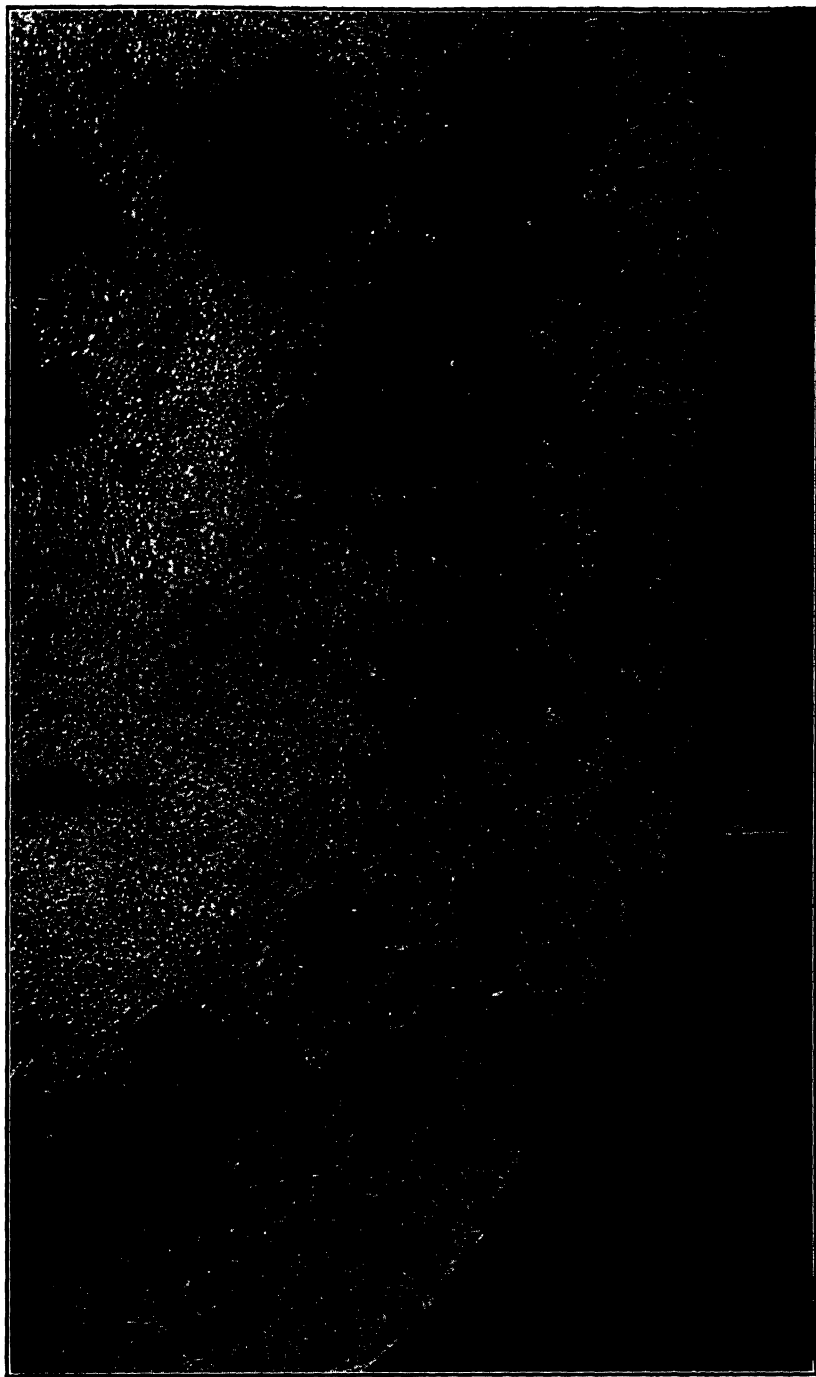
FIG. 30.—INGOT H. AXIAL SECTION, BOTTOM END. × 2. Hole-contour lines. To the right, Dendritic structure in skin, globular, upset structure in main portion of rim zone. rim hole with marked contraction showing bubble contour.
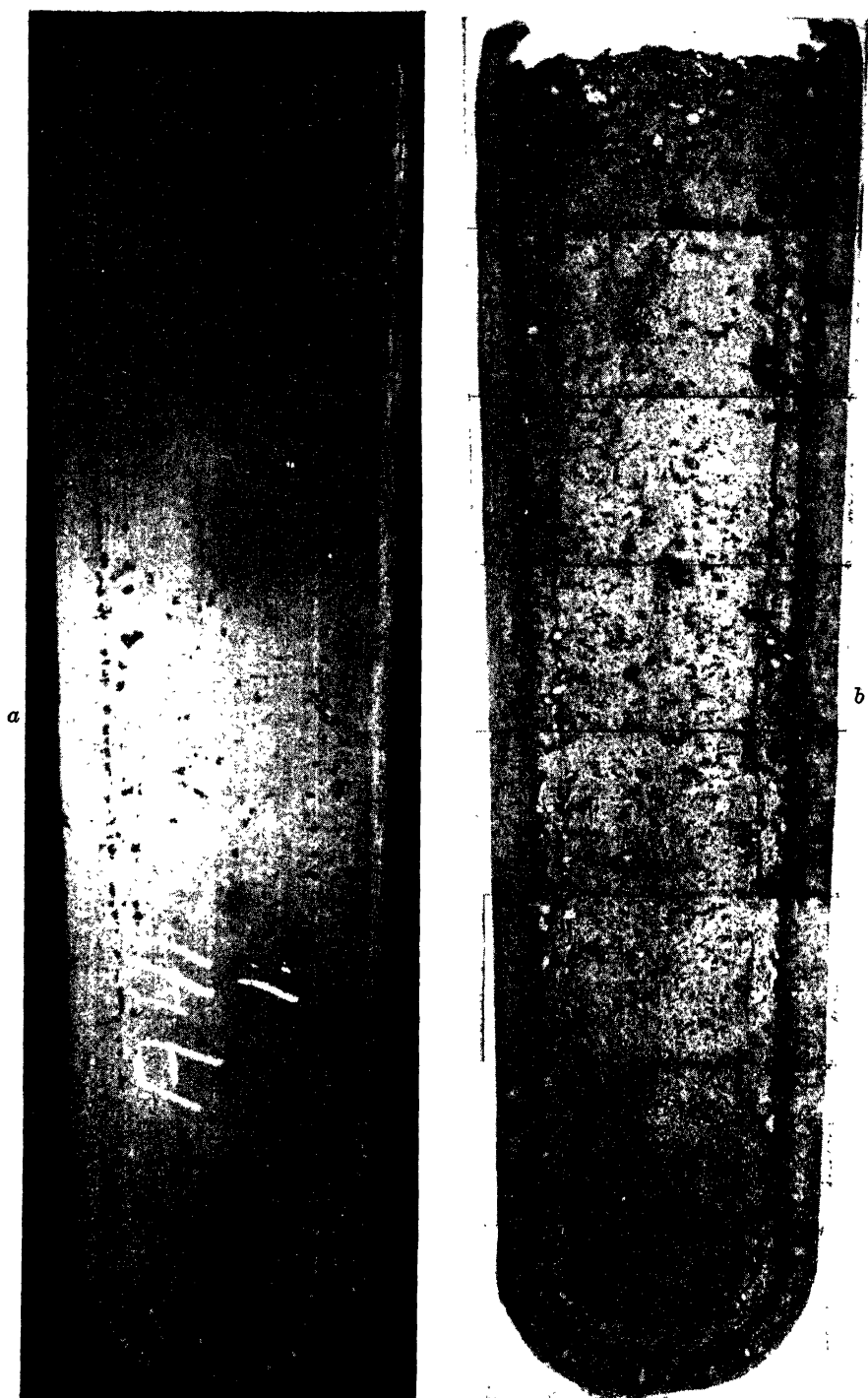
Fig. 31.—For descriptive legend see opposite page.

again toward a maximum at the axis. The latter coincides with an axial blowhole segregate visible on Fig. 17b. The upper level is consistently higher in the three elements than the lower one.

4. In the core, upper level, the mean concentrations of carbon, phosphorus and sulphur are moderately higher than the ladle analysis. In the core, lower level, the mean concentration of carbon is somewhat higher, of phosphorus equal to, and of sulphur lower than the ladle analysis. Hence, it appears that the lower central portion shows a definite negative segregation. This conclusion applies to carbon as well, if it be assumed that the ladle sample was not completely killed, and consequently, gas was given off when it froze.

Ingot F3; 37 grams aluminum per ton (Fig. 49). Upper level. The results agree on the whole with those of ingot F1, upper level, but the rim zone is higher and the core lower in all three elements. At the axis is a maximum, probably due to a blowhole segregate. The fact that nowhere in the rim zone is the carbon content lower than the ladle analysis confirms the assumption that the sample was not completely killed.

Ingot G; ladle analysis 0.046 per cent C, 0.007 per cent P and 0.025 per cent S (Fig. 50). Upper level.

1. Phosphorus is low and uniform until a depth of 40 mm., then rises steeply to the end of the rim zone and thereafter less steeply to a maximum beyond the intermediate holes, then falls somewhat and finally rises somewhat.

2. Sulphur falls to a minimum at a depth of 40 mm., then varies like phosphorus, only more so.

3. Carbon is uniform to 40-mm. depth, then falls to a minimum at about the end of the rim zone, and then rises continuously to the axis.

The results described here agree as a whole with earlier results,[104,110,133] and more particularly with those reported by Swinden.[127]

Oxygen was determined by the vacuum-fusion method. It was assumed that the samples ought to be free from porosity, and the ingots were therefore rolled before sampling. A detailed analysis from many positions in the section, therefore, being out of the question, the oxygen determinations were limited to: 10-mm. round rods taken from rim zone and core—according to sulphur print—of 100-mm. round or square billets, and 11-mm. round rods turned from 12-mm. round rolled bars, representing the average in a transverse section. The following ingots were examined: F, treated in casting in the same manner as ingot F1 of Table 1; G, same manner as ingot G and K as ingot K1. The results are given in Table 2, and may be summed up as follows: The oxygen content

FIG 31.—INGOT I. C, 0.17; MN, 0.60 PER CENT. REPEATED OSCILLATIONS DURING FREEZING. UNETCHED AXIAL SECTION AND SULPHUR PRINT. X 0.15.
Few rim holes. Marked sulphur segregation toward inner boundary of rim zone. Two sets of intermediate holes. Lower end of core uniform and sound.

is considerably higher in ingot G with 0.046 per cent carbon than in ingots F and K with 0.14 and 0.21 per cent carbon, respectively, the difference between the latter two being small. In ingot G it is about twice as high in the core as in the rim zone. In ingots F and K it is highest at the bottom, and the same for rim zone and core. It falls toward the top, somewhat more in the core, the top showing less oxygen in the core than in the rim zone (the high value in ingot F, top, rim zone, may be accidental). Some investigations of the oxygen distribution were made earlier by Bardenheuer and Müller[71] and by Geiger.[103]

The distribution of carbon, phosphorus, sulphur and oxygen thus found in the ingots present several points of interest, which will be discussed later (p. 225).

TABLE 2.—*Determinations of Oxygen Content in Various Parts of Some Ingots*
PER CENT

Size of Billet or Bar	100-mm. Round Billet				100-mm. Square Billet		12-mm. Round Bar		
Ingot No.	G		F		K		G	F	K
Carbon content, per cent	0.046		0.14		0.21		0.046	0.14	0.21
Position in section	Rim zone	Core	Rim zone	Core	Rim zone	Core			
Top			0.017 0.017 0.014	0.009 0.009	0.011 0.012	0.009 0.010			
Half height	0.027 0.027	0.063 0.056	0.011 0.012	0.012 0.013	0.012 0.011	0.011 0.012	0.044 0.041	0.012 0.012	0.012 0.012
Bottom			0.016 0.018	0.018 0.020	0.018 0.013 0.014	0.015 0.015			

OTHER OBSERVATIONS MADE

Attempts were made to determine the *linear rate of freezing of the rim zone* by adding various elements during the rimming period. The method has been suggested by Hadfield,[46] who added copper. Small amounts—about 0.1 per cent—of nickel, cobalt and copper were tried but no discontinuity was found on the etched sections. An addition of 0.02 per cent of sulphur,[47] was, however, found to produce a visible line of discontinuity in the sulphur print. Fig. 51 (p. 210) shows a print of a transverse section taken 200 mm. from the top of ingot K5 to which additions were made ½, 1, 2, 3, 4 and 5 min. after casting. It shows that
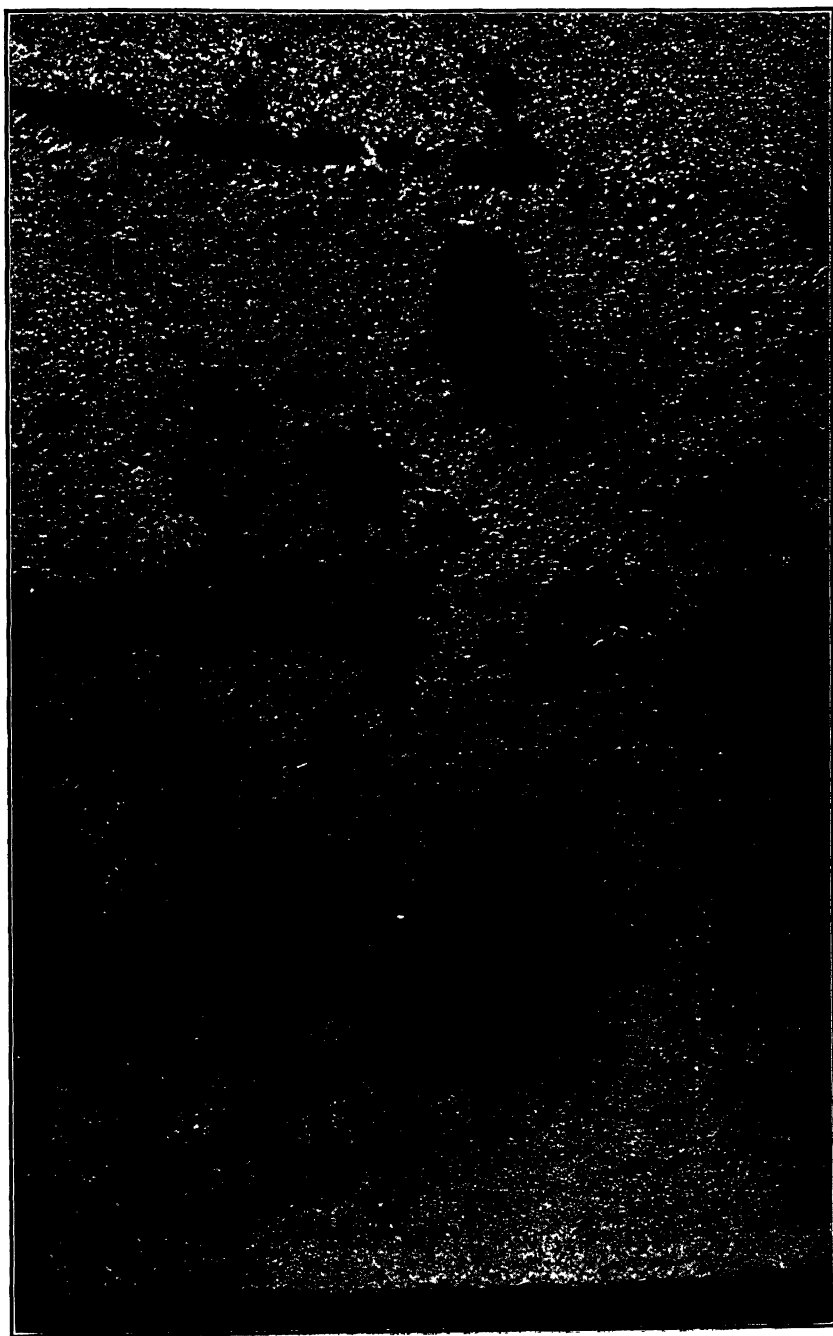
FIG. 32.—INGOT I. RIM ZONE AND CORE, HALF HEIGHT. × 2.
Numerous hole-contour lines.

the rate of freezing is not uniform around the circumference. The following formula agrees roughly with this and other similar tests that were made: $D = 0.85\sqrt{t}$, where D is thickness of freezing wall in inches and t is time in minutes after the steel in casting reached the section in question. The formula is in good agreement with earlier publications.[121]
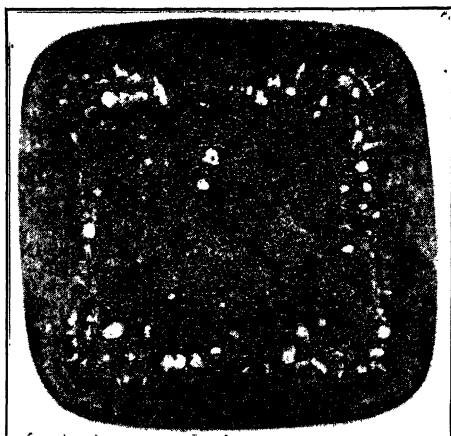
FIG. 33.—INGOT IA. SULPHUR PRINT OF CROSS SECTION 20 CENTIMETERS FROM TOP. × 0.15.

The *sound of the impact of the steel stream* in top-casting as well as the *sparking of the metal* give useful indications as to the subsequent behavior in rimming, and the position of the rim holes in the ingot.* Steel similar to ingot G when cast gives a soft impact, sparks are thrown out already at the beginning, and immediately after casting the top surface is brought into lively movement by gas rising at the mold walls. Steel similar to ingot K2 gives a hard impact; the top surface after casting is quiet for some time, giving off no sparks.

As pointed out by other investigators, a moderate and continuous sinking of the steel level during rimming indicates the formation of a rim zone with few or no rim holes, whereas after early sinking soon followed by rising the rim holes will be found to extend to a height in proportion to the amount of rising.

Ingot B was found to contain somewhat transparent, gray, in transmitted light brownish yellow, spherical *slag inclusions*, both in rim zone and core, up to several tenths of a millimeter in size, occasionally exceeding 1 mm. Usually they had a finely dotted structure (Fig. 52) and probably consist of (Mn,Fe)O in a matrix of silicate, sometimes with

FIG. 34.—FRACTURE OF RIMMING-STEEL INGOT.

sulphide. They will be called silicate inclusions. When such a drop has happened to be surrounded by segregated liquid, it absorbs sulphide and distinct grains of sulphide are found in the inclusion.

---

* According to observations made by S. Wohlfahrt.

Fig. 53 shows MnS, separated primarily, in a matrix of MnS, (Mn,Fe)O and transparent silicate. Fig. 54 shows a large inclusion found in an axial blowhole segregate, deformed by being forced into an interstice in the freezing metal. The sulphide absorption is here limited to a certain depth. MnS particles in the surrounding metal indicate its segregated character.

The large silicate inclusions are assumed to have existed in the liquid before freezing began or possibly to have formed through oxidation during rimming. Smaller silicate inclusions, possibly of lower silica content, are also found, which probably were separated after enrichment of the liquid metal in oxygen during freezing. They may contain sulphide, usually as droplets (Fig. 55). Fig. 56 shows an inclusion of this kind in which the sulphide droplets have shrunk after the silicate solidified, possibly owing to separation of iron on the adjacent metal.

In Table 3 are given two analyses of scum accumulated on top of a rimming-steel ingot, C = 0.10 per cent; sample I taken immediately after casting, sample II just before applying a cooler plate a few minutes afterward.* Similar analyses have been recorded by Ruhfus.[33] The composition of the scum will be discussed later.

TABLE 3.—*Analysis of Scum from Rimming-steel Ingot*
PER CENT

Constituent	Sample I	Sample II
FeO	29.43	20.26
Fe$_2$O$_3$	9.14	5.28
MnO	42.31	57.15
MgO	5.00	4.90
CaO	1.50	0.90
Al$_2$O$_3$	3.50	2.80
SiO$_2$	8.40	8.00
P$_2$O$_5$	0.172	0.076

GENERAL DISCUSSION OF SOLIDIFICATION PROCESS

The following is an attempt to explain in a general way the phenomena occurring during the solidification of a rimming-steel ingot. This explanation is based on observations and theories previously published as well as on the results of the present investigation.

CONDITION OF LIQUID STEEL BEFORE CASTING

For obtaining a true rimming-steel ingot, the metal should contain appropriate amounts of carbon and oxygen, causing a sufficient gas evolution during solidification. Carbon monoxide is the major constituent of the gas evolved and other gases present will have only little

* The samples were taken at Domnarfvet steel works by S. Wohlfahrt.

a

b
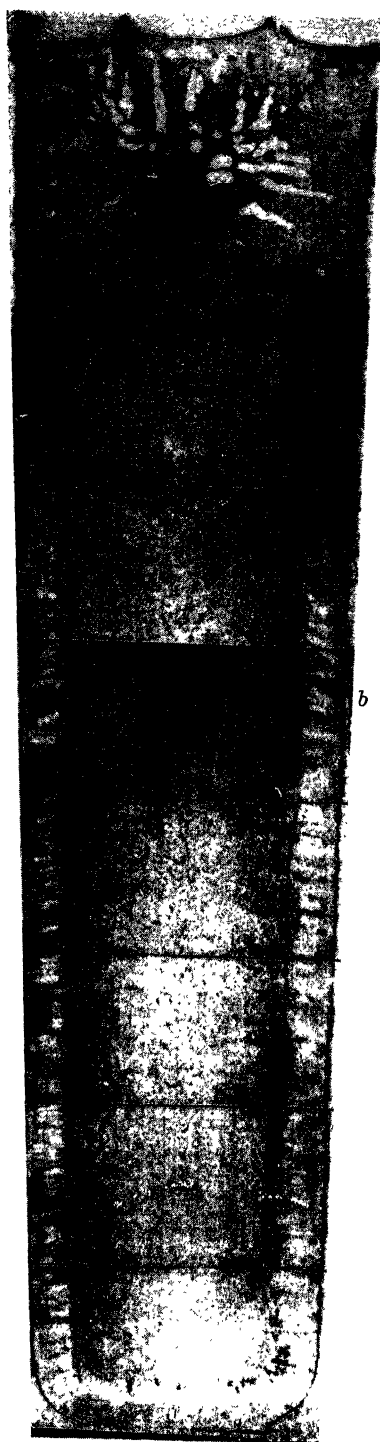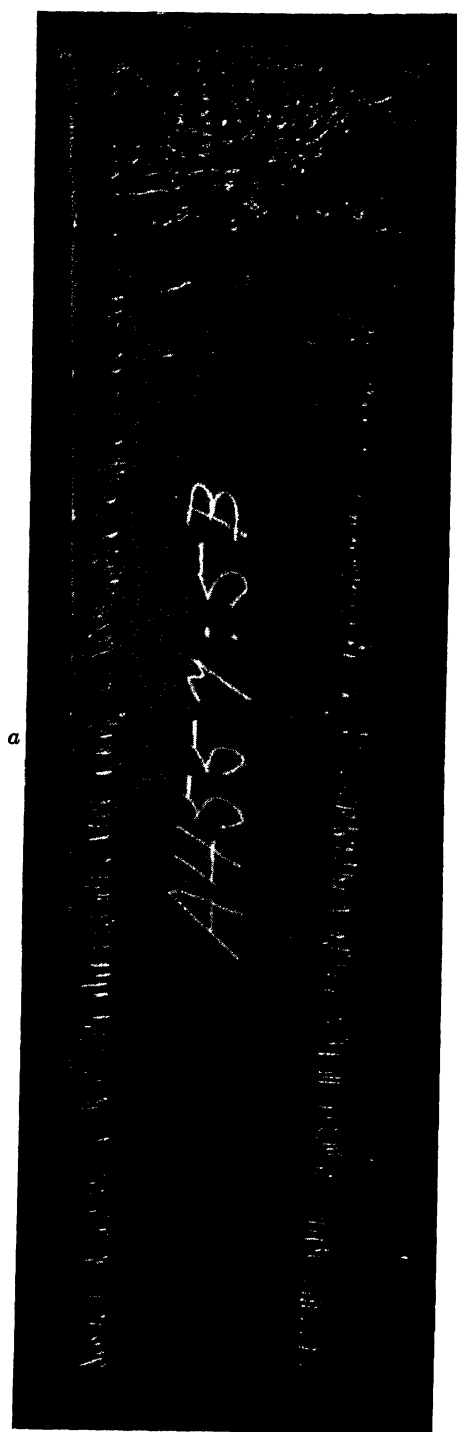
Fig. 35.—For descriptive legend see opposite page.

influence. The rate of carbon removal is generally considerable up to the moment of tapping, and thus it is to be expected that the actual carbon-oxygen product will be greater than the equilibrium value. As has been mentioned earlier, the change of this equilibrium value with temperature is small. The temperature may have, however, some influence on the rate of reaction and thus on the actual carbon-oxygen product, an increase in temperature generally decreasing the deviation from equilibrium. The rate of oxygen supply from the furnace slag might also be increased, thereby more or less compensating the effect first mentioned.
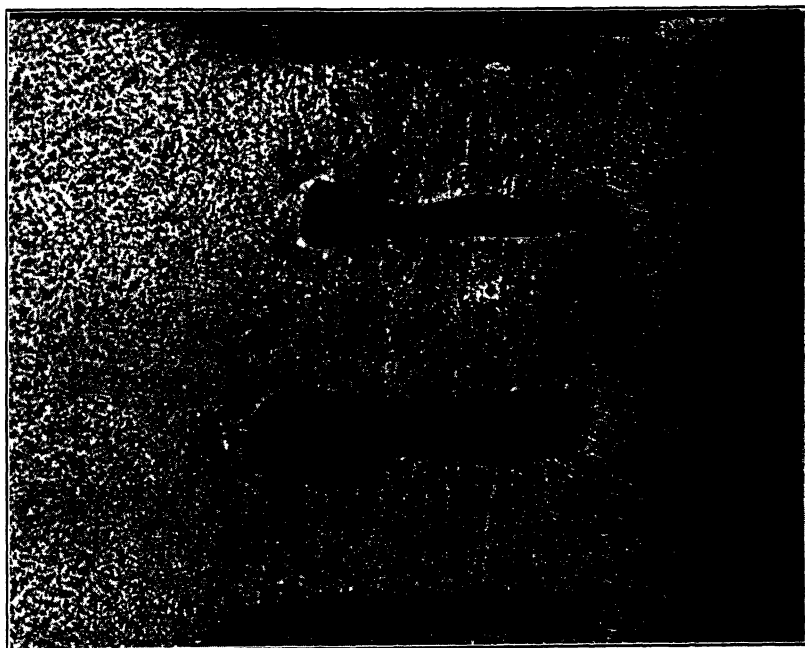
FIG. 36.—INGOT K1. RIM ZONE AND PART OF CORE, NEAR BOTTOM. × 2.
Dendritic structure in skin, upset dendritic structure in rest of rim zone. Compressed rim holes with blunt inner end and point segregates. Outer region of core largely dendritic.

There seems to be no unanimous opinion on the influence of temperature on the actual carbon-oxygen product. Observed cases of insufficient gas evolution and rising in the molds when the steel was very hot, as well as excessive gas evolution and formation of boot-leg or box-hat ingots when its temperature was too low,[24,54] may have been caused more

FIG. 35.—INGOT K1. C, 0.21; MN, 0.65 PER CENT. EARLY CAPPING. UNETCHED
AXIAL SECTION AND SULPHUR PRINT. × 0.14.
Narrow rim zone. Rim-hole point segregates. Sloping segregate bands rising from rim holes and intermediate holes. V-segregates and absence of core holes in greater part of core. Near top marked freezing center with segregate, surrounded by long blowholes pointing toward center.

directly through the influence of the casting temperature. If the steel is cast very hot the solidification rate will be comparatively slow at first, and therefore also the rate of gas evolution.

It may be taken as certain that the liquid rimming steel is generally "supersaturated" with respect to carbon monoxide, when tapped into the ladle. Some carbon monoxide may be given off during tapping. Boiling in the ladle, however, which sometimes occurs, is probably caused by the mixing of the steel with oxidizing furnace slag. Manganese additions of
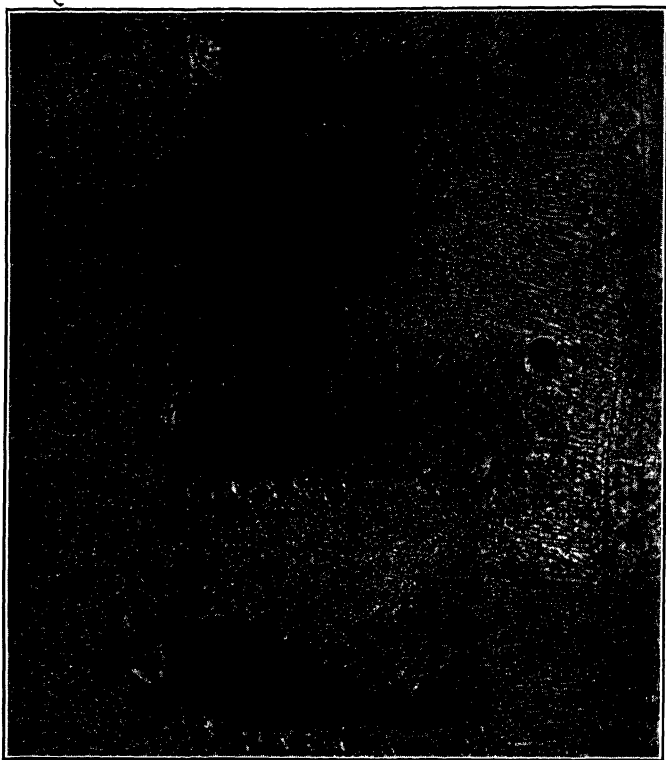
FIG. 37.—INGOT K1. RIM ZONE AND PART OF CORE, ONE-THIRD FROM TOP. × 2.
Rim zone dendritic with series of hole-contour lines and rim channels. Compressed intermediate holes.

ordinary magnitude should not cause any "deoxidation," no oxide phase being formed (p. 161); if the carbon content of the ferromanganese is considerable, it may cause a "manganese boil." Boiling when some cold object is immersed in the liquid steel may be explained by solidification around this object.

The silicon content of rimming steel is generally low, the order of magnitude being about 0.01 per cent. It seems probable that even this small amount of silicon is present partly as undissolved oxide slag, as the affinity between silicon and oxygen is great. If the oxygen content of

the steel is low, however, a considerable part of the silicon may be in solution. For instance, if the oxygen content is 0.02 per cent the dissolved silicon will be about 0.01 per cent at 1500° C., provided the manganese content is lower than 0.15 per cent.[97] That is, the silicon content may in some cases have a perceptible influence on the quantity of gas evolved while the steel solidifies.
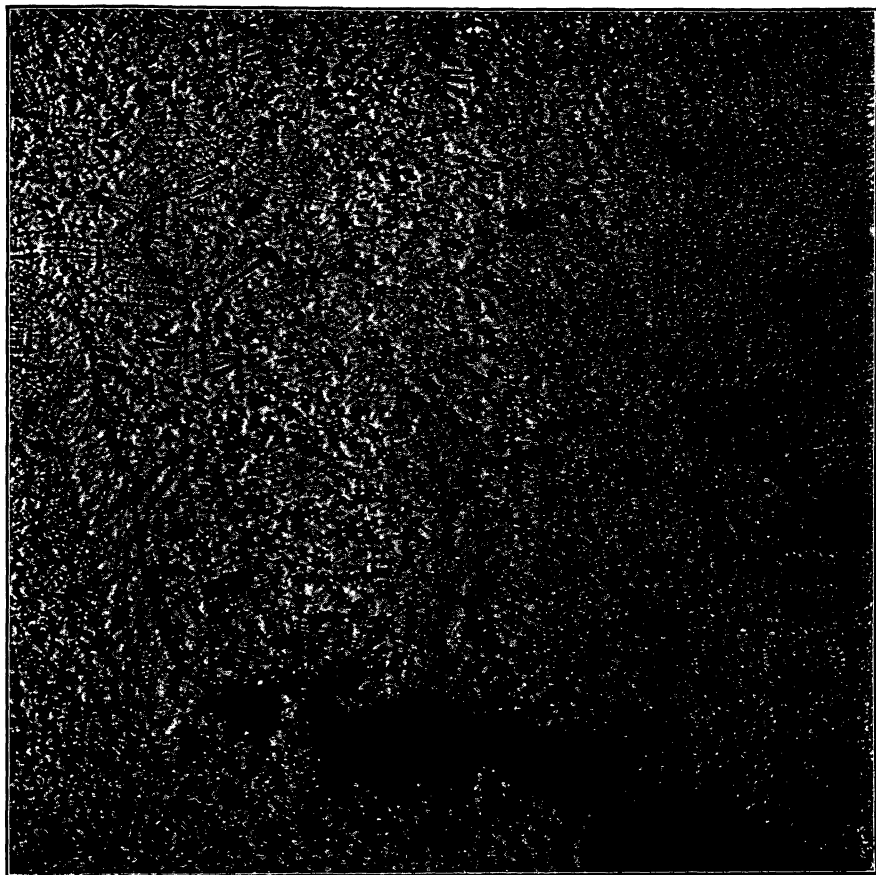
FIG. 38.—INGOT K1. PART OF RIM ZONE AND CORE, NEAR TOP. X 2.
Hole-contour lines, sloping segregate bands. Largely dendritic structure in core.

Aluminum is often added to the liquid steel in order to adjust the gas evolution. The affinity between aluminum and oxygen is very great and for the purpose of the following discussion it is sufficient to assume that the aluminum added is completely oxidized. The Al_2O_3 may combine with FeO, MnO or SiO_2. It may be assumed, however, that the quantity of oxygen eliminated from the liquid steel is roughly equal to the aluminum quantity added.

FIG. 39.—INGOT K1. AXIAL SECTION, ONE-FOURTH FROM TOP. × 0.6.
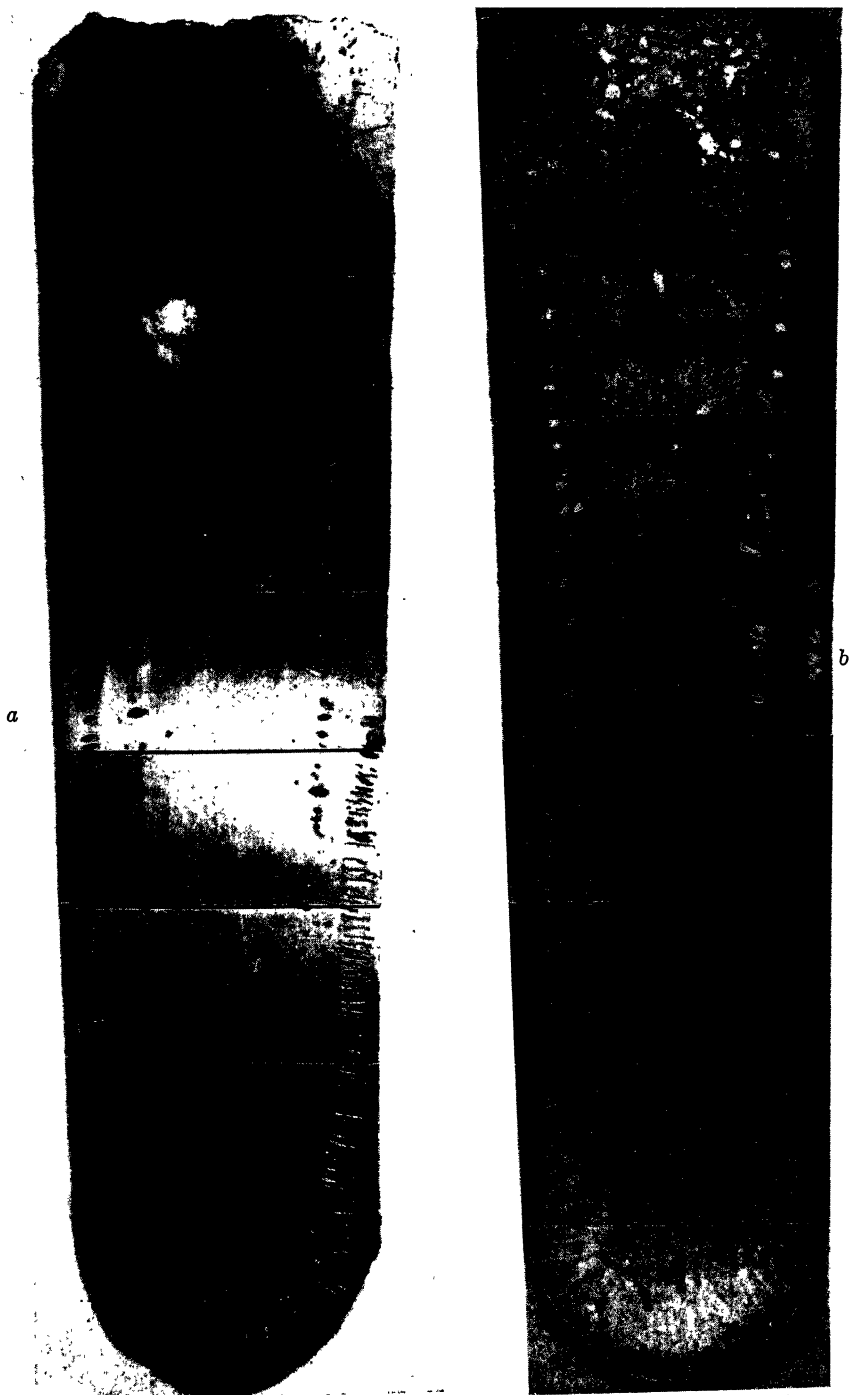
FIG. 40.—INGOT K2.   C, 0.21; MN, 0.65 PER CENT.   NORMAL FREEZING.   UNETCHED
AXIAL SECTION AND SULPHUR PRINT.   × 0.14.
Rim holes in lower half.   High freezing center.

THE RIMMING PERIOD

When the steel solidifies very rapidly, the gas evolution may be suppressed. Thus, the superficial layer of an ingot will generally solidify without gas evolution. The rate of solidification decreases as
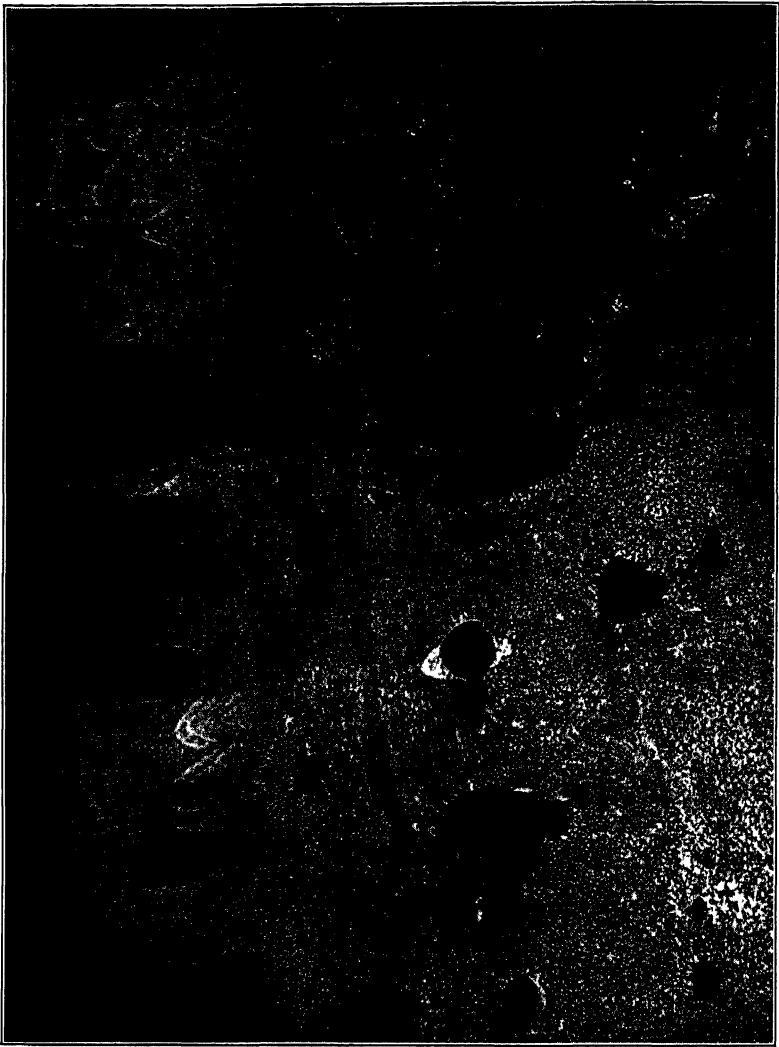
FIG. 41.—INGOT K2. RIM ZONE AND PART OF CORE, HALF HEIGHT. × 1.
Thin dendritic skin. Series of hole-contour lines at inner ends of rim holes. Upset structure. Marked intermediate and core-hole segregates.

the solid layer becomes thicker and at a certain thickness gas evolution will start in the liquid adjacent to the solid steel, where carbon and
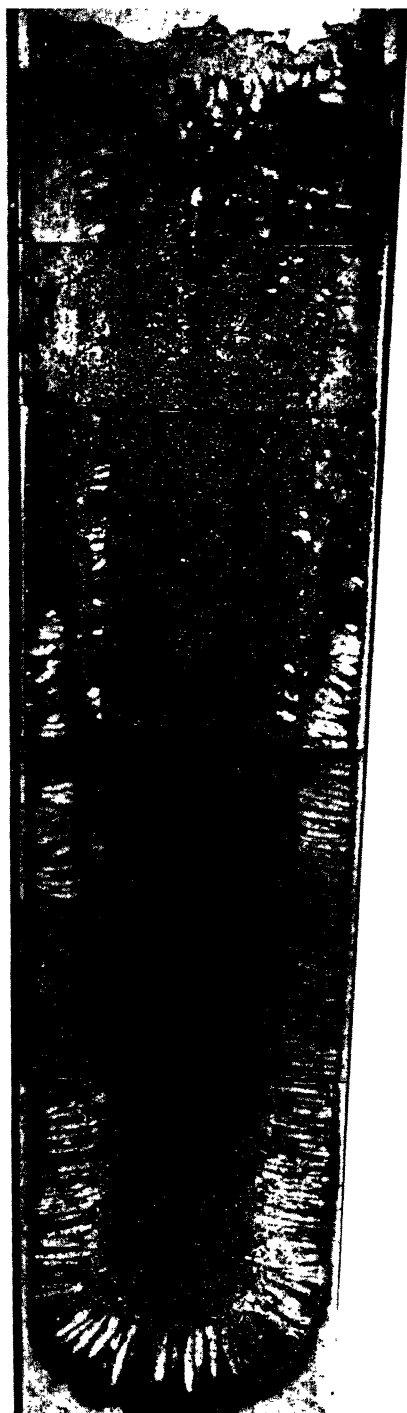
FIG. 42.—INGOT K3. C, 0.21; MN, 0.65 PER CENT. MOLD GAS COLLECTED. × 0.15.
Similar to Fig. 40, but fewer core holes.
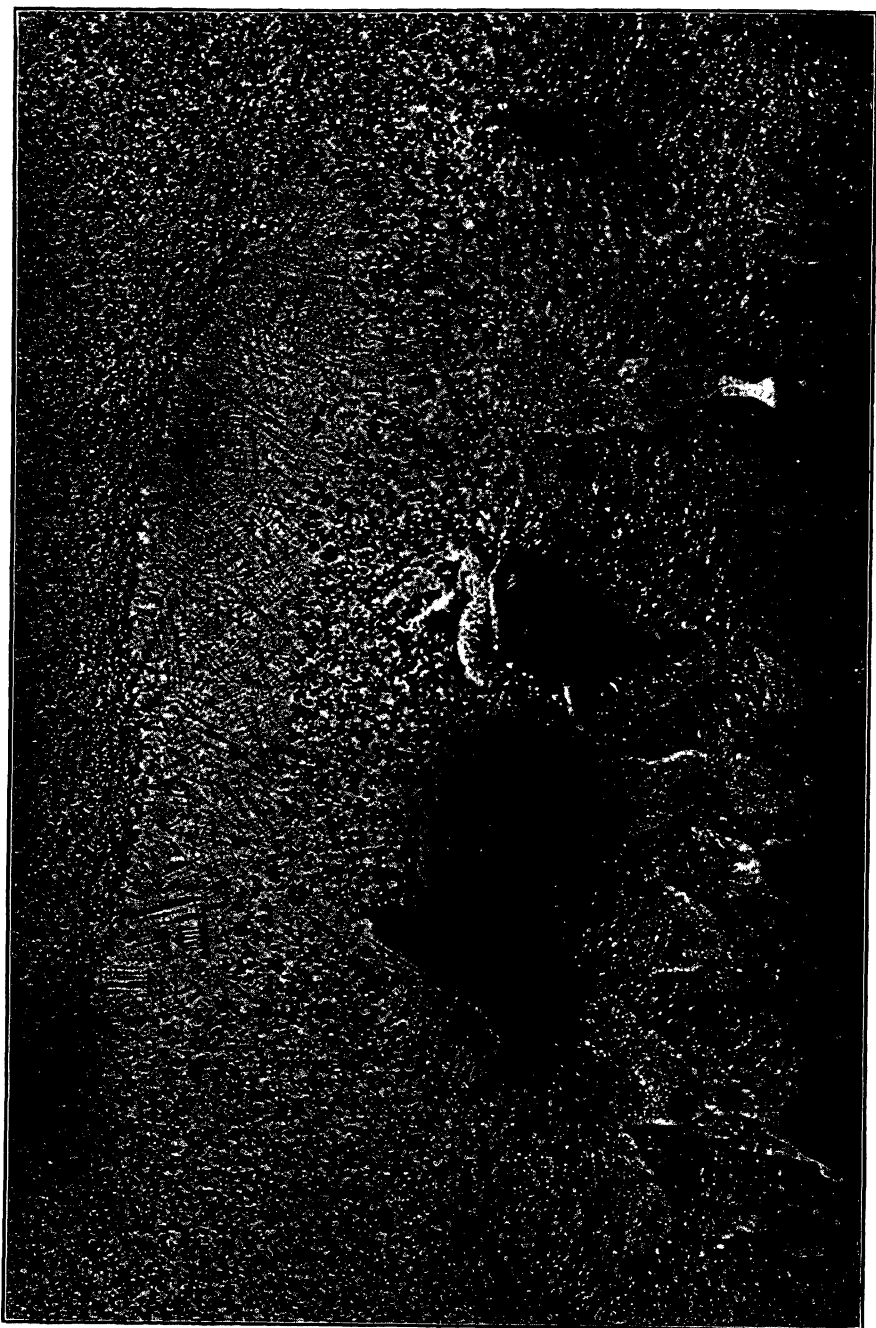
FIG. 43.—INGOT K3.   PART OF RIM ZONE AND CORE, ONE-THIRD FROM BOTTOM.   × 2.
   Point segregates and hole-contour lines at inner ends of rim holes.   Large segregate in outer region of core.
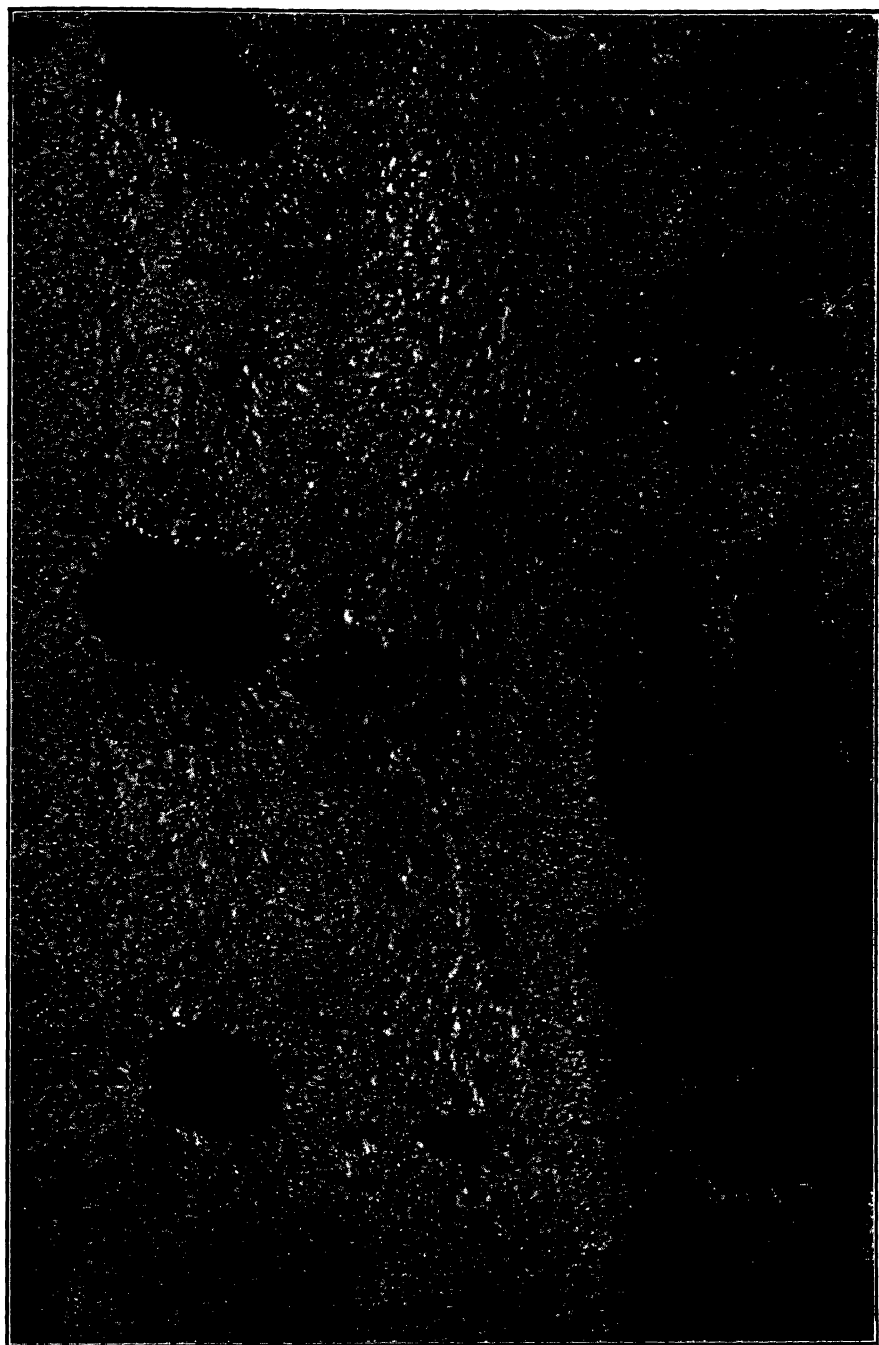
FIG. 44.—INGOT K3. PART OF RIM ZONE AND CORE, HALF HEIGHT. × 2.
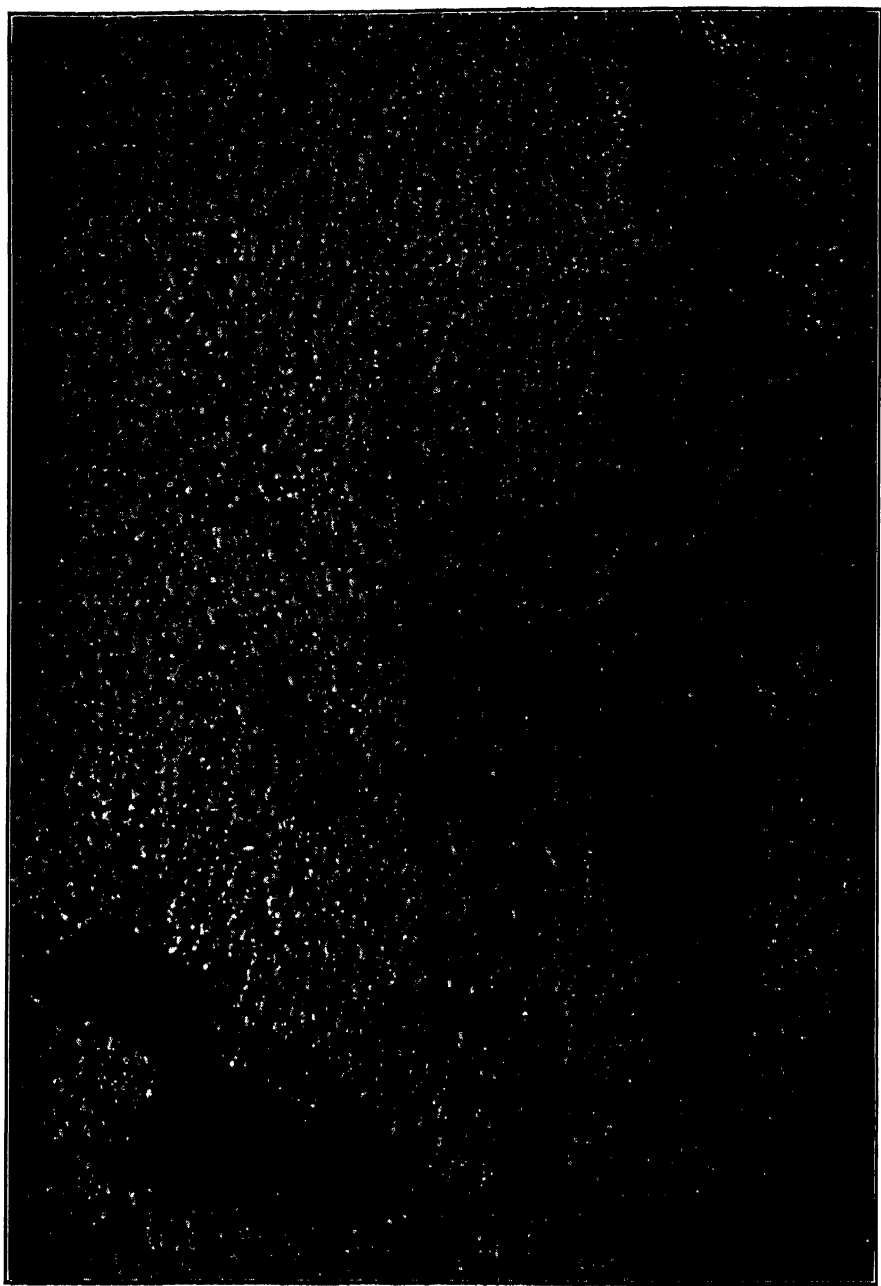
Fig. 45.—Ingot K3. Part of rim zone and core, one-fourth from top. × 2.
Transition from dendritic structure in rim zone to globular structure in core.

Fig. 46.—Ingot K4.   C, 0.21; Mn, 0.65 per
cent.   Heat-insulating mold cover.   ×0.15.
Sulphur print.   Top crust perforated by core
material.   Intermediate hole region merges into
external core-hole region.   Large hole segregates
along axis.

207
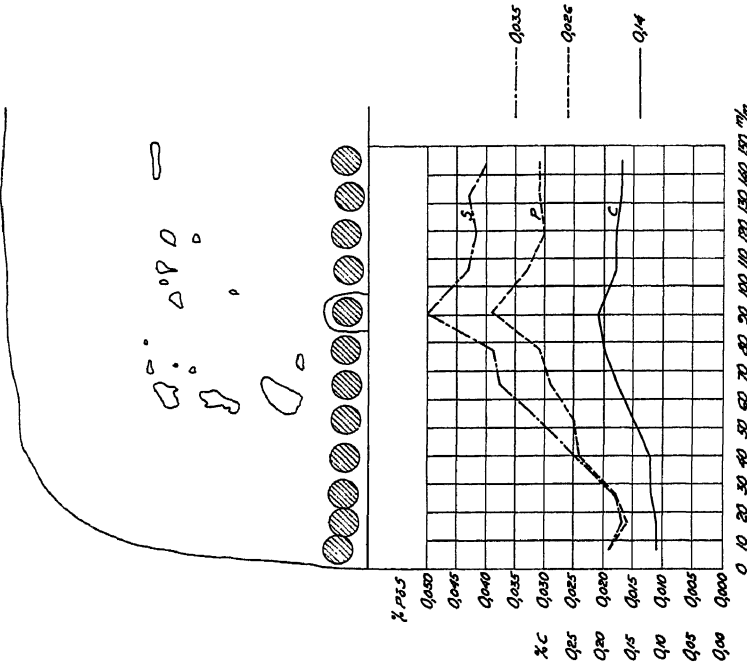
FIG. 47.—INGOT F1.
DISTRIBUTION OF C, P AND S 0.1 FROM BOTTOM.
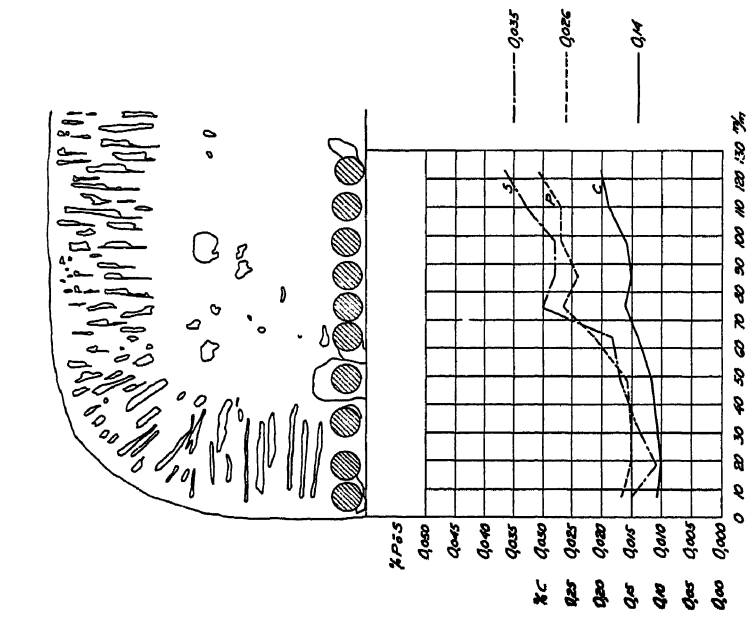
FIG. 48.—INGOT F1.
DISTRIBUTION OF C, P AND S 0.6 FROM BOTTOM.

Fig. 49.—Ingot F3.
Distribution of C, P and S 0.6 from bottom.

Fig. 50.—Ingot G.
Distribution of C, P and S 0.6 from bottom.
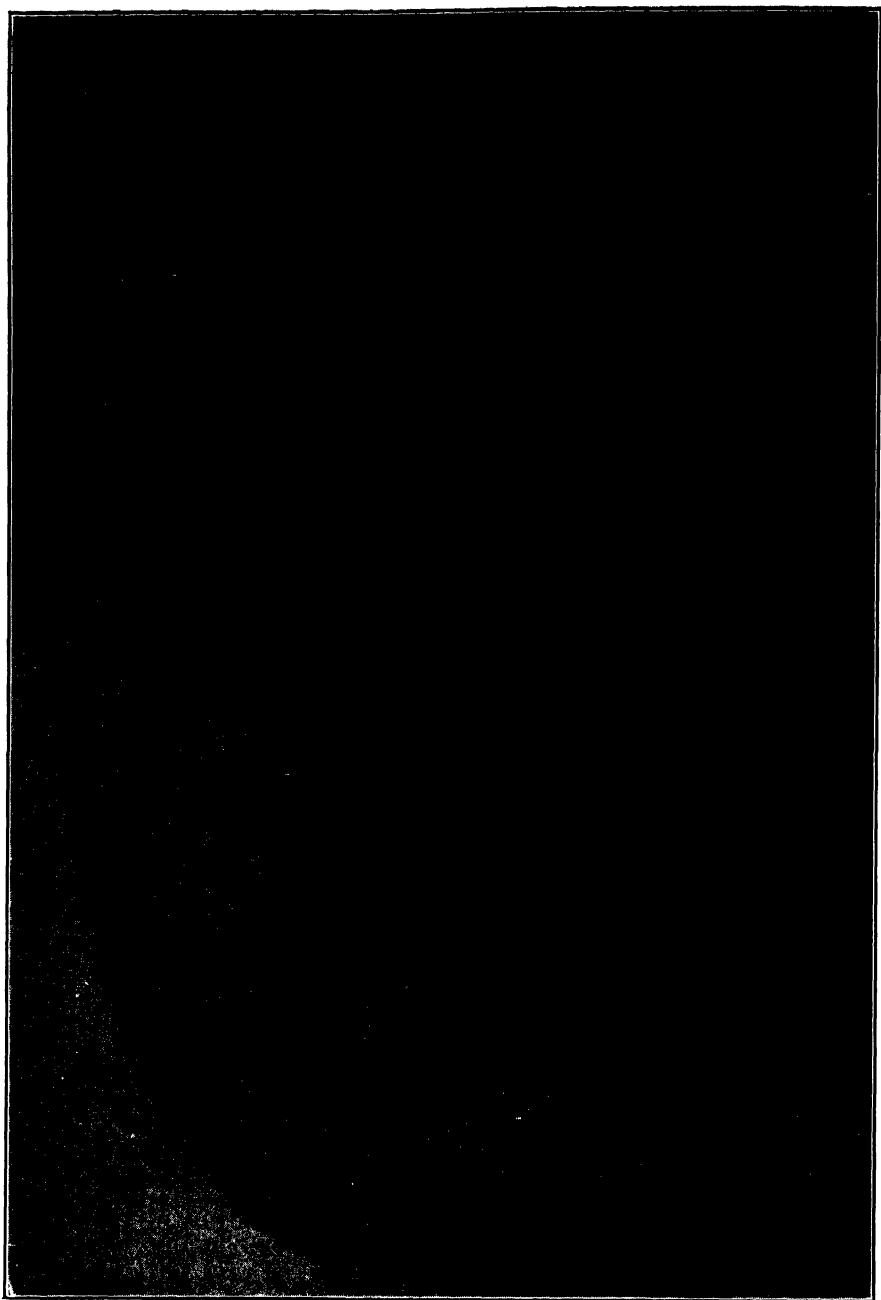
FIG 51.—INGOT K5. SULPHUR PRINT OF CROSS SECTION 20 CENTIMETERS FROM BOTTOM.   × 1.
Sulphur additions ½, 1, 2, 3, 4 and 5 min. after casting.
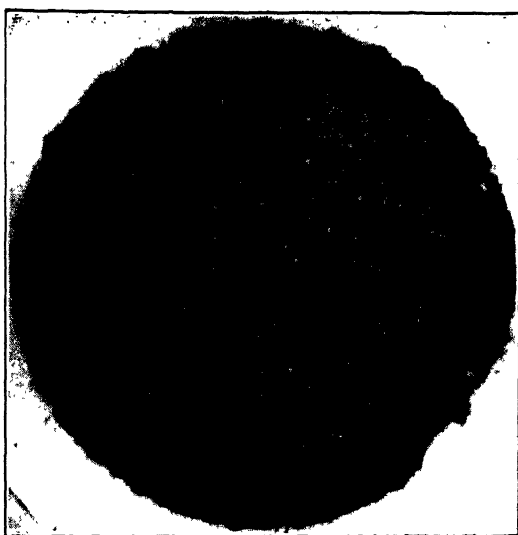
Fig. 52.—Ingot A. Large silicate inclusion, fine structure. × 1000.

Fig. 53.—Ingot A. Large silicate inclusion, coarser structure. × 1250
Primary (Mn,Fe)S in groundmass of (Mn,Fe)S, (Mn,Fe)O and silicate.

oxygen accumulate.   The surface layer solidifying without gas evolution may be extremely thin in some cases and rather thick in others, as will be seen in the following paragraphs.

FIG. 54.—INGOT A.   BIG SILICATE INCLUSION, DEFORMED, IN SEGREGATE AREA.
× 150.
    Manganese sulphide separated in surface zone of inclusion and in adjoining areas of the steel.
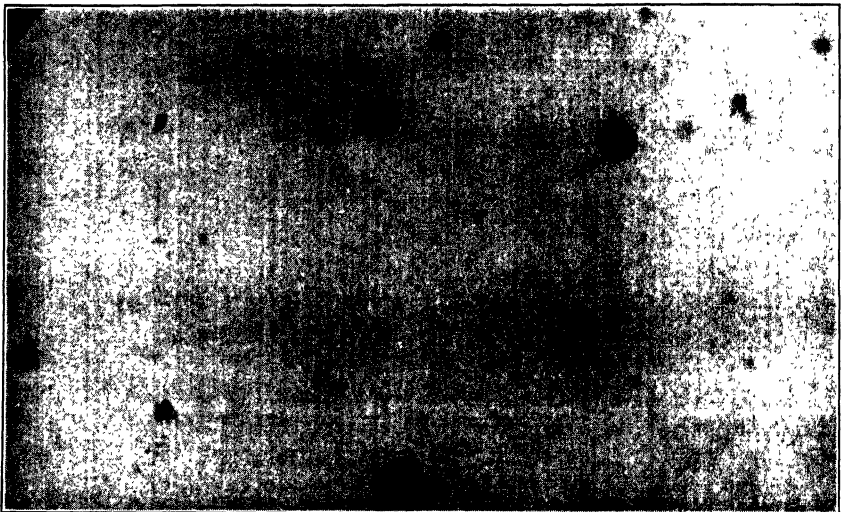
FIG. 55.—INGOT A.   SMALL SILICATE INCLUSIONS, SOME WITH MANGANESE SULPHIDE.
× 750.

The gas forms bubbles sticking to the solid steel as a consequence of the capillary forces, which may be measured by the surface tension. Carbon and oxygen will diffuse from adjacent regions of liquid steel, supersaturated with respect to the carbon monoxide, to the bubbles already formed, causing them to grow. At the same time the steel solidifies around the outer side of the bubbles (that is, the side toward the ingot surface), thereby forming pits or "bubble seats" in the solid wall.

When the size of a bubble exceeds a certain value the surface tension is insufficient to counterbalance the floating power and the bubble or part

Fig. 56.—Ingot A. Silicate inclusion, cruciform in section with shrunk manganese sulphide. × 1500.

of it will rise to the surface; a remainder of the bubble may be left in the "seat" mentioned. A great number of bubbles rising along the solid walls will set up a circulation current in the liquid interior of the ingot, upward in the outer part and downward in the axial part. This circulation current is characteristic of the rimming period and is essential for the segregation during this period.

While the top surface of an ordinary ingot is still open, the pressure in the bottom part exceeds that in the top part by 50 to 100 per cent. According to Herty et al.,[107] this should cause the gas evolution to be slower in the bottom part. Probably their conclusion is correct. Still, the relation between gas evolution and pressure is undoubtedly rather complicated, as will be explained later (p. 218).

The reaction between rising gas bubbles and the surrounding liquid steel will probably proceed very nearly to equilibrium, the total surface

of the bubbles being very large and the reaction rate in the liquid steel being generally very high.[93]   Thus, the liquid steel freed from its bubbles at the top surface may be assumed to be saturated with respect to carbon monoxide of atmospheric pressure. This liquid forms the descending part of the circulating current and when it arrives at the bottom end it is unsaturated with respect to the bubbles forming there. It will dilute the residual liquid present, hence the weight of gas evolved on solidification of a unit weight of steel in the lower part of the ingot will be further reduced.

The volume of a bubble containing a certain weight of gas will be 50 to 100 per cent greater in the upper part than in the lower part of the ingot. Also, the amount of gas rising through a horizontal section of the liquid interior is that dislodged in the whole ingot part below the section in question.

Hence, the volume of rising gas is very much greater near the top than near the bottom. Consequently the liquid-steel current is more rapid in the top part than in the bottom part of the ingot; that is, a rather great part of the stream lines do not extend into the latter part, and the movement in the liquid steel may be described as a ring vortex with a vortex line in the upper part of the ingot. This difference in speed may be accentuated in ingots that are narrow in proportion to their length, particularly big-end-up ingots.

Let us now consider the mechanism by which blowholes and some related structural features of the rim zone are formed. If the gas quantity is very small a bubble may grow at the same rate as the surrounding steel and no gas will be dislodged. Then the bubble will grow into an elongated blowhole. No current will be generated in the liquid steel, and there is no rimming action. This will occur in ingots of semikilled steel.

If the gas evolution is stronger a bubble may be partly or wholly dislodged, and this process will be accelerated by the current caused by the bubbles rising through the liquid. The details of this process are illustrated by Fig. 57. A bubble is assumed to adhere to the solid steel (Fig. 57a). The wall of solid steel grows inward and at the same time the bubble grows (Figs. 57b and 57c). The inward surface of the bubble retains its spherical shape while its outward part, now surrounded by solid steel and assuming the character of a blowhole, becomes tapered. The bubble is assumed to grow more rapidly than the wall of solid steel; that is, the part of the bubble protruding into the liquid steel becomes larger. When this part has reached a certain size, depending upon the velocity of the liquid metal current, it will be dislodged and form a rising bubble.

If it be postulated that movement is slow, or no movement exists, there will be enough gas left afterward to form a somewhat protruding

bubble (Fig. 57d_1). The next layer of steel solidified will form the beginning of a contraction of the blowhole (Fig. 57e_1) but new gas evolved will later change this into an expansion (Fig. 57g_1). It is in the nature of this mechanism that the growing blowhole assumes the shape of a surface of revolution with periodic contraction and expansion, the axis of which is at right angles to the interface where the bubble is seated. In this way rim holes are probably formed on continuous freezing from a mold wall during conditions of gas evolution and moderate or slow movement in the liquid metal. The fact that rim holes usually deviate somewhat upward from the direction postulated naturally follows from the deformation of the protruding bubble caused by the rising current of liquid metal. The deviation increases toward the top, probably owing to the increasing velocity of the metal current.
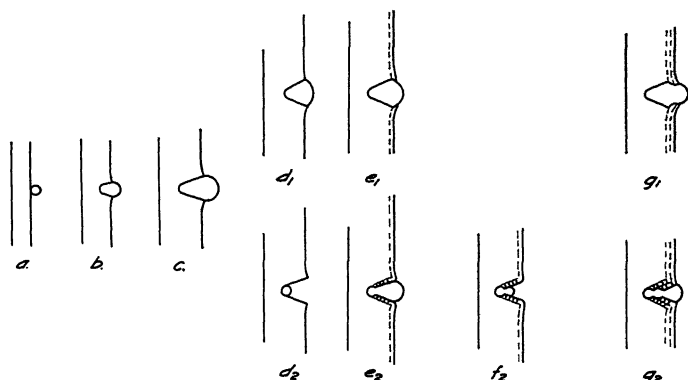
FIG. 57.—DIAGRAM SHOWING FORMATION OF RIM HOLE AND RIM CHANNEL.

If, however, after a rim hole has commenced to form, the metal moves very rapidly past the bubble, so much gas will be removed that the liquid enters the tapered blowhole (Fig. 57d_2). Next, a layer of steel will solidify on the tapered hole wall, the remnant of gas growing meanwhile so as to force the liquid out of the hole (Fig. 57e_2). Another rapid movement will again remove most of the gas (Fig. 57f_2) and the phenomenon repeats itself (Fig. 57g_2). It is suggested that *rim-hole contour lines* (Figs. 20, 25, 32, 37, 41) and *rim channels* (Figs. 9, 10, 20, 21, 28, 37) are formed in this way, in a periodic manner. It is noteworthy that rim channels have no tendency to deviate upward, which may be seen when rim holes and rim channels exist side by side. The explanation probably is that there is no protruding bubble that may be deformed. Rim channels near the surface of the ingot often show various directions, probably a result of irregular thickness of the freezing wall. It is not necessary that there be a continuous channel. After a tapered hole or seat has once formed, a bubble of such small size may remain at the bottom of the seat that the entering liquid freezes over it. A new bubble may then form

separated from the former one. Still, it may be that continuous channels of varying diameter are a common occurrence, although their continuity is seldom seen in a section. The contour lines seen in a section are usually rounded, obviously because they are not generally sectioned through their axes. The etching contrast that makes these lines appear is probably due to the rapid freezing of a layer of steel in contact with the walls of the blowhole, which had cooled for some time out of contact with liquid metal. It seems more difficult to explain how the so-called *arrow segregates* (Figs. 10, 20), indicated in Figs. $57e_2$ to g_2, are formed. Possibly, when the liquid suddenly touches the cooler hole walls, stresses are developed in the solidifying layer, which defórm it, and thus give rise to the separate segregate lines. The distance from the channel to which the segregates extend probably indicates the size of the hole from which the channel formed. Sometimes, "arrow pores" are seen (Figs. 10, 20), possibly also a result of the stresses suggested.

It has often been observed that adjacent rim holes show a common periodicity of contraction and expansion. In a region of similar pressure and freezing rate, the rim holes will grow at a similar rate and almost at the same time reach the size of bubble that cannot longer be carried by the hole. A temporary acceleration of the movement will then sweep away the surplus gas from all the bubbles, with the result that all rim holes in the neighborhood receive a contraction. From that moment the holes will widen at a similar rate until the bubbles reach a labile size again, the process thus repeating itself. Figs. $7b$, 8, $11b$, 12, $19a$ and 58 illustrate these features. Possibly the growth of two adjacent bubbles to such a size that they touch each other and coalesce sometimes is a decisive factor in causing the dislodgment. Fig. 58, among others, also illustrates the fact that the thickness of the freezing wall may be irregular.

It is well known that blowholes ordinarily are present in the lower part of the rim zone, whereas such holes are generally absent in the upper part.[40] The explanation of this fact as a consequence of movement caused by rising bubbles[51] is generally accepted. The presence of rim channels and hole-contour lines in the upper part of the rim zone confirms the explanation mentioned.

If the ingot height is decreased sufficiently no rim holes will be present even in the bottom end of the ingot.[85,91,98] Indeed, it seems as though the distance from the ingot top to the uppermost rim holes changes but slightly when the total height of the ingot is varied. Hence, it appears that a variation in the volume of gas rising from lower levels is less important than a variation in the volume of gas evolved at the level in question; that is, the effect of pressure on the volume of gas evolved from a unit quantity of steel seems to be great—too great to be explained as a result only of the corresponding difference in volume of a constant quantity of gas. If this estimation is correct the quantity of gas, by

FIG. 58.—RIM HOLES IN EARLY CLOSED INGOT IV, ONE-SIXTH FROM BOTTOM. AXIAL SECTION, UNPOLISHED, UNETCHED. ×4.

Synchronized contractions and expansions, blunt inner ends.

weight, must be considerably smaller in the lower part of the ingot. Presumably the circulation current has only slight, if any, influence during the first stage of solidification. Thus the conclusion is that an increase in pressure by 50 to 100 per cent will probably reduce the gas quantity evolved by more than the amount corresponding to the difference in the equilibrium conditions.

Let us now return to the moment when the gas evolution is just beginning. The bubbles have been described as forming at the surface of a wall of solid steel. This description is, however, only approximate. When the first layer is solidifying, before the gas evolution has started, the conditions are similar to those prevailing in a killed-steel ingot. Thin stems and branches of dendritic crystals grow into the liquid and segregating substances accumulate in the residual liquid in the interstices. After gas evolution has started there is, as seen from "bled" ingots, between the rim holes possibly present, an apparently solid wall growing with a rather smooth surface toward the liquid interior. This appearance is, however, misleading, since it may be concluded from deformation structures observed in this wall (the rim zone of completely solidified ingots) and from the "sweat" in the rim holes (p. 181) that residual liquid may be present in a rather large part of the wall at the moment when the ingot top is closed and the pressure begins to rise. The extent of the region in which residual liquid is present between the δ iron crystals depends on the magnitude of the freezing range.

The pressure inside a gas bubble is higher than in the surrounding steel because of the surface tension, and the difference is inversely proportional to the radius of the bubble. If this law held for infinitely small bubbles there would never form any bubble nuclei even at a high supersaturation. When a bubble is extremely small, however, its increase will be determined by probability laws.[60] The probability that a bubble nucleus will form in a certain volume of supersaturated liquid steel is proportional to the time available. Hence, if the solidification is very rapid no nuclei will form; that is, the gas evolution will be completely suppressed.

In the very surface layer of an ingot the rate of solidification will be extremely high, and for the reasons given the gas evolution will be suppressed there. In some cases this "chilled" layer is rather thick (as for instance in Fig. 36). When it has reached a certain thickness bubble nuclei form and may grow to rim holes. It might be supposed that from this moment on the gas evolution should approximately be determined by the equilibrium conditions. If the curve TUV in the Fe-C-O equilibrium diagram, Fig. 2 (p. 155), is reasonably correct the oxygen content of the solid steel should be very low. The actual oxygen content of the rim zone is, according to Table 2 (p. 192), much higher. The values reported are averages for the rim zone, with exception of the innermost and outermost portions.

Although gas is freely evolved at the growing wall, the conclusion seems inevitable that that gas quantity represents only part of the amount corresponding to full equilibrium being attained on freezing.

The explanation probably is to be found in the mechanism of freezing as already described. In the front layer of the wall, crystals grow, enclosing liquid in a proportion depending upon the magnitude of the freezing range of the steel. The enrichment in carbon and oxygen at the actual front is counteracted by the admixture of circulating liquid, and it may be roughly assumed that the thin liquid layer between the front crystals is thus kept in equilibrium with the gas. This effect, however, does not extend far back into the solid-liquid aggregate. As the latter gradually completes its freezing the carbon and oxygen contents of the enclosed liquid increase. Still, it is suggested that, with the exception mentioned later, no gas is evolved during this later stage of freezing; in other words, the average composition of a solid-liquid layer just behind the front remains practically unchanged during its subsequent freezing. This conclusion is supported by the high carbon-oxygen product found on analysis and by the absence in the structure of blowholes likely to have formed behind the front of the wall. Why the gas evolution is suppressed in spite of the comparatively slow freezing and fairly low strength of the solid structure must be left for future investigations to decide.

The exception mentioned refers to the evolution of gas from the liquid constituting part of the wall of rim holes and bubble seats. In this way the composition of a thin adjoining layer may be affected by diffusion.

The fact that the carbon-oxygen product obtained on analysis of the rim zone is considerably lower for ingot G (0.046 per cent C) than for ingots F (0.14 per cent C) and K (0.21 per cent C), as seen from Table 2, probably results from the narrower freezing range and thus more compact freezing structure of the former.

As mentioned, the quantity of gas evolved during the rimming period seems to be less in the lower part of the ingot than in the upper one. The corresponding ratio between the pressures is less than 2:1, for ingots of normal height. The gas quantity represents the difference between the average oxygen (or carbon) content of the liquid and that of the solid steel. According to our previous hypothetical but plausible assumption, as indicated in Fig. 2, the oxygen content of the solid steel is low; hence if it were doubled by a corresponding increase in the pressure, the gas evolution would be reduced very little.

Thus the influence of pressure on the gas evolution, if really as great as previously assumed, probably results from an increase in the deviation from the equilibrium conditions. An obvious result of the increase in pressure is that the concentration of carbon and oxygen in the residual liquid when gas evolution begins will be greater. That is, carbon and

oxygen are concentrated in more narrow interstices between the steel crystals, and their diffusion to gas bubbles already formed is impeded. Then, however, we come across the question again, why new bubble nuclei do not form in these narrow interstices. At the end of the solidification the potential gas equilibrium pressure will be very high here, probably some tens of atmospheres.

As mentioned, rimming steel usually contains small amounts of silicon; some part of it is dissolved and the rest is present as silica or silicate. During solidification part of the silicon in solution combines with oxygen, and if the oxygen content of the steel is low, as at relatively high carbon contents, the gas evolution may possibly be noticeably reduced. At usual manganese contents the liquid steel is not saturated with respect to the $(Fe,Mn)O$ phase; that is, the manganese will not have any influence during the first stage of solidification, if carbon monoxide is given off freely. The formation of oxide phase may, perhaps, be facilitated by manganese if the solidification is rapid enough to cause the gas evolution to be partly suppressed, the degree of suppression being thereby increased. Sulphur and phosphorus, if present in large amounts, might have a similar effect by increasing the quantity of residual liquid in the apparently solid wall.

The rim holes are separated from the outer ingot surface by a *skin* of sound steel. The skin must be sufficiently thick to withstand oxidation when the ingot is heated for rolling; if not, the product will show "roaks" or "seams." The skin may form in two different ways.

The assumption nearest at hand is that it forms by suppression of the gas evolution through "chilling" of the outer layer of steel (ref. 27, p. 149; ref. 88: "a thin outer skin of 'chilled' crystals," ref. 133). Really, in the ingots of the heat K previously described, and also in some other ingots of relatively high carbon content, the structure of the skin is clearly dendritic and hole-contour lines and rim channels are not present. Thus it may be concluded that in these cases the skin has solidified without gas evolution.

The ingots of heats A, B, C and D, the carbon content of which is about 0.08 per cent, are different, the skin showing clearly hole-contour lines (Fig. 13) and rim channels (not visible in the region reproduced in Fig. 13 but in Figs. 8, 15 and 16). That is, gas has been evolved when the skin solidified and its relative soundness is caused by removal of the gas bubbles, in the same way as they are removed normally by the "rimming action" in the upper part of the ingot. The formation of rim holes in the lower part of these ingots may be explained as a consequence of sufficient decrease in the gas evolution so that the bubbles are not removed. The decrease in gas evolution will be caused by the decrease in the rate of solidification as the solidified layer becomes thicker and by

mixing with the unsaturated steel descending in the axial part of the ingot interior.

The gas evolution may be so lively as to make the whole rim zone almost free from blowholes. In ingot G, with 0.046 per cent carbon, rim holes are present only in the very bottom end; rim channels begin close to the ingot surface (Fig. 28).

It is suggested that the rimming class of steel with respect to the formation of the skin may be divided into two subclasses. The types of skin will be described in the following pages as "chilled skin" and "rimmed skin." The low-carbon ingots described here belong to the rimmed-skin class; the ingots with relatively high carbon content to the chilled-skin class. Although the greater part of the rimming steel made at present undoubtedly belongs to the former class, steel of the latter class is probably made in sufficient quantity to justify the classification suggested.

An assumption near at hand is that a rimmed skin should form when the liquid steel is highly supersaturated with respect to carbon monoxide, and a chilled skin when the steel is only slightly supersaturated or unsaturated. The observed connection between carbon content and skin would then imply that the supersaturation is higher at low carbon contents. For instance, heat G should have been much more supersaturated than heat K, in spite of the addition of 0.02 per cent aluminum to heat G. The most plausible measure of the supersaturation is the difference between the equilibrium pressure of the liquid steel in question and the actual pressure. The equilibrium pressure, according to our assumptions, is proportional to the carbon-oxygen product. There seems to be no reason why the product should be greater at low carbon contents. This question should be decided experimentally.

Another assumption that should be tested is that the gas evolution is more easily suppressed at a certain supersaturation if the carbon content is high; that is, the oxygen content low. The silicon content of the steel, though low, may also have some influence (p. 199), more noticeable if the total oxygen content of the steel is not too great as compared with the oxygen that may combine with the silicon.

The rimmed skin will generally be thicker at carbon contents approaching that of the balanced composition, because of the great quantity of gas evolved when a unit weight of steel solidifies (p. 159); often rim holes may be completely or almost completely absent.

Probably there is a range of carbon content somewhere around 0.15 per cent in which the skin may be rimmed if the supersaturation of the liquid steel is relatively high and chilled if it is low. In this overlapping range a sufficiently thick skin may be obtained in two ways. If the skin is of the rimmed type, the supersaturation—that is, for a given carbon

content the oxygen content of the steel—should be high enough to prevent the bubbles from forming rim holes during a sufficient period. If the skin is of the chilled type the steel should be only slightly supersaturated or unsaturated, in order to delay gas evolution as long as possible without causing the steel to rise in the mold.

At an intermediate degree of supersaturation the skin will probably be rather thin. Heat F may be taken as an example of this kind. The structure of the skin is clearly dendritic in the lower end and hole-contour lines have not been observed here. At half the ingot height, however, hole-contour lines are visible in the skin outside the rim holes.

The *distance between adjacent rim holes* is very large as compared with the dimensions of the dendritic crystals that may form the outer part of the rim zone, as in the ingots from heats F and K (Figs. 23, 36, 41). The blowholes have sometimes been described as growing between "columnar crystals." It is more adequate to describe the crystals as forming between the bubbles seated on the freezing wall and growing in advance into the liquid. This is true, although the first nucleus of a bubble will probably develop in the interstices between dendritic crystals, as mentioned already. When once a bubble has formed, carbon and oxygen will diffuse from the adjacent liquid steel, thereby lowering the supersaturation and the probability of formation of new nuclei, and the extent of this diffusion will probably determine the distance between neighboring rim holes.

Sometimes the bubble parts of two growing rim holes will touch each other and unite, and in this way two holes may grow into one.

The top level, during rimming, changes under the combined influence of the following factors: (1) shrinkage on freezing lowers it, (2) a decrease in the volume of gas in the liquid lowers, an increase raises it, (3) formation of blowholes in the freezing wall raises it.

As is well known, a rim declining inward indicates that the rim zone contains few or no rim holes, a horizontal rim a moderate amount. If rim holes form in the greater part of the rim zone, the metal will rise above the original level and no rim, in the original sense of the word, will form.

Rising ingots are the result of slow gas evolution, which may be caused by high casting temperature, retarding the solidification of the outer layer; by presence of some silicon dissolved in the liquid steel, for instance, from working at a high temperature in an acid furnace or converter; or by a relatively high carbon content, causing the quantity of gas evolved to be small even if the supersaturation was rather great. The addition of aluminum to the liquid steel may cause rising, as is well known and has been demonstrated again in this investigation (pp. 167 and 178, ingot F3).

Boot-leg or *box-hat* ingots are obtained if gas is evolved at an excessive rate immediately on casting. The metal rises as a result of the rapid growth of the numerous bubbles, which thus occupy a considerable part of the volume. The gas evolution will soon slow up and the liquid, freed from the greater part of its bubbles, will rapidly sink back to a lower level, leaving in the upper part of the mold only thin walls. The cause of the rapid gas evolution may be high supersaturation with respect to carbon monoxide or a low casting temperature; it is rather difficult to separate these factors (p. 195). The first ingots of a heat may rim normally, and the last ones tend to form boot-leg ingots, probably because the casting temperature falls. At carbon contents about 0.05 per cent, the tendency to boot-leg formation will be rather great because both solidification and the elimination of a certain degree of supersaturation—as expressed in terms of carbon-oxygen product—involve the evolution of great gas quantities (p. 147).

The influence of the *casting speed* will depend on the type of skin. During casting a layer of steel solidifies close to the mold wall, and the outer part of this layer always solidifies under low pressure. In the case of a *rimmed skin* its thickness may be increased by slow casting, facilitating the gas evolution at a time when rim holes might otherwise have begun to form. In the case of a *chilled skin* slow casting may reduce the thickness of the skin in the lower part of the ingot, the gas evolution beginning at a higher rate of solidification when the pressure is lower. If in the latter case the ingot is cast extremely rapidly the gas evolution will begin in the upper part and rim holes may form there, the skin being thin on account of the low pressure. At an intermediate casting speed, the gas evolution may begin at the same time in the lower and upper ends, and the bubbles rising from below may aid in removing the bubbles in the upper part, thereby eliminating the trouble of a thin skin. The skin may even be of the chilled type in its lower part, and of the rimmed type in its upper part, because of gas bubbles rising from below before casting is finished.

It has sometimes been stated that *bottom-casting* will give a thicker skin. According to Wohlfahrt this effect is rather due to the slow casting generally associated with that method. If the steel is of the strongly gas-evolving type a well centered falling stream will tend to accelerate the upward movement at the mold walls and thus assist in forming a thick skin, whereas bottom-casting would tend to have an opposite effect.

During the rimming period, the circulating steel may be *oxidized by the air* at the open top surface, and also through spark particles falling back into the steel. Judging from observations made by Helmer[139] such oxidation may noticeably affect the gas evolution. It was found that when the mold top was covered temporarily with a plate the metal rose.

When the plate was removed the gas reaction and circulation increased and the normal level was again established.

Agitation of the mold during rimming, as described on p. 185 (ingot I Fig. 31) will assist in producing a sound rim zone. It may cause additional segregation, depending on the manner in which it is carried out.

The structure ordinarily formed during the early period of rimming —as far as we have succeeded in developing it—is either dendritic or rather indistinct with a certain amount of hole contour lines, but always fine. At a certain distance from the surface the structure usually begins to change and to resemble a globular structure that gradually becomes coarser, although not as coarse as in the interior of the ingot. Hence it may be concluded that crystal nuclei have commenced to form in the liquid metal, a phenomenon favored by the continuous agitation. The crystals grow in number and size and the moving mass shows signs of becoming viscous. It might be that its "scrubbing" action on the protruding bubbles is thereby increased so as to stop the growth of the rim holes. At all events, their growth is usually discontinued at a certain depth before rimming is completed. Their inner ends ordinarily contract to a rounded point, sometimes succeeded by repeated hole-contour lines (Figs. 41, 43). The inner part of the rim zone is then free from holes, but may contain rim channels.

As the moving mass grows thicker, the rim at the top begins to close. After it has closed some gas will accumulate under the crust, the pressure will gradually rise, bubbles evolved at the freezing wall will adhere and grow only as fast as shrinkage permits, and the movement will virtually cease. The increasing pressure may break the top crust, and the expanding bubbles may rise and start a rapid movement temporarily. Perhaps this process is repeated. After this has happened for the last time, a set of bubbles will form that will constitute the *intermediate holes*.

The closing of the ingot top is generally accelerated in the later stage by placing a cooler plate or *cap* on the ingot top. Thereby the repeated breaking through of the top crust, causing "nigger heads" to form, is prevented. A really early closing, however, is possible by means of a firmly attached cover, as used for ingot K1 in this investigation. In most cases when early closing is planned, molds with only a small top opening are used.

It may be supposed that the composition of the steel will affect the formation of the top crust. If the temperature range of solidification is great the top crust will probably only slowly become strong enough to resist the increasing pressure. The range of solidification will be great if the sulphur and phosphorus contents are high. As to the carbon content, the balanced composition corresponds to the smallest solidification range. If this line of reasoning is correct and the effects assumed

are not counterbalanced by other effects of the substances mentioned, for instance on the gas evolution, troubles in the formation of the top crust should occur rather seldom in steel with a balanced composition and low sulphur and phosphorus contents.

COMPOSITION OF RIM ZONE

The schematic diagram of Figs. 5 and 6 will now have to be adjusted, due account being taken of several factors that may affect the composition of the steel freezing during the rimming period.

It will be assumed that the liquid metal is saturated; i.e., in equilibrium with the gas phase $CO(+CO_2)$. The following factors will have to be considered:

1. The first layer of steel frozen in contact with the mold walls may not give off any or all of the gas it should were equilibrium reached; in other words, supercooling of the gas reaction may occur.

2. When the δ iron crystals grow the mother liquor may remain between the growing crystals to a greater or lesser extent, depending upon the efficiency with which it is carried away by the moving metal and replaced by metal from the interior. If no gas is given off in the first stage of freezing, there will be little or no "dilution" effect from that source.

3. Assuming that rapid gas evolution and circulation of the metal have been established, the dilution effect on the outer layer of liquid will have as its counterpart a gradual "concentration" effect on the main mass of liquid metal, and, in consequence, the composition of the solid solution forming will also be more and more concentrated. The terms "dilution" and "concentration" as used here for the liquid metal, when gas is freely given off, should be qualified by the statement that they apply to phosphorus, sulphur, etc., but that of the two elements carbon and oxygen one changes in reverse direction to the other, owing to the shape of line PQR (Fig. 2). Only for the balanced composition both are unchanged.

4. Mother liquor is enclosed between the growing dendritic crystals and also when free crystals become attached to the wall. As discussed on p. 218, this mother liquor will freeze without giving off gas, thus causing the carbon and oxygen contents to be higher than the equilibrium values on curve TUV. Toward the end of the rimming period the circulation will slow down and in consequence the proportion of mother liquor enclosed will probably increase, thus raising the average carbon and oxygen contents. The freezing of this mother liquor will not be completed until some time after the top is closed. The increased pressure will then prevent gas from being evolved in the inner part of the rim zone, although carbon and oxygen may reach high values.

To evaluate with any accuracy the effect of these various factors on the composition of the succeeding layers of the rim zone is, of course, impossible in the present state of our knowledge, but an attempt will be made to demonstrate their resultant trend.

To begin with, let us take the case of a binary alloy passing through its freezing range. If the metal is quiet and the rate of freezing is rapid enough to prevent major diffusion in the liquid in front of the growing crystals, the mean composition of the succeeding layers of the solidified alloy will be constant and equal to the composition of the original liquid. If, however, the liquid circulates rapidly enough, and if diffusion in the solid is slow, the layers first formed will be purer, the ones later formed increasingly impurer than the average, in respect of the component lowering the melting point. The freezing point is lowered continuously, and the composition of the layers approaches the solidus curve in proportion as the movement is efficient in mixing the liquid.

In Fig. 59, P represents the original liquid metal, having a higher carbon content than the balanced composition. We assume that the first layer solidifies quietly without gas evolution. Its mean composition will then be P. While the next layer freezes some gas is given off, which brings the mean composition to A_0. At the same time, however, some circulation may be caused by rising bubbles. This will move the mean composition toward the solidus, roughly along the arrow to B_0. The general mixing will bring the composition of the main liquid to P_1. The following layer will freeze under increased gas evolution, thus bringing its mean composition to A_1 from where the increased circulation will displace it to B_1, and so forth: B_2, B_3 . . . The direction AB in each case results from the partial displacement of mother liquor of high carbon and oxygen content, by liquid from the main mass. The last layers will include some mother liquor that will have no opportunity to give off gas, since it will freeze after the top has become closed and the pressure has increased. That will displace the composition from C_n towards P_n to B_n.

The trend of the carbon and oxygen concentrations in the succeeding layers of the rim zone, provided no gas is given off at first, will then be as follows: The skin near the surface will have the same composition as the cast liquid metal. Then carbon and oxygen will decrease together to a certain depth, where carbon will reach a minimum and start to increase again, oxygen still decreasing. At a still greater depth oxygen may reach a minimum and start to increase somewhat. In the main liquid, carbon will increase and oxygen decrease constantly. The mass of metal remaining to form the center of the ingot would be a mixture of liquid P_n and crystals B_n having the same composition D_n.

If gas is evolved immediately on freezing, the first layer frozen will have a composition corresponding to a point on the B curve removed from

P; in other words, there will be little or no fall in carbon content from the surface inward.

A liquid metal Q of lower carbon content than the balanced composition will form a rim zone varying in carbon and oxygen along a curve like QEF. In this case oxygen will first reach a minimum and then possibly carbon. In the main liquid, carbon will decrease and oxygen increase during the whole rimming period. If, however, gas evolution sets in at the start, as usually happens in steels of this kind, the first part of the curve will be missing.

If the metal has the balanced composition, carbon and oxygen will segregate together and reach their minimum simultaneously.

As to the elements not taking part in the gas reaction, phosphorus, sulphur and manganese, their distribution follows in principle what has been said above about a binary alloy. Owing to the slow circulation in the beginning, the dilution effect will at first be slight. The concentrations will decrease with the accelerated movement to a minimum and then rise often beyond the original values.

At what depth the respective minima are reached cannot be deduced from the qualitative reasoning presented here.

The hydrostatic pressure should have the effect that carbon and oxygen at a certain depth beneath the surface, in the lower part of the ingot, will be higher than at the same depth nearer to the top. The slower circulation postulated in the bottom part should cause a smaller dilution effect there than at the top.

These two conclusions are not, however, borne out by the curves in Figs. 47 and 48, for unknown reasons. Otherwise, the trend of the curves in Figs. 47 to 50 agrees on the whole with the conclusions drawn from theoretical reasoning. For instance, the concentration minima in the rim zone of the rising ingot F3 (Fig. 49) that may be assumed to have frozen under less rapid movement than ingot F1, are higher than in the latter (Fig. 48). The fact that carbon decreases through the whole rim zone of ingot G with 0.046 per cent carbon (Fig. 50) agrees with case Q in Fig. 59.

The oxygen distribution found in ingots F, G, and K (Table 2) is particularly interesting. The falling values in the rim zone toward the top (with the exception mentioned on p. 192) agree well with the postulated effects of hydrostatic pressure and movement during freezing. The tendency toward low values in the core, as compared with those of the rim zone of ingots F and K, at first surprising, may be explained as follows: Above, in Fig. 59, the mean composition of the liquid with suspended crystals, which will form the core of the ingot, was for an ingot of higher carbon content assumed to be D_n. It is conceivable that the mean composition of the part of the rim zone that was analyzed is G, which has a higher oxygen concentration than D_n.

Freezing after Top Is Closed

At the moment when the top surface is finally closed the interior of the ingot normally consists of a mass of liquid metal mixed with numerous small crystals, the mixture on account of the preceding circulation having a fairly uniform temperature and composition. A set of bubbles is probably attached to the inner surface of the rim zone, where they remain because the previous movement in the crystal-liquid mixture is subsiding, this in its turn following from the fact that from now on the volume of gas evolved is determined mainly by the shrinkage. A temperature gradient is now soon established in the outer zone of the interior mass. In this zone freezing proceeds and some gas is evolved: the "intermediate bubbles" grow under increasing pressure.

The rim zone, if free from holes, is unaffected by the increased pressure. If, however, as often occurs in the lower part of the ingot, rim holes are present, the innermost portions of the hole walls, being often fairly thin and probably still containing some mother liquor, will yield under increased pressure. There will be an upsetting effect—*upset structure*—and probably a tendency to distortion. The holes that are filled by gas of lower pressure will be compressed, from the inner point and sideways, and a sweat of numerous droplets of mother liquor may be squeezed onto their surface. On account of the transverse compression a certain longitudinal ridge effect in the arrangement of the droplets will be produced. This process will apply to the inner, hotter part of the blown rim zone, often to the greater part of it. If the inner points of the rim holes are surrounded by a sufficiently mobile aggregate—or, after early closing, by an aggregate consisting mainly of liquid—a quantity of this will be forced into the hole this way, forming a blunt-end *hole-point segregate*. Under the increased pressure the liquid may perhaps dissolve some gas. The irregularly deformed shape of the inner ends of rim holes is illustrated in Figs. 23, 58, upset structure in Figs. 24, 30, 36, hole-point segregate in Figs. 36, 37, 43, 44, 58, and rim-hole sweat may be discerned in Fig. 58.

In describing the structure of the center portion of the ingots examined, references have been made to compressed holes, upset structure, blow-hole segregates and symmetrical deformation lines, and the conclusion was reached that during the freezing of this portion, from the rim zone inward, and often from one end of the ingot toward the other, the pressure is continually growing, blowholes formed at an earlier stage being afterward compressed, as new blowholes are developed at a higher pressure elsewhere. We will now consider the possible theoretical implication thereof.

As already mentioned, shortly after the top has closed a temperature gradient will be established in a zone next to the rim zone. Freezing

proceeds throughout this zone, the crystals growing and the mother liquor becoming enriched in carbon, oxygen, and other solutes. The accompanying shrinkage allows more gas to be evolved. The gas given off comes from the outer part of this zone, which may be called subzone 1, because the enrichment of the liquid and the consequent pressure of carbon monoxide is greater there, the freezing of the inner part of the zone proceeding at present without gas evolution. If it were possible for the gas to stay entirely within subzone 1, where it is evolved, freezing would be expected to continue inward in the manner
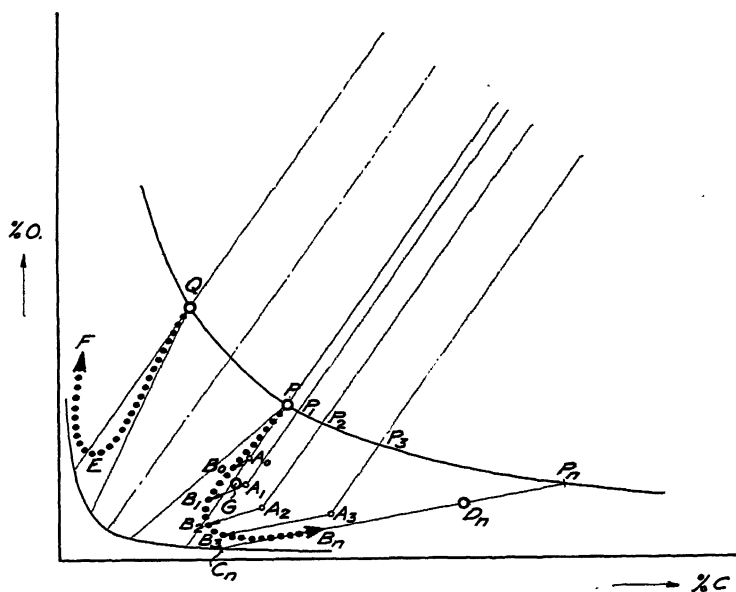
FIG. 59.—COMBINED EFFECT OF MORE OR LESS COMPLETE GAS REACTION AND CIRCULATION MIXING ON COMPOSITION OF SUCCESSIVE LAYERS OF RIM ZONE FOR HIGHER AND LOWER CARBON CONTENT OF METAL.

indicated with gas evolution in subzone 1 going on only until subzone 2 had reached the same carbon monoxide pressure as subzone 1. This would be possible before subzone 1 was wholly frozen, although the former would always be hotter, because the liquid of the latter, in giving off gas, would lose some carbon and oxygen and, consequently, its carbon monoxide pressure would be overtaken by that of subzone 2, where no gas has been evolved. In this manner, it might be argued, a freezing zone would travel inward through the central region, blowholes being successively formed in an outward subzone, only to be later compressed. The pressure would rise rapidly at first as the carbon monoxide pressure of the external subzone would reach a high value corresponding to the composition of its enriched mother liquor, and then more slowly as the final carbon monoxide pressure in each subzone would

be slightly higher than in the preceding one. At any moment, the pressure in the gas-evolving subzone would be transmitted to the internal mass enclosed by it. The fact that gas of low pressure, in the form of the intermediate bubbles, was already present at the start, would make the initial pressure curve less steep, since the first gas given off would join those bubbles.

In this reasoning, however, no account has been taken of the size of blowholes formed. The assumption that the gas would remain within the subzone where it is given off is evidently not true, judging from the observations made. It is likely, under ordinary conditions, that any bubble formed during this period, including the intermediate bubbles, before it is compressed, reaches a considerable size, greater than the width of the gas-evolving zone. The bubble, having a pressure determined by the composition of the liquid in the gas-evolving zone, penetrates to a depth where the liquid has less carbon monoxide pressure. The consequence ought to be that a reaction sets in, whereby gas evolved somewhere in the outward end of the bubble is continuously being dissolved by the surrounding liquid in the inward portion, particularly at the inner end, where freezing is least advanced. The transport of carbon and oxygen through the blowholes inward during freezing of central portions will produce a corresponding segregation of those two elements, which will tend to delay the freezing of the axial region and cause the pressure curve to be less steep at the beginning and steeper at the end.

It might be expected that this process would favor the preservation of the bubbles once formed and make them grow all the way to the axis, since, by increasing the carbon and oxygen contents in the mass surrounding those ends, their inner ends would be predisposed to evolve gas in preference to other regions of the same temperature. This arrangement of the blowholes may, in fact, be seen in the top of the early closed ingot K1 (Fig. 36), where freezing took place in liquid containing few crystal nuclei, and has also been often observed in the top portion of semikilled ingots. Under such circumstances there would be no deformation from within—no upset structure. This arrangement of blowholes and the absence of deformation are, however, in rimming-steel ingots an exception. Generally, the core holes are well distributed and show signs of having been compressed and deformed, with resulting formation of segregate. It is suggested that, in the earlier stages of freezing of the core, downward convection currents and falling crystals may interfere with the growth of the blowholes. Furthermore, as the crystals grow the diffusion in the mother liquor will become more restricted, and regions between and at a distance from the blowholes will become supersaturated and form new blowholes that may outlive the ones formed earlier. At a later stage, the growth of the crystals into one continuous mass will further promote these effects.

The ideas submitted here, in an attempt to explain the various details seen in the structure of the core, may be correct or not, but it cannot be doubted that all the evidence is consistent with the conception that, normally, freezing proceeds inward under evolution of gas at a growing pressure whereby blowholes formed earlier are more or less compressed and the aggregate between them deformed. Blowhole segregates with no visible blowholes attached may occur because the blowhole may be situated outside of the section but it might also happen that blowholes are wholly compressed, the gas being redissolved.

The maxima in carbon, phosphorus and sulphur concentrations beyond the intermediate holes found in ingots F1 and F3 (Figs. 47 to 49) and also found by Swinden[127] are probably due to the accumulation of mother liquor in front of the freezing wall during the period when the top is beginning to freeze over and, in consequence, circulation is slowing down, also to the effect of blowhole segregates common in this zone (Figs. 21, 27b), sometimes forming a continuous layer (Figs. 43, 44). The absence of a similar maximum in carbon in ingot G (Fig. 50) may be considered to confirm the theoretical conclusions given above for the composition of the mother liquor in a steel of lower carbon content than the balanced composition.

Owing to the greater pressure in the lower part of the ingot, the gas-evolving zone will there be associated with a higher total pressure, a liquid richer in carbon and oxygen and a lower temperature than in the upper part. Therefore, this zone does not coincide exactly with an isothermal but is somewhat nearer to the surface in the lower part.

During the period when the interior contains crystals suspended in the liquid but not yet forming a continuous mass, a slow sedimentation of the crystals is believed to go on. This would cause the lower part of the central region to be purer and the upper part impurer than would otherwise be the case. If, according to the idea expressed by Dickenson[61] for killed ingots, slag inclusions are carried down by the falling crystals, the oxygen content would hereby be affected in the opposite direction to the one caused by the sedimentation of crystals in itself. The distribution of carbon, phosphorus and sulphur in the central region of ingot F1 (Figs. 47 and 48) and the reversed oxygen distribution in the same ingot (Table 2), as well as various data given in the literature agree with those assumptions.

The freezing process converges toward a point, generally the hottest part of the interior, the "heat center" according to Benedicks and Löfquist (ref. 75, p. 226). We prefer, however, the term "freezing center," because segregation from sedimentation and difference in hydrostatic pressure may cause the two centers not to coincide. In the freezing center, the last stages of freezing and the gas evolution will take place in an aggregate where the crystals have to a great extent grown

together. The gas finally evolved will, therefore, tear this coherent mass of crystals apart, thus forming a blowhole of irregular outline. At the same time part of the mother liquor flows together into a marked segregate (Figs. 17, 18, 26, 27, 40).

In the early stage of freezing of the interior, the region enclosed within the gas-evolving zone is composed of a mobile aggregate of uniform pressure—disregarding the hydrostatic part of the pressure. As freezing proceeds inward the gas-evolving zone traverses layers of increasing compactness. The rigidity of the enclosed region will, at a certain stage, reach a point where pressure differences will not be transmitted rapidly enough for a uniform pressure to be established. Different parts of the ingot may then, to some extent, freeze independently of each other. If the pressure in the gas-evolving zone, and therefore in the enclosed region also, mounts faster in one end of the ingot, the pressure gradient will cause an axial displacement of the more or less coherent aggregate, with result-ing symmetrical deformation lines. This presupposes, of course, that blowholes in the region of lower pressure will be compressed at a corresponding rate.

As an example, a big-end-up ingot having rim holes in its lower half (ingot F2, Fig. 18), may be chosen. In the period when the interior assumes a certain rigidity, owing to the heat-insulating properties of the rim holes, the freezing will proceed, and the pressure grow, faster in the upper part, thus causing a deformation downward noticeable as sloping lines in the layer adjoining the intermediate holes (cf. Fig. 22, external deformation lines, p. 179). In the next stage, however, owing to its smaller mass, the lower part will freeze faster, and its pressure will exceed that of the upper part. Thus, a deformation upward sets in (Fig. 22, intermediate lines). Finally, a freezing center will be established near the top and the still higher pressure reached will cause deformation downward again (Fig. 22, system of lines near axis). In Fig. 18b this sequence of deformation lines may be seen on the sulphur print about halfway up the ingot. All the time blowholes are formed in the temporary region of pressure maximum. Similar symmetrical deformation lines, usually less complicated, will be seen in Figs. 7a and 7c, 15, 16, 19b, 35b, 40b, 42. The deformation lines along the axis always point away from the final freezing center, with its irregular blowhole and segregate, whether this is situated in the lower part (Figs. 7, 15, 16) or in the upper part (Figs. 19b, 35b, 40b, 42).

The presence of long, irregular blowholes with segregates and cracks along the axis in ingot G (Fig. 27) points to the conclusion that the freezing center of this ingot extended from about 0.25 to 0.9 of the ingot height; in other words, it solidified practically simultaneously along this part of the axis.

The *final pressure* in the solidified ingot will depend on several factors:

1. Composition of the steel:

a. A low carbon content means a lower final pressure. The liquid will reach the oxide line at a lower carbon content (Fig. 2).

b. The presence of manganese has a similar effect, since oxide will begin to separate at a lower oxygen content (the deformation lines in ingot B (Fig. 11) are less marked than in ingot A (Fig. 7), C (Fig. 15) and D (Fig. 16)). If it be assumed that the last parts of residual liquid contain 0.5 per cent carbon, the pressure calculated is 50 atmospheres if no manganese is present and 25 atmospheres if the manganese content is 0.4 per cent.

c. An aluminum addition *per se* will cause oxygen to be removed. Thus, less carbon will be consumed in gas evolution and more carbon should ordinarily remain in the liquid at the time of closing. This would lead to a greater final pressure.

2. Early closing will increase the final pressure by retaining more carbon and oxygen in the interior of the ingot (ingot K1, Fig. 35*b*).

3. Conditions favoring diffusion in the solid phase, such as slow cooling, may be expected to restrict the increase of carbon and oxygen in the liquid and thus to limit the final pressure at a lower value.

Some effects of *early closing* of the ingot top, as observed in ingot K1, have been described on pp. 179 and 182. The rim zone is comparatively thin, as seen in Figs. 35 and 40; this is an obvious consequence of the interruption of the rimming process.[52] The major part of the core is free from blowholes and its structure is rather similar to that of a killed-steel ingot. The following explanation of this remarkable fact is suggested.

After the closing of the ingot top the gas evolution was retarded by the increasing pressure. The sloping segregate lines previously described and explained (p. 182) indicate that gas was evolved at the inner boundary of the solid wall, even in the lower part of the ingot. Because of the early closing the pressure increased to a rather high value while there were still only few free crystals suspended in the main mass of liquid steel. Under the quiet conditions then prevailing the suspended crystals settled in the liquid, thus gradually building up a deposit of relatively pure crystals with a small amount of residual liquid in the interstices. As a consequence the liquid moved upward and the average content of carbon, oxygen, and other segregating elements became greater in the upper than in the lower part of the ingot. The cooling in the lower region being slow, the composition within the crystals would be equalized to a considerable extent by diffusion and the residual liquid in the deposit probably solidified without its carbon-oxygen product reaching the value necessary for gas evolution at the existing pressure.

Thus it may be explained that after a certain stage of solidification of the core gas was developed only at the top. The bubbles formed here have grown into elongated blowholes pointing toward the freezing center, probably because the quantity of free crystals present here was small as a result of the sedimentation and did not interfere with the continuous growth of the wall and its blowholes.

Obviously, V-segregates are due to deformation caused by a pressure gradient, when freezing in its later stages proceeds along the axis. In a killed-steel ingot, the pressure is continuously being reduced on the low-pressure side, and the amount of deformation is largely determined by shrinkage. In a rimming-steel ingot like ingot K1, the pressure is continuously being increased on the high-pressure side, and yielding of blowhole regions will increase the amount of deformation.

The effects of *delayed closing of the top* have already been dealt with in connection with the description of ingot K4 (Fig. 46, p. 207). Comparing this ingot with ingot K1 (Fig. 35, p. 196), it may be concluded that an early and efficient closing of the top of a rimming-steel ingot may be utilized to form a central region, the major part of which is practically free from local cavities and segregates, whereas delayed closing means a blown central region, which may contain segregates along the axis.

SLAG INCLUSIONS AND INGOT SCUM

Turning to the subject of inclusions, the following may be stated. In the ternary system Fe-C-O, if no oxidation took place during rimming, oxide inclusions might form in the external layer of the rim zone in consequence of suppressed gas evolution, but as soon as gas is freely evolved no oxide, or very little, would ordinarily form until some time after the top had been closed and the liquid under increasing pressure had reached the oxide solubility line (Fig. 2). In the presence of manganese in ordinary amounts, the same would hold true, but the oxide in the central region would form earlier. The small quantity of silicon present will probably be largely oxidized before casting and, of the remainder, oxide will be continuously formed during cooling, the inclusions formed consisting mainly of MnO, FeO and SiO_2. When the oxide solubility line is reached, greater quantities of oxide of lower silica content will begin to form.

Oxidation during rimming may cause the formation of large oxide (silicate) drops; also, remnants of furnace slag and eroded ladle lining and runner bricks will probably form large inclusions.

The analyses of ingot scum recorded in Table 3 (p. 195) show that furnace slag and lining material formed part of the mass separated. The change in composition is consistent with the view that oxidation from the air during rimming also contributes to the slag formed, the increase in manganese and decrease in iron content following from the change in

metal-slag equilibrium with falling temperature and from the growing manganese content of the liquid metal.

Sulphur, in the amount commonly present—free-cutting steel is not considered here—will be in solution in the liquid metal at the time of casting. During freezing, the mother liquor will be gradually enriched in sulphur and sulphide will appear in two ways: (1) the oxide (silicate) phase will contain a certain amount of sulphide in solution, which during further cooling will be thrown out as a separate phase (Figs. 53 to 56); (2) at a certain stage of enrichment, sulphide separates from the mother liquor (Fig. 54) as in killed steel.[36] In the cases investigated, there was enough manganese to form manganese sulphide.

REACTION BETWEEN GAS IN BLOWHOLES AND SURROUNDING SOLID STEEL DURING COOLING

The gas collected by Müller from blowholes in his drilling experiments[6,8] consisted mainly of hydrogen, and its carbon monoxide content was very low, whereas that of the mold gas was rather high. Howe, discussing these results (ref. 27, p. 142), concluded that the gas forming the blowholes had a fairly high content of carbon monoxide, which was reabsorbed during the cooling of the ingot. It is also a well-known fact that the surface of blowholes, particularly those in the inner part of the ingot, sometimes is discolored.

An attempt will be made to discuss the possible reactions that may take place during cooling between the gas enclosed in a blowhole and the surrounding steel, on the basis of the tentative Fe-C-O equilibrium diagram put forth. The conclusions, of course, will be only qualitative.

Among the boundary surfaces of the δ-iron single-phase space in the Fe-C-O diagram (Fig. 2), two are of particular interest for the present discussion. The oxide saturation surface, starting from the curve *ETL* on the solidus surface, rapidly retreats toward lower oxygen concentration with decreasing temperature, as indicated by the saturation curve in the Fe-O diagram to the left in Fig. 2. The equilibrium with $CO + CO_2$ is represented by a surface extending from the curve *TUV*. Probably this surface is approximately parallel to the temperature axis, just as the corresponding gas saturation surface of the liquid steel. Of course, the deviation of the gas equilibrium surface from the vertical direction may become noticeable at low temperatures. Its position depends on the pressure. These two saturation surfaces of the δ iron intersect along a sloping curve, extending from *T* toward lower temperature and oxygen content and higher carbon content. The relative positions of the two surfaces are indicated in Fig. 60.

As already pointed out, the pressure of the gas (mainly $CO + CO_2$) within a rim hole, on freezing, will be approximately the sum of one atmosphere and the hydrostatic pressure. The gas will be approximately

in equilibrium with the surrounding steel. On cooling, the following changes affecting gas-metal equilibrium may take place: (1) compression of the hole from the high pressure developed in the interior of the ingot, (2) thermal pressure fall, (3) allotropic transformation in the steel, and (4) separation of oxide from the steel after the saturation surface has been passed.

A change making the actual gas pressure less than the equilibrium gas pressure of the metal (such as item 2) will cause the latter to give off carbon and oxygen to form more gas. A change in the opposite direction (such as items 1 and 4) will cause the gas to oxidize and carburize the steel—gas will be "absorbed." Regarding the change in oxygen solubility at the A_4 and A_3 transformations, too little is known to justify any conclusions. Roughly, it may be said that the compression mentioned may cause the steel to absorb some carbon and oxygen at high temperatures, that at a lower temperature oxide will be separated from the steel, and that the gas will oxidize and carburize the steel surface. A thin film of oxide will probably be formed and the carbon may be dissolved in the steel, form cementite or be deposited as free carbon, depending on conditions. Because of the small gas quantity involved, any oxide film formed on the wall of a rim hole will probably be too thin to be visible.

FIG. 60.—SECTION PARALLEL TO TEMPERATURE AXIS THROUGH Fe-C-O DIAGRAM FROM Fe TOWARD CO. (1) One-phase space of liquid steel at ordinary pressure; (1 + 2) same as 1 at a high pressure; (3) one-phase space of δ iron at ordinary pressure; (3 + 4) same as 3 at a high pressure.

The last portions solidifying in the wall of a core hole will have such a high oxygen content that oxide is formed. The gas pressure and thus the gas quantity will be high. On cooling, the formation of an oxide skin will begin immediately and proceed as described before. Thus the oxide skin of a core hole will be thicker than that of a rim hole; still, the quantity of carbon and oxygen in the blowhole gas is always minute and the skin may be visible occasionally as a discoloration of the blowhole surface.

The presence of manganese in the steel will not alter these reactions fundamentally. The oxide saturation surface will be displaced toward lower oxygen contents. The pressure of the gas in a core hole will be lowered and thereby the thickness of the oxide skin decreased.

Accumulation of hydrogen in the blowholes has been discussed already (p. 151).

SUMMARY

The results of an investigation into the structure and freezing process of rimming-steel ingots, carried out by a committee working under the auspices of Jernkontoret, in Stockholm, are presented.

1. The observations and views of previous investigators of rimming-steel ingots have been reviewed, with particular reference to the nature of the gases liberated during freezing, and their effect on the formation of blowholes and on the structure and composition of the steel.

2. The laws of freezing for rimming steel of various carbon and manganese contents under different conditions have been outlined as deduced from a tentative iron-carbon-oxygen diagram, modified by manganese, in which the gas phase is also included.

3. As a consequence of the reaction: carbon (in solution) + oxygen (in solution) → $CO + CO_2$ (gas), there exists a balanced composition characterized by the carbon and oxygen concentrations of the liquid remaining unaltered as long as gas is freely evolved during freezing. This composition is probably not far from 0.06 per cent carbon and 0.04 per cent oxygen, if the gas is given off at atmospheric pressure. For metal having higher carbon content, carbon will increase and oxygen decrease in the liquid metal during freezing under gas evolution; for metal of lower carbon content the opposite holds true.

4. After the top of the ingot has closed, gas is evolved in limited volumes, mainly corresponding to the shrinkage, under continuously growing pressure as the carbon and oxygen concentrations in the liquid and the solid increase, composition and pressure being interrelated as indicated by the equilibrium diagram.

5. A series of rimming-steel ingots, with carbon varying from 0.046 to 0.21 per cent, have been studied by chemical analysis, sulphur prints and etched sections.

6. Details of primary structure, blowholes and segregates in the different ingots examined have been described. From those observations the mechanism of formation of the skin, rim holes, rim channels, intermediate and core holes, deformation structures of different type and several forms of segregate has been deduced.

7. The distribution of carbon, phosphorus, sulphur and oxygen in the different zones of the ingot has been determined in a few cases and been found to agree on the whole with the distribution deduced from consideration of the equilibrium diagram and the known or postulated variables associated with the freezing process.

8. Various effects of the growing pressure during freezing of the core on the structure of rim zone and core have been observed, and mechanisms of their formation have been suggested. Factors affecting the manner in which the pressure grows have also been suggested.

9. Effect of composition, temperature and casting conditions on the structure of the ingot have been discussed.

The investigation of ingot structure was carried out in the Metallographic Department of Tekniska Högskolan in Stockholm. The oxygen determinations were made at Metallografiska Institutet in Stockholm, the chemical analyses reported in Figs. 47 to 50 under the direction of Mr. Enlund at Degerfors, a number of sulphur prints were prepared at Kallinge and Nykroppa.

ACKNOWLEDGMENTS

APPENDIX.—Preparation and Etching of Ingot Sections

In etching the polished section of an ordinary rimming-steel ingot that has received no heat-treatment, the true primary structure of the rim zone may not be distinctly developed, whatever etching may be tried. There are two reasons for this: (1) the structure is fine and the local differences in phosphorus concentration, etc., which exist in this zone, are very slight; (2) upon the primary structure is superimposed a secondary structure that originates in the following way (ref. 56, p. 81). The metal, owing to its low carbon content, freezes to δ-iron crystals, dendritic or globular. During cooling, δ iron is transformed, at A_4, into γ iron, austenite. The austenite crystals growing from the surface inward ordinarily assume an elongated or columnar shape, their main direction being perpendicular to the A_4 isothermal. For that reason they become curved at corners, a feature not occurring in the primary crystals. The austenite precipitates ferrite in the range A_3-A_1, the remainders forming pearlite at A_1. Within each austenite grain or column a Widmannstätten structure is thus formed, with ferrite and pearlite alternating in uniform orientation. This latter structure is developed by etching in copper-bearing solutions also, and if, as in the rim zone, the primary structure is fine and indistinct, the secondary

structure, with contrasts in orientation between neighboring regions that were previously austenite grains, may practically be the only one revealed. The fine details of primary structure that should give information as to the actual manner of freezing are not discovered, and the secondary structure is sometimes believed to be the freezing structure.

In order to eliminate this misleading secondary structure, the ingots or ingot sections have been heated to about 1000° C., quenched in water and annealed at about 700°. By this treatment a fine structure of ferrite with small rounded particles of cementite is produced. The primary structure, which is, of course, unaffected by the heat-treatment, will then appear alone on suitable etching. Common etching methods do not, however, give good contrasts in the rim zone. The following program of preparation and etching has been found successful—except for ingot G with 0.046 per cent carbon—and has been used throughout the present investigation:

Grinding on a series of emery cloths and emery papers down to Hubert 00 or 000,
Polishing on cloth with levigated alumina,
Etching once in 0.25 per cent HNO_3 in alcohol (mild pre-etching),
Etching four times in 1 part Stead's solution + 2 parts H_2O + 3 parts alcohol,
Etching two times in 1 part Stead's solution + 3 parts alcohol,
Etching one to four times in 1 part Stead's solution + 2 parts alcohol.

The etching solution is rapidly poured over the surface* and by tilting this back and forth the solution is made to flow over all parts uniformly until all the copper is deposited. The section is then washed well in running water and rubbed with a piece of cotton soaked in dilute ammonia, until the copper is thoroughly dissolved, again washed with water (not too cold), then with alcohol and quickly wiped dry with a clean towel. It is then etched again without delay.

As the presence of blowholes renders washing difficult and may cause discolored spots to form around them, it is advisable to plug the holes before grinding. This can be done with plaster of Paris that is dried and then allowed to absorb Bakelite solution, which is hardened by heating to 130°.

REFERENCES

1. K. Styffe: Iakttagelser under ett besök i England 1862 rörande jernhandteringen. *Jernkontorets Annaler* (1864) 340.
2. L. E. Boman: Das Bessemern in Schweden in seiner jetzigen Praxis. Leipzig, 1864.
3. F. Gautier: Solid Steel Castings. *Jnl.* Iron and Steel Inst. (1877, I) 40.
4. H. Bessemer: *Jnl.* Iron and Steel Inst. (1877, I) 81.
5. F. C. G. Müller: Untersuchungen über den Bessemerprocess. *Ber.* deut. chem. Gesellschaft (1878) 11, 536.

---

* Certain curved lines visible on some of the structures shown are due to temporary arrests in applying the solution (compare Fig. 21).

6. F. C. G. Müller: Ueber die in Eisen und Stahl eingeschlossenen Gase. *Ber. deut. chem.* Gesellschaft (1879) **12**, 93.

7. A. Davis: Consolidation of Fluid Steel. *Jnl.* Iron and Steel Inst. (1879, II) 479.

8. F. C. G. Müller: Ueber die Gasausscheidungen in Bessemergüssen. *Ztsch.* Ver. deut. Ingenieure (1879) **23**, 493.

9. J. Parry: On Hydrogen and Carbonic Oxide in Iron and Steel. *Jnl.* Iron and Steel Inst. (1881, I) 183.

10. H. Bessemer: *Jnl.* Iron and Steel Inst. (1881, I) 197.

11. F. Stubbs: *Jnl.* Iron and Steel Inst. (1881, I) 199.

12. C. Walrand: Structure de l'acier coulé. *Annales industrielles* (1882) **14**, 234.

13. A. Pourcel: Notes on Manufacture of Solid Steel Castings. *Jnl.* Iron and Steel Inst. (1882, II) 509.

14. E. W. Richards: *Jnl.* Iron and Steel Inst. (1882, II) 519.

15. F. C. G. Müller: Ueber die Gasausscheidungen in Stahlgüssen. *Stahl und Eisen* (1882) **2**, 531.

16. C. A. Caspersson: Om den vid bessemerblåsningen rådande värmegradens inflytande på de bekomna götens egenskaper. *Jernkontorets Annaler* (1882) 295.

17. C. A. Caspersson: Influence of Heat in the Bessemer Blow on the Nature of the Ingots. *Jnl.* Iron and Steel Inst. (1883, I) 480.

18. A. Ledebur: Eisen und Wasserstoff. *Stahl und Eisen* (1882) **2**, 591.

19. A. Pourcel: Gasausscheidungen in Stahlblöcken. *Stahl und Eisen* (1883) **3**, 48.

20. F. C. G. Müller: Zur Berichtigung. *Stahl und Eisen* (1883) **3**, 79.

21. H. Wedding: Blasenbildung im Flusseisen. *Stahl und Eisen* (1883) **3**, 199.

22. F. C. G. Müller: Neue Experimental-Untersuchungen über den Gasgehalt von Eisen und Stahl. *Stahl und Eisen* (1883) **3**, 443.

23. A. Ledebur: Bruchstücke aus dem Gebiete der Eisenhüttenkunde. Zur Theorie der Gasentwicklung beim Flusseisen. *Stahl und Eisen* (1883) **3 : 2**, 599.

24. E. G. Odelstjerna: Om Martinmetalls beredning och användning. *Jernkontorets Annaler* (1883) 34.

25. F. Guthrie: On Eutexia. *Phil. Mag.* (1884) **17**, 462.

26. A. Ledebur: Altes und Neues vom Eisen. *Stahl und Eisen* (1886) **6**, 143.

27. H. M. Howe: The Metallurgy of Steel, I. New York, 1890.

28. K. Styffe: Aluminum såsom raffineringsmedel för andra metaller. *Jernkontorets Annaler* (1892) 275.

29. A. Pourcel: Segregation and Its Consequences in Ingots of Steel and Iron. *Trans.* A.I.M.E. (1893) **22**, 105.

30. A. R. von Dormus: Studien und Betrachtungen über die Ungleichmässigkeits-erscheinungen des Stahlschienen-Materials. *Ztsch.* Oesterreich. Ing. und Arkit. ver. (1896) **48**, 191.

31. L. Tetmajer: Metamorphosen der basischen Schienenstahlbereitung und des Prüfungsverfahrens der Stahlschienen. *Schweizerische Bauzeitung* (1896) **28**, 130.

32. H. Wedding: Ausführliches Handbuch der Eisenhüttenkunde, I, 1131. Braunschweig, 1896.

33. A. Ruhfus: Ueber Saigerungen im Flusseisen. *Stahl und Eisen* (1897) **17**, 41.

34. J. A. Brinell and A. Wahlberg: Hållfasthetsprof, och andra undersökningar å diverse metaller och ämnen. *Jernkontorets Annaler* (1901) 195.

35. A. Wahlberg: Influence of Chemical Composition on Soundness of Steel Ingots. *Jnl.* Iron and Steel Inst. (1902, I) 333.

36. A. Ledebur: Handbuch der Eisenkunde, III (4. Aufl.) 915. Leipzig, 1903.

37. J. E. Stead: *Jnl.* Iron and Steel Inst. (1905, II) 224.

38. R. Baumann: Schwefel im Eisen. *Metallurgie* (1906) **3**, 416.
39. H. M. Howe: Piping and Segregation in Steel Ingots. *Trans.* A.I.M.E. (1907) **38**, 3.
40. E. von Maltitz: Blowholes in Steel Ingots. *Trans.* A.I.M.E. (1907) **38**, 412.
41. C. B. Wheeler: Report of the Tests of Metals . . . made with the United States Testing Machine at Watertown Arsenal. Government Printing Office, Washington, 1910.
42. F. Wüst and H. L. Felser: Der Einfluss der Seigerungen auf die Festigkeit des Flusseisens. *Metallurgie* (1910) **7**, 363.
43. P. L. T. Héroult: Presence and Influence of Gases in Steel. *Trans.* Amer. Electrochem. Soc. (1910) **17**, 135.
44. J. E. Stead: Notes on the Welding Up of Blowholes and Cavities in Steel Ingots. *Jnl.* Iron and Steel Inst. (1911, I) 54.
45. H. Le Chatelier: La réduction de l'oxyde de fer et les gazogènes. *Rev. de Mét.* (1912) **9**, 509.
46. R. Hadfield: On a new Method of Revealing Segregation in Steel Ingots. *Jnl.* Iron and Steel Inst. (1912, II) 40.
47. H. M. Howe: *Jnl.* Iron and Steel Inst. (1912, II) 68.
48. E. Heyn: Die technisch wichtigen Eigenschaften der Metalle und Legierungen: 419–432, Metallische Stoffe und Gase; A. Martens: Handbuch der Materialienkunde für den Maschinenbau, II A. Berlin, 1912.
49. C. A. Edwards: The Physico-Chemical Properties of Steel, 86. London, 1916.
50. W. Mathesius: Die physikalischen und chemischen Grundlagen des Eisenhüttenwesens, 115, 352. Leipzig, 1916.
51. H. D. Hibbard: Effervescing Steel. *Trans.* A.I.M.E. (1920) **62**, 160.
52. A. Johansson: Direkt valsning av göt från icke eldade värmegropar. *Jernkontorets Annaler* (1920) 149.
53. P. Oberhoffer: Das schmiedbare Eisen, 202. Berlin, 1920.
54. H. D. Hibbard: Finishing Melting Temperatures of Simple Ingot Steels. *Trans.* A.I.M.E. (1925) **71**, 476.
55. O. von Keil and A. Wimmer: Beitrag zur Kenntnis der Gussblock- und Gasblasenseigerung. *Stahl und Eisen* (1925) **45**, 835.
56. P. Klinger: Beitrag zur Kenntnis der beim Giessen und beim Erstarren des Stahles entwickelnden Gase. *Stahl und Eisen* (1925) **45**, 1640.
57. C. Peirce: Making Rimmed Steel. *Trans.* A.I.M.E. (1926) **73**, 1026.
58. L. F. Reinartz: *Trans.* A.I.M.E. (1926) **73**, 1036.
59. A. L. Feild: *Trans.* A.I.M.E. (1926) **73**, 1045.
60. M. Volmer and A. Weber: Keimbildung in übersättigten Gebilden. *Ztsch. phys. Chem.* (1926) **119**, 277.
61. J. H. S. Dickenson: A Note on the Distribution of Silicates in Steel Ingots. *Jnl.* Iron and Steel Inst. (1926, I) 177.
62. B. Osann: Lehrbuch der Eisenhüttenkunde, II, 186. Leipzig, 1926.
63. C. H. Herty, Jr., J. M. Gaines, B. M. Larsen, W. A. Simkins, R. L. Geruso and S. P. Watkins: The Physical Chemistry of Steel Making: The Solubility of Iron Oxide in Iron. Min. and Met. Investigations, *Bull.* 34 (1927).
64. E. Améen and H. Willners: En studie över gaser i flytande stål. *Jernkontorets Annaler* (1928) 195.
65. Second Report on the Heterogeneity of Steel Ingots. Sec. V, A Study of Carbon Steel Ingots other than "Killed." *Jnl.* Iron and Steel Inst. (1928, I) 477.
66. F. B. McKune: *Trans.* A.I.M.E. (1929) **84**, 255.
67. A. L. Feild: *Trans.* A.I.M.E. (1929) **84**, 256.
68. J. E. Carlin: Physical Chemistry of Rimmed Steel. *Trans.* Amer. Soc. Steel Treat. (1929) **16**, 293.

69. A. Hultgren: Crystallisation and Segregation Phenomena in 1.10 per cent Steel Ingots. *Jnl.* Iron and Steel Inst. (1929, II) 69.

70. P. Bardenheuer and C. A. Müller: Untersuchungen über das Verhalten der Begleitelemente des Eisens, insbesondere des Sauerstoffs bei der Seigerung des Stahles, mit Beiträgen zur Sauerstoffbestimmung. *Mitt.* K.W.I. Eisenforschung (1929) **11**, 255.

71. P. Bardenheuer and C. A. Müller: Untersuchungen über die Seigerung in beruhigten und nicht beruhigten Flussstahlblöcken. *Mitt.* K.W.I. Eisenforschung (1929) **11**, 273.

72. C. H. Herty, Jr., J. M. Gaines, H. Freeman and M. W. Lightner: A New Method for Determining Iron Oxide in Liquid Steel. *Trans.* A.I.M.E. (1930) **90**, 28.

73. C. H. Herty, Jr.: *Trans.* A.I.M.E. (1930) **90**, 42.

74. H. Schenck: Amerikanische Forschungsarbeiten über die physikalische Chemie der Stahlerzeugungsverfahren. *Stahl und Eisen* (1930) **50**, 1782.

75. C. Benedicks and H. Löfquist: Non-Metallic Inclusions in Iron and Steel, 226. London, 1930.

76. H. C. Vacher and E. H. Hamilton: The Carbon-oxygen Equilibrium in Liquid Iron. *Trans.* A.I.M.E. (1931) **95**, 124.

77. E. C. Bitzer: Characteristics of Rimmed Steel. *Blast Furnace and Steel Plant* (1931) **19**, 249.

78. A. Stadeler and H. Thiele: Der Einfluss der Kokillentemperatur auf die Lage der Randblasen und auf die Seigerungsverhältnisse in weichen Flusstahlbrammen. *Stahl und Eisen* (1931) **51**, 449.

79. E. Herzog: *Stahl und Eisen* (1931) **51**, 458.

80. W. Oertel and A. Schepers: Eigenschaften beruhigt und unberuhigt vergossenen Stahles. *Stahl und Eisen* (1931) **51**, 710.

81. H. Dünwald and C. Wagner: Thermodynamische Untersuchungen zum System Eisen-Kohlenstoff-Sauerstoff. *Ztsch. anorg. Chem.* (1931) **199**, 321.

82. P. Bardenheuer and H. Wünnenberg: Ein Beitrag zur Frage der Verarbeitbarkeit von beruhigtem und unberuhigtem Stahl. *Mitt.* K.W.I. Eisenforschung (1931) **13**, 63.

83. G. Phragmén: Termodynamik, en kort lärobok med tillämpningar på metallurgiska problem. Stockholm, 1931.

84. H. C. Hibbard: *Trans.* A.I.M.E. (1933) **104**, 134.

85. W. Eichholz and J. Mehovar: Untersuchung über die Eigenschaften von Stahlblöcken in Abhängigkeit von den Herstellungsbedingungen unter besonderer Berücksichtigung des Harmet-Verfahrens. *Archiv. Eisenhüttenwesen* (1932) **5**, 449.

86. A. Hultgren and G. Phragmén: Några iakttagelser vid undersökning av strukturen hos 1, 10 proc. kolstålsgöt. *Värmländska Bergsmannaföreningens Annaler* (1932) 116.

87. H. Dünwald and C. Wagner: Thermodynamische Untersuchungen zum System Eisen-Kohlenstoff-Sauerstoff. Entgegnung auf die Bemerkung von W. Krings. *Ztsch. anorg. Chem.* (1932) **205**, 205.

88. Fourth Report on the Heterogeneity of Steel Ingots—Principles Involved in the Making of Rimming Steel. Iron and Steel Inst. (1932) 68.

89. H. Schenck, W. Riess and E. O. Brüggemann: Ueber die Geschwindigkeit und die Gleichgewichtskonstante der Kohlenstoffreaktion bei der Herstellung flüssigen Stahls. *Ztsch. Elektrochemie* (1932) **38**, 562.

90. N. A. Ziegler: Solubility of Oxygen in Solid Iron. *Trans.* Amer. Soc. Steel Treat. (1932) **20**, 73.

91. S. Caspersson and K. E. Johansson: Blåsbildningen i 12″ göt av basisk martin med kolhalt ca. 0.05%. *Jernkontorets Annaler* (1932) 375.

92. F. Körber and W. Oelsen: Ueber die Beziehungen zwischen manganhaltigem Eisen und Schlacken, die fast nur aus Manganoxidul und Eisenoxidul bestehen. *Mitt.* K.W.I. Eisenforschung (1932) **14**, 181.
93. R. Perrin: Nouvelles méthodes de métallurgie. *Rev. de Mét.* (1933) **30**, Mem. 71.
94. Fifth Report on the Heterogeneity of Steel Ingots. Iron and Steel Inst. (1933) 4.
95. C. A. Edwards and H. N. Jones: A Study of the Influence of Varying Oxygen and Carbon Content in Iron upon the Position of Blowholes in Steel Ingots. Fifth Report on Ingots, Iron and Steel Inst. (1933) 39.
96. C. Benedicks: *Jnl.* Iron and Steel Inst. (1933, II) 423.
97. F. Körber and W. Oelsen: Die Grundlagen der Desoxydation mit Mangan und Silizium. *Mitt.* K.W.I. Eisenforschung (1933) **15**, 271.
98. J. H. Nead and T. S. Washburn: Manufacture of Rimmed-steel Ingots. *Metals and Alloys* (1934) **5**, 43.
99. A. G. Egler and J. L. Tatman: *Jnl.* Iron and Steel Inst. (1934, I) 238.
100. E. Herzog: Rüttelversuche bei erstarrendem Stahl. *Stahl und Eisen* (1934) **54**, 462.
101. B. Kalling: Den kemiska jämviktslärans betydelse för de metallurgiska processerna. *Jernkontorets Annaler*, tekniska diskussionsmötet (1934) 96.
102. W. R. Fleming: On the Manufacture of Rimming Steel. *Trans.* Amer. Soc. Metals (1934) **22**, 532.
103. H. L. Geiger: *Trans.* Amer. Soc. Metals (1934) **22**, 542.
104. H. Meyer: Die Seigerung in Stahlblöcken. *Stahl und Eisen* (1934) **54**, 597.
105. F. Badenheuer: Die Bildung von Schattenstreifen in silizierten Stahlblöcken. *Stahl und Eisen* (1934) **54**, 1073.
106. H. Schenck: Einführung in die physikalische Chemie der Eisenhüttenprozesse, II—Die Stahlerzeugung. Berlin, 1934.
107. C. H. Herty, Jr., C. F. Christoffer, H. Freeman and J. F. Sanderson: Physical Chemistry of Steel Making. The Control of Iron Oxide in the Basic Open-Hearth Process. Min. and Met. Investigations, *Bull.* **68** (1934).
108. C. A. Edwards: Gases in Metals. *Trans.* A.I.M.E. (1935) **117**, 13.
109. T. Swinden and W. W. Stevenson: Some Experiments on Gases in Iron and Steel, and Their Effect on the Solidification of Ingots. Sixth Report on Ingots, 137. Iron and Steel Inst. (1935).
110. J. H. Andrew and E. M. Trent: Segregation in Steel Ingots, Sixth Report on Ingots, 173. Iron and Steel Inst. (1935).
111. C. A. Edwards, R. Higgins, M. Alexander and D. G. Davies: Influence of the Casting Temperature upon the Position of Blowholes in Steel Ingots of Varying Oxygen and Carbon Content. Sixth Report on Ingots, 193. Iron and Steel Inst. (1935).
112. E. Gregory: Sixth Report on Heterogeneity of Steel Ingots. Discussion, Correspondence, and Committee's Reply (1936) 7.
113. W. H. Hatfield: Heterogeneity of Steel Ingots. *Iron and Steel Ind.* (1935) **9**, 57.
114. F. Körber and W. Oelsen: Die Wirkung des Kohlenstoffs als Reduktionsmittel auf die Reaktion der Stahlerzeugungsverfahren mit saurer Schlacke. *Mitt.* K.W.I. Eisenforschung (1935) **17**, 39.
115. A. Jackson: Rimming Steels. *Iron and Steel Ind.* (1936) **9**, 179.
116. B. Kalling and N. Rudberg: Provkokill för noggrann bestämning av kol och syre i stålbad. *Jernkontorets Annaler* (1936) 138.
117. G. L. Danforth, Jr.: Rimmed Steel Quality. *Blast Furnace and Steel Plant* (1936) **24**, 781.
118. F. Körber and W. Oelsen: Die Auswirkung der Silizid-, Phosphid- und Karbidbildung in Eisenschmelzen auf ihre Gleichgewichte mit Oxyden. *Mitt.* K.W.I. Eisenforschung (1936) **18**, 109.

119. W. P. Rees: Sixth Report on the Heterogeneity of Steel Ingots. Discussion, Correspondence, and Committee's Reply (1936) 59.
120. J. Chipman and A. M. Samarin: Effect of Temperature upon Interaction of Gases with Liquid Steel. *Trans.* A.I.M.E. (1937) **125**, 331.
121. J. Chipman and C. R. FonDersmith: Rate of Solidification of Rimming Ingots. *Trans.* A.I.M.E. (1937) **125**, 370.
122. T. S. Washburn and J. H. Nead: Structure of Rimmed-steel Ingots. *Trans.* A.I.M.E. (1937) **125**, 378.
123. C. H. Herty, Jr.: *Trans.* A.I.M.E. (1937) **125**, 398.
124. L. F. Reinartz: *Trans.* A.I.M.E. (1937) **125**, 398.
125. B. M. Larsen: *Trans.* A.I.M.E. (1937) **125**, 399.
126. H. D. Hibbard: *Trans.* A.I.M.E. (1937) **125**, 399.
127. T. Swinden: Rimming Steel—A Study of Composition Variation from Outside to Centre. Seventh Report on Ingots. Iron and Steel Inst. (1937) 15.
128. T. Swinden and W. W. Stevenson: Some Further Experiments on Gases in Iron and Steel and Their Effect on the Solidification of Ingots. Seventh Report on Ingots, 139. Iron and Steel Inst. (1937).
129. F. Körber: *Jnl.* Iron and Steel Inst. (1937, I) 356-P.
130. R. L. Cain: Open-hearth Proceedings, 1937, 104. A.I.M.E.
131. F. Körber: Der Einfluss der Beimengungen auf die Reaktionen zwischen Eisenschmelzen, Eisen-Mangan-Silikaten und fester Kieselsäure. *Jernkontorets Annaler* (1937) 319.
132. G. Phragmén: *Jernkontorets Annaler* (1937) 343.
133. J. W. Halley and T. S. Washburn: Distribution of the Metalloids in Rimmed-steel Ingots. *Trans.* A.I.M.E. (1938) **131**, 195.
134. L. Guillet: Acier calmé, acier effervescent. *Rev. de Met.* (1937) **34**, 493.
135. K. C. McCutcheon and J. Chipman: Evolution of Gases from Rimming-steel Ingots. *Trans.* A.I.M.E. (1938) **131**, 206.
136. A. McCance: Application of Physical Chemistry to Steel-making. Iron and Steel Inst. Symposium on Steel-making (1938) 331.
137. B. Matuschka: Solidification in Open-topped and Closed-topped Ingot Moulds. *Jnl.* Iron and Steel Inst. (1938, I) 109-P.
138. A. Hultgren and G. Phragmén: Stelningsförlopp och struktur i göt av otätat stål. *Jernkontorets Annaler* (1938) 377.
139. G. Helmer: *Jernkontorets Annaler* (1938) 460.
140. H. D. Hibbard: Freezing of Rimmed Steel. *Iron Age* (1938) **142**, 69.

The Dendritic Structure of Some Alloy Steels

By Daniel J. Martin,* Member, and James L. Martin,† Junior Member A.I.M.E.

The dendritic pattern of steels shown by deep etching is used extensively as a guide in the inspection and control of the great majority of steels used in ordnance construction and for many applications in industry. The value of macroexamination lies in the fact that it enables a qualified observer to make deductions concerning the general quality of relatively large pieces of metal. Not the least of these general characteristics is the nature and extent of the dendritic segregation in the steel, either in the cast condition or after mechanical or thermal treatments.

Previous Work

Detailed methods for macroetching were outlined by Yatsevitch[1] and have been standardized by the American Society for Testing Materials. A comprehensive study of the occurrence, origin, and the chemical and crystalline nature of the dendritic structure was given by Keshian.[2] The marked persistence of dendritic segregation in nickel steels is fully recognized and has been discussed by Sauveur and Reed[3] and by others.

Very little, however, has been written on the effect of the various elements on the macrostructure of steels, and the purpose of this report is to submit evidence concerning the influence of chromium, nickel and molybdenum on the macrostructure of some 4 by 4-in. ingots cast and treated under closely controlled conditions.

Methods and Results

The ingots to be described were made in a 60-lb. high-frequency induction furnace at the Watertown Arsenal. Heats were made from a single lot of materials; were molten for the same length of time; tapped at approximately the same temperature into a standard mold preheated in each case to 150° ± 10° C.; and stripped and buried in ashes after 10 min. in the mold. Transverse disks were taken from the same location in

* Captain, Ordnance Department, U. S. Army, West Point, N. Y.
† Assistant Metallurgist, Watertown Arsenal, Watertown, Mass.
[1] References are at the end of the paper.

each ingot and were etched 35 min. in a solution of 37.5 per cent HCl, 12.5 per cent H_2SO_4, and 50 per cent H_2O at the simmering point of the solution. The chemical compositions of the disks so treated are shown in Table 1.

TABLE 1.—*Chemical Compositions of Disks*[a]

Ingot	Composition, Per Cent								
	C	Mn	Si	P	S	Ni	Cr	Mo	V
A	0.38	0.80	0.35	0.007	0.015		1.21	0.65	0.21
B	0.44	0.60	0.14	0.007	0.016	1.26		0.68	0.20
C	0.41	0.73	0.23	0.007	0.015	1.22	1.20	0.65	0.21
D	0.41	0.67	0.20	0.007	0.015	2.38	1.20	0.60	0.20
E	0.38	0.70	0.25	0.009	0.017	3.75	1.17	0.89	0.20
F	0.43	0.66	0.24	0.007	0.014	2.36		0.61	0.21
G	0.37	0.59	0.28	0.012	0.018	3.57		0.65	0.21
H	0.42	0.67	0.28	0.009	0.016			1.04	0.10
I	0.42	0.68	0.39	0.011	0.016			2.08	0.10
J	0.44	0.56	0.34	0.009	0.019			4.07	0.12

[a] Analyses by A. Sloan, Watertown Arsenal.

The first series of ingots is intended to show the structures obtained in these steels: (1) without nickel, (2) without chromium, and (3) with both nickel and chromium present. These structures are depicted in Fig. 1. In ingot A the dendritic structure is not readily apparent. The dendrites were so small that their structure could be seen only with great difficulty. This implies either (1) that larger dendrites did not exist in this steel or (2) that, if they did, their patterns were erased by subsequent diffusion. Since all of these ingots were treated alike, the normal effect of diffusion cannot be considered a cause for differences in the size of dendritic pattern. Ingot B developed a somewhat larger pattern, the traces of which are more pronounced in the macrostructure; ingot C, containing both nickel and chromium, shows the growth of large dendrites and a segregation not easily overcome. However, with nickel present, it is evident that the chromium intensifies the effect of the nickel.

Fig. 2 shows the effect of increasing the nickel content in this composition of steel. Ingot C has already been considered. Ingots D and E indicate the structures obtained with two and three times the nickel content of ingot C. It would seem that the size and persistence of dendritic segregation is increased to some degree with 2.38 per cent Ni but that more nickel than this has but little added effect.
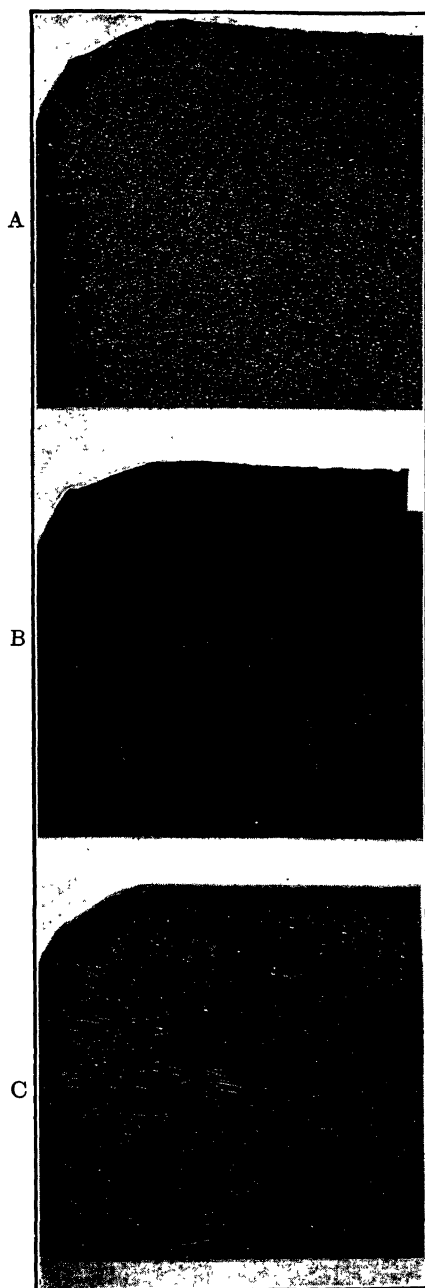
FIG. 1.—MACROSTRUCTURES OF INGOTS
A, B AND C, ¼ SECTION.   × 1.
Ingot A: Ni, 0; Cr, 1.20
Ingot B: Ni, 1.20; Cr, 0
Ingot C: Ni, 1.20; Cr, 1.20
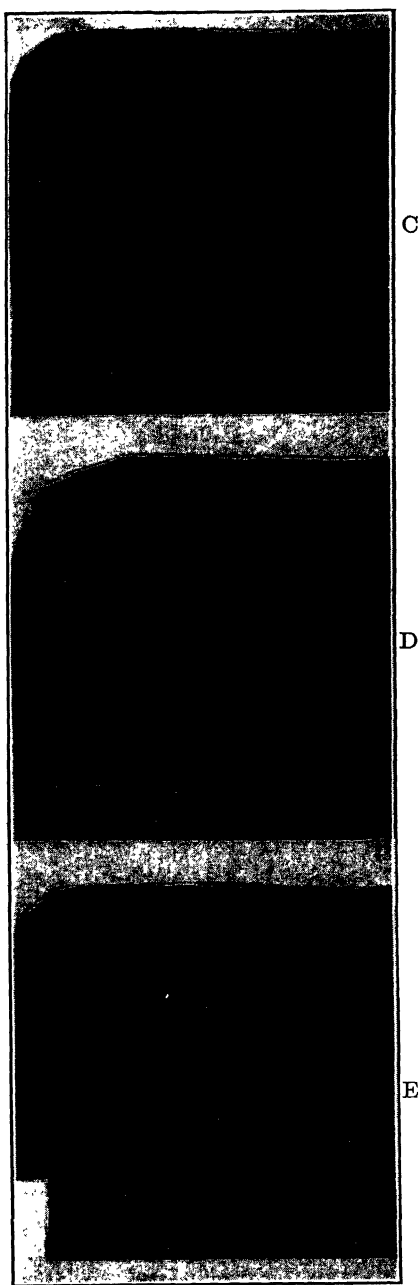
FIG. 2.—MACROSTRUCTURES OF INGOTS
C, D AND E, ¼ SECTION.   × 1.
Ingot C: Ni, 1.20; Cr, 1.20
Ingot D: Ni, 2.40; Cr, 1.20
Ingot E: Ni, 3.80; Cr, 1.20
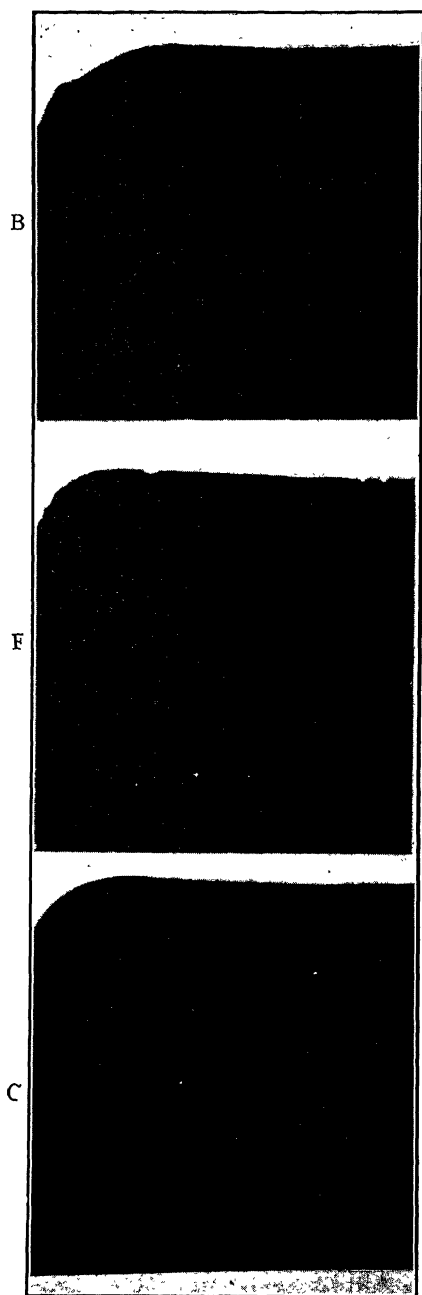
FIG. 3.—MACROSTRUCTURES OF INGOTS
B, F AND G, ¼ SECTION.   × 1.
Ingot B: Ni, 1.20
Ingot F: Ni, 2.40
Ingot G: Ni, 3.60
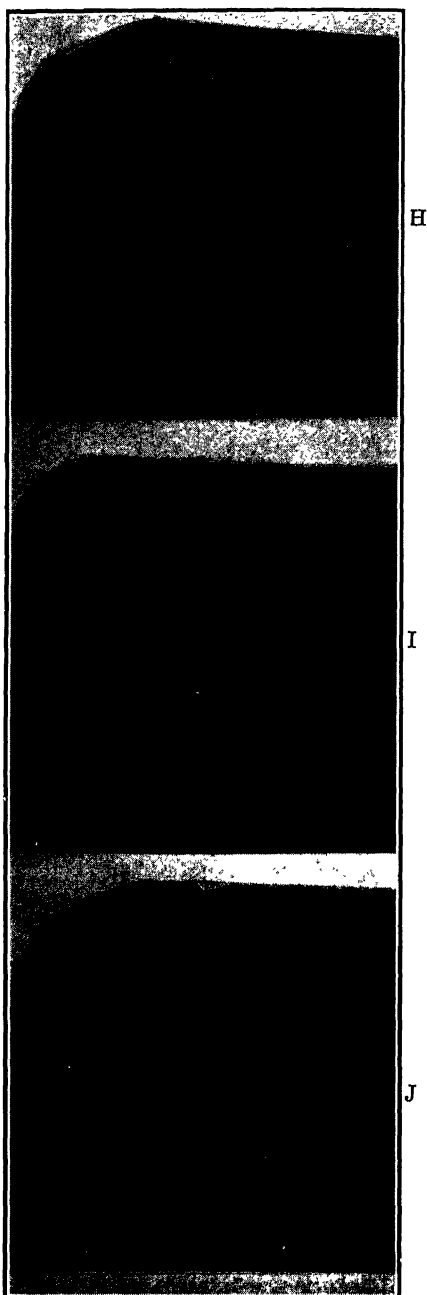
FIG. 4.—MACROSTRUCTURES OF INGOTS
H, I AND J, ¼ SECTION.   × 1.
Ingot H: Mo, 1
Ingot I: Mo, 2
Ingot J: Mo, 4

For purposes of comparison, a third series of ingots of the same general composition, but without chromium, is shown in Fig. 3. The structure of the comparable ingots B, F and G are shown to develop in the same manner, generally, as C, D and E of Fig. 2. However, in Fig. 3 the dendrites were somewhat smaller in size and the patterns much more delicately outlined.

The effect of molybdenum is shown in Fig. 4. Ingots H, I and J, containing 1, 2 and 4 per cent Mo., exhibit a structure quite different from the ingots previously discussed, with a tendency toward the usual type of pattern, under the same conditions of etching, only as the molybdenum increases above some 3 per cent.

A general observation can be made with respect to the color of the macroetched disks from the various ingots, although it is difficult to illustrate with photographs. Nickel gives to the disks a white or silvery color. Chromium causes a definite blackening of the structure, and molybdenum produces a very definite brown color.

DISCUSSION OF RESULTS

During the course of these experiments it was found that the technique employed in polishing and etching had relatively little effect upon the results, provided only that the time of etching was closely observed and held constant. Somewhat misleading results could be obtained by etching any one disk in any series for less than 35 min. but overetching did not prove harmful. Disks were repolished and etched several times without any apparent change in the results reported. It should also be noted that the brown color imparted by molybdenum is characteristic and can be distinguished from rusty surfaces obtained by improper drying after etching by the fact that rusty disks are very unevenly browned whereas those containing molybdenum are uniform in color.

An explanation of the observed results might be satisfactorily approached from a number of different points of view. For example, Bailey[4] has shown that the thermal conductivity of metals at high temperatures is reduced by the presence of impurities and that the reduction is proportional to the content of impurity. It may be argued, therefore, that the larger dendrites will result when the solidified shell of the ingot has lower thermal conductivity and thereby holds the interior temperature of the ingot at some range between the liquidus and solidus for a longer period of time, hence permitting greater time for the growth of the dendrites.

The inference to be drawn would be that the larger the percentage of the usual impurities plus alloys, the larger would be the size of the dendrites as shown by the pattern remaining at room temperature. Such a conclusion might be justified if each impurity were known to have the

same effect in lowering the thermal conductivity. If this were true, ingots A and B, Fig. 1, should have about the same structure, but they do not. Data concerning the effect of the various elements at high temperature are not available. However, it may be offered in speculation that the added elements chromium, nickel and molybdenum may affect the thermal conductivity somewhat after the order of their own conductivities with respect to iron at room temperature. If this were true, the chromium steels would be expected to have the poorest conductivity and the molybdenum steels by far the best. The necessary deduction would then be that the dendritic pattern of ingot A should be somewhat larger than that of ingot B, which is not the case. It must be recognized that the thermal conductivity should have an effect on the dendritic structure, but, with the data available, it does not seem possible to explain the observed results.

A much more satisfactory explanation seems to be possible on the basis of Giolitti's diagram,[5] reproduced and modified as shown in Fig. 5.

It is apparent that the temperature range in which the dendrites can grow is represented by the vertical distance between the liquidus and the solidus. For alloy Y this range is represented by m. Other alloys of the system such as X and Z will have, respectively, smaller and larger temperature ranges than Y; hence, other things being equal, less and more time for the dendrites to grow than for the alloy Y. Consequently it should be expected that the size of the dendrites will increase from alloy X to alloy Z and that, though both may be large, the difference in size for differences in composition will be less near the middle of the LS loop than at either end.

If it may be assumed that the addition of nickel, chromium, molybdenum, or any other element changes the distance m either by reason of the nature of the element or by its effect upon the thermal conductivity, surface tension, viscosity, or some other physical property of the alloy, the size of the resulting dendrites would seem to depend upon this change in the equilibrium diagram and the distance m between the liquidus and the solidus at the chosen percentage composition. It is a known fact that the diagram is altered by the addition of alloying elements. Andrew and Binnie[6] report a lowering of the liquidus by additions of nickel and chromium together to the extent of 4.4 to 5° C. for each per cent of nickel and chromium combined. They also determined that the solidus is lowered by additions of molybdenum. Their conclusion, however, that nickel and nickel-chromium steels are more homogeneous than others because of a lessening of the solidification range seems hard to justify in view of the well-known tendency toward persistent dendritic segregation in these steels. It is felt that additions of these elements tend more toward increasing the downward slope of the L-S loop and, if this is so, the actual temperature range of solidification would be increased and the

results more in accord with the data presented. Evidence that this is true for the effect of chromium at least is indicated in the work of Tofante, Sponheuer, and Bennek,[7] which shows a decided increase in the slope of the loop with various additions of chromium.

Persistence of the dendritic segregation may also be explained by Fig. 5, after the method set forth by Giolitti.[5] The first crystal of alloy Y will have a composition indicated at O and the last liquid to solidify the composition indicated at P. If no diffusion took place upon
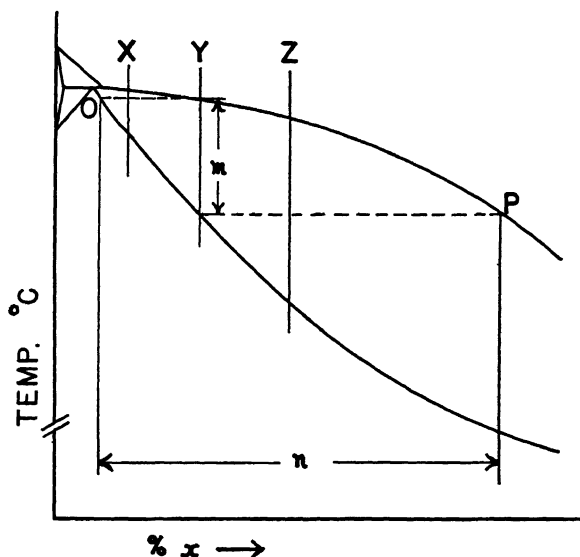
FIG. 5.—EQUILIBRIUM DIAGRAM, IRON IRON-CARBIDE SYSTEM (*after Giolitti[5]*).

solidification and cooling, the extent of segregation at room temperature is shown by the horizontal distance n, which would be the maximum segregation for the alloy. The magnitude of n varies with the shape and slope of the L-S loop and the particular alloy composition in the system under consideration. Of course, the value of n will not give a true picture of conditions for various alloys because of the tendency of any cast alloy to homogenize during and after solidification. The size of the observed dendritic pattern obviously is some function of these two variables, a study of which, it is hoped, may be made the subject of a subsequent report. At the present time it may be sufficient to indicate that nickel is known to retard the rates of diffusion as shown by Sauveur and Reed[3] and others. Increasing percentages of nickel were shown, in Figs. 2 and 3, to result in increased size of the dendritic pattern. This is felt to be due to the effect of nickel on the diffusion rate rather than to its effect on the L-S loop.

CONCLUSIONS

The structures reported upon were obtained on 4-in. ingots, and may not, therefore, be considered to apply to larger ingots of industrial size. However, in so far as these small ingots are concerned, it may be concluded that:

1. The effects of chromium, nickel and molybdenum on the size and the persistence of the dendritic segregation depend upon their effect upon the size and shape of the liquidus-solidus loop of the iron iron-carbide diagram, as shown in Fig. 5, and upon their effect on diffusion during and after solidification.

2. The typical colors imparted to the macrostructure by nickel, chromium and molybdenum are white, black and brown, respectively.

3. The size of the dendrite increases rapidly with additions of nickel up to 3 per cent and more slowly thereafter.

4. Chromium intensifies the effect of nickel.

5. The size and persistence of typical dendritic segregation does not become marked with much less than 4 per cent molybdenum.

ACKNOWLEDGMENT

REFERENCES

1. M. G. Yatsevitch: The Macrostructure of Steel. *Army Ordnance* (Jan-Feb. 1931).
2. H. G. Keshian: Dendritic Steel. *Trans.* Amer. Soc. Steel Treat. (1930) **17**, 321–382.
3. A. Sauveur and E. L. Reed: Dendrites in Nickel Steel. *Trans.* Amer. Soc. Steel Treat. (1931) **19**, 89–96.
4. L. C. Bailey: The Thermal Conductivity of Certain Approximately Pure Metals and Alloys at High Temperatures. *Proc.* Royal Soc. (1931) **A-134**, 57–76.
5. F. Giolitti: Heat Treatment of Soft and Medium Carbon Steel. New York, 1921. McGraw-Hill Book Co.
6. J. H. Andrew and D. Binnie: Third Report on Heterogeneity of Steel Ingots, Sec. 2. *Jnl.* Iron and Steel Inst. (1929) **119**, 309–346.
7. W. Tofante, A. Sponheuer, and H. Bennek: *Archiv Eisenhuttenwesen* (1935) **8**, 499–506.

DISCUSSION

(Cyril Wells presiding)

G. F. COMSTOCK,* Niagara Falls, N. Y.—The method of etching steel sections in hot acid, as used by the authors, is widely used for indicating the degree of heterogeneity, but serves particularly well to bring out unsoundness, segregation, and

---

* Metallurgist, The Titanium Alloy Manufacturing Co.
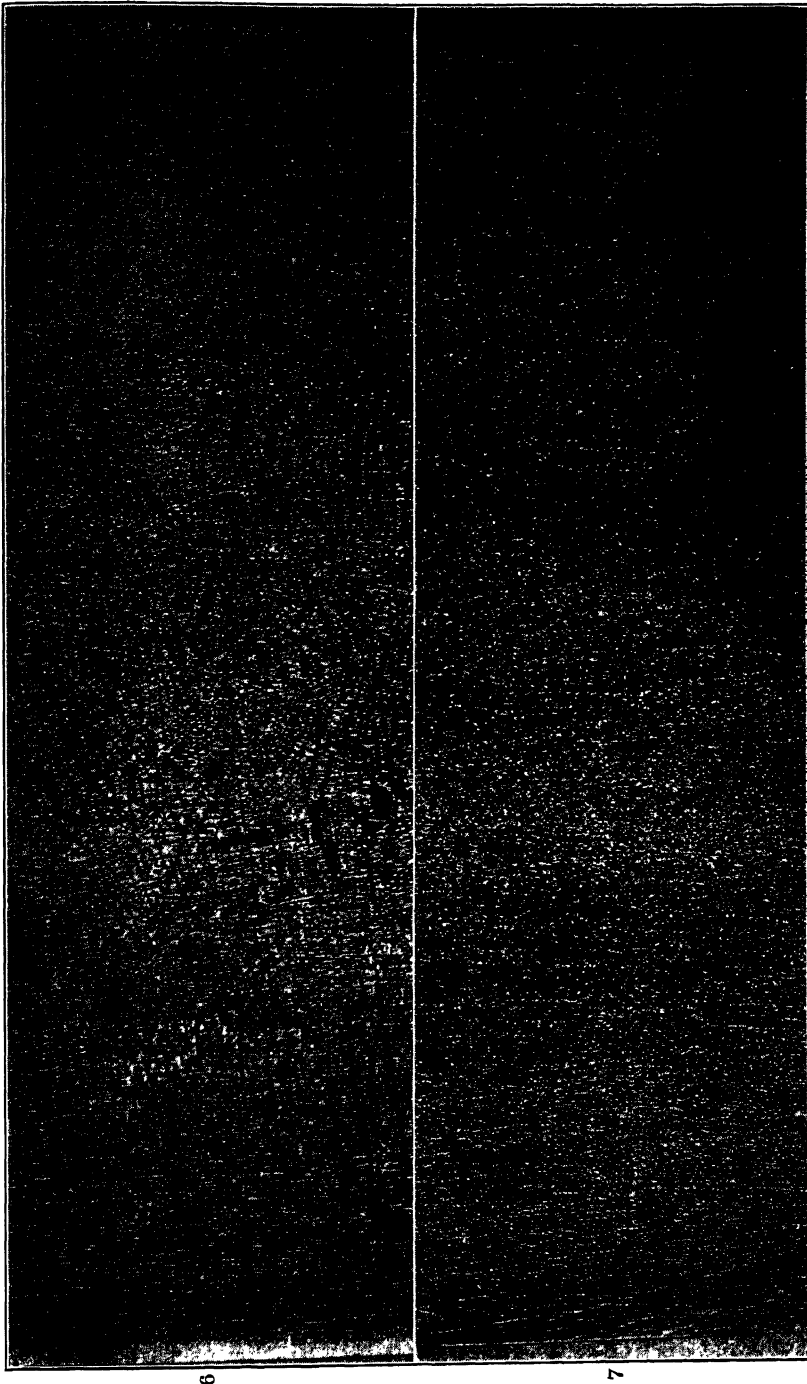
Fig. 6.—Section of small ingot of 0.40 per cent carbon steel, etched by Humfrey's method and magnified about 2.5 diameters, showing dendrites. No titanium was added to this ingot and it was poured at about 2925° F.

Fig. 7.—Section of ingot similar to that shown in Fig. 1, except that it contains 0.105 per cent titanium. The pouring temperature, etching and magnification were the same. Note the absence of dendrites.

the distribution of sulphides and possibly some other types of inclusions. Although it often shows dendrites also in steels where this structure is prominent, a more effective method for making visible the dendritic structure in all steels is that described by Humfrey.[8] This method involves etching the steel first with a neutral solution of copper-ammonium chloride, and replacing it gradually with a similar solution acidified. After washing and drying, the etched surface is rubbed with an abrasive paper of moderate fineness, and the dendrites then stand out clearly as bright areas outlined by dark depressions not reached by the abrasive. This method does not require a specially high polish on the surface to be etched, nor great skill in application, and is more certain to show dendrites clearly when they are present than any of the hot acids more commonly used for macrographic work.

The authors' comparison of various steels on the basis of dendritic structure is interesting, but might it not be possible that the greater distinctness of this structure in the nickel steels as compared with the chromium steels was due merely to the clearer attack of the etching reagents on the former? The pouring temperature of the steel is also a very important factor in dendrite formation, as they are not found in steel that is poured very cold.

It would be interesting to have a fuller discussion from the authors as to the effects of a dendritic structure on such steel properties as are important from their point of view; in other words, how detrimental are dendrites in steel for practical purposes?

If it is desired to eliminate a dendritic structure from a given steel, which must be poured fairly hot, there is no better method than to add titanium. This was shown to be effective with various kinds of steel in 1935, by Valenta and Poboril,[9] and the accompanying photographs (Figs. 6 and 7) illustrate some results recently obtained in the Metallurgical Research Laboratory of the Titanium Alloy Manufacturing Co. with a plain 0.40 per cent carbon steel. The one of the nontitanium ingot is typical of every ingot made without titanium, and the other is typical of all the titanium-treated ingots, without exception. The sections were prepared by Humfrey's method, as outlined above. To secure this result mere deoxidation with titanium is not sufficient, but a residual titanium content of at least 0.08 to 0.1 per cent seems to be required. The reason for this effect is probably that titanium carbide or cyanonitride separates from the steel in the form of fine, scattered crystals before general solidification, and these crystals act as nuclei to cause more steel crystals to start in a given volume, so that none of the steel crystals can then grow so large.

---

[8] *Jnl.* Iron and Steel Inst. (1919) **99**, 273.

[9] Valenta and Poboril: Influence of Titanium on Primary Crystallization. Research Rept. No. 20 from Skoda Works, Pilsen. Int. Foundry Congress, Brussels, Sept. 1935.

Occlusion and Evolution of Hydrogen by Pure Iron

By George A. Moore,* Junior Member, and Donald P. Smith,† Member A.I.M.E.

In spite of many investigations of the occlusion of hydrogen in iron, the nature of the process and the reasons for the accompanying effects upon the metal are still open questions. This is in large part due to three causes: (1) the difficulty of obtaining iron of adequate purity as starting material; (2) the occurrence of allotropic transformations, which complicate the effects; and (3) the fact that the body-centered cubic modification does not lend itself readily to crystallographic investigation.

The present paper attempts a critical review and correlation of the somewhat scattered and disconnected existing observations, and an experimental determination of the extent to which the conclusions that appear to follow from these are applicable to iron of really high purity, studied under well-defined conditions.

Review

Although only a comparatively few investigations have so far been made on the pure system iron-hydrogen, there is a much larger volume of literature which throws some light on the problem but falls short of a place in the systematic investigations, either because no attempt was made to measure equilibrium conditions or because the metal used was not iron or the gas not pure hydrogen. Such results have been variously dismissed in the past as of no importance, or as too complicated to try to explain; or they have been explained in terms of any of a dozen or more pictures, each of which is contradicted by data from other sources. The present importance of these data thus arises from their very mass and diversity, which present a picture of occlusion as a phenomenon whose variability cannot be ignored. We have attempted to organize the literature into groups comprising similar experiments or data leading to similar conclusions, thus of necessity sacrificing accuracy of historical order.

Lattice Occlusion.—Throughout this discussion, the term "lattice occlusion" will be used to denote the formation of a simple solid solution of a gas in a metal lattice, usually of interstitial distribution. The word

"solution" would probably be simpler, and synonymous to most readers, but unfortunately this word has been expanded in meaning by some workers to include a number of possible forms of occlusion, which are by

FIG. 1.—LATTICE OCCLUSION OF HYDROGEN BY IRON.
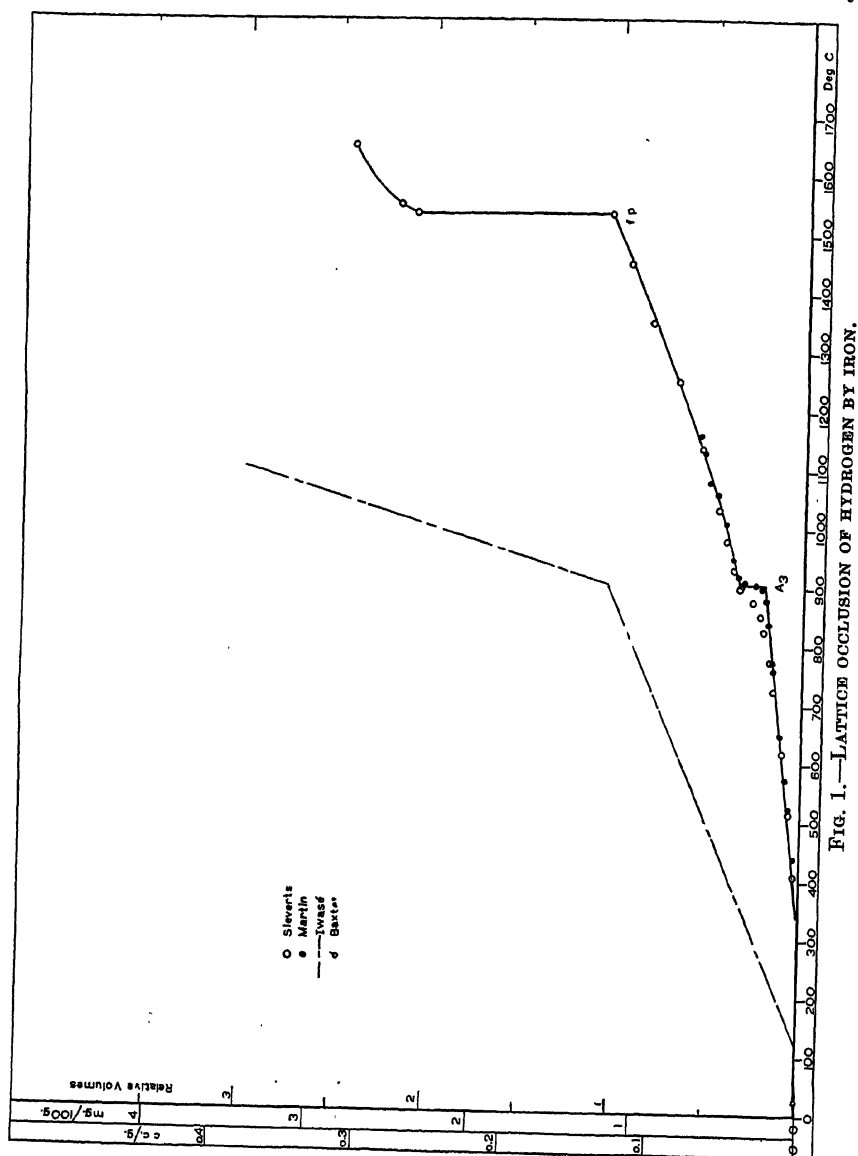
no means solution in the crystallographic sense and hence may convey unintended meanings. As *a priori* considerations as to what data can represent such lattice occlusion, we may assume that the values must be equilibrium figures, reversible with respect to temperature and pressure,

that there must be a thermodynamically sound dependence upon temperature and pressure, and that the values should not vary with the physical condition of the metal. While these are obviously necessary conditions, it is by no means certain that they cannot be counterfeited to a considerable extent by other forms of occlusion. Therefore the values should be interpreted as representing only maxima for lattice occlusion. Data in this connection come largely from three groups of investigators, all using essentially the same method; change of pressure in a closed system. These data are represented by the papers of Sieverts, Iwasé and Martin.

The first observation of which we have record is that of Baxter[1] in 1899, who states that the solubility of hydrogen in finely divided iron at room temperature is zero. This point has never been adequately checked, so the exact meaning of "zero" must still be left in some doubt, but may reasonably be taken to mean too small to measure. The bulk of the lattice occlusion data comes from the work of Sieverts[2,3] with Beckmann,[2] Jurisch,[4] Müller, and Krumbhaar, in the period 1907–1911, and is shown plotted in Fig. 1. Sieverts[2] reports that he was unable to find any occlusion by soft iron wire below 400°, but that earlier investigators found gas retained at these temperatures by other forms of iron. Since the latter do not appear to represent equilibrium conditions, discussion of them will be deferred to a later section. In general, the results of the investigations by Sieverts lead to the conclusion that lattice occlusion is small or nil at room temperature and increases with rising temperature, and that the quantity occluded is proportional to the square root of the pressure, thus indicating complete dissociation of the hydrogen in the lattice. A brief confirmation of these points was made by Neumann[5] in 1914.

In 1926, Iwasé[6] attempted a redetermination of the equilibrium system, obtaining solubilities about five times as great as those of Sieverts. He did not, however, take sufficient precautions to purify his iron, but used it practically as imported (from Germany) with only ten minutes' vacuum treatment. His high results may therefore be due to oxide, as suggested by Sieverts[6] or to a number of other causes. Even Iwasé found no occlusion below 100°. In 1929 Sieverts[7] published a general review in which are included the data from the earlier papers; and in 1931, with Hagen,[8] he refuted Iwasé by measuring the occlusion of iron powder, properly prepared, obtaining results identical with earlier figures for the massive metal. Borelius,[9] from theoretical considerations, has shown that the true temperature dependence of solubility should be of the form $S = ce^{\frac{-E_s}{2kT}}$, in which the value of E_s in the alpha range is given by Smithells[13] as 15,600 cal.

---

[1] References are at the end of the paper.

In 1929, Martin[10] published a careful redetermination of the equilibrium occlusion of hydrogen by iron, using metal of 99.98 per cent purity. He obtained results in almost perfect agreement with those of Sieverts, except at the critical point, where he observed a much sharper discontinuity. This sharp break is theoretically sound and has been accepted by Sieverts.[8] Martin's results also are plotted in Fig. 1.

With regard to the lattice occlusion in the delta range, there is as yet no certain information. Schenck and Luckemeyer-Hasse[11] have reported a sudden drop in solubility at the A_4 point, but the experiments of Sieverts and Zapf[12] fail to show such a change.

Total Occlusion.—As we have seen, the lattice occlusion of hydrogen by iron is practically nil at low temperature and reaches not quite one relative volume just below the melting point. There is, however, a considerable mass of data in the literature showing for various irons occlusions anywhere from a few hundredths of one volume up to 370 volumes. In most cases the exact condition of the sample is not given, or, as for the cast irons, is too complicated to allow of much interpretation of the results. In many cases, no analysis of the gas was made, but judging by the analyses that have been reported, the hydrogen content must normally be well over 50 per cent. These data, converted to a common unit, relative volumes, are summarized in Table 1.

Among the possible sources of gas, in addition to that occluded by ferrite, in the lattice and otherwise, there may be: occlusion by other constituents than ferrite; reaction between various constituents, or with the crucibles; enclosed gas in blowholes; etc. Troost and Hautefeuille[27] and Parry[28] both considered reactions to be contributing factors. Schmitz[29] showed the actual existence at high temperature of equilibria of the form $FeX + H_2 = Fe + 2XH$ where X represents carbon, silicon, etc. Satoh[30] demonstrated occlusion of hydrogen by iron nitride. Table 1 shows that in general the gas content of the cast irons is much higher than that of the medium range of steels, but that the gas again increases on approaching pure iron, a fact that we take as suggesting that reaction gas is an important factor only when impurities are present in rather large amount. Müller[31,32] demonstrated that considerable gas could be removed from steel by the act of drilling a hole in it, obtaining up to one volume, largely hydrogen. Stead showed that by using a very blunt drill and taking thin shavings, the gas recovery may be increased about ten times. Similarly, Baker[34] demonstrated that about half the gas content of steel may be removed by rolling. On the other hand, it will be noticed that cold-worked metal often contains (Belloc[33]) or takes up more gas than when cast or annealed. When gas is removed by working, it is usually assumed that it was present in blowholes, but according to the work of Baker[34,35] this cannot be a completely general explanation, since he found that unsound steels, full of blowholes, normally contain

TABLE 1.—*Gases in Iron and Its Alloys, Total Occlusion*

Investigator	Reference	Date	Material and Method	Temperature, Deg. C.	Relative Volumes		Percentage of H₂
					Gas	H₂	
Graham.......	14	1866	Soft Fe., hot evolution	?		0.42–0.46	
Graham.......	15	1867	Meteoric Fe, evolution	Red	2.85		86
			Horseshoe nails, evolution	Red	2.66		35
			Malleable Fe, evolution	Red		<1.0	
Parry.........	16	1873	Gray pig, hot vac.	?	55.		Mostly
			Wrought iron, hot vac.	Red to white	<7.8		
			W. I. degassed, absorbs	?		13.13	
			W. I. degassed, evolves	?		10.75	
Troost and Hautefeuille.	27	1873	Gray cast iron, evolution	800°	0.262		74.07
			Gray cast iron, saturated, evolution	800°	0.733		94.42
			Cast steel, evolution	800°	0.0346		22.72
			Cast steel, saturated, evolution	800°	0.1226		82.05
			Soft Fe, evolution	800°	0.291		23.78
			Soft Fe, saturated, evolution	800°	0.219		71.94
Troost and Hautefeuille.	17	1875	Soft Fe ingot, evolution	800°		⅓	
			Gray cast iron, evolution	800°		1.0	
Parry.........	28	1874	Gray pig, absorbs	?		20	
Müller........	31	1879	Drilling:				
			Bessemer steel, no Mn	Room	0.60		88.8
			Bessemer + Mn	Room	0.45		77.0
			Open-hearth steel	Room	0.25		67.8
			Crude Fe, cupola	Room	0.35		83.3
Stead.........			?? Drilling	Room	7–11		
Parry.........	18	1881	Spiegeleisen, evolution	Dull red	2		81.05
			White cast iron, evolution	Dull red	2		84.00
			Gray cast iron	Dull red	21		89.70
			Clean steel	Dull red	13		52.01
			Wrought iron	Dull red	2		54.10
			Gray iron, evolution	High	370	205	
			Gray iron, reheated, absorbs	High		20	
			Bessemer steel, evolution	1083°	70.5		
			Bessemer steel, reheated, absorbs	1083°		10.536	
Neumann and Streintz......	20	1892	Reduced iron occludes	?		19.17–9.38	
Heyn.........	21	1900	Mild steel	800		0.16	
Boudouard....	22	1907	Merchant iron	445	1.61		Rich
			Merchant iron	1100	0.2–4.0		Rich
Rugan and Carpenter.......	23	1909	High-silicon cast iron, evolution	900	22.2		88
Belloc.........	33	1909	Nickel steel, evolution:				
			Turnings	780(?)	3.3		
			Wire, C.D.	780(?)	9.7		
			Wire, ann. vacuo	780(?)	2.4		
			Wire, ann. H₂	780(?)	2.5		
			Wire, ann. N₂	780(?)	2.2		
Goerens.......	24	1910	Steels, evolution	850–980	0.09–0.91		
Charpy and Bonnerot....	25	1911	Steel, evolution:				
			Plate	950	2.82		
			Broken pieces	950	3.14		
			Hard Martin	950(?)	7.70		
			Hard electric	950(?)	5.90		
			Hard crucible	950(?)	5.42		
			Soft electric	950(?)	2.44		
			Soft Martin	950(?)	3.22		
			Extra soft Martin	950(?)	5.50		
			Extra soft Thomas	950(?)	8.33		
Baker.........	26	1909	0.90 steel, evolution:				
			Sound, as cast	900(?)	10.4		52
			With blowholes	900(?)	less		
Baker.........	34	1911	Steel, as cast	500	8–10		Up to 98
			Steel, rolled	500	4–5		

much less gas than similar steels from sound ingots, indicating that while the blowhole was once full of gas, it is able to retain less upon cooling than would be retained by a similar volume of solid iron. Tammann and Schneider[36] have also shown that both the rate and quantity of hydrogen occlusion vary with the physical state of the iron.

Electrochemical Occlusion.—Of equal importance with the large amounts of hydrogen which are sometimes occluded from the gas by iron alloys are the amounts of hydrogen of electrochemical origin that have been found to be taken up near room temperature and sometimes retained for considerable periods of time. While there are several theoretical points with regard to the mechanism of such occlusion, which cannot well be considered at this time, it should be apparent that this gas cannot all be in the lattice, since even if the true solubility at one atmosphere is appreciable, the dissociation pressure over a solution of 200 or so volumes would be far beyond the breaking strength of the iron. The data will be found in Table 2.

TABLE 2.—*Total Electrochemical Occlusion of Hydrogen by Iron*

Investigator	Reference	Date	Method	In	Temperature, Deg. C.	Relative Volumes		Percentage of H_2
						Gas	H_2	
ELECTROLYTIC IRON								
Meidinger............	37	1862	Evolution	H_2O	100	NH_3(?)	Copious	
Cailletet.............	38	1875	Evolution	H_2O	60–70		Intense	
			Evolution	vac.	?		240	
Lenz................	39	1869	Evolution		?	185		Chiefly
			Reabsorption	H_2O	Room	3.8		Chiefly
Müller..............	40	1909	Combustion				12–68	
Haber...............	41	1898					16–85	
Roberts-Austen	42	1887					17–20	
IRON CATHODICALLY CHARGED WITH HYDROGEN								
Thoma..............	46	1889	Coulometer	HCl	Room		10	
Franzini.............	47	1930	Voltameter	NaOH	Room		60	
Körber and Ploum....	48	1933	Very Pure Fe				zero	
OCCLUSION ON PICKLING IN ACID								
Graham.............	50	1868	Immersion	HAc	Room		0.57	
Thoma..............	46	1889	Immersion	HCl, d.	Warm		2.0	

For electrolytic iron, in addition to the data listed, Okochi,[43] with the aid of the X-ray, concluded that the greater part of the hydrogen in the iron is expelled on heating from 100° to 500° and that the *small portion remaining* is present as a *solid solution*.

TABLE 3.—*Relationship of Occlusion Units for Iron*

d_{Fe} = 7.86 grams per c.c.   At. Wt. Fe = 55.84
d_{H_2} = 8.99 × 10⁻⁵ grams per c.c.   At. Wt. H = 1.0078

Relative Volume, Normal Temperature and Pressure	C.C. per Gram Met.	Mg. per 100 Grams Met. = Wt. % × 10³	Atom Per Cent	H/M Ratio (Atom)
1	0.1272	1.1438	0.0633	6.3374 × 10⁻⁴
7.860	1	8.990	0.4956	4.9812 × 10⁻³
0.8743	0.1112	1	0.0554	5.5408 × 10⁻⁴
17.51	2.228	20.033	1	0.0111
1577.9	200.75	1804.79	50	1

In iron charged with hydrogen at the cathode of an electrolytic cell, Bellati and Lussana[44] observed that iron is more permeable than nickel, palladium or platinum, in opposition to the fact, more recently discovered,[7] that the lattice occlusion, for nickel and palladium at least, is much greater. Ramsey[45] first suggested that the hydrogen is dissociated during electrochemical occlusion, but this is also true for lattice occlusion, so his assignment of the differences in magnitude to this cause alone is no longer valid. Thoma[46] found when he cut his wires that the evolution of hydrogen was especially large at the cut surfaces. Tammann and Schneider[36] found in this case, also, that the amount of occlusion varies with the physical condition of the iron. Körber and Ploum[48] found that the purest iron cathodes did not occlude, but that occlusion was normal in the presence of small amounts of various impurities. However, they did not show that the various samples were in the same physical condition, so it may well be that there is only an indirect correlation due to the modification of structure by impurities.

Cailletet[49] appears to have been the first to observe occlusion upon the simple immersion of iron in acid (H₂SO₄, dil.). Using two plates welded together, he built up an internal pressure of 35 cm. of Hg, but does not report the actual amount occluded. Graham[50] reports that the hydrogen occluded by his iron could not be removed in vacuum except by heating nearly to redness. Some more recent related points will be considered below in connection with diffusion.

Adsorption.—Some mention should be made of the adsorption of hydrogen on the surface of iron, especially since our results will be found to show a certain similarity in form with the kinetics of activated adsorption. The magnitude, however, will at once be seen to be altogether different, in spite of the masking tendency inherent in the fact that adsorption studies are generally on very finely divided material having a large surface per unit weight.

Physical adsorption appears to be limited to temperatures well below the range of our experiments. Nikitin[52] found it to vanish at −80°, but

at lower temperature to attain a value of 1.65 c.c. per gram, or 13 rel. vol. Benton and White[53] found no physical adsorption above 0°. Dureau and Teckentrup[54] found adsorption, partly physical, at 18°, but report that the total amounts at most to a monomolecular layer.

Activated, or chemical, adsorption has generally been observed in the range from 0 to 500°, and appears to be much smaller than the physical. Dew and Taylor[55] report a low at 110° of 0.0028 c.c. per gram (0.022 rel. vol.) and about four times this amount at their top temperature of 305°. For a supported iron catalyst, 0.1 per cent Fe, Pease and Stewart[56] found adsorption at 0° of 0.005 c.c. per gram, about half that of similar materials containing copper or silver. Benton and White[53,57] report 0.0055 c.c. per gram (0.043 rel. vol.) at 0°. Such values are obviously far too small to represent any important contribution to our results.

Some of these investigators, however, have reported a different type of effect, which is much slower than adsorption, of greater magnitude, and largely irreversible. This effect has been variously termed absorption, solution (!), secondary activated adsorption, etc. Nikitin[52] found better than 1 c.c. per gram (7.6 rel. vol.) at 380° and 2 c.c. per gram (15.7 rel. vol.) at 510°. Benton and White,[53] running experiments for as much as 35 days without reaching equilibrium, report:

TEMPERATURE, DEG. C.	C.C. PER GRAM	RELATIVE VOLUME
0	0.0602	0.473
110	0.0453	0.356
210	0.0328	0.258

The time factor here eliminates any explanation assigning these results to the external surface, but it should also be noted that they are higher than the true solubility anywhere in the alpha range and that the temperature coefficient is strongly negative. They are, therefore, due neither to adsorption nor to lattice occlusion, and should be considered in terms of gas that is inside the boundaries of the metal but not inside the lattice.

Evolution.—The process of evolution of occluded gas from a metal into a vacuum must always be controlled by two factors, the relative freedom of diffusion and the driving force, or internal equilibrium pressure of the gas. This last must be a function of the temperature and of the amount and condition of the occluded gas. Considering a lattice occlusion of the type shown in Fig. 1, it is thermodynamically necessary that, once given a solution of fixed concentration at any temperature, upon raising the temperature the equilibrium pressure of this solution must *decrease* correspondingly with the increase of solubility at one atmosphere. Considering also that diffusion occurs entirely within the lattice, there may well be a threshold temperature below which no diffusion takes place, but above this temperature diffusion must be uniformly free, though finite in rate. On exposing such an ideal system, at a suitable temperature, to

an external vacuum, evolution would be immediate and would continue until essentially all the gas was gone, decreasing in rate only in proportion to the equilibrium pressure or more likely the square root of the same, and thus approximately to the same function of the concentration. With a given residual pressure externally, the most gas could be removed at the *lowest* temperature at which diffusion takes place.

Since this is exactly the picture normally implied when one speaks of hydrogen dissolved in iron, it is most surprising that so little comment has been raised by the fact that for the past 70 years numerous investigators have been doing this experiment, always obtaining results directly contrary to the theory. As early as 1868, Graham,[50] referring to the iron-hydrogen system, made the very pertinent observation: "It does not follow that, because a gas is occluded by a metal, under a pressure of one atmosphere, at low temperature, the gas will also escape into a vacuum at the same temperature, a much higher temperature being often required for the expulsion of the gas than for its first absorption." Subsequent work has amply confirmed this statement. Parry[16,18] stated that iron evolved gas at red to white heat for seven days and then gave off a new portion on raising the temperature, and also that absorption was not reversible. Boudouard[22] reported that additional gas was evolved on raising the temperature, and that more gas could be obtained by cooling to room temperature after a first extraction and then reheating to the same temperature. Baker[34] found that evolution began below 400°, increasing at 600° and again at 787°, then fell off, and that there was no indication of any equilibrium dissociation pressure. He suggested that the gas (98 per cent H_2) is "imprisoned in the pores of the steel." Charpy and Bonnerot,[25] working entirely at 950°, on steels, found that the velocity of evolution decreases very sharply with time, that the amount is not proportional to the weight of the sample, even when used as pieces of the same size, and that an external pressure somewhat decreases the initial rate of evolution, which does not, however, drop off as fast as before, and thus tends eventually to equalize the amounts of gas removed. Langmuir and Sweetser[58] appear to have been the first to apply our present method of heating a ribbon out of contact with its surroundings, obtaining nearly three times as much hydrogen at 1100° as at 800° (silicon steel). Several investigators have found that evolution increases to a marked extent at the critical points, among them being Belloc[59] for soft steel at A_0 and A_3, Esser[60] for electrolytic iron at A_3, and Brace and Ziegler[61] for iron just below the A_4 point. This last is a little doubtful, however, since their heating appears to have been very rapid for so large a sample.

While most of the papers just mentioned present only incomplete data for disconnected observations, there are others that afford more definite information, particularly with regard to the composition of the

gases concerned.   Thus Belloc[59] found soft steel to give off only carbon monoxide at low temperature, hydrogen first appearing at 400° and increasing in amount and proportion at higher temperatures.   He noted also that gas was very irregularly distributed, the amount being greatest at the centers of his bars, and that the proportions of different gases also varied from point to point.   He found no indication of the existence of a definite dissociation pressure.   Baker[26,35] reported evolution of hydrogen at 300°, with a maximum at 600°, above which the rate fell off to 900°, and again rose.   The gas from his steels was over 90 per cent H_2 at lower temperatures.   On reheating a sample he obtained additional gas. Tammann[62] found that hydrogen is evolved from cold-worked iron at 530° to 600°, where softening begins.   In general, he observed that evolution begins at the recrystallization temperature, but that additional hydrogen may be expelled at higher temperatures.   Nikitin[52] found that hydrogen absorbed by iron powder began to come off at 330°.

The following six papers give essentially complete rate curves against either time or temperature: Belloc,[33] pumping to apparent exhaustion on each occasion, found successive releases of gas on raising the temperature; and making seven successive complete extractions at the same temperature of 780°, the metal resting three days at room temperature in a high vacuum after each extraction, he found that the original apparently complete extraction corresponded to only about one-third of the total gas removable at this temperature.   Ryder,[63] using a directly heated ribbon of silicon steel, measured and analyzed the total additional gas given off after raising the temperature in steps of 50°.   He found small evolutions of hydrogen up to 750° and then a rapid rise to his top temperature of 900°.   He also reported that he had essentially similar results with pure iron, the temperature of first rapid emission shifting with the A_2 point. Pilling,[64] using electrolytic iron, nearly pure except for 0.11 per cent H_2 content, found the rate of evolution low at 30° but increasing to a sharp maximum at 250°, then decreasing to a minimum at 400°, and increasing to a lower maximum at 650°.   Borelius and Gunneson[65] found temperature periods in the emission of occluded hydrogen and nitrogen from iron, but devoted their attention to a series of acceleration points in the rate of emission, whose meaning so far escapes us.   The maximum rates for their emission occur at 30°, 350°, 570°, and 680° for hydrogen.   Hugues[66] gave a series of curves for electrolytic iron which are quite similar to our own.   The gas expelled was 49 to 51 per cent H_2.   The total amount removable increased in a nearly linear manner from 50° to 1000°.   At a given temperature the total gas removed increased for about 2 to 4 hr. and then became nearly constant.   He gave a differential rate curve at 730°, which shows an induction period of 10 to 20 min., a high rate at 30 min. decreasing rapidly to about the end of the first hour, and then more slowly until it is practically nil at the end of the sixth hour, at which

point subsequent experiment showed that at least one-third of the original gas still remained in the sample. He was convinced that there is no compound present. Guillet and Roux[67] gave data for a rate curve on a cementation steel. On first heating, evolution started at about 400° and reached a maximum rate at about 800°. The gas was of about equal parts hydrogen and carbon monoxide.

Throughout all of these experiments there are apparent indications that the gas evolved was *not* from a true solution, or lattice occlusion, but rather that it had been retained in a more mechanical manner. We incline to believe that rift occlusion has been a very large contributing factor in all cases. However, the nature of the experiments has been such that in any given case another explanation can always be suggested, although no other appears to cover all cases. We have found no case where the explanation is limited to rift occlusion by the simultaneous observance of *all* of the following necessary precautions: that the iron be of sufficient purity to contain no second phase beyond ferrite; that there be no appreciable nonmetallic solid inclusions; that there be no blowholes or other gross openings; that there be no evolution of gas from or reaction with crucibles, etc.; and that the composition of the gas be so close to pure hydrogen that the evolution of other gases, especially carbon monoxide, may be regarded as incidental. It is for these reasons that we have attempted to measure gas evolution under better defined conditions.

Diffusion.—The diffusion of gases through metals is a problem in itself, but one so closely connected with occlusion that some mention is in order here. Diffusion, other than through microscopic holes, must always be the resultant of three processes, any one of which in a given case might control the rate. These are, in order of occurrence: the condensation, adsorption, or penetration process at the first surface; the process of motion through the body of the metal; and the evolution or evaporation from the second surface. In iron-hydrogen, we should expect, on account of the irreversible effects already noted, that the third process would be slower than the first. With respect to the passage through the metal, the gas might go by way of the lattice, through rifts, or even possibly along the grain boundaries. In any event, we should expect the possibility of diffusion to be limited by the possibility of occlusion in the corresponding condition. It would be a direct contradiction to suppose that diffusion was occurring through the lattice, for example, at a temperature at which direct measurements have shown the lattice occlusion to be nil.

We will not attempt to make a complete review of diffusion, especially since most work refers to several metals, but only to mention a few points to indicate that the effect in this case may be more complicated than is generally supposed. Deville,[69] one of the first discoverers,[68] makes a significant remark, which we should like to repeat: "Dans les métaux, la

porosité résulte de la dilatation que la chaleur fait éprouver aux espaces intermoléculaires; elle est en relation avec la forme des molécules que l'on peut toujours supposer régulières, et avec leur alignment qui détermine le clivage ou les plans de facile fracture des masses cristallisées." Deville's data were very limited, but we think this represents a penetrating viewpoint for the year 1864. Other early workers in the field were Cailletet,[70] Menshing and Meyer,[71] and Biltz.[72] Andrew,[73] in 1918, gave a theoretical consideration in which he ascribed the bulk of the occlusion and diffusion to the "amorphous cement" at the slip planes and grain boundaries. Andrew's ideas would now benefit from a restatement, on account of the present disrepute of the amorphous cement theory, but it appears that he was not at all sure of the amorphous nature of the occluder, regarding palladium black as a typical example.

Most of the recent work has been devoted largely to finding mathematical formulas for the diffusion rate. Thus Lombard[74] confirms the square root dependence on P for diffusion of H through Fe and[75] finds an exponential dependence on temperature. He also[76] thinks the rate depends on the physical condition of the metal, and may depend on the allotropic changes. His temperature range is too short to show the latter, or to give any information as to the lower temperature ranges. Khitrin[77] confirms the Richardson[76] formula in general, but finds a maximum rate at 500°. Smithells and Ransley[79] confirm Edwards (below) in that the rate is the same through a single crystal as through fine-grained iron, and introduce the Langmuir adsorption isotherm to explain the fact that their own and other data show abnormally high rates at low pressure. This results in a well fitting curve, but gives a formula so flexible that their mechanistic interpretation is by no means the only one possible. It should also be noted here that in general the rate is abnormally high at low temperature as well as low pressure, a point not explained by the above modification. Baukloh and Keyser[80] find diffusion only above 500°, which is "not wholly intercrystalline." There is a break at A_3 such that the rate in gamma iron is *less* than in alpha. Baukloh and Guthmann[81] find the same for chromium steels. For Armco iron they find that the grain boundary not only does not aid diffusion, but actually impedes it. The experiments by Ham on sheets composed of two metals indicate that the processes at the second or exit face often have a significant effect in controlling the diffusion rate. Ham and Sauter[82] find that iron heat-treated in nitrogen may show a diffusion rate for hydrogen from 10 to 15 times normal, the original rate returning after baking out at higher temperatures. They show that for very slow rates the diffusion rate is proportional to the first power of the pressure, and for the fast rates to the square root of the pressure; while it is in general intermediate between the two, thus indicating that at least part of the hydrogen is diffusing as molecules; i.e., *not* through the lattice. Ham[83] fits the data

to a general exponential formula, but needs new constants for each temperature range (400° to 700°, 770° to 840°, 848° to 900°, 900° to 954°) since the diffusion changes sharply at the critical points.

Diffusion of Electrochemical Hydrogen.—The first observation of the diffusion of hydrogen released by pickling iron in acid was by Cailletet,[49] who observed that the nascent hydrogen would diffuse to the center of a hollow iron cell at room temperature, building up a pressure inside but not diffusing back. Graham[50] ascribes this to penetration of the acid itself, which of course has been amply refuted. Johnson[51] found nascent hydrogen diffusing for 17 cm. up an iron wire, one end of which was exposed to acid. Charpy and Bonnerot[87] found the diffusion of nascent hydrogen to be irreversible up to 26 atmospheres. Fuller[88] found the rate on pickling to be doubled if the tube had previously been used; and the rate for cathode hydrogen 7 to 10 times as great in a pickled tube as in a new one. He also found that the low rate was restored if the tubes stood for three days, or were heated to 130° for 4 hr. The original rate was about 14 times greater at 90° than at room temperature, and was different for different electrolytes. Schmidt and Lücke,[89] by measuring electrode potential, concluded that for thin foils cathode hydrogen diffuses through more rapidly than it can re-enter an electrolyte, while for thicker foils the hydrogen passes into the electrolyte as fast as it comes through. Borelius and Lindblom[90] attempted to relate cathode current density to equivalent pressure, finding $p = 17,000$ I, which they admit is probably far from correct even if gas and cathodic diffusion proceed in the same manner.

There are a few investigations from a more mechanistic viewpoint. Williams and Homerburg[91] found that stresses up to the yield point produced a marked increase in the rate of diffusion of cathode hydrogen, and that slag and inclusions of oxides and sulphides, if present, especially at the grain boundaries, are attacked and removed, thus providing an easy path of diffusion. Such an effect, however, could not occur in a homogeneous single-phase sample. For a single crystal of pure iron, Edwards[92] found the diffusing of nascent hydrogen to occur at the same rate as for the same material in fine-grained form, indicating that the boundaries are not a factor for pure material. Mahin,[93] by observation with the microscope, found that the diffusing hydrogen was evolved quite uniformly over the surface of the grain, not concentrated at the boundaries. Additional confirmation of this point has been made by Körber[94] and others.

Diffusion at High Pressure.—While gaseous hydrogen does not ordinarily diffuse through iron at room temperature, Bridgman[95] found that this does occur at 9000 atmospheres. Poulter and Uffelman[96] found steel to permit the passage of hydrogen at only 4000 atmospheres, after which treatment the hydrogen would go through freely at 100 atmospheres.

The opening of pores could only be detected under the microscope after several treatments. The gas was evolved as a uniform distribution of fine bubbles, too small to be seen individually without a microscope.

We should like to note that throughout all of this work there is the suggestion that while lattice diffusion undoubtedly predominates in certain temperature and pressure ranges, there is also a factor of a more mechanical nature. We do not believe this to be due to gross cracks in normal cases, nor to the grain boundaries, at least in pure material. As will be shown later, diffusion along rifts at the slip planes may be a considerable factor. It is not at all certain that such diffusion would follow the same mathematical law as effusion through larger holes.

Critical Points.—The famous "hydrogen points" of Roberts-Austen,[97] if reproducible, would afford valuable information for the occlusion problem. Such points have been found for electrolytic iron by Müller,[40] Guillet and Portevin[98] and others beside the original observer. They occur at different positions in the different samples and vary in number from 2 to 10 or 11. The points disappear with the gradual loss of hydrogen and are not generally restored by recharging. They have not, however, been found for less saturated irons. Charpy and Bonnerot[25] found no effect of degassing on the critical points of steel. Rawdon, Hidnert and Tucker,[99] found no such points for iron heated in hydrogen, but observed a slight absorption of heat from room temperature to 200° for cathodically charged iron, corresponding to the release of gas; and some irregularity near 370°. Esser[60] found an increasing magnitude of the volume change at A_3 with the expulsion of hydrogen. Rugan and Carpenter[23] found a slight contraction of length and increase of diameter when the gas was expelled from a sample of cast iron. Sieglerschmidt[100] reports that electrolytic iron shows an increased thermal expansion near 600°, but does not report any additional points. Esser and Cornelius[101] find the only effect of heating in hydrogen to be a splitting of the A_3 transition.

It would appear, therefore, that there is nothing in the thermal data of sufficient certainty to cause any modification in the inferences from lattice occlusion data already discussed. Whatever effects may occur correspond to very high concentration of hydrogen and could be in equilibrium only at high pressures. They might indicate the temporary existence of another phase, but could equally as well be due to secondary effects.

X-ray Structure.—The X-ray data on the iron-hydrogen system are very limited, comprising only three papers. Okochi[43] observed that the greater part of the hydrogen occluded in electrolytic iron is expelled on heating to 100° to 500° and that the *small part remaining* is present as a solid solution (lattice occluded). Rawdon, Hidnert and Tucker[99] found no effect on structure on heating iron in hydrogen. Wever and Pfarr[102]

found both distention and line broadening, indication of an interstitial solid solution plus a disruption of the regular grain structure. This last would be expected in rift occlusion.

Mechanical Properties.—The hardness and brittleness of electrolytic iron, as well as embrittlement on cathode charging of iron or on pickling in acid, have often been observed. Among those who observed these effects without any particularly satisfactory attempt at explanation are Lenz,[39] Cailletet,[38] Heyn,[21] Fuller,[103] Cournot,[104] Cazard and Hugues,[105] Guillet and Roux,[67] and Bardenheur and Ploum.[106] It appears that in some cases at least part of the embrittlement due to hydrogen is the result of the reaction of the hydrogen with slag, and sulphide or oxide inclusions, largely at the grain boundaries. Andrew[107] thinks this may be a factor. Large importance is attached to this effect by Williams and Homerberg[91] and by Baukloh and Guthmann.[61] Thanheiser[108] ascribes blistering on pickling to the same cause.

Hardness has been ascribed to the formation of a solid solution by Benedicks,[109] Merica,[110] Guillet and his co-workers[111] and by Majima.[112] The last concludes: "H exists in two forms in iron. Part is occluded mechanically and has no specifically marked effect on the strength of the iron. Part of the H, however, is present in the iron in some form of solid solution and causes the brittleness of the metal." The only objection to assigning hardness to the solid solution is the known very low concentration of the latter at ordinary temperatures.

It has been often suggested that the hardness of electrolytic iron is due largely to its structure and not to the gas content, since softening is not usually coincident with the main evolution of hydrogen. This viewpoint is supported by the work of Story,[113] Okochi,[43] Hugues,[66] and Guichard et al.[114] The similar viewpoint for iron hardened by charging is supported by Andrew,[107] who states that brittleness is due rather to induced molecular rearrangement than directly to the hydrogen. This last may well include the effect of rift occlusion such as has been demonstrated in this laboratory for nickel[123] and palladium.[122] Andrew's view[73,107] that the main occluder is "additional amorphous cement produced by cold work" would in modern terminology refer to disrupted material at the slip planes. He shows[107] one photomicrograph in which there is a fine structure suggestive of the effect of hydrogen on nickel, but the resolution is not sufficient to permit any definite conclusion. Pilling[64] also observed a fine structure and thought he had an "unstable compound" formed, but was also unable to resolve the patterns. Pfeil[115] found a little grain-boundary effect at low temperature, but found that more generally his iron was weakened *on the cubic cleavage planes.* He used both ordinary and single-crystal iron and thought that cracks due to machining strains were in some way intensified by the occluded hydrogen. Alekseev and Polukarov[116] dispute this for really pure hydrogen, but must have

observed the same effect, since they ascribe it to impurities such as AsH_3 in the hydrogen.

Electrical Resistance.—While the electrical resistance of a metal increases upon formation of a solid solution, there are other factors besides lattice occlusion that can bring about a change in this case. Thus any change in dimensions will have its effect, as will a strain, or still more, an opening up of structure. Sieverts[117] attempted to determine the order of the change to be expected from the formation of the solid solution by using the same law observed for palladium, obtaining values of 0.04 per cent at room temperature and 0.33 per cent at the melting point. He was not able to observe any change during gas occlusion. Johnson[51] appeared to find an increase of resistance after pickling, but had to allow for the iron dissolved, and so could not make an accurate measurement. Belloc[33] found a 10 to 12 per cent decrease after expelling the gas from his wire, which is a value so large that it must be due to changes in structure on annealing, rather than to the gas directly. Guillet and Portevin[98] found a slight elevation of resistance for electrochemical occlusion and from it set the limit of solid solution in their electrolytic iron at 0.008 per cent (7 rel. vol.), and in a cathodically charged bar at 0.006 per cent (5.2 rel. vol.), values higher than the one atm. isotherm, but much lower than the total amount recoverable. Several workers in M. A. Schurmann's[118] laboratory have obtained increased resistance upon gas occlusion by a process of many successive chargings and dischargings. This method produces a metal having a very definite open structure, so that the increase of resistance may be due largely to mechanical causes.

Magnetic Properties.—Corresponding with the mechanical hardness of electrolytic iron or the hardening upon occlusion of hydrogen, there is a similar increase of magnetic hardness. This was first observed by Mattheissen[119] and confirmed by Cailletet[38] and by Cazard and Hugues.[105,66] Cioffi[120] found magnetic softening upon treatment of iron with hydrogen and subsequent degassing, but does not think it due directly to the hydrogen. Reber,[121] investigating the changes produced by cathode charging, finds them to persist after the expulsion of the gas. His conclusions appear well founded and are in accord with the suggestions we have made with regard to rift occlusion. We quote:

> It is suggested that the iron is locally cold-worked by nonuniform distribution in it of hydrogen in excess of the solubility limit at room temperature, and that uniformly distributed hydrogen up to this limit has very little effect on ferromagnetic properties. The small time difference for the hardening effect on different thickness rings makes it seem probable that H^+ is being fed at once to all points of weakness through many channels of low resistance, rather than entering by plane diffusion from the exposed surface.

APPARATUS

The apparatus used in this investigation is basically similar to that commonly used to determine the gas content of metals, but a few modifi-

cations have been made to overcome recognized sources of error. When using an exterior source of heat most workers since Parry[18] have either observed or suspected a more or less continuous evolution of gas from the boat and combustion tube, necessitating large and uncertain blank corrections. At higher temperature, also, it is never certain that gas is not diffusing in through the tube itself. Therefore we decided to heat the samples by passing current directly through them, using as electrodes and supports heavy copper tubes, which could be water-cooled. The clamps that came in actual contact with the samples were made from coin silver, which to the best of our knowledge is not an occluder, thus eliminating any possibility of emission of gas from the electrodes, even if locally heated at the contact point. The part of the vacuum system immediately surrounding the sample was made separable from the rest at two ground joints, allowing easy access to the sample. This piece was of fused quartz, but inasmuch as the samples were not in actual contact with the wall, the temperature never went much above 100° and the use of quartz was a needless refinement. Since placing a thermocouple in direct contact with a small, directly heated sample would probably change its temperature and also introduce a possible source of gas, we were forced to rely on an optical pyrometer for our temperature determinations. Pressure was observed by means of two McLeod gauges of different compression ratios, supplemented by a manometer for values above one millimeter. Before the third run, provision was made for checking the purity of the evolved gas by adding a compression bulb and Plücker tube, allowing the gas to be analyzed by its emission spectrum. The complete system is shown in Fig. 2.

The furnace section is shown at A. The T-shaped quartz tube has two ground joints tapered in the same direction, and can be slid up over the long electrode to expose the sample. When in use, the joints are sealed with Picein and protected by water jackets, as shown. The sample, in the form of a ribbon, is rigidly clamped in the upper silver electrode. A silver block weighing about 20 grams clamps on the lower end and serves to keep the sample straight and out of contact with the walls. This block is in turn connected to the lower electrode jaw by a pure silver ribbon, which is pleated to allow free motion of the block. The low-voltage, high-amperage current for heating the sample is supplied from a variable step-down transformer giving nominal outputs of from 1 to 45 volts from a 110-volt primary. The main current control is on the primary side, a 220-volt source being connected through a power resistance and bank of constant current ballast tubes to the 110-volt winding. A smaller resistance across this winding allows up to the full current of one tube to be shunted past. By switching the tubes in or out and varying this shunt, any current from zero to the capacity of the tube bank can be passed through the transformer and held constant. When the drop across the tube bank is adjusted to the middle of the working range, the

tubes will absorb a fluctuation of from 20 to 30 volts on the lines without allowing any noticeable variation in the secondary current through the sample.
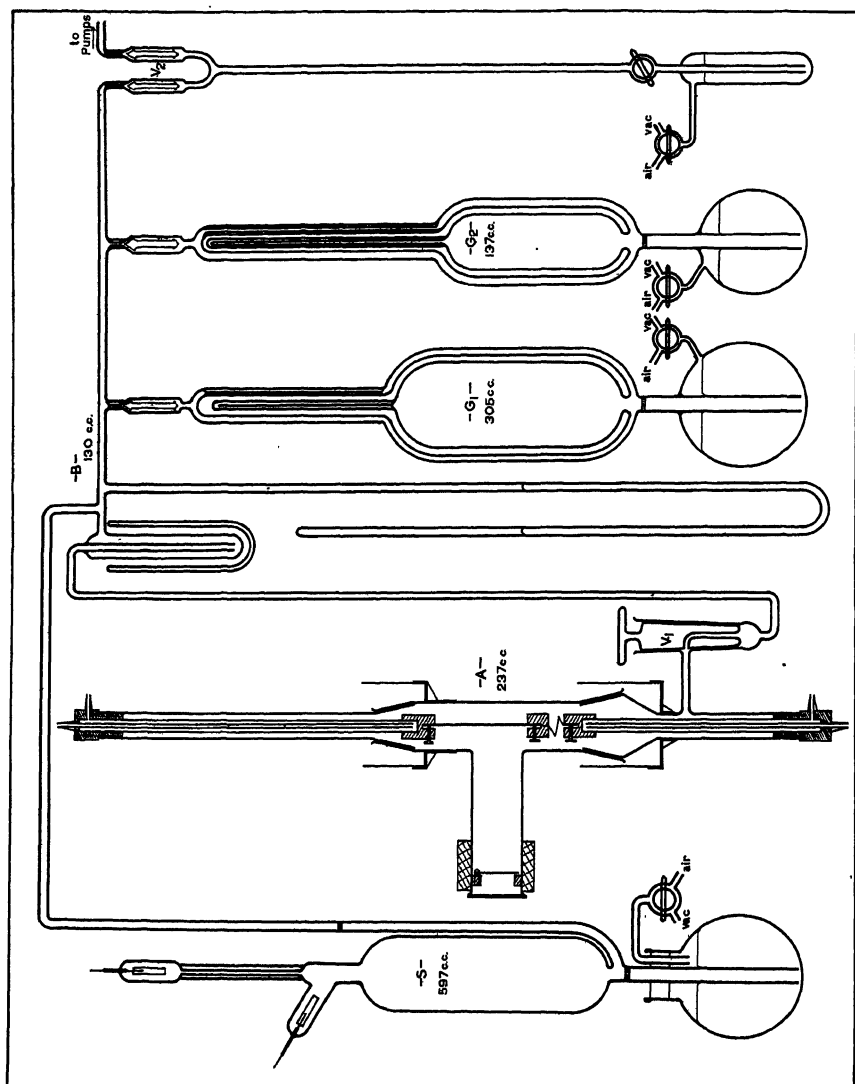
FIG. 2.—APPARATUS FOR MEASURING GAS EVOLUTION.

When first testing this furnace arrangement with a straight furnace tube, we found that, as the melting point of the sample was approached, there was an appreciable amount of sputtering of the metal onto the walls, producing a film, which made the optical pyrometer readings inaccurate. A side tube about 6 in. long was therefore added, closed at its outer end

by a flat quartz window through which observations could be made. As a further protection of the window, a small magnetically operated door was installed, which remained closed except when we were actually reading the temperature. A ring of phosphor bronze fitted snugly into the side tube served to support a sheet of the same high-purity iron used as samples. A coil, consisting of about 40 turns of No. 18 bell wire, wound outside the tube was connected to a 6-volt battery through a key near the pyrometer. When energized, this coil swung the iron door up to the top of the side tube and out of the line of vision. The pyrometer was a Hickok–Leeds and Northrup standard model and was calibrated against the melting points of nickel, copper and iron in the furnace, and against a standard thermocouple for the lower ranges. As used, it would detect a variation of two or three degrees from any fixed temperature, but could only be relied on for absolute values within about 15°. Temperatures below red heat could be estimated only by applying the same law to the heating current through the sample as is used for the pyrometer current at higher temperature.

The tube for spectroscopic analysis is shown at S. The heavy electrodes were supported on tungsten rods running through Pyrex seals about 1 in. long. For the electrodes proper, Monel metal rod was found most satisfactory, although pure sheet nickel was used successfully for a while. The common aluminum electrodes could not be used because of their large affinity for oxygen and their usually large gas content. The compression bulb under the discharge tube, 597 c.c. in volume, was operated by connections to the air and to a water pump, similarly to the McLeod gauges, and made it possible to bring gas from a pressure of less than 10^{-4} mm. up to sufficient density to give a good emission spectrum. The spectroscope used is a Gaertner wave-length spectrometer, equipped with a small camera interchangeable with the eyepiece, and having a stepslide over the slit so that a logarithmic series of exposures could be made.

Since the mercury pump was operated only to obtain a vacuum at the start of each isotherm, and was then cut off, sometimes for several days, during the course of the run, it was necessary to exclude all leaks completely. The one stopcock between the furnace and the liquid-air trap was found indispensable, since no mercury could be permitted in this section and a shutoff of some kind was needed whenever the liquid air was removed from the trap. By using a large cock, of about 25 by 100 mm., having the lower end completely enclosed; and by pouring a layer of melted stopcock grease into the cupped top, all leaks at this point were eventually eliminated. The connection between the pump and the high-vacuum system was made through a mercury cutoff. Sufficient mercury almost to fill the Y was confined between the two float valves and a stopcock about 50 cm. down the central arm, at which point the back

pressure of the mercury was sufficient to prevent any possibility of leakage. Thus confined, the mercury seal is impervious to gas up to a pressure considerably above one atmosphere. Similar float valves at the top of the McLeod gauges served both to prevent spilling mercury over into the rest of the system and to give definite cutoff points to aid in holding the volume constant at known values. The compression bulbs not immediately needed could thus be subtracted from the constant-volume system by the simple expedient of running the mercury up to the marks at the beginning of a run. At the spectrum tube, a barometric riser was used and the constant-volume point indicated by a marking band, thus making it necessary to adjust the level at this point before making any reading. This proved to be so much bother that the insertion of a float valve at this point would have been highly advisable. The constant-volume points for any of the bulbs when open were taken as those at which the mercury just cut off, or opened, the lines, and therefore seldom had to be considered.

The spectrum tube and bulb were normally opened at or near the end of an isotherm run, at which time the furnace section A was closed off at the stopcock. The spectrum normally showing the absence of appreciable quantities of any gases but hydrogen and oxygen, a fairly good quantitative analysis could be made by opening all the bulbs and passing a discharge from one terminal of the Plücker tube to the mercury cutoff near the pump, and to the mercury at the bottom of the gauges. In the course of about half an hour the oxygen would all be converted to water and absorbed in the liquid-air trap. One-third of the change in volume, then, represented the content of free oxygen in the gas. Upon then removing the liquid air and allowing the trap to reach room temperature, the pressure would increase corresponding to the total volume of water, some of which had been produced by the removal of the oxygen, the balance being free water evolved during the course of the run, but not observed in the original pressures.

The general method of taking an isothermal evolution curve was as follows: With the furnace closed off and the liquid-air trap warm, the system was pumped down to about 10^{-6} mm. The furnace connection was then opened and the bulk of any gas there allowed to rush through the warm trap before the liquid air was put on a few minutes later. Evacuation was then continued until the whole system reached a pressure of about 10^{-6} mm., the gas on the walls being driven out with a high voltage discharge. When this pressure was reached, the spectrum tube and bulb were closed off by letting the mercury up to the constant-volume marker. Exactly one minute before zero time, gauge I was closed, the mercury being allowed to run up to the float valve without any attempt at a reading. About 30 sec. before the zero, the mercury in the Y cutoff was allowed to start rising at a rate sufficient to close off

the tube within 5 sec. of the zero.   The heating current was then started, or increased, at the moment when the pump was cut off.   Gauge II could then be closed for the first reading as early as one minute after the start of the run.   The pressure base value, being preserved in gauge I, could subsequently be read when convenient.   Normally, the pressure in the system was on the scale of the lower compression gauge after about one minute, so the high-compression gauge I was left closed throughout the run unless an expansion of volume appeared advisable.

RESULTS

A. The iron used in this investigation was a sample of hydrogen-purified carbonyl iron kindly supplied by Dr. R. F. Mehl.   It had the following analysis: C, <0.005 per cent; S, <0.002; O_2, <0.002; N_2, <0.001; Al, 0.002; Cr, 0.012; Mn, 0.005; Si, 0.030; Cu, 0.017; Ni, 0.013. It had been saturated with hydrogen at 880°.   A similar piece in bar form gave an analysis of 0.0002 per cent H_2.   The metal was rolled into sheet about 0.06 mm. thick, then cut into ribbons about 4 mm. wide by 185 mm. long.

In all, three runs were made.   Of these, No. 1, preliminary in nature and serving only to show that the evolution was not such as would be expected from a lattice solution, will not be reported in detail.   Run 2 was on a sample weighing 0.4818 grams, whose only exposure to hydrogen was for a few minutes at low pressure while the apparatus was being flushed out at the start of the run.   The sample for run 3 weighed 0.4016 grams and was soaked in hydrogen in the apparatus for 55 days at one atmosphere and about 25°.

B. The total amount of gas evolved after various times and temperatures is shown for run 2 in Fig. 3.   Three scales of volume are given, the inside being relative volumes for this sample, plotted cumulatively, and others being cubic millimeters at room temperature and 760 mm., plotted both cumulatively and separately for each isotherm.   The isotherms were run consecutively on the same sample without intermediate treatment.   In this run the spectroscopic apparatus had not been added, so no analysis of the gas was made.   No correction for room temperature was made.   A large liquid-air trap was used at this time, necessitating a considerable correction as the liquid air evaporated.   This took the form of a revision of the effective volume of the system when assuming it for calculating purposes as at uniform temperature.   This change of volume was determined by trial on the empty system containing a fraction of a millimeter of hydrogen, a curve being taken over 24 hr. and then applied in calculating the results of the run.   In run 2 this correction amounted to about 100 c.c. for a full trap, accurate only to 3 or 4 c.c., thus limiting the accuracy of the volume (some 700 c.c.) to about 1 per cent.   In run 3, the trap was made much smaller, thus reducing this

correction to 7 c.c. for a full trap, known to a fraction of a cubic centimeter, and making the effective volume of the system good to about 0.1 per cent. The variation of room temperature was a larger error in both
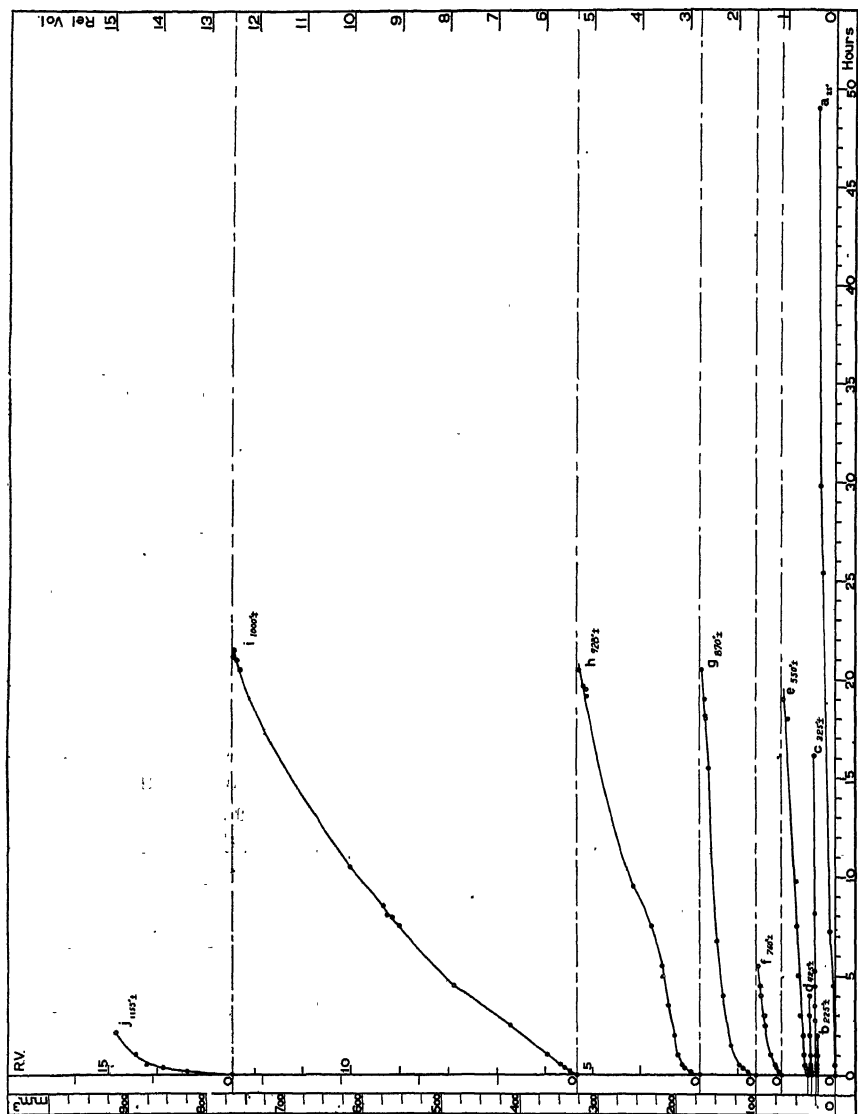
FIG. 3.—ISOTHERMAL EVOLUTION OF GAS FROM PURE IRON, RUN 2.

cases, although measured to 0.1° in run 3. No correction was made for the Knudsen effect in the furnace, since this was constant for any isotherm and relatively small in any case, inasmuch as the furnace body never went above 100°.

In run 3, with the saturated sample, an effort was made to reduce all errors to as small a value as possible in order to determine whether the irregularities in the previous run were real. The spectroscope was added and its results checked by burning and freezing out the oxygen as water.
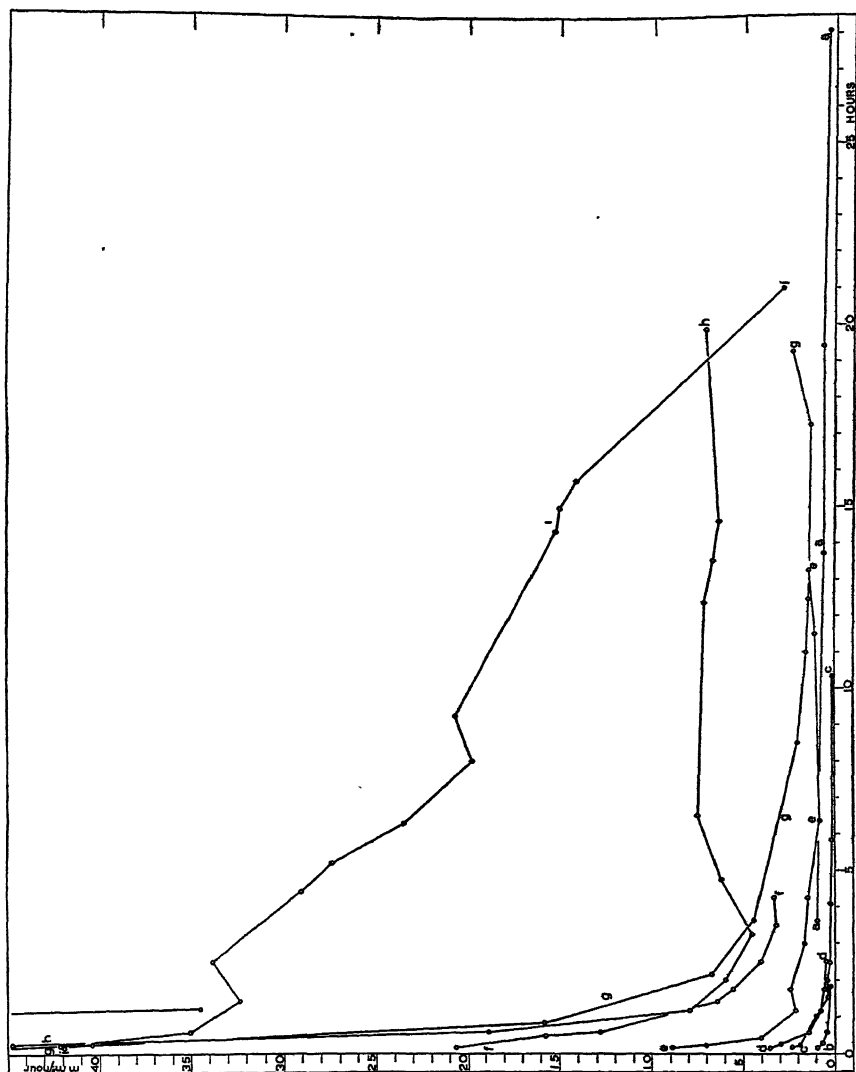
FIG. 4.—RATES OF EVOLUTION, RUN 2.

Room temperature was noted and accurate corrections made for the liquid-air trap, as noted above. The results, reduced to normal temperature and pressure, are shown in Fig. 5, and are accurate to at least one part in 1000 above the base line for the isotherm considered. This is better than the scale of plotting demands, so all visible variations are

TABLE 4.—*Abstract of Data on Evolution of Hydrogen from Pure Iron*

Run	Temperature, Deg. C.	Pressure, Mm.	Rate, Cu. Mm. per Hr.	Average Rate, Cu. Mm. per Hr.	Total Volume, Cu. Mm.	Time, Hr.°Min.'
2-a						
Initial............		0.000333	0.716	0.966		
Maximum.......	26	0.0162	1.53	0.966		
Minimum........	22		0.117	0.358		
Final............			0.117	0.358	21.96	49° 00'
2-b						
Initial............		0.000018	0.420	0.941		
Maximum.	225	0.000821	1.286	0.941		
Minimum........	200		0.132	0.260		
Final............			0.308	0.260	0.308	2° 00'
2-c						
Initial............		0.000065	3.28	2.33		
Maximum........	325	0.005728	3.28	2.33		
Minimum........	300		Zero	0.184		
Final............			0.197	0.188	4.650	16° 10'
2-d						
Initial............		0.000067	2.76	3.56		
Maximum........	430	0.003570	3.975	3.56		
Minimum........	420		0.337	0.478		
Final............			0.415	0.478	3.264	4° 00'
2-e						
Initial.......:....		0.000187	9.918	8.899		
Maximum........	600	0.03286	12.375	8.899		
Minimum........	550		0.255	0.841		
Final............			5.146	1.46	31.565	19° 00'
2-f						
Initial............		0.000348	19.00	20.67		
Maximum........	770	0.03436	21.16	20.67		
Minimum........	738		1.96	3.34		
Final............			2.88	3.34	30.246	5° 30'
2-g						
Initial............		0.000805	40.62	47.43		
Maximum........	880	0.0764	60.62	47.43		
Minimum........	833		Zero	1.367		
Final............			2.76	2.355	68.905	20° 30'
2-h						
Initial............		0.000266	78.23	44.727		
Maximum........	943	0.1659	78.23	44.727		
Minimum........	900		2.115	4.53		
Final............			6.868	7.127	156.108	20° 30'
2-i						
Initial............		0.001058	48.95	41.916		
Maximum........	1037	0.4641	48.95	42.155		
Minimum........	972		Zero	2.864		
Final............			Zero	2.864	437.8	21° 30'

TABLE 4.—(Continued)

Run	Temperature, Deg. C.	Pressure, Mm.	Rate, Cu. Mm. per Hr.	Average Rate, Cu. Mm. per Hr.	Total Volume, Cu. Mm.	Time, Hr.°Min.'
2-j						
Initial............		0.00208	103.14	216.81		
Maximum........	1158	0.1677	352.74	221.63		
Minimum........	1148		23.878	34.508		
Final............			23.878	34.508	148.98	2° 07'

Grand total gas 901.683 cu. mm. = 14.71 rel. vol. (corrected)

Run	Temperature, Deg. C.	Pressure, Mm.	Rate, Cu. Mm. per Hr.	Average Rate, Cu. Mm. per Hr.	Total Volume, Cu. Mm.	Time, Hr.°Min.'
3-a						
Initial............		0.001576	2.23	10.874		
Maximum........	26.4	0.1232	13.89	10.874		
Minimum........	23.6		0.040	0.432		
Final............		0.05051	0.040	0.432	114.87	96° 30'

$O_2 = 6.702$ per cent:$H_2 = 93.298$ per cent:plus $H_2O = 40.020$ per cent

Run	Temperature, Deg. C.	Pressure, Mm.	Rate, Cu. Mm. per Hr.	Average Rate, Cu. Mm. per Hr.	Total Volume, Cu. Mm.	Time, Hr.°Min.'
3-b						
Initial............		0.000074	70.8	50.7		
Maximum........	450	0.07997	70.8	50.7		
Minimum........	430		0.14	0.211		
Final............		0.03879	1.25	0.380	82.77	99° 30'
3-c						
Initial............		0.000049	1.26	0.282		
Maximum........	450	0.03411	1.26	0.496		
Minimum........	430		Zero	0.169		
Final............		0.03366	0.09	0.496	20.728	91° 57'

Total both runs: 103.50 mm.³

$O_2 = 10.205$ per cent:$H_2 = 89.795$ per cent:plus $H_2O = 90.488$ per cent

Run	Temperature, Deg. C.	Pressure, Mm.	Rate, Cu. Mm. per Hr.	Average Rate, Cu. Mm. per Hr.	Total Volume, Cu. Mm.	Time, Hr.°Min.'
3 d						
Initial............		0.00157	56.3	33.64		
Maximum........	777	0.1597	56.3	33.64		
Minimum........	695		Zero	0.585		
Final............		0.04762	1.420	0.80	122.83	96° 45'

$O_2 = 11.524$ per cent:$H_2 = 88.476$ per cent:plus $H_2O =$ zero

Run	Temperature, Deg. C.	Pressure, Mm.	Rate, Cu. Mm. per Hr.	Average Rate, Cu. Mm. per Hr.	Total Volume, Cu. Mm.	Time, Hr.°Min.'
3 e						
Initial............		0.00113	40.33	117.2		
Maximum........	965	0.9942	159.6	117.2		
Minimum........	910		Zero	2.65		
Final............		0.5759	0.41	2.65	948.5	215° 00'

$O_2 = 0.669$ per cent:$H_2 = 99.331$ per cent:plus $H_2O = 4.60$ per cent

Run	Temperature, Deg. C.	Pressure, Mm.	Rate, Cu. Mm. per Hr.	Average Rate, Cu. Mm. per Hr.	Total Volume, Cu. Mm.	Time, Hr.°Min.'
3-f						
Initial............		0.00396	138.5	109.4		
Maximum........	1080	1.0521	138.5	109.4		
Minimum........	1070		9.5	10.29		
Final............		0.5703	23.	10.29	1003.2	47° 00'

$O_2 =$ zero:$H_2 = 100$ per cent:$H_2O =$ zero

Grand total: 2293 cu. mm. = 44.88 rel. vol. permanent gas

plus 183.3 cu. mm. = 3.587 rel. vol. H_2O

$H_2 = 97.636$ per cent:$O_2 = 2.364$ per cent:plus $H_2O = 7.992$ per cent

real. The dotted portion of curve f, Fig. 5, represents standing at 25° when the run was stopped overnight, and is the only case where an isotherm was interrupted. The short vertical lines cutting the various curves represent reductions in pressure by expansion of the system
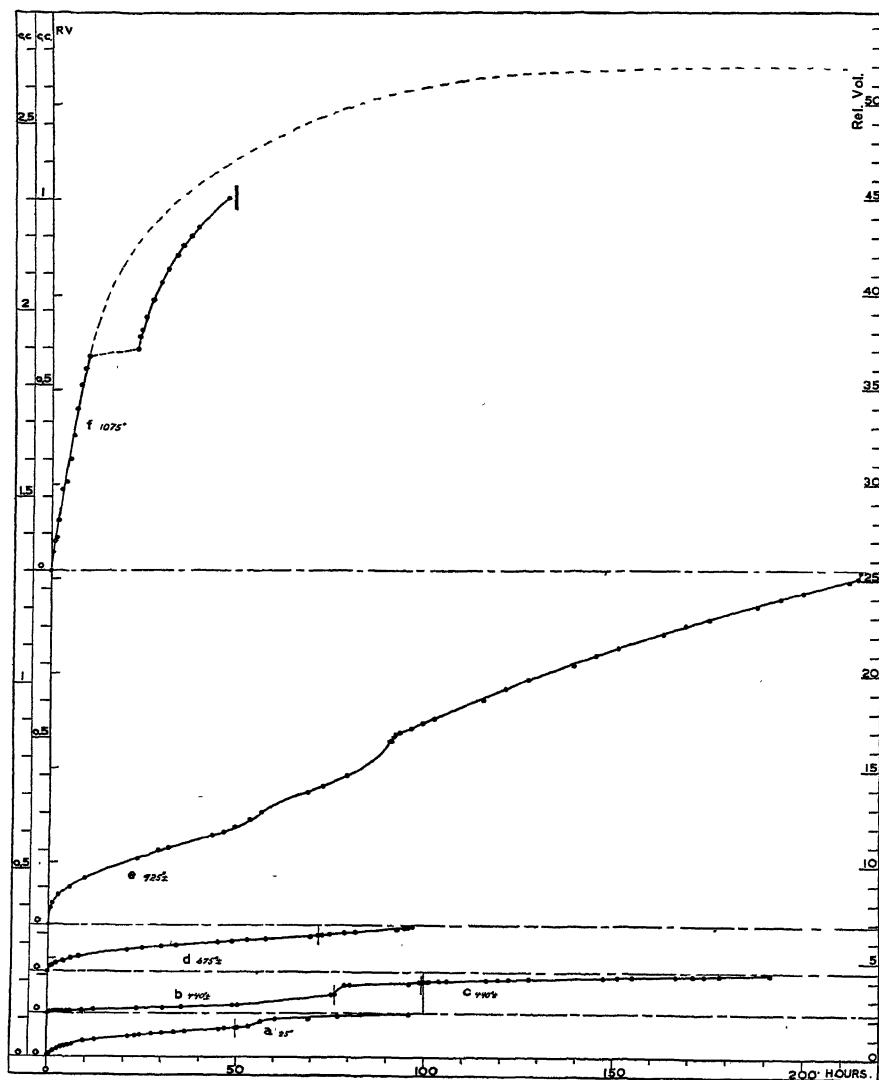
FIG. 5.—ISOTHERMAL EVOLUTION OF GAS FROM PURE IRON, RUN 3.

whenever the pressure approached 1 mm. For curve c, Fig. 5, the system was exhausted to 10^{-4} mm., but the temperature was held at the same value. The temperature and pressures, as well as other data for these and other curves will be found in Table 4.

C. The rates of evolution of gas in cubic millimeters per hour, uncorrected for area of sample, have been calculated directly from the original data. These were found in all cases to show very large fluctuations,
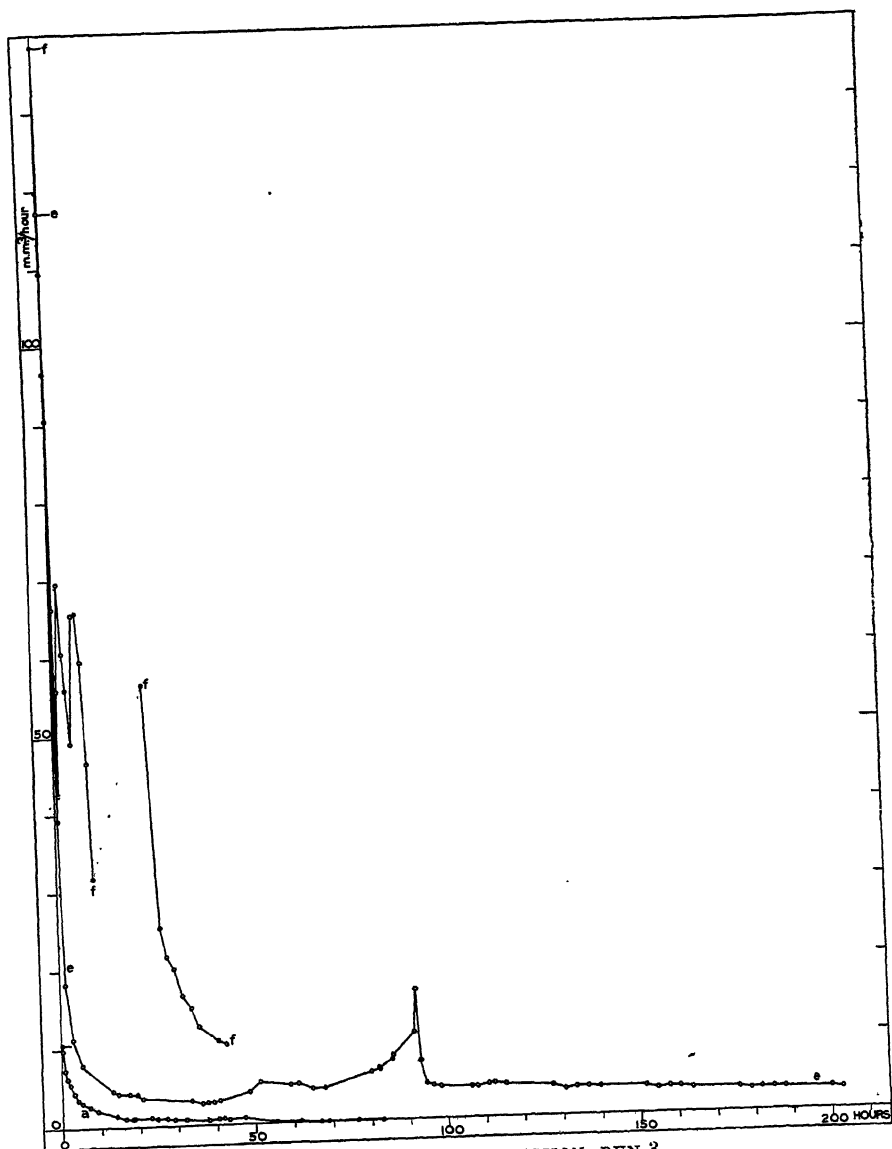
FIG. 6.—RATES OF EVOLUTION, RUN 3.

which usually amounted to from 2 to 20 times the probable error. In order to eliminate the possible compounding of errors due to the appearance of the same reading with opposite sign in two successive rates, the

figuring of rates over longer periods was considered advisable.   Three
reading periods were taken; i.e., the rate was struck between each reading
and the fourth following, and plotted against the mean time between the
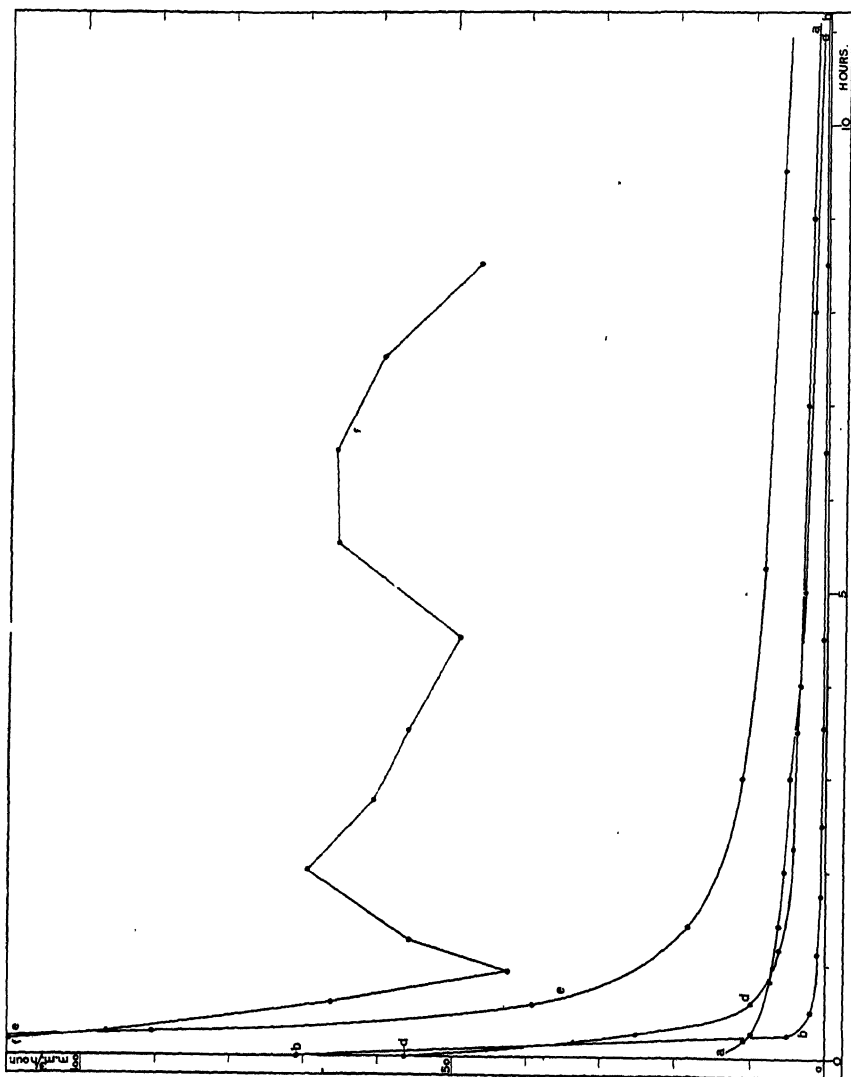
FIG. 7.—RATES OF EVOLUTION, RUN 3.

two.   All the rates shown are figured in this way except in Fig. 8, where
both methods were used.   Since in this case successive rates are com-
pletely independent, the displacement of two points in the same direction
presumably represents a real fluctuation and of three points almost
certainly a real fluctuation.   Making due allowance for the new smaller
value of the probable error, the relative improvement in smoothness of

the curves is greater than would correspond to the reduction in error alone, but they still show variations several times the probable error. Fig. 4 shows the complete rate curves for run 2; Fig. 6 three complete
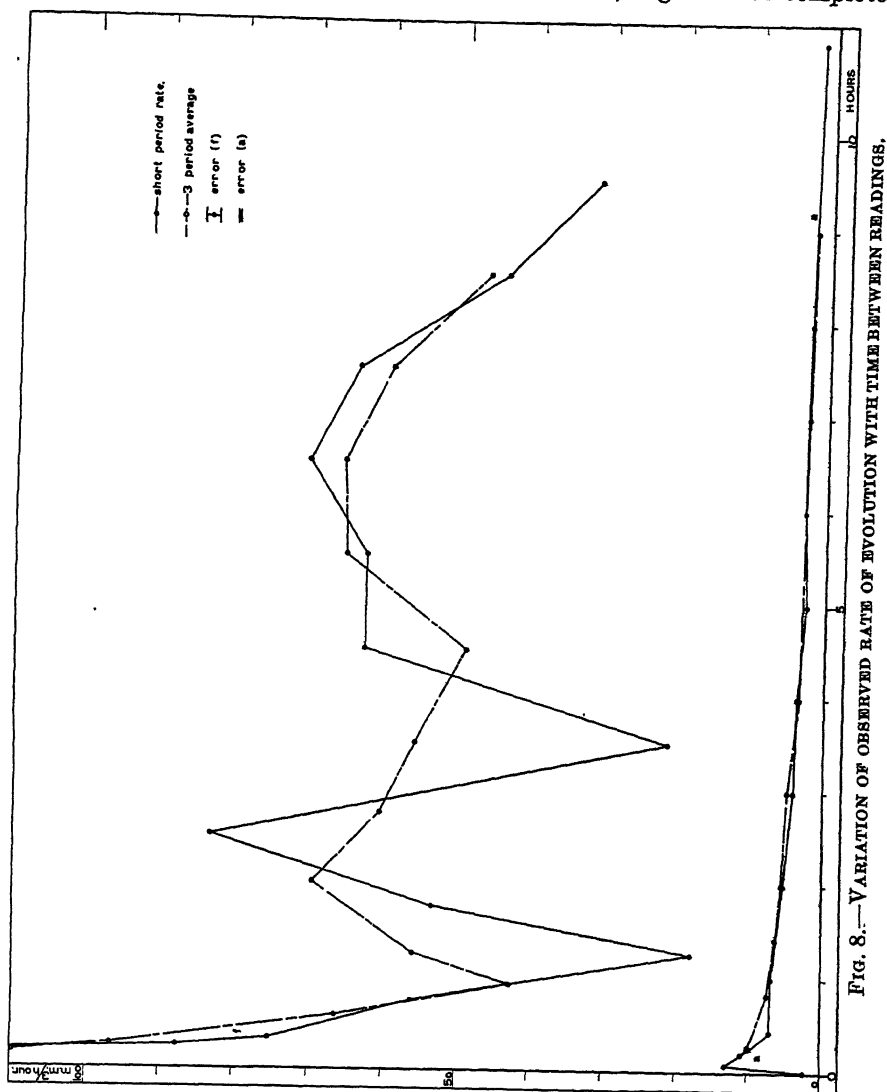
FIG. 8.—VARIATION OF OBSERVED RATE OF EVOLUTION WITH TIME BETWEEN READINGS.

curves for run 3; Fig. 7 the first 10 hr. for each isotherm of run 3, and Fig. 8 two of the same curves figured both for two and four readings.

D. It must be admitted that our measurement of temperature was not very accurate, so we do not put too much faith in the absolute values of the gas content and rate variation with temperature, but would like to call attention to the magnitude and general form of the gas content,

shown in Fig. 9, as compared with the lattice occlusion values which are there replotted from Fig. 1. The presumably small unknown gas content at the end of the run should be added to all values. In Fig. 10 are shown curves for both the initial rate of evolution at various temperatures
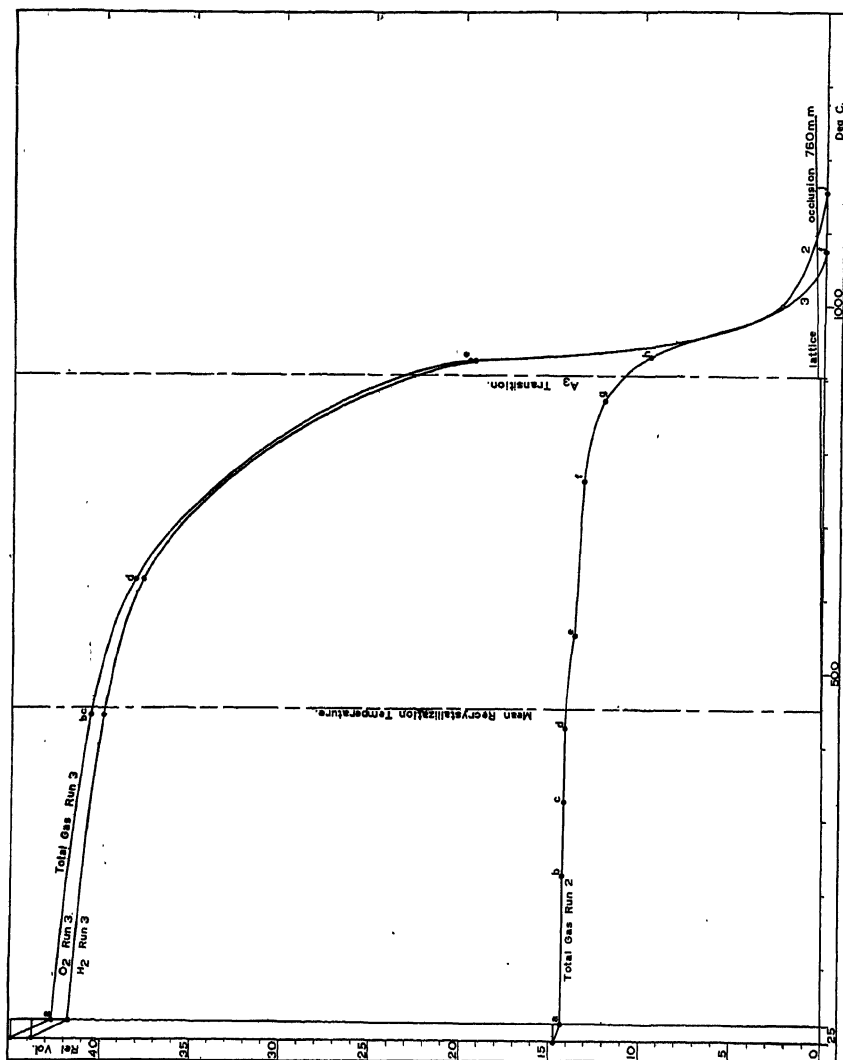
FIG. 9.—OBSERVED GAS CONTENT OF PURE IRON AFTER ANNEALING IN VACUO.

and the basic or final rate after the latter levels off. Since it appears that the initial rates may depend largely on the change of temperature between isotherms, these rates are also shown divided by the number of hundreds of degrees step-up of temperature from the previous run. Since the curves cross several times, the points have been identi-

fied by run number and isotherm letter in this figure, corresponding to the previous figures.

E. Some mention should be made of the change in properties of the iron upon such thorough degassing. The original material was similar
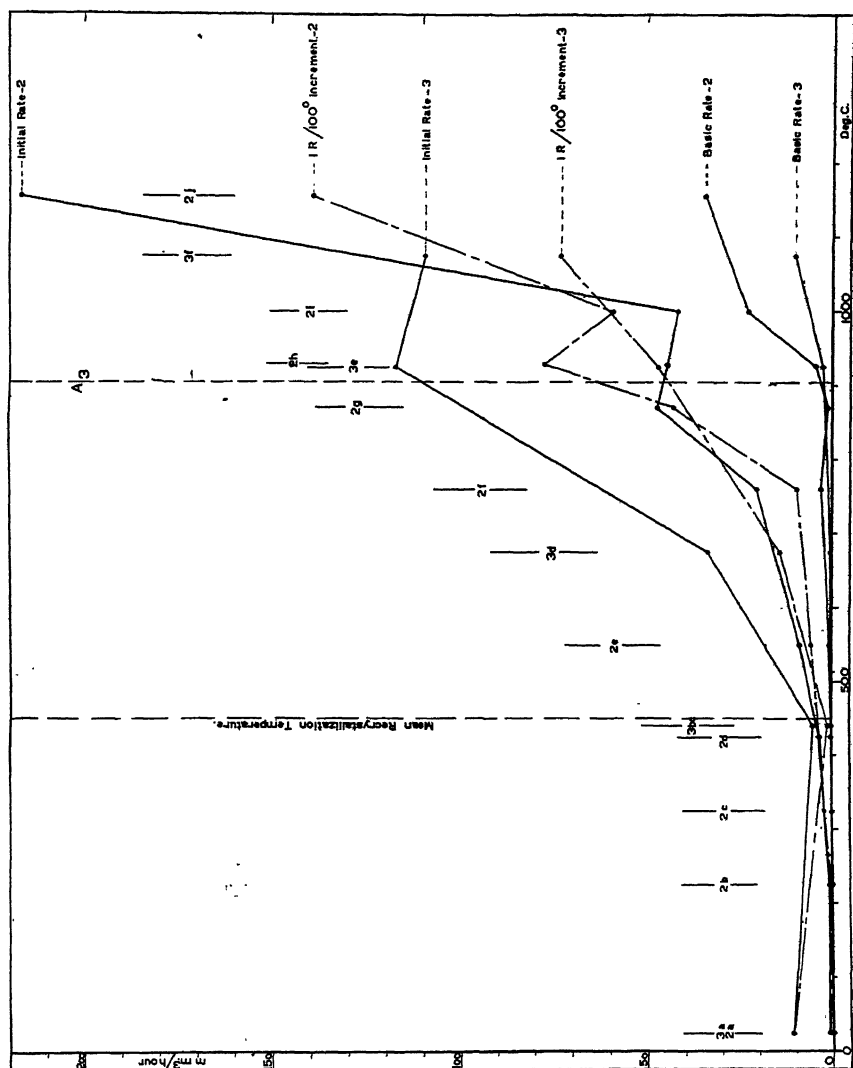
FIG. 10.—RATES OF EVOLUTION AT VARIOUS TEMPERATURES.

in properties to Armco and similar commercially pure iron, and was hard from the rolling. After the degassing anneal, the metal had assumed both the appearance and relative softness of platinum foil and remained exposed to laboratory air in a wet bottle for over one year without a sign of tarnish. It did not, however, retain its stainless properties after being

strained. Immersed in water saturated with air, the iron did not rust, but rather etched cleanly, as would be expected in dilute acid.

DISCUSSION OF RESULTS

We have already considered the comportment that would be expected if the occlusion of hydrogen by iron were a simple lattice occlusion and the process of evolution one of diffusion through the lattice (p. 263). In this case the expected hydrogen content would be zero at room temperature, about 0.2 rel. vol. at 880° (where this iron was first saturated) and not over 1 rel. vol. just below the melting point. After exhausting at a given temperature, no more gas would be expected to come off upon raising the temperature. The isothermal rate would be roughly proportional to the square root of the total hydrogen concentration.

On the contrary, however, it was found that rolled iron soaked in hydrogen at 25° takes up as much as 45 rel. vol. of gas, or over 200 times the amount in the lattice. Of this, only a certain relatively small fraction can be removed at a given temperature in finite time. The portion that can be removed increases with temperature over the whole range of the experiments.

The rate of evolution is *not* rationally related to the amount of gas in the sample. This rate appears to be the sum of two factors, the "initial" and "basic" rates. The initial rate starts high and falls off very rapidly. It develops upon suddenly increasing the temperature to a value higher than any the sample has previously reached, but does not develop on heating again in high vacuum to the temperature of the preceding run; i.e., it depends on the change of temperature as well as its absolute value. It appears to represent evolution from rifts which, owing to the expansion of the metal, have been put in direct communication with the surface.

An initial rate may sometimes be developed at constant temperature (Fig. 5a, b) if the system containing some of the evolved gas is suddenly expanded, indicating that gas of more deep-seated origin has been transferred to the crevices and there retained by the external pressure. This effect, however, is only transient and does not involve any change in the basic rate, and thus bears only a superficial resemblance to the attainment of an equilibrium pressure, a process that we have *not* been able to observe.

The basic rate is small compared with the initial rate. It decreases slowly with time, but becomes infinitesimal while gas still remains in the sample. The controlling factor here is presumably diffusion through the lattice.

Both the initial and basic rates are relatively small below the recrystallization range. The initial rate increases after passing through the recrystallization point and again above the A_3 transition; while the basic

rate is practically independent of temperature up to 450°, then increasing only slightly to the A_3, after which it rises sharply.

The total rate is subject to a series of random fluctuations, varying in magnitude from the lower limit of observation up to at least 10 times the probable error, and varying greatly also in duration. Many of these fluctuations are so large that it does not seem reasonable to attribute them to errors of observation, therefore it is highly probable that they are the result of the discontinuous formation of small bubbles within the surface of the metal, in a manner similar to that which we have previously demonstrated[123] for nickel-hydrogen.

At higher temperatures, minima of longer duration were observed (run 3, e and f; Figs. 6 and 7), which look as though the previous treatment had left a grossly unequal distribution of gas in the sample, thus giving a higher or lower rate as the immediate source of the gas is either a concentrated or less concentrated region.

CONCLUSION

At ordinary temperature high-purity iron, in rolled condition, absorbs as much as 200 times the quantity of hydrogen that corresponds to the lattice occlusion, or true solubility. In the cold-worked metal, therefore, much hydrogen must be contained in voids of some sort, and not in the lattice itself.

In spite of the positive temperature coefficient of lattice solubility, the "saturated" worked metal evolves hydrogen when the temperature is raised, whence again the hydrogen cannot be dissolved solely in the lattice.

Only a minor portion of the contained hydrogen is thus evolved at constant temperature before the rate of evolution becomes immeasurably small. This fact, also, excludes any possibility that the evolution is an approach to solubility equilibrium.

With successive increases, each new temperature brings about renewed evolution, which consists always of a relatively rapid emission, followed by a very much slower one. The rates of evolution bear no rational relation to the total hydrogen content, but appear to be accidental and irregular, showing chance maxima and minima. Rates of this character must result from localized inequalities of hydrogen concentration and a variable resistance to escape.

Our present results hence afford evidence that occlusion is greater in cold-worked iron than in iron that has been fully annealed, and that in the former a large part of the hydrogen is contained in crevices or voids. It appears that rift occlusion, somewhat similar to that already found for nickel and palladium, must in this case account for the majority of the observed occlusive effects; i.e., that in addition to saturation of the lattice a much larger portion of gas is condensed in slip rifts or other small openings, where it is subsequently trapped, by readjustment of the metal.

so that it cannot diffuse out, even into a vacuum. It is only upon further readjustment, occurring upon heating, that the rifts again open and allow the gas to pass to the surface. Apparently these rifts comprise not only the principal seat of occlusion, but also, when available, a preferred path of diffusion.

As to the exact nature of these voids, our present observations show only that they are increased in capacity by cold-working. The possible relation is evident, to the much discussed "mosaic" or "block" structures of metals, regarding which some especially relevant papers have been cited in the foregoing review. Attention has been directed also to the many evidences that the crevices in question are intragranular, and not situated at the grain boundaries. From analogy, only, to palladium and nickel, for which direct evidence has been found that the occluding crevices are rifts along the planes of slip, produced during deformation, we therefore presume them to be similar in iron; recognizing the possibility, however, that in the body-centered cubic crystals of alpha iron the production of twinning voids also may play a role. Further studies by metallographic and other methods are still much needed.

BIBLIOGRAPHY

References listed under the same number are normally reprints, translations, or abstracts of each other, or otherwise contain essentially the same information.

Lattice Occlusion

1. G. P. Baxter: *Amer. Chem. Jnl.* (1899) **22**, 351–360.
2. P. Beckmann: Dissertation, 1907. Leipzig.
   A. Sieverts: *Ztsch. phys. Chem.* (1907) **60**, 129–201.
3. A. Sieverts: *Ztsch. phys. Chem.* (1911) **77**, 591–613.
4. E. Jurisch: Dissertation, 1912. Leipzig.
5. B. Neumann: *Stahl und Eisen* (1914) **34**, 252.
6. K. Iwasé: Tohôku Imp. Univ. *Sci. Repts.* (1926) [1] **15**, 531–566.
7. A. Sieverts: *Ztsch. Met.* (1929) **21**, 37–44.
8. A. Sieverts and H. Hagen: *Ztsch. phys. Chem.* (1931) **A-155**, 314–317.
9. G. Borelius: *Ann. Phys.* (1927) **83**, 121.
10. E. Martin: *Metals and Alloys* (1930) **1**, 831–835; *Stahl und Eisen* (1929) **49**, 1861; *Archiv Eisenhüttenwesen* (1929) **3**, 407–416.
11. H. Schenck and L. Luckemeyer-Hasse: *Archiv Eisenhüttenwesen* (1932) **6**, 209–322; *Technische Mitt. Krupp* (1933) **1**, 121–126.
12. A. Sieverts and G. Zapf: *Ztsch. phys. Chem.* (1935) **A-172**, 314–315.
13. C. J. Smithells: Gases and Metals. New York, 1937. John Wiley & Sons.

Total Occlusion

14. T. Graham: *Phil. Trans.* Roy. Soc. London (1866) **156**, 415–439.
15. T. Graham: *Proc. Roy. Soc.* London (1867) **15**, 502–503.
16. J. Parry: *Jnl.* Iron and Steel Inst. (1873-II) 429–432.
17. L. Troost and P. Hautefeuille: *Compt. rend.* (1875) **80**, 788–791; *Ann. chim. phys.* (1876) [V] **7**, 155–177.
18. J. Parry: *Jnl.* Iron and Steel Inst. (1881-I) 183–194.
19. F. C. G. Müller: *Stahl und Eisen* (1883) **3**, 443–454.
20. G. Neumann and F. Streintz: *Wiener Monat.* (1892) **12**, 656.

21. E. Heyn: *Stahl und Eisen* (1900) **20**, 837–844; *Metallographist* (1903) **6**, 39–48.
22. O. Boudouard: *Compt. rend.* (1907) **145**, 1283–1284; *Metallurgie* (1908) **5**, 277; *Rev. de Mét.* (1908) **5**, 69–74; *Bull.* Soc. Chim. (1908) [4] **3**, 247.
23. H. F. Rugan and H. C. H. Carpenter: *Metallurgie* (1909) **6**, 706–716.
24. P. Goerens: *Stahl und Eisen* (1910) **30**, 1514–1518; *Iron Age* (1910) 1026; *Metallurgie* (1910) **7**, 384–395.
25. G. Charpy and S. Bonnerot: *Compt. rend* (1911) **152**, 1247–1250.
26. T. Baker: *Carnegie Schol. Mem.*, Iron and Steel Inst. (1909) **1**, 219–229.
27. L. Troost and P. Hautefeuille: *Compt. rend.* (1873) **76**, 482–485, 562–566.
28. J. Parry: *Jnl.* Iron and Steel Inst. (1874-I) 92–102.
29. F. Schmitz: *Stahl u. Eisen* (1919) **39**, 373–381.
30. S. Satoh: *Bull.* Chem. Soc. Japan (1930) **5**, 291–303 (in Japanese); *Chem. Absts.* (1931) **25**, 2092; *Nature* (1931) **128**, 457.
31. F. C. G. Müller: *Ber.* Deut. chem. Ges. (1879) **12**, 93–95.
32. F. C. G. Müller: *Ber.* Deut. chem. Ges. (1881) **14**, 6–14.
33. G. Belloc: *Ann. chim. phy.* (1909) [8] **18**, 569.
34. T. Baker: *Carnegie Schol. Mem.*, Iron and Steel Inst. (1911) **3**, 249–259.
35. T. Baker: *Trans.* Faraday Soc. (1919) **14**, 228.
36. G. Tammann and J. Schneider: *Ztsch. anorg. allgem. Chem.* (1928) **172**, 43–64; G. Tammann: *Ztsch. Elektrochem.* (1929) **35**, 26.

Electrochemical Occlusion

37. H. Meisinger: *Dinglers Jnl.* (1862) 163, 283–284; *Neues Jarb. prakt. Pharmacie* **16**, 295.
38. L. Cailletet: *Compt. rend.* (1875) **80**, 319–321.
39. R. Lenz: *Bull.* Acad. St. Petersburg (1869) **14**, 337; *Jnl. prakt. Chem.* (1869) **108**, 438–448.
40. A. Müller: *Metallurgie* (1909) **6**, 145–160.
41. F. Haber: *Ztsch. Elek.* (1898) **4**, 410.
42. W. C. Roberts-Austen: *Jnl.* Iron and Steel Inst. (1887-I) 71.
43. M. Okochi: *Bull.* Inst. Phys. Chem. Res., Tokoyo (1923) **2**, 13–22; *Chem. Absts.*, **18**, 3030.
44. M. Bellati and S. Lussana: *Atti* R. Ist. Veneto (1890) [7] **1**, 1173–1218.
45. W. Ramsay: *Phil. Mag.* (1894) [5] **38**, 206–218; *Ztsch. phys. Chem.* (1894) **15**, 518.
46. M. Thoma: *Ztsch. phys. Chem.* (1889) **3**, 69–102; *Centralblatt Electrotecknik* (1889) **11**, 131.
47. T. Franzini: *Rend.* R. Ist. Lombardo (1930) [2] **63**, 465–482.
48. F. Körber and H. Ploum: *Ztsch. Elek.* (1933) **39**, 252–255.
49. L. Cailletet: *Compt. rend.* (1868) **66**, 847.
50. T. Graham: *Proc.* Roy. Soc. London (1868) **16**, 422–427.
51. W. H. Johnson: *Proc.* Roy. Soc. London (1875) **23**, 168–180.

Adsorption

52. N. I. Nikitin: *Jnl.* Russian Phy. Chem. Soc. (1926) **58**, 1081–1094; *Ztsch. anorg. Chem.* (1926) **154**, 130–143.
53. A. F. Benton and T. A. White: *Jnl.* Amer. Chem. Soc. (1931) **53**, 3301–3314; (1931) **54**, 1820–1830.
54. F. Dureau and C. H. Teckentrup: *Ann. Physik* (1932) **12**, 927–960.
55. W. A. Dew and H. S. Taylor: *Jnl. Phys. Chem.* (1927) **31**, 281.
56. R. N. Pease and L. Stewart: *Jnl.* Amer. Chem. Soc. (1927) **49**, 2783–2787.
57. A. F. Benton: *Trans.* Faraday Soc. (1934) **28**, 202–218.

Evolution

58. I. Langmuir and S. P. Sweetser: Publication unknown (1912).   Quoted by W. E. Ruder: *Trans.* Amer. Electrochem Soc. (1916) **33**, 202.

59. G. Belloc: *Compt. rend.* (1907) **145**, 1280–1283; (1908) **147**, 244; *Bull.* Soc. d'Encour. (1908) **110**, 492; *Rev. de Mét.* (1908) **5**, 469, 571; *Metallurgie* (1908) **5**, 386, 730.
60. H. Esser: *Stahl und Eisen* (1927) **47**, 341.
61. R. H. Brace and N. A. Ziegler: *Trans.* A.I.M.E. (1928) **78**, 544; N. A. Ziegler: *Trans.* A.I.M.E. (1929) **84**, 428.
62. G. Tammann: *Ztsch. anorg. Chem.* (1920) **114**, 278–280.
63. H. M. Ryder: *Trans.* Amer. Electrochem. Soc. (1918) **33**, 197–202.
64. N. B. Pilling: *Trans.* Amer. Electrochem. Soc. (1922) **42**, 9–17.
65. G. Borelius and F. Gunneson: *Nature* (1924) **113**, 82–83.
66. B. Hugues: *Rev. de Mét.* (1925) **22**, 764–775.
67. L. Guillet and A. Roux: *Compt. rend.* (1926) **183**, 717; *Rev. de Mét.* (1929) **26**, 1–11

Diffusion, Normal Hot

68. H. St. Clair Deville and L. Troost: *Compt. rend.* (1863) **56**, 977–983, [Pd]; **57**, 965–967, [Fe].
69. H. St. Clair Deville: *Compt. rend.* (1864) **59**, 102–107.
70. L. Cailletet: *Compt. rend.* (1864) **58**, 1057.
71. J. Menshing and V. Meyer: *Ztsch. phys. Chem.* (1887) **1**, 151.
72. W. Biltz: *Ztsch. phys. Chem.* (1892) **9**, 152–157.
73. J. H. Andrew: *Trans.* Faraday Soc. (1918) **14**, 233.
74. V. Lombard: *Compt. rend.* (1927) **184**, 1557–1559.
75. V. Lombard: *Jnl. chim. phys.* (1928) **25**, 587, 604.
76. V. Lombard: *Rev. de Mét.* (1929) **26**, 343–350 and 519–531.
77. L. N. Khitrin: *Jnl. Exptl. Theoret. Phys.* (U. S. S. R.) (1934) **4**, 160–170; *Compt. rend.*, **28**, 7096.
78. O. W. Richardson: *Phil. Mag.* (1904) **7**, 260.
79. C. J. Smithells and C. E. Ransley: *Nature* (1934) **134**, 814; *Proc.* Roy. Soc. (1935) **A-150**, 172–197.
80. W. Baukloh and H. Kayser: *Ztsch. Met.* (1935) **27**, 281–285.
81. W. Baukloh and H. Guthmann: *Ztsch. Met.* (1936) **28**, 34–40.
82. W. R. Ham and J. D. Sauter: *Phys. Rev.* (1935) [2] **47**, 337.
83. W. R. Ham: *Phys. Rev.* (1936) [2] **49**, 643.
84. W. R. Ham: *Trans.* Amer. Soc. Metals (1937) **25**, 536–570.
85. C. B. Post and W. R. Ham: *Jnl. Chem. Phys.* (1937) **5**, 913–919.
86. W. R. Ham and W. L. Rast: *Trans.* Amer. Soc. Metals (1938) **26**, 885–902.

Diffusion, Electrochemical

87. G. Charpy and S. Bonnerot: *Compt. rend.* (1912) **154**, 592–594.
88. T. S. Fuller: *Trans.* Amer. Electrochem. Soc. (1919) **36**, 113–129.
89. G. C. Schmidt and T. Lücke: *Ztsch. Phys.* (1922) **8**, 152–159.
90. G. Borelius and S. Lindblom: *Ann. Phys.* (1927) [4]**82**, 201–226.
91. R. S. Williams and V. D. Homerburg: *Chem. and Met. Eng.* (1924) **30**, 589–591; *Trans.* Amer. Soc. Steel Treat. (1924) **5**, 399–412.
92. C. A. Edwards: *Jnl.* Iron and Steel Inst. (1924) **110**, 9–43.
93. E. G. Mahin: *Proc.* Indiana Acad. Sci. (1927) **37**, 272–276.
94. F. Körber: *Ztsch. Met.* (1929) **21**, 45.

Diffusion, High Pressure

95. P. W. Bridgman: *Rec. Trav. Chim.* (1923) **42**, 568–571. *Proc.* Amer. Acad. Arts and Sci. (1924) **59**, 173–211.
96. C. Poulter and L. Uffelman: *Physics* (1932) **3**, 157–158.

Critical Points

97. W. C. Roberts-Austen: *Proc.* Inst. Mech. Engrs., 5th Rept. Alloys Research Com. (1899) 35–68.
98. L. Guillet and A. Portevin: *Compt. rend.* (1913) **156**, 702–705.
99. H. S. Rawdon, P. Hidnert and W. A. Tucker: *Trans.* Amer. Soc. Steel Treat. (1926) **10**, 233–256.
100. H. Sieglerschmidt: *Mitt.* Deut. Materialprüfungsanstalt (1930) **13**, 135–139.
101. H. Esser and H. Cornelius: *Trans.* Amer. Soc. Steel Treat. (1933) **21**, 733–740.

X-Ray Structure

102. F. Wever and B. Pfarr: *Mitt.* Kaiser-Wilhelm Inst. Eisenforschung (1933) **15**, 147–148.

Mechanical Properties

103. T. S. Fuller: *Genl. Elec. Rev.* (1919) **23**, 702–711.
104. J. Cournot: *Compt. rend.* (1920) **171**, 170; *Rev. de Mét.* (1920) **17**, 568–570.
105. B. Cazard and B. Hugues: *Rev. de Mét.* (1925) **22**, 218–222.
106. P. Bardenheur and H. Ploum: *Mitt.* Kaiser-Wilhelm Inst. Eisenforschung (1934) **16**, No. 11, 129–136.
107. J. H. Andrew: *Trans.* Faraday Soc. (1914) **9**, 316–329.
108. G. Thanheiser: *Ztsch. tech. Phys.* (1929) **10**, 143–146.
109. C. Benedicks: *Ztsch. phys. Chem.* (1901) **36**, 529–538.
110. P. D. Merica: *Met. and Chem. Eng.* (1917) **16**, 496–503.
111. L. Guillet and J. Cournot: *Compt. rend.* (1931) **192**, 787–789.
    L. Guillet, A. Roux and J. Cournot: *Compt. rend.* (1931) **193**, 685–687.
112. M. Majima: *Bull.* Inst. Phys. and Chem. Res., Tokyo (1922) **1**, 136–144; *Chem. Absts.* (1924) **18**, 3030.
113. O. W. Story: *Trans.* Amer. Electrochem. Soc. (1914) **25**, 489–527.
114. M. Guichard: *Compt. rend.* (1930) **190**, 1417; (1931) **192**, 623–625.
    Guichard, Clausmann, Billon and Lanthony: *Compt. rend.* (1931) **192**, 1096–1098; *Chem. et Ind.*, Spec. No. (April 1934) 472–473; *Bull. Soc. Chim.* (1936) [5] **1**, 679–688.
115. L. B. Pfeil: *Proc.* Roy. Soc. London (1926) **A-112**, 182–195.
116. D. N. Alekseev and M. N. Polukarov: *Jnl.* Russian Phys. Chem. Soc. (1926) **58**, 511–517; *Ztsch. Elek.* (1926) **32**, 248–252.

Electrical Resistance

117. A. Sieverts: *Int. Ztsch. Metallog.* (1912) **3**, 37–56.
    F. Müller: Dissertation. Leipzig, 1911.
    F. Loessner: Dissertation. Leipzig, 1911.
118. H. Kleine: *Ztsch. Phys.* (1925) **33**, 391–407.
    T. Skutta: *ibid.* (1930) **65**, 385–403.
    H. Jellinek: *ibid.* (1930) **66**, 543–557.

Magnetic Properties

119. A. Matthiessen: *Phil. Mag.* (1858) [4] **15**, 80.
120. P. P. Cioffi: *Phys. Rev.* (1932) [2] **39**, 363–367.
121. R. D. Reber: *Physics* (1934) **5**, 297–301.

Princeton Laboratory

122. D. P. Smith and G. J. Derge: *Trans.* Electrochem. Soc. (1934) **66**, 253–269.
123. G. A. Moore and D. P. Smith: *Trans.* Electrochem. Soc. (1937) **71**, 545–563.

DISCUSSION

(James T. MacKenzie presiding)

A. SIEVERTS,* Jena, Germany.—Two papers, both of which appeared in September 1938, one in Japan, the other in Germany, are missing from the section on lattice occlusion in the bibliography of the paper by Moore and Smith.

Keizo Iwasé and Masazi Fukusima[124] have determined anew the solubility of hydrogen and nitrogen in electrolytic iron and *ferrum reduction*, and have obtained results that agree excellently with those of earlier work by P. Beckmann, E. Jurisch, A. Sieverts, E. Martin and H. Schenck. Iwasé rejected his earlier measurements, because "neither the degree of vacuum in the apparatus nor the purity of the samples used in his measurement were satisfactory." A further confirmation of the old values was supplied by the work which A. Sieverts, G. Zapf and H. Moritz,[125] published in September 1938, without knowledge of the Japanese investigation. The solubilities of hydrogen in iron from the two papers may be briefly tabulated as in Table 5.†

TABLE 5.—*Summary of Two Recent Papers*

	H_2 per 100 Grams Fe, C.C. (N.T.P.)					
Degrees, Centigrade..................................	500°	700°	A_3	900°	1100°	1200°
Iwasé and Fukusima:						
Electrolytic iron.........................	0.5	1.6	2.8	4.6	7.2	8.5
Reduced iron...........................	0.7	1.9	3.2	4.5	6.8	8.0
Sieverts, Zapf, Moritz......................	0.6	1.8	3.0	4.7	7.0	8.2
Average older values........................	0.7	1.7	2.9	4.5	6.6	7.7

The *lower* curve of Fig. 1 in Moore and Smith's paper is also essentially correct. This also holds for higher temperature to beyond the melting point. The intermediate slight jump in solubility found at A_4 would scarcely become apparent at the scale of the figure.

The sentence on page 265, "It would be a direct contradiction to suppose that diffusion was occurring through the lattice . . . at a temperature at which direct measurements have shown the lattice occlusion to be nil," is certainly correct. However, the lattice occlusion may become very small without cessation of diffusion as a consequence, as the example of platinum-hydrogen shows.[126]

G. DERGE,‡ Pittsburgh, Pa.—Anyone at all acquainted with the subject of gases in metals is very much indebted to these authors for their review and analysis of the literature dealing with hydrogen in iron. Owing to the confusion that exists, we are also indebted to them for their experimental investigation of the subject.

Recent theoretical developments in physical metallurgy seem to require some sort of irregularity or discontinuity in the crystal lattice. In his theory of plastic deformation, G. I. Taylor refers to these as "dislocations." The Wagner-Schotky concept of

---

* Chemical Laboratory, Friedrich Schiller University.
[124] K. Iwasé and M. Fukusima: *Sci. Repts.* Tohoku Imp. Univ. (1938) [1] **27**, 162.
[125] A. Sieverts, G. Zapf and H. Moritz: *Ztsch. physik. Chem.* (1938) **A-183**, 19.
† Incidentally, it may be mentioned that the solubilities of nitrogen in iron between 800° and 1300° C. also agreed closely in the two papers.
[126] *Ber.* Deut. Chem. Ges. (1912) **45**, 221.
‡ Metals Research Laboratory, Carnegie Institute of Technology.

the mechanism of diffusion involves vacant lattice points. The present paper, along with other publications by Professor Smith and his students, provides an experimental investigation into the nature and reality of such imperfections, and it seems to me that the concepts thus presented merit the careful consideration of those who are interested in these phases of the science of metals.

C. S. BARRETT, * Pittsburgh, Pa. (written discussion).—The photographs of rolled metals after hydrogen treatment that have been presented in this paper and in other papers by Dr. Smith and his collaborators show a banded appearance of the grains that is very striking. There is close resemblance between these markings and the strain markings I like to call deformation bands, † which are caused by fragmenting of the grains during deformation into regions (generally lamellae) of differing orientation. It seems probable that the markings after hydrogen treatment are another manifestation of deformation bands, or at least are related to them in some way.

N. P. GOSS,‡ Youngstown, Ohio.—The unusually large amount of hydrogen evolved when a cold-rolled pure iron saturated with hydrogen is heated to elevated temperatures is most interesting. This in an indirect way may give a method for the determination of the internal surface created during cold-working. It would be of unusual interest to determine whether a pure iron stressed elastically also absorbs large volumes of hydrogen.

It is well known that cold-working a metal fragments the grains into smaller lattice blocks, which differ in orientation from the parent grain, and the density of the metal decreases. This has been attributed to lattice distortion (slight increase in lattice parameter) by many authorities. The results obtained here seem to support the theory advanced several years ago by myself and others, and does not support the lattice distortion theory.

It has, for example, been shown consistently that the rate of diffusion through iron depends upon the grain size. This can only be interpreted to mean that the hydrogen has a greater tendency to diffuse along the grain boundaries than through the body of the grain. Cold-working may be considered to increase the internal surface or generation of more grain boundary. The creation of more internal surface also must increase the *free space*. The decrease in density need not be associated with lattice distortion, but may be considered as entirely due to the increase of internal surface, which demands more free space. The mechanism may be described briefly as follows, and the following assumptions must be made:

1. The lattice is not deformed or dilated by cold-working.

2. The grains are not fragmented without limit; i.e., the fragments are finite in size.

Cold-working simply causes the lattice blocks to rotate and glide on the slip planes of the type {110}. When this occurs, new internal surface is created, and the spacing between the displaced blocks is slightly increased. This means that more free space has been developed, and this will account for the slight decrease in density. The development of so much internal surface and, therefore, more free space by cold-working, permits more hydrogen to be stored in these voids of the plastically deformed iron.

The authors have not only presented some very valuable information on the occlusion and evolution of hydrogen from cold-worked metals, but also have provided a new tool with which to investigate certain phenomena that occur when a metal is practically deformed. I wish that the authors would give some consideration as to

---

* Metals Research Laboratory, Carnegie Institute of Technology.

† See papers beginning on pages 296 and 327 of this volume.

‡ Physicist, Cold Metal Process Co.

whether or not this method could be successfully applied to problems concerning plastic deformation. For example, I would like to ask the authors if they have considered determining the relationship between the volume of occluded hydrogen gas and the amount the pure iron has been cold-worked. (Another way of saying the same thing is the relationship between the volume of occluded gas emitted and the density of the metal.)

G. A. MOORE AND D. P. SMITH (authors' reply).—Professor Sieverts has kindly called attention to two papers of importance omitted from our bibliography. While both of these appeared after the close of our search, it must be admitted that our list of references is incomplete. Indeed we have in a few cases wittingly omitted publications that seemed to be of little present interest in relation to occlusion.

With regard to the possibility that lattice occlusion may be very small, yet sufficient to permit a certain amount of diffusion, it may be remarked that the various types of experiment differ much in sensibility, so that the point at which the quantity of hydrogen becomes negligible remains somewhat uncertain. It seems to us clear, however, that the greatest solubility of hydrogen in the iron lattice, which would accord with Professor Sieverts's results, and with recent confirmatory findings of others, is far too small to account for such ready diffusion as would be necessary to explain the initial rapid evolution of gas, observed in the present study.

We should also like to point out that it is by no means certain that diffusion experiments, especially of the transfusion type, are capable of distinguishing between lattice diffusion and that of the other kind. Hence we do not regard platinum-hydrogen as a valid example of lattice diffusion unaccompanied by lattice solution. Electrical experiments, now in progress here, are yielding indications that, while Professor Sieverts is entirely right as to the extremely small value of the lattice occlusion in platinum-hydrogen, there exists a much larger rift occlusion; and that the rift hydrogen is highly dissociated and therefore presumably able to diffuse according to mathematical laws similar to those which apply to a dissolved gas.

The discussions by Dr. Barrett and Dr. Derge touch upon highly important questions of plastic deformation. While we regard occlusion studies as capable of yielding much valuable information with regard to structural features in a range of dimensions otherwise difficult to investigate, the present paper affords indications only of the existence of discontinuities in the iron lattice, and does not enable us to draw well-founded conclusions as to their character.

In reply to Dr. Barrett's comments, we think it indisputable that the banded appearance of nickel and palladium, after subjection to hydrogen, is closely connected with the deformation bands of Dr. Barrett's investigations; but we do not believe that the two are identical. The hydrogen patterns lie within the deformation bands and appear to pertain to rifts within these larger features of the structure. In the absence of micrographic evidence for iron, we can only surmise that the rift system is somewhat similar in this case also.

We agree with Mr. Goss that experiments to determine the effect of elastic deformation upon occlusion would have interest. We are also inclined to regard our present results as affording evidence of structural changes that probably are better described as "fragmentation" than as "lattice distortion"; but they do not exclude the simultaneous occurrence of the latter. With one statement of the commentator we are obliged to disagree. He says that "It has been shown consistently that the rate of diffusion through iron depends upon the grain size. This can only be interpreted to mean that the hydrogen has a greater tendency to diffuse along the grain boundaries than through the grain." The negative results of Edwards[92] and of later experimenters,[79,93,94] and the directly contrary findings of Baukloh and Guthmann,[81] seem to us to support amply the opposite conclusion. Taken in conjunction with

our own results, this would imply that the "free space" produced by deformation is within the grains, rather than in the grain boundaries.

In any severely worked metal, the area of slip planes is greater, by several orders of magnitude, than that of the grain boundaries. Hence, if the production of internal surfaces and free spaces were to occur simultaneously at the boundaries and the slip planes, the influence of the latter would greatly predominate. We therefore regard it as less forced to explain rift occlusion in terms of effects upon the slip planes, quite apart from the definite micrographic evidence that has been found for palladium and for nickel. Indeed, we are at a loss to understand why the grain boundaries are so often regarded as the typical internal surfaces; whereas in reality they are probably the least extensive, the least understood, and the most easily contaminated, of the possible varieties.

With regard to Mr. Goss's other considerations upon the roles of lattice deformation and fragmentation, our present results do not seem to warrant any conclusions. It is perhaps possible that occlusion studies could be conducted with such accuracy that determinations of occluded hydrogen versus density could be made to afford information as to the parts played by lattice expansion and by fragmentation, in causing the expansion of the metal, as Mr. Goss suggests. Duplication of results might, however, prove to be very difficult, in such a series of experiments, because of the presence of extraneous factors. Moreover, it seems likely that the periods required for the attainment of equilibrium would be long, perhaps as great as one thousand hours per specimen! We are constrained to leave such studies to others.

Structure of Iron after Compression

By Charles S. Barrett,* Member A.I.M.E.

The experiments reported in this paper have been fruitful in disclosing the mechanism of the deformation of iron in compression. They have established the nature of "deformation bands," "etch bands," or "X-bands," that have been a recognized but little understood feature in the structure of cold-worked metals since the early days of metallography, and have shown the role of the bands in the development of preferred orientations by cold-working. The work has also shown the relation of the orientation of individual grains to the preferred orientation of the aggregate.

Some of the methods previously used in the determination of the indices of slip planes and slip directions are shown to be untrustworthy in the presence of deformation bands. The conclusion is reached that many slip planes and slip directions must operate during each stage in the compression of a single crystal, and that theories failing to take account of this require revision. In conducting the experiments a method of compression has been used by which extreme reductions can easily be reached, even to the limit set by the metal's capacity to deform without fracture.

The work is a portion of a research program on the plastic properties of iron and steel. It is being used as a foundation for studies of orientations resulting from recrystallization and is being extended to other metals and other types of deformation.

Previous Work

The previous experiments are few and have given confusing results. Ono[1] compressed a polycrystalline alpha-iron specimen between two flat plates of a testing machine and found that severe deformation oriented the crystals into a duplex preferred orientation, one set of crystallites having a cube diagonal of the body-centered cubic lattice parallel to the compression axis, and another set having a cube axis parallel to the compression axis. We shall speak of this structure as a double fiber texture of the type [111] + [100]. Wever[2] also made an X-ray determination of the texture

* Member of Staff, Metals Research Laboratory, and Lecturer, Department of Metallurgy, Carnegie Institute of Technology, Pittsburgh, Pa.

[1] References are at the end of the paper.

of polycrystalline iron after compression to 80 per cent reduction in thickness between two conical compression plates that were designed to minimize surface friction.[3] Contrary to Ono, Wever found merely a single fiber texture, with [111] parallel to the axis of compression.

A common feature of the microstructure of cold-worked iron is a banded appearance of individual grains. The bands are distinguishable from slip lines by the fact that they may be seen after repolishing and etching, and from Neumann bands by their lack of crystallographic uniformity in parallelism and width and by their varying contrast with varying degrees of cold-work. Rosenhain[4] considered them to be layers of amorphous metal left on slip planes after slip had taken place; Howe was unsatisfied with this theory and devoted an entire chapter to the "X-bands," as he called them, in his book.[5] He seems to have regarded them as regions in which the orientation had changed without reaching a twinned orientation, but he began and ended his discussion with the statement that their nature had yet to be discovered. Pfeil[6,7] published numerous photographs of the bands in compressed crystals of iron and concluded that they consisted of regions of differing orientation arising from movement on parallel sets of slip planes that differ in the bands from those active in the parent crystal. There have been no detailed quantitative studies of them or of their significance with regard to preferred orientations. Deformation bands in nonferrous metals are common; these are discussed later in the paper.

The theories of the mechanism of the production of deformation textures have been somewhat confusing. It seems fairly certain that when compression causes slip to occur homogeneously on a single set of parallel slip planes the lattice as a whole must rotate directly toward the position that would put those planes perpendicular to the axis of compression (the pole of the slip planes thus rotating directly toward the axis). But the theoretical difficulties arise in deciding how many differently oriented slip planes can operate at each stage in the compression, what happens to the crystal when several planes are operating simultaneously, and what importance should be attached to the bending of lamellae (bend gliding) and to disturbances at the boundaries of slip planes (local distortion). The experiments of many investigators on face-centered cubic single crystals have indicated that slip begins on the single set of slip planes having the greatest resolved shear stress and continues on these until the resultant rotation of the crystal brings an approximately equal shear stress on a second set of planes, which then operates in competition with the first. This simple mechanism, however, is inadequate to explain some of the deformation textures of polycrystalline metals, as Boas and Schmid[8] and others have pointed out.

Among the theories for polycrystalline metals are Polanyi's,[9] in which lattice rotation is attributed to simultaneous slip on all crystallographi-

cally equivalent slip planes and directions, or slip systems; Wever's,[10-13] in which the mechanism of bend gliding is added to lattice rotation; and Boas and Schmid's,[8] in which lattice rotation is assumed to result from slip on the three systems subjected to the highest stress and capable of producing the observed change of shape of the specimen. In addition to the uncertainty as to how many potential slip systems are active, there was for a long time an uncertainty as to the number of possible slip planes in iron crystals, but it has recently been rather conclusively shown by Gough[14] and by Barrett, Ansel and Mehl[15] that with small strains the deformation occurs on planes of the type (110), (112), and (123), and in directions of the type [111]. The deformation bands discussed in this paper have not been taken into consideration in any theories of deformation textures, yet undoubtedly they are a major factor in the development of many textures of ferrous and nonferrous alloys.

<h3 align="center">EXPERIMENTAL PROCEDURE</h3>

Materials.—All experiments were made with hydrogen-purified mild steel in the form of cylindrical specimens cut from $\frac{1}{2}$-in. diameter rods. The material was prepared in the Metals Research Laboratory by Dr. M. Gensamer, and has been described elsewhere.[16] The treatment reduced the carbon content to the limit detectable under the microscope and made substantial reductions in sulphur and oxygen. A grain size of 120 grains per square millimeter was obtained from the purification process, and single crystals were grown from this by a strain-anneal treatment.

Methods of Compression.—The specimens were compressed in three different ways: (1) between polished lubricated plates in a testing machine; (2) between conical plates in a testing machine, with the cone angle designed to compensate for friction at the plate surface; and (3) by a "compression-rolling" technique described below. The method of flat plates was inconvenient at great reductions of thickness and was thought to introduce a considerable amount of inhomogeneity in the deformation because of surface friction. Conical plates, while designed to eliminate fully the effect of friction at the plates,[3] were difficult to use and inapplicable at great reductions. The third method, which we refer to as "compression-rolling," was found entirely satisfactory for the work and a very effective means of compressing specimens of any size into thin sheets. It consisted of rolling a specimen in many passes, the specimen being rotated in its own plane several degrees between each pass in such a way as to produce deformation equivalent to uniaxial compression. Before using this method extensively, however, it was first established by X-ray tests that the method produced textures in large-grained and small-grained samples that were identical with those produced by the conventional methods of compression. The rolls used were 8 in. in diameter and were

run slowly (15 r.p.m.) to minimize heating; a typical compression involved 25 passes for a reduction from 0.156 in. to 0.010 in. (93 per cent total reduction in thickness), the specimen never becoming warm to the touch. Between passes the specimen was turned in its own plane about 20° or 30°, so that the specimens retained an approximately circular cross section at all times, maximum and minimum diameters seldom differing more than $\frac{1}{8}$ in. from an average diameter of 1.5 or 2.5 in. This was not true of the bicrystals, however, for the grain boundary in a bicrystal showed greater resistance than the body of the crystals to spreading.

Since it was found that the orientations were developed in their most ideal state with extreme reductions, the compression-rolling was always continued until cracks began to form at the periphery—usually to 93 per cent to 97 per cent reduction in thickness. A close approximation to the final texture was reached, of course, much earlier in the process (in one case around 72 per cent and in another 77 per cent), so that after the equilibrium conditions were reached the specimens usually received from 70 to 90 per cent further reduction.* This severe cold-work in the equilibrium state should serve to remove any doubts about the stability of the orientations present.

Orientation Determinations.—A preliminary selection of single crystals was made by observing the reflection of light from the cube etch-pit faces developed by etching in dilute nitric acid. After the crystals were cut from the rods, their ends were ground and etched and their orientation determined within $\frac{1}{2}$° by back-reflection Laue photographs,[17] in which the Laue spots were found to be satisfactorily sharp. Included crystallites were rarely seen in the crystals, and when they were noticed the crystals were discarded.

Orientation changes were measured at various stages in the compression process by the rotating-crystal method,[18] using radiation from a molybdenum target X-ray tube directed at the compressed surface (after etching) at an angle of 10° from the surface. In one instance this method was supplemented by the optical method of reflection from etch pits, and in another by plotting a pole figure[19] from surface reflections of molybdenum radiation.

The final orientations were determined in three ways. Laue photographs were the most useful, using tungsten or molybdenum radiation, with the beam penetrating the sheet. When the compression-rolling left the metal 0.006 in. thick or less, the X-ray beam penetrated the entire sheet; thicker sheets were etched to 0.005 in. before being X-rayed. No difference between the structure of the etched and unetched sheets was found, which indicates that surface effects were negligible. Samples from

---

* In terms of effective deformation, $ln(t_0/t)$, where t_0 is the initial and t the final thickness, these textures appeared at effective deformations of 1.27 to 1.47 and were maintained during further deformation of 1.20 to 2.30.

the crystals compressed between flat or conical plates were prepared by cutting thin strips from the centers of the disks and reducing them to 0.004 in. by grinding and etching. With these the X-ray beam penetrated what had been the exact center of the compressed disk. The Laue method was checked and supplemented by a special arrangement of the optical method, which will be described in the subsequent paragraphs, and also in several instances by the rotating-crystal method.

EXPERIMENTAL RESULTS

Fine-grained Iron.—The compression texture of polycrystalline iron having 120 grains per square milli-meter is found to be a double fiber texture, [111] + [100], with more of the material having [111] than [100] directions parallel to the compression axis. This result was obtained with: (1) a specimen compressed 87 per cent between flat plates (with machining into a cylinder at two stages in the process), (2) a specimen compressed between cones to a reduction of 80 per cent at the center, and (3) specimens compression-rolled 94 and 95 per cent in 30 passes. The [111] and [100] orientations are clearly evident on every X-ray pattern but are seen best when the X-ray beam is inclined at a small angle to the plane of the com-pressed sheet, for then the cube planes lying parallel to the compressed surface reflect strongly, as in Fig. 1.*

FIG. 1.—PATTERN OF COMPRESSED FINE-GRAINED IRON.
X-ray beam at 14° to compression plane. Spot at top center is reflection from (200) parallel to compression plane, proving the [100] texture; nearly all other prominent spots are from [111] texture. 87 per cent compression between flat plates.

To prove that initial textures in the hot-rolled purified rod did not influence the result, a specimen was prepared with its compression axis in a radial instead of a longitudinal direction in the original bar. After 95 per cent compression by rolling, this yielded a pattern showing orienta-tions of the same kind as those of Fig. 1.

The texture is independent of the manner of compression and of the amount of compression after the texture has been developed, except for some differences in the angular range of scattering around the mean

---

* The textures may be determined by the spots at the following angles in Fig. 1, measuring from the projection of the compression axis on the film (vertically downward on the print): (110) 23°, 85°, 145°; (200) 50°, *85°*, 120°, *180°*; (211) 55°, 82°, 113°, *145°*, 160°. The italicized readings are from the [100] texture only; all others coincide with predictions for the [111] texture.

position, and confirms the conclusion of several investigators that the change of shape, and not the manner of obtaining it, is the governing factor in developing the different types of preferred orientations.

The microstructure of polycrystalline compression specimens shows that many individual grains are oriented with either a [111] axis or a [100] axis parallel to the direction of compression. But an important feature of the microstructure is that many individual grains possess a banded structure, with [111] and [100] orientations in adjacent bands.

Optical Method of Revealing Textures.—The orientation of grains and bands can be seen in a striking manner by a special illumination of the etched surface. Fig. 2 illustrates the method used. Fig. 2a was made with the specimen tilted some 15° out of the focal plane of the camera lens and with diffuse light incident at a small angle to the surface from the side nearest the lens. Since crystals having a [111] axis normal to the surface have their cube planes 54° from the surface, this arrangement permits the cube faces of etch pits to reflect light into the camera, whereas it does not permit crystallites with the [100] orientation to reflect into the camera. Therefore, the [111] crystallites appear light and the [100] dark. But when the light source is shifted so as to reflect from planes *parallel* to the compressed surface, the [100] texture areas then appear light and the [111] areas dark, as in Figs. 2b and 2c. The ratio of dark and light areas indicates that [111] is the predominating texture, confirming the conclusion from the X-ray patterns.

Large-grained Iron.—The features noted in fine-grained material were found again in large-grained specimens containing 2 to 20 crystals per cubic centimeter. The banded structures are present as before. Typical structures are reproduced in Fig. 3; the contrast between adjacent bands increases with the amount of cold-work from reductions of 20 or 30 per cent up to 50 or 70 per cent. The bands sometimes have an approximate regularity, as in Fig. 3b, but in general are wavy and irregularly spaced. It is evident from Figs. 2 and 3 that these bands are identical with those discussed by Pfeil, and since they have been described in detail by him,[6,7] no further study of their shape and distribution was made. There are many reasons to believe that their outward form and their inner structure are conditioned by the initial orientation of a grain and the type of deformation (i.e., the directions of flow). The fine structure evident in Fig. 3a and also present but less evident in Fig. 3b might well be the same banding phenomenon on a very fine scale, the scales of the two standing in the ratio of perhaps 100 to 1. This is suggested by the similarity between this fine structure and the structure of deformed grains in aggregates.

When a large-grained specimen was compressed 90 per cent, the individual grains were found to have orientations of exactly the same types (as proved by both optical and X-ray methods) as those found in compressed single crystals, which are discussed below. There can be no
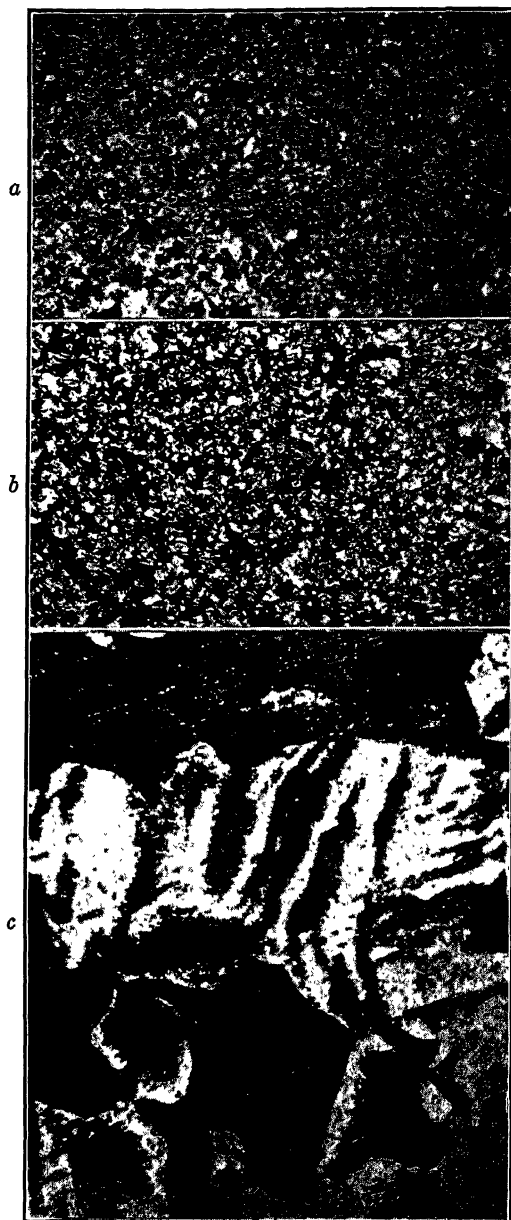
FIG. 2.—COMPRESSED SURFACE OF POLYCRYSTALLINE IRON AFTER 55 PER CENT REDUCTION IN THICKNESS.

Dilute nitric etch. Illumination adjusted to reveal individual components of textures.

a. [111] orientation appears light, [100] dark. × 5.
b. [100] orientation appears light, [111] dark. Same field as a. × 5.
c. [100] orientation appears light, [111] dark. Shows banded structure. × 100.

doubt that the behavior of the lattice is independent of grain size, at least in its major features.

Single Crystals.—When single crystals of the shape of right cylinders are compressed along the axes of the cylinders, four different types of final orientation result, depending upon the initial orientation of the lattice with respect to the axis of compression. These orientations have been determined by Laue photographs, rotating crystal photographs, and etch-pit observations.

a   b
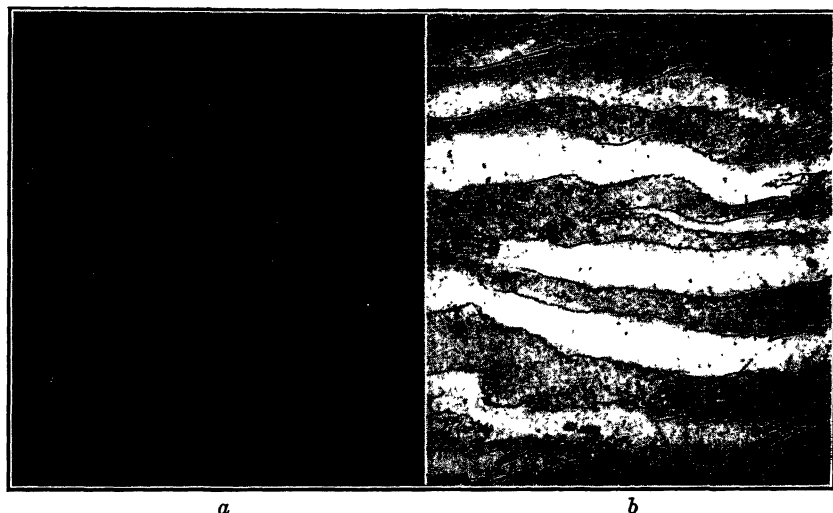
FIG. 3.—DEFORMATION BANDS IN LARGE-GRAINED IRON.
Section perpendicular to axis of compression, polished and etched after deformation. Etchant was 10 per cent picric acid, 0.5 per cent nitric acid in alcohol.
    a. Compressed 46 per cent between flat plates, × 100.
    b. Compressed 68 per cent between flat plates, × 100.

(A) The Cube Orientation [100].—All crystals with the axis of compression initially within about 22° of a cube axis rotate into a final orientation that yields the diffraction pattern of Fig. 4 when the X-ray beam is parallel to the axis of compression (normal to the sheet). The symmetry of the pattern indicates that the compressed sheet is a distorted single crystal, with a cube axis parallel to the axis of compression and two cube axes in the plane of the sheet. From the radial spread of the inner (110) and (200) streaks on the film, it can readily be calculated that the range of orientation about this mean position is only 8° to 10°; the circumferential spread of the streaks is of the same order. Plotted on a pole figure, the asterism streaks are approximately circular areas centered about the mean positions.*

---

* Wadlund[20] recently published Laue photographs of undeformed rock salt in which similar asterism was found associated with sharp Laue spots. Zachariasen[21] proposed the theory that the asterism was due to two-dimensional cross-grating diffraction arising at the boundaries of mosaic blocks. The author[22] showed that the con-

The nature and divergence of the orientations is represented by the arrangement of blocks in Fig. 5. The model has been photographed looking vertically down along the axis of compression, the cubic blocks representing orientations of various regions in the surface of the sheet.

Laue photographs taken with the beam striking five different spots on the surface of a crystal were identical, showing that the orientations were uniform (except for a narrow band at the edge). Etching in dilute nitric acid leaves the surface of the sheet practically unpitted and appearing as
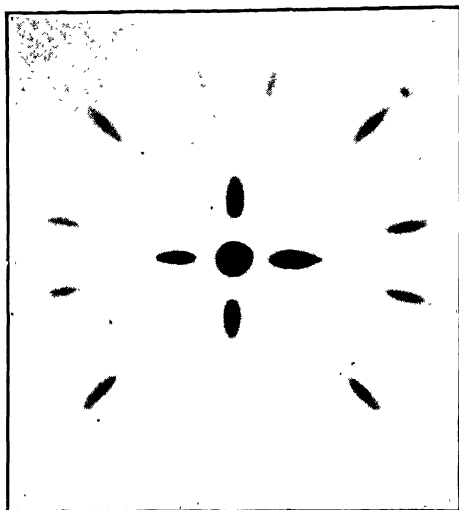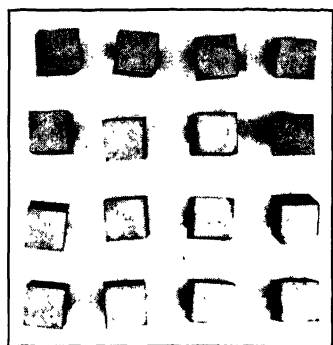
FIG. 4.   FIG. 5.

FIG. 4.—LAUE PATTERN AFTER COMPRESSION ON AN AXIS NEAR [100].
Fourfold symmetry proves [100] orientation; deviations from the mean orientation are 8° to 10°. X-ray beam parallel to compression axis.

FIG. 5.—MODEL OF CUBE ORIENTATIONS OF FIG. 4.
Cubes represent lattice orientations over surface of compressed sheet viewed from point on axis of compression. Picture is turned 45° with respect to Fig. 4.

if it had not been attacked by the acid. The model (Fig. 5) explains this appearance: the planes exposed by etching are the cube planes that are oriented as are the faces of the blocks in Fig. 5, thus etching exposes the cube faces parallel to the surface of the sheet (those represented by the tops of the blocks).

(B) *The Octahedral Texture* [111].—A crystal with the [111] direction 17° from the compression axis rotated during compression until [111]

ventional explanation of asterism—the result of orientation divergence—was adequate to explain all features of the pattern; he maintained that since orientation divergence is known to be present in rock salt, asterism is a necessary consequence and cannot be advanced as proof of an alternative theory. In the deformed crystals of the present study there is no justification for doubting the conventional explanation; a scatter of orientations is to be expected, and its range may be deduced with confidence from the length and width of the striae by the methods in general use since 1925.[23]

became coincident with the axis. The Laue photograph, Fig. 6, shows again a distorted single-crystal pattern with a scatter very similar to the preceding case, although exaggerated in Fig. 6 by the heavy exposure of the film. A model of the orientation is shown in Fig. 7, in which the blocks are arranged with their body diagonals normal to the plane of the sheet. In a later section it is shown that the specimens giving Laue patterns of these A or B types are not strictly homogeneous, as they appear on the X-ray films, but may contain up to 2 or 3 per cent of material of the other orientation.*

(C) *A Cube Orientation Coexistent with an Octahedral Orientation.*—All crystals compressed along an axis that was near neither [100], [111], nor
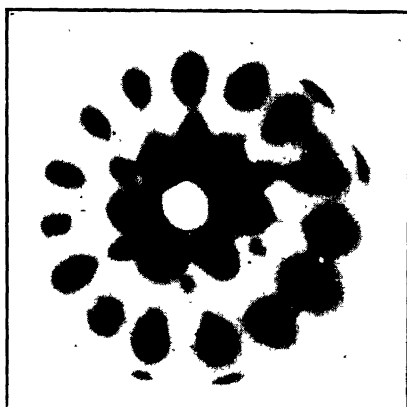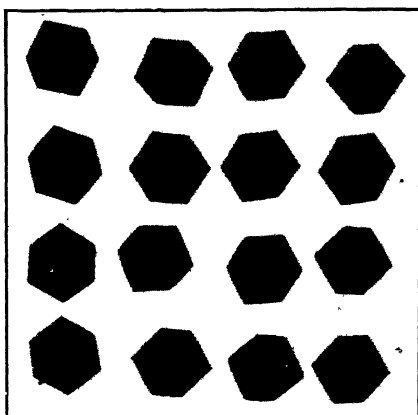
FIG. 6.   FIG. 7.
FIG. 6.—LAUE PATTERN AFTER COMPRESSION ON AN AXIS NEAR [111].
Three-fold symmetry proves [111] orientation, with a small orientation divergence.
FIG. 7.—MODEL OF OCTAHEDRAL ORIENTATION OF FIG. 6.
Blocks with their lower corners resting on compression plane are viewed from point on axis of compression.

[110] directions of the lattice resulted in the two coexistent orientations described under A and B above. A compression-rolled specimen of this type is shown in Fig. 8a, under illumination designed to make the [111] texture appear light, and in Fig. 8b, under illumination making the [100] texture appear light. The Laue photograms of these crystals are of the type reproduced in Fig. 9, and the orientations are those indicated in Fig. 10. The appearance of the etched surface (Fig. 8) might lead one to expect large areas of each orientation, but these areas are not purely a single orientation, and they do not extend throughout the thickness of the

* There seems little doubt that the small traces of a second texture present could be eliminated by compressing a crystal exactly along [111] or [100]. The types of orientation found in these disks would make particularly useful specimens for magnetic study; magnetic torque measurements on these would be much more easily interpreted than measurements on ordinary rolled iron specimens having complex orientations. See L. P. Tarasov.[24]

sheet, as the X-ray and microscopic evidence shows; Laue patterns show substantially the same proportions of the orientations at different spots on the sheet.   There appears to be a rather constant relation in orienta-

a   b
FIG. 8.—PHOTOGRAPH OF SHEET HAVING CUBE AND OCTAHEDRAL ORIENTATIONS.
a. [111] orientation light, [100] dark.
b. [100] orientation light, [111] dark.
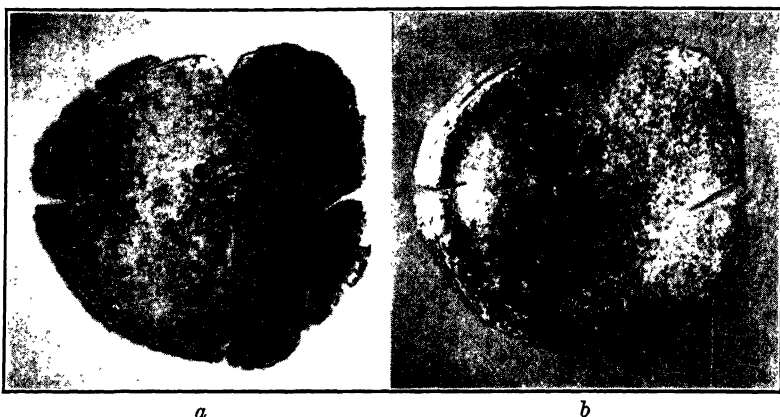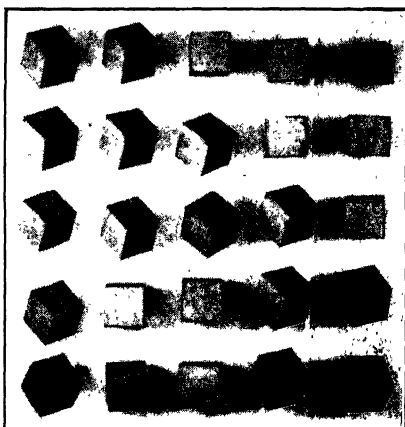
FIG. 9.   FIG. 10.
FIG. 9.—LAUE PATTERN AFTER COMPRESSION ON AXIS REMOTE FROM [111], [100] AND [110].
Shows both [100] and [111] orientations in crystal No. 17 after 94 per cent reduction by compression-rolling.   X-ray beam parallel to compression axis.
FIG. 10.—MODEL OF COEXISTENT CUBE AND OCTAHEDRAL ORIENTATIONS OF FIG. 9.
A deformation band crosses picture from upper left to lower right corners.   Picture is turned 45° with respect to Fig. 9.

tion between the [100] and [111] components of the texture in most of the crystals studied.   As indicated by the model, or the Laue pattern, there is one (110) plane that is parallel in the two components of the texture, and that (110) plane is parallel to the axis of compression.   Deviations from this relationship were usually little greater than deviations from the

mean in one of the components.   It should be remarked that this orientation relationship differs only about 15° from that in twinning, but careful study of a number of films from different specimens gave ample proof that it was not actually the relationship in twinning.   Perhaps a further study would be fruitful in which the relative orientations in the two components of the texture around the axis of fibering are given greater attention and related to the original orientation of the crystal.   It was not felt that these details were sufficiently useful to be given attention in the present experiments, although in most cases the data have been recorded.

(D) *Multiple Orientations.*—Crystal No. 5 compressed along an axis 5° from [110] gave Laue patterns like the one reproduced in Fig. 11.   These
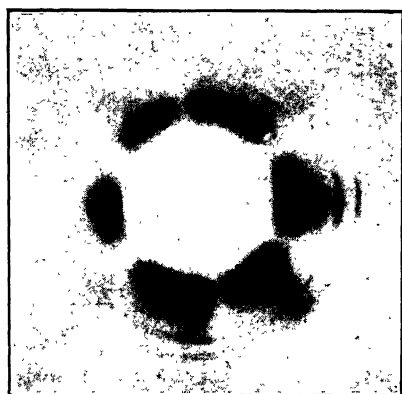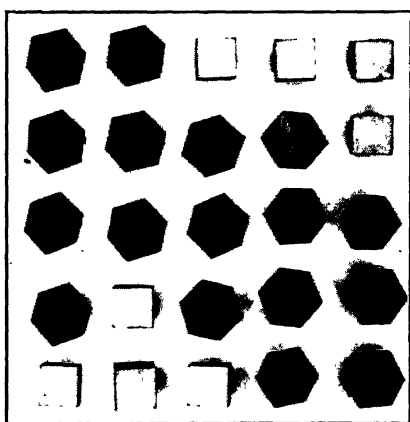
FIG. 11.   FIG. 12.

FIG. 11.—LAUE PATTERN AFTER COMPRESSION ON AN AXIS NEAR [110].
   Specimen No. 5 compression-rolled 93 per cent.   X-ray beam parallel to compression axis.
   FIG. 12.—MODEL OF CUBE AND MULTIPLE OCTAHEDRAL ORIENTATIONS OF FIG. 11.

result principally from a sharp [100] orientation coexistent with multiple [111] orientations and have been so represented in the model of Fig. 12; close inspection of the original film of Fig. 11 discloses faint spots from a second [100] orientation differing 45° from the first, but this weaker orientation has not been included in the model.   The crystal fragments having [111] axes normal to the sheet do not have identical azimuthal positions around the normal but are scattered through an angle of 25° or 30° around the normal.

Relative Amounts of [100] *and* [111] *Orientations in a Specimen.*—The relative prominence of the two orientations in a specimen showing both types is a function of the initial orientation of the specimen, as will be seen from the summary of the compression-rolling experiments in Table 1. The last column of this table lists the relative intensities of the two components, as judged by visual inspection of Laue photographs; numerical intensities were assigned so that their total arbitrarily equals 5.   The rela-

TABLE 1.—*Summary of Compression-rolling Experiments*

Crystal No.	Thickness, In.		Number of Passes	Compression, Per Cent	Orientation		
					Initial, Degrees from		Final, with Relative Intensities as Subscripts
	Initial	Final			100	111	
3a	0.163	0.008	23	95	10	46	100_5
3b	0.163	0.008	23	95	40	32	$100_3 + 111_2$
4	0.139	0.008	24	94	28	31	$100_4 + 111_1$
5	0.131	0.009	22	93	40	35	$100_2 + 111_3$
7	0.102	0.006	20	94	26	31	$100_4 + 111_1$
8a	0.170	0.010	22	94	11	47	100_5
11	0.156	0.010	25	93	38	20	$100_2 + 111_3$
12	0.157	0.010	25	94	39	18	$100_1 + 111_4$
13	0.184	0.005	22	97	14	41	100_5
16	0.186	0.006	25	97	26	34	$100_4 + 111_1$
17	0.177	0.010	∗ 26	94	48	12	111_5
22a	0.149	0.007	21	95	29	38	$100_4 + 111_1$
23a	0.197	0.008	22	96	33	23	$100_1 + 111_4$
24a	0.217	0.007	24	97	39	18	$100_1 + 111_4$
25	0.209	0.009	20	96	22	37	100_5
26	0.255	0.005	82	80	19	38	100_5
27	0.162	0.005	68	72	36	23	$100_2 + 111_3$

tions given in Table 1 are shown graphically on the stereographic projection of Fig. 13, where the initial orientation of the cylindrical axis of each specimen is represented by a small circle in a unit stereographic triangle, which gives the lattice orientation in the specimen. The relative amounts of [100] and [111] material in each crystal after compression is indicated roughly by the relative amounts of white and black area within the circle.

A microscopic investigation after etching in dilute nitric acid proved an effective supplement to the X-ray determinations, for small areas of differing orientation were found that were too minute to register on most Laue patterns. By means of the microscopic work it was possible to answer the question, "Is there a minute amount of material of octahedral orientation in a specimen that gives a Laue pattern showing only cubic orientation?"

FIG. 13.—STEREOGRAPHIC PROJECTION OF INITIAL ORIENTATIONS.
Relative prominence of [100] orientation (white segments of circles) and [111] orientation (black segments of circles) in each crystal after compression are indicated.

Visual estimates of the relative amounts of material of [100] and [111] orientations were made of several specimens. This was done at a magnification of 500 diameters, and only areas larger than 0.001 mm. were considered. A number of factors conspire to make these estimates inaccurate, but they are presented to show the general trends.

The crystals (see Table 1 for initial orientations) and the estimated percentage of the total area having the [111] texture follow: No. 3a, 0.3 per cent; No. 8a, 0.6 per cent; No. 13, 1 per cent; No. 25, 1.5 per cent; No. 16, 6 per cent; No. 12, 60 per cent; No. 17, 98.5 per cent. There can be no doubt that, even in specimens appearing by X-rays to be of a single
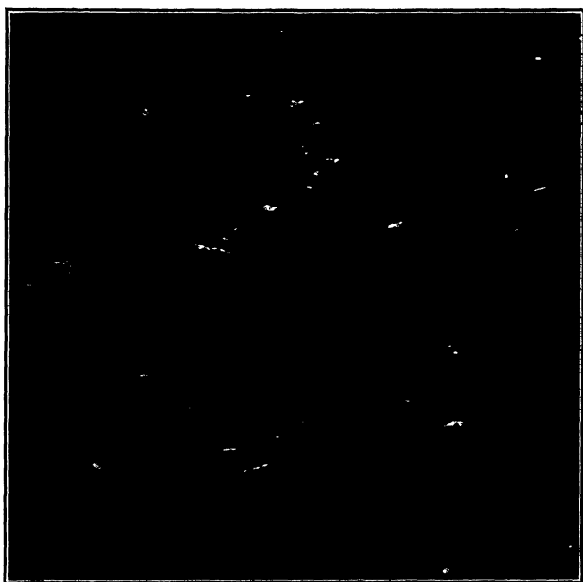
FIG. 14.—PHOTOGRAPH COMPRESSED SPECIMEN No. 25.
Dilute nitric etch, × 4. Light streaks are of [111] orientation, not detected by X-rays.

orientation, there is a small amount of the second orientation. The distribution of the small areas of [111] orientation in specimen No. 25 can be seen as white areas against the dark [100] background of Fig. 14.

The optical work (as well as the X-ray work, where applicable) established the fact that the percentage of [111] material increases continuously as the initial orientation departs from [100] and approaches [111]. It may be concluded from this that there is not a direct correspondence between imperfections of any sort in the original crystals and the two orientation components, for a continuous variation of imperfections with initial orientation would not be expected.

Model of the Compression Texture.—From the data on single crystals and the fact that no difference in behavior was found between isolated

crystals and the grains of an aggregate, it becomes easy to construct a model of the orientations in the deformation texture of polycrystalline iron. The final orientations in each grain are determined by the initial orientation with respect to the effective axis of compression in the grain and very little, if any, by the position of the grain in the specimen. A model of the aggregate is given in Fig. 15, viewed, as in the previous models, from a point on the axis of compression.

Fig. 15.—MODEL OF ORIENTATIONS IN COMPRESSED POLYCRYSTALLINE IRON.
Grains in surface of compression represented in their final orientations, some with deformation bands, others without.

Rotation into Equilibrium Orientations.—The progressive change of orientation with increasing compression was traced with rotating crystal photograms, the specimen rotating in its own plane. After each step in the compression-rolling process 0.001 to 0.004 in. was removed from each compressed surface of the specimen by etching before the specimen was mounted on the X-ray goniometer.

Specimen No. 26 had an initial orientation with its axis 19° from [100] and 38° from [111]. The progressive change in orientation shown on these films is plotted in the stereographic projection of Fig. 16, where circular areas represent the scatter of orientations of the specimen axis

(the compression axis) with respect to the crystal lattice orientation, represented by the unit stereographic triangle, for the various stages signified by the figures for percentage reduction.* Two important features are to be noted: (1) the axis rotates directly toward [100] along approximately the shortest path, and (2) the scatter of orientations first increases, then, after reaching the final orientation (at about 77 per cent), decreases until it is of the order of ±3°. The pole figure is not intended to indicate the exact shape of the scattered areas that are drawn as circles, for these details were not made evident with the X-ray method used.

Specimen No. 27 had an initial orientation—36° from [100] and 23° from [111]—that gave a double orientation after compression. The pole
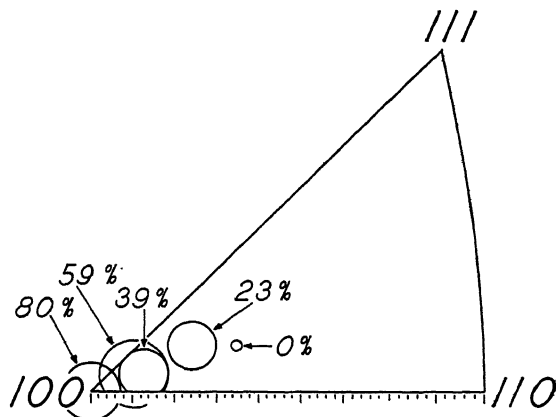
FIG. 16.—POLE FIGURE SHOWING ROTATION OF CRYSTAL No. 26 DURING COMPRESSION.
Circular areas represent orientations of compression axis with respect to lattice at per cent reduction indicated. Scale of degrees is given at bottom of figure.

figure constructed from rotating crystal patterns for various stages in the compression-rolling is shown in Fig. 17. This crystal first increased its spread in orientation without much alteration of the mean orientation. Then at 20 or 30 per cent reduction it began to divide itself into regions rotating in different directions, some going directly toward [111] and others directly toward [100], the final orientations being reached between

---

* Molybdenum radiation, collimated by ¾-mm. pinholes, was incident at 10° on the specimen surface. A flat film was placed parallel to the axis of rotation, thus 80° from the incident beam. The percentage reduction was calculated from the thickness reductions by rolling alone, disregarding reductions by etching. The initial thickness was 0.255 in., and the final was 0.005 in. Nine photographs were made during the 82 passes of the compression-rolling. Etching altered the effective reduction at each stage; while the various stages have been designated by the percentage reduction exclusive of etching, a more significant figure for the cold-work at each stage is the effective deformation $ln(t_0/t)$ calculated for each stage and summed up for successive stages. The correspondence between nominal percentages and effective deformation figures for the experiment is as follows: 23 per cent = 0.27; 39 per cent = 0.51; 59 per cent = 1.00; 80 per cent = 3.06.

65 and 70 per cent reduction.   In this case also the scatter from the mean positions increased until the final orientations were reached, at which time the scatter was about 5° from the mean.   The X-ray patterns are not as sensitive as microscopic methods for detecting the early stages of the formation of differently rotating regions, because X-ray diffraction averages together all the slightly deviating orientations, while the microscope sees only the differences in orientation.*

Generation of Deformation Bands.—The experiment on crystal No. 27 discloses the orientation history of the banded structure, for the two differently rotating areas of Fig. 17 are actually the bands seen in photomicrographs such as Figs. 2c and 3, and often visible to the naked eye on the etched surface as deformation progresses.   The gradual increase in contrast between adjacent deformation bands with increasing cold-work
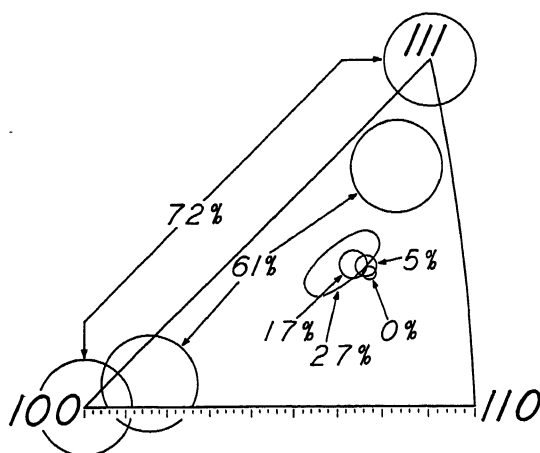
FIG. 17.—POLE FIGURE SHOWING ROTATION OF CRYSTAL No. 27 DURING COMPRESSION.

is the result of the increasing difference in orientation between adjacent bands, with the consequent difference in orientation of the etch pits in the bands.   The fundamental nature of these bands was thus correctly inferred by Howe[5] and by Pfeil[6,7] from the etching characteristics of the bands, from needle-point impressions in the bands, and from the directions of slip lines in the bands, although earlier observers did not quantitatively determine any of the orientations or relate them to the development of the deformation texture of single crystals or polycrystalline iron.

---

* Specimen No. 27 was initially 0.162 in. thick.   After compression-rolling and etching in 8 stages (68 passes) it was reduced to 0.005 in.   The effective deformation at the stages plotted in Fig. 17 are related to the nominal percentages as follows: 5 per cent = 0.05; 17 per cent = 0.19; 27 per cent = 0.34; 61 per cent = 1.19; 72 per cent = 2.53.

Calculations of Shear Stresses on Slip Planes.—For the interpretation of the lattice rotations and the equilibrium deformation textures, it should be helpful to know the possible slip planes and directions and the resolved shear stresses calculated for each system under the various conditions of our experiments. As previous work did not indicate how many slip systems could be active at any stage of the deformation, the stresses on all systems were calculated. While no rigorous conclusions have yet been derived from the calculations, we feel that they are sufficiently fundamental to be presented here; it is hoped that the rather novel manner of presenting them will aid others in finding useful correlations between the stresses and the plastic behavior of iron crystals. A few conclusions can be drawn immediately from them and are presented in the discussion that follows.

In alpha iron there are four [111] slip directions, around each of which are arranged three (110) planes, three (112) planes, and six (123) planes.[14,15] The 12 slip planes that are approximately equally spaced around each slip direction make up the total of 48 slip systems of each crystal. The resolved shear stresses on these 48 systems for a unit compressive stress were calculated for crystals of 11 different orientations spread over the unit stereographic triangle, a total of 528 stresses.[*]

A graphic method of representing these stresses is almost necessary if any relations between them are to be seen, so the following scheme was devised. The orientations of the crystals are plotted on stereographic projections, the axis of compression in each crystal being represented in the usual way as a point in a unit stereographic triangle. Each resolved shear stress is plotted as a vector. The origin of the vector is the point representing the crystal orientation. The length of the vector is proportional to the resolved shear stress on the given slip system per unit compressive stress applied to the crystal. The direction of the vector represents the rotation of the lattice that would result if that slip system alone were operating. The vector is therefore drawn tangent to the stereographic great circle passing through the origin of the vector and the pole of the slip plane.

All vectors for a single specimen should be thought of as lying in a plane tangent to the reference sphere, and in this plane they point as closely as possible toward the pole of the slip plane. It may be helpful to think of these vectors as forces pulling tangentially at the ends of the specimen axis (the axis constitutes a radius of the reference sphere) and tending to produce rotation of the specimen axis about its pivot at the

---

[*] Computations were made to two figures, using angles measured on a 15¾-in. stereographic net[19] and applying the formula $S = \cos a \cos b$, where S is the resolved shear stress per unit compressive stress applied to the crystal, a is the angle between the axis of compression and the pole of the slip plane, and b is the angle between the axis of compression and the slip direction.
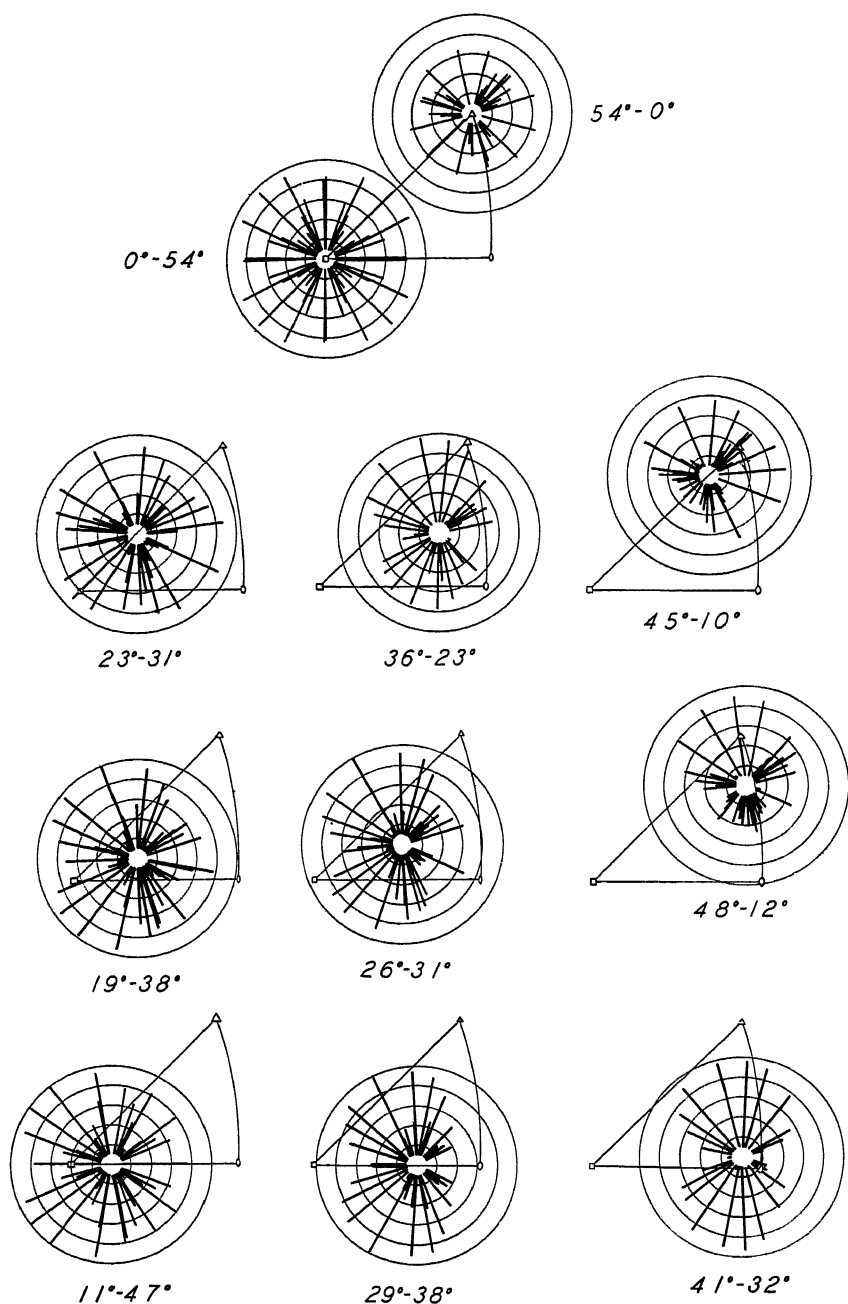
FIG. 18.—DIAGRAMS OF RESOLVED SHEAR STRESSES ON SLIP SYSTEMS OF IRON.
Each radial line has a length proportional to resolved shear stress on a slip plane and shows stereographically the direction of rotation expected from slip on that plane during compression. Numbers give position of axis relative to [100] and [111] respectively.

center of the sphere. The vectors defined in this way, however, cannot be combined by the laws of vector addition or subtraction to any advantage in describing the deformation mechanism, so it is not intended that they be considered as ordinary force vectors. The plots are reproduced in Fig. 18. The numbers appearing below each plot are the angles between the specimen axis and the [100] and [111] directions of the lattice respectively. For example, the group of vectors in Fig. 18 designated as 0°–54°, applies to a crystal whose axis is parallel to [100] and 54° from [111]. Concentric circles have been added to represent stress magnitudes of 0.1, 0.2, 0.3, 0.4, and 0.5.

DISCUSSION OF RESULTS

Comparison with Theory.—Boas and Schmid's theory of deformation textures,[8] the most fully developed and successful one published to date, merits careful comparison with the present findings. This theory predicts a [111] compression texture in polycrystalline aggregates when (110) planes alone act as slip planes, and a double texture, [111] + [100], in agreement with experiment, when additional slip planes of the type (112) are assumed. While the theory has not been carried through for (110) + (112) + (123) slip, it can be seen from the stress vectors in Fig. 18 or from the calculations of Fahrenhorst and Schmid[25] that the correct polycrystalline texture would also be predicted under these assumptions.*

While the theory is successful in predicting the polycrystalline texture of iron, it fails to describe the detailed behavior of single grains in the aggregate and isolated single crystals: It predicts that a crystal will rotate until the axis of compression coincides with a plane of symmetry in the crystal, after which the axis will rotate in the symmetry plane until either the [100] or [111] position is reached. The mechanism actually observed, on the other hand, involves in the general case a partitioning of the crystal into bands and a rotation of the material in each band toward the [100] or [111] position, along the most direct route.

Number of Active Slip Systems.—It is apparent that the actual mechanism involves deformation on more than one slip system in the crystal as a whole but on a given set of systems within a single band, since lattice rotation is heterogeneous over the whole but homogeneous throughout a single band or a considerable portion of the band. It may further be concluded that several slip systems in each band must operate in addition to the most highly stressed one, for were this not so the specimen axis could

---

* It would be an interesting experiment to obtain the compression texture of an iron-silicon alloy containing 4 or 5 per cent silicon, for slip has been noted only on (110) planes in such alloys[15] and a single deformation texture would be predicted by Boas and Schmid's theory. Plans are being made to conduct this test on the same material used in the slip-plane research.

not follow a great-circle route to the final orientation—the longest vectors of Fig. 18 seldom point directly toward [100] or [111]. When a crystal reaches the [100] orientation (Fig. 18, plot 0°–54°), there are four systems under equal maximum stress that must have an equal tendency to become active, and since there are 12 systems under stress equal to or greater than 0.45, and 20 under stress equal to or greater than 0.40, it is probable that a great many of these also participate in the deformation. Similarly, in the [111] position, plot 54° to 0°, nine systems under stress of 0.31 to 0.32 must operate, and the 21 systems equal to or greater than 0.25 may be expected to do so.

In the absence of a rigorous analysis of the mechanics of rotation during multiple slip in a banded structure, it seems scarcely profitable to discuss at length the probable number of active systems in the cases shown in the plots. Indeed, it seems not unlikely that a statistical view of the mechanism is as profitable as any, since flow may be appreciable in varying amounts on a considerable number of the less stressed systems. The vectors for crystal No. 27, for example, lend qualitative support to this view (cf. plot 36°–23°, Fig. 18). The four vectors greater than 0.40 in this diagram tend to rotate the crystal more toward [111] than [100], and it is only by going to shorter vectors that a tendency to produce other than a pure [111] texture seems to be evident, yet both [100] and [111] components were prominent after compression-rolling. Recent observations[14,15] on slip lines in iron also support the idea that a number of planes operate, since these observations indicate approximately equal slip resistance on (110), (112) and (123) planes. The idea is consistent with recent theories of Polanyi,[26] Taylor,[27] Becker,[28] Orowan,[29] and Burgers,[30] in which movement on slip planes is thought to vary exponentially with applied stress as a consequence of the action of thermal vibrations in aiding the applied stresses to overcome potential barriers.

Generation of Deformation Bands.—The first effect of compression is to increase the range of orientation in the crystal. This might be ascribed to various causes such as imperfection, inclusions, variations in hardness, finite lengths of slip lines, and Lüders lines or flow lines. On the other hand, this scatter might be a result of some specific instability of the crystal under compression that causes certain regions to slip on one set of planes and adjacent regions to slip on another. If the latter is true, and certain of the experimental results seem to indicate it, a fundamental property of crystals subjected to stress remains a mystery awaiting solution.

Once the scatter in orientation has occurred, it accentuates itself. The crystal in this state is a pseudopolycrystalline aggregate in which interference at "grain boundaries" between differently oriented bands becomes important. In the first place, there must be a tendency for movement on any one slip system to be restrained by the neighboring band, this reaction to the movement being greatest on the plane on which

movement occurred, but having large components on all similarly oriented planes such as to tend to shift further movement to very differently oriented slip planes or slip directions. From Chalmer's work on bicrystals of tin[31] it may be concluded that this reaction increases with increasing difference in orientation of the adjacent regions.

Secondly, the differently directed slip in adjoining regions must serve to alter the stress system; three-dimensional stresses must exist and must vary from point to point in the crystal, increasing the heterogeneity of the strain. A third factor of importance is the change in resolved shear stresses taking place as the orientation of a small region or band changes. The various plots of Fig. 18 are concerned with this factor, but it must be remembered that these plots are calculated assuming ideal uniaxial stress, which is correct enough on the average but must be subject to variations from point to point in the interior of the specimen because of the first and second factors discussed above. These factors all act to accentuate the scatter, and none act to reduce it until equilibrium orientations are reached.

When the deformed grains have reached [100] or [111] positions, the third factor, orientation, must predominate. Crystallites thrown out of the equilibrium positions by either the first or second mechanism are returned to it by the third. In terms of the vector scheme, this comes about by a shortening of the vectors that point away from the equilibrium position and a lengthening of the vectors that point back toward it.

Origin of Multiple Orientations.—The vector plot 41°–32° (Fig. 18) suggests a simple explanation for the multiple orientations that arise in crystal No. 5, to which the plot applies. All major vectors point in the general direction of two different [111] poles, located at equal angles above and below [110]. (Only one of these is shown in the plot.) An inhomogeneous structure would be anticipated from the vector arrangement, with different portions of the crystal rotating directly toward the two [111] poles and having different azimuthal orientations after reaching the equilibrium positions. From the symmetry of the lattice as reflected in the symmetry of the vectors, it can also be seen that there should be about equal probabilities of fragments rotating to either of two different [100] positions.

Deformation Bands in Body-centered Cubic Metals.—The experiments of this paper have dealt with deformation bands formed in iron by compression only, but bands are encountered in iron deformed in other ways as well. Ordinarily rolling produces abundant bands (see, for example, a photograph of Armco iron published by Jeffries and Archer.[32] Considering the similarity between compression-rolling and straight rolling, this is only to be expected. Brearley[33] observed them as early as 1910 in the necked region of a tensile-test piece. Dr. Gensamer, of this laboratory, has noted deformation bands in cold-drawn steel wire, and one of his

students, Mr. J. G. Kura, has found them associated with Neumann bands in hydrogen-purified iron that was compresed by impact. Bands thus seem to be common in ferrite deformed in many ways—perhaps in all ways.

The pronounced lamellar structures Elam[34] found in beta brass crystals elongated in tension must have been analogous to the deformation bands of ferrite, for she remarked, "In some crystals there were alternate bands, resembling lamellar twinning. These bands persisted when a crystal section was polished and etched, unlike slip bands which are usually purely surface markings." Johnson[35] had previously observed strain markings in beta brass, and from their similarity to Neumann bands had concluded (without crystallographic analysis) that they were deformation twins, while Bengough[36] had thought they were the result of the precipitation of the alpha phase along slip planes. Clark[37] and Van Wert[38] took the latter view; Mathewson,[39] A. J. Phillips,[40] and D. W. Smith[41] the former. Greninger clarified the matter by pointing out that two kinds of strain markings are found after straining beta copper-zinc and copper-tin alloys. One kind has a close resemblance to Neumann bands in its metallographic appearance (although it is crystallographically different) and occurs only in metastable phases as a result of transformation of thin lamellae into a transition phase, a mechanism analogous to martensite. A second kind of marking[42,43] resembles the deformation bands discussed in this paper in many respects. However, since Greninger did not observe definite evidence of the latter bands in his samples after repolishing and etching, he concluded that they did not involve any considerable difference in orientation, although he noted some orientation differences too small to measure. But the key to Greninger's observations of these bands, and to other studies to be mentioned later that have given mysterious results, lies in the amount of deformation used. The very light compression in Greninger's experiments could have produced only very slight differences in orientation, if the formation of bands in beta brass is in any way similar to the formation of deformation bands in ferrite. Had the deformation been carried further, undoubtedly the differences would have been magnified, and etch bands of increasing visibility would have been found.

It is significant that beta brass has a body-centered cubic lattice that deforms by slip on {110} planes alone,[43] as contrasted with the lattice of iron, which deforms by slip on {110} + {112} + {123} planes, and yet beta brass is capable of forming deformation bands. Therefore, a great multiplicity of slip systems is not essential to the occurrence of this phenomenon.

Bain and Jeffries[44,45] have published a photomicrograph of a twisted crystal of tungsten showing a structure somewhat resembling deformation bands.

Deformation Bands in Face-centered Cubic Metals.—Mathewson and Phillips[46] have described bands in rolled alpha brass that resemble the deformation bands of iron in their etching characteristics and in their growth in number and prominence with increased cold-work. Johnson[47,48] has reported them in rolled copper and alpha brass, Adcock[49] in rolled cupronickel (80 per cent copper, 20 per cent nickel), Elam[50] in rolled silver, and Rosenhain[51] in cupronickel manganese. Samans[52] made microscopic and X-ray observations of bands in 70:30 brass specimens that had been rolled to a reduction of 50 per cent. His conclusion that the bands resulted from mechanical twinning was probably the result of an accidental choice of a degree of rolling for which deformation bands would reach positions approximately equivalent to twinning.*

A series of observations at different reductions is the best method for distinguishing deformation bands from twins when such uncertainties arise; Mathewson and Phillips' studies at various reductions indicate rather strongly, for example, that Samans' bands must have been deformation bands resembling those in iron instead of twins.

Experiments we are conducting on compression-rolled fine-grained alpha brass and on cold-drawn wires of the same material show that both compression and wire drawing produce double fiber textures, from which the implication is strong that the banding mechanism is related to the face-centered cubic deformation textures in a way analogous to the relation between banding and texture in the iron discussed in this paper. It should be pointed out, however, that banding might be possible in some metals having only a single fiber texture, since distinguishable orientations can exist around the axis of fibering. The double (or multiple) [111] orientations observed in the present experiments are examples of this possibility.

Whenever banding is prominent in the microstructure of metals, there can hardly be any question that it is a primary factor in determining the nature of preferred orientations. A detailed analysis of rolled crystals, similar to the present study of compressed crystals, should yield a new insight into the complex orientations in cold-rolled materials. The same can be said of the textures of recrystallized material, for the mechanism of recrystallization is closely tied up with deformation bands, as many published photographs have shown.

Deformation Bands vs. Local Distortion at Slip Planes.—Goucher,[53] with tungsten crystals deformed under tensile stresses, Taylor,[54] Yamaguchi,[55] and Burgers and Louwerse,[56] with aluminum crystals under homogeneous compression between lubricated flat plates, found rather

---

* At one time the author thought the equilibrium [100] and [111] orientations in his severely compressed iron specimens bore a twinned relation to each other, but careful analysis of the films disproved this, as did the progressive changes in orientation during compression.

wide ranges of orientation in the deformed crystals. In all these cases there should have been no bend gliding resulting from external constraint at the grips or compression plates, and a new theory was required to explain the inhomogeneities in orientation. The theory advanced by Taylor and adopted by all the later investigators named was that local distortion of a crystal occurs at the slipping surfaces within it, the distortion being in the nature of a rotation of crystalline fragments. Rotations were observed from 2° to 15° in most cases, but increased with increasing deformations up to 20° and more; the direction of rotation was that to be expected of rollers placed between the slipping surfaces. The theory has been given a prominent place in recent discussions of work-hardening* and of recrystallization.†

There is a surprising similarity between the orientation ranges accompanying some of the deformation bands in the experiments reported in this paper and the orientation ranges in the experiments just cited, on which Taylor's "local distortion" theory is based. It should be pointed out that none of the X-ray data in these experiments actually disclosed the *location* of the crystallites with scattered orientations—the data revealed only average conditions in the specimens. That the disturbances were located at slipping surfaces was merely inferred from the type of scatter observed (and in some of the experiments there was an incomplete determination of the type of this orientation scattering). Is it not possible that deformation bands have been mistaken for disturbances localized at slip planes in this series of studies? There should be a detailed experimental study capable of disproving deformation-band effects before this series of experiments can lend support to the theory of fragmentation and rotation at slip planes.

Another question requiring further study concerns the nature of the fine structure in large deformation bands. We have suggested, in connection with Fig. 3, that the fine lines in a band are merely minute deformation bands. An alternative explanation is that they are the local distortions at slip planes discussed in this section. It is difficult to choose between these two theories at present.

Significance of Deformation Bands in Slip-plane Determinations.— All determinations of the indices of slip planes and slip directions are untrustworthy when a crystal assumed to deform homogeneously divides, on the contrary, into deformation bands of appreciable difference in orientation. The methods employed by Taylor and Elam are particularly susceptible to this criticism, for they are based on the assumption of homogeneous deformation and uniform orientation throughout a

---

* See, for example, H. J. Gough's Edgar Marburg Lecture,[57] and W. G. Burgers' article in Houwink.[30]

† See ref. 56 and W. G. Burgers' chapter in Reports of the International Conference on Physics, 2, Phys. Soc. (London) (1935).

crystal, yet they involve sufficient deformation to reorient the lattice in deformation bands. Elam's experiments[34] on beta brass elongated in tension, using these methods, led to the conclusion that the slip lines coincided with crystallographic planes only in the early stages of deformation, and that with greater elongations both the slip planes and slip directions became noncrystallographic. Her observations of deformation bands, however, lend support to the view that differently oriented regions developed in the tests. Thus, while slip planes and directions may have appeared to deviate from crystallographic planes and directions under the assumption of a homogeneous deformation, they did not necessarily alter their crystallographic character *within each band*. It appears more logical to drop the assumption of homogeneity (unless it can be substantiated by rigorous X-ray data) than to drop the idea of slip on crystallographic planes and directions, which has proved such a fruitful and successful one in many developments of experiment and theory. Taylor's earlier distortion measurements on beta brass[58] and the measurements of Taylor and Elam on iron[59] are similarly open to question. It is not likely that the "undistorted planes" of their experiments were entirely unaffected by deformation bands, even though the deformations used were not extreme.

On the other hand, slip-plane determinations based on very slight deformations need not be questioned from this standpoint. In this category, for instance, are the work on ferrite by Gough[14] and by Barrett, Ansel, and Mehl[15] and the work on beta brass by Greninger.[43]

SUMMARY

A method of compressing specimens by rolling them successively in many different directions permitted deformation up to the limit set by the capacity of the material to flow without fracture. This and more conventional means of compression were applied to alpha iron, and the results were analyzed by a special optical method, as well as by standard X-ray methods.

Single crystals or individual grains of alpha iron do not, in general, seek a single orientation during deformation by compression. A crystal initially having [100] near the compression axis will end as a distorted crystal with [100] parallel to the axis, while one starting with [111] near the axis will end as a distorted crystal with [111] parallel to the axis; all others cease to be single crystals and produce the structure known in the literature as deformation bands, etch bands, or X-bands. The crystalline material in the bands rotates progressively as deformation continues, in a direct manner so as to bring [111] in one band and [100] in another band into positions parallel to the axis. The fraction of a crystal possessing each orientation depends upon the initial orientation. This mechanism is responsible for the compression texture of polycrystalline

iron, which we have redetermined and find to be a double fiber texture with [111] and [100] parallel to the compression axis. The orientations are illustrated with models.

It is concluded that slip occurs on a considerable number of slip systems to produce these effects; a graphic representation of all possible slip systems and their resolved shear stresses is presented. Deformation bands have probably introduced errors in the slip-plane determinations of Taylor and Elam on alpha iron and beta brass and may possibly have been mistaken for local distortion at slip planes by several experimenters. Deformation bands analogous to those in iron apparently form in other metals, both face-centered and body-centered, and it is suggested that in such cases deformation bands are important factors in the development of deformation textures and recrystallization textures.

REFERENCES

1. A. Ono: X-ray Examination of Inner Structure of Strained Metals, IV—Alpha Iron Plastically Strained in Extension, Compression and Torsion. *Mem. Coll. Eng. Kyushu Imp. Univ.* (1925) **3**, 267.
2. F. Wever: Compressed Structures of Cubically Crystallized Metals. *Ztsch. tech. Physik* (1927) **8**, 404.
3. E. Siebel and A. Pomp: Die Ermittlung der Formanderungsfestigkeit von Metallen durch den Stauchversuch. *Mitt. K-W. Inst. Eisenforschung, Dusseldorf* (1927) **9**, 157.
4. W. Rosenhain: Metals, Crystalline and Amorphous. *Engineering* (1913) **96**, 510.
5. H. M. Howe: Metallography of Iron and Steel. New York, 1916. McGraw-Hill Book Co.
6. L. B. Pfeil: Deformation of Iron with Particular Reference to Single Crystals. *Carnegie Schol. Mem.*, Iron and Steel Inst. (1926) **15**, 319–380.
7. L. B. Pfeil: Effect of Cold Work on Structure and Changes Produced by Subsequent Annealing. *Carnegie Schol. Mem.*, Iron and Steel Inst. (1927) **16**, 153–210.
8. W. Boas and E. Schmid: Zur Deutung der Deformationstexturen von Metallen. *Ztsch. tech. Physik* (1931) **12**, 71.
9. M. Polanyi: Über Strücturänderungen in Metallen durch Kaltbearbeitung. *Ztsch. Physik* (1923) **17**, 42.
10. F. Wever and W. E. Schmid: *Mitt. K-W. Inst. Eisenforschung, Düsseldorf* (1929) **11**, 109.
11. F. Wever and W. E. Schmid: *Ztsch. Metallkunde* (1930) **22**, 133.
12. W. E. Schmid: *Ztsch. tech. Physik* (1931) **12**, 552.

13. F. Wever: Texture of Metals after Cold Deformation. *Trans.* A.I.M.E. (1931) **93**, 51.
14. H. J. Gough: Behavior of a Single Crystal of Alpha Iron Subjected to Alternating Torsional Stresses. *Proc. Roy. Soc.* (London) (1928) **A-118**, 498.
15. C. S. Barrett, G. Ansel and R. F. Mehl: Slip, Twinning and Cleavage in Iron and Silicon Ferrite. *Trans. Amer. Soc. Metals* (1937) **25**, 702.
16. M. Gensamer and R. F. Mehl: Yield Point in Single Crystals of Iron under Static Loads. *Trans.* A.I.M.E. (1938) **131**, 372.
17. A. B. Greninger: A Back-reflection Laue Method for Determining Crystal Orientation. *Trans.* A.I.M.E. (1935) **117**, 61–74. *Ztsch. Krist.* (1935) **91**, 424–432.
18. E. Schmid and W. Boas: Kristallplastizität, 41–51. Berlin, 1935. Julius Springer.
19. C. S. Barrett: The Stereographic Projection. *Trans.* A.I.M.E. (1937) **124**, 29.
20. A. P. R. Wadlund: Radial Lines in Laue Spot Photographs. *Phys. Rev.* (1938) **53**, 843.
21. W. Zachariasen: Comments on the article by A. P. R. Wadlund. *Phys. Rev.* (1938) **53**, 844.
22. C. S. Barrett: Radial Lines in Laue Spot Photographs. *Phys. Rev.* (1938) **53**, 1021.
23. C. S. Barrett: Internal Stresses. *Metals and Alloys* (1934) **5**, 131, 154, 170, 196, 224.
24. L. P. Tarasov: *Jnl. Applied Phys.* (1938) **9**, 192.
25. W. Fahrenhorst and E. Schmid: Über die plastische Dehnung von α-Eisen-kristalle. *Ztsch. Phys.* (1932) **78**, 383.
26. M. Polanyi: *Ztsch. Physik* (1934) **89**, 660; *Ztsch. Metallkunde* (1925) **17**, 94.
27. G. I. Taylor: *Proc. Roy. Soc.* (London) (1934) **A-145**, 362, 388, 405; *Proc. 4th Int. Cong. Applied Mechanics,* Cambridge (1934) 113; *Ztsch. Krist.* (1934) **89**, 375.
28. R. Becker: *Physik. Ztsch.* (1925) **26**, 919.
29. E. Orowan: *Ztsch. Phys.* (1934) **89**, 605, 614, 634; (1935) **97**, 573; (1936) **98**, 382.
30. W. G. Burgers and J. M. Burgers: *Nature* (1935) **135**, 960; *Trans.* Roy. Acad. Sci., Amsterdam (1935) **15**, sec. 1, No. 3, 173. A summary by Burgers is given by R. Houwink: Elasticity, Plasticity, and Structure of Matter. Cambridge Univ. Press, 1937.
31. B. Chalmers: Influence of Difference of Orientation of Two Crystals on Mechanical Effect of Their Boundary. *Proc. Roy. Soc.* (London) (1937) **A-162**, 120.
32. Z. Jeffries and R. S. Archer: Crystalline Structure of Metals. *Chem. and Met. Eng.* (1921) **24**, 771.
33. H. Brearley: The Use of Microscopic Methods. Sheffield Soc. Engrs. and Metallurgists (1909–1910) 17–18, Fig. 56.
34. C. F. Elam: Distortion of Beta Brass and Iron Crystals. *Proc. Roy. Soc.* (London) (1936) **A-153**, 273.
35. F. Johnson: Some Features in the Behaviour of Beta Brass When Cold Rolled. *Jnl.* Inst. Metals (1920) **24**, 301.
36. G. D. Bengough: Discussion of paper by Johnson. *Ibid.*, 311.
37. F. H. Clark: A Study of the Heat Treatment, Microstructure and Hardness of 60:40 Brass. *Trans.* A.I.M.E. (1927) *Proc.* Inst. Metals Div., 276.
38. L. R. Van Wert: Some Observations in Heat Treatment of Muntz Metal. *Trans.* A.I.M.E. (1929) **83**, 498.
39. C. H. Mathewson: Discussion of paper by Clark. *Idem,* 299.
40. A. J. Phillips: Discussion of paper by Van Wert. *Idem,* 505.
41. D. W. Smith: A Study of the Segregate Structures in Copper-tin and Silver-zinc Alloys. *Trans.* A.I.M.E. (1933) **104**, 48.
42. A. B. Greninger and V. G. Mooradian: Strain Transformation in Metastable Beta Copper-zinc and Beta Copper-tin Alloys. *Trans.* A.I.M.E. (1938) **128**, 337.

43. A. B. Greninger: Deformation of Beta Brass. *Trans.* A.I.M.E. (1938) **128**, 369.
44. E. C. Bain and Z. Jeffries: Mixed Orientation by Plastic Deformation. *Chem. and Met. Eng.* (1921) **25**, 775.
45. Z. Jeffries and R. S. Archer: The Science of Metals, Fig. 60. New York, 1924. McGraw-Hill Book Co.
46. C. H. Mathewson and A. Phillips: Recrystallization of Cold-worked Alpha Brass on Annealing. *Trans.* A.I.M.E. (1916) **54**, 608.
47. F. Johnson: Influence of Cold Rolling upon Mechanical Properties of Oxygen-free Copper. *Jnl.* Inst. Metals (1919) **21**, 335.
48. F. Johnson: Discussion of paper by Adcock. *Jnl.* Inst. Metals (1922) **27**, 94.
49. F. Adcock: Internal Mechanism of Cold Work and Recrystallization in Cupronickel. *Jnl.* Inst. Metals (1922) **27**, 73.
50. C. F. Elam: Discussion of paper by Adcock. *Idem*, 94.
51. W. Rosenhain: Discussion of paper by Adcock. *Idem*, 96.
52. C. H. Samans: The Deformation Lines in Alpha Brass. *Jnl.* Inst. Metals (1934) **55**, 209.
53. F. S. Goucher: On the Strength of Tungsten Single Crystals under Tensile Stress. *Phil. Mag.* (1924) [6] **48**, 229, 800.
54. G. I. Taylor: Resistance to Shear in Metal Crystals. *Trans.* Faraday Soc. (1928) **4**, 121.
55. K. Yamaguchi: Internal Strain of Uniformly Distorted Aluminum Crystals. Sci. Papers Inst. Phys. Chem. Research (Tokyo) (1929) **11**, 151.
56. W. G. Burgers and P. C. Louwerse: Über den Zusammenhang Zwischen Deformations-vorgang und Rekristallisationstexture bei Aluminium. *Ztsch. Phys.* (1931) **67**, 605.
57. H. J. Gough: Edgar Marburg Lecture. *Proc.* Amer. Soc. Test. Mat. (1933) pt. 2, **33**.
58. G. I. Taylor: Deformation of Crystals of Beta Brass. *Proc.* Roy. Soc. (London) (1928) **A-118**, 1.
59. G. I. Taylor and C. F. Elam: Distortion of Iron Crystals. *Proc.* Roy. Soc. (London) (1926) **A-112**, 337.

DISCUSSION

(R. H. Aborn presiding)

A. B. GRENINGER,* Cambridge, Mass.—The information presented by Dr. Barrett, and more particularly the interpretation of the data, is certainly welcome to those who have long been dissatisfied with the currently accepted homogeneous picture of metal crystal deformation. I agree with Dr. Barrett's remarks on deformation bands in beta brass. Severe deformation of these crystals produces bands for which orientation differences are readily detected; however, these bands are considerably more irregular than those produced with light deformation.

Many questions come to mind regarding the origin and nature of these deformation bands; many of these will undoubtedly be answered in Dr. Barrett's future work. A most fascinating problem concerns the interrelation between slip lines and deformation bands. Is it not possible that many of our *visible* slip lines may be fine deformation bands and that the main difference between the two is one of dimension? It is, of course, not necessary that bands and slip lines have the same orientation habit; this was clearly shown by the work on beta brass to which Dr. Barrett refers.

---

* Assistant Professor of Metallurgy, Graduate School of Engineering, Harvard University.

Dr. Barrett has stated that deformation bands "seem to be common in ferrite deformed in many ways—perhaps in all ways." A microscopic study of fatigue failure is being made by R. W. Vose, of the Materials and Structures Laboratory at Harvard. Fatigue specimens of Armco iron were polished and etched at the region of maximum stress concentration, and the behavior of the specimen was observed microscopically during the fatigue loading. The main microstructural feature in the
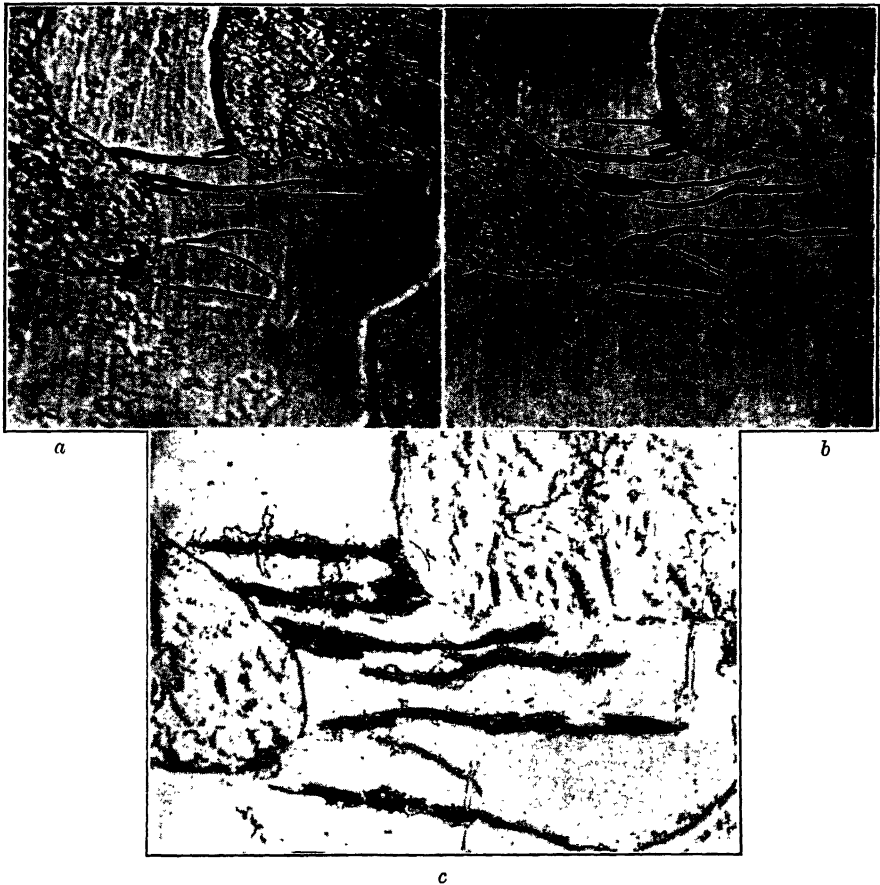
FIG. 19.—ARMCO-IRON FATIGUE SPECIMEN.

30,000 lb. per sq. in.: a, after 1,000,000 cycles, × 420; b, after 2,000,000 cycles, × 420; c, after 4,000,000 cycles, × 640. All three photographs show same specimen area. Experiment and photographs by R. W. Vose.

behavior of the specimen was the appearance and growth of bands within the ferrite grains. These bands are formed and grow even under conditions that will not start a fatigue crack in 6,000,000 cycles (Fig. 19). The bands are visible after repolishing and etching in Nital, and it is probable that they belong to the classification of deformation bands. A systematic study of these bands produced by fatigue loading (preferably in a face-centered cubic metal of large grain size) should yield valuable information regarding the genesis and growth of deformation bands.

C. S. BARRETT (author's reply).—Dr. Greninger's discussion again raises the question, "Are bands sometimes mistaken for slip lines?" I have discussed the matter

on page 320, but there is one bit of evidence that tends to support this idea that is not mentioned in the paper; namely, the contour of the surface at a slip line.   Greenland[60] has remarked that, at least in mercury crystals, slip lines do not break up the surface into abrupt sharp-edged steps such as one would expect from the nature of the glide mechanism, but instead they mold the surface into rounded humps or into steps with rounded edges.   There are, however, several possible explanations of the lack of sharpness other than the one we are discussing, so this is not very convincing evidence.

Mr. Vose's photographs, showing bands that are visible in fatigue specimens after repolishing and etching, appear to be regions in which some sort of reorientation or fragmentation has occurred.   There have been exhaustive studies of these bands on the polished surfaces of fatigue specimens,[61] and there can scarcely be any doubt that they are masses of tightly spaced, parallel slip lines, which are usually resolvable at high magnifications.   They occur with stresses both above and below the fatigue limit, and thus signify cold-work rather than fatigue damage.

Localized groupings of slip lines like these could be expected to result in heterogeneous orientation changes, thus probably forming bands very similar to the deformation bands formed during static compressing.   The nature of the rotations, however, might be different since a grain of a given orientation would probably alter its shape differently in the two cases.   X-ray studies of the orientations in individual small grains after fatigue have shown marked similarities with the orientations of grains in a slightly elongated tensile specimen[62] and still further suggests that the markings in Dr. Greninger's discussion are analogous in many respects to those under discussion in this paper and in the following paper of this series (which follows on page 327 of this volume).   The lattice of each grain of a polycrystalline metal is progressively distorted into wider ranges of orientation when it is subjected to increasing elongation in tension or compression or increasing stress amplitude in fatigue.   The increasing scatter in orientation is as much a characteristic feature of the deformation of grains of an aggregate as the path of the mean orientation of the grain or the mean orientation of a band.   It is probable that the grains of an aggregate are subjected to such heterogeneous strains that the lattice rotations are frequently more complex than those plotted in Figs. 16 and 17, and that deformation bands are then more irregular in shape.

[60] K. M. Greenland: Slip Bands on Mercury Single Crystals.   *Proc.* Roy Soc. (1937) **163-A**, 29–34.

[61] For example, see: J. A. Ewing and J. C. W. Humfrey: The Fracture of Metals under Repeated Stress.   *Phil. Trans.* Roy. Soc. (1902) **200-A**, 241.

H. J. Gough and D. Hanson: The Behavior of Metals Subjected to Repeated Stresses.   *Proc.* Roy. Soc. (1923) **104-A**, 538.

[62] C. S. Barrett: Distortion of Grains by Fatigue and Static Stressing.   *Metals and Alloys* (Jan. 1937).

Structure of Iron after Drawing, Swaging, and Elongating in Tension

By Charles S. Barrett,* Member, and L. H. Levenson, † Junior Member A.I.M.E.

Plastic flow in metal crystals and the changes in orientation resulting from it are generally understood to take place by the following fundamental mechanisms: (1) slip on crystallographic planes, (2) homogeneous crystal rotation resulting from the slip, (3) bending of the lattice between the planes of slip, and, under certain circumstances, (4) twinning. This paper and a preceding one on iron subjected to uniaxial compression[1] concern two additional processes that must now be added to this list: (5) the formation of deformation bands, and (6) the bending and rotation of these bands.

The present investigation yields a new understanding and definiteness to the common terms so loosely used when speaking of cold-worked metals —"grain fragmentation," "elongated grains," and "deformation twins," "deformation bands," "etch bands," or "X-bands." Bands have been noted on the polished and etched surfaces of cold-worked metals by various investigators for more than 25 years,‡ yet their nature and their significance have been so little understood that they are not treated in the most comprehensive modern texts on the deformation of crystals. The experiments in this series show that they are one of the fundamental processes in the deformation of metals, of importance in the development of preferred orientations, in work-hardening (since they have the effect of reducing the effective grain size and interfering with slip), and in the recrystallization process.

The present experiments were performed on the same stock of material that was used in the earlier compression experiments[1]—hydrogen-purified mild steel in which the carbon content had been reduced to the limit detectable under the microscope and in which single crystals could be grown by a strain-anneal treatment.[2]

---

* Member of Staff, Metals Research Laboratory and Lecturer, Department of Metallurgy, Carnegie Institute of Technology, Pittsburgh, Pa.

† Research Assistant, Metals Research Laboratory, Carnegie Institute of Technology, Pittsburgh, Pa.

[1] References are at the end of the paper.

‡ A list of references to the literature on the subject is included in the paper of reference 1.

DEFORMATION TEXTURE OF POLYCRYSTALLINE WIRES

When polycrystalline iron wire is cold-drawn through circular dies and etched so as to remove the outer layers, which in all drawn wires are known to deviate somewhat in orientation from the ideal orientation of the core,[3–7] a preferred orientation is developed in which [110] lattice directions become parallel to the wire axis. This has been confirmed a number of times since its discovery by Ettisch, Polanyi and Weissenberg,[8] but it was thought worth while to check it with material from different sources, to look for faint traces of a second orientation, and to see whether swaging or combinations of drawing and swaging altered the results. The usual [110] deformation texture, with no trace of other textures, was found in purified mild steel after drawing or after swaging followed by drawing, in iron-vanadium after drawing, in iron-silicon after drawing or after swaging and drawing, and in purified Armco iron after swaging.
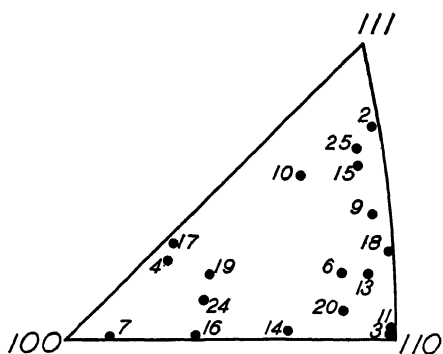
FIG. 1.—INITIAL ORIENTATION OF EACH CRYSTAL USED.
Cylindrical axes are plotted as points in unit stereographic triangle.

DEFORMATION TEXTURE OF SINGLE CRYSTALS

Drawn Crystals.—Nine single crystals of different orientations were drawn into wires, and the orientations developed in them by the drawing were determined. The orientations of these crystals and those used in experiments to be mentioned later are represented in the stereographic projection in Fig. 1, where the initial direction of the elongation axis is plotted as a point appropriately related to the cube, octahedral, and dodecahedral directions of the lattice in the crystal, which are represented by the three vertices of the stereographic triangle. The crystals used in the wire-drawing experiments, Nos. 2, 3, 4, 6, 7, 13, 16, 18, 19,* are well scattered over the unit stereographic triangle and thus are a fair sample of all possible orientations.

The final deformation texture in all these crystals was the same as in polycrystalline wires; namely, a fiber texture with the [110] direction in the wire axis and a random orientation around the axis, regardless of whether in the early stages the crystals were drawn or swaged. This was found in X-ray patterns at the following percentages of reduction in area

---

* The crystals were all cylindrical except Nos. 2 and 3, which were approximately square in cross section.

in the crystals noted:* Nos. 2, 4, 6, 7 and 13 at 99 per cent and Nos. 16 and 18 at 95 per cent. The final orientations may have been reached with somewhat smaller reductions than these, however. Crystal No. 18 was swaged to a reduction of 74 per cent and then drawn so as to make a total reduction of 95 per cent. By this time the final [110] texture had been reached and was retained when this area was further reduced 90 per cent by drawing. The [110] texture, therefore, is stable and is uninfluenced by the amount of deformation received after reaching the final position. In crystals that were photographed with the X-ray beam parallel to the axis (Nos. 2, 3, 13 and 16) the Debye rings were complete, indicating a random orientation around the axis.

Swaged Crystals.—To simulate the deformation of a grain in a polycrystalline aggregate and to reduce coring effects so common in drawn wires, a number of crystals 0.25 to 0.36 in. in diameter were mounted in a close fitting hole drilled in the center of a 0.50-in. dia. fine-grained rod of the same material, and the assembly reduced by swaging. The positions of the crystals in the pipe were then determined by a radiograph, and they were removed by carefully filing away the pipe

FIG. 2.—DIFFRACTION PATTERN OF CRYSTAL No. 15 AFTER 80 PER CENT REDUCTION BY SWAGING.
X-ray beam parallel to axis. Shows large range of orientations around axis.

segments. While these swaging experiments were useful for microstructure studies, they did not involve reductions sufficiently heavy to align [110] directions in the crystals with the axis of elongation and thus to prove conclusively that the [110] position is the stable one. In view of the other experiments in the series, however, this cannot be doubted.

X-ray photograms made with the beam parallel to the axis revealed, by the circumferential lengths of the arcs, the amount of spread in orientation around the wire axis, which we shall speak of as the spread in azimuth. This azimuthal spread increased with increasing deformation, the arcs merging into continuous circles as the final equilibrium texture was reached, as in the example shown in Fig. 2. It was noted that without exception, spread in angles between a [110] direction and the wire axis was always much less than the spread in azimuth, and usually was only about ± 4°. In a number of the photograms there were indications

---

* All percentages given in this paper indicate percentage reduction in area of cross section.

of more than one orientation, and deformation bands were suspected. Microscopic studies of these bands were then undertaken.

DEFORMATION BANDS IN POLYCRYSTALLINE WIRES

Drawn Wires.—Fig. 3 shows the appearance of the cross section of a wire after a small reduction by drawing and rather severe etching in dilute

FIG. 3.—DEFORMATION BANDS IN TRANSVERSE SECTION OF POLYCRYSTALLINE IRON WIRE.   × 100.
Reduced 30 per cent by drawing.   Dilute nitric etch.

nitric acid, which develops etch pits having cube planes as faces.   Some of the grains have been "fragmented" into bands having an orientation different from the matrix in which they form, and reflecting light differently.   The general appearance is almost identical with the appearance of the compressed surface of iron deformed in compression (cf. Fig. 2 of ref. 1).

These deformation bands begin to appear at a very small reduction in area—the exact point perhaps depending upon the grain size or other conditions—and at first are difficult to see, but they increase in contrast with increasing deformation, indicating an increasing difference in

orientation across the boundary of each band.   At 25 per cent reduction bands were noted in grains of all sizes from 3 mm. down to 0.015 mm. in diameter.   It may be anticipated that under proper conditions they can be found in grains of any size in the range of ordinary materials, though perhaps more frequently in the larger grains.

At low deformations a section parallel to the axis of the wire may show bands at any angle to the axis.   The bands, which usually occur in parallel sets within a grain, are approximately flat lamellae.   As the deformation progresses these lamellae are forced to swing into a position more and more closely parallel to the axis of the wire, because of the

FIG. 4.—ELONGATED BANDS AND GRAINS IN LONGITUDINAL SECTION OF WIRE.   × 500.
    Polycrystalline, 120 grains per sq. mm., reduced 95 per cent by drawing.   Dilute nitric etch.

decrease in diameter and the increase in length of the wire.   The microstructure is then of the type shown in Fig. 4, in which most, though not all, of the striations are axial.   Assuming homogeneous deformation, the amount of rotation at any degree of elongation can readily be calculated: If a plane lies at an angle θ_0 from the axis before deformation and at an angle θ after deformation, which reduces the diameter from D_0 to D and increases the length from L_0 to L, then

$$\tan \theta = (D/D_0) \cdot (L_0/L) \cdot \tan \theta_0 \qquad [1]$$

and, since $L_0D_0{}^2 = LD^2$ because the volume remains unchanged, it follows that

$$\tan \theta = (D/D_0)^3 \tan \theta_0 \qquad [2]$$

Somewhat more involved calculations will give the percentage of the planes or the percentage of the traces that will fall within any given angle from the axis at any deformation, assuming a random orientation of the

original lamellae. This percentage steadily increases with deformation and could be used, in fact, to estimate the amount of elongation that had been undergone by a wire.

It is emphasized that the familiar "elongated grains" in wires, which extend so nearly axially after severe deformation, are not to be identified in general with the original grains, but rather with the individual bands within these grains.

Swaged Wires—Tensile Specimens.—There appears to be no marked difference between the microstructures produced by small amounts of reduction by drawing, swaging, or elongation in tension; bands of the same appearance are seen in all cases. For example, bands were seen in a polycrystalline rod pulled in tension to a reduction of 20 per cent. There can be no doubt that polycrystalline iron when elongated by any type of cold-work contains deformation bands.
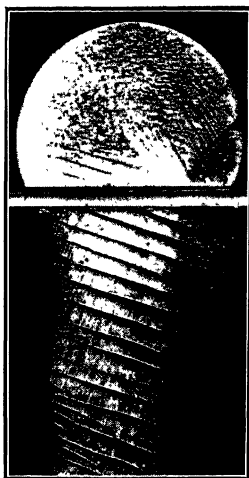
FIG. 5.—TRANSVERSE AND LONGITUDINAL SECTIONS OF CRYSTAL No. 10. × 5. Reduced 11 per cent by drawing. Dilute nitric etch.

DEFORMATION BANDS IN SINGLE CRYSTALS

Bands in single crystals are best for detailed studies, for the width of the bands is then sufficiently great to permit a determination of the lattice orientation within each band. When the deformation of the crystals is small, the crystallographic planes that form the bounding surfaces of the bands may also be determined.

Drawn Crystals.—Crystal No. 10, a long crystal having its cylindrical axis 24° from [110] and 39° from [100], was turned on a lathe, using small cuts, to a series of segments having the following diameters: 0.258 in., 0.266 in., 0.275 in., and 0.284 in. It was then drawn through a die to reduce all sections to 0.250 in., the reduction in the different segments being 6 per cent, 11 per cent, 17 per cent, and 22 per cent, respectively. The segments were then sectioned transversely and longitudinally. Deformation bands were seen in all segments, although only a few could be distinguished in the least deformed segment; all were straight or curved only slightly.

A back-reflection Laue X-ray photogram of the segment deformed 6 per cent permitted an orientation determination after drawing and showed that there had been a rotation of the lattice of only 2° in the portion of the crystal struck by the beam (a spot on the center of the longitudinal section). The bands, therefore, began to form before there was any appreciable rotation of the crystal, probably at the beginning of the deformation. In the segment deformed 11 per cent, the bands appear

as in Fig. 5. The directions of the traces of these bands on the transverse and longitudinal sections adjoining the common edge were plotted on a stereographic projection reproduced in Fig. 6, in which the plane of the projection is the cross-section plane.[9] The intersections of the dashed lines are the poles of the bands located from the directions of the traces of bands appearing on both surfaces. The dashed line near the circumference at the lower left represents the data from a band seen on one surface only.* The poles of the cube and octahedral planes determined by the Laue photogram of the adjacent segment (which had
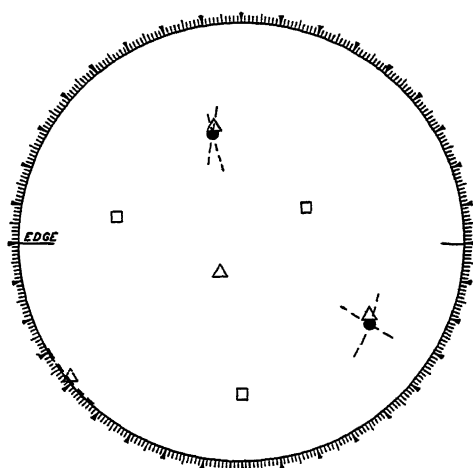
FIG. 6.—ANALYSIS OF CRYSTAL NO. 10 SHOWING THAT BANDS ARE ON {111} PLANES.
Stereographic projection on transverse plane. Filled circles are poles of bands; squares and triangles are poles of {100} and {111} planes located by X-rays.

received less deformation) are shown by squares and triangles, respectively. The bands have formed on {111} planes, since the poles of the bands lie very close to the poles of {111} planes located by X-ray data (the triangles). Additional confirmation of the orientation of the crystal was obtained from a back-reflection Laue photogram of the segment shown in Fig. 5. In spite of the cold-work and increased blurring of the Laue spots, two zones of spots could still be detected on the photogram lying in a position identical, within the limits of error of the work, with the two principal zones of the less deformed segment indicating a mean orientation substantially identical with that plotted in Fig. 6. A stereographic projection was made for the segment deformed 22 per cent, and bands on the same three planes of the type {111} were again clearly identified. In some region of the crystal that was not exposed by the

---

* The camera used in taking pictures of the specimens of Figs. 5 and 7 inverted the image of the surfaces; the stereographic projections refer to the actual specimens rather than their inverted images.

metallographic polishing, the fourth {111} plane may have exhibited bands also.

Crystal No. 19, with its cylindrical axis 26° from [110] and 22° from [100], was drawn from a diameter of 0.377 in. to 0.303 in., a reduction of 31 per cent in area, with the production of numerous sets of bands shown in transverse and longitudinal section in Fig. 7. (It is sometimes difficult to show all the sets of bands well on a single photograph, for each is most favorably seen when the incident light is adjusted to it alone.) The analysis of the data from the specimen of Fig. 7 is shown stereographically in Fig. 8, a projection on the cross-section plane. Dashed lines and their intersections (filled circles) represent the loci of poles capable of accounting for the observed traces of the bands. These, however, cannot be the position of the bands in the undeformed crystal. If it is assumed that they formed before appreciable elongation took place, and that the deformation was homogeneous, equation 2 can be used as a correction formula giving the displacement of the poles toward the center of the projection necessary to make the projection apply to the undistorted crystal. The poles corrected in this manner lie on the dot-dash lines and at their intersections, marked by the open circles. There is good agreement between these corrected poles of the bands and an orientation of the lattice indicated by the squares (cube
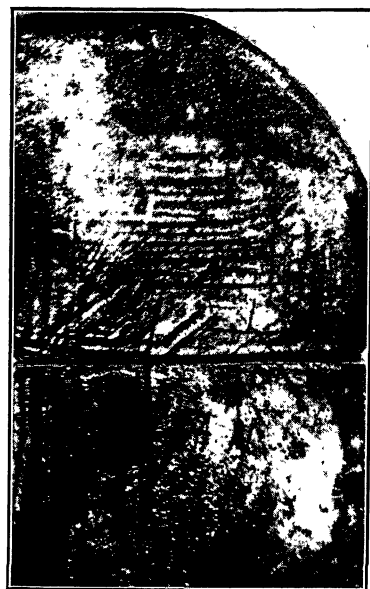
FIG. 7.—TRANSVERSE AND LONGITUDINAL SECTIONS OF CRYSTAL No. 19. × 5.
Reduced 30 per cent by drawing. Dilute nitric etch.

poles) and triangles (octahedral poles). The agreement is best when all directions are read from bands near a single spot in the crystal. It follows from the projection that three sets of bands have formed in [100] planes and at least two sets on [111] planes of the crystal.

Fig. 9 is a projection of the same crystal on which are plotted the poles of cube planes within individual bands. These have been determined by a simple optical goniometer operating with the light reflected from the cube-faced etch pits of individual bands, using only the more reliable type of reflections (those from pit faces nearly parallel to the surface). The poles of the reflecting cube planes are shown as open circles, each being labeled with a letter indicating on what plane the band formed. For example, the alternating bands on the cube plane A, whose pole is at the left side of Figs. 8 and 9 and whose traces are vertical

in Fig. 7, have cube axes in orientations indicated by the circles A and
A'. The orientation difference across the boundary of the bands of the
A set is therefore represented by the separation of the A-A' pairs of
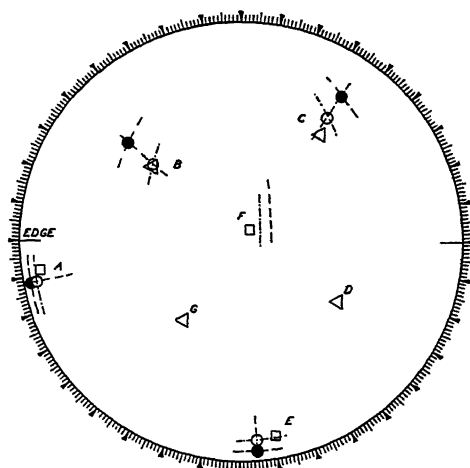
FIG. 8.—ANALYSIS OF CRYSTAL NO. 19 SHOWING THAT BANDS ARE ON {100} AND
{111} PLANES.
    Stereographic projection on transverse plane. Poles of bands indicated by filled
circles for deformed crystal, open circles for undeformed crystal (calculated); squares
and triangles are poles of {100} and {111} planes.
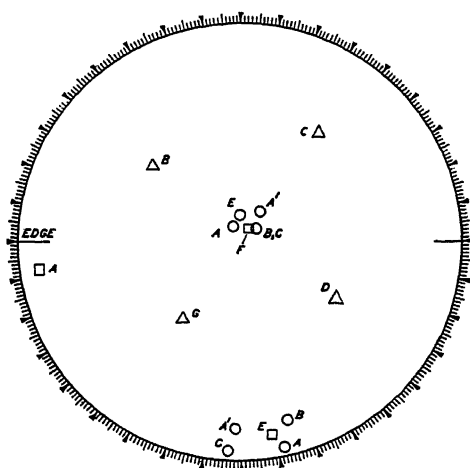
FIG. 9.—ORIENTATIONS OF LATTICE WITHIN INDIVIDUAL BANDS OF CRYSTAL OF
FIGS. 7 AND 8.
    Open circles are poles of {100} planes, located by optical reflections from etch pits.
Letters indicate bands to which they refer.

circles. Great accuracy is not claimed for these optical determinations,
but the accuracy is sufficient to prove three important points regarding
the mechanism of banding:

1. The bands are not twins. The difference in orientation between any band and any other is of the order of 15° or less, which is far less than is encountered in twinning.

2. The lattice in bands that have formed on different crystallographic planes is rotated in several different directions from the mean orientation of the whole. Each parallel set of bands rotates away from the parent orientation in a manner peculiar to itself.
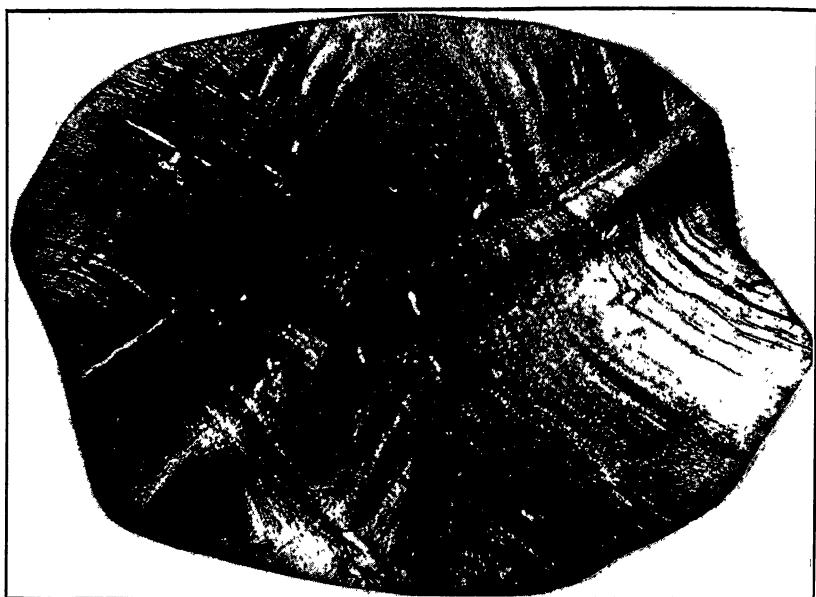
FIG. 10.—TRANSVERSE SECTION OF CRYSTAL No. 16 AFTER 90 PER CENT REDUCTION BY SWAGING. × 25.
Shows curvature of deformation bands. Dilute nitric etch.

3. The mean orientation of the bands is equal to or close to the original orientation, indicating that banding began in the early stages of the deformation.

That these bands are not twins and do not originate as twins is also established by the proof in Figs. 6 and 8 that the bands form on {100} and {111} planes and not on the twinning planes, which are of the form {112} in iron.[10]

Swaged Crystals.—The crystals that were swaged while mounted in an iron pipe show the behavior of deformation bands after more severe deformation.

Crystal No. 13, examined at 36 per cent reduction, had developed bands on two sets of {111} planes; the orientation difference across the boundaries of one of the sets was between 15° and 20°. (This crystal was originally 9° from [110] and 43° from [100].) Crystal No. 17, at 80 per cent reduction, also showed two sets of {111} bands.

Crystal No. 16 was examined at reductions of 84 per cent, 90 per cent, 96.8 per cent, and 97.5 per cent, and was found in every case to have inter-penetrating sets of bands exhibiting a very marked curvature in the cross-section plane. This is shown in Fig. 10, which was taken after 90 per cent reduction. The longitudinal sections are largely free from this curvature (Fig. 11). (The initial orientation was 26° from [110] and 19° from [100].)

Crystals 11 and 15 also showed curved bands when examined at reductions of 63 per cent and 75 per cent, respectively. Since the bands in these crystals always appear curved on the cross section and straight on the longitudinal section, it follows that they are bent only around an axis parallel or nearly parallel to the axis of elongation, and it seems
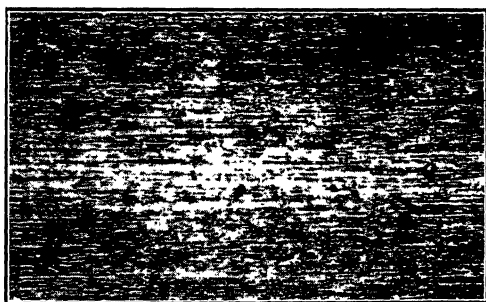
FIG. 11.—LONGITUDINAL SECTION OF CRYSTAL No. 16 AFTER 97.5 PER CENT REDUC-
TION BY SWAGING AND DRAWING.   × 100.
Shows alignment of deformation bands with elongation axis.   Dilute nitric etch.

obvious that their curvature is the cause of the large azimuthal spread in orientation evident in X-ray patterns like Fig. 2. It is surprising that crystal No. 11 had an initial orientation only 1½° from [110], a stable orientation, yet it deformed inhomogeneously with as many bands as the others, the bands marking out {111} planes. X-ray diffraction patterns of this crystal prove that the bands are visible only because of a difference in orientation around the axis, for the Debye rings in patterns made with the X-ray beam parallel to the axis contain only long arcs, while those made with the beam normal to the axis show only sharp spots.

The microstructure of the longitudinal section of these crystals, as shown, for example, in Fig. 11, resembles in a striking manner the appear-ance of a polycrystalline cold-drawn wire, owing to the elongated deforma-tion bands which resemble so closely the elongated grains and bands in polycrystalline wires. Fig. 10 shows that in spite of a certain amount of freedom of the crystal to assume a noncircular cross section by forcing an uneven displacement of the surrounding fine-grained material, there has been severe warping of the bands.

Crystals Elongated by Tension.—Crystal No. 24, which had its axis approximately 20° from [100] and 26° from [110] (as determined by optical

reflections from etch pits) developed one parallel set of bands having an orientation that differed only 5° to 7° from the matrix at a deformation of approximately 40 per cent. Similar bands formed in the fillets of the tensile specimen, where the elongation was less, and these were more difficult to see because of their smaller orientation difference.

Crystal No. 25, initially about 47° from [100] and 24° from [110], developed bands so pronounced that they could be seen on the surface of the specimen without etching, in the manner of Lüders lines. These most
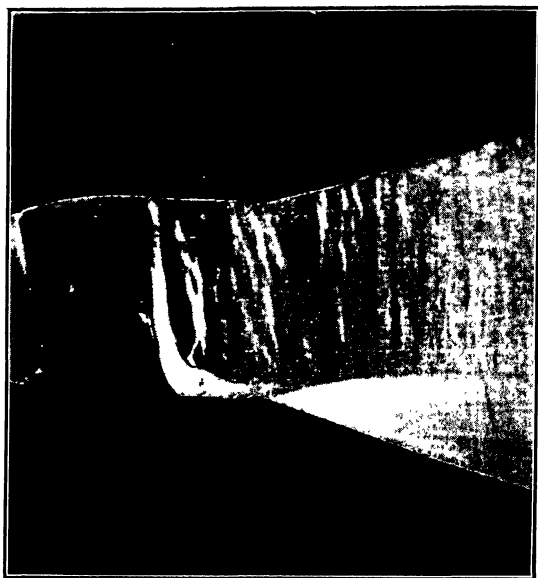
FIG. 12.—LONGITUDINAL SECTION OF CRYSTAL NO. 25 PULLED IN TENSION TO A MAXIMUM REDUCTION OF ABOUT 40 PER CENT AT NARROW END. × 5.
Shows increasing contrast of deformation bands with increasing elongation. Dilute nitric etch.

prominent bands formed on a single set of {111} planes and had a lattice orientation some 15° removed from the adjoining material at a point where the reduction was approximately 40 per cent. Fig. 12, a section through a portion of the specimen parallel to the axis, confirms in a striking way the conclusion that the orientation difference across the boundaries of a deformation band increases with increasing deformation. In the narrow portion of the specimen that was reduced about 40 per cent the bands are contrasty, but in the less deformed fillet of larger diameter the contrast decreases until the bands become invisible. The matrix itself exhibited a changing orientation across the cross section, one side differing about 9° from the other side, and for a half millimeter or so around each small included crystallite this distortion was accentuated. The bands in crystals 24 and 25 showed very little curvature in the cross-

section plane, indicating that the curvature discussed in the preceding section arises from lateral constraints that are present in all cases except the tensile tests of single crystals.

Crystal No. 20, with its axis 7½° from [110] and 38° from [100], was pulled in tension until it failed. The specimen necked down to a sharp, even knife-edge, which was perpendicular to the direction of loading and parallel to a [110] direction of the lattice. Five different cuts were made through the highly deformed region of the specimen and examined metallographically, but no bands were seen on any of the surfaces. Probably this represents the only condition in which an iron crystal can elongate appreciably without the formation of bands.

MODELS ILLUSTRATING DEFORMATION OF A CRYSTAL

The experiments reported above show that iron crystals undergoing plastic elongation are unstable and subdivide into bands regardless of whether or not there are constraints imposed upon them by adjacent crystals or die walls. (The only exception to this rule appears to be a crystal elongated by pulling in tension in the direction of the face diagonal [110].) The bands represent regions in which the lattice is rotating away from the initial orientation. When the bands have a width about equal to their spacing, as frequently occurs, it is probably incorrect to speak of bands embedded in a matrix and more correct to speak of an alternating set of parallel bands. The bands usually form on octahedral planes of the original crystal and less frequently on the cube planes, and rotate away from the parent orientation in different directions. These fundamental characteristics may be illustrated by models consisting of blocks, representing the cubic unit cells, mounted on the transverse and longitudinal sections of a cylinder. Fig. 13 represents a crystal of cylindrical shape having its axis parallel to the cube axis of the crystal lattice. Fig. 14 shows the same crystal after it has been slightly elongated by pulling in a tensile machine, swaging, or drawing through a die. A deformation band has formed on an octahedral plane and is shown by the white lines, within which the orientation differs slightly from that of the rest of the crystal. The model is qualitative only and is not intended to show the exact direction of the lattice rotation in any part of the crystal, nor the exact amount of rotation, which steadily increases with increasing deformation.

After further deformation in the wire die, the bands become curved in the cross-section plane, and in the longitudinal plane they become aligned more nearly parallel to the wire axis, while within each band a rotation of the lattice brings a face diagonal of the unit cubes into parallelism with the wire axis. The orientations are then somewhat like the model of Fig. 15, although in reality they are more complex than can be shown in so simple a model. Fig. 15 indicates only one set of curved bands,

whereas usually there are several other sets that cut across these, and sometimes small bands are to be found within large bands, to add further to the complexity. The result of these alterations in the crystal is to produce a preferred orientation of the complete fiber texture type, with crystalline fragments possessing all orientations around the axis of the wire but with all fragments having a [110] direction parallel to this axis (neglecting the outer zones of the wire where disturbances of the flow direction are encountered). At this stage, deformation bands are visible
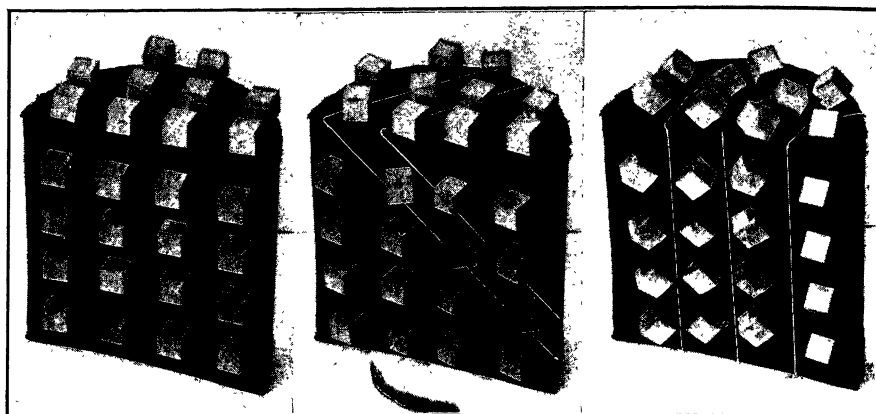
FIG. 13.   FIG. 14.   FIG. 15.

FIG. 13.—MODEL OF CRYSTAL HAVING CUBE AXIS PARALLEL TO CYLINDRICAL AXIS.
Blocks represent orientation of unit cells.

FIG. 14.—MODEL OF CRYSTAL OF FIG. 13 AFTER SLIGHT ELONGATION.
A deformation band, bounded by {111} planes of original lattice, has an orientation different from rest of crystal.

FIG. 15.—MODEL OF CRYSTAL AFTER SEVERE ELONGATION.
Shows curvature of deformation bands about cylindrical axis, alignment of bands with axis, and alignment of cube face diagonals with axis.

only because of a difference in orientation of a restricted type across their boundaries, a difference around the axis of elongation, as indicated in the model.

DISCUSSION OF RESULTS

The fragmentation of single crystals and of grains in an aggregate into deformation bands and the subsequent behavior of these bands are fundamental factors which have been overlooked in theories of crystalline flow, deformation textures, work-hardening, and recrystallization. The previously accepted elements, (1) slip on one or more crystallographic planes, (2) homogeneous crystal rotation resulting from slip, (3) bending of the gliding lamellae (biegegleitung), and (4) twinning, are inadequate to describe the changes occurring in a crystal during plastic flow. There must be added to this list: (5) the formation of deformation bands, and (6) the bending and the rotation of these bands and the crystalline mate-

rial within them. An additional element in this list, which has been proposed by Taylor, Yamaguchi, Burgers and Louwerse, is a "local distortion" involving small regions of the crystal at the surfaces where slip has occurred. It was pointed out in the preceding paper of this series[1] that evidence advanced in support of this theory could not be accepted unless deformation bands were proved to be absent, since bands would have given somewhat similar results in their experiments. The tensile experiments in the present paper add further emphasis to this statement, for the spread in orientation over the cross section of elongated crystals is very similar to the spreads observed by the earlier investigators mentioned and attributed by them to local disturbances at slip planes. Furthermore, preliminary results being obtained in this laboratory with the deformation of aluminum crystals indicate that aluminum, which is the metal used in most of the experiments on "local distortion," is by no means free from the tendency to form bands during deformation.

The present investigation establishes a new mechanism—perhaps the principal mechanism—by which static stressing (and possibly in some cases also dynamic stressing) can cause the changes in X-ray patterns of polycrystalline metals that have been the subject of much attention in recent years by various investigators, including Gough and Wood[11] and one of the authors.[12] It was concluded by the latter that "the distortion of a grain proceeds by a reorienting of the parts with respect to each other by bending or perhaps by fragmenting. The range of orientation increases continuously with the increasing severity of cold-work and does not appear to be limited at any stage to two degrees" (as had been concluded by Gough and Wood[11]). But the details of this mechanism could not be established without supplementing the X-ray photograms with data from the microscope and optical goniometer, as has been done in the present paper.

The banding mechanism is also important in the interpretation of the results obtained with the various devices[13-15] for investigating plastic deformation on a microscopic scale within individual grains. It thus must be considered in connection with the interesting problems having to do with grain boundary vs. intragranular distortion.

Failure to take account of the heterogeneous nature of the deformation process in single crystals has unquestionably confused many previous experimenters, as was pointed out in the preceding paper. A case of this that is directly related to the present discussion is Elam's[16] recent attempt to analyze the slip systems in iron and beta brass by measurements on crystals elongated in tension, and it accounts for her failure to obtain a conclusive analysis. That deformation bands were actually present in her crystals is obvious from her photographs and comments and from the fact that the "twinlike" markings she observed were bounded by {100} planes in one crystal of beta brass and {100} together with {111} planes

in iron crystals, though her comparison of the markings with twins and Lüders lines is rather misleading, for deformation bands do not have the usual features of these processes.[1,17] Earlier investigations that must have been similarly confused are the determination of the slip systems in iron and beta brass by Taylor and Elam[18,19] based on distortion measurements, and the work of Fahrenhorst and Schmid[20] on iron.

An investigation of bands in rolled iron, which is the subject of a paper now in the course of preparation at this laboratory, is disclosing a behavior whose complexity would well have been anticipated from the complexities observed in these more symmetrical deformations.

ADDENDUM, JANUARY 14, 1939

G. I. Taylor[21] has recently developed a theory of deformation textures of aluminum that should prove a valuable step toward an understanding of the origin of deformation bands in all metals. He calculates that in grains of polycrystalline aluminum during compression or elongation five slip systems must operate in order to produce the required change in shape, these being the five for which the work of deformation is less than for any other five that could produce this change of shape. His calculations show numerous orientations in which two or more groups of five slip systems would give minimum values for the work. A grain having one of these orientations would have a tendency to rotate in two or more directions, and Taylor remarks that the direction of rotation could be a result of any combination of these, and thus be any direction within a considerable range.

Our studies suggest that in iron (and probably in most metals), as a result of having more than one group of slip systems equally favored, the grains divide into deformation bands, with alternate groups of systems operating in alternate bands, rather than rotating homogeneously in a direction intermediate between the demands of each of the favored groups.

SUMMARY

A specific type of "grain fragmentation" occurs in swaged and drawn iron wires and tensile specimens, and doubtless in all iron rods, wires, and tubes formed by cold formation, and in grains from a diameter of 0.02 mm. or smaller up to single crystals. It consists of the formation of deformation bands on crystallographic planes of the forms {100} and {111} in the early stages of deformation. The lattice within a band rotates away from the parent orientation an amount that gradually increases with the deformation. The direction of this lattice rotation depends upon the crystallographic plane on which the band has formed. After greater deformation the parallel sets of bands become curved and also rotate into a position parallel to the wire axis, while the lattice within each band rotates so as to bring a [110] direction parallel to the axis. The curving

of the bands, their interpenetration, and the lattice rotation within them are thus able to generate a [110] fiber texture in a single crystal or grain such that fragments possess all azimuthal positions around the wire axis. The "elongated grains" seen in longitudinal sections of iron wires are frequently deformation bands. Deformation bands account for the failure of some investigators to get conclusive results regarding the slip directions and slip planes from investigations with tensile specimens.

REFERENCES

1. C. S. Barrett: Structure of Iron after Compression. Page 296, this volume.
2. M. Gensamer and R. F. Mehl: Yield Point in Single Crystals of Iron under Static Loads. *Trans.* A.I.M.E. (1938) **131**, 372.
3. E. Schmid and G. Wassermann: The Texture of Hard-drawn Wires. *Ztsch. Physik* (1927) **42**, 779.
4. W. A. Wood: Measurements on the Degree of Orientation in Hard-drawn Copper Wires. *Phil. Mag.* (1931) **11**, 610–617.
5. G. Greenwood: The Cold Working of Platinum Wires and the Fibrous Textures thereby Produced. *Ztsch. Krist.* (1929) **72**, 309–317; Fiber Texture in Nickel Wires. *Ibid.* (1931) **78**, 247.
6. T. Fujiwara: Effects of the Direction of Drawing on the Arrangement of the Microcrystals in Aluminum Wire and on its Tensile Strength and Broken Fracture. *Mem. Coll. Sci. Kyoto Imp. Univ.* (1932) **A-15**, No. 1, 35–42.
7. W. G. Burgers: Differences in Space Lattice Disturbance and Texture between Surface and Central Zones of Drawn Single-crystal and Multicrystal Tungsten Wires. *Ztsch. Physik* (1929) **58**, 11–38.
8. M. Ettisch, M. Polanyi and K. Weissenberg: Fibrous Structure of Hard-drawn Metals. *Ztsch. phys. Chem.* (1921) **99**, 352.
9. C. S. Barrett: The Stereographic Projection. *Trans.* A.I.M.E. (1937) **124**, 29.
10. C. S. Barrett, G. Ansel and R. F. Mehl: Slip, Twinning and Cleavage in Iron and Silicon Ferrite. *Trans.* Amer. Soc. Metals (1937) **25**, 702.
11. H. J. Gough and W. A. Wood: A New Attack on the Problem of Fatigue in Metals Using X-ray Methods of Precision. *Proc. Roy. Soc.* (London) (1936) **154-A**, 510.
12. C. S. Barrett: Distortion of Grains by Fatigue and Static Stressing. *Metals and Alloys* (Jan. 1937).
13. G. Seumel: Experiments on the Influence of Grain Boundaries on the Deformation of Test Bars Consisting of Many Crystals. *Ztsch. Krist.* (1936) **93**, 249.
14. H. Unkel: A Study of the Deformation of the Macrostructure of Some Two Phase Alloys by Cold Rolling. *Jnl.* Inst. Metals (1937) **61**, 171.
15. F. N. Rhines and R. Ward: The Microgrid. A Method for the Observation of Plastic Deformation on a Microscopic Scale. *Metals and Alloys*, in press.
16. C. F. Elam: Distortion of Beta Brass and Iron Crystals. *Proc.* Roy Soc. (London) (1936) **A-153**, 273.
17. M. Gensamer: The Yield Point in Metals. *Trans.* A.I.M.E. (1938) **128**, 104.
18. G. I. Taylor: Deformation of Crystals of Beta Brass. *Proc.* Roy. Soc. (London) (1928) **118-A**, 1.
19. G. I. Taylor and C. F. Elam: Distortion of Iron Crystals. *Proc.* Roy. Soc. (London) (1926) **112-A**, 337.
20. W. Fahrenhorst and E. Schmid: Plastic Elongation of Alpha Iron Crystals. *Ztsch. Phys.* (1932) **78**, 383.
21. G. I. Taylor: Plastic Strain in Metals. *Jnl.* Inst. Metals (1938) **62**, 307–324.

DISCUSSION

(Alden B. Greninger presiding)

N. P. Goss,* Youngstown, Ohio.—The authors state that four changes may take place when a metal is plastically deformed, and they feel that two other factors must be added in order to have a more complete picture of plastic deformation; namely, (5) formation of deformation bands, (6) bending and rotations of these bands.

FIG. 16.—LOW-CARBON STEEL WIRE, 0.04 PER CENT CARBON. × 2000.
Descriptive legend at the foot of this page.

Fig. 16.—Annealed. Tensile strength, 42,000 lb. per sq. in. Grains differ in "fine structure," large one appearing granular, and some of surrounding grains "lamellar." Grains that have "lamellar" fine structure in the annealed condition will naturally appear banded when drawn through a die. This is obvious when the cold-drawn "fine-structure" structures are examined.

There are many kinds of "fine structures" in annealed metals, and these influence the deformed texture. It is therefore very important to know what the "fine structures" of the annealed grains look like, before the metal is deformed.

* Physicist, Cold Metal Process Co.

However, in the four changes that are presented as accepted by the authors, one is questionable; that is, bending of the lattice between slip planes when a metal is plastically deformed. Such a condition would mean that the lattice is elastically deformed, and the atom planes bent, warped, etc. If this were true, the X-ray patterns of elastically deformed lattices would show a shift in the spectral lines, or the $K\alpha$ and doublets would be diffused.

I have been able to show by experiment that in alpha iron, alpha iron carbon steels up to and including 0.90 per cent C, 18-8 and other low-alloy steels, cold-rolled as much as 90 per cent without intermediate heat-treatment, the $K\alpha$ lines could be sharply resolved, and no shift observed. This can be accomplished when the X-ray technique is improved so that a nearly parallel beam is realized. The exact conditions were given in a recent paper.[22] It should be pointed out that all other papers dealing with cold-rolled steels always stated that cold-working distorted the lattice because the X-ray diffraction patterns always had diffused $K\alpha$ doublets. The fault in many instances was in the X-ray technique.

Again, the appearance of radial asterism on X-ray diffraction patterns of slightly deformed metals can only be attributed to block displacement, but has also been interpreted to indicate warped or bent lattice planes by some authorities. I need not go into detail here for the mechanism of plastic deformation is adequately explained by Jeffries and Archer.[23] Elam,[24] for example, points out that the elongation of Laue spots was at one time considered to mean only the gradual distortion of the lattice involving alteration of the plane spacings. This theory was advanced by Czochralski, and has been shown by Nusbaum, Goss and others[25] to be an incorrect explanation.

FIG. 17.—LOW-CARBON STEEL WIRE, 0.04 PER CENT CARBON; 40 PER CENT REDUCTION IN AREA. × 2000.

However, even though it has been shown that radial asterism does not mean lattice distortion, several papers published by Dr. Barrett indicate that he still considers radial asterism to be associated with lattice distortion. He based it, however, on a peripheral widening of the Laue spot, which he considered to be a much more sensitive indicator. I would like to ask Dr. Barrett whether he still interprets the

[22] N. P. Goss: Study of the Lattice Distortion in Alpha Iron. Presented at A.I.M.E. Meeting, February 1939.

[63] Z. Jeffries and R. S. Archer: Science of Metals, chapters V and VI. McGraw-Hill Book Co.

[24] C. F. Elam: Distortion of Metal Crystals, 169. Oxford.

[25] C. Nusbaum and N. P. Goss: Grain Distortion in Metals during Heat Treatment. Preprint, Amer. Soc. Metals, Sixteenth Annual Convention, New York, October 1934.

peripheral broadening of Laue spots to mean lattice distortion or curved atomic planes, or if he now accepts the interpretation of Nusbaum, Goss and others.

In my opinion, before adding further speculative ideas to explain the mechanism of plastic deformation, it would be better to settle certain of the controversial lattice-distortion theories; the X-ray experimental evidence considered to support this theory is based on faulty evidence, which started with the interpretation given by Czochralski.

The experimental evidence, which fails to support this theory, exists in abundance; for instance:

1. The compressibility of the annealed and cold-worked metal are the same.

2. The heat content of a metal is slightly increased by cold-working. (If the lattice were dilated, a decrease in heat content would be acquired.)

3. Magnetostriction does not alter the permeability of silicon strip steel.

Bain and Jeffries[26] examined a plastically deformed crystal with the X-ray and found that it produced a mixed orientation. I cite this paper to show that it has been known a long time that cold-working produces a mixed orientation of the "fine structure."

A series of "fine structure" photomicrographs are presented in Figs. 16, 17 and 18, to show that cold-working merely fragments and reorientates the "blocks" of the fine structure, but no evidence of banding can be seen. The grains of Fig. 16 have become elongated and one can see that the fine structure has been distorted and the blocks tend to lie in a common direction because they have become oriented in a definite direction with respect to the direction of working.

The identity of each grain has been preserved and the grain boundary is still sharply defined. There is no evidence of banding as advocated by the authors. Of course, the fine structure cannot be observed at the low magnification used by the authors. The preparation of their specimens was not clearly stated. To show fine structure, the specimens must be carefully polished and etched.

The fine structure of the grains cannot be fragmented without limit, which is confirmed by the fine-structure photomicrograph of Fig. 19 and also by the X-ray reflection diagram of Fig. 20. The grains still retain their identity even after a reduction of 99.8 per cent. Each grain appears as a so-called band. Because of the drastic cold-working, however, the structure inside each grain is not banded, but the fine structure is strongly fibered. It can also be observed that the fine structure consists of a number of small "discrete blocks," which appear to be "lined up" in the direction of working. To interpret completely all that is shown in this fine-structure pattern would be a long story. However, it does seem to substantiate the X-ray data that the blocks cannot be made smaller than about 10^{-5} cm.

The authors also say that only one orientation texture is developed; i.e., the [110] direction of the grain fragments tends to coincide with the axis of the wire, and that no other textures are present. I have made hundreds of Laue diagrams of cold-drawn iron and commercial steel wires, and found several textures present. The [211] direction along the wire axis was prominent even in wires drafted from 10 to 99.9 per cent. However, the [110] fibering is by far the most prominent.

It is true that homogeneous deformation is an essential assumption from a theoretical point of view. Such an assumption must be made if the subject is to be developed mathematically, and requires all lines that were linear before deformation to remain after the deformation. This makes it easy to apply tensor analysis or the dyad of Gibbs. However, this does not mean that the degree of deformation does not vary from point to point in a deformed single crystal or crystal aggregate.

---

[26] *Chem. and Met. Eng.* (1921) **25**, 775–777.
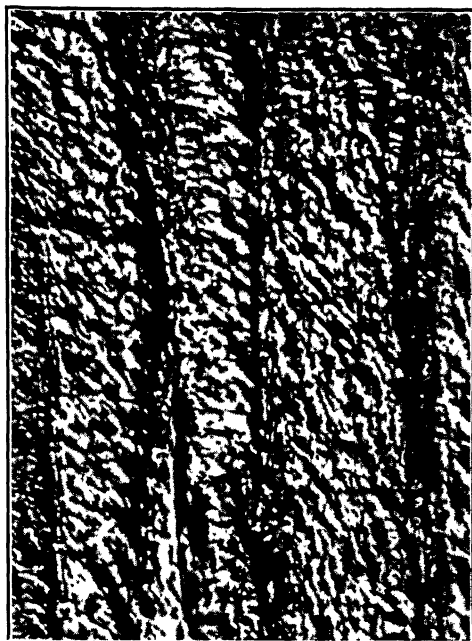
FIG. 18.—LOW-CARBON STEEL WIRE, 0.04 PER CENT CARBON, 80 PER CENT REDUCTION IN AREA. × 2000.
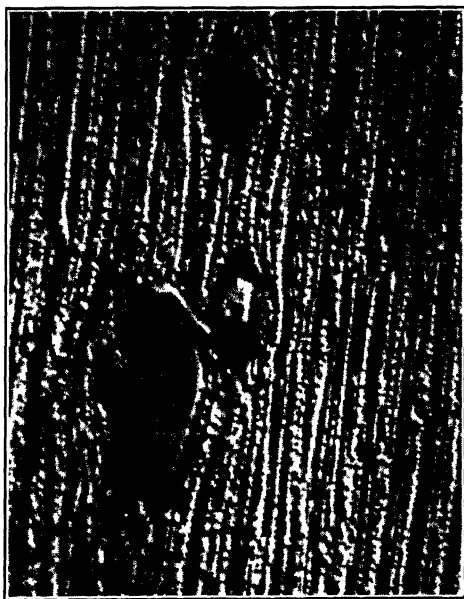
FIG. 19.—LOW-CARBON STEEL WIRE, 0.04 PER CENT CARBON, 99.8 PER CENT REDUCTION IN AREA. TENSILE STRENGTH, 194,000 LB. PER SQ. IN. × 2000.
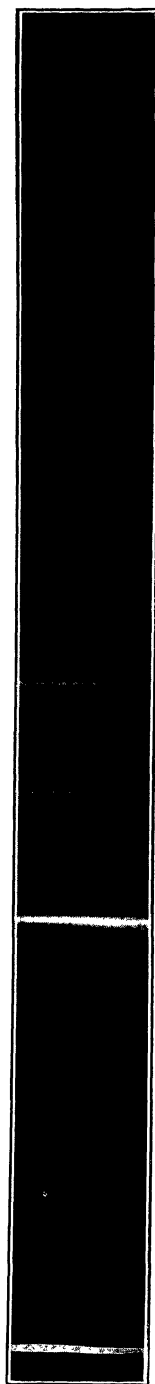
FIG. 20.—ARMCO INGOT IRON, 0.02 PER CENT CARBON. Reflection diagram. No radiation. Zirconic filter 0.010 in. thick. X-ray beam defined by two slits 0.015 by 0.375 in. spaced 3.5 in. apart. Angle of incidence on specimen 25°. All of the $K\alpha$ doublets of first order lines are resolved (the sharpness is only a function of beam sharpness). Cold-rolled from 0.079 to 0.019 in. Cold-working has fragmented the grains into smaller units, but not without limit. The crystal fragments are not smaller than 10^{-5} cm. The cold-working has created more internal surface, and therefore more "free space" around each crystal fragment, causing a slight decrease in density. The lattice is not distorted.

In a polycrystalline metal it is more difficult to realize uniform homogeneous plastic deformation because of: (1) grain-size variation, (2) difference in orientation of the grains, (3) variation in chemical composition from grain to grain, (4) variation in the "fine structure" of the grains.

The authors say: "the distortion of a grain proceeds by reorienting of the parts with respect to each other by bending or perhaps by fragmenting." It is difficult to understand what they have in mind; i.e., how can reorientation of the parts take place by a bending mechanism? The grain would first of all have to be fragmented, and then these fragments would gradually be oriented. I should like to have the authors state more clearly what they mean by "bending" and the reorienting mechanism in general.

Cold-working breaks up the grains into smaller units, creating new orientations, thus creating more internal surface and more "free space," which explains the slight decrease in density of cold-worked metals.

I should like to have the authors present X-ray diagrams to prove that the lattice is bent between slip planes. The X-ray technique must be given so that the experimental conditions may be known. Also to have them present "fine-structure" photomicrographs, to show the structure of the iron they used in the annealed condition. Samples representative of those used in this investigation would be suitable.

M. H. PAKKALA,[*] Kearny, N. J.—The authors say that the deformation bands form at low reductions and eventually lie parallel to the axis of extension. They imply that these bands, formed at low reductions, remain perfectly intact (apart from slight bending and twisting) up to 90 to 98 per cent reductions. This does not appear very clear in view of the possible number of other crystallographic planes that may be introduced into the process, unless the whole mass that is crossed by deformation bands rotates as a whole.

I should be interested to know whether the authors have studied the recrystallized grains that grow from an aggregate of deformation bands or elongated crystal grains. The excellent photomacrographs exhibited by Dr. Sachs[27] in an article on

* Research Laboratory, U. S. Steel Corporation.
[27] G. Sachs and R. Karnop: Zur Kinetik der Rekristallisation. *Mitt.* deut. Mat. prüfgsamt. (1930) **13**, 86–92.

recrystallization in single crystals, which had been given various percentages of extension, show that such a study would not be too difficult; and, indeed, Sachs did determine the various orientations but he was studying the effect of alloying elements and impurities on the recrystallization of aluminum. I have observed under a microscope a considerable number of partial and fully recrystallized textures of low-carbon steels, but one does not always have the X-ray facilities in a steel mill for making orientation studies of these textures. However, I did note that, where the original crystalline structure was not completely obliterated by cold-rolling or drawing. the growth of recrystallized grains began at the old grain boundaries and not in any possible deformation band within a grain. This observation may or may not be related to the present subject of discussion, but I should like to know whether the authors did any work along this angle or whether they intend to do so.

G. SACHS,* Cleveland, Ohio.—I wish to congratulate Dr. Barrett and his co-workers for their interesting discovery, which changes the picture we have today on the deformation of crystals. I have, however, a few questions about points that are not yet quite clear to me.

It has always been assumed that a crystal that is forced to a given shape will glide on more than one gliding system, several systems being always sufficient to produce any desired shape. Dr. Barrett's work shows that the process is rather a different one, the crystal being split up into a number of parts, each of which deforms in a different way. The changes of orientation have been followed up by Dr. Barrett, but there is nothing said about whether, judging from these changes, only a single gliding system operates in each of these crystal fragments, or several. Furthermore, it is only natural that a single crystal in such complicated operations as drawing, swaging or rolling must be split into a number of fragments to produce a preferred orientation that is as manifold as that of a polycrystalline material, and, as has been observed before, exactly the same.[28]

But it is not quite clear whether an undisturbed single crystal would have a tendency to do so in a tensile test, especially in its parts, which are quite free from any disturbance by the fillets, etc. The parts of this paper that deal with such a process do not state clearly whether the formation of bands is caused by such irregular disturbances or is actually a process that is invariable connected with any deformation of crystals.

Dr. Barrett also gives some figures that indicate the relative orientation of the fragments after different amounts of deformation. He says that in all cases the crystals move in such a way that a (110) line approaches the axis of the test rod. I should be very much interested to learn which way an originally identical direction perpendicular to this one moves, giving as far as I understand a steadily increasing scattering, approaching a fiber structure with eventually an orientation of this direction at random. How large is this scattering after different deformations?

C. S. BARRETT AND L. H. LEVENSON (authors' reply).—The principal points of Mr. Goss' discussion may be summarized as follows:

1. Iron shows a "fine structure" when polished, etched, and viewed microscopically. The "fine structure" differs from grain to grain (Fig. 16), and is altered by deformation (Figs. 17, 18, 19) into a "mixed orientation" noted by Bain and Jeffries. The appearance of the initial "fine structure" is important, for it influences the deformation texture. Mr. Goss offers Figs. 17, 18 and 19 to disprove our conclusion that bands form in grains of cold-drawn wire.

---

* Assistant Professor of Metallurgy, Case School of Applied Science.

[28] G. Sachs and E. Schiebold: *Naturwiss.* (1925) **113**, 964–968.

2. The fiber texture of iron wire includes some [211] in addition to the main orientation, [110].

3. Cold-rolling does not introduce elastic distortion in steel, because Goss and Nusbaum have been able to resolve the $K\alpha$ doublets of molybdenum diffracted by cold-rolled steel (Fig. 20). What part does lattice bending play in reorientation, in radial asterism, and in peripheral widening?

We will reply to these points in order.

1. The "fine structure" that is seen under the microscope on a polished and etched surface is merely the appearance produced by the etch pits so familiar to metallographers, and first observed, according to Desch, in 1816. Under suitable conditions the pits are bounded by crystallographic planes of low indices but more often the bounding planes deviate somewhat from crystallographic planes. The appearance of the etched surface differs from grain to grain because the orientations of the grains—and consequently the etch pits—differ from grain to grain; it is altered by deformation because the orientations of the grains are altered. Fragmentation of grains is revealed by suitable etching (Figs. 3, 4, 5, 7, 10, 11 and 12), but is sometimes obscured by unsuitable etching, as was pointed out by Bain and Jeffries in 1921, and as appears to be true of some of Mr. Goss's photomicrographs. The "fibers" of Mr. Goss's Fig. 19 probably consist of bands as well as individual grains, but these are indistinguishable in the print; a suggestion of bands is seen in Fig. 17. Since the behavior of a grain is conditioned by its initial orientation with respect to the axes of strain, it follows that the appearance of the etched surface is related to its behavior during deformation, but the way to an understanding of the relationship is not, as Mr. Goss suggests, through qualitative studies of the surface roughed by etching, but by a study of the underlying orientation relationships. The orientations may be determined, as has been done in this paper and others of this series, by reflecting light from suitably developed etch pits or by X-ray diffraction.

2. The [211] texture Mr. Goss believes he has seen in "hundreds of Laue diagrams" is not present in our samples. Very sensitive tests for this texture may be made by placing the wire at an angle of 73° to a beam of molybdenum X-rays, or at 40° to a beam of cobalt X-rays. Both of these tests were made on wires that had been drawn to a reduction in diameter of 90 per cent and deeply etched. No trace of a [211] texture was found; all spots confirmed the [110] texture. Strong (220) reflections were observed in the molybdenum pattern, however, that suggest an explanation of Mr. Goss's conclusion. The (220) $K\beta_1$ reflection of molybdenum from alpha iron occurs at a reflecting angle of 18.1° and therefore produces a spot very near the place Mr. Goss was expecting to find a (211) $K\alpha$ reflection from a [211] texture, which has a reflecting angle of 17.6°. We therefore believe he disregarded the presence of molybdenum $K\beta_1$ radiation in his X-ray beam, assigned incorrect indices to his spots, ignored the fact that other spots did not confirm the [211] texture, failed to check his results with X-rays of other wave lengths, and thus arrived at an incorrect interpretation of the fiber texture. It is also possible that he did not etch away the surface layers, where orientations are usually not as "ideal" as at the center of the wire.

3. Mr. Goss doubts that cold-work widens diffraction lines, but offers no evidence to the contrary. He has not submitted a photogram of annealed steel made with experimental conditions identical with those of Fig. 5, to which the latter can be compared, so it is impossible to judge the amount of line widening. It is incorrect, of course, to assume that the doublet resolution will be destroyed by a small amount of widening.

That cold-work widens diffraction lines has been established by so many well-known experiments by leading investigators throughout the world, there seems little need for listing here the many reports in the literature confirming this.

Elastic strain is not held to be the only factor in reorienting the grain fragments during cold-work, or in causing either asterism or peripheral widening in Laue patterns of cold-worked metals; plastic strain is always an important factor. In some nine papers by one of the present authors in which elastic and plastic strain were under discussion in connection with grain reorientation or the spreading of Laue spots, the stand has never been taken that elastic strain is the only mechanism; if a contrary impression has been received from these it has been through misunderstanding.

Mr. Pakkala's pertinent discussion raises the question of whether the bands remain intact throughout the deformation. Without any extensive tests of the point, we are convinced that bands, once they are formed, never redissolve. This follows from the fact that the boundary of a band is equivalent to a grain boundary in that it separates two regions of differing orientation. The authors are developing the technique of determining the orientation differences between bands more accurately, and are reporting some results on bands in aluminum.[29] While it seems clear that the boundaries cannot redissolve, it is not equally certain that the identity of a given band can be retained throughout an indefinite amount of cold-work, for bands that form later may grow within it or possibly cut across it.

We do not see any difficulty in visualizing the rotation of the bands toward positions more nearly parallel to the wire axis. Consider the pattern made on the ends and on the cylindrical surface of the wire by bands that intersect these surfaces. If deformation continues, it seems obvious that these patterns on the surfaces will remain geometrically similar except for a uniform reduction in diameter and increase in length (assuming for the moment no curving or growth of the bands). This will bring the planes of the bands more nearly parallel to the axis of extension. The deformation of the lattice within the bands occurs by crystallographic slip on many sets of slip systems; at any one instant and in any one small region of the band the number of slip systems operating is presumably five,[21] but the five that are active must change with deformation and with location. A further discussion of the heterogeneous nature of the flow will be found in the succeeding paper of this series.[29]

It seems highly probable that the orientations of recrystallized grains are related to the orientations of the deformed material in which they appear, and thus are influenced by the presence of deformation bands. Pfeil noted that recrystallized grains can form along deformation bands, and in this laboratory a swaged iron-silicon alloy (1.95 per cent Si) that had been partially recrystallized was observed to have small recrystallized grains located in a string along curved deformation bands. We are now attempting to correlate deformation and recrystallization orientations; in fact, this idea was back of the whole series of investigations of deformation structures.

In reply to Dr. Sachs' question as to whether one or several slip systems operate within a single deformation band, we would state that the observed lattice rotations within the bands require more than one slip system. This question has been discussed in a previous paper by one of the authors[1] and also by G. I. Taylor,[21] who points out that five systems are necessary for producing an arbitrary homogeneous strain with minimum work. The sets of slip systems active in neighboring bands must of course be different, since their lattices rotate in different directions from a common initial orientation.

Dr. Sachs states that it is only natural that a single crystal must divide into a number of fragments to produce the same preferred orientation as that of polycrystalline material and that this has been observed before. Sachs and Schiebold, indeed, found in 1925 that a drawn single crystal of aluminum gave an X-ray pattern similar to that of drawn polycrystalline aluminum. However, we have found that this is by

no means true in general. We find that compressed single crystals of both iron[1] and aluminum[29] have only very limited azimuthal positions in the final texture, and that rolled single crystals of iron show only a portion of the polycrystalline texture. The complete polycrystalline texture observed in a single grain or crystal of drawn iron is probably caused by the extreme curvature of the bands at high deformation. We find, furthermore, that the fragmentation is not irregular, but consists of deformation bands bounded by crystallographic planes—at least under reasonably favorable conditions of strain.

The question is raised by Dr. Sachs as to whether deformation bands are caused by "disturbances" or are invariably formed. We have always found certain orientations that do not produce bands with the deformations we have studied, but whether the other orientations lead to banding as a result of disturbances or as a result of a fundamental property of a perfect lattice subjected to perfectly homogeneous strain is a matter of opinion. The fact that bands form on crystallographic planes suggests that they are a fundamental mechanism in deformation, and this is also suggested by the fact that they have been observed in aluminum even when extreme care has been used to insure homogeneous deformation.[29,30,31]

In answer to Dr. Sachs' last question, the spread in an azimuthal direction, around the wire axis, increases continuously with deformation until a complete fiber texture is reached. This spread varies with the initial orientation, and with the method of producing the elongation, but is roughly $\pm 20°$ at about 80 per cent reduction in area, and is always much greater than the spread about any axis normal to the wire axis. Referring to the single crystals whose orientations are plotted in Fig. 1, the following had a spread in azimuth of 15° to 25° each way from the mean orientation (estimated from transmission photograms): No. 13 at 74 per cent reduction, No. 14 at 68 per cent, No. 15 at 75 per cent, No. 16 at 84 per cent and 90 per cent, No. 17 at 90 per cent, No. 18 at 74 per cent. Those having less than this were No. 13 at 36 per cent with about $\pm 10°$ spread, No. 14 at 45 per cent with $\pm 5°$ spread, and No. 17 at 80 per cent with $\pm 5°$ spread. Crystal No. 15 at 80 per cent had the large spread indicated by the rings in Fig. 2. It was noted that, without exception, the spread in the angle between a [110] direction and the wire axis was always much less than the spread in azimuth and was only about $\pm 4°$ in most of the cases.

[30] C. F. Elam: An Investigation of Some Banded Structures in Metal Crystals. *Proc.* Roy. Soc. (1928) **121-A**, 237.

[31] G. I. Taylor and W. S. Farren: The Distortion of Crystals of Aluminum under Compression. *Proc.* Roy. Soc. (1926) **111-A**, 529.

.

Magnetic Torque Studies of the Texture of Cold-rolled and of Recrystallized Iron-silicon Alloys

By Leo P. Tarasov,* Junior Member A.I.M.E.

Magnetic torque studies of ferromagnetic single crystals have been carried out in a number of laboratories during the last decade[1,2] and some work has been reported on polycrystalline material showing preferred orientation. Goss[3] used the method extensively in developing electrical sheet with desirable magnetic properties, but he used it as a control rather than as a means of studying the texture. Bozorth[4] made a quantitative correlation of a torque curve he obtained from some cold-rolled iron with the texture as determined from X-rays, but did not extend his studies beyond the one specimen. Other studies, which have been reported from time to time[2,5] have also been incomplete in the sense that no effort was made to study a whole series of samples, differing only in degree of cold reduction or in the annealing temperature, in order to ascertain the effect of such treatments on the texture as revealed by torque measurements. It is the purpose of this investigation to make such a study, mainly in order to see how useful the method can be made when used under favorable circumstances and to find what kind of a correlation can be expected between magnetic and X-ray studies of texture. Before proceeding further, it is desirable to say a little about single crystals, so as to make clear the concepts involved in magnetic torque measurements.

Magnetic Torque Method

It is fairly well known nowadays that single crystals of ferromagnetic substances have directions of easy magnetization and of hard magnetization. In Fig. 1 are reproduced typical magnetization curves for a single crystal of iron, which show that in a $<100>$ direction saturation occurs at low fields compared to those required to saturate the same crystal in a $<110>$ or a $<111>$ direction. (The magnetization intensity I is defined by the equation $B = H + 4\pi I$.) At fields high enough to

cause saturation in all three directions, it would seem from these curves that we should not be able to detect any difference in magnetic properties between various directions in a crystal, but it is actually found that no matter how high the magnetizing field may be the intensity of magnetization still varies with direction.   What really happens is that the direction of I_s, the saturation intensity, coincides with the direction of the applied field H only if the latter is along a direction of easy or of hard magnetization.   In all other cases, I_s deviates a little from H, the angle of deviation depending on the orientation of H with respect to the crystal axes.
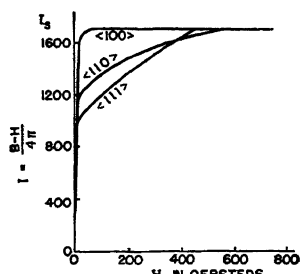
The effect of this deviation can best be understood in a specific example, say a single crystal of iron cut into a circular disk whose plane is (1$\bar{1}$0).   This disk thus contains the [001], [110] and [111] directions, the first two being directions of easy magnetization and the last of hardest magnetization.   If this disk is held in a strong and uniform magnetic field so that it can rotate around its axis, and if the field is always parallel to the plane of the disk, the field will tend to rotate the disk so as to bring one of the "easy" axes just mentioned parallel to the field.   The reason for this is that the energy of the single crystal in the magnetic field is a minimum in these directions, as can be shown mathematically, and the disk tries to get into a condition of minimum energy.   This is shown
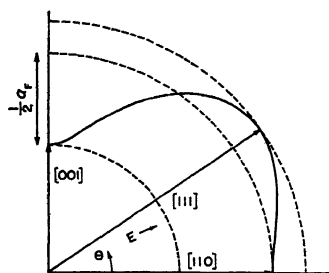
FIG. 2.   FIG. 3.

FIG. 2.—MAGNETIC ENERGY AS A FUNCTION OF ANGLE IN (1$\bar{1}$0) PLANE OF IRON.
FIG. 3.—TORQUE CURVE FOR (1$\bar{1}$0) PLANE.
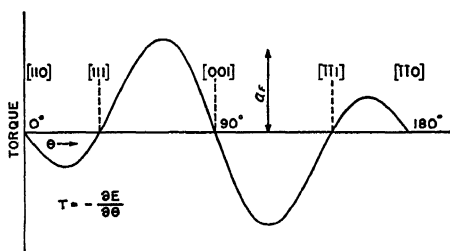
graphically in Fig. 2, where the energy is plotted against direction, using polar coordinates.   The plane of the disk, which is (1$\bar{1}$0), lies in the plane of the paper.   An external mechanical torque can be applied to the disk so as to prevent this rotation, and a plot of the magnetic torque for various positions of the disk in question is found to give the curve shown in Fig. 3, where θ is the angle in the plane of the disk between H and [110].

If the torque per unit volume is denoted by T and the energy per unit volume by E, the relation between them is given, as usual, by $T = -\dfrac{\partial E}{\partial \theta}$ and Figs. 2 and 3 show roughly why the torque curve is alternately positive and negative. I_s coincides with H not only in the [110] and [001] directions but also in the [111] direction, and in all these cases the torque acting on the specimen is zero. There is, however, a noticeable difference between the first two directions and the last one, in that the last is very unstable, corresponding to an energy maximum. Experimentally, this means that although no torque will be experienced by a disk when the field is in a [111] direction, any slight disturbance will cause the disk to move away from this position, whereas for the other types of directions the disk will be restored to the original position. These positions are easily distinguishable experimentally and thus furnish a convenient means of determining the correct sign to be given to the torque, which should be such that the torque curve has a negative slope when passing through a stable zero of torque.*

All that has been said applies with suitable modifications to a single crystal disk whose plane has any other orientation with respect to the cubic axes. Tarasov and Bitter[6] have developed torque equations for the general case. It is there shown that

$$T/a_F = A_1 \sin 2\theta + A_2 \sin 4\theta + B_1 \cos 2\theta + B_2 \cos 4\theta \qquad [1]$$

where a_F is the anisotropy constant† expressed in ergs per cubic centimeter and A and B are numerical coefficients whose magnitudes depend solely on the orientation of the plane of the disk with respect to the cubic axes. The anisotropy constant, which is a direct measure of the difference between the energies of magnetization in the directions of easy and of hard magnetization, can be obtained either from magnetization curves of a single crystal[4] or from its torque curve.[6] The foregoing applies only to the case in which there is just *one* anisotropy constant, which is positive, as is practically true in regard to iron, steel, and iron-silicon; for a discussion of what happens when this condition is not fulfilled, we refer the reader to Bozorth's article.[4]

Of the two types of instruments used in measuring magnetic torque, the more usual is a torsion instrument[1] in which the restoring torque is obtained by twisting the wire attached to a chuck holding the disk. The axis of the disk is along the wire. The other method, used in the

---

* It should be noted that the opposite convention is used in the papers by Akulov and Brüchatov and by Sixtus; the one recommended here, used by Bozorth and his collaborators and by Bitter, seems more desirable because it conforms to the usual definition of torque as the *negative* derivative of the energy with respect to angle.

† The anisotropy constant is defined by $E = 2a_F(\alpha_1{}^2\alpha_2{}^2 + \alpha_2{}^2\alpha_3{}^2 + \alpha_3{}^2\alpha_1{}^2)$ where the α's are the direction cosines of the direction of magnetization with respect to the cubic axes. Others have used an anisotropy constant K_1 which is $2a_F$.

present investigation, involves the use of an analytical balance with the chuck so fixed to the center of the balance arm that the axis of the disk passes along the knife edge.[6] The restoring torque is then due to the weights which bring the balance to equilibrium.* A field of about 2500 oersteds is desirable so as to avoid certain distortions of the torque curve that occur at lower fields.

TORQUE METHOD APPLIED TO POLYCRYSTALLINE MATERIAL
Texture and Torque Curves

Work in recent years with X-rays,[7] magnetic torque measurements[1-5] and optical reflection[2] has shown that preferred orientation occurs in cold-rolled and hot-rolled steel, both before and after annealing treatments. The results have been expressed either in terms of ideal orientations with deviations therefrom or by pole figures.[8]

It is evident that with a perfectly random distribution of grain orientations the magnetic torques of the individual grains must cancel completely. At the other extreme, when all the grains are lined up in much the same way, the torque curve must approach that of the corresponding single crystal. Such cases are rarely met with in practice. Ordinarily we find that rolled steel, whether it is in the deformed or in the recrystallized state, has a magnetic torque curve with an amplitude ranging roughly from one-fourth to one-half that of a single crystal whose orientation is similar to the preferred orientation of the strip. It is possible to use special deformation and heat-treating schedules to produce strip with a torque curve having an amplitude much closer to that of a single crystal,[3] but these highly developed textures will not be considered here because this work was purposely limited to studying the effect of *simple* heat-treatments on the torque curves and the texture.

A perfectly random orientation is not the only texture that can give zero torque for all angles in the disk, since it can be shown that in iron and steel a texture for which a {111} plane is always in the rolling plane would give the same result.† This is true also of any texture that is perfectly random around the normal to the rolling plane; the zero torque which is always observed in such a case is simply due to the symmetrical arrangement of the particles around the axis of the disk. A quite arbitrary texture composed of two preferred orientations, both with {100} in the rolling plane but with the cube edge of one along the face diagonal of the other, also shows no torque in any position. This last is so arbitrary that it is not likely to occur, but the others probably

---

* From the author's experience with both types of apparatus, the torsion type is to be preferred on the grounds of both speed and accuracy.

† This statement is true only if the equation in the second footnote of page 355 is valid. Sometimes an additional, usually unimportant, term is added to this equation and in that case the torque in a {111} plane is not always zero.

do and yet their presence cannot be detected by the torque method. The possibility of preferred orientations that do not give rise to any torque curve should always be kept in mind.

The results shown in the experimental torque curves are only fairly reproducible when made on 1-in. disks punched from various parts of the same lot of material but the discrepancies are never serious and are merely indicative of the variation of texture as between the different parts. If a given lot of material is to be so heat-treated that only slight changes in the torque are expected, it is preferable to make measurements on the same disk before and after the treatment; otherwise the change may be masked by the spread between samples. With this precaution slight changes in the torque curve are easily detectable.

Most of the torque curves made for both the deformation and the recrystallization textures reveal at least a slight asymmetry; in other words, the cosine terms in the torque equation are not quite zero, as they would be if the planes normal to the disk and containing either the rolling or the cross direction were planes of symmetry, as is assumed in the ideal case. Although this asymmetry is normally not serious, it is generally better to take measurements throughout 180° instead of half that range. The reasons for the existence of this asymmetry are unknown at present and not much can be done about it except to neglect it.

Unlike most other magnetic phenomena, torque is not strain-sensitive, at least as a first approximation. Little is known about the nature of the effect of strains upon the torque curves but the effect, when present, is small enough to be neglected in this type of investigation. Roughly speaking, it can be said that a tension strain contributes a term to the torque equation proportional to the strain and a compression strain of the same magnitude contributes the same term but with its sign changed. To the extent that the tension and compression strains balance each other, their contributions to the torque will cancel. Later we shall see that strains can affect the torque curve to a slight extent but not nearly enough to invalidate any texture study.

Method of Expressing Torque Data

The expression of torque data in terms of arbitrary units, such as milligrams or divisions, or of absolute units, such as ergs per cubic centimeter, is not very useful in the study of texture because nothing is said about how the amplitude of the curve compares with that for a suitable single crystal. This information can be included easily by expressing the torque, hence the coefficients of the sine and cosine terms, on a relative basis such that a single crystal with {100} in the plane of the disk would give a curve with unit amplitude. The equation for such a single-crystal disk is simply $T/a_F = -\sin 4\theta$, which means that in 180° there

will be two positive peaks and two negative peaks, all of unit amplitude. Instead of unit amplitude, it may often be convenient to express results in percentages, the {100} single crystal giving an amplitude of 100 per cent. This is the same as setting a_F equal to 100 per cent instead of equal to some definite energy per unit volume. Such a procedure requires a knowledge of a_F which is unfortunately lacking at the present time. The author has recently found that a_F varies more or less linearly · with silicon content from about 2.4×10^5 ergs per cu. cm. for pure iron to about 0.9×10^5 ergs per cu. cm. for iron with 7 per cent Si. The effects of all other elements (except nickel and cobalt) are completely unknown. But even a rough knowledge of a_F is useful in comparing specimens of the same chemical composition. For instance, a 10 per cent error in a_F will cause a corresponding error in the scale of the torque curve, but it will be of no great importance that a texture that was thought to give torque peaks 40 per cent of the possible maximum should have actually given peaks only 36 per cent of that value. In the present work, a_F was somewhat arbitrarily set at 1.57×10^5 ergs per cu. cm. for the strip containing 3 per cent Si.
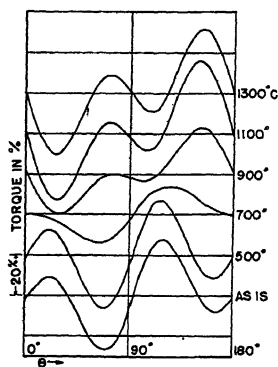
FIG. 4.—TYPICAL TORQUE CURVES FOR POLYCRYSTALLINE MATERIAL.
The curves are for specimens that had been cold-rolled 40 per cent (H2) and annealed for one hour at the temperatures indicated.

Although it is possible to describe torque curves in terms of their peaks, this method is unsatisfactory in dealing with any texture giving a transitional type of torque curve, as shown in the third curve from the bottom in Fig. 4. The coefficients A_1 and A_2 of the sine terms of the torque equation are far more useful because they specify unambiguously both the size and the type of the torque curve. The asymmetry of the curves, which was mentioned previously, is due to the coefficients B_1 and B_2, especially the former. This information was obtained with the help of a number of complete harmonic analyses of typical torque curves, and it was found that both cosine terms could be dropped legitimately, since they were small compared to the sine terms.

On the basis of these harmonic analyses, it was decided that measurement of torque at four suitably chosen points would suffice to determine A_1 and A_2. Let us assume that the torque equation is in the complete form $T = A_1 \sin 2\theta + A_2 \sin 4\theta + B_1 \cos 2\theta + B_2 \cos 4\theta$, where the torque and the coefficients are in the same units. Setting the zero for θ so that the zero torque near the cross direction falls at $\theta = 90°$, we can measure T_1 at $+67\frac{1}{2}°$, T_2 at $+22\frac{1}{2}°$, T_3 at $-22\frac{1}{2}°$, and T_4 at $-67\frac{1}{2}°$. Then it is easy to show that

$$A_1 = \frac{(T_2 - T_3) - (T_4 - T_1)}{\sqrt{8}} \qquad [2]$$

and

$$A_2 = \frac{(T_2 - T_3) + (T_4 - T_1)}{4}$$

Measurements at these four angles give a sufficiently accurate knowledge of the torque curve for all work with polycrystalline material.

COLD-ROLLING TEXTURES

Material

The greatest part of the work reported here was performed upon an alloy of iron containing 3 per cent silicon. The reasons for choosing this composition were its availability in suitable form, its commercial usefulness, and the absence of a gamma phase, which is present if the silicon content is below 2 per cent and which would interfere with the study of the recrystallization texture. This material,* labeled series H, contained 2.98 per cent Si, 0.071 per cent C and 0.18 per cent Mn. The reductions are shown in Table 1, where the last column gives the ratio of the initial to the final thickness during the cold-rolling process.

TABLE 1.—*Reductions in Thickness*

Specimen	Final Thickness, Mils		Percentage Cold-rolled	t_0/t_1
	Hot-rolled	Cold-rolled		
H1	25	20	20	1.25
H2	33	20	40	1.65
H3	50	20	60	2.5
H4	100	20	80	5.0
H5	50	10	80	5.0
H6	100	10	90	10.0
H7	20	(20)	0	1.00
H8	22	20	10	1.10
H9	20	(20)	0	1.00
H10	22	20	10	1.10
H11	25	20	20	1.25
H12	100	5	95	20.0
H13	100	8	92	12.5
H14	100	6	94	16.7
H15	100	4	96	25.0
H16	100	3	97	33.3

* This strip was obtained in various stages of deformation from the Research Laboratory of the General Electric Company, and a considerable number of the heat-treatments described later were carried out at the same place through the kindness of Mr. W. E. Ruder.

After being hot-rolled at a temperature somewhere in the neighborhood of 850° C., lots H1 through H6 were normalized at 870° C., pickled, and then cold-rolled on a four-high Steckel mill with working rolls of 2-in. diameter. H7 through H11 were hot-rolled from $\frac{1}{2}$ by 2 by 30-in. bars of the same material. H7 and H8 were hot-rolled at 900° C., while the others were hot-rolled at 950° to 975° C. The lots that were to be cold-rolled were normalized at 900° C., pickled, and then cold-rolled on a four-high mill with 2¾-in. diameter working rolls. H12 through H16 were cold-rolled on the same rolls, starting from strips about 1 by 11 in. cut from H6.

Because the recrystallization texture of series H could not be easily reconciled with the pole figures published by Barrett, Ansel and Mehl,[7] Dr. Barrett kindly furnished a few of their specimens on which torque measurements were made. These were labeled series J. Samples JE and JB contained 2.07 per cent Si while JD contained 4.61 per cent; the first had been cold-rolled 75 per cent, from 232 to 57 mils, and the other two had each been cold-rolled 94.5 per cent, from 250 to 14 mils. Further details are to be found in the original paper.

Torque Studies

All torque measurements were made on punched disks 1 in. in diameter. The method of representing results has already been described. Samples were run in duplicate until it was established that variations between samples of the same lot could be treated as negligible. The lowest curve of Fig. 4 is the one for the 40 per cent cold-rolled material in its deformed state; the other curves are for annealed samples of the same lot and will be discussed later. It was observed that as the degree of deformation was increased to 80 per cent the larger peaks grew in size and at the same time the difference between them and the lesser peaks diminished. (We are considering here only the cold-rolling textures.) Beyond 80 per cent cold reduction, the peaks continued to grow larger but the *difference* between the larger and the smaller peaks began to increase. Restated in terms of A_1 and A_2, these changes are shown in Fig. 5, which summarizes all the torque data for the specimens in their cold-rolled condition. The specimens have been divided into several groups, based on their final thickness, and are distinguished by symbols. Although a smooth curve is drawn through the points for the series H disks, it is possible that a family of such curves should be drawn, one for each final thickness. Lack of suitable material prevented an investigation of this point.

The common method of plotting some quantity against the percentage of reduction in thickness was not used because this meant unjustifiable crowding of points at the high reductions. The much more logical procedure was used of plotting A_1 and A_2 against log (t_0/t_1), where t_0

and t_1 are the initial and final thicknesses, respectively. In this way
we do not lose sight of the fact that as much may happen to the metal
in being rolled to half its thickness, whether this be a reduction of 50
per cent starting from the original thickness, or a change of reduction
from 90 to 95 per cent, also based on the original thickness. The fact
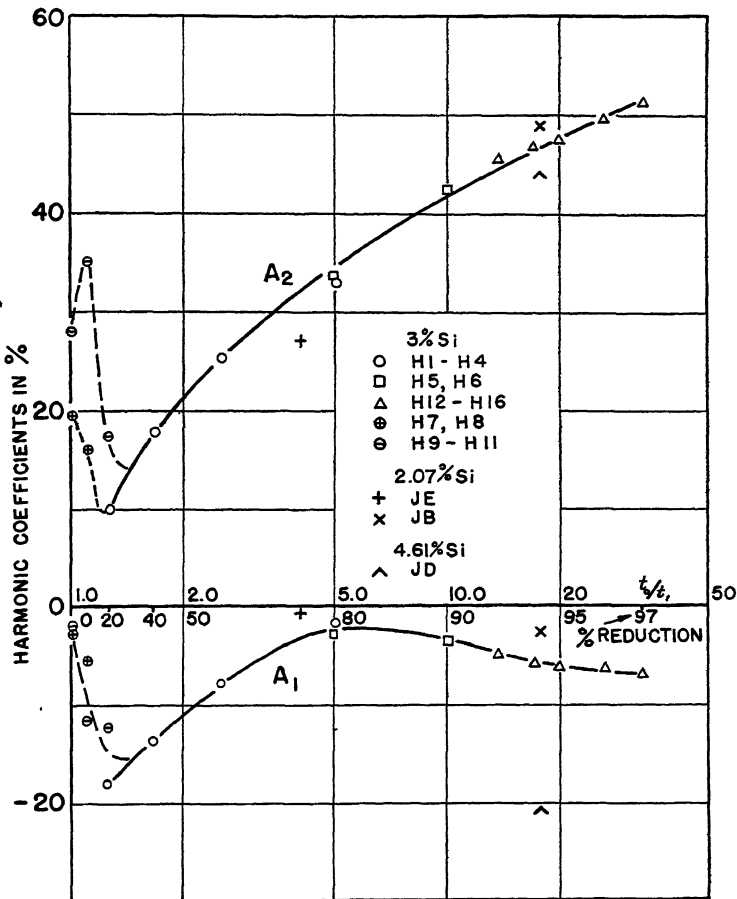
FIG. 5.—A_1 AND A_2 AS FUNCTIONS OF THE AMOUNT OF COLD-ROLLING.

that A_2 does vary almost linearly when plotted as just described shows
the correctness of this statement.

After the smooth solid curves of Fig. 5 were obtained, an extension
of the curve to reductions of less than 20 per cent looked very promising.
Some of the same material, which was still in bar form, was hot-rolled
at 900° C. to 22 mils and some to 20 mils. The former was then cold-
rolled down to 20 mils, so that zero and 10 per cent cold reductions
were available. The encircled crosses are nowhere near the solid curve
and the curve would have to undergo a very sudden and unexpected

change of slope in order to pass through these points.   A change in the hot-rolling temperature to 950° C. or so gave the encircled dashes, which are farther than ever from the solid curve.   These results show how sensitive is the texture of hot-rolled and of slightly cold-rolled material to slight changes in the hot-rolling technique.   No further studies were made along this line because the problem appeared too complicated for a brief investigation.   When more is known about the nature of recrystallization itself, as distinguished from recrystallization that accompanies hot deformation, a thorough study of hot-rolling should be of great interest.

X-Ray Studies of the Rolling Texture

Within the past few years several excellent papers have appeared[8] on the cold-rolling textures of iron, mild steel and iron-silicon alloys, all based on the pole-figure method originated by Wever.[9]   Wever was able to show that such a pattern could be explained fairly well by a combina-
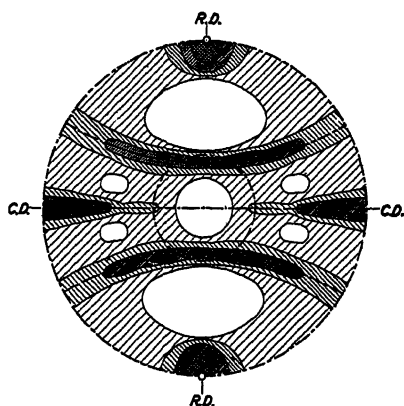
FIG. 6.—{110} POLE FIGURE FOR 4.6 PER CENT SILICON ALLOY COLD-ROLLED 95 PER CENT. SPECIMEN JD. (Barrett, Ansel and Mehl.[7])

tion of compression and limited tension textures, which were predicted on theoretical grounds for single crystals of body-centered metals by Boas and Schmid.[10]   The complete tension texture can be visualized best as the totality of all orientations obtained by placing a cube so that a cube face is in the rolling plane and the cube edges of this face are at 45° to the rolling and cross directions, and then rotating the cube freely about the rolling direction. As an alternative way of saying the same thing, let R and C be the rolling and cross directions and N the normal to the rolling plane; then this texture would be described as having (001) perpendicular to N with [110] parallel to R, the whole rotated freely around R.   The limited tension texture is the same except that the rotation around R is limited to 40° or 50° from the original position.   The compression texture is formed by freely rotating the cube around the body diagonal, which remains parallel to N; in other words, (111) is perpendicular to N.

At the present time work by Gough[11] and by Barrett, Ansel and Mehl[12] indicates that slip in iron and iron-silicon up to 4 per cent Si takes place not only along {110} planes but along {112} and {123} as well.   If the silicon content is greater than 4 per cent, slip is confined to the {110} planes.   It was because of this difference that Barrett, Ansel and Mehl[7] investigated by means of X-rays the deformation and recrystal-

lization textures of both 2.07 and 4.61 per cent Si alloys. Their pole figures show that, in spite of the possible difference in the slip mechanism, the textures for the 95 per cent cold reduction are very nearly the same, the main difference being that the scatter around R is 40° to 45° in each direction for the low-silicon alloy and 55° to 60° for the other. The high-silicon texture is shown in Fig. 6. In both cases, cold-rolling to increasing reductions in thickness does not decrease the scatter in orientation around R, but simply increases the fraction of crystals having the limited tension texture.

Correlation of Torque and X-Ray Studies

An idealized texture can usually be deduced from a pole figure, and this texture will be sufficiently good for calculating the torque curve corresponding to the pole figure. Such calculations, based on the pole figures published by Barrett, Ansel and Mehl, and on the torque equations given previously for single crystals of any orientation, are outlined elsewhere.[13] The calculated harmonic coefficients A_1 and A_2 can be expected to differ from the measured ones by a factor of two or so, since a pole figure does not indicate how much of the texture is completely random, or what is just as bad, distributed symmetrically around N. If the texture is composed half of the idealized one and half of the random one, obviously the measured coefficients will be only half as large as calculated on the basis of the idealized texture. But if it is found that the ratio of the measured coefficients to the calculated ones is not approximately the same for A_1 and A_2, some wrong assumption must have been made about the idealized texture, usually in the nature of an oversimplification. The results for the most interesting of the cold-rolled specimens are indicated graphically in Fig. 7.

FIG. 7.—COMPARISON OF CALCULATED AND MEASURED VALUES OF A_1 AND A_2 FOR SOME COLD-ROLLED SPECIMENS.

H6— 90% CR, 3% Si
JB— 95% CR, 2% Si
JD— 95% CR, 4.6% Si

The calculations are based on the limited tension texture described previously; and in order to take care of the random orientations, these values are arbitrarily divided by two. The calculations for H6 and for JB assume a scatter around the mean position of 45°, and for JD, of 55°, in accordance with the pole figures previously mentioned.[7]

The agreement in those for H6 and JB can be said to be perfect, but the large discrepancy in the calculated and measured values of A_1 for JD cannot be easily explained. It is impossible to state whether this difference is to be ascribed to a change in the slip mechanism associated with the change in the silicon content or to a variation in the cold-rolling procedure, because the low-silicon strip JB (and also all of series H) was

rolled at room temperature, while the high-silicon JD had to be rolled at 150° C. so as to avoid cracking on account of brittleness. The importance of these results lies in the fact that, whatever may be the reason for the change, the torque measurements here clearly indicate a difference in texture between two specimens that have been deformed the same amount and have practically the same pole figures.

We shall now see how this anomalous behavior can be explained by the fact that a pole figure cannot furnish us complete information about the distribution of the orientations of the particles that make up the polycrystalline material. In order to establish uniquely the orientation of a particle—that is, of its crystal axes—it is necessary to know only the orientations of two of the planes of this particle. This is a simple enough matter for a single crystal, but when the problem is to find the orientation distribution of a large number of particles from a knowledge of the orientation distribution of two sets of planes, we see that there is no unique way of pairing individual planes from the two sets.
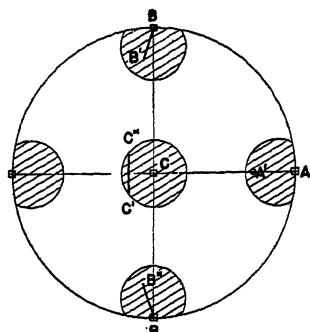
FIG. 8.—POLE FIGURE OF {100} PLANES OF AN ARTIFICIAL TEXTURE, SHOWING INDEFINITENESS OF PARTICLE ORIENTATIONS.

To make this clearer, there is shown in Fig. 8 the pole figure for the {100} planes of an artificial texture. If we first consider a single crystal of which two of the cube faces are at A and B, it is evident that the third cube face must be at C, 90° from both A and B. Let us now assume that we have a sharply defined texture as shown by the shaded regions. If we take some particle of which the cube face is at A', the only thing we know about one of its other cube faces is that it is somewhere on the line $B'BB''$, all points of which are 90° from A'. The central shaded region is of no help in determining the particle orientation, for all that we know about the third cube face is that it is 90° from A' and 90° from an unknown point on the line $B'BB''$—in other words, on the line $C'C''$.

When the texture is sharply defined, as in the artificial one of Fig. 8, the possible particle orientations are limited and there is no difficulty in stating with fair accuracy the distribution of particle orientations. But when there are several gradations of intensity in a pole figure, and these regions take up most of the area, it may be possible to set up several arrangements of particle orientations, all of which would give a distribution of planes in accordance with the pole figure. Since the torque curve depends on the manner in which the *particles* are oriented, it is not surprising to find a case in which different types of torque curves are associated with approximately the same X-ray texture.

To return briefly to Fig. 7 and to JD, one of the possible ways of reconciling the calculated and measured values of A_1 is to assume that in addition to the ordinary limited tension texture with R for its axis, there is a considerable amount of a tension texture with C as an axis. This additional texture must be drastically limited in its extent so as to conform with the pole figure. In order to check the validity of this assumption, it would be necessary to make a more detailed X-ray study of this unusual texture shown by JD.

RECRYSTALLIZATION TEXTURES

Torque Studies

Samples with a number of different degrees of deformation were annealed for 1 hr. at a series of temperatures 200° apart, from 300° to
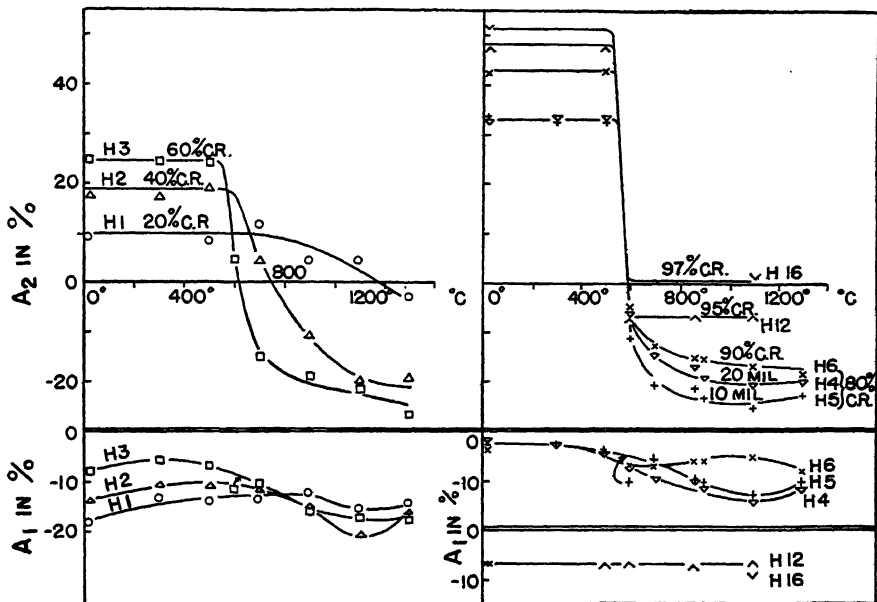
FIG. 9.—A_1 AND A_2 AS FUNCTIONS OF ANNEALING TEMPERATURE FOR VARIOUS AMOUNTS OF COLD-ROLLING.
All specimens were annealed for one hour.

1300° C., and also at 600° C., which is close to the recrystallization temperature. The effect of these heat-treatments on the harmonic coefficients is shown in Fig. 9, where the coefficients are plotted against annealing temperature for a given degree of cold reduction. The curve marked $H2$ can be compared with the torque curves of Fig. 4 in order to get a better understanding of the coefficients A_1 and A_2.

The time of one hour was chosen because the larger part of any orientation transformation can usually be expected to take place in this

or even a much smaller interval. This is not necessarily true of transformations taking place at the lowest possible temperature, but in such a case very long heat-treatments would be necessary to attain equilibrium. The curves for A_2 thus do not show equilibrium conditions in the region between the horizontal portions of the curves, but measurements made on samples similarly treated for 24 hr. show that no serious error is made unless the temperature happens to be within a few degrees of the recrystallization temperature.

These curves show clearly how the sluggishness of the recrystallization decreases as the amount of cold-work is increased. Another interesting feature is the decrease in the absolute value of A_2 as the amount of cold-rolling is increased beyond 80 per cent. In this case there is good reason to believe, on the basis of published X-ray evidence, that the recrystallization texture is not being weakened by increasing the cold-work, but that it is becoming of such a nature as to cause the resulting torque to cancel out more completely. Nothing can be deduced about the process of recrystallization from the curves for A_1, but the fact that changes in A_1 occur far below the recrystallization temperature (as given by the curves of A_2) can be related to strain relief at these lower temperatures.
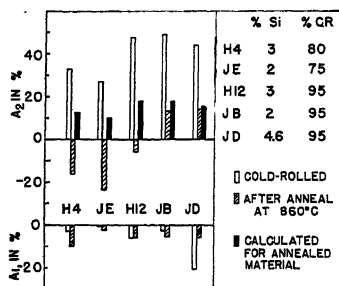
FIG. 10.—COMPARISON OF A_1 AND A_2 FOR CERTAIN COLD-ROLLED SPECIMENS BOTH BEFORE AND AFTER A RECRYSTALLIZING ANNEAL.
Also shown are the values of these coefficients calculated on the assumption that the recrystallization texture can be obtained from the cold-rolling texture by a simple rotation, as described in the text.

Bitter[14] has shown that strains can be expected to affect A_1 without affecting A_2 in the least, and this is seen to be true here.

The negative value of A_2 that was found to be characteristic of series H in the recrystallized condition could not be reconciled with the published pole figures, as will be discussed later. It was for this reason that series J was investigated. In order to eliminate all possible sources of error, these samples were given the same heat-treatment as that used in the X-ray study;[7] namely, very slow rates of heating and cooling with a maximum temperature of 860° C. Experiments performed later on various recrystallized samples of series H showed that the torque curves depended only on the highest temperature at which the annealing took place and not at all on the rate of cooling or of heating. For this reason it is entirely proper to compare material from series H subjected to a 1-hr. anneal with the samples of series J. Other heat-treatments could not be tried with the J samples because very little material was available.

The results shown in Fig. 10 are quite unexpected. JE behaves as if it were an H specimen, which would be considered entirely normal

were it not for the fact that JB, with the same composition but a some-what greater cold reduction, is found to have A_2 definitely positive instead of negative.   Yet the corresponding specimens in series H, which contains 3 per cent Si and thus has the same slip mechanism as JB and JE, do not show any traces of similar behavior.   The results are not accidental because they were duplicated on other specimens annealed according to approximately the same schedule some time later.   In view of the large difference that exists between JB and JD in the cold-rolled state, at least in so far as A_1 is concerned, the complete agreement between the coefficients in the annealed condition is also somewhat surprising.   ·

The Recrystallization Texture

The pole figures that have been published for recrystallized iron, mild steel, and iron-silicon[7] agree fairly well in their main features.   The differences are chiefly those arising from the different amounts of scatter around the common ideal texture. The best pole figure to consider is the one for JD, because it shows unusually little random orientation for a recrystallized texture (Fig. 11).   It happens that although this texture looks complicated, it can be visualized clearly if it is thought of as the result of rotating the ordinary cold-rolling texture 17° each way about the sheet normal.   The same holds true for the low-silicon alloy JB.   As regards JE, which was cold-rolled only 75 per cent, its texture was not given by means of a pole figure, but was stated to be of the same general type as that for JD, except that it was less completely developed.
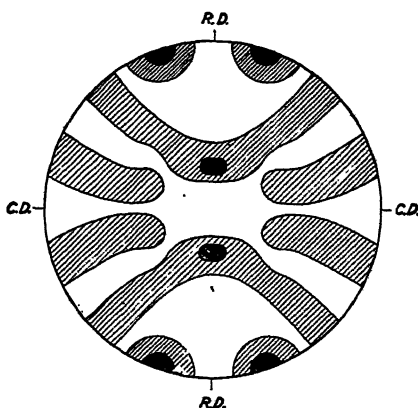
FIG. 11.—{110} POLE FIGURE FOR 4.6 PER CENT SILICON ALLOY COLD-ROLLED 95 PER CENT AND RECRYSTALLIZED AT AND BELOW 860° C.   SPECIMEN JD.   (Barrett, Ansel and Mehl.[7])

Correlation of Torque Data with the Pole Figures

If the recrystallization texture is considered as obtainable from the cold-rolled texture by a simple rotation of the latter through 17° either way around N, the torque curve of the rolling texture can be modified by multiplying A_1 by cos $(2 \times 17°)$ and A_2 by cos $(4 \times 17°)$ to give the calculated coefficients for the recrystallization texture.   The values of A_2 so computed are shown in Fig. 10 next to the measured ones.   Similar calculations for A_1 would not have much significance because of the

comparatively large changes that occur in this coefficient at temperatures below recrystallization and that in all likelihood are connected with strain relief.

Although the calculated and measured values of A_2 are in excellent agreement for both JB and JD, this is not true for any of the samples in series H nor for JE, where we find that the disagreement extends to the sign of A_2. The clue to this disagreement seems to be that JE, of which the pole figure is known to be fairly diffuse,[7] but of the same type as JD (Fig. 11), gives a torque curve which at first sight does not conform to the X-ray data; on the other hand, JD has a concentrated recrystallization texture with which the torque curve agrees very well. Since the highly concentrated texture leads to the correct positive value of A_2, it seems that the negative value of A_2 found for the poorly developed texture of JE must be attributed to the negative contributions to A_2 of the lightly shaded portions of its pole figure, these negative contributions being sufficient to more than balance the positive contributions of the heavily shaded regions. This interpretation is reasonable because the X-ray blackening of the film caused by a given number of reflecting planes spread thinly over a large area of the pole figure is less than that caused by an equal number concentrated in a small area, yet the magnetic torque exerted by the particles of the first group may in certain cases be much greater than that exerted by particles of the other group.

It has been assumed that it is proper to compare the low-silicon JE with the high-silicon JD rather than with the low-silicon JB. That the silicon content is different should not invalidate the conclusions that have been drawn, since JB could have been substituted for JD throughout on account of the similarity of their recrystallization textures, as found from both the X-ray and the magnetic torque measurements. The only reason for using JD and not JB was that the pole figure of the former was available and the other was not.

Since it is quite certain that there is no significant difference between the recrystallization textures of a 2 per cent and a 3 per cent Si iron, the explanation of the negative value of A_2 given previously for JE must also hold for all of the specimens of series H. It is interesting to note that as the degree of cold-rolling increases beyond 80 per cent, A_2 changes gradually for the completely recrystallized specimens from about -20 per cent towards zero per cent (Fig. 9). In terms of the foregoing explanation, this behavior means that the lightly shaded areas of the recrystallization pole figures are becoming of less importance as the degree of cold-work is increased, and thus the negative contributions to A_2 are decreased. No explanation can be offered at present as to why a 95 per cent cold-rolling was sufficient to give a satisfactory positive value of A_2 for JB after recrystallization, whereas in the series H samples even a 97 per cent reduction left A_2 far from a similar positive value.

A torque curve similar to those for the recrystallized samples in series H was obtained by Sixtus[2] who used 3.5 per cent Si iron that had been cold-rolled 85 per cent with an intermediate anneal and was then given a final anneal at 1100° C. The intermediate anneal was responsible for more than doubling the coefficients obtained with the corresponding disk from series H, but X-ray work by Bozorth[15] on similarly treated material showed that the texture consisted in large part of (110) planes in the rolling plane. This type of texture is completely ruled out unless there has been an intermediate anneal, as is evident from the pole figures of iron-silicon recrystallized without the intermediate anneal, as in Fig. 11.

At present, therefore, the only logical correlation of the X-ray and magnetic torque results seems to be the one already outlined. It is important to notice that we can have a texture which on the basis of torque studies alone may be erroneously classified as a (110) texture, similar to that found by Bozorth and Sixtus, but which X-ray work shows to be definitely of a different type.

Grain Size

The grain size was measured for a few typical samples and it was found that the grain size varied with the history of the specimen in the expected manner. On the American Society for Testing Material's scale, the grain size was around No. 6 for the specimen recrystallized at and below 900° C., and No. 3 for those at 1100° C. Nothing could be found in the grain size to account for any of the anomalous torque results.

SUMMARY

The chief purpose of this investigation was to make a magnetic torque study of various simple deformation and recrystallization textures of iron-silicon, and to find what sort of a correlation can be expected between these results and the textures found with the use of X-rays. The magnetic torque method is based on the experimental fact that most ferromagnetics have crystallographic directions of easy magnetization and of hard magnetization, and that a single-crystal disk of such a material suitably held in a strong magnetic field tends to turn so as to make one of its easy directions parallel to the external field. The same behavior will be shown by a disk of polycrystalline material, provided the grains have a suitable preferred orientation. A knowledge of the torque exerted by such a disk gives a limited amount of information about its texture.

The problem turned out to be more difficult than was first expected, because while in a few instances there was excellent agreement between the two methods, in the rest there was just as complete disagreement. This disagreement between magnetic and X-ray results could, however, be made to disappear by postulating that the lightly shaded regions of a

pole figure arise from a large number of suitably oriented particles whose contribution to the torque curve outweighs the contributions of the particles represented by the heavily shaded regions of the pole figure.

The *highly cold-rolled* specimens of iron-silicon gave torque curves in good agreement with the published pole figures if it was assumed that half of the particles were randomly oriented and thus did not contribute to the torque curve. An exception to this good agreement was found for a high-silicon disk, for which it was necessary to assume the presence of a subsidiary texture capable of explaining the torque data and yet not contradicting the pole figure.

A little work was done on *hot-rolled* and *slightly cold-rolled* specimens, but the spread of the results showed the great sensitivity of these textures to slight variations in the process of deformation.

In regard to the *recrystallization* texture, two specimens gave torque curves in excellent agreement with the published X-ray work; all the rest had torque curves of an entirely different kind, which could be interpreted only by assuming that the lightly shaded regions of the pole figures played a very important part in determining the torque.

A minor but interesting change in the torque curves was noted when the specimens were annealed below the recrystallization temperature. This change is thought to be associated with strain relief.

A very useful field for the application of the magnetic torque method appears to be in checking the textures as determined by X-rays; in case of marked disagreement, further X-ray work is indicated. It is possible that some of the discrepancies can be traced to the qualitative nature of present-day pole figures. There is no doubt that if pole figures can be made more quantitative, torque measurements can be interpreted with greater precision. Torque studies should also prove valuable in determining the most interesting textures that should be studied in detail with X-rays.

REFERENCES

1. H. J. Williams: Some Uses of the Torque Magnetometer. *Rev. Sci. Inst.* (1936) **8,** 56.
2. K. J. Sixtus: Magnetic Anisotropy in Silicon Steel. *Physics* (1935) **6,** 105.
3. N. P. Goss: New Development in Electrical Strip Steels. *Trans. Amer. Soc. Metals* (1935) **23,** 511.
4. R. M. Bozorth: Determination of Ferromagnetic Anisotropy in Single Crystals and in Polycrystalline Sheets. *Phys. Rev.* (1936) **50,** 1076.
5. N. S. Akulov and N. Brüchatov: Über eine Methode zur quantitativen Untersuchung der Walztextur. *Ann. Physik* (1932) **15,** 741.
6. L. P. Tarasov and F. Bitter: Precise Magnetic Torque Measurements on Single Crystals of Iron. *Phys. Rev.* (1937) **52,** 353.
7. C. S. Barrett, G. Ansel and R. F. Mehl: Preferred Orientations in Iron-silicon Alloys. *Trans.* A.I.M.E. (1937) **125,** 516. (This reference contains a good bibliography of the X-ray work.)
8. C. S. Barrett: The Stereographic Projection. *Trans.* A.I.M.E. (1937) **124,** 29.
9. F. Wever: Texture of Metals after Cold Deformation. *Trans.* A.I.M.E. (1931) **93,** 51.
10. W. Boas and E. Schmid: Zur Deutung der Deformationstexturen von Metallen. *Ztsch. tech. Physik* (1931) **12,** 71.
11. H. J. Gough: Behavior of a Single Crystal of Alpha Iron Subjected to Alternating Torsional Stresses. *Proc. Roy. Soc.* (London) (1928) **A118,** 498.
12. C. S. Barrett, G. Ansel and R. F. Mehl: Slip, Twinning and Cleavage in Silicon Ferrite. *Trans. Amer. Soc. Metals* (1937) **25,** 702.
13. L. P. Tarasov: Thesis, Physics Department, M.I.T., 1937.
14. F. Bitter: Introduction to Ferromagnetism, 219. New York, 1937. McGraw-Hill Book Co.
15. R. M. Bozorth: Orientation of Crystals in Silicon Iron. *Trans. Amer. Soc. Metals* (1935) **23,** 1107.

DISCUSSION

(L. W. McKeehan presiding)

H. MUSSMANN* AND H. SCHLECHTWEG,* Essen, Germany.—It is generally known that when a dish is held in a magnetic field it exerts around its axis normal to the lines of force a magnetic torque, which tends toward a definite limit as the field intensity increases. The curve plotted to give this limit for various directions of the field is known to be composed of a second and a fourth harmonic. By observing their behavior, Mr. Tarasov was able to study the recrystallization of cold-rolled *transformer* material with 3 per cent Si. We were already acquainted with the excellent results he achieved in this way and have found them to be correlated in an interesting manner with what we had previously observed in soft iron. The results we obtained at that time are shown in Figs. 12 and 13, but only in as far as the fourth harmonic coefficient is concerned, since this is the main point of interest here. With the 3.18 per cent Si alloy material we also found the inversion of signs reported by Mr. Tarasov but at considerably lower temperatures, particularly in slightly cold-rolled specimens; complete agreement with our experience in respect of temperature at the point of sign reversal is restricted to high degrees of cold deformation (60 per cent and over). We consider worth noting, especially in view of our results with soft iron (Krupp WW iron), that with increasing deformation the minimum value of the fourth coefficient

---

* Fried. Krupp Aktiengesellschaft.

first drops down to negative values only to rise again until at an 80 per cent cold reduction it reaches zero; this is where the practically disappearing fourth harmonic coefficients, which Mr. Tarasov also observed, are found to occur.

The recrystallization process in *soft iron*, which can be deformed with considerably greater ease, may perhaps permit further penetration into this mechanism. It is interesting that after slight cold deformation (about 20 per cent) the recrystallization process is characterized by the appearance of additional positive values of the fourth harmonic coefficient (type A). After high degrees of cold-rolling—50 and 60 per cent, for instance—a behavior is observed that is similar to that of the above-mentioned Si alloy material (type B) whereas, with medium deformation in the 40 per
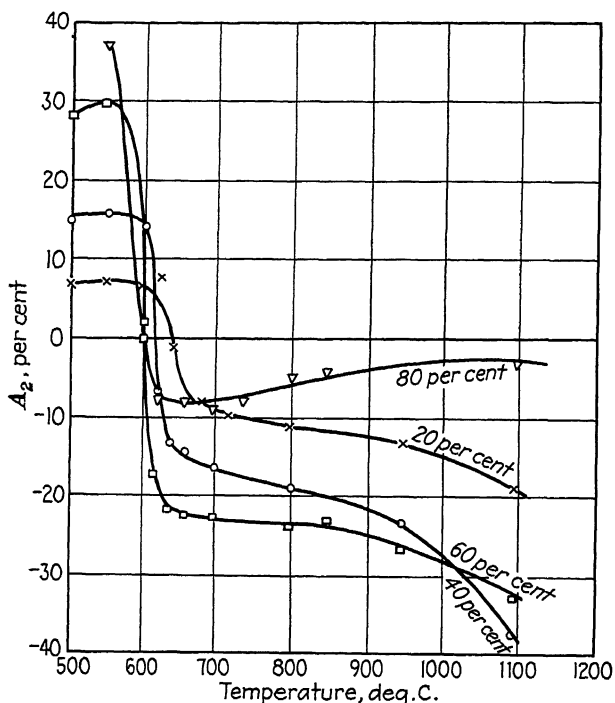
FIG. 12.—TRANSFORMATION MATERIAL (3.18 SILICON).

cent range, both types are superimposed. In soft iron, additional positive portions of the fourth harmonic coefficient were also observed when deformation was high, as 80 per cent. Just as in transformer material, where the reversal of sign, which is connected with the turning point of the curve, is shown to shift at lower temperatures as the degree of cold-rolling increases, the same phenomenon is also found in soft iron at the turning point temperature; i.e., the temperature at which the greatest modification takes place in the material. Actually, after annealing to above the A_3 point the torque in the magnetic field practically disappears.

Mr. Tarasov's observations are only in agreement with our own experience in as far as behavior according to type A was not found in the recrystallization tests with silicon-alloy material. The reason for this may lie in the fact that a definite degree of deformation which, with soft iron, would still result in behavior according to type

A, will already cause such far-reaching modifications in the more brittle silicon alloy as could only be enforced in soft iron by cold-rolling to about 55 per cent, producing type B.

It may be of interest, by the way, that with a roll of slightly different crown the fourth harmonic coefficient is particularly liable to assume different values below the temperature of its turning point, which, as mentioned, may possibly coincide with a reversal of sign, depending on the material used. This difference, however, seems to disappear again above this temperature. On the other hand, this may possibly be the initial point of an explanation of the phenomenon that Mr. Tarasov
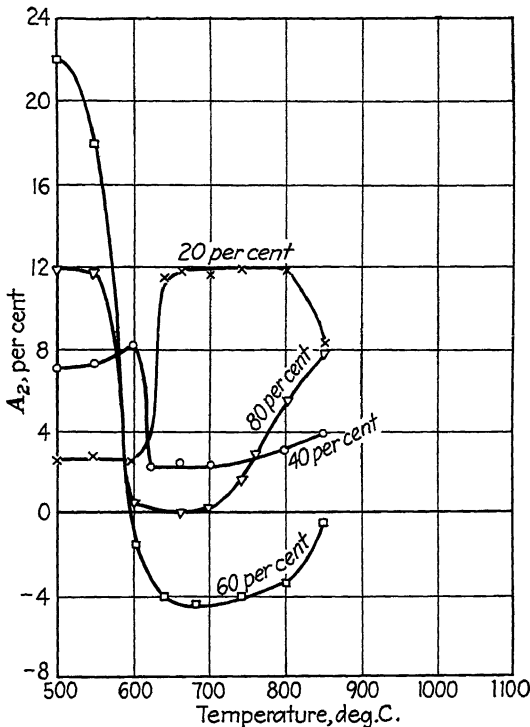
Fig. 13.—Krupp's soft iron.

found the temperature of the sign reversal of the fourth harmonic coefficient to be higher than we did.

According to Mr. Tarasov's statement, which is also in agreement with our experience, the second harmonic coefficient does not depend to such a high degree on the annealing temperature as does the fourth harmonic coefficient. While generally varying between 5 and 15 per cent for transformer material, it attains, in the best of circumstances, some 8 per cent in soft iron, or less when the degree of cold deformation is higher.

Occasionally, when studying specimens of very low degrees of deformation, curves are encountered that do not show symmetry on the reverse hand after half a period of 90°. In such cases, Mr. Tarasov points out, it is no longer possible to use his method of determining the different harmonic coefficients; we usually determined

the various harmonic coefficients in these cases by a simple graphic method, adding or deducting the curve that had been displaced by 90°.

We intend to publish our experiments in the *Forschungsberichte Krupp* in the near future.

C. S. BARRETT,* Pittsburgh, Pa.—Some of the recrystallization treatments that the author has been studying with magnetic torque measurements are closely related to some that G. Ansel and I have studied with X-ray diffraction. In view of the differences between these two methods of investigating the textures of deformed and recrystallized metals, a brief comparison of results should be interesting.

Silicon steel containing 2.07 per cent Si (the material discussed in the paper by Barrett, Ansel, and Mehl[16]) after cold-rolling to a reduction in thickness of 95 per cent was given various annealing treatments. A strip was clamped while elastically bent and was annealed for 48 hr. at 520° C. At the end of this time the permanent set in the strip indicated that less than 2 per cent of the initial stress remained. Diffraction patterns and microscopic examination showed, however, only partial recrystallization. The patterns of this specimen and of a specimen annealed 120 hr. at the same temperature indicated that the usual recrystallization texture was developing, although in both cases some of the original rolling texture remained. Subsequent annealing at 580° C. completed the recrystallization in both these specimens and the usual recrystallization texture was found (this is described in the reference cited). The usual texture was also obtained by heating the specimen gradually from 100° to 580° in 8 hr. and cooling at the same rate. Likewise, specimens of 4.61 per cent Si gave the same recrystallization texture when heated from 100° to 860° in 8 hours and cooled at the same rate, or when put into a furnace at 1093° C. for 2 minutes. Thus varying the final annealing treatment can at most lead to varying degrees of recrystallization and not to various kinds of texture. If any stresses are relieved in individual grains before they recrystallize, the stress relief is without effect on the final texture.

The author has drawn a rather sharp break in his curves of torque constant versus temperature, but we believe they should be so drawn. We have noted that in 95 per cent cold rolled material it is possible to have no recrystallization at one temperature in 12 hr., and yet have complete recrystallization in 12 hr. at a temperature only 20° higher.

There appears little hope that the magnetic method will contribute much that will aid in solving the mysteries of deformation and recrystallization textures, but it has already proved itself of value in industrial applications where its sensitivity to slight changes in rolling and annealing schedules can be made use of even though the exact meaning of the results in terms of orientations remains uncertain or unknown.

G. EDMUNDS,† Palmerton, Pa.—Have any attempts been made to correlate the fiber structures as indicated by these studies, in addition to the X-ray diffraction studies, with such properties as tensile strength versus direction of testing, the development of ears on drawn cups, and other things that concern the plastic deformation of the metal? Such studies have not always correlated well with X-ray determinations of structures, although there have been definite cases reported in which some correlation of the type has been found. Mr. Tarasov has presented here a method for noting differences of a nature that are hidden from the X-ray, and it would be interesting if he could give us information on any correlations of the type referred to.

J. J. B. RUTHERFORD,* Kearny, N. J.—The author mentioned that some of these steels were the same as the materials used by Mehl and some of his co-workers in recent experiments. Mehl described that the 4.6 per cent Si steel was impossible to cold-roll in the usual process that applied to other materials. In fact, I think he had to go to a temperature of about 150° C. to cold-roll his material. Can the author comment on the differences in behavior introduced by rolling the 4.6 Si steel at 150° as against the room temperature that was used for the 2 and 3 per cent Si steel.[7]

L. P. TARASOV (author's reply).—It is very interesting to see that the torque data of Dr. Mussmann and Dr. Schlechtweg on silicon steel recrystallized after various amounts of cold-rolling follow at least qualitatively the curves of Fig. 9. The lack of good quantitative agreement is of equal interest because it shows how much the texture can be affected by the deformation history. The disagreement is especially strong for specimens that had only small amounts of cold-rolling before recrystallization, and this is in line with the difficulty that was experienced in getting reproducible *cold-rolled* textures for specimens with only 10 or 20 per cent of cold reduction.

The complexity of the torque data for cold-rolled and recrystallized iron serves as a good illustration of why it may be decidedly worth while to make a preliminary torque study of the texture of a ferromagnetic material before proceeding with X-ray work. The torque method, as previously stated, makes possible a quick survey of the conditions necessary to give rise to each of several types of texture that may be encountered; X-ray work then permits a detailed study of the characteristics of these textures; and, in some cases, at least, the best interpretation of the X-ray data can be made with the help of the magnetic torque curves.

The X-ray studies described by Dr. Barrett are certainly interesting in the light they throw on the effect of strains upon recrystallization. As compared to his value of 20° C. for the difference between the temperatures of no recrystallization and complete recrystallization, some subsequent torque studies on 95 per cent cold-rolled iron and iron alloys have shown this range to be somewhat larger; say, 50° or 75° C. The nature of the material undoubtedly has much to do with the amount of this spread.

In reply to Mr. Edmunds, I did not try to correlate any of the physical properties with the results of the magnetic torque measurements, since the main purpose of this work was to check the torque method against the texture as deduced from X-ray studies. Very recently (May, 1939) Dr. W. M. Saunders, Jr., finished some work at the Massachusetts Institute of Technology, which showed a qualitative relationship between the type of earing and the magnetic torque data. This work is described in his doctorate thesis, entitled "Earing of Low-carbon Strip Steel," which has not yet been published.

Regarding the effect of cold-rolling at 150° C., about which Mr. Rutherford inquires, the value of A_1 is shown in Fig. 7 to be many times larger for JD, cold-rolled at 150° C., than for the steels cold-rolled at ordinary temperatures. Because JD contained 4.6 per cent Si and the others considerably less, it was not possible to say at that time whether the large value of A_1 was due to the rolling temperature or to the composition. Some work was done subsequently on a 3 per cent Si steel that was cold-rolled from 250 to 14 mils at 150° C., like JD. In this case A_1 was practically the same as for JD, so that we can safely attribute the unusual magnitude of A_1 to the cold-rolling temperature and not to the composition. These results also show that the texture is affected more by a change in the cold-rolling temperature than by a change in the composition.

---

* U. S. Steel Corporation Research Laboratory.

Influence of Atmosphere and Pressure on Structure of Iron-carbon-silicon Alloys

By Alfred Boyles,* Member A.I.M.E.

THE experiments described below are a continuation of work on the graphitization of cast iron conducted as part of the program of fundamental research at Battelle Memorial Institute. In previous work it was found that melting in hydrogen increased the amount of eutectic carbide appearing in certain alloys and in others produced marked changes in the size of the graphite flakes. These effects seemed to be closely related to the amount of sulphur and manganese present in the material studied. Iron-carbon-silicon alloys did not respond to hydrogen in the same manner as cast iron and there was no evidence to show that hydrogen was able to stabilize the carbide in such alloys unless additions of sulphur were made. The two alloys examined contained about 2 per cent of silicon. The present paper is concerned with alloys of lower silicon content and describes the structural changes produced by melting in various atmospheres at pressures ranging from a partial vacuum up to 300 lb. per sq. inch.

FIG. 1.—APPARATUS FOR MELTING UNDER PRESSURE.

A, inlet for gas.
B, outlet for evacuation.
C, power lead.
D, thermocouple.
E, plug for access to furnace.
F, crucible.

EXPERIMENTAL METHOD

The experimental technique was similar to that previously employed, so that direct comparison might be made with earlier work. Alloys were

prepared from Westinghouse electrolytic iron, graphite and silicon carbide. These were melted by induction in a magnesia crucible and sand-cast into bars of such shape that pieces weighing about 50 grams could be broken off for remelting. A typical charge is shown in Fig. 33.

TABLE 1.—*Analyses of the Iron-carbon-silicon Alloys*

Alloy No.	Composition, Per Cent			
	Carbon	Silicon	Sulphur	Manganese
11...................................	3.03	0.47	0.008	0.00
12...................................	3.14	0.73	0.008	0.00
13...................................	3.12	0.97	0.006	0.00
14...................................	3.21	1.23	0.005	0.00

Remelts were made in alundum crucibles (Grade RA84) using the same Globar furnace previously employed. Each melt was brought up
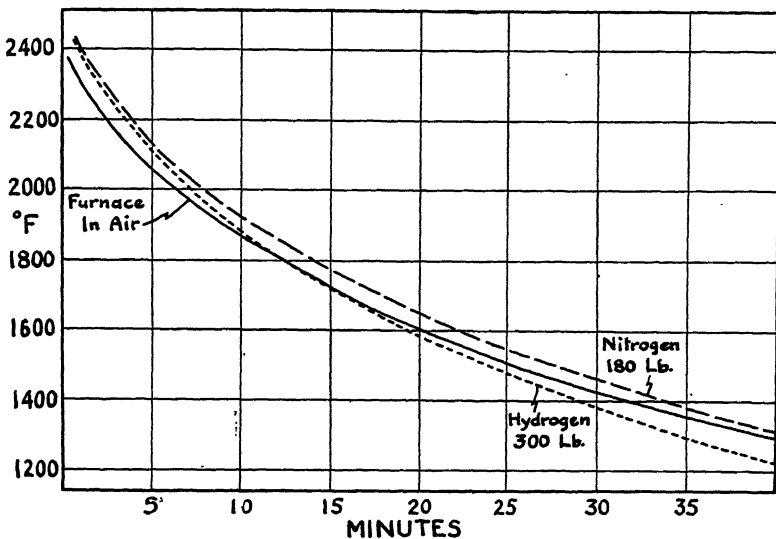
FIG. 2.—COOLING CURVES FOR VARIOUS MELTING CONDITIONS.

to 2500° F., held 30 min. at this temperature and allowed to cool slowly with the furnace. The cooling rate is shown in Fig. 2. Melts of each alloy were made in vacuo, in air, and in hydrogen.

In order to extend the work to pressures above atmospheric, the entire Globar furnace was enclosed in a vessel made from pipe fittings, a section of which is shown in Fig. 1. A cylinder of gas was attached at *A* and a vacuum pump at *B*. With the charge in place, the vessel was evacuated for about 18 hr., the lowest pressure attainable being about 1 mm. of mercury. *B* was then closed and the gas introduced to give a

pressure somewhat below the maximum desired. As the furnace warmed up the pressure gradually increased and was finally adjusted when 2500° F. was reached, which required from 2 to 3 hr. Each melt was held 30 min. at 2500° F. and allowed to cool with the furnace under pressure. Fig. 2 shows typical cooling curves, which do not differ greatly from the cooling curve of the furnace in open air. The platinum-platinum rhodium thermocouple required constant attention when working with hydrogen. It was checked frequently and kept in calibration by cutting away the affected part.

DESCRIPTION OF THE MELTS

The melts are described in the following paragraphs and summed up in Table 2.

Test No. 199.—Melting in vacuo gave fine graphite in a ferrite matrix. Pearlite occurs in the central part of the primary dendrites (Fig. 3). There is no eutectic or proeutectoid carbide.

Test No. 211.—Melting in air gave a fully pearlitic matrix containing fine graphite and some irregular flakes (Fig. 4). Proeutectoid carbide occurs as fine needles.

Test No. 205.—Melting in hydrogen gave a fully pearlitic matrix containing a mixture of irregular graphite and eutectic carbide. Needles of proeutectoid carbide are very prominent (Fig. 5).

Test No. 258.—Melting in hydrogen at a pressure of 100 lb. per sq. in. gave a pearlitic matrix containing eutectic carbide (Fig. 6). No graphite formed in this melt. Needles of proeutectoid carbide occur in the primary dendrites. The melt as a whole resembled Fig. 23 and contained numerous cavities formed by the evolution of gas during freezing.

Test No. 260.—Melting in nitrogen at a pressure of 100 lb. per sq. in. gave a fully pearlitic matrix with a mixture of fine graphite and irregular flakes (Fig. 7). The entire melt is shown in Fig. 24. It contains numerous interdendritic cavities and has a layer of extruded metal on top. Traces of eutectic carbide occur near the bottom.

Test No. 200.—Melting in vacuo gave fine graphite in a ferrite matrix (Fig. 8). No eutectic or proeutectoid carbide occurs. The entire melt is shown in Fig. 25. Pearlite occurs along the ribs of the primary dendrites and is concentrated at the boundaries of the eutectic cell structure, forming a coarse network. This melt as a whole contains less pearlite than the preceding alloy melted under the same conditions.

Test No. 212.—Melting in air gave a pearlitic matrix containing mixed fine and coarse graphite (Fig. 9). The entire melt is shown in Fig. 27. A few spots of ferrite occur near the surface. Traces of proeutectoid carbide are visible as fine needles in Fig. 9.

Test No. 206.—Melting in hydrogen gave a fully pearlitic matrix in which most of the graphite occurs as long flakes (Fig. 10). Pro-

TABLE 2.—*Description of the Melts*

Test No.	Melting Conditions	See Fig.
MELTS OF ALLOY No. 11 (C, 3.03 PER CENT; Si, 0.47 PER CENT)		
199...........................	In vacuo (pressure 2 mm. of Hg)	3
211...........................	In air at atmospheric pressure	4
205...........................	In hydrogen at atmospheric pressure	5
258...........................	In hydrogen at 100 lb. per sq. in.	6
260...........................	In nitrogen at 100 lb. per sq. in.	7 and 24
MELTS OF ALLOY No. 12 (C, 3.14 PER CENT; Si, 0.73 PER CENT)		
200...........................	In vacuo (pressure 2 mm. of Hg)	8 and 25
212...........................	In air at atmospheric pressure	9 and 27
206...........................	In hydrogen at atmospheric pressure	10 and 29
257...........................	In hydrogen at 100 lb. per sq. in.	11
242...........................	In hydrogen at 150 lb. per sq. in.	
243...........................	In hydrogen at 300 lb. per sq. in.	
240...........................	In nitrogen at 180 lb. per sq. in.	12
241...........................	In nitrogen at 300 lb. per sq. in.	
MELTS OF ALLOY No. 13 (C, 3.12 PER CENT; Si, 0.97 PER CENT)		
201...........................	In vacuo (pressure 2 mm. of Hg)	13
213...........................	In air at atmospheric pressure	14
207...........................	In hydrogen at atmospheric pressure	15 and 31
259...........................	In hydrogen at 100 lb. per sq. in.	
244...........................	In hydrogen at 150 lb. per sq. in.	16 and 23
261...........................	In nitrogen at 150 lb. per sq. in.	17
MELTS OF ALLOY No. 14 (C, 3.21 PER CENT; Si, 1.23 PER CENT)		
202...........................	In vacuo (pressure 2 mm. of Hg)	18
214...........................	In air at atmospheric pressure	19
208...........................	In hydrogen at atmospheric pressure	20
245...........................	In hydrogen at 150 lb. per sq. in.	21
262...........................	In nitrogen at 150 lb. per sq. in.	22

eutectoid carbide appears as fine needles. The entire melt is shown in Fig. 29. There is no free ferrite.

Test No. 257.—Melting in hydrogen at a pressure of 100 lb. per sq. in. gave eutectic carbide in a pearlitic matrix (Fig. 11). No graphite formed. The melt as a whole resembled Fig. 23 and contained numerous cavities. The melts made in hydrogen at pressures of 150 and 300 lb. per sq. in. were very much like the one shown.

Test No. 240.—Melting in nitrogen at a pressure of 180 lb. per sq. in. gave a fully pearlitic matrix with small irregular graphite flakes (Fig. 12). Traces of proeutectoid carbide occur as needles. The melt as a whole resembled Fig. 24 and contained numerous cavities. The melt made in

Fig. 3.   Melted in vacuo.
Fig. 4.   Melted in air.
Fig. 5.   Melted in hydrogen.
Fig. 6.   Melted in hydrogen at 100 lb.
   per sq. in.
Fig. 7.   Melted in nitrogen at 100 lb.
   per sq. in.
        All etched in HNO_3.
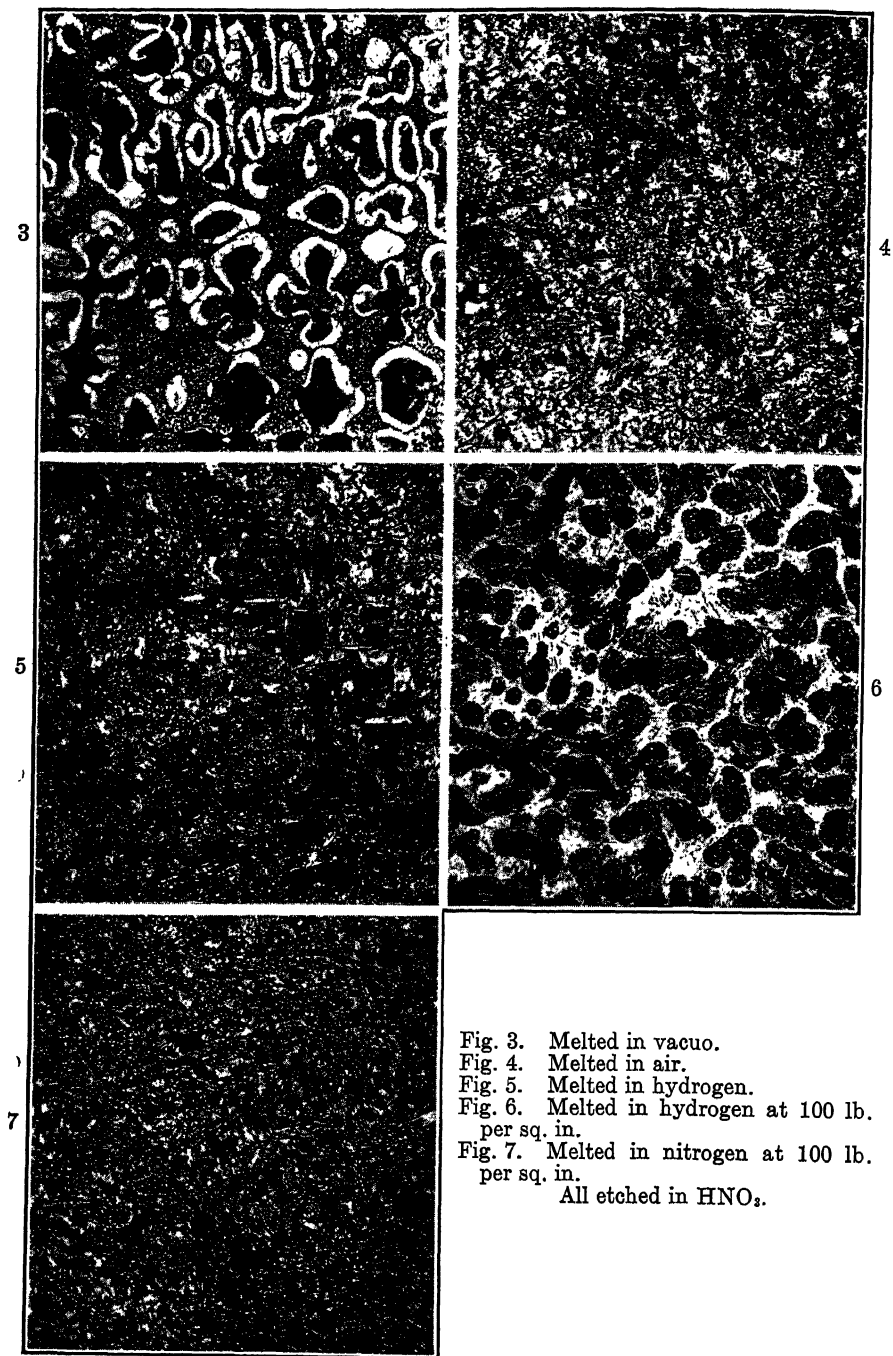
FIGS. 3–7.—ALLOY No. 11 (C, 3.03 PER CENT; SI, 0.47 PER CENT).   × 40.
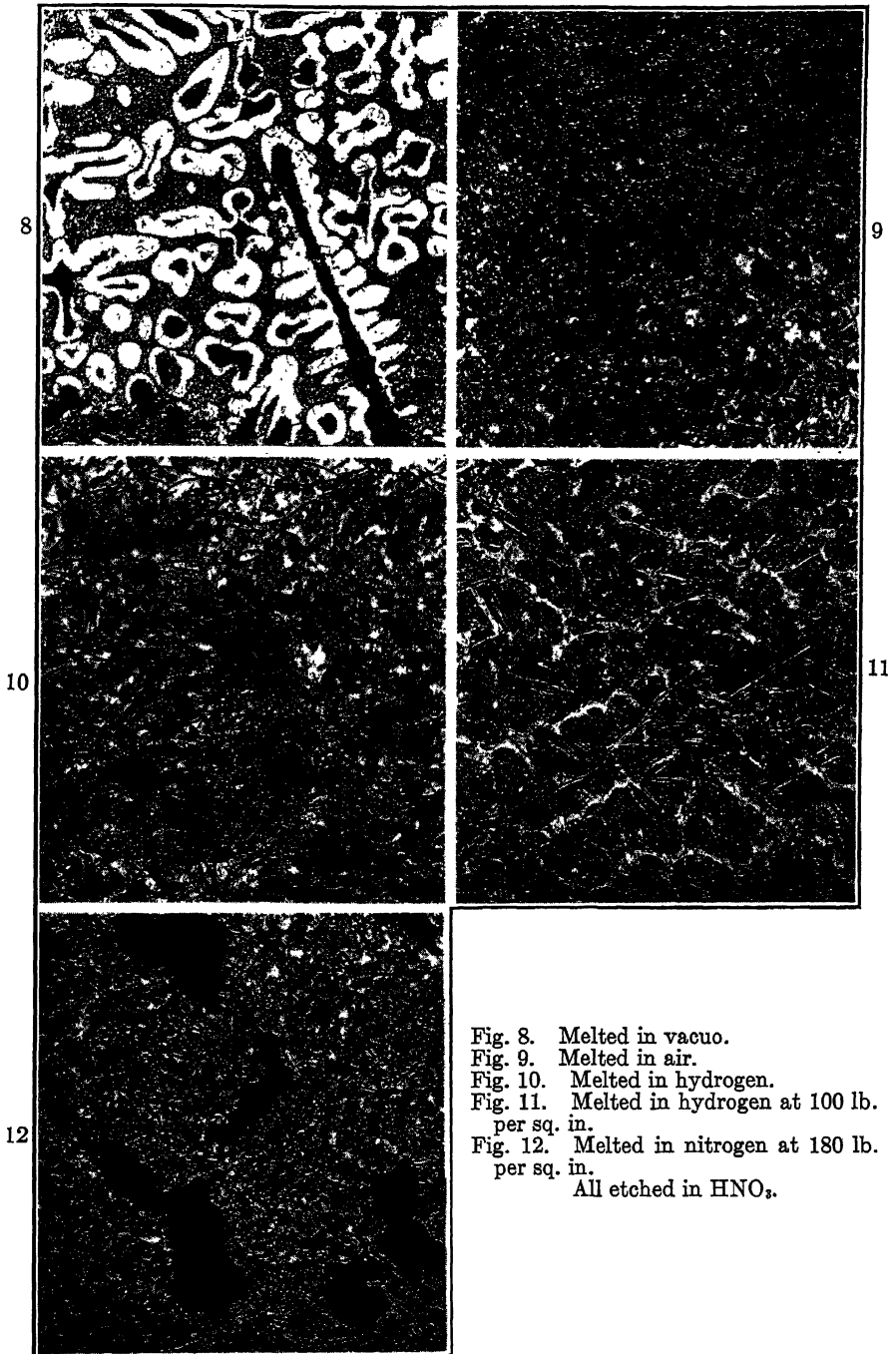
Fig. 8.   Melted in vacuo.
Fig. 9.   Melted in air.
Fig. 10.   Melted in hydrogen.
Fig. 11.   Melted in hydrogen at 100 lb.
  per sq. in.
Fig. 12.   Melted in nitrogen at 180 lb.
  per sq. in.
      All etched in HNO₃.

FIGS. 8–12.—ALLOY NO. 12 (C, 3.14 PER CENT; SI, 0.73 PER CENT).   × 40.

FIG. 13.   Melted in vacuo.
FIG. 14.   Melted in air.
FIG. 15.   Melted in hydrogen.
FIG. 16.   Melted in hydrogen at 150 lb.
  per sq. in.
FIG. 17.   Melted in nitrogen at 150 lb.
  per sq. in.
            All etched in HNO₃.
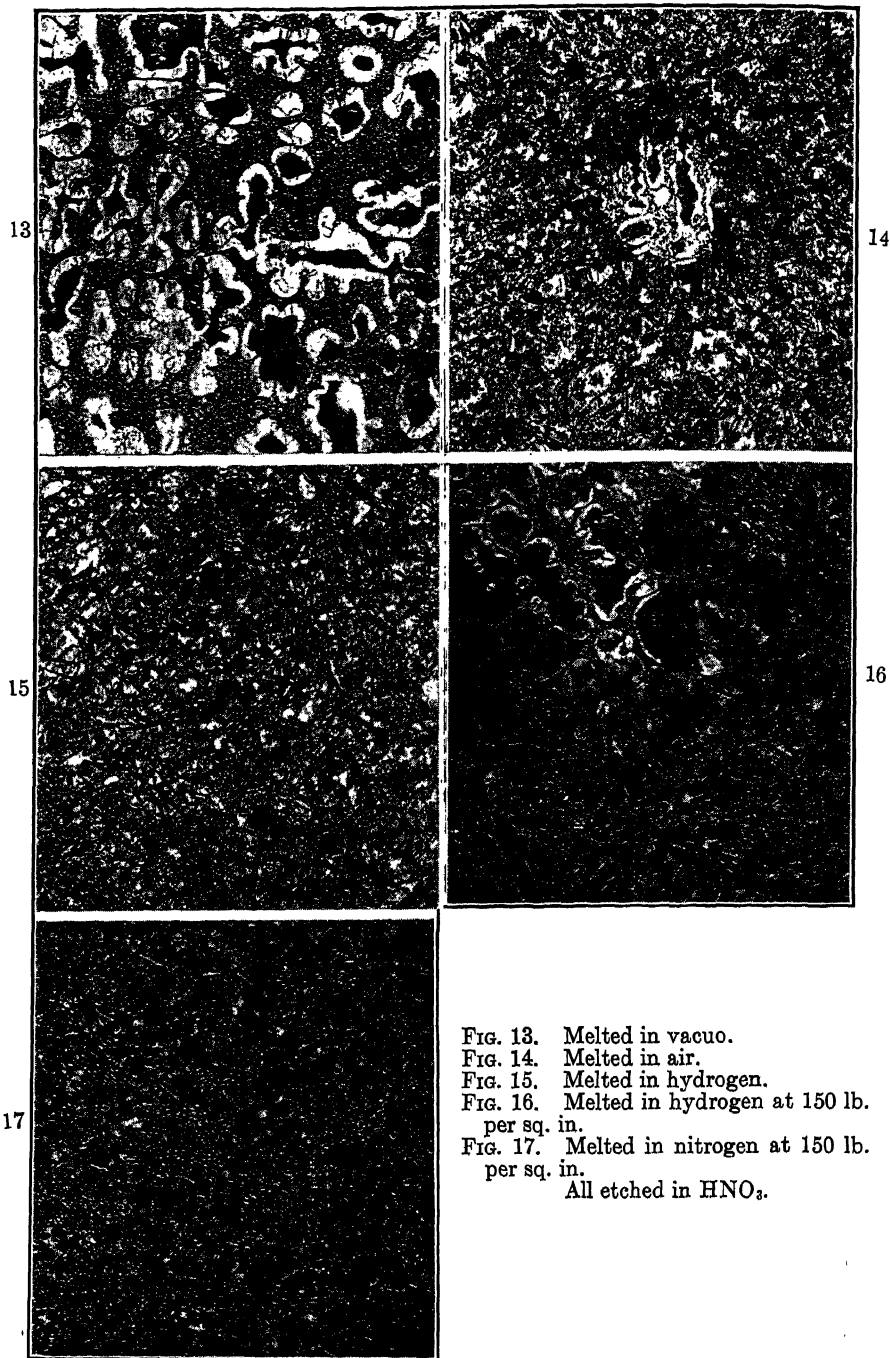
FIGS. 13-17.—ALLOY No. 13 (C, 3.12 PER CENT; SI, 0.97 PER CENT).   × 40.

Fig. 18.   Melted in vacuo.
Fig. 19.   Melted in air.
Fig. 20.   Melted in hydrogen.
Fig. 21.   Melted in hydrogen at 150 lb.
  per sq. in.
Fig. 22.   Melted in nitrogen at 150 lb.
  per sq. in.
     All etched in HNO_3.
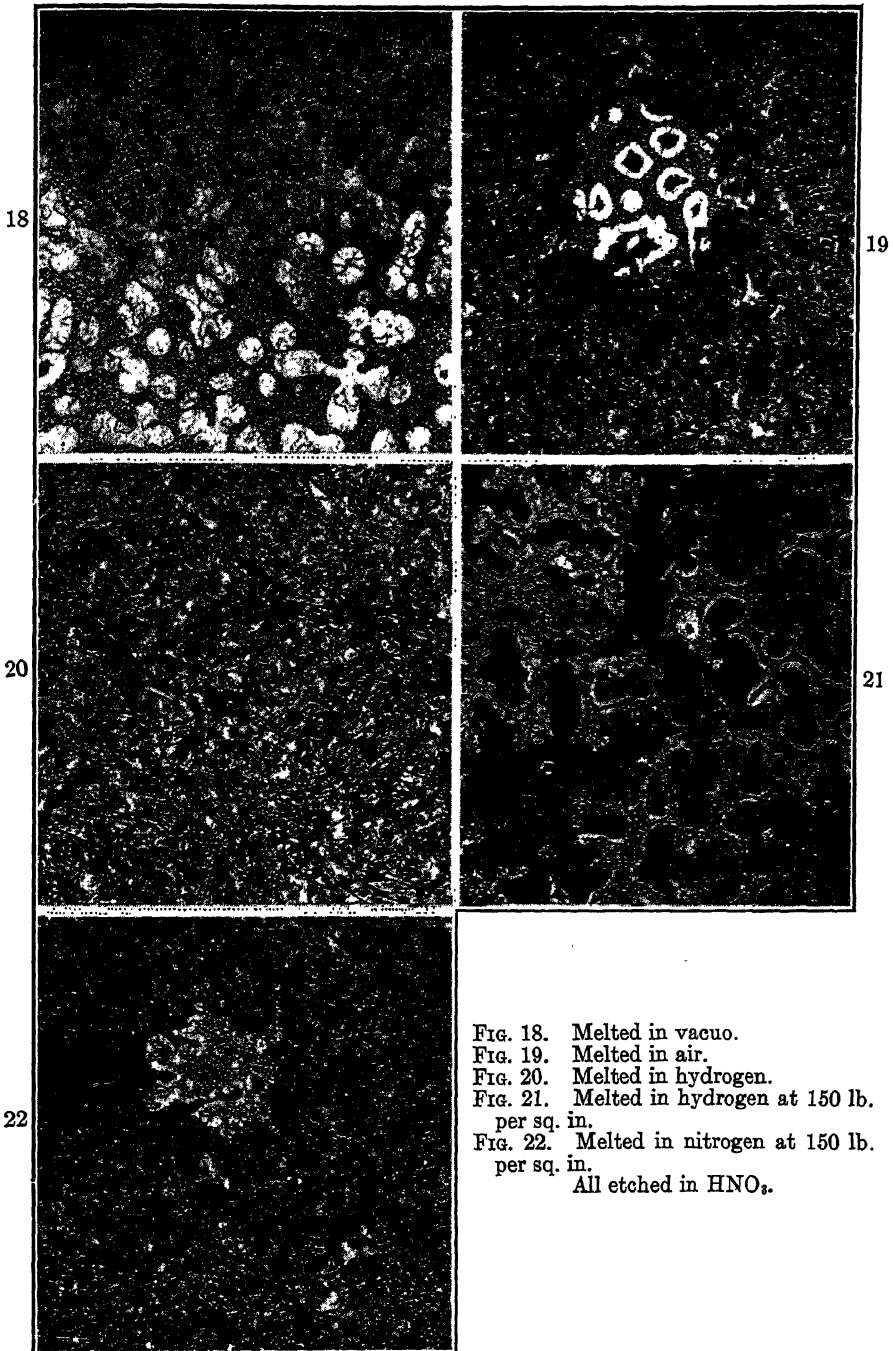
Figs. 18–22.—Alloy No. 14 (C, 3.21 per cent; Si, 1.23 per cent).   × 40.

nitrogen at 300 lb. pressure (No. 241) differed only in containing a greater number of cavities.

Test No. 201.—Melting in vacuo gave fine graphite in a ferrite matrix (Fig. 13). Pearlite occurs in the primary dendrites and is concentrated at the cell boundaries in the manner shown in Fig. 25. There is no eutectic or proeutectoid carbide.

Test No. 213.—Melting in air gave a pearlitic matrix containing scattered spots of ferrite (Fig. 14). Graphite ranges from small to fairly large flakes. There is no eutectic or proeutectoid carbide.

Test No. 207.—Melting in hydrogen gave a pearlitic matrix with graphite ranging from small to large flakes (Fig. 15). Some ferrite occurs near the surface of the melt (Fig. 31). There is no eutectic carbide but needles of proeutectoid carbide are present.

Test No. 244.—Melting in hydrogen at a pressure of 150 lb. per sq. in. gave the structure shown in Fig. 16. Most of the melt is composed of pearlite and eutectic carbide but spots of fine graphite occur, in the center of which ferrite appears. The entire melt is shown in Fig. 23. It contains numerous cavities and has a layer of extruded metal on top. The melt made in hydrogen at 100 lb. per sq. in. had the same type of structure.

Test No. 261.—Melting in nitrogen at a pressure of 150 lb. per sq. in. gave a fully pearlitic matrix containing medium sized graphite flakes (Fig. 17). There is no eutectic carbide but some needles of proeutectoid carbide occur.

Test No. 202.—Melting in vacuo gave fine graphite in a ferrite matrix (Fig. 18). Only a few traces of pearlite occur and these are in the boundaries of the eutectic cell structure.

Test No. 214.—Melting in air gave a pearlitic matrix with scattered spots of ferrite (Fig. 19). The graphite ranges from very fine to large flakes. There is no eutectic or proeutectoid carbide.

Test No. 208.—Melting in hydrogen gave a pearlitic matrix with some ferrite at the outer surface of the melt. Most of the graphite occurs as large flakes. There is no eutectic carbide but a few needles of proeutectoid carbide are present (Fig. 20).

Test No. 245.—Melting in hydrogen at a pressure of 150 lb. per sq. in. gave the structure shown in Fig. 21. The central part of the primary dendrites is pearlite. Fine graphite occurs in a ferrite matrix. It should be noted that the entire structure in Fig. 21 resembles the graphitized spot in Fig. 16.

Test No. 262.—Melting in nitrogen at a pressure of 150 lb. per sq. in. gave a structure resembling the melt made in air (compare Fig. 22 with Fig. 19). Fine graphite occurs in the ferrite areas surrounded by medium sized flakes in a pearlitic matrix. There is no eutectic or proeutectoid carbide.

DISCUSSION OF THE STRUCTURES

The changes produced by the various melting conditions may be summarized as follows:

1. Vacuum melting produces fine graphite, always associated with ferrite. Pearlite occurs chiefly in the boundaries of the eutectic cells and its amount decreases as the silicon is raised.

2. Melting in hydrogen at atmospheric pressure increases the size of the graphite flakes and produces eutectic and proeutectoid carbide, the amount of which decreases as the silicon is raised.

3. Melts made in air are intermediate as regards graphite flake size and amount of proeutectoid carbide.

4. Melting under pressure in hydrogen prevents graphitization in the first two alloys. With 0.97 per cent Si fine graphite appears in spots associated with ferrite. With 1.23 per cent Si this type of graphitization occurs over most of the melt.

5. Melts made under pressure in nitrogen show structures resembling those made in air but contain more proeutectoid carbide.

An attempt will be made to interpret these changes in terms of the amount of hydrogen in solution at the time of freezing as judged from the circumstances of melting. It will be assumed that the chief effect of melting under pressure is to increase the amount of gas dissolved by the molten metal. This is justified by the fact that melting in nitrogen at elevated pressures does not stabilize the carbide to any extent, whereas melting in hydrogen does. The mechanical effect of pressure on the expansion due to graphitization may therefore be neglected in the range of pressure under consideration. The amount of hydrogen dissolved by a given alloy is dependent on the partial pressure of the hydrogen in the furnace and the temperature, which was 2500° F.

Arranged in the order of probable increase in hydrogen content of the alloys, the melting conditions are as follows: vacuum melting, melting in air, melting in hydrogen at atmospheric pressure and melting in hydrogen at pressure above atmospheric. In alloy No. 11 low hydrogen gives fine graphite and ferrite (Fig. 3). With increasing hydrogen the graphite flakes become larger and free carbide appears (Figs. 4 and 5) and finally the entire melt becomes white (Fig. 6). Alloy No. 12 shows a similar behavior. In alloy No. 13 the same trend occurs (Figs. 13, 14 and 15) but areas of fine graphite associated with ferrite appear in the melt of highest hydrogen content (Fig. 16). In alloy No. 14 all the eutectic carbide managed to graphitize (Fig. 21), producing a structure similar to the graphitized spots in alloy No. 13.

The change in graphite flake size in these alloys resembles changes previously observed in cast iron melted under circumstances conducive

to a change in its hydrogen content.[1]   In the cast iron it was found that as the hydrogen increased the graphite flakes increased in size, reached a maximum and finally grew smaller again.   Increasing additions of sulphur to an iron-carbon-silicon alloy containing 2 per cent Si produced a similar series of flake sizes, and remelting the same pieces in hydrogen at atmospheric pressure gave mottled structures in alloys above 0.15 per cent S.[2]

From the work just described, it appears that lowering the silicon in iron-carbon-silicon alloys produces substantially the same effect as increasing the sulphur in so far as the response to hydrogen is concerned. For a given melting condition, the amount of eutectic and proeutectoid carbide increases as the silicon is lowered and as the hydrogen is increased.

This conclusion does not apply to the carbide of the eutectoid.   In alloy No. 14 increased amounts of ferrite appear at both ends of the series; i.e., in melts made in vacuo and in melts made under pressure in hydrogen (Figs. 18 and 21).   In alloy No. 13 the ferritic areas are closely associated with white iron (Fig. 16).   A similar phenomenon often occurs in chill tests of gray iron, in which a ferritic zone is found between the white portion and the gray pearlitic part.[3]

For this reason the effect of a faster cooling rate on the iron carbon-silicon alloys was investigated.   The crucible was supported by an alundum tube, which in turn rested on a polished steel rod passing through a brass bushing in the lower stopper of the Globar furnace tube. At any time the crucible could be lowered so as to bring it into the cold part of the furnace without changing the atmosphere and pressure in the furnace tube.   In this way melts were made in vacuo, in air and in hydrogen and cooled rapidly.   These were melted in the usual way and held 30 min. at 2500° F.   Cooling curves were not obtained but optical readings on melts made in air indicated that a temperature of 1500° F. was reached in five minutes.

STRUCTURE OF FAST COOLED MELTS

Alloy No. 11 (Si 0.47 per cent) was fully white when melted in hydrogen at atmospheric pressure.   Melting in air gave a few scattered areas of fine graphite while melting in vacuo gave numerous spots of fine graphite resembling those shown in Fig. 30.

Alloy No. 12 (Si 0.73 per cent) melted in vacuo had the structure shown in Fig. 26, which consists of ferrite, pearlite and fine graphite. There is no eutectic or proeutectoid carbide.   Comparison with Fig. 25 shows that fast cooling has increased the amount of pearlite, which is concentrated at the boundaries of the eutectic cells.

---

[1] References are at the end of the paper.

Melting in air and fast cooling gave the structure shown in Fig. 28. Ferrite occurs at the centers of the eutectic cells while the rest of the matrix is pearlitic. Small islands of eutectic carbide are scattered
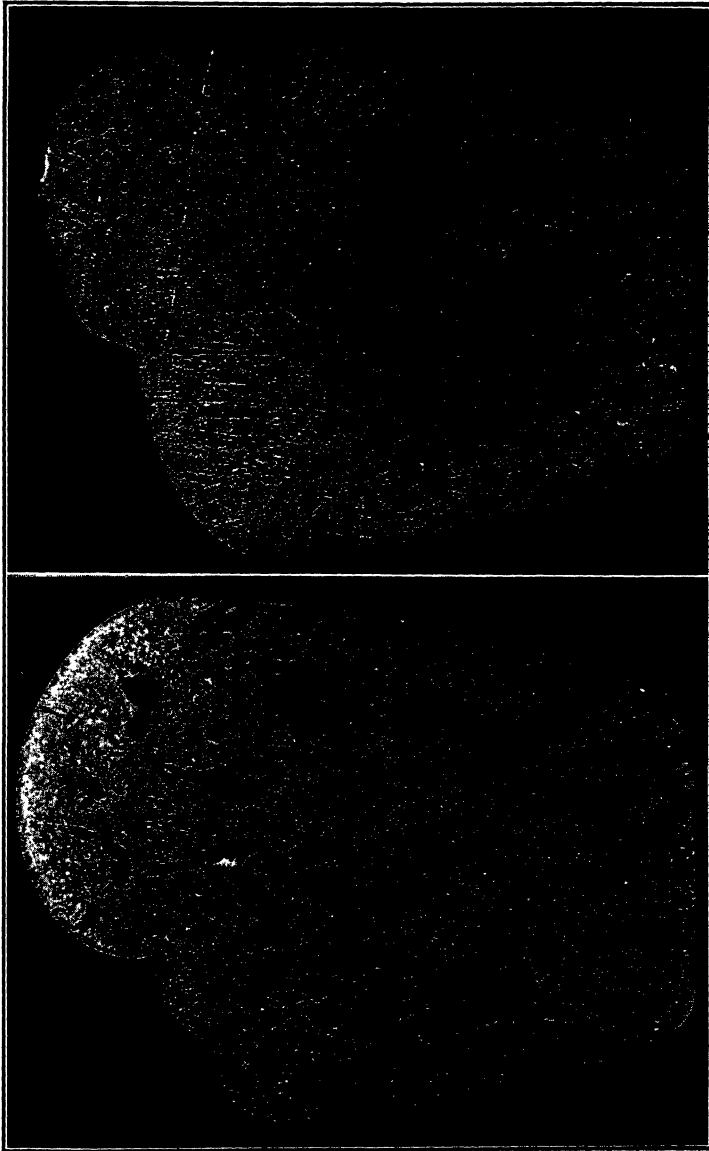
FIG. 23.

FIG. 24.

FIG. 23.—ALLOY NO. 13 MELTED IN HYDROGEN AT A PRESSURE OF 150 LB. PER SQ. IN. ETCHED, ×3.
FIG. 24.—ALLOY NO. 11 MELTED IN NITROGEN AT A PRESSURE OF 100 LB. PER SQ. IN. ETCHED, ×3.

throughout the interior and the bead extruded on top has a white core. Very fine graphite occurs over most of the melt. Comparison with the melt slowly cooled in air (Fig. 27) shows that fast cooling has produced:

(1) a marked increase in the amount of ferrite, (2) an increase in the amount of eutectic carbide, (3) a decrease in the amount of proeutectoid carbide.   (The fine needles in Fig. 9.)
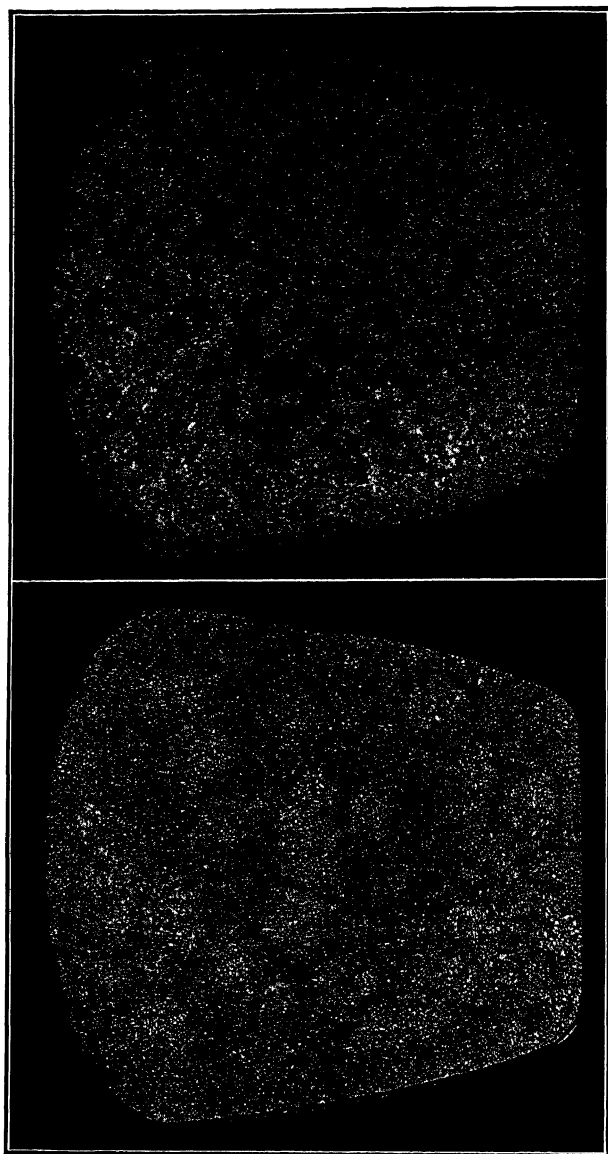
FIG. 25.—ALLOY NO. 12 MELTED IN VACUO AND SLOW-COOLED. ETCHED. ×3.
FIG. 26.—ALLOY NO. 12 MELTED IN VACUO AND FAST-COOLED. ETCHED. ×3.

Melting alloy No. 12 in hydrogen and fast cooling gave the structure shown in Fig. 30.   Most of the melt is white and consists of pearlite and eutectic carbide.   Fine graphite occurs in spots and around the cavities near the center.   In the interior of these spots freeferrite appears.

Comparison with the melt slow-cooled in hydrogen shows a very great increase in the amount of eutectic carbide.   It should also be noted that no free ferrite occurs in the slow-cooled melt (Figs. 29 and 10).
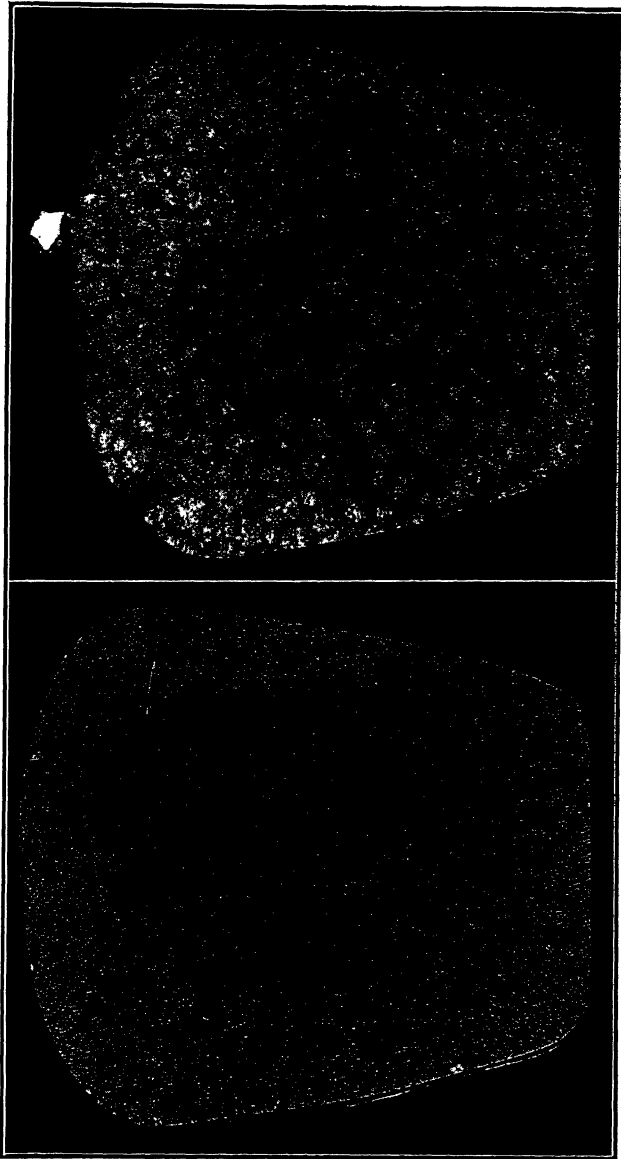
FIG. 27.

FIG. 28.

FIG. 27.—ALLOY NO. 12 MELTED IN AIR AND SLOW-COOLED.   ETCHED.   X 3.
FIG. 28.—ALLOY NO. 12 MELTED IN AIR AND FAST-COOLED.   ETCHED.   X 3.

Alloy No. 13 (Si, 0.97 per cent) melted and fast-cooled in vacuo resembled Fig. 26 except that the amount of pearlite was less.   Graphite occurred as very fine particles.

Melting in air and fast cooling gave a structure resembling Fig. 32. Here the outer part is ferrite with pearlite along the ribs of the dendrites (*A* in Fig. 35). The interior is a mixture of ferrite and pearlite. Graph-
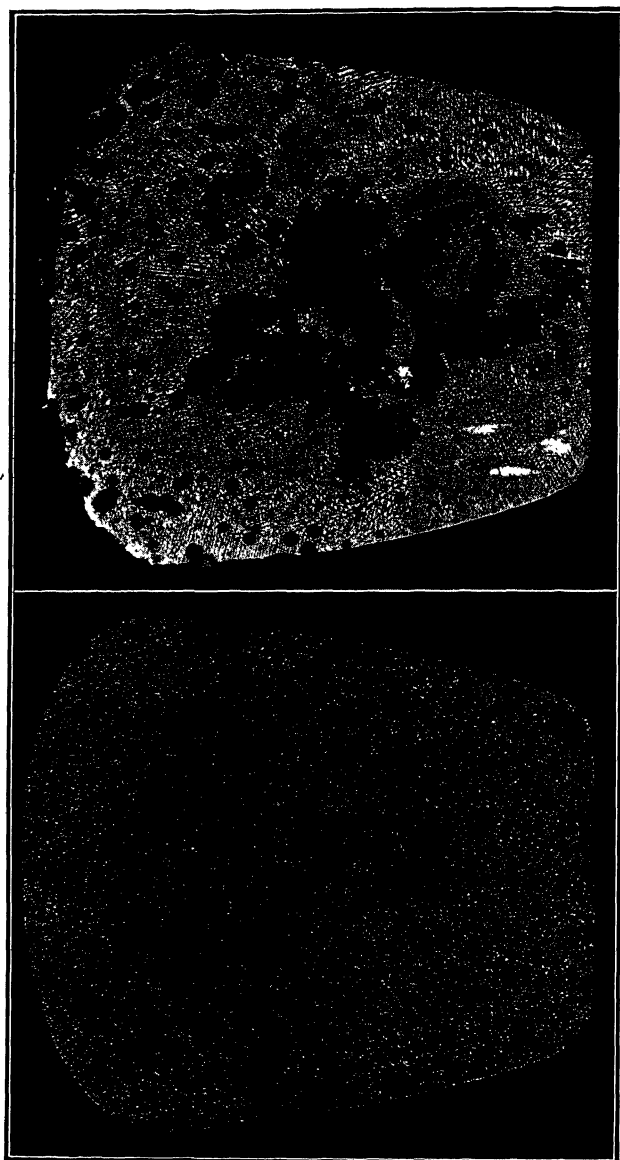
Fig. 29.

Fig. 30.

Fig. 29.—Alloy No. 12 melted in hydrogen and slow-cooled. Etched. ×3.
Fig. 30.—Alloy No. 12 melted in hydrogen and fast-cooled. Etched. ×3.

ite occurs as very fine particles. Several small islands of eutectic carbide appear in this melt (*B* in Fig. 35). There is no proeutectoid carbide in the graphitized portion.

Melting in hydrogen and fast cooling gave substantially the same result as melting in air. The entire melt is shown in Fig. 32. Comparison with the melt made in hydrogen and slow-cooled shows a remarkable increase in the amount of ferrite (compare Fig. 32 with Fig. 31). At the same time fast cooling produced more eutectic carbide.

The results with alloy No. 14 (Si 1.23 per cent) were similar in that fast cooling produced more ferrite than slow cooling in melts made in air and in hydrogen. No eutectic carbide occurred in these melts.

It appears from these experiments that similar structural changes may be obtained either by increasing the cooling rate or by increasing the amount of hydrogen by melting under pressure. For example, alloy No. 12 is white when melted and fast-cooled in hydrogen at atmospheric pressure (Fig. 30) and also when melted and slow-cooled in hydrogen at a pressure of 100 lb. per sq. in. (Fig. 11). Alloy No. 13 melted and fast-cooled in hydrogen at atmospheric pressure shows islands of eutectic carbide associated with fine graphite (similar to Fig. 35). The same alloy melted in hydrogen at a pressure of 150 lb. per sq. in. and slow-cooled shows fine graphite in a ferritic matrix, closely associated with eutectic carbide (Fig. 16). The difference here is one of degree rather than of kind.

The structure of the original sand-cast bars offers additional evidence on the effect of cooling rate. Fig. 33 is a section of alloy No. 14 as cast. The light circular areas have the structure shown at A in Fig. 34, consisting of fine graphite in a matrix of ferrite. Only a little pearlite occurs along the ribs of the primary dendrites. The darker areas in Fig. 33 have the structure shown at B in Fig. 34 and consist of pearlite and eutectic carbide. The junction of the white and gray portions is very sharp. Alloy No. 13, as cast, had a structure resembling Fig. 33 except that the graphitized areas were less numerous. Alloys No. 11 and No. 12 were white throughout.

The structures shown in Fig. 34 and in Figs. 35 and 16 are of the same type and it is worth while to speculate as to how they might have been formed. On the basis of previous work on the mechanism of freezing,[1] it may be assumed that the cell structure shown in Fig. 33 formed during the freezing of the eutectic and that each circular area represents a crystallization center. The first part of the eutectic to freeze, therefore, managed to graphitize. The question arises as to whether graphitization occurred directly on freezing or whether a carbide eutectic froze first.

We might imagine crystallization of the eutectic liquid just beginning at one of the cell centers shown in Fig. 33 and assume that a carbide eutectic formed similar to that at B in Fig. 34. As solidification progressed the heat liberated locally held this spot at temperature long enough for graphitization to start, resulting in fine graphite like that at A

in Fig. 34.   Meanwhile additional carbide eutectic was freezing around the graphitized area.   This in turn continued to graphitize as the front of solidification advanced.   It is obvious that the first part to freeze
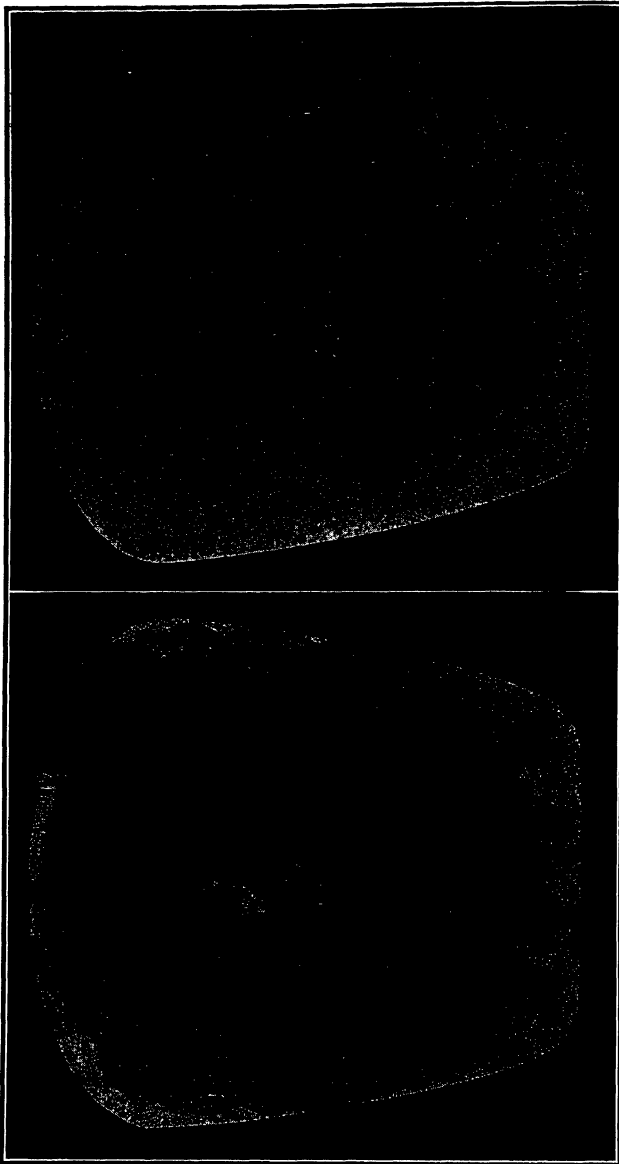
FIG. 31.
FIG. 31.—ALLOY NO. 13 MELTED IN HYDROGEN AND SLOW-COOLED.   ETCHED.   ×3.
FIG. 32.—ALLOY NO. 13 MELTED IN HYDROGEN AND FAST-COOLED.   ETCHED.   ×3.
FIG. 32.

would have greatest opportunity to graphitize and that continued cooling of the sample might bring the process to an end before all the carbide eutectic was completely broken down.   Patches of eutectic carbide
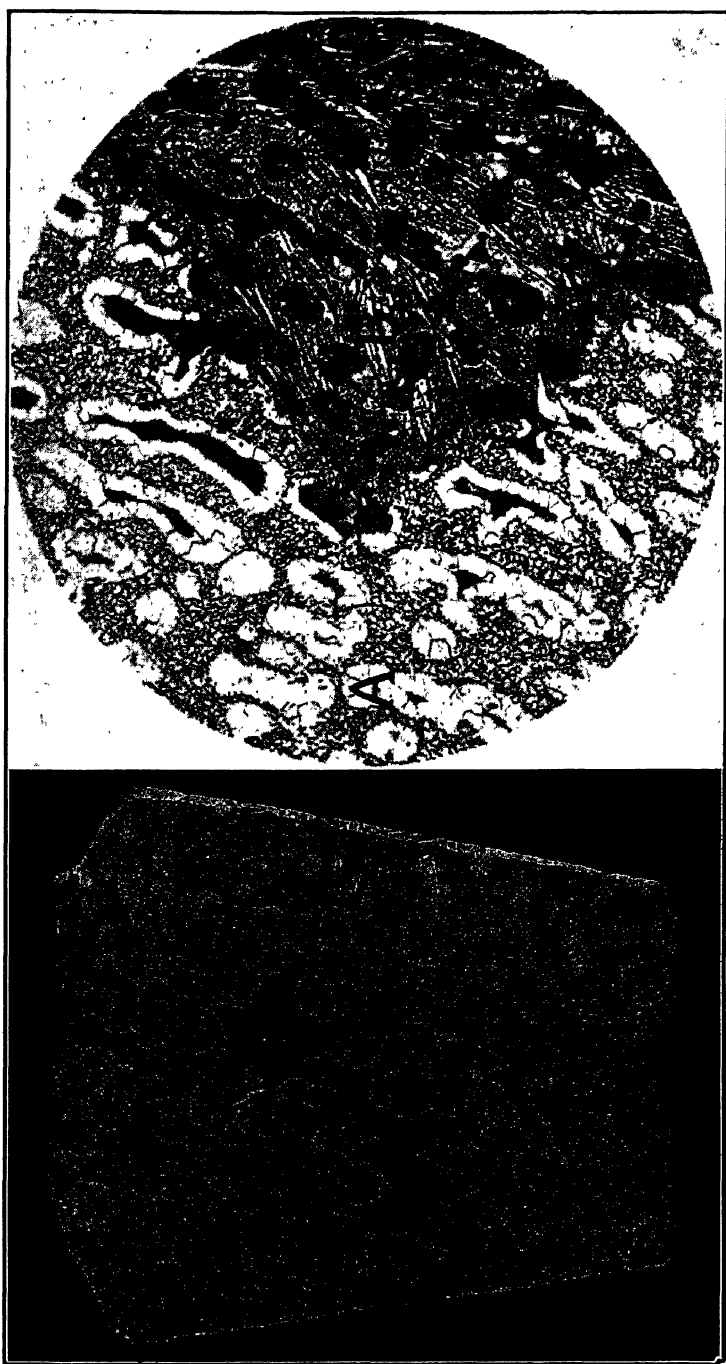
Fig. 33.

Fig. 34.

Fig. 33.—Alloy No. 14 as cast. Etched. × 3.
Fig. 34.—Detail of structure shown in Fig. 33. Etched in HNO₃. × 150.

would thus be left at various places between the crystallization centers, as shown in Fig. 33. Such a mechanism would effectively prevent the growth of long flakes and would leave a "graphite eutectic" in immediate juxtaposition to a carbide eutectic, as shown in Figs. 16, 34 and 35.

The mechanism postulated here offers an explanation for the similarity of structure occurring in fast-cooled melts and those made under pressure. Both are attributed to delayed graphitization produced in the former by rapid cooling and in the latter by excessive hydrogen
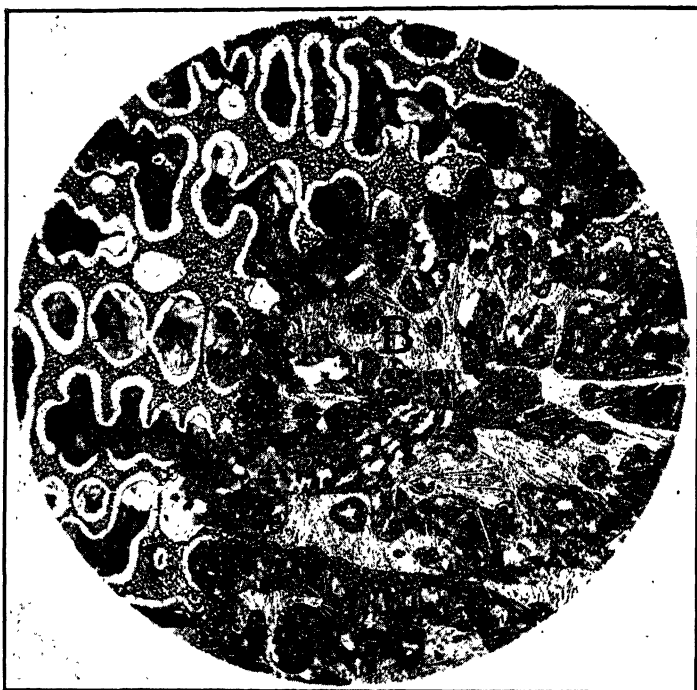
FIG. 35.—ALLOY NO. 13 MELTED IN AIR AND FAST-COOLED. ETCHED IN HNO₃.
× 100.

content. It does not offer any reason as to why ferrite should be associated with fine graphite of this type.

Parke, Crosby and Herzig have proposed an explanation for the occurrence of a ferritic zone between the carbidic and the pearlitic regions in thin cast-iron wedges.[3] They conclude that the graphite in the ferritic part formed in the solid state, the ferrite resulting from dissociation of solid cementite. The structures shown by these authors resemble in many ways those found in the iron-carbon-silicon alloys, which may have originated in the same manner. Work is being continued on this problem, which seems, from the behavior of the pure alloys, to be a characteristic of the iron-carbon-silicon system.

Summary

From melts made under different atmospheres at various pressures, the following conclusions are drawn:

1. Hydrogen stabilizes the eutectic carbide in iron-carbon-silicon alloys containing very little sulphur and manganese. The effect diminishes as the silicon content is increased.

2. Melting under pressure in hydrogen increases the stabilizing effect.

3. Similar structural changes are obtained by increasing the cooling rate or by melting under pressure in hydrogen.

References

1. A. Boyles: The Freezing of Cast Iron. *Trans.* A.I.M.E. (1937) **125**, 141–203.
2. A. Boyles: The Formation of Graphite in Gray Iron. *Trans.* Amer. Foundrymen's Assn. (1938) **46**, 297–340.
3. R. M. Parke, V. A. Crosby and A. J. Herzig: Notes on the Graphitization of Gray Cast Iron. *Metals and Alloys* (1938) **9**, 9–14.

Kinetics of the Decomposition of Austenite at Constant Temperature

By J. B. Austin* and R. L. Rickett,* Associate Member A.I.M.E.

Measurements of the rate of decomposition of austenite at constant temperature are commonly represented by plotting the percentage transformed on linear coordinates against time on either a linear or a logarithmic scale, a method that yields a curve that in shape resembles an integral sign (Fig. 1). A graph of this kind is not always convenient because extrapolation to the beginning or end of the transformation, or even interpolation, may be uncertain unless there are a large number of observations, which seldom happens; furthermore, the degree of consistency of a set of measurements is difficult to judge from such a curve. It is desirable therefore to find some mode of plotting, or even better to find a standard variety of graph paper, that gives a straight line instead of the integral shape. The straight line has many advantages; the number of readings required to fix the position of the curve is greatly reduced, interpolation is easy and rapid, extrapolation can be carried out with greater confidence and, finally, the consistency of the measurements is readily estimated from the scatter of the points. The last advantage is particularly valuable when the data are obtained by direct microscopic examination alone, because they are influenced by the skill of the observer in estimating the relative size of areas, possibly also by undetected inhomogeneity of the specimen. A search for ways of representing the observations as a straight line yielded two methods which are described in this paper. The paper also includes an account of some interesting relations brought to light in applying these methods to the available experimental data.

Usually the best way to derive such a method of plotting is to base it on established principles of chemistry and physics, as has been done, for example, for the temperature variation of the equilibrium constant of a chemical reaction. But so little is known of the mechanism of the decomposition of austenite, and so little is available in the way of well established background for changes of this kind, that it is simpler to rely upon purely empirical means. The general plan therefore is to study existing data with a view to finding some function of the direct observations that will

reduce the data to a straight line, a device for treating observations that often offers advantages and has been widely used.

The first data taken for study were the original dilatometric measurements made by Davenport and Bain.[1] Their investigations, which included six steels of different composition and covered the temperature range from 340° C. (644° F.) to room temperature, are particularly suitable because the observations were carefully made, were almost completely objective and furnished a practically continuous record of the transformation. Inspection of their results, such as the typical set given in Fig. 1, shows that the rate curves can be roughly grouped into two classes. At the higher temperatures the curves have but one step, which in shape resembles that of an integral sign, whereas at the lower temperatures the decomposition appears to take place in two steps. There is no sharp demarcation between the two groups, one merging into the other gradually, but in general the simple ∫ shape* is characteristic of temperatures above 260° C. (500° F.) and the two-step curve appears below 200° C. (400° F.).

The data for the higher temperatures were studied first because the curves are simpler in this range. These isothermal rate curves are not unlike the reaction velocity curve for a monomolecular reaction, but a closer comparison reveals discrepancies that cannot be satisfactorily explained on the basis that the decomposition of austenite is monomolecular or even bimolecular. There can be no doubt therefore that the transformation of austenite is a relatively complex reaction. The form of the curves suggests the logistic, or autocatalytic, curve which is widely used in statistical studies of population and in representing the velocity of an autocatalytic chemical reaction. Its equation is:

$$\log \frac{P}{100 - P} = k't + C' \qquad [1]$$

where P is the amount of growth, or the amount transformed, at the time t, expressed in percentage of the total growth or transformation, and k' and C' are arbitrary constants.

There is one important difference, however, between the curves of Fig. 1 and the ordinary autocatalytic curve given by equation 1, for this equation represents a curve that is symmetrical about the point for 50 per cent transformation when time is plotted on a linear scale, whereas the curves for the decomposition of austenite are symmetrical when time is plotted on a logarithmic scale as in Fig. 1. Consequently, it is to be expected that a better fit should be obtained by modifying equation 1 to give:

---

[1] References are at the end of the paper.

* In this discussion the isothermal rate curves are described as ∫-shaped, whereas the curve showing the variation of rate with temperature is called the S curve.

$$\log \frac{P}{100 - P} = k \log t + C \qquad [2]$$

or

$$\frac{P}{100 - P} = D t^k \qquad [3]$$

where D is a new arbitrary constant.
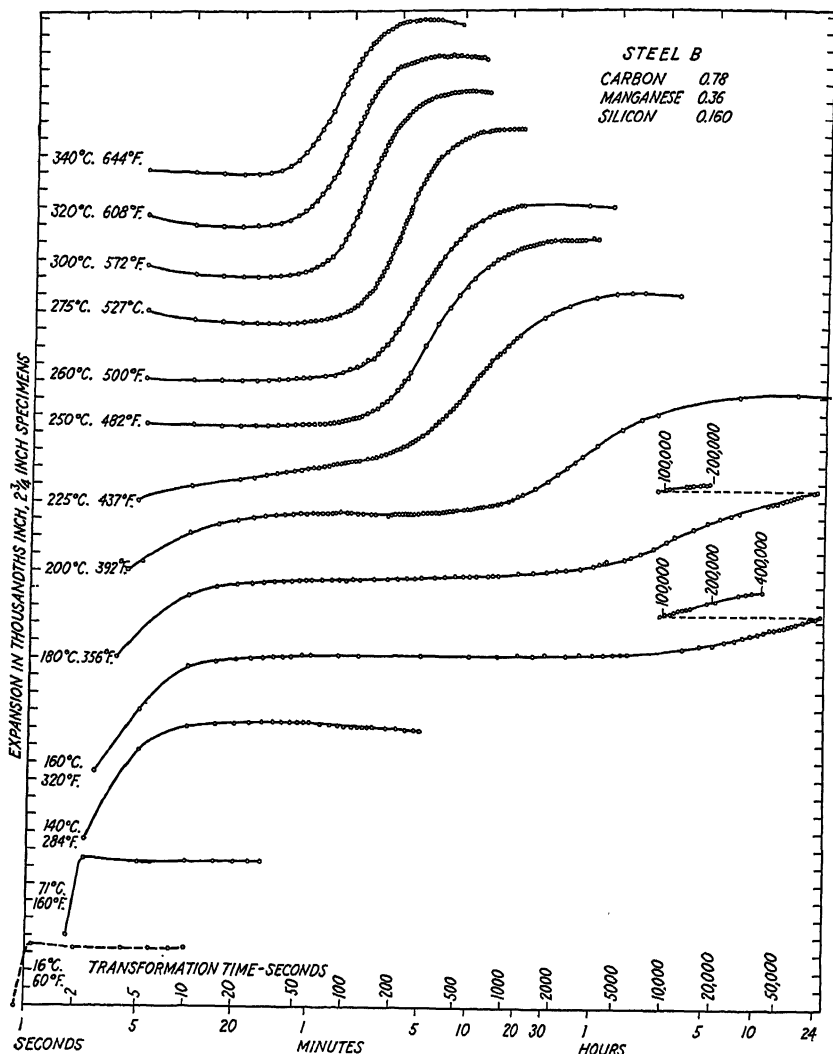
FIG. 1.—ISOTHERMAL RATE CURVES FOR THE DECOMPOSITION OF AUSTENITE IN STEEL B. After Davenport and Bain.[1]

If the data do follow this relation, a plot of $\log P/(100 - P)$ against $\log t$ should give a straight line. In making such a graph it is convenient

to use the tables giving values of $P/(100 - P)$ for a given value of P that are included in many chemical texts on the discussion of the conductance of solutions.*

The conversion of values of $P/(100 - P)$ and t into logarithms, which is necessary if ordinary graph paper is used, can be avoided by the use of double-logarithmic coordinate paper, but this method has in practice the disadvantage that the values of $P/(100 - P)$ cover a range of several orders of magnitude and a very large sheet of double-log paper is necessary.
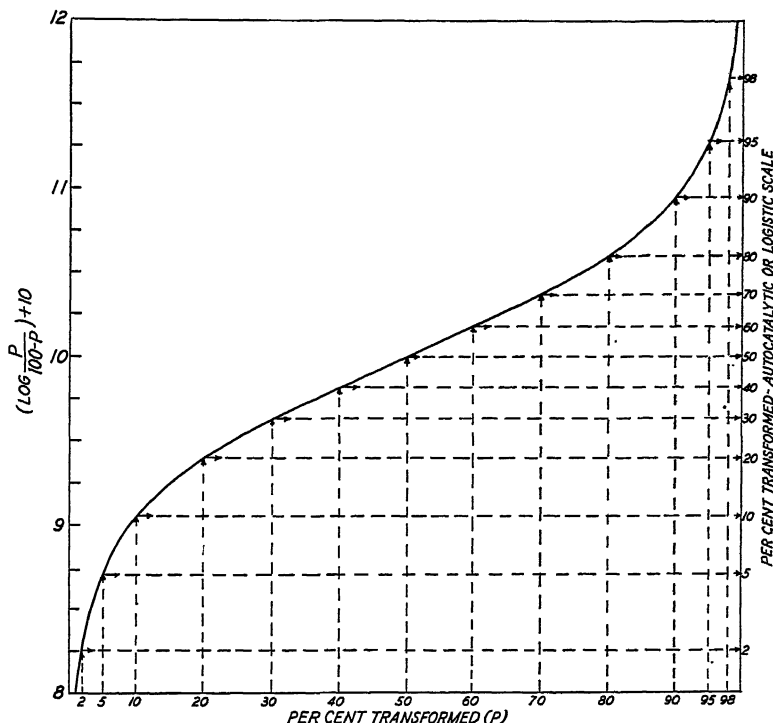
FIG. 2.—DERIVATION OF THE "AUTOCATALYTIC" SCALE.

The difficulty can be overcome by using the logistic or autocatalytic scale described by E. B. Wilson,[2] which is constructed from the curve relating $\log P/(100 - P)$ with P as is shown in Fig. 2. A curve is first drawn by plotting values of $\log P/(100 - P)$ (on the left-hand axis) against P as ordinate. The intercept on the curve corresponding to different values of P is then projected on the right-hand axis and gives a scale whose intervals are such that they bear the same relation to P as $\log P/(100 - P)$. If this scale is used as ordinate, values of P may be plotted directly. As the curve in Fig. 2 extends to infinity for zero per cent or 100 per cent

---

* See, for example, Findlay: Practical Physical Chemistry, 163. New York, 1923. Longmans, Green and Co.

transformation, the scale cannot be used for extrapolating to the beginning or the end of the reaction, but it is easy to extrapolate to, say, 1 per cent or 99 per cent transformation, which is equally useful and more definite, for the terms "beginning" and "end" have little significance when applied to a reaction of this kind, since "beginning" and "end" should be defined in terms of the initial or final movement of atoms or of the transformation of unit cells, and such quantities are not observable by ordinary methods of studying reaction velocity.

Graph paper having the autocatalytic scale as ordinate and a linear scale as abscissa can be purchased, but with these coordinates it is necessary to plot the logarithm of time, which requires a calculation. An alter-
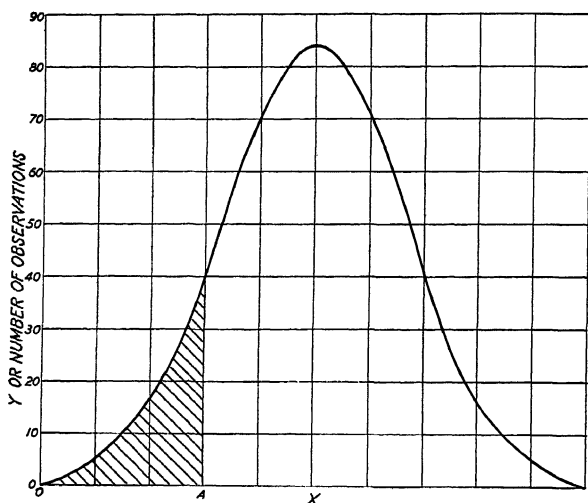
FIG. 3.—TYPICAL "PROBABILITY" CURVE.

native that we have found useful is to rule the autocatalytic scale on the linear axis of semilog graph paper, giving a chart upon which P and t may be plotted directly. In using paper of this kind the autocatalytic scale is best terminated at 1 per cent and 99 per cent transformation. One reason for this has already been given but another is that a precise determination of the fraction transformed becomes increasingly difficult for very small or very large percentages. The use of 1 per cent and 99 per cent permits the estimation of the approximate time necessary for complete transformation of austenite in a steel to be heat-treated by the Austempering method [cf. *Steel* (1937) **100**, 42–45] and at the same time avoids going into the range where the data are not precise and errors in calculation are magnified by the extension of the scales.

Another curve of similar shape, which looks as though it might fit the data for the decomposition of austenite, is the integral of the probability function. If the probability function itself is plotted on linear coordi-

nates, it gives the "probability" curve shown in Fig. 3. This is also the form of the so-called frequency curve for a series of observations that are controlled by chance alone. For example, if a record is made of a large number of throws of a pair of dice, and if the number of times each possible sum turns up is plotted as a function of the sums, the results give a curve of this type, provided the dice are true and the thrower has no special skill.

The integral of the probability curve, or the cumulative frequency expressed as a percentage of the total number of throws, gives a curve of the type shown in Fig. 4. For example, the integral of the probability function between the limits $x = 0$ and $x = a$, which is represented by
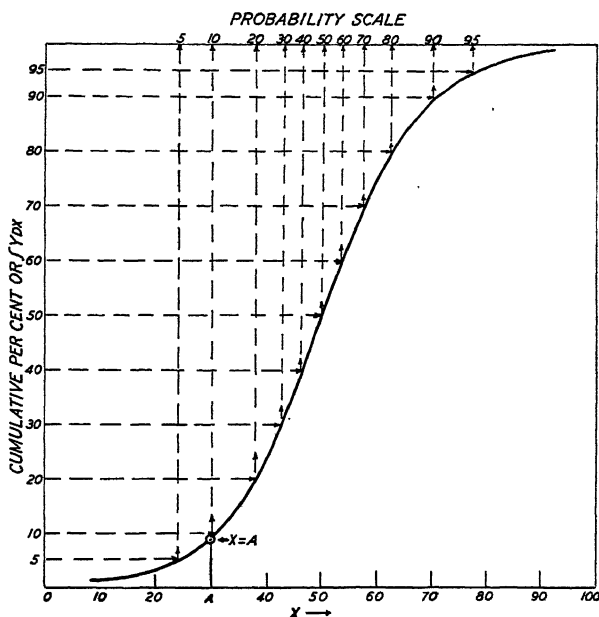
FIG. 4.—DERIVATION OF "PROBABILITY" SCALE FROM INTEGRAL OF "PROBABILITY" . CURVE SHOWN IN FIG. 3.

the shaded area in Fig. 3, gives a point on the curve of Fig. 4 for $x = a$. Or with the frequency curve, the fraction of the total number of readings that lie below the value a gives a point for a in Fig. 4.

The ∫-shaped curve so obtained closely resembles the curves for the rate of decomposition of austenite and also the autocatalytic curve of Fig. 2, and, as with the autocatalytic curve, it can be used to derive a scale that permits data conforming to it to be plotted on a straight line. This probability scale is derived by the same process used for the autocatalytic scale, as is illustrated in the diagram. It consists in drawing intercepts on the curve for even values of the integrated probability function and then projecting these intercepts on the other axis (Fig. 4). If, therefore, the data for the decomposition of austenite fit this curve, they will give a

straight line if the percentage transformed is plotted on the probability scale against time on a logarithmic scale.

The probability scale differs from the autocatalytic scale in being more extended at the ends, but each appears to offer a good chance of giving the desired result therefore both have been tried.   Graph paper having the probability scale as ordinate and a logarithmic scale as abscissa can be purchased, and on this type of paper P and t can be plotted directly.
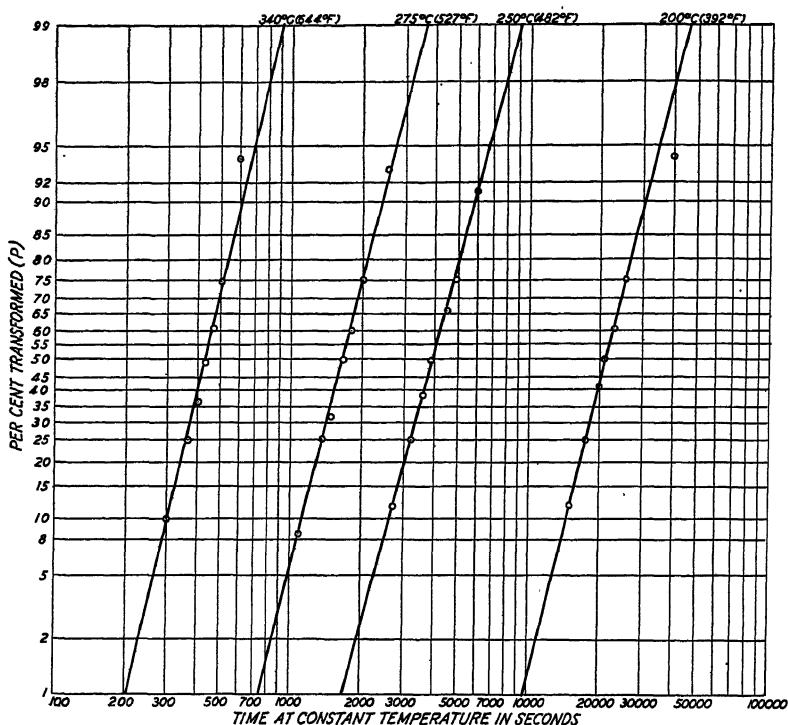
FIG. 5.—DILATOMETER DATA OF DAVENPORT AND BAIN FOR STEEL A PLOTTED WITH LOGARITHMIC SCALE FOR TIME AND THE "AUTOCATALYTIC" SCALE FOR PERCENTAGE TRANSFORMATION.

As with the autocatalytic scale, the probability scale is terminated at 1 per cent and 99 per cent transformation, because no useful purpose is served by going beyond these limits and the extension of the scale becomes so great that experimental errors, which are most likely to occur at the ends of the scale, are greatly magnified.

As a first test of these methods, the dilatometric measurements of Davenport and Bain[1] have been plotted in both ways.   In treating these data the reasonable assumption has been made that the fraction of the total increase in length that is covered up to a given time represents the percentage of austenite that has decomposed in that interval.   In all, 16 sets of data, including at least one set for each of the six steels, have

been plotted and in every case the result is a straight line on each type of plot. There are occasional deviations when the amount transformed is below 5 per cent or above 95 per cent, but it is difficult to say definitely whether these are real departures or represent uncertainties in operation or errors in calculation of the percentage transformation from the change in length that have been magnified by the extended scale.

Typical examples of the results obtained with these data are shown in Figs. 5 and 6, which give the measurements for steel A plotted on "log-autocatalytic" paper and on "log-probability" paper, respectively.

As a further check, an additional series of 15 sets of data taken from the literature, chiefly from the publications of the Kaiser Wilhelm-Institut für Eisenforschung, were tested. These measurements were all
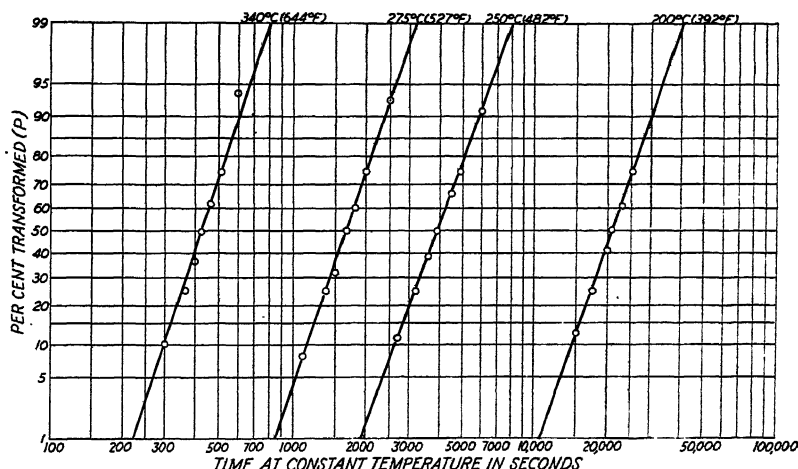
FIG. 6.—DILATOMETER DATA OF DAVENPORT AND BAIN FOR STEEL A PLOTTED WITH A LOGARITHMIC SCALE FOR TIME AND THE "PROBABILITY" SCALE FOR PERCENTAGE TRANSFORMATION.

made with automatic or semi-automatic apparatus and were not restricted to the dilatometric method. Some, for example those of Fig. 7, were made by following the change of ferromagnetism. In taking such data from published articles it was frequently necessary to read values from relatively small diagrams, so that high accuracy is not possible. Consequently, the conclusions drawn from results with these data are not as well founded as those based upon the direct observations of Davenport and Bain.

In view of the consistency with which the most reliable measurements plot on a straight line on either "log-autocatalytic" or "log-probability" scales, it seems justifiable to conclude that both types of graph can be successfully used. And judging from the data we have tested, neither type of plot has any marked advantage over the other. It may well be

that when a much larger number of measurements is available one kind will give a better straight line than the other but at present no definite choice can be made. As a matter of convenience, the fact that "log-probability" paper can be purchased gives this method some advantage, but if there were enough demand for "log-autocatalytic" paper, it could undoubtedly be obtained as well.

It should be noted that the fact that the data plot on a straight line on "log-probability"-"log time" coordinates rather than on "log-probability"-time coordinates means that we are dealing here with a skewed probability curve instead of a symmetrical one such as is shown in Fig. 3. Moreover, the closeness with which the data follow a probability curve, even though it be skewed, raises the question of whether it may not be simpler for many purposes to look upon the decomposition of austenite at constant temperature as a statistical process of which the rate is governed by chance rather than to seek a detailed mechanism of the transformation.

FIG. 7.—MAGNETIC MEASUREMENTS OF WEVER AND HÄNSEL[5] PLOTTED ON "LOG-PROBABILITY" PAPER.

Although the two methods give a straight line, and in that respect are equivalent, there is some difference between them in the time for 1 per cent and 99 per cent transformation as derived by extrapolating the lines. This is illustrated by Table 1, which compares the times for steel A as read from Figs. 5 and 6 with estimates of the time for the "beginning" and "end" of the reaction made by inspection of the original ∫-shaped curves. Comparing the two methods of plotting, the log-probability method indicates a longer "starting" time but a faster reaction than does the other way, but the differences are not of great significance from the point of view of heat-treatment. For example, at 250° C. (482° F.) the log-autocatalytic graph shows that the reaction is 1 per cent complete in 1700 sec., or about 28 min., whereas the log-probability plot indicates 1900 sec., or about 32 min. The difference for 99 per cent transformation is somewhat greater, the log-autocatalytic method giving 9200 sec. or about 2½ hr., whereas the log-probability curve gives just 2 hr. This may appear to be quite a difference but in terms of percentage transformation it is relatively small. Thus, if the

TABLE 1.—*Comparison of Time Required for* 1 *Per Cent and for* 99 *Per Cent Transformation in Steel A as Calculated by Different Methods*

Temperature	Time, Seconds					
	1 Per Cent Transformation			99 Per Cent Transformation		
	"Auto-catalytic Curve"	"Proba-bility Curve"	"Beginning" Read Directly from Curves Similar to Those in Fig. 1	"Auto-catalytic Curve"	"Proba-bility Curve"	"End" Read Directly from Curves Similar to Those in Fig. 1
340° C. (644° F.).....	205	230	155	910	810	700
275° C. (527° F.).....	740	850	500	3,650	3,200	3,300
250° C. (482° F.).....	1,700	1,900	1,300	9,100	7,200	10,000
200° C. (392° F.).....	9,500	10,500	3,600	46,000	42,000	100,000

log-autocatalytic plot should be the more accurate but the log-probability curve was actually used, and a sample was heated at this temperature for only 2 hr. instead of 2½ hr., it would still be 97 per cent transformed.

This point serves to emphasize the extreme slowness with which the last few per cent austenite decomposes under some conditions and to demonstrate that in practical austempering operations it may be necessary to strike a balance between the cost of converting the last traces of austenite and the possible improvement in quality of steel that results therefrom. For instance, Fig. 5 shows that at 250° C. (482° F.) 95 per cent of the austenite is decomposed after 1 hr. 54 min., whereas it takes 2 hr. 30 min., or 36 min. more, to get an additional 4 per cent decomposed. The cost of transforming that last 4 per cent is therefore disproportionately high and it may well be that in many applications the difference in the properties of the steel corresponding to the last 4 per cent does not justify such increased expense.

The slow rate at the beginning and end of the reaction also serves to explain the differences between the times for 1 per cent and 99 per cent decomposition and the time for the "beginning" and "end" as read from the original curves. At the higher temperatures, where the reaction is fast, there is no great difference, but as the temperature is lowered and the reaction becomes slower the discrepancy becomes greater.

One of the most interesting points that appeared in studying the data of Davenport and Bain is the fact that in the temperature range in which the simple ∫-shaped curves appear the rate curves for a given steel at different temperatures are parallel. This is illustrated by the lines shown in Figs. 5 and 6 for steel A, but it was observed for other steels as well. It indicates that the ratio of the time required for 99 per cent transformation to that required for 1 per cent transformation is the same over the temperature range included in the figures—or, another way of expressing

it is that the exponent k in equation 3 is independent of temperature. The interpretation to be placed on this behavior is not clear, but this does not prevent it from being a possible aid in the critical examination of a set of measurements. Thus, it appears probable that the data should not only plot on a straight line but that the rate curves for different temperatures over a considerable range should have the same slope.

This parallelism is most marked in the measurements of Davenport and Bain but is not evident to the same degree in the other data studied, although there are some indications of it. Why this should be true is not clear. It may be that it is characteristic of dilatometric data only,
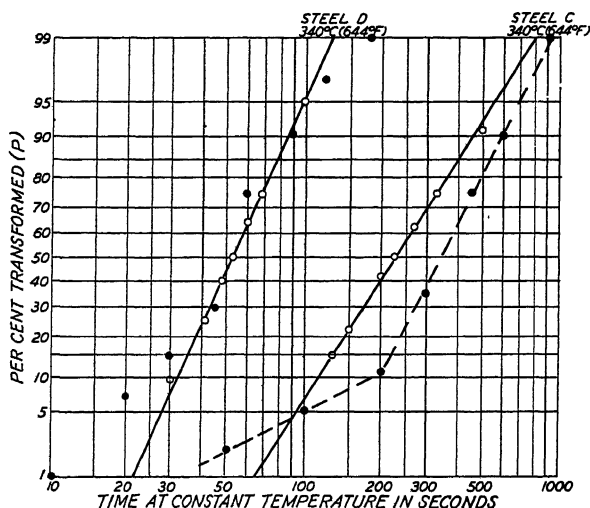
Fig. 8.—Comparison of rate data obtained by microscopic examination of quenched specimens (black disks) with dilatometer curves (circles) for same steel at same temperature.

since there is ample evidence to show that different methods of observation yield different results, or it may be due to errors in taking the published data from small diagrams. Whatever the cause, the phenomenon is so clearly evident in the dilatometric data that it cannot possibly be coincidence. Further discussion of it is reserved until a later section.

With the general form of the curves established by essentially objective methods it is of interest to see how closely this form is approached by measurements made by a more subjective method, such as microscopic examination of specimens quenched after different periods of exposure to the constant temperature. Examination of a large number of data obtained by this method has shown that they vary widely in consistency. Some plot reasonably well on a straight line, others show marked curvature and do not even remotely resemble a straight line. In a few cases in which a linear plot was obtained, the lines for different temperatures

are parallel but in general this is not true. Typical examples of the results obtained with the microscope are shown in Fig. 8 where they are compared with the dilatometer curve for the same steel at the same temperature. The curves for steel D, shown at the left, agree fairly well; those for steel C, on the right, show very poor agreement. Both sets of data show a discrepancy between the dilatometer measurements and the microscope observations at the beginning of the reaction, the microscope indicating a greater amount of transformation in a given time than the dilatometer. The marked curvature shown by the curve for the microscope observations in this range has been observed for a great number of steels and can be interpreted in either of two ways: (1) It may represent a real action, which is observed under the microscope but which is not recorded by the dilatometer, or (2) it may indicate a tendency on the part of the observer to estimate too high a percentage of transformation product when only a small amount of it is present. An observational error of this sort is understandable, since the estimation of the relative magnitude of two areas becomes increasingly difficult as the size of one area decreases relative to the other. There is similar deviation at the end of the reaction, but on the average this does not seem to be so marked as the deviation for a small fraction transformed.

If the accumulation of further evidence should show that this is an observational error, in making measurements by the microscopic method it would be better to make more observations in the range 25 to 75 per cent transformation and to extrapolate to lower or higher percentages than to make direct observations near the beginning or end of the transformation.

The dilatometric measurements of Davenport and Bain do not extend beyond 340°C. (644° F.) but there is ample evidence from microscopic data on the same steels to show that the rate curves plot on a straight line at all temperatures between the nose of the S curve (that is, where the transformation goes fastest) and the temperature at which the martensite reaction appears. It is also evident from the microscopic data and from other measurements, such as those shown in Fig. 7, that if they are not complicated by the appearance of proeutectoid ferrite the rate curves for the transformation of austenite to pearlite and ferrite also give a linear plot. And even when proeutectoid ferrite does appear, it seems likely that the rate of transformation of the remaining austenite has the same general form, although the available data are not sufficient to establish this beyond question.

The parallelism of the rate curves for different temperatures, however, appears on the basis of present evidence to be confined to the range between the temperature of the nose of the S curve and the temperature at which martensite begins to appear; in other words, it holds for the range in which austenite transforms to bainite.

Turning now to the data for temperatures below about 200° C. (400° F.), that is, in the range in which the rate curves no longer have the single ∫-shape (Fig. 1), it is clear that the whole curve does not give a straight line when plotted on log-autocatalytic or log-probability paper. But it has been found that the second step in the curve, which has the same shape as the curves for higher temperatures, does give a straight line. That is, if one neglects the initial rise and takes the length at the flat
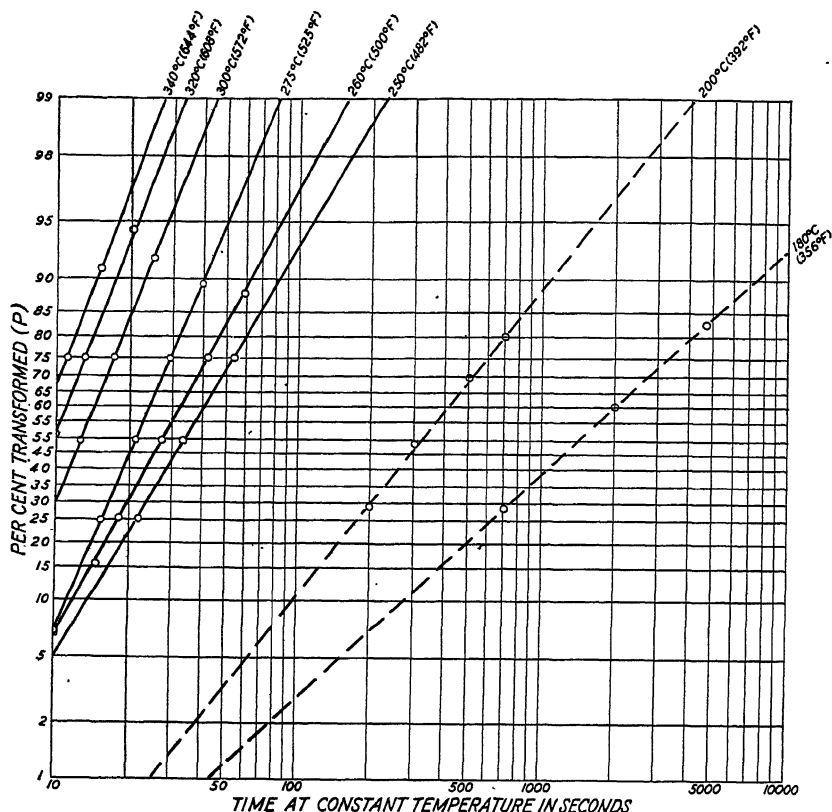
FIG. 9.—MEASUREMENTS BY DAVENPORT AND BAIN FOR STEEL B PLOTTED ON "LOG-AUTOCATALYTIC" PAPER.

Solid lines are transformation curves when there is apparently but one step; dashed lines indicate rate for second step in two-step curves.

portion of the curve as the starting level of a second reaction, the rest of the curve gives a linear plot. This is shown by the data for steel B in Fig. 9. What essentially has been done in this method of dealing with the data is to change the basis of calculation from the percentage of austenite that has disappeared to the percentage of some final product, which is appearing. The product that appears in the second step cannot be identified from the rate curves alone, but whatever it is, the rate of its appearance gives a straight line when plotted by the methods given.

VARIATION OF RATE OF TRANSFORMATION WITH TEMPERATURE

From 340° C. (644° F.), the highest temperature at which the dila-tometer measurements of Davenport and Bain were made, down to about 250° C. (480° F.) the isotherms are parallel for each of the steels studied (Figs. 5 and 6). The slope of the curve varies from steel to steel, but it is constant for any given steel, which, as already pointed out, indicates that k in equations 2 and 3 is independent of temperature within this range. The influence of temperature enters therefore only through the arbitrary constant C in equation 2 or D in equation 3. This constant varies inversely with temperature, which suggests at once that the loga-
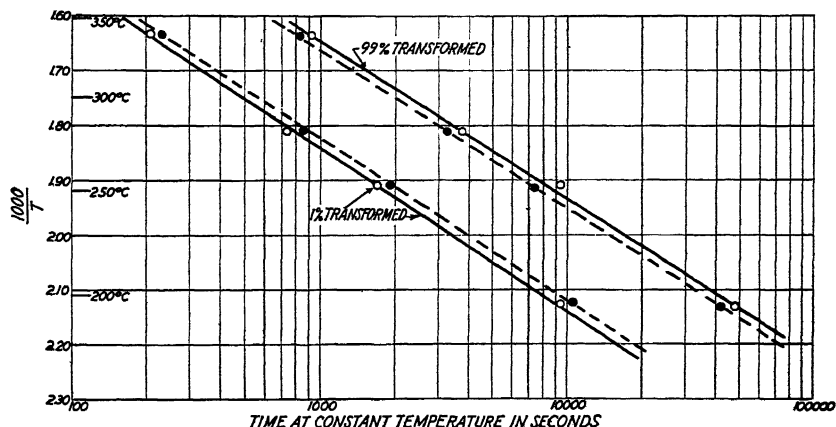
Fig. 10.—LINEAR VARIATION WITH TEMPERATURE OF LOGARITHM OF TIME REQUIRED FOR 1 PER CENT AND 99 PER CENT TRANSFORMATION (STEEL A).
Solid lines represent values obtained by extrapolation on "log-autocatalytic" paper (Fig. 5); dashed lines represent extrapolated values obtained on "log-proba-bility" paper (Fig. 6).

rithm of the constant may be proportional to the reciprocal of the absolute temperature, a type of relation that is known to hold for the temperature variation of a rate of chemical reaction or diffusion. As the rate of transformation of austenite in this temperature is probably controlled by a rate of diffusion it is not unreasonable to expect that such a relation should hold. If the logarithm of the constant is inversely proportional to the absolute temperature T, it follows that the logarithm of the time required to complete any given fraction of the transformation also varies linearly with $1/T$.

As a test of this relation, the time required for 1 per cent and for 99 per cent transformation in steel A has been plotted as a function of tempera-ture, with results shown in Fig. 10, in which time is plotted as abscissa on a logarithmic scale and the reciprocal of the absolute temperature on the Centigrade scale is plotted as ordinate on a linear scale. Steel A was selected because its isotherms are parallel over a larger temperature range

than are those for any other steel studied.   The differences between the two sets of lines give a good indication of the differences to be expected in using the two methods.   It is evident from the diagram that within this temperature range the logarithm of the time required for a given fraction of the austenite to decompose is proportional to $1/T$.

This result is useful in two ways; it provides an easy and accurate means of interpolating to obtain data for a temperature at which no direct measurements are available and it provides a criterion by which the consistency of a set of experimental data can be judged.   The use of such curves for extrapolation, however, is not recommended, because there are definite limits at both high and low temperatures to the range in which this relation holds.   At low temperatures it fails as soon as the simple isothermal curve begins to change to the more complex two-step type, and at high temperatures it fails when the rate of transformation begins to decrease; that is, at the nose or S_1 point of the so-called S curve. (See, for example, the curves of Fig. 7, which represent data obtained at such temperatures.)   In general, it should not be extended to a temperature above about 550° C. (or 1000° F.) nor to a temperature below about 250° C. (480° F.), and deviations above 250° C. (480° F.) are not uncommon.   There are, on the other hand, a few instances, such as steel A, in which the relation holds as low as 200° C. (380° F.).

Within the range 550° C. (1000° F.) to 250° C. (480° F.), however, we are justified in representing the variation in the logarithm of the constant by:

$$\log C = \frac{a}{T} + b \qquad [4]$$

where a and b are constants.   And combining this relation with equation 2 we have:

$$\log \frac{P}{100 - P} = k \log t + \frac{a}{T} + b \qquad [5]$$

which represents the decomposition of austenite as a function of time and of temperature within the limits stated.

It has already been pointed out that in the range in which the isothermal curves are of the two-step type the second step gives a straight line on log-probability or log-autocatalytic paper, but that these straight lines do not have the same slope.   It is also observed that the slope of such lines begins to change before the isothermal curve shows two clearly defined steps.   This is shown by the data for steel B in Fig. 9.   The curves for temperatures down to and including 275° C. (525° F.) have the same slope.   The curves for 260° C. (500° F.) and 250° C. (482° F.) have a distinctly smaller slope, even though the isothermals (Fig. 1) seem to have the simple one-step shape.   It is of interest, therefore, to

see how the time for 1 per cent and 99 per cent transformation varies with $1/T$ for this steel, and this has been done in Fig. 11, using the log-autocatalytic plot for extrapolating. The same type of curve, of course, is obtained for any other percentage transformation.

Above 275° C. (525° F.) the points fall on two parallel straight lines just as they did with steel A (Fig. 10). Just below 275° C. (525° F.), however, there comes a break. The points representing time for 99 per cent transformation lie on a straight line but the slope of the line is different. The points for the beginning of the reaction (1 per cent transformation) show a curious curvature around 250° C. (482° F.) but at still lower temperatures lie once more on a straight line. To sum up,
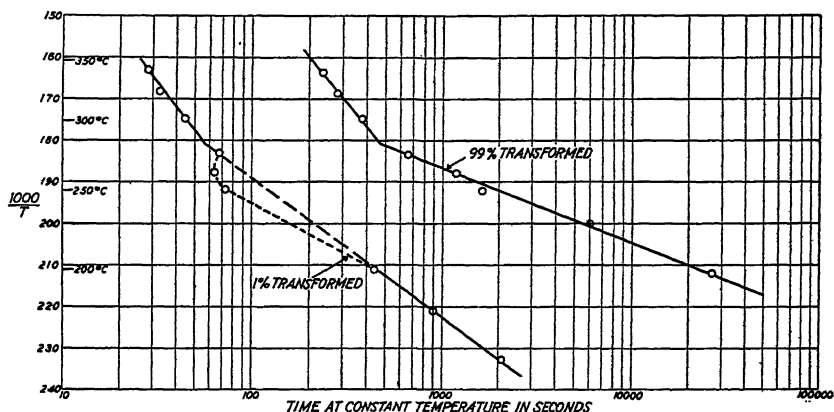
FIG. 11.—VARIATION WITH TEMPERATURE OF TIME REQUIRED FOR 1 PER CENT AND 99 PER CENT TRANSFORMATION, STEEL B.

Lines above 250° C. are for curves that appear to consist of one step. Lines for temperatures below this are for second step of two-step curves. Dashed lines indicate that portion of plot in which true position of the lines is uncertain.

in the temperature range where the isothermal curves have the simple one-step shape, the lines on the temperature-time chart are parallel straight lines; at lower temperatures, where the isothermal curves have two clearly defined steps, the time for the beginning or end of the second step also gives a straight line on the time-temperature chart, but these lines are not parallel but diverge rapidly as the temperature is lowered. In the intermediate range, the curve for the beginning of a transformation has a curvature as shown in the figure.

This curvature is rather curious and the fact that above and below this range the data lie on a straight line suggests that the curvature does not represent a true behavior but that the reaction is here complicated by the presence of some other factor. The nature of this complicating factor is not difficult to find. It lies in the first step of the low-temperature reaction, which has not yet been considered in this discussion.

At temperatures below about 200° C. (392° F.) the first step is obviously completed before the second begins (Fig. 1) and there is no

difficulty in separating the two.   In this range it is also clear that as the temperature is lowered the first step starts sooner and, once started, goes more rapidly to completion.   At 225° C. (437° F.) the first step has so fused into the second that it is impossible to separate them (Fig. 1). Accordingly no data for this temperature are included in any of the figures.   Above 225° C. (437° F.) the stepwise appearance of the iso-thermal curve has disappeared, but in view of the fact that the rate of the reaction represented by the first step is known to be slowing up at the higher temperatures it is reasonable to suppose that it still goes on, that it contributes something to the total change in length, and that it thereby affects to some extent the course of the isothermal curve in the early stages of transformation.   If these plausible assumptions are made, the anomalous results obtained at 250° C. (482° F.) and 260° C. (500° F.) are easily explained because the true change in length resulting from the second step alone is smaller than the observed change and this alters the apparent fraction transformed as calculated from the length changes. It is our belief, therefore, that if the data for the second reaction could be separated, the points for the beginning of transformation would fall on the dashed line of Fig. 11 rather than on the curved dotted line.

Although the evidence clearly indicates the existence of two consecu-tive reactions at the lower temperatures, it does not give any certain identification of the nature of these reactions.   Indeed, such an identifica-tion is impossible from kinetic data alone.   The metallographic data obtained with the microscope help out in this respect but are insufficient at present to give a complete explanation of the kinetic measurements.

At the temperatures at which the isothermal curves have a common slope, there seems little doubt that the reaction whose progress is observed is the decomposition of austenite to give the structure known as bainite. Moreover, it is almost certain that the first step at the lower temperatures represents the transformation of a part of the austenite to martensite. But this immediately raises several questions.   Why does not all the austenite go to martensite?   Why does some of it appear to remain for a relatively long time and then start a slow change to some other struc-ture?   And what is this other structure?   Is it a different kind of mar-tensite?   These questions are unanswerable at present and indicate the need for a more detailed metallographic investigation of the changes taking place below 200° C. (392° F.).

At temperatures at which austenite transforms to lamellar pearlite the isotherms appear to have different slopes.   Comprehensive data of the same accuracy as the dilatometer curves for lower temperatures are lacking but the measurements that are available (for example, those of Fig. 7) indicate that this is true.

The original time-temperature curves given by Davenport and Bain, that is, the so-called S curves, were concerned primarily with the dis-

appearance of austenite and are correctly drawn from this point of view. If one considers the different reactions, however, it is more convenient to plot the data on a reciprocal temperature scale, which results in an S curve such as the schematic one shown in Fig. 12. The dashed lines in this figure indicate uncertainty as to the course of the lines.

A difficulty arises in this type of plot in determining the temperature at which to terminate the lines for the second reaction at low temperatures, because this curve shows only the rate of transformation and does not give the amount. As the temperature is lowered the fraction of the total amount of austenite that transforms in the first step increases and
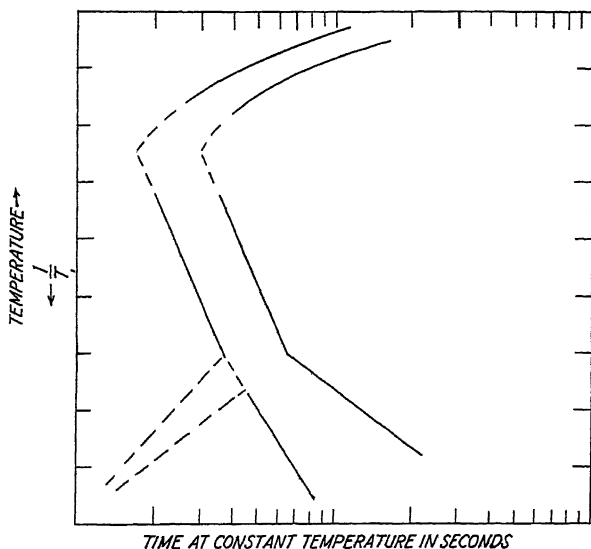
FIG. 12.—TEMPERATURE VARIATION OF RATE OF TRANSFORMATION OF AUSTENITE. DASHED LINES ARE USED TO DENOTE UNCERTAINTY IN POSITION.

the fraction that transforms in the second step decreases correspondingly. It may well be, therefore, that at room temperature or below all the austenite decomposes in the first step, so that the second reaction does not occur at all. In this case the rate obtained by extrapolating the straight lines representing the beginning and end of the second step has no significance.

It should be noted that this discussion of the variation of rate of transformation with temperature is based upon data for only six steels, which cover but a limited range of composition. In view of this fact, the conclusions drawn should not be too broadly generalized until there is further experimental evidence to justify such extension, because it is conceivable that some of the high-alloy steels may behave differently. Nevertheless, it has been found that scattered rate data for the transformation in other materials, such as cast iron[3] and iron-cobalt-tungsten alloys[4] plot on a

straight line, which suggests that the methods of plotting described may prove to have a wide usefulness. There are even indications that data on the rate of aging or of precipitation-hardening also give a straight line on these coordinates.

SUMMARY

1. Measurements of the rate of decomposition of austenite at constant temperature can be made to plot on a straight line, if time is plotted on a logarithmic scale and the percentage transformed is plotted on either the "autocatalytic" or the "integrated-probability" scale. Graph paper that has the "probability" scale as ordinate and a logarithmic scale as abscissa is obtainable and is useful for plots of this kind.

2. The straight-line plot permits easy and rapid interpolation and also permits extrapolation to 1 per cent and 99 per cent transformation, which are convenient points to take as the beginning and end of the transformation. It has a further use as an aid in judging the consistency of a set of measurements from the scatter of the points.

3. The isothermal rate curves for a given steel plotted in this manner have the same slope over the temperature range in which austenite transforms to bainite. Moreover, within this same range the time required for completion of a given fraction of the transformation varies inversely with the absolute temperature; that is, $\log t = \dfrac{a}{T} + b$. For a given steel the constant a is independent of the fraction chosen, so that the lines representing the 1 per cent and 99 per cent transformation are parallel. These relations have a special usefulness in a critical study of experimental data.

4. Below about 250° C. (482° F.) the isothermal rate curves show two steps instead of one. The rate at which the second reaction goes on is also represented by a straight line on "log-autocatalytic" or "log-probability" paper. The logarithm of the time required for completion of a given fraction of the transformation varies inversely with the absolute temperature, but the lines for different percentage transformation do not have the same slope.

5. There appear to be two reactions taking place at temperatures below 200° C. (382° F.). The first, which is probably the formation of martensite, starts sooner, and goes on faster, as the temperature is lowered. The second, whose nature is not yet clearly recognized, becomes increasingly slower with decreasing temperature.

REFERENCES

1. Davenport and Bain: Transformation of Austenite at Constant Subcritical Temperatures. *Trans.* A.I.M.E. (1930) **90**, 117.
2. E. B. Wilson: *Jnl.* Nat. Acad. Sci. (1925) **11**, 451.
3. Murphy, Wood and Girardi: Amer. Soc. Metals Preprint (Oct. 1937) Fig. 18.
4. Sykes: *Trans.* Amer. Soc. Metals (1937) **25**, 953, Fig. 59.
5. Wever and Hänsel: *Mitt.* K. W. I. Eisenforschung (1937) **19**, 47–56, Fig. 8a.

DISCUSSION

(A. Allen Bates presiding)

E. S. DAVENPORT,* Kearny, N. J.—We have applied the method of analysis suggested by the authors to isothermal transformation data that we have been accumulating for some time on a number of commercial low-alloy steels. In general, our experience confirms that of the authors in that somewhat more consistent results are obtained from the dilatometer than from microscope observations. This was to be expected, perhaps, in view of the uncertainty involved in a visual estimate of the extent of transformation, particularly near the beginning and end of the reaction.

This has led us to place more and more reliance on dilatometric observations, and we have recently constructed and are now using a dilatometer capable of operating at all temperatures up to the Ae₁ temperature. This instrument has performed satisfactorily and we have again found substantial agreement between our visual estimates with the microscope and the dilatometric data. Dilatometric methods, of course, give no information as to the nature and structure of the product being formed out of the austenite, and we will always find it necessary to turn to the microscope for this essential information.

---

* Research Laboratory, U. S. Steel Corporation.

Reaction Kinetics in Processes of Nucleation and Growth

By WILLIAM A. JOHNSON* AND ROBERT F. MEHL,† MEMBER A.I.M.E.

IT is now recognized that several important types of reactions in metallic systems proceed by the formation of nuclei and the growth of these nuclei. The process of freezing is a simple example of this, as Tammann pointed out years ago.[1] Tammann held that the rate of freezing is determined by a rate of nucleation, expressed as the number of nuclei formed per unit volume of unfrozen liquid per second, and a rate of growth of these nuclei, expressed as the linear rate of radial growth in units of length per second. For isothermal freezing the conception is simple; for ordinary freezing, extending over a range of temperature, it is not as simple, for the values of the two constants must change with change in temperature. There is ample evidence that the postulated mechanism is correct even though a quantitative derivation of the rate of isothermal or of ordinary freezing in terms of the two constants has been lacking.

In recent years other reactions have been found to proceed in a similar fashion. It has been well established, particularly by Bain,[2-8] that the formation of pearlite from the eutectoid decomposition of the solid solution austenite proceeds in such a way, and Polanyi and Schmid, Tammann and Crone, Karnop and Sachs, and others[9-11] have shown that the process of recrystallization proceeds in a similar way.

Isothermal reaction rates have been determined for eutectoid decomposition by a number of investigators. Bain's[2-8] work on the formation of pearlite from austenite is especially valuable in this respect—the type of isothermal reaction curve obtained, as illustrated in Fig. 13, showed an initial slow rate, accelerating to an intermediate maximum rate which then decelerated to the completion of the reaction; similar curves have been obtained by Wever and his collaborators.[12] Other eutectoid decompositions show similar behavior: for example, the decomposition of the beta eutectoid in the copper-aluminum system, studied by Smith

and Lindlief;[13] of the beta eutectoid in the aluminum-zinc system;[14] and of the "FeO," wüstite, phase in the iron-oxygen system (in this case the initial slow rate is absent or minor).[15] The proeutectoid rejection of ferrite in the decomposition of austenite has certain similarities,[16] though this reaction is more nearly comparable to simple precipitation from a solid solution. The rates of allotropic changes in tin[17] and in sulphur[18] have been studied, but the data are not of general use, for nucleation in these cases, occurring chiefly on the surface of the sample, is dependent on the shape of the sample used and on the nature of the liquid in which the samples are immersed; the isothermal reaction curves are not readily reproducible.

The analysis of isothermal reaction curves is more readily made when there are no concentration changes in the unreacted matrix during the reaction, for such concentration changes will certainly cause a variation in the rate of nucleation or the rate of growth during the reaction, greatly complicating the analysis; the process of freezing of a pure metal or of a congruently freezing alloy, the process of recrystallization of a metal or alloy following cold-work, and the process of eutectoid decomposition of a solid solution phase, however, all proceed without concentration changes in the unreacted matrix. For such reactions, which thus include processes of great industrial and metallurgical importance, an analysis of the isothermal reaction curve is important, both for the purpose of providing an explanation for the exact form of the curve and of providing assistance in determining the values of the basically important factors of the rate of nucleation and the rate of growth.

It has been conventional in the past to compare such isothermal reaction curves with chemical reaction curves of various orders. Thus Chaudron and Forester[15] stated that the isothermal reaction rate for the decomposition of "FeO" varies with the fourth power of the percentage of undecomposed "FeO"; Bain[2-8] compared the isothermal reaction curve for the formation of pearlite from austenite with the first order chemical reaction curve, but also pointed out discrepancies in the comparison; similar comparisons have been made by Fraenkel and Goez[14] for the decomposition of the beta phase in the aluminum-zinc system and by McBride, Herty and Mehl[16] for the proeutectoid rejection of ferrite from austenite. Such comparisons are of little use. The rate of many reactions may be expressed as dependent upon the momentary value of some quantity, but though in some reactions this has been of assistance in discovering the underlying mechanism of the reaction, in others, among which are those being considered here, it is purely an empirical and approximate representation of rate data. In first order reactions in a single homogeneous phase, in gases or liquids, the dependence of the rate upon the momentary concentration of the reactant is explicable on the basis that the rate is determined by the probability of

the formation of activated molecules through the energy redistribution following favorable collision, and in such cases the quantities in the first order reaction equation have real meaning in terms of concentration of reactant and resultant. There are no true concentration variables in any of the reactions cited above (in the formation of pearlite from austenite, for example, there is no concentration variation within any phase throughout the progress of the reaction) and there is no fundamental similarity to any reaction proceeding in a homogeneous phase. The reactions considered here are heterogeneous reactions which proceed by nucleation and by growth at an interface; for such reactions it is obvious that a quantitative expression for the rate of decomposition derived by the use of quantities of real physical significance—namely, the rate of nucleation and the rate of growth—will be far more useful.

Various attempts have been made to describe the isothermal reaction curve in terms of certain constants; Krainer[19] proposes to superimpose a reaction curve of the first order on the isothermal curve for the formation of pearlite and to characterize the experimental curve by the rate constant for the first order reaction and by the time intercept of the first order reaction curve, which he designates as the "nucleation time"; such attempts, while perhaps somewhat useful for comparison among similar data, are of no analytical use because the terms have no real meaning.

J. B. Austin and R. L. Rickett[20] recently demonstrated that the isothermal reaction curve for the formation of bainite from austenite in eutectoid steels (isothermal reaction temperatures between 570° and 200° C.) and less certainly for the formation of pearlite can be plotted as straight lines "if time is plotted logarithmically and the percentage transformed on either the 'autocatalytic' or the 'integrated-probability' scale." As the authors point out, the result is empirical and not in terms of a known mechanism of reaction; it is of assistance in appraising the accuracy of rate data and in comparing rate data for different temperatures. There is no apparent relation between this result and the mechanism by which the reactions are believed to proceed.

Several writers have pointed out that isothermal reaction curves for different temperatures of reaction and for different alloy steels can be brought into approximate coincidence by displacement on the logarithmic time scale;[21-23] the coincidence is only fair, however, and, at the moment, of uncertain significance; it adds nothing to the knowledge of the basic factors determining the rate of reaction.

The only attempts to derive the isothermal curve in terms of rates of nucleation and growth thus far recorded are that by Göler and Sachs,[24] that by Tammann,[22] and that by Fraenkel and Goez.[18] Göler and Sachs assumed a constant rate of nucleation in a unit volume of untransformed matrix and a constant rate of radial growth of these nuclei to spheroids (and to other geometric forms). The analysis, however, did not allow

for the impingement of growing spheroids and the resultant retardation in the reaction rate—accordingly, it gave a rate continuously increasing with time; it assumed general nucleation, that is, nuclei forming at random positions in the matrix, and thus did not provide for nucleation at grain boundaries as often observed in the formation of pearlite. Tammann used a simple arithmetical method, which bore the same limitations; Tammann's selection of isothermal reaction curves for comparison from the work of Bain was unfortunate, for these curves apply to the formation of lower bainite, which appears not to proceed by a process of nucleation and growth.[25] Fraenkel and Goez attempted to calculate the rate of transformation in terms of the rate of nucleation and the rate of growth, but assumed all nuclei to form at the first instant and did not provide for impingement, though the factors that determine the full form of the isothermal reaction curve were accurately described in a qualitative way.

An analysis of the isothermal reaction curve thus requires an expression in terms of the rate of nucleation and the rate of growth. When nucleation is exclusively or largely at the grain boundary, it requires an additional term for the matrix grain size. Such analyses are presented herewith, which: (1) reproduce the form of the observed isothermal reaction curve, (2) permit predictions to be made concerning the influence of of the several variables on the rate of reaction and on the shape of the reaction curve, and (3) offer methods by which the determination of rates of nucleation and growth may be greatly facilitated.

General Nucleation

The Analysis

The following analysis pertains to reactions in which nuclei form at random throughout the matrix, without regard for the matrix structure. Such an analysis should apply to the process of congruent freezing and to recrystallization in pure metals and in one-phase alloys. It will be assumed in this derivation: (1) that the reaction proceeds by nucleation and growth; (2) that the rate of nucleation, N_v, expressed in number of nuclei per unit of time per unit of volume, and the rate of radial growth G, expressed in units of length per unit of time, are both constant throughout the reaction; (3) that nucleation is random, without regard for matrix structure; and (4) that the reaction product forms true spheres except when during growth impingement on other growing spheres occurs. Departures from these simple assumptions will be discussed later. The small volumes of reaction product grown from single nuclei will hereinafter be termed "nodules."

An expression for the extent of reaction at any reaction time in terms of N_v and G is required, which provides for the impingement of growing

nodules of reaction product and the resultant inactive impingement interface. The derivation of the equation is given in Appendix A.* This derivation is obtained by the following scheme: The rate of growth of a sphere nucleated at some arbitrary time is calculated; the rate of growth of an actual nodule—a sphere that has suffered impingement and thus distortion from sphericity during growth—is a fraction of the rate of growth of the sphere; this fraction is simply the fraction of untransformed matrix; this determines the rate of growth of one nodule, which, multiplied by the number of nodules nucleated at the same time, gives the rate of growth of all nodules nucleated at this arbitrary time; sum-
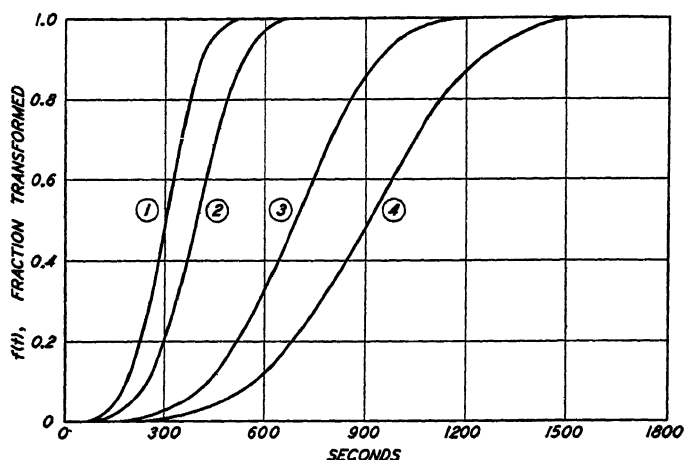
FIG. 1.—REACTION CURVES FOR GENERAL NUCLEATION FOR VARIOUS VALUES OF N_v AND G. ABSCISSA SCALE LINEAR.
Curve 1 is for N_v = 3000 per cm.³ per sec., G = 3 × 10⁻⁵ cm. per sec.
Curve 2 is for N_v = 1000 per cm.³ per sec., G = 3 × 10⁻⁵ cm. per sec.
Curve 3 is for N_v = 3000 per cm.³ per sec., G = 1 × 10⁻⁵ cm. per sec.
Curve 4 is for N_v = 1000 per cm.³ per sec., G = 1 × 10⁻⁵ cm. per sec.

ming such expressions for all times of nucleation gives the rate of transformation; integrating this expression gives an equation for the fraction transformed as a function of time, the expression required (equation 1):

$$f(t) = 1 - e^{-\frac{\pi}{3}N_v G^3 t^4} \qquad [1]$$

in which $f(t)$ is the fraction transformed and t is the time expressed in the same units as N_v and G.

Properties of the Plot

Equation 1 is plotted in Fig. 1 for a series of values of N_v and G, with $f(t)$ as ordinate and t as abscissa. It has become conventional to record

* The appendixes A, B, C, D, and E, in which are given the full details of the derivation of this and later equations may be obtained in the form of microfilm, from the American Documentation Institute, 2101 Constitution Avenue, Washington, D. C. The A.D.I. number is 1182 and the price $0.45 in microfilm and $2.70 in photoprint.

the time axis logarithmically on such diagrams in order that widely differing reaction curves may be plotted on a single diagram; Fig. 2 is such a plot.* These plots may be simplified by taking values of the quantity $\sqrt[4]{N_vG^3} \times t$ as abscissas, in which case one curve suffices to represent the family of curves in Figs. 1 and 2, as shown in Figs. 3 and 4.

The derivation obtained by Göler and Sachs[24] gives curves that are nearly identical with those in Figs. 1 to 4, up to about 5 per cent reaction (a difference of 0.1 to 0.2 per cent), but which differ increasingly at higher percentages of reaction.
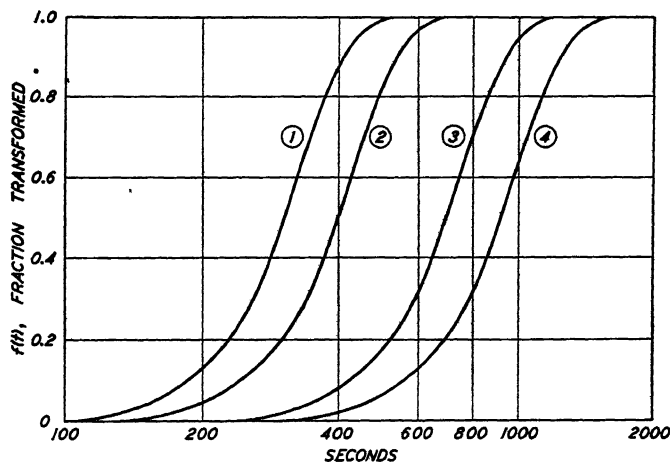
FIG. 2.—REACTION CURVES SHOWN IN FIG. 1, BUT WITH ABSCISSA SCALE LOGARITHMIC.

It may be seen from Figs. 3 and 4 that the amount of transformation depends solely on the value of the term $\sqrt[4]{N_vG^3} \times t$ and not on individual values of N_v, G, and t. Accordingly, identical reaction curves can be obtained for an infinite number of pairs of values of N_v and G for which the product N_vG^3 is the same. It follows that if two curves coincide at any point they coincide throughout.

The curves in Figs. 1 and 2 for various values of N_v and G all have the same shape: i.e., by contracting or extending the time axis linearly they can be brought into coincidence; this will be the criterion for shape. This is a characteristic of reactions that exhibit general nucleation, but not of

* Caution must be exercised in inspecting reaction curves plotted with time logarithmically, for the logarithmic plot distorts the curve, extending it at short time periods and condensing it at long. Plotted in this way, all reaction curves appear to start more slowly than they actually do—even a first order reaction curve, which begins with maximum velocity, appears when plotted this way to begin with a slow velocity and then to accelerate. It should also be noted that there is no zero on the logarithmic plot, and the displacement of a given curve to the right or the left depends solely on the logarithmic value chosen as the origin. These comments apply as well to the second section of this paper as to the first, and apply as well to experimental as to calculated curves.

reactions in which the locus of nucleation is dependent upon structure, as shown in the second section.

The relative effects of N_v and G upon the reaction curve may be seen in Figs. 1 and 2. A given change in the rate of growth exerts a much
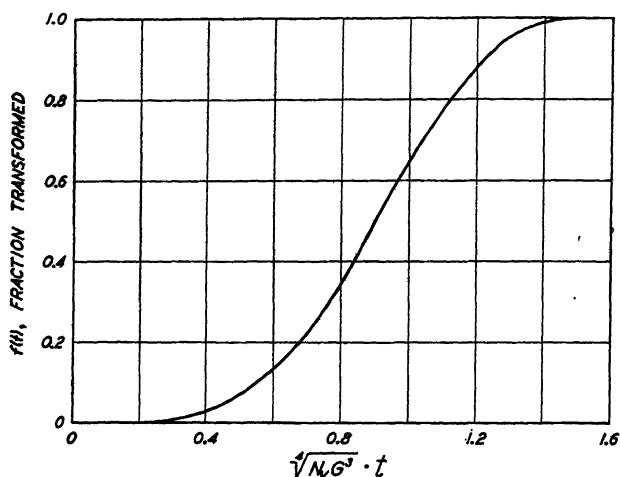
FIG. 3.—MASTER REACTION CURVE FOR GENERAL NUCLEATION, ABSCISSA SCALE LINEAR.
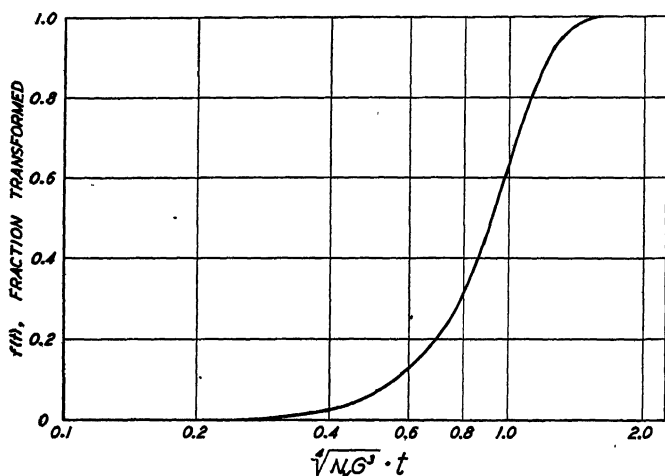
FIG. 4.—MASTER REACTION CURVE FOR GENERAL NUCLEATION, ABSCISSA SCALE LOGARITHMIC.

greater influence on the reaction curve than a corresponding change in the rate of nucleation; this is evident from the fact that G occurs in the third power in the product $N_v G^3$ whereas N_v occurs in the first.

It is conceivable that the rate of growth of the nodules might vary with the crystal direction in the transforming phase. Such variation would lead to ellipsoids (or more complicated shapes) rather than spheres, but

the shape of the reaction curve would remain the same. The coefficient of t^4 in the exponential term of equation 1 would be changed, however, and the time of reaction would thus also be changed.

Effect of Variation in N_v and G during Reaction

It is known that in certain recrystallization processes (*vide infra*) N_v and G are not constant throughout the reaction; it is necessary, therefore, to study the effect of this variation upon the reaction curve. The derivation given in Appendix A can be modified to apply to any assumed varia-
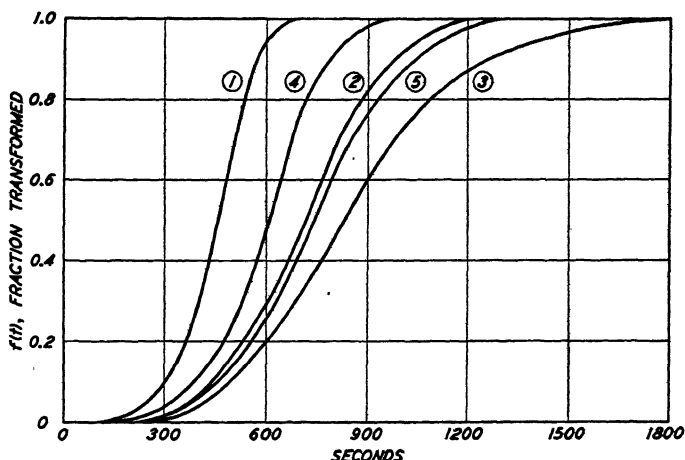
Fig. 5.—Reaction curves for general nucleation showing effect of variations in N_v and G during reaction.

Curve 1 is for G increasing linearly with time from 1×10^{-5} cm. per sec. at beginning of reaction to 3×10^{-5} at end (99.9 per cent), N_v constant, equal to 1000 per cm.³ per sec.

Curve 2 is for G, constant, equal to 1×10^{-5} cm. per sec., N_v, constant, equal to 1000 per cm.³ per sec.

Curve 3 is for G decreasing from 1×10^{-5} cm. per sec. at beginning of reaction to 0.33×10^{-5} cm. per sec. at end, N_v, constant, equal to 1000 per cm.³ per sec.

Curve 4 is for N_v increasing from 1000 per cm.³ per sec. at beginning of reaction to 10,000 at end, G constant, equal to 1×10^{-5} cm. per sec.

Curve 5 is for N_v decreasing from 1000 per cm.³ per sec. at beginning of reaction to zero at end G, constant, equal to 1×10^{-5} cm. per sec.

tion in N_v and G; one illustration of such a modification of the analysis is given in Appendix B. If it is assumed that N_v and G vary during reaction linearly with time in such a way that $N_v = N_{v0} (1 + \beta t)$ and $G = G_0 (1 + \alpha t)$, in which α and β are constants, a suitable expression may be obtained (equation 2):

$$f(t) = 1 - \exp\left\{-\pi N_0 G_0^3\left[\frac{t^4}{3} + \frac{t^5}{15}(9\alpha + \beta) + \frac{t^6}{30}\alpha(11\alpha + 4\beta) \right.\right.$$
$$\left.\left. + \frac{t^7}{210}\alpha^2(16\alpha + 19\beta) + \frac{t^8}{48}\alpha^3\beta\right]\right\} \quad [2]$$

Reaction curves for several values of α and β are plotted in Fig. 5. The effect of such variation in G on the shape of the reaction curve is shown in Fig. 6, in which three of the five curves of Fig. 5 are replotted, each on a different scale, in such a way that they coincide at 50 per cent reaction. Variation in G during the reaction gives different shapes to the curves. The curve for G increasing during the progress of the reaction, curve 1 lies below the reference curve (for which N_v and G are constant during the reaction) up to 50 per cent reaction and above, beyond 50 per cent; the curve for G decreasing during the reaction shows the opposite behavior. Variation in G during the reaction exerts a more
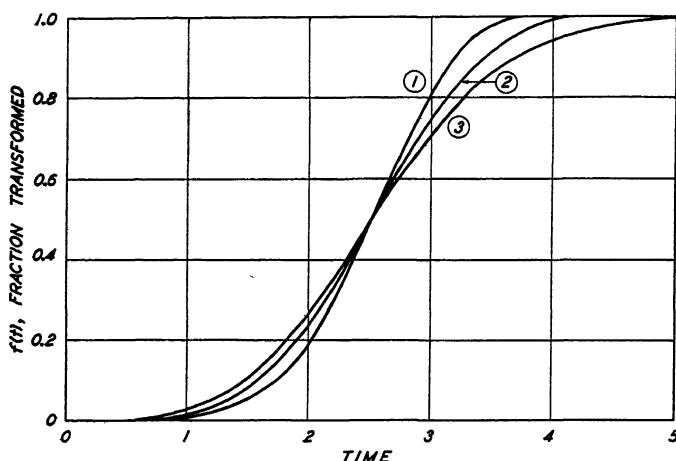
FIG. 6.—CURVES 1, 2 AND 3 OF FIG. 5 REPLOTTED ON ABSCISSA SCALES CHOSEN SO AS TO GIVE COINCIDENCE AT 50 PER CENT REACTION, SHOWING EFFECT OF VARIATIONS IN G DURING REACTION ON SHAPE OF REACTION CURVE.

marked influence on the reaction curve than variation in N_v; replotting curves 4 and 5 of Fig. 5 yields curves nearly indistinguishable from curve 2, and accordingly they are not replotted in Fig. 6.

Distribution of Nodule and Patch Sizes

It will be shown that the above expressions are useful in determining N_v and G. In applying them for this purpose, it will be convenient to consider the distribution of nodule sizes in space and of nodule areas, which we shall call "patches," on a plane of polish. The calculations that lead to the distribution functions given below are contained in full in Appendix C.

In the discussion to follow, the distribution function $P(x)$ of a set of objects whose characteristic measure (volume or radius) is x is defined in such a way that the number of objects with measure between x and $x + dx$ is $P(x)\,dx$. The distribution function, $\eta(\bar{\phi})$, of nodule volumes,

$\bar{\phi}$, for a completely reacted sample has been calculated by finding the number of nodules formed in a short time interval and the average volume of these nodules. This function is given by the parametric equations

$$\eta(\bar{\phi}) = \frac{(N_V/G)^{3/2}e^{-2\alpha^4}}{8\sqrt{3\pi}\int_\alpha^\infty e^{-v^4}[(v - \alpha) - 2\alpha^3(v - \alpha)^2]dv} \qquad [3]$$

$$\bar{\phi} = 4\sqrt[4]{27\pi}(G/N_V)^{3/4}e^{\alpha^4}\int_\alpha^\infty e^{-v^4}(v - \alpha)^2dv$$

where α is the parameter and v is an integration variable. Equation 3 is plotted in Fig. 7; the method of plotting is described in detail in the discussion of Fig. 9.
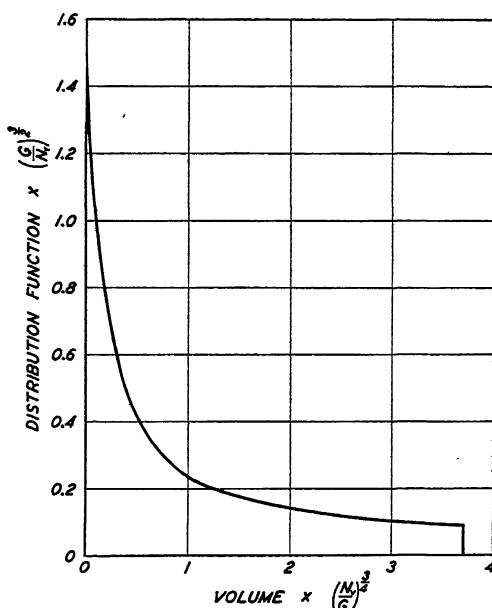
FIG. 7.—DISTRIBUTION CURVE IN SPACE FOR AVERAGE NODULE VOLUME.

The total number of nodules per unit volume of completely reacted sample, n_e, may be obtained by integrating equation 3 with respect to $\bar{\phi}$. The result is

$$n_e = 0.896(N_v/G)^{3/4} \qquad [4]$$

Since metallic samples are opaque, the distribution function in equation 3 is not directly applicable, but the distribution function for patches on a plane of polish can be derived from it on the assumption that the nodules are spheres whose volumes equal those of the corresponding nodules. With this assumption, the spacial distribution function, $\eta(\bar{\phi})$, which is in terms of volume, becomes $\psi(r)$ in terms of the corresponding

radius r; $\psi(r)$ is

$$\psi(r) = \frac{\sqrt{\pi/12}(N_v/G)^{3/2}e^{-2\alpha^4 r^2}}{\int_\alpha^\infty e^{-v^4}[(v - \alpha) - 2\alpha^3(v - \alpha)^2]dv} \qquad [5]$$

where r is given by the relation $\bar{\phi} = \frac{4}{3}\pi r^3$ and the other terms have the same meaning as in equation 3. Equation 5 is plotted in Fig. 8; the method of plotting is described in detail in the discussion of Fig. 9. Although Figs. 7 and 8 both represent the distribution of nodules in space, they are of quite different shape because the distribution curve of Fig. 7 is plotted as a function of volume while that of Fig. 8 is plotted as a
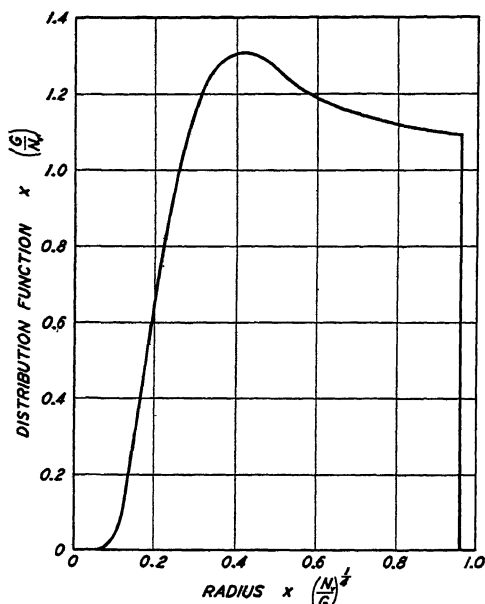
FIG. 8.—DISTRIBUTION CURVE IN SPACE FOR AVERAGE NODULE RADIUS.

function of radius. The distribution function, $\theta(\rho)$, for patches of radii ρ on a plane of polish is then given by[26]

$$\theta(\rho) = 2\rho \int_\rho^{r_{max}} \frac{\psi(r)dr}{\sqrt{r^2 - \rho^2}} \qquad [6]$$

where $\psi(r)$ is given by equation 5 and r_{max} is the radius of the largest sphere. Equation 6 is plotted in Fig. 9.

The number of patches of radius between ρ and $\rho + d\rho$ is the area under the curve between the abscissas ρ and $\rho + d\rho$, as illustrated in Fig. 9. This curve has been derived for the general case (all values of N_v and G), and thus the scales of the ordinate and abscissa axes are generalized. The abscissa is radius, and the units are as shown; to

illustrate, assuming $G = 16 \times 10^{-6}$ cm. per sec. and $N_v = 100$ per sec. per cm.^{3}, then $(G/N_v)^{1/4} = 0.02$ cm. The maximum radius is thus
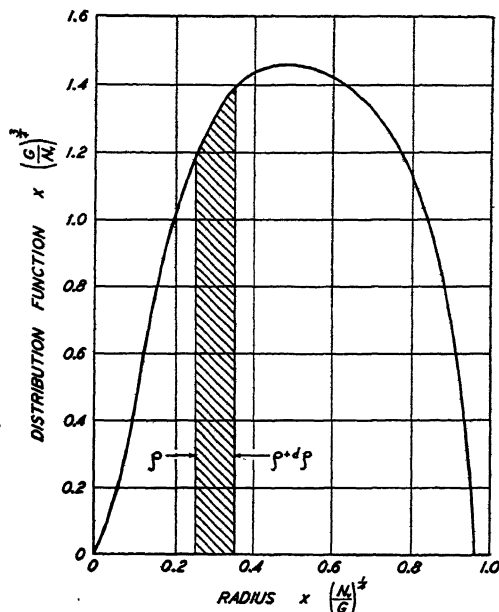
FIG. 9.—DISTRIBUTION CURVE ON PLANE OF POLISH FOR AVERAGE PATCH RADIUS.

$0.96 \times (G/N_v)^{1/4} = 0.96 \times 0.02$ cm. $= 0.0192$ cm.; intermediate radii are obtained in the same way; *i.e.*, by multiplying the abscissa values plotted in Fig. 9 by $(G/N_v)^{1/4}$. The ordinate values are obtained in a similar manner; thus, in the example given, the maximum value of the distribution function is $1.47 \times (N_v/G)^{3/4} = 1.47 \times 1/(0.02 \text{ cm.})^3 = 183,750$ per cm.^{3} Thus Fig. 9 is a master distribution curve for patches (nodule areas on a plane of polish) for a system that has reacted to completion by nucleation and growth with N_v and G constant throughout the reaction. Figs. 7 and 8 are also master plots from which distribution functions for particular values of N_v and G may be obtained by the simple calculations described for Fig. 9.

FIG. 10.—CORRESPONDENCE OF EXPERIMENTAL (FULL CURVE) AND CALCULATED DISTRIBUTION CURVE (DOTTED). Experimental and calculated curves obtained as described in Appendix C.

The total number of patches per unit area of a completely reacted sample, n_T, may be found by integrat-

ing equation 6 with respect to ρ. The result is

$$n_T = 1.01(N_v/G)^{\frac{1}{2}} \qquad [7]$$

The distribution curve obtained by Scheil and Wurst[27] for the patch sizes in recrystallized Armco iron may be compared with the distribution curve calculated here. Changing the ordinate units so as to refer the data to a square millimeter area (Appendix C) and plotting the curve in the manner employed in Fig. 9, produces the curve shown in Fig. 10; the calculated distribution curve on this same figure is one derived for the same total number of patches. In general the agreement is good.

Application and Use of Analysis

The analysis given may be applied quantitatively to reactions for which the assumptions made in the derivation are valid. These are: (1) that the reaction proceeds by nucleation and growth, (2) that the distribution of nuclei is random, without regard for structure, and (3) that the rate of nucleation and the rate of growth remain constant throughout the reaction.

The application of the analysis to the process of freezing may be made only with certain limitations. When nucleation at the surface of the system is pronounced and extensive columnar growth occurs, the requirement of general nucleation is obviously not met. Similarly, in ordinary nonisothermal freezing, N_v and G will vary in a complicated fashion with the temperature, and this circumstance is difficult to provide for in an analytical way. It is possible also that the mobility of small nodules in a partially frozen melt should tend to decrease the importance of the impingement factor somewhat. But for the slow freezing of metal in the interior of an ingot, where equiaxed grains are obtained, the analysis may find an application.

The decomposition of austenite to pearlite in many cases shows pronounced grain-boundary nucleation,[2-8] and the nodules usually do not grow across the grain boundaries of the austenite matrix. This process, though meeting the other requirements, fails to meet those of general nucleation and of growth restricted only by impingement on other growing nodules. In some steels[25] general nucleation is pronounced, though apparently always accompanied by grain-boundary nucleation; in such cases the proper analysis must be a combination of that given above for general nucleation and that following in the next section on grain-boundary nucleation. It should also be pointed out that the formation of "lower" bainite from austenite almost beyond question is not a process of nucleation and growth,[25] and the analysis should not be applied to this.[22]

The application of the analysis to recrystallization is on more certain ground. This process is also one of nucleation and growth; in the recrys-

tallization of heavily deformed aggregates, nuclei appear to form at random and to grow without regard for the grain structure of the recrystallizing material. Nuclei form usually in twins or slip planes, but these regions are distributed sufficiently uniformly that the nucleation may be considered random. In some cases, however, N_v and G change during recrystallization; such a change in G has been shown for tin by Polanyi and Schmid[9] and for lead and zinc by Tammann and Crone,[10] though Karnop and Sachs[11] reported that G remains constant during the recrystallization of aluminum.

The reaction and distribution curves derived above may be used in the determination of N_v and G in any reaction that meets the requirements of the analysis. If the experimental reaction curve and the distribution curve of patch sizes are of the same shapes as the calculated reaction and distribution curves, it may be concluded that N_v and G remain constant throughout the course of the reaction; if the experimental reaction curve does not agree with the calculated curve, it may be concluded that either N_v or G or both are not constant; if N_v increases and G decreases during the reaction, the reaction curve may be indistinguishable from the reaction curve calculated for constant N_v and G, but the distribution curve would show a marked distortion, so that both should be used in applying this test.

If it is known that N_v and G remain constant for a given process, it is not necessary to have complete reaction and distribution curves for calculating N_v and G. If the fraction of transformation at a known time t is determined experimentally, the value of $\sqrt[4]{N_v G^3} \times t$ corresponding to this fraction of transformation is easily read from the reaction curve in Figs. 3 and 4; since the time is known, $\sqrt[4]{N_v G^3}$ is obtained. If the total number of patches per unit area on a polished surface is measured, the value of $(N_v/G)^{1/2}$ may be obtained from equation 7; from the values of $\sqrt[4]{N_v G^3}$ and $(N_v/G)^{1/2}$ determined in this way, the values of N_v and G may be calculated.

If it is known that N_v and G are constant, and if either one of these quantities is determined experimentally, the other may be calculated. This may be done either by counting the number of patches per unit area, which gives the value of $(N_v/G)^{1/2}$, or by determining the fraction of transformation in a given time, which gives the value of $\sqrt[4]{N_v G^3}$; by substituting in either of these quantities the one constant determined, the other may be calculated. This should greatly lighten the extreme labor required in the experimental determination of N_v and G.

GRAIN-BOUNDARY NUCLEATION

The Analysis

The derivation of the reaction equation when nucleation occurs exclusively at the grain boundary—as, for example, in the formation of pearlite

from austenite in certain steels,[*] presents special though not insurmountable difficulties. In this case we assume: (1) that the reaction proceeds by nucleation and growth, (2) that the rates of nucleation and growth remain constant throughout the reaction, (3) that nucleation is exclusively at grain boundaries, (4) that the matrix is composed of spherical grains of radius a, (5) that the nodules grow only into the grain in which the nuclei originated and do not cross grain boundaries, and (6) that the rate of transformation is retarded by impingement of growing nodules on one another and on grain boundaries. These are conditions for the formation of pearlite from austenite. Items 3, 4, 5 and 6 distinguish this case from the case of general nucleation.

We require an expression for the extent of reaction at any reaction time in terms of a rate of grain-boundary nucleation, N_s, expressed as number of nuclei per unit of time per unit of grain-boundary area; a rate of growth G; and a matrix grain size a, which provides for the impingement of growing nodules of reaction product and the resultant inactive impingement interface. The provision for impingement in this case is more difficult than in general nucleation, for there is no simple relation of impingement to the extent of reaction, and a different approach is required.

The derivation of the equation is given in Appendix D. The matrix is assumed to be constituted of spherical grains. The rate of transformation of a single grain is calculated and from this the rate of transformation of the aggregate of grains may be found. Nuclei are assumed to form at the surface of the grain and to grow inward; an arbitrary thin spherical shell within the grain and concentric with it is considered; the growing nodules intersect this shell; the rate of increase in the area of the shell contained within a particular nodule is calculated; multiplication of this rate by an impingement factor involving the area of the shell, the area of the shell contained within the particular nodule considered, and the fraction of the shell contained within all nodules, yields the rate of transformation of the shell due to the single nodule considered; integration of this rate for all times of nucleation yields the total rate of transformation of the shell. Integration of this gives the fraction of the shell transformed as a function of time (the fraction *untransformed* is given by equation 8b); integration of this over the whole grain gives the fraction of the grain transformed as a function of time (the fraction *untransformed* is given by equation 8a); correcting this equation for the most probable time of formation of the first nucleus in each grain yields the required equation for the fraction of transformation as a function of time, equation 8.

$$F(z) = 4\pi\lambda \int_0^z e^{-4\pi\lambda\alpha} \xi(z - \alpha)d\alpha \qquad [8]$$

where $\qquad z = \dfrac{G}{a} \times t \qquad$ and $\qquad \lambda = \dfrac{a^3 N_s}{G}$

where $\qquad \xi(z) = \begin{cases} 3 \int_{1-z}^{1} y^2 [1 - \omega(z,y)] dy \text{ when } z \leq 1 \\ 3 \int_{0}^{1} y^2 [1 - \omega(z,y)] dy \ \text{ when } z \geq 1 \end{cases}$ [8a]

where $\omega(z,y) = \begin{cases} 1 & \text{when } 0 \leq z \leq (1-y) \\ \left[\dfrac{(1+y)^2 - z^2}{4y} \right] \left\{ (y)^{(1+y-z)} \left[\dfrac{(1+y+z)}{(1+y-z)} \right]^{(1+y)} \right. \\ \qquad\qquad \left. \left[\dfrac{(1+y)^2 - z^2}{4} \right]^{z} e^{2(1-y-z)} \right\}^{4\pi\lambda} \\ \qquad\qquad \text{when } (1-y) \leq z \leq (1+y) \\ 0 & \text{when } z \geq (1+y) \end{cases}$

[8b]

and where α and y are integration variables, whose limits are $0 \leq \alpha \leq \infty$ and $0 \leq y \leq 1$.

Equation 8 was evaluated numerically by Simpson's rule. The method is briefly as follows. The desired value of the parameter λ is chosen; for any assumed value of z, say z_1, a curve $\omega(z_1,y)$ can be calculated from equation 8b. Using this value of $\omega(z_1,y)$, which is a function of y, $\xi(z_1)$ can be calculated from equation 8a. Repeating this process for a series of values of z yields a curve $\xi(z)$ as a function of z. For any desired value of z, say z_2, a curve $\xi(z_2 - \alpha)$ can be constructed from $\xi(z)$; this curve can then be used to determine $F(z_2)$ from equation 8. Repeating this process for a series of values of z yields the desired reaction curve.

For values of λ not less than 3, the approximate formulas given previously[25] hold very well.

$$F(z) = \begin{cases} 3 \int_{1-z}^{1} y^2 [1 - g(y,z)] dy & \text{when } z \leq 1 \\ 3 \int_{0}^{1} y^2 [1 - g(y,z)] dy & \text{when } z \geq 1 \end{cases}$$

where $g(y,z) = \begin{cases} \exp. \ \{ -\pi\lambda[z^3/3y - z/y \\ \quad (1-y)^2 + 2/3y(1-y)^3] \} & \text{when } (1-y) \leq z \leq (1+y) \\ 0 & \text{when } z \geq (1+y) \end{cases}$

Equation 8 may be plotted in a number of ways. A family of curves could be plotted in which the grain size a and the rate of nucleation N_s were kept constant and various values assumed for the rate of growth G; another family could be plotted in which a and G were kept constant and N_s varied; and a third plotted in which G and N_s were kept constant and a varied; the use of these curves would then consist in finding which curve in these three families agreed with the experimental reaction curve. The multitude of comparison curves would render this method very

laborious. A much shorter method is to plot the equation in terms of the two factors in which it is written; namely, $\lambda = \dfrac{a^3 N_s}{G}$ and $z = G/a \times t$. Equation 8 is plotted in this fashion in Fig. 11, in which the time scale is linear, and in Fig. 12, in which the time scale is logarithmic, for a series of values of λ.

In applying this analysis, the plots given in Figs. 11 and 12 are sufficient for all purposes; it is not at all necessary to perform the computations outlined above, which have been described merely to demonstrate the method by which the plots were obtained. The use of these plots in the treatment of data is simple. They are master plots. The ordinate is $F(z)$, the fraction transformed. The abscissa is not simply time, but z, the actual time multiplied by G/a; the factor G/a is designated as the time-scale factor. The plot shows a family of curves, each characterized by a different value of $\lambda = \dfrac{a^3 N_s}{G}$. The value of this quantity determines the shape of the curve, and we shall designate this quantity λ as the shape factor. Curves for values of λ not shown may be obtained easily by interpolation. Any experimental reaction curve may be compared to these curves.

It is obvious from Figs. 11 and 12 that if N_s, G and a are known, the shape factor $\dfrac{a^3 N_s}{G}$ can be calculated and the shape of the curve determined; furthermore the time-scale factor G/a can be calculated and the horizontal or time extension of the curve determined. This should give a curve that coincides with the experimentally observed curve. Although a is readily determined, there have been no good determinations of N_s and G,[25] and an absolute comparison cannot be made on this basis. It has been shown, however, that curves of the form given in Figs. 11 and 12 can be fitted to experimental reaction curves with a high degree of perfection, as shown in Fig. 13.*

The number of nodules in each completely reacted grain of the matrix is a function only of the shape factor λ. This function is plotted in Fig. 14; the derivation of the equation is given in Appendix E. Since the volume of a single grain is $\tfrac{4}{3}\pi a^3$, the number of nodules per unit volume is found by multiplying the number of nodules read from Fig. 14 by $\dfrac{3}{4\pi a^3}$. This analysis cannot be extended, however, to the calculation

---

* The very slow initial rate of the decomposition of austenite has led some investigators to call this initial period an incubation or induction period, inferring that the system is "preparing" to react, that the major reaction has not yet begun. This is not necessary; it may be seen from Figs. 11 and 12 (and also from Figs. 1 and 2) that an initial slow rate is an inevitable result of the process of nucleation and growth. The logarithmic plotting exaggerates the initial slow rate.
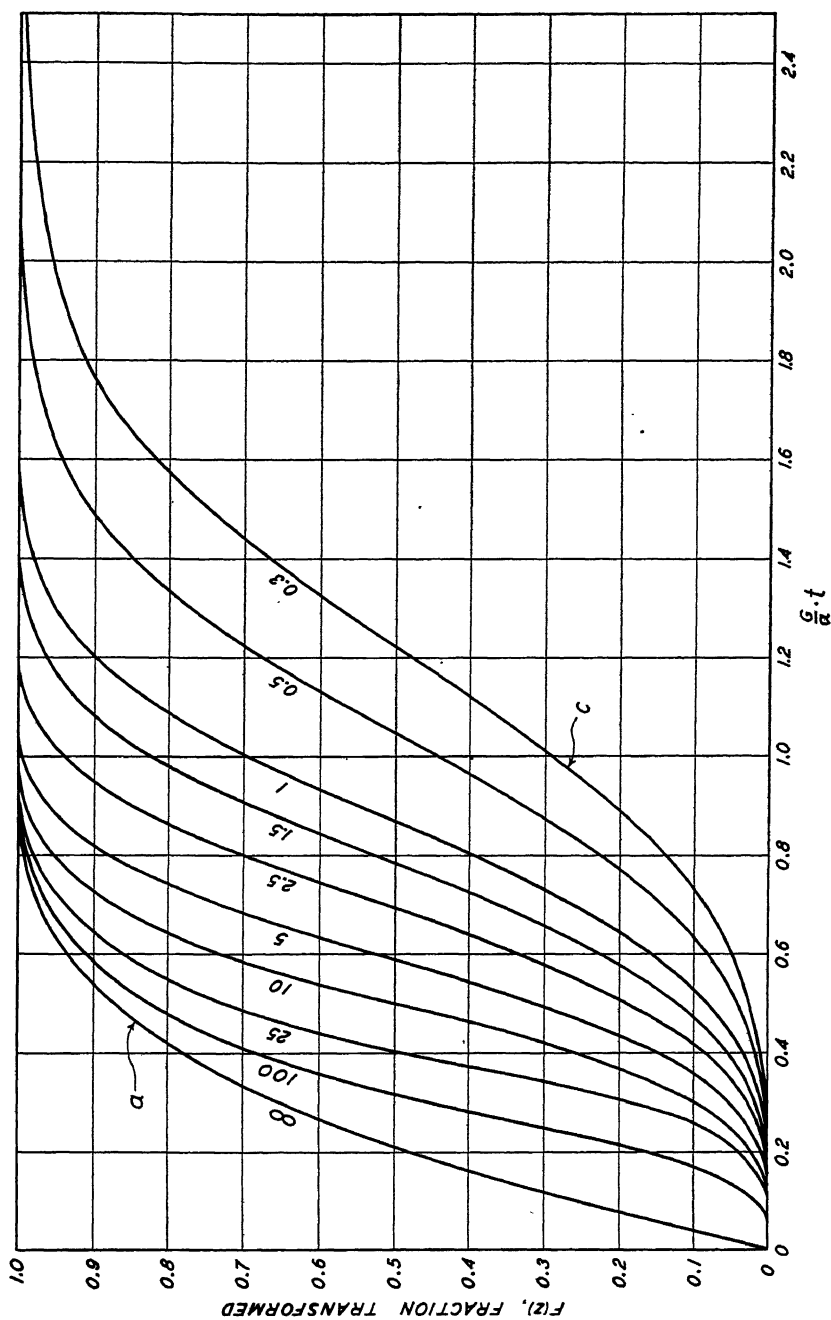
FIG. 11.—MASTER REACTION CURVES FOR GRAIN-BOUNDARY NUCLEATION, ABSCISSA SCALE LINEAR.
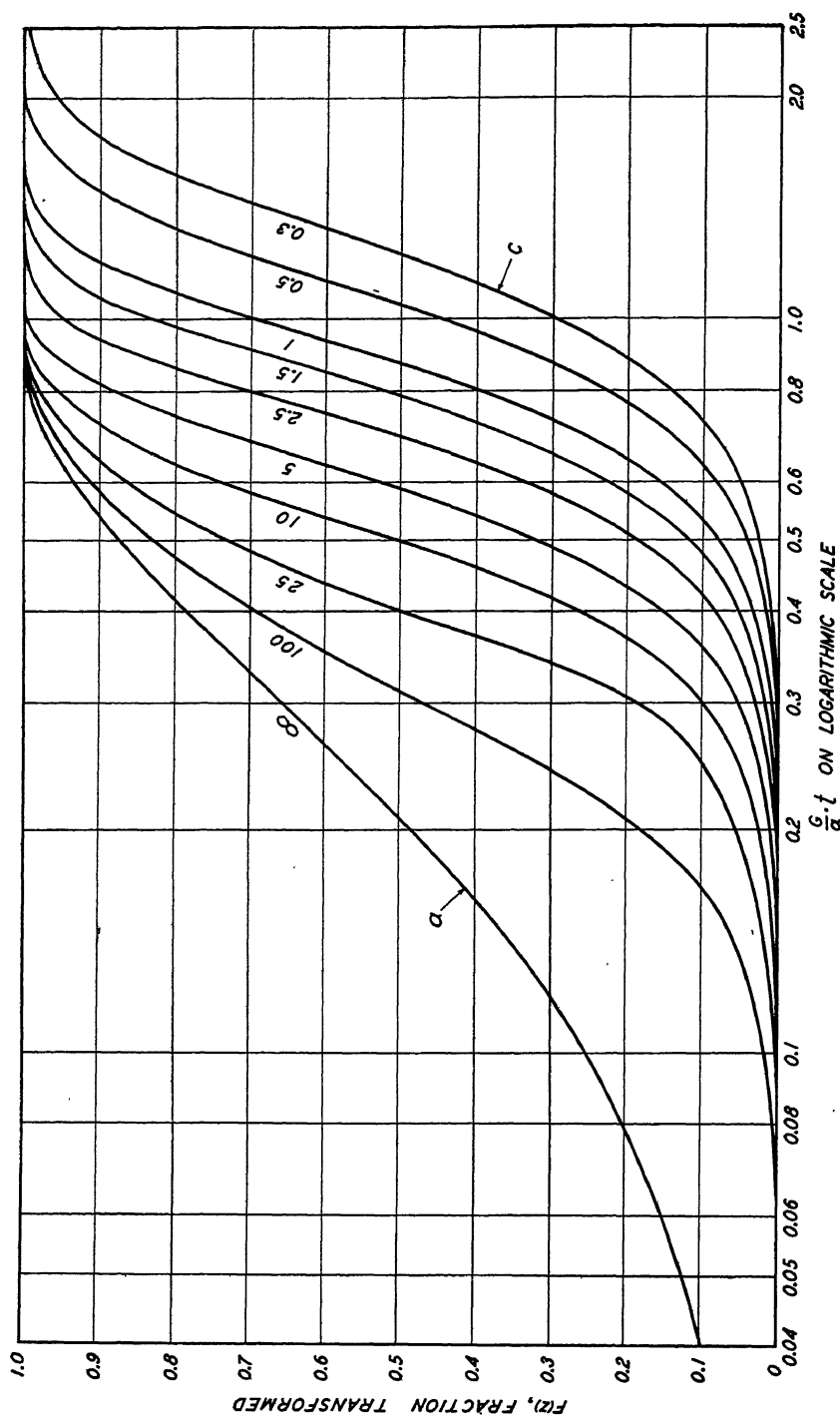
FIG. 12.—MASTER REACTION CURVES FOR GRAIN-BOUNDARY NUCLEATION, ABSCISSA SCALE LOGARITHMIC.

of the number of nodule intersections on the plane of polish—patches—nor to the distribution of patch areas, for the nodules in this case do not approximate spheres, as in general nucleation. Accordingly, no correlation between N_s, G, and a, and a distribution function of nodule size can be made until the statistical shape of the nodule is studied.

No one has made a careful study of the number of pearlite nodules that can form in a single grain of austenite, but it appears that the num-
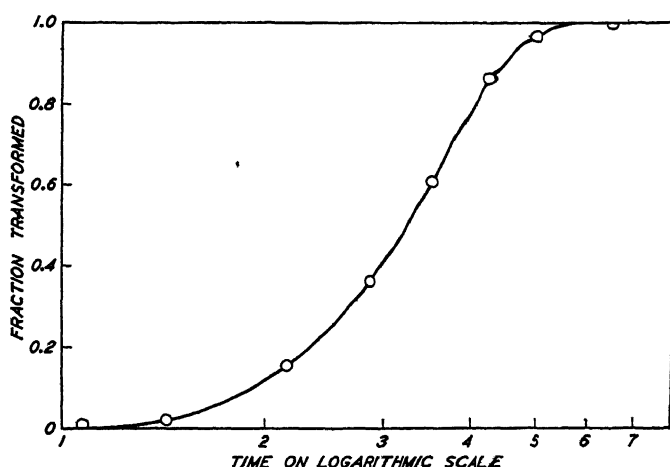
FIG. 13.—CORRESPONDENCE OF EXPERIMENTAL (FULL CURVE) AND CALCULATED REACTION CURVES (CIRCLES).
Experimental curve from Fig. 9, E. S. Davenport and E. C. Bain, *Transactions,* Amer. Soc. Metals (1934) **22**, 894. Calculated curve obtained as described in text. Abscissa scale logarithmic.
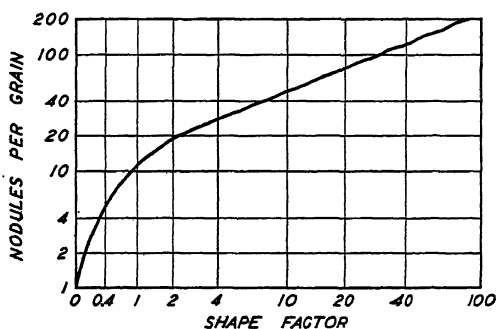
FIG. 14.—RELATION OF NUMBER $\bar{n}$ OF NODULES PER GRAIN TO SHAPE FACTOR λ.
The abscissa is log $(1 + \lambda)$. The ordinate corresponding to any value of $\bar{n}$ is proportional to log $\bar{n}$.

ber rarely, if ever, falls below 4 or 5, corresponding to a value of λ of approximately 0.3. Since the discussion of the effect of changes in N_s, G, and a on the shape of the reaction curve which follows is limited to the formation of pearlite from austenite, curves with shape factors under

0.3 will not be considered. For reactions other than the austenite-pearlite eutectoid decomposition, lower values of λ may have to be employed.

Effect of Grain Size

The effect of grain size may be sought by inquiring what the effect of increasing the grain size a will be upon the shape of the curve and upon the time scale. It can be seen from Fig. 11 that increasing a will increase the factor $\dfrac{a^3 N_s}{G}$ and will alter the shape of the curve toward that of curve (a); and conversely, a decrease in a will alter the shape of the curve toward that of curve (c); samples of the same steel with different grain sizes will therefore exhibit reaction curves of somewhat different shapes. With increasing grain size the distance the nodule must traverse to reach the center of the grain becomes greater, and this increases the reaction time. Thus an increase in a decreases the value of the time-scale factor G/a, and the time of reaction is increased. The grain size in commercial heat-treating steels varies essentially between American Society for Testing Materials numbers 10 and 1, corresponding to a range in a of 1 to 23. Increasing a by a factor of 23, and maintaining N_s and G constant, will increase the total reaction time by from 5 to 23 times, depending on the particular values of N_s and G obtaining.

The effect of grain shapes other than spheres is in general to increase the rate of reaction, since any other shape has a greater ratio of grain surface to grain volume and an increase in surface area engenders an increase in reaction rate. Mixed grain sizes, the so-called "duplex" grain structure, often occur. As shown in Fig. 11, the *shape* of the reaction curve varies with grain size, and the *displacement* of the curve on the time axis also varies. It would be expected that the reaction curve for a steel with mixed grain size would lie between those for the largest and smallest grain sizes in the sample, and this is true, but the curve is not identical with the curve calculated for the *average* grain size—it varies from this both in shape and (to a minor degree) in position with respect to the time axis, as shown in Fig. 15. A consideration of the phenomena at play in a duplex structure will suggest what this variation should be: the small grains will react quickly, and this will displace the first part of the curve upward (increasing percentage of reaction), whereas the large grains will react relatively slowly, and this will displace the latter part of the reaction curve downward (decreasing percentage of reaction). The actual effect of a duplex structure depends on the particular distribution of grain sizes present; it is not the same when only grain sizes No. 2 and No. 6 are present as when all grain sizes from No. 2 to No. 6 are present. In the first case the reaction curve will not be smooth—i.e., the small grains will have reacted almost completely before the large ones have reacted appreciably, and there may be a hump in the

reaction curve as a result. If the mixture of grain sizes is continuous, the reaction curve will be smooth. The disposition of the curves for different grain sizes shown in Fig. 15 depends on the relative values of N_s and G. Thus, the higher the value of the ratio N_s/G, the greater will be the separation of the curves for the different grain sizes.

Effect of Rate of Nucleation

Any discussion of the effects of rate of nucleation and rate of growth on the reaction curve is complicated by the fact that any influence that alters one often alters the other. Thus, while nonmetallic inclusions such as alumina probably affect only the rate of nucleation, alloying elements
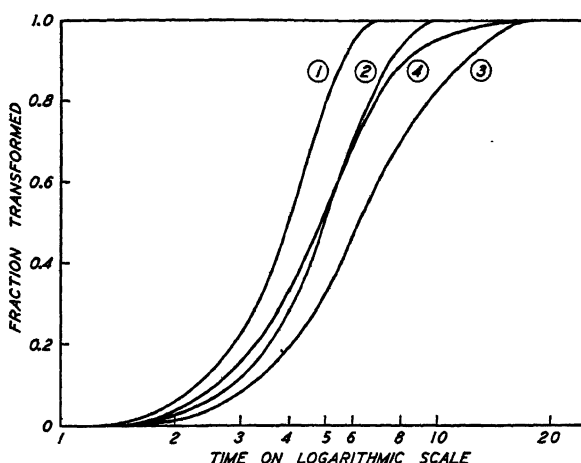
FIG. 15.—SHOWING EFFECT OF GRAIN SIZE AND EFFECT OF MIXED GRAIN SIZE ON REACTION CURVE.

Curve 1 is for A.S.T.M. grain size No. 6, curve 2 for grain size No. 4, curve 3 for grain size No. 2, curve 4 for a mixture of equal parts of grain sizes Nos. 6, 4 and 2. Note that reaction curve for mixture, curve 4, is not identical with reaction curve for average grain size, No. 4, curve 2.

probably exert an influence on both the rate of nucleation and the rate of growth. Variations in the rate of nucleation N_s will have no effect on the time-scale factor G/a, and will affect the reaction curve only by altering its shape. An increase in N_s will alter the shape of the curve toward that of curve (a), Fig. 11; the curve is thus displaced upward and correspondingly the time for a given percentage of reaction will be shorter by the amount of lateral displacement, right to left, which this incurs. It is a striking result of this analysis that altering the shape factor between 0.3 and ∞ results in a decrease in the time of reaction of only 70 per cent. If the grain size and the rate of growth are kept constant, and this variation in λ is effected by changing the rate of nucleation alone, the greatest possible variation in the rate of nucleation can have only a relatively small effect on the rate of reaction.

Effect of Rate of Growth

It can be seen from Fig. 11 that increasing G will alter the shape of the reaction curve toward that of curve (c), and decreasing G, toward that of curve (a); increasing G will also alter the time-scale factor, displacing the reaction curve toward shorter times. Any change in G produces opposite and nearly equal effects to those produced by the same change in a.

The chief factors in determining the rate of reaction are the grain size a and the rate of growth G; as stated, N_s is of much less influence relatively. Although the effects of variations in a and G are nearly equal though opposite, in reality G is a far more important variable, for it can be varied over a very much greater range. In commercial steels the grain size varies essentially between A.S.T.M. numbers 1 and 10, corresponding to a range in a of 1 to 23; but G can be varied over a very wide range, a range of many orders of magnitude, either by altering the temperature of reaction or, more important, by the addition of alloying elements. It is in this circumstance that lies the reason for the fact that the effect of grain size on the rate of reaction is a minor one compared to the effect of alloying elements.

The analysis of the reaction curve for the case where N_s is very low compared to G is interesting. In this case the generation of one nucleus in a grain results in the complete reaction of that grain before another grain is nucleated. The rate of reaction will thus be proportional to the rate of nucleation, which in turn is proportional to the number of grains still available for nucleation; that is, to the number of unreacted grains. This will accordingly furnish a reaction curve identical with that for a first-order reaction. But only in this very exceptional case will the first-order reaction curve be reproduced in form.

Conditions for Identical Reaction Curves

Two identical reaction curves (both with respect to shape and time) will be obtained when the two factors a^3N_s/G and G/a are identical in the two steels. The conditions under which this is possible can readily be appraised. For a given steel at a fixed reaction temperature, both N_s and G are constant, and only a can be varied; a cannot be varied to obtain identical constants and thus to obtain identical reaction curves. For a given steel reacting at a series of temperatures, N_s, G, and a are all variable, but in order to get identical factors and therefore identical reaction curves, N_s and G would have to change with temperature in opposite directions which, as has been shown,[25] is not observed in the formation of pearlite. For two different steels reacting at a series of temperatures, N_s, G, and a are again all variable, and it is possible that the stated condi-

tions can be met; coincidental reaction curves are theoretically possible and will be found if proper values of N_s, G and a appear.

The effect of variation in N_s and G during reaction can be discussed qualitatively; a quantitative discussion would require a knowledge of the type of such variation which is not available. When such data become available the appropriate modification of the analysis given in Appendix D can be made. A considerable increase in N_s will result in a relatively small effect on the reaction curve, since it has been shown that the maximum possible variation in time of reaction for maximum variation in N_s is only 70 per cent (note that this is for an increase in N_s for grain-boundary nucleation alone and does not pertain to any variation in intragranular nucleation). Variation in G, however, will exert an important influence on the rate of reaction since this will affect the time-scale factor.

Uses of Analysis

The analysis is of value in the experimental study of isothermal reaction rates, for it may be used greatly to facilitate the determination of the basic constants N_s and G, the rate of nucleation and the rate of growth.

1. With a known, approximate values of N_s and G can be obtained from the isothermal reaction curve alone if the reaction curve is determined accurately. The procedure is as follows: Plot the experimental curve with time logarithmic to the same scale as given in Fig. 12 (the same abscissa distance for each power of 10); superimpose the experimental and the master curves in Fig. 12, and shift curves laterally until the experimental curve is brought into coincidence with one of the master curves; this will give the value of a^3N_s/G. Choose any point on the time axis; read the value of $G/a \times t$ at this point from the master curve and the value of t from the experimental curve; with a known, G can be calculated; since a^3N_s/G has been determined, and since a and G are known, N_s can be calculated. The errors will accumulate in N_s, but since N_s is less important than either G or a this is not disturbing.

2. If more accurate values of N_s than those given in paragraph 1 are desired, an experimental determination of G is required. The procedure is as follows: With G and a known, the experimental curve may be plotted on Fig. 12 directly by multiplying the experimental times by G/a, and the curve with which it coincides selected; from the value of a^3N_s/G for this curve and the known values of a and G, N_s may be calculated.

3. If more accurate values of G than those given in paragraph 1 are desired, an experimental determination of N_s is required. The procedure is as follows: The experimental curve may be fitted to the master curve as in (1); equally good fits can be obtained with λ values varying within a narrow range. For each λ value within this range a value of N_s and G may be calculated as in (1); from this series the N_s value closest to the

experimentally determined N_s value may be selected, and the accompanying G value is that desired.

In determining rates of nucleation and rates of growth, therefore, the analysis should be of assistance in shortening experimental studies. The analysis applies only, it must be emphasized, to a process that proceeds by nucleation at grain boundaries exclusively and by radial growth from these nuclei. In applying it, it is necessary first to ascertain that the process conforms to these conditions. The formation of bainite at low temperatures and the formation of martensite in steels, though perhaps starting at grain boundaries, do not proceed by radial growth, and accordingly the analysis must not be applied to these reactions. The fact that the formation of bainite at low temperatures gives a reaction curve very similar in appearance to that for the formation of pearlite is thus wholly deceptive. For reactions in steel the analysis applies therefore only to the formation of pearlite.

No studies of the statistical shape of pearlite nodules have been made, and the patch-area distribution curve accordingly has not been calculated, but it seems possible to make a successful study of this sort and to derive the desired distribution curve. If a method were available for determining the number of patches after complete reaction, a relation between this number and N_s, G, and a could be derived, and this would be of assistance in determining N_s and G in a manner comparable to the method used in the first section.

The possible shapes of reaction curves for grain-boundary nucleation as given in Fig. 11 include a curve for $\lambda = \infty$ which starts with maximum velocity, whereas the reaction curve for general nucleation always starts with a zero velocity and then accelerates. An experimental curve of the shape given by the curve $\lambda = \infty$ in Fig. 11 may thus be taken as proof of grain-boundary nucleation, whereas curves of any other shape will not in themselves distinguish between the two types of nucleation. The reaction curve for the decomposition of the phase "FeO"[15] is of the shape $\lambda = \infty$ in Fig. 11, and it may be concluded that nucleation in this transformation is restricted to the grain boundary.

SUMMARY

An analytical expression is derived for the rate of reaction in a reaction proceeding by nucleation and growth when nucleation occurs without regard for matrix structure and the nuclei tend to grow into spherical nodules. The effects upon the reaction curve of variations in the rate of nucleation N_v, and in the rate of growth G, have been derived from the analytical expression. Distribution curves are derived for the sizes of nodules and for the corresponding areas on the surface of polish. The application of the analysis to the process of freezing and recrystallization is discussed. The calculation of N_v and G from easily obtained experi-

mental data is described. If N_v or G is known, the other may be calculated from fewer experimental data.

An analytical expression is derived for the rate of reaction in a reaction proceeding by nucleation and growth when nucleation is restricted to the grain boundaries and the nuclei tend to grow to half-spherical nodules. The effects upon the reaction curve of variations in matrix grain size a, in the rate of grain-boundary nucleation N_s, and in the rate of growth G, have been derived from the analytical expression. Conditions for identical reaction curves are given. The application of the analysis to actual reactions, particularly the formation of pearlite from austenite, is discussed. It is shown: (1) that if a is known and the experimental reaction curve known accurately, N_s and G can be calculated with fair accuracy, and (2) that if a and the experimental reaction curve are known and either N_s or G is known, the other can be calculated with improved accuracy.

These analyses serve not only to reproduce the form of isothermal reaction curves in terms of the constants N (N_v or N_s) and G, but serve also to assist in the determination of these basically important constants.

REFERENCES

1. G. Tammann: States of Aggregation. Translation by R. F. Mehl. New York, 1925. D. Van Nostrand Co.
2. E. S. Davenport and E. C. Bain: *Trans.* A.I.M.E. (1930) **90**, 117.
3. E. C. Bain: *Trans.* A.I.M.E. (1932) **100**, 13.
4. E. C. Bain: *Trans.* Amer. Soc. Metals (1932) **20**, 385.
5. E. C. Bain: *Year Book* Amer. Iron and Steel Inst. (1934) 86–119.
6. J. R. Vilella, G. E. Guellich and E. C. Bain: *Trans.* Amer. Soc. Metals (1936) **24**, 225.
7. J. G. Zimmerman, R. H. Aborn and E. C. Bain: *Trans.* Amer. Soc. Metals (1937) **15**, 755.
8. E. C. Bain: *Jnl.* Iron and Steel Inst. (1938) **138**, 33P.
9. M. Polanyi and E. Schmid: *Ztsch. Physik* (1925) **32**, 684.
10. G. Tammann and W. Crone: *Ztsch. anorg. allg. Chem.* (1930) **187**, 289.
11. R. Karnop and G. Sachs: *Ztsch. Physik* (1930) **60**, 464.
12. Series by F. Wever and collaborators, beginning 1930: F. Wever and N. Engel, *Mitt.* K.W.I. Eisenforschung, Düsseldorf (1930) *Abh.* 150. The first paper on isothermal reaction rates was by F. Wever and H. Lange: *Ibid.* (1932) *Abh.* 201. The most recent paper was by F. Wever and A. Rose: *Ibid.* (1938) *Abh.* 359.
13. C. S. Smith and W. E. Lindlief: *Trans.* A.I.M.E. (1933) **104**, 69.
14. W. Fraenkel and W. Goez: *Ztsch. Metallkunde* (1925) **17**, 12.
15. G. Chaudron and H. Forester: *Compt. rend.* (1924) **178**, 2173–2176.
16. D. L. McBride, C. H. Herty, Jr. and R. F. Mehl: *Trans.* Amer. Soc. Metals (1936) **14**, 281.

17. E. Cohen and C. van Eijk: *Ztsch. phys. Chem.* (1899) **30**, 616.
18. W. Fraenkel and W. Goez: *Ztsch. anorg. Chem.* (1925) **144**, 45.
19. H. Krainer: (*a*) *Archiv Eisenhüttenwesen* (1936) **9**, 619; (*b*) *Ztsch. Elektrochem.* (1937) **43**, 503–509.
20. J. B. Austin and R. L. Rickett: This volume, page 396.
21. F. Wever and H. Hänsel: *Mitt. K. W. I. Eisenforschung, Düsseldorf* (1937) *Abh.* 318.
22. G. Tammann: *Ztsch. anorg. allg. Chem.* (1933) **214**, 407.
23. G. B. Upton: *Trans. Amer. Soc. Metals* (1934) **22**, 690.
24. F. v. Göler and G. Sachs: *Ztsch. Physik* (1932) **77**, 281–286.
25. R. F. Mehl: The Physics of Hardenability. Amer. Soc. Metals Preprint (Oct. 1938).
26. A. Huber: *Ztsch. Physik* (1934–1935) **93**, 227.
27. E. Scheil and H. Wurst: *Ztsch. Metallkunde* (1936) **28**, 340–343.

DISCUSSION

(Gilbert E. Doan presiding)

G. E. DOAN,* Bethlehem, Pa.—These mathematical studies in the rate of development of crystalline grains bring a quantitative aspect into Tammann's descriptive theory of nucleation and grain growth, which cannot help but remind one of the more extensive mathematical definition given to our knowledge of metallic structures by J. Willard Gibbs in the Phase Rule. One approach prescribes only the number of crystalline phases, it is true, while the other deals with the rate of development of any one phase. But both lead, by a process of mathematical analysis, toward an increase in the degree to which metallic systems may be treated quantitatively.

The very rarity of mathematical contributions in metallurgy will cause the reader of this paper to be reminded all the more strongly of that earlier basic mathematical contribution. When one realizes that ·experiment and description, followed by hypothesis, is the program followed by at least 99 per cent of our metallurgical research —in age-hardening, in work-hardening, in investigation of constitutional diagrams, in metallic property studies, and even in Bain's studies of decomposition rates—one finds that the mathematical contributions fall naturally into a class by themselves, a class of the very highest value.

Little or no progress was made in understanding the factors that determine the number of phases at equilibrium until Gibbs set up the system in mathematical form. Likewise little progress has been made up to the present in understanding the isothermal reaction curve in metallic systems. Perhaps this paper, with its keen analytical approach, is a fundamental step in that direction.

S. E. MADIGAN,† Waterbury, Conn.—Congratulations are due the authors of this paper for their stimulating application of mathematics to metallurgy. A continuation of this effort to make mathematics a metallurgical tool should be of great value.

The agreement of their results with experimental data is very encouraging. It is also pleasing to see the elimination of the rather awkward conception of an incubation period before nucleation begins. The assumptions involved in the calculations for grain-boundary nucleation can, of course, be applied only to special cases. The results from the assumption of random nucleation can also be applied only with great caution.

The authors suggest that this latter assumption can be applied to single-phase alloys especially after severe working. This, however, is purely relative and is funda-

---

* Professor of Metallurgical Engineering, Lehigh University.
† Chase Brass and Copper Co., Inc.

mentally incorrect.   As stated by Elam,[28] recrystallization starts at grain boundaries and slip planes; thus in a severely worked alloy, although there are a multitude of possible nucleation points, the process is still not completely random.   While the present work does not include any factor for original crystal size or cold-work in single-phase alloys, it is well known[29] that both of these factors affect recrystallization.

In an investigation still in progress in the Laboratories of Chase Brass and Copper Co., Inc., some interesting observations have been made in this direction.   Alpha brasses with varying degrees of cold-working have been subjected to long-time anneals at temperatures slightly above the recrystallization point.   The nucleation number was found to increase with increasing cold-work.   After 15 days at 500° F. severely worked specimens of 70-30 brass had completely recrystallized, although some coalition occurred on further heating.   After the same heat-treatment specimens less severely worked showed only a few nucleation centers and were completely recrystallized only after 200 days.   At the end of this period, as was to be expected, the grain size was much smaller for the severely worked material than for the other.

It is possible that the line of attack used by the authors can be extended to include the effect of original grain size and working on variations in N and G.   Probably, however, a more fundamental basis must be used, such as that applied by Stranski, Volmer and others to crystallization from vapors and melts.

In crystal physics such problems have been attacked by the use of the thermo-dynamical concept of free energy relations.   As an example, the adsorption of small crystals by larger ones (coalition) has been successfully explained by a consideration of the surface energies and the energy of sublimation.   Since for stability the free energy must be a minimum, nucleation should start at points of high energy; i.e., at slip planes and crystal boundaries.   That such regions of high energy exist within metals has been shown by C. G. Maier[30] and others.   In order that nucleation may start, an energy of activation must be supplied by thermal agitation, electrical discharge, etc.   This concept of activation energy has been used by Ehring, Ewell[31] and others in applying the modern theory of reaction rates to such problems as diffusion, plasticity and viscosity, and might be applied successfully to recrystallization.

Stranski[32] has developed a successful theory of crystallization from vapors and melts, which gives both nucleation number and crystallization velocity in terms of the more fundamental values of sublimation energy and surface energy.   Stranski obtained a distribution function given by the expression

$$\frac{dZ_a}{da} = Ce^{-\frac{\varphi}{2r_0^2}\left(\frac{4a^3}{a_3} - 6a^2\right)/kT}$$

where a = edge length of a cubic crystallite,

a_3, edge length of a three-dimensional nucleus,

r_0, edge length of a unit cell,

$\dfrac{dz_a}{da}$, distribution function for number of crystallites of size a,

φ, work function,

C, constant,

kT, has usual thermodynamic significance.

The nucleation number is given by

$$N = Ar_0(a_3^2 e^{-W_2/kT})^3 e^{-E_0/3kT}$$

[28] C. F. Elam: Distortion of Metal Crystals.   Oxford Univ. Press.

[29] L. W. Eastwood, A. E. Bousu and C. T. Eddy: *Trans.* A.I.M.E. (1935) **117**, 246.

[30] C. G. Maier: *Trans.* A.I.M.E. (1936) **122**, 121.

[31] R. H. Ewell: *Jnl. Applied Physics* (1938) **9**, 252.

[32] Stranski: *Phys. Ztsch.* (1935) **36**, 393.

and the crystallization velocity by

$$G = Ar_0(a_2 e^{-W_2/kT})^2 e^{-E_2/2kT}$$

where a_2 = edge length of a two-dimensional nucleus,

W_2, two-dimensional work function,

E_s, surface energy,

E_e, edge energy.

It is interesting that the curve for $\dfrac{dZ_a}{da}$ is, of the same shape as the experimental data of Scheil and Wurst in Fig. 15 of the present paper. Stranski has compared his value for the recrystallization velocity with the data of Volmer and Marder[33] for supercooled glycerin, with excellent results.

It would be rather difficult to compare Stranski's theory directly with available data on metals, but a similar consideration of the recrystallization problem from the fundamental standpoint of free energies might yield a solution showing the effect of crystal size and working upon the recrystallization process.

F. C. HULL,* Pittsburgh, Pa.—In the derivation of their reaction equations for grain-boundary nucleation the authors have assumed: (1) a constant rate of nucleation, (2) a constant rate of growth, (3) a single grain size, (4) that the nuclei are statistically distributed with respect to their position at the boundary of a given grain and from grain to grain, and (5) that pearlite nodules do not grow across grain boundaries. The fact that these assumptions may not be fully justified does not detract from the theoretical value of the analysis, but it would make it extremely difficult to use the master curves as an aid in the experimental determination of rates of nucleation and growth. Observations made by the writer indicate that the master curves will not be as helpful in experimental determinations of the rates of nucleation and growth in steels as the authors had hoped.

Only a few words need to be said about the constancy of austenitic grain size. Statistical calculations reveal a range of grain sizes in space in steels which ordinarily would be considered as having a uniform grain size. This variation from constancy does affect the shape of the reaction curve, as the authors have shown, and would be a source of error in trying to match an experimental reaction curve with the master curves.

The writer has obtained data that indicate that there is a considerable variation of rate of nucleation with time during the isothermal decomposition of austenite. The rate of growth of pearlite was found to be constant. The steel investigated was a medium-hardening carbon tool steel, containing 1.01 per cent C, 0.16 per cent Si, 0.15 per cent Mn, 0.011 per cent P, 0.011 per cent S, 0.05 per cent Cr and 0.03 per cent Ni. Aluminum additions were made in the ladle. Samples cut from a forged bar were heated 1 hr. at 875° C. and oil-quenched, then heated ½ hr. at 1100° C. and transformed different times in a lead bath at 680° C. Transformation was halted by an ice-water quench. The radius of the largest pearlite nodule in a plane section of each sample has been plotted versus the corresponding reaction time in Fig. 16. The fact that the points lie close to a straight line indicates that the linear rate of growth of pearlite is constant. The slope of the line is equal to G, or 4.3×10^{-3} mm. per sec. in this instance. The intercept on the time axis corresponds closely to the time required for the specimen to reach the temperature of the lead bath.

Using the statistical methods employed by Scheil,[34] the number of pearlite nodules per cubic millimeter was calculated for various reaction times (Fig. 17). Up to about

[33] Vollmer and Marder: *Ztsch. phys. Chem.* (1931) **154-A**, 97.
* Westinghouse Graduate Fellow in Metallurgy, Carnegie Institute of Technology.
[34] Scheil: *Ztsch. Metallkunde* (Nov. 1936) 340.

16 sec. (corresponding to 20 per cent total transformation) each nodule usually represents a single nucleus, but thereafter nodules from different nuclei impinge, and a calculation of the number of transformed volumes is no longer a measure of the total number of nuclei formed during the reaction.   The points in Fig. 17 do not lie on a straight line through the origin, as they should if the rate of nucleation were constant.
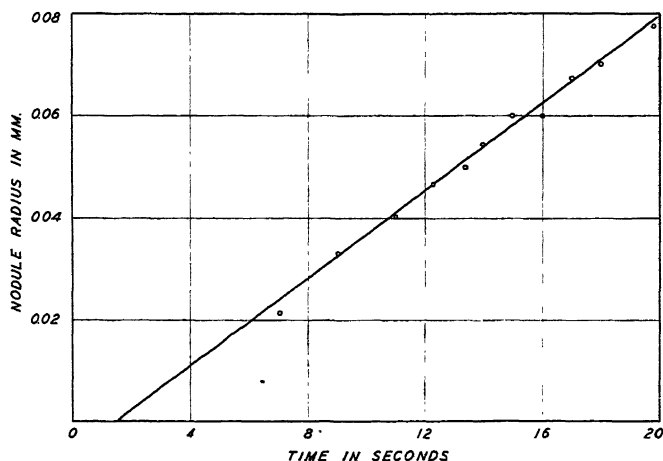
FIG. 16.—NODULE RADIUS VERSUS TIME IN FORMATION OF PEARLITE AT CONSTANT TEMPERATURES.
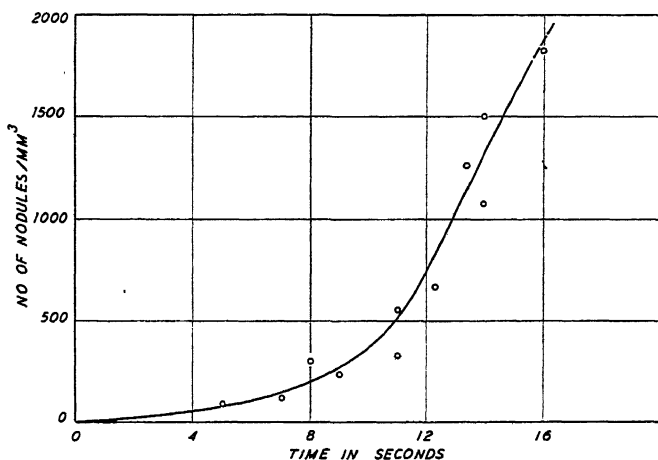
FIG. 17.—NUMBER OF NODULES PER MILLIMETERS CUBED VERSUS TIME IN FORMATION OF PEARLITE AT CONSTANT TEMPERATURE.

The actual rate of nucleation, expressed as number of nuclei per cubic millimeter of untransformed austenite per second, has been obtained as a function of time by dividing the slope of the curve in Fig. 17 at each point by the corresponding percentage not transformed (Fig. 18).   It is highly probable that the rate of nucleation decreases after reaching a maximum, but this study has not been completed.

Observations made by the writer on partially reacted steels cast doubts on the validity of the authors' fourth and fifth assumptions; namely, that nuclei are statistically distributed, and that nodules do not cross boundaries.   Under the conditions

of heat-treatment used in this research an average austenite grain diameter of about 0.05 mm. (A.S.T.M. grain size 6) was developed, which is only a fraction of the diameter of many of the pearlite nodules. In the transformation of fine-grained steels or in coarse-grained steels at temperatures near the critical, there is usually only one nucleus per grain, for the whole grain is transformed before another nucleus appears. Under such conditions of nucleation, transformation continues in grains adjoining the one in which the original nucleus formed. This means that either: (1) pearlite can grow across a grain boundary, or (2) that strains resulting from transformation increase the rate of nucleus formation in the vicinity of the transformed region. It is conceivable that the heat evolved during transformation may have to be considered. It is observed that nuclei form preferentially near grains in which transformation has begun. Such a cluster of nuclei soon grows together to form a single nodule and transformation continues around this nodule as though we were dealing with a case of
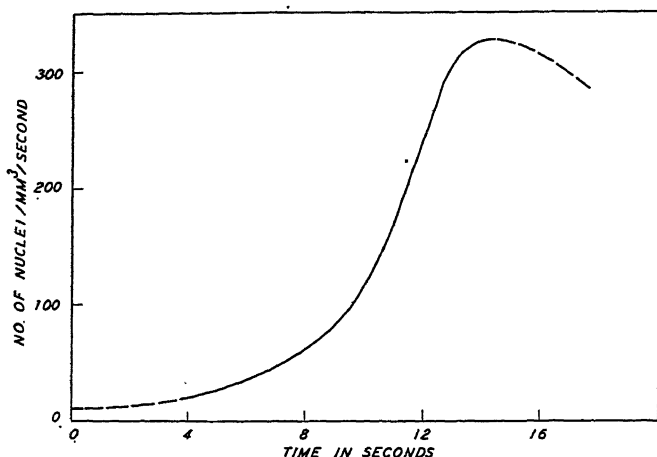
FIG. 18.—RATE OF NUCLEATION VERSUS TIME IN ISOTHERMAL DECOMPOSITION OF AUSTENITE.

Note that N is given as number of nuclei per cubic millimeter of untransformed austenite per second.

general nucleation. It is apparent that the factor determining the rate of transformation is the number of original nuclei rather than the ones that form close to an advancing interface. When the rate of nucleation is high and many nuclei form at the boundaries of all the grains, the authors' assumptions are more nearly justified.

J. E. DORN* AND E. P. DE GARMO,* Berkeley, Calif.—Reaction kinetics have fundamental importance in practically every phase of metallurgical practice. Scarcely a process exists that is not dependent upon the two variables change of properties and time. For heat-treatment of steel, reaction kinetics have a special significance that has been vividly demonstrated by the investigations of Bain, Davenport and others. These experiments have resulted in a more accurate knowledge of the principles involved in the art; they have accounted for a new method of heat-treatment involving the isothermal decomposition of austenite at temperatures from 400° to 800° F. that yields a product that is only slightly less hard but exceedingly tougher than tempered martensite; they have also established the recognition of a new microconstituent, bainite; numerous additional achievements of isothermal reaction studies could be appended to the preceding itemization.

* Department of Mechanical Engineering, University of California.

Up to the present time the reaction curves obtained in these investigations had only empirical significance. For example, the shape of the reaction curve for the decomposition of austenite into pearlite were not correlated with the processes of nucleation and growth that were involved in this reaction. The present paper by Johnson and Mehl is indeed a most welcome and important contribution in this respect. At this time, when the value of more accurate metallurgical control is so widely appreciated, the true industrial importance of the present theoretical paper can scarcely be estimated. Perhaps the most apparent consequence centers about the so-called induction period, which the present authors have indicated to be inherent in the mechanism for nucleation and growth. If this is true it will be possible to establish a fairly accurate criterion for the time-temperature relationships during a continuous quench that will permit the formation of 50 per cent martensite. Such a criterion correlated with the heat-transfer equations would successfully yield the information we desire concerning the hardenability of steels. Furthermore, the authors' conclusions concerning the induction period (although not yet unquestionably established) deny the long-debated point concerning intermediate steps in the decomposition of austenite to pearlite. We cannot at present predict all of the consequences of this excellent paper.

In our laboratories at the University of California some studies on rates of reactions are in progress. (The results will be published upon completion of this work.) For volume nucleation and growth we have obtained an expression

$$f(t) = 1 - e^{\sum_{1}^{\infty}(-1)^m A_m t^{4m}}$$

where

$$\sum_{1}^{\infty}(-1)^m A_m t^{4m} = -\left(\frac{\pi G^3 N v}{3}\right)t^4 + 0.01428\left(\frac{\pi G^3 N v}{3}\right)^2 t^8$$
$$-0.001057\left(\frac{\pi G^3 N v}{3}\right)^3 t^{12} + \cdots$$

seven terms of the series being required for 0.1 per cent accuracy in the final solution. For $\sqrt[4]{\frac{\pi G^3 N}{3}}\,t < 0.9$, our results agree very well with those of the authors. Above this value our reaction curve lies below that reported, but the deviation never exceeds 5 per cent. This difference arises because Johnson and Mehl assumed that the rate of nucleation is independent of the amount of untransformed material whereas we assumed that the rate of nucleation is proportional to the untransformed volume.

The analytical approach to transformation by grain-boundary nucleation and growth that Johnson and Mehl used is unique and represents the first method that yields a reasonable solution to this difficult problem. They are to be congratulated upon having formulated a simple and reasonably adequate criterion for calculating the impingement factor for this problem.

A previous paper by Dr. Mehl (ref. 25) contained an equation for the transformation curve, which we believe is slightly more accurate than that given in the present analysis. It must be evident that due to: (1) the application of differentials in the rate of nucleation equation and (2) the application of the impingement factor that was used, the present analysis does not represent what takes place in a single grain but is representative of the average reaction of a great number of grains. If this be so, is it necessary to correct for the most probable time of formation of the first nucleus when in differential language discrete nuclei have no significance? We believe that this correction is inherent: (1) in the statistical differential statement

that the rate of nucleation is proportional to the grain-surface area and (2) in the assumption made in establishing the impingement factor. In this light, equation $8a$ yields the final result, provided this equation is accurate.

It appears to us that in the derivation of equation $8a$, as given in Appendix D, several additional overcorrections were employed. Perhaps the authors would be willing to elucidate further on these points. The divisor in the impingement factor is the total area of the shell of radius x outside the nodule considered. Should not this area be $4\pi X^2 - S_1$, where S_1 is the area included in the impeded nodule and not in the area included in the nodule provided it has suffered no impingement? We have also failed to understand why the rate of growth of the first nucleus was added to the solution of D-5 which we believe already contains this factor in a statistical manner. Because of the application of differential methods, the time of formation of the first nucleus is spread over a small-time range such that at times less than the most probable time of formation only a fraction of a nucleus is nucleated. From a statistical point of view this means that at a time less than the most probable only a fraction of the grains considered have nucleated.

We tried to incorporate into the Johnson-Mehl analysis the added assumption that the rate of nucleation is proportional to the untransformed surface of the grain. This yielded

$$f(t) = \frac{3}{a^3}\int_{a-Gt}^{a} x^2 \left(1 - e^{-\frac{2\pi a^2 G}{x}\left\{\sum_0^\infty (-1)^m \left(t - \frac{a-x}{G}\right)^{3m+2}\left[t + (3m+2)\frac{(a-x)}{G}\right]\right\}}\right) dx$$

where the coefficients of the series are known. If all except the first term of this series is neglected the equation agrees with that previously reported by Mehl. The agreement between the results is good up to $\frac{Gt}{a} = 0.6$, beyond which point our reaction curves lie slightly below those reported by Mehl.

It is apparent, in view of the idealizations used in this analysis, that the theoretical reaction curves are only first approximations to the experimental reaction curves. Exact agreement between theory and experiment, therefore, is rather fortuitous. This is especially true when the reaction data are compiled by microscopic investigations on plane surfaces and then interpreted in terms of the volume transformed without adequately taking into consideration the probability factor involved in such alterations.

It may be important to note that microscopic investigations on rates of nucleation cannot yield an independent value of the nucleation constant. If pearlite nodules are half spheres the probability of "seeing" a nodule of radius r nucleated at the surface of an austenite grain of radius a is

$$P = \frac{2}{\pi}\arcsin\frac{r}{2a} + \frac{r}{a\pi}\arccos\frac{r}{2a}$$

To a first approximation (valid only for small values of z) the number of nodules seen per grain cut by the polished plane is

$$Z = 4\lambda\left[2z - \arcsin\frac{z}{2} - \left(1 - \frac{z^2}{2}\right)\arccos\frac{z}{2} + \left(4 - \frac{z}{2}\right)\sqrt{1 - \frac{z^2}{4}} - 2.4292\right]$$

At present, therefore, the nucleation constant cannot be determined independently of the growth constant.

We wish to congratulate both authors on their excellent contribution. The tremendous amount of work devoted to the preparation of this paper is scarcely revealed by its modest presentation.

M. Avrami,* New York, N. Y.—It is a remarkable but not unfamiliar fact that theorists and experimenters in a given field may, for considerable periods of time, use divergent concepts to describe the same set of phenomena. It is even more striking when one and the same individual advances the theoretical concepts and performs many of the experiments that disagree with his own theory and lead others to a different picture. We have exactly such a situation in the theory of the mechanics of phase change, advanced by Tammann, which the authors of this paper have followed and attempted to make quantitative.

Tammann assumes a constant rate of spontaneous nucleation of the new phase either throughout the volume or upon the grain surfaces of the old phase. The rate of this nucleation, as it would occur if the old phase were perfectly uniform, may be calculated, following Volmer and others, from thermodynamic considerations. We find, however, that the assumption of constant rate of nucleation (proportional to the transforming volume or surface) is generally contradictory to the experimental facts. The work of many experimenters, including, recently, Hammer[35] and Scheil-Lange Weise,[36] has shown that, as transformation proceeds, the rate of observed nucleation decreases much faster than in proportion to the untransformed region, so that the total number of growth nuclei approaches a definite saturation value characteristic of the degree of undercooling. It is as though only a certain number of *germ nuclei*, which, becoming activated, can serve as nuclei for growth to grains of observable size, are originally present, and as transformation proceeds these become used up. These germ nuclei already exist in the old phase and their effective number can be altered by temperature and duration of superheating. It is in this way that the kinetics of phase change is conditioned by previous treatment, a fact well known to all experimenters in this field. The germ nuclei may be heterogeneities of any sort to which the nucleation mechanism is sensitive—for instance, strained regions in the lattice, foreign particles with an adsorbed layer of the new phase, prephase fluctuations of the type recently considered by Frenkel,[37] or tiny "blocks" or "crystal molecules" of the new phase of the sort contemplated in one form or another by Zwicky, Smekal, Goetz, and many others.[38]

Besides the direct evidence for the existence of these germ nuclei there is a great deal of indirect evidence; e.g., in the fact that the grain-size distribution in the resulting microstructure of a new phase shows far fewer small crystals than is to be anticipated on the constant-nucleation-rate hypothesis. This may be seen in the data of Tammann-Crone[10] on cadmium and aluminum, and of Scheil-Lange Weise[36] on the austenite-pearlite transition. Göler-Sachs and Huber[24,26] have commented on this discrepancy without being able to explain it. Huber suggests that it requires a fundamental conceptual change. It does. We find an immediate explanation in terms of the idea that the germ nuclei get used up as the reaction proceeds.

The above and related considerations have led me to develop the theory of the kinetics of phase change upon the basis that the new phase is nucleated by germ nuclei whose number can be altered by previous treatment of the old phase.† The

---

* School of Mines, Columbia University.

[35] C. Hammer: *Ann. Physik* (1938) **33**, 445.

[36] E. Scheil and H. Lange-Weise: *Archiv Eisenhüttenwesen* (1937–38) **11**, 93.

[37] J. Frenkel: *Jnl. Chem. Physics* (July 1939).

[38] C. H. Desch: The Chemistry of Solids. Cornell Univ. Press, 1934.

† This work is contained in a series of papers, which will appear shortly in the *Journal of Chemical Physics*. A less mathematical treatment will also be ready soon.

density of germ nuclei diminishes through activation of some of them to become growth nuclei for grains of the new phase and ingestion of others by these growing grains. The quantitative relations between the density of germ nuclei, growth nuclei, and transformed volume have been derived and expressed in terms of a *characteristic time scale* for any given substance and process. The geometry and kinetics of a crystal aggregate, under both isothermal and nonisothermal treatment, have been studied and a number of empirical results, including those of Krainer, Austin-Rickett, Wever-Hensel, Tammann, and Upton, mentioned by the authors, have been derived as approximations under the proper circumstances from the general theory. The effect of the theory is to emphasize the importance of the specific nucleation rate, rather than the rate of grain-growth G, as the factor determining the time scale of the phenomena. This result, which stands in direct contradiction to the statement of the authors, is in agreement with the conclusions of several investigators (see, for instance, Scheil-Lange Weise[36]).

From yet another point of view it may be seen that the basic premise of the authors is unsatisfactory. Their theory for volume (or "general") nucleation leads to isothermal reaction curves all having the same shape (on a logarithmic time plot as in Fig. 2). In order to obtain the experimentally observed diversity of shapes, such as are found in the decomposition of austenite, they are compelled to resort to a surface nucleation theory. Now, there is no reason why the assumption of random distribution of grain centers throughout the volume should not be applicable with good approximation even where nucleation takes place exclusively at the grain boundaries, just so long as the structure is fine-grained. The results of a random volume nucleation theory should check approximately with those of a theory that explicitly takes into account the distribution along grain boundaries. The diversity of isothermal curve shapes in random volume nucleation is immediately realized upon the introduction of the germ nucleation theory.

In certain extreme cases, where there are almost no germ nuclei present and the substance is greatly supercooled, the spontaneous nucleation throughout the volume will effect phase change. In these circumstances the assumption made by Göler-Sachs and the authors is verified. Their theory is then included in the general one as the special limiting case in which there is a very numerous and uniformly dense distribution of germ nuclei with a correspondingly small specific nucleation rate. Let us proceed to see whether the authors' results follow correctly from their basic premises in this case. If, for brevity, we denote by the adjective "extended" the volume of any grain had its growth been unimpeded by impingement upon any other grain, we may state one of their fundamental steps as follows: The ratio of the rate of growth of an actual "nodule" to the rate of growth of its extended volume is equal to the fraction of untransformed matrix per unit volume. Karnop-Sachs (ref. 11) have previously made a mathematically equivalent assumption. Considerable doubt may be raised as to its validity, on the following grounds: The fraction of untransformed matrix measures the ratio of nonoverlapped to extended volume of any *random volume region*. We cannot too easily assume that it also measures the corresponding ratio in what is effectively a *selected surface region;* i.e., the layers of grain increments in an element of time. The assumption requires more rigorous justification. It does turn out to be correct, primarily because of the assumed complete randomness. The rigorous justification is given in the aforementioned work to appear in the *Journal of Chemical Physics*. But even though this fundamental assumption is justified, the authors' results must be corrected, since, in calculating the total actual extended volume, they unwarrantably set it equal to the total extended volume of all the grains that would have appeared if there had been no diminution in untransformed volume. This is equivalent to assuming a constant rate of nucleation per unit total (not untransformed) volume. The argument given by the authors in appendix A to justify

this procedure is in error, since the contribution to the transformed volume, of those grains that would have appeared inside the already transformed regions, is not a fraction of their extended volume *but definitely zero*. A functional equation somewhat in the manner of Göler-Sachs must be solved to allow for the continually decreasing volume of nucleation. (This has been done much more generally in the theory previously referred to.) Thus, even in the special case that they have treated, of constant nucleation rate per unit untransformed volume, we must regard the authors' results as only an approximation, which becomes progressively poorer as transformation proceeds.

WILLIAM A. JOHNSON AND ROBERT F. MEHL (authors' reply).—We are grateful to Dr. Doan for his kind comments on this paper. While a mathematical analysis of known and recognized behavior may add no new practical result directly, it has been the experience of those who have engaged in such work that it furnishes a clearer understanding of the relative importance of cooperating factors and thus improves one's judgment on practical problems; furthermore, quantitative analytical work frequently brings to light unexpected factors, which when controlled furnish practical improvements.

Dr. Madigan's discussion is valuable and pleasant to receive. We are not in disagreement with him as to the assumption of general nucleation in recrystallization; fundamentally nucleation in recrystallization is in fact not random but preferred, presumably, at positions of maximum strain energy—slip lines, etc. These positions, however, are perhaps sufficiently randomly distributed throughout a drastically cold-worked sample that the assumption may prove permissible. The point can be studied experimentally: the recrystallization of silicon-ferrite can be accomplished in such a way that the recrystallized grains grow in nearly perfect sphericity in an unrecrystallized matrix; the determination of N_v and G should be easy to make. Work on this problem is now being pursued in our laboratory. This we believe to be the proper method to study recrystallization. It is very interesting to know that Dr. Madigan is performing a similar study on brass; we should expect some difficulty in a lack of sphericity in the growing grains and in distinguishing between the recrystallized grains and the matrix.

We agree also on the importance of nucleation theory in reactions of this type. One of us has recently used this theory in discussing the formation of pearlite from austenite (ref. 25); the importance of activation energies in this theory as well as in other connections is well recognized.[39] Unfortunately, the theory has not been fully developed for solid-solid reactions. The results of the theory for condensation reactions can be applied to solid-solid reactions only qualitatively, for the formal theory requires interface energies at solid-solid interfaces upon which we have no information. This is being discussed in a paper soon to be published.[40] In view of this, it is our opinion that rapid progress is more likely to be made by experimental determinations of N_v and G and the variation of these—so far as recrystallization is concerned—with original grain size, percentage of deformation (and type of deformation), solute concentration in solid solutions, recrystallization temperature, etc. The effect of original grain size, percentage of deformation, etc., to which Dr. Madigan refers, should not be included in the reaction equations given in the present paper, for this will manifest itself purely upon the values of N_v and G, which are to be substituted in the reaction equation to provide the reaction curve.

[39] R. F. Mehl: Diffusion in Solid Metals. *Trans.* A.I.M.E. (1936) **122**, 1.

[40] R. F. Mehl and L. K. Jetter: Mechanism of Precipitation from Solid Solutions. Amer. Soc. Metals (Oct. 1939).

We are pleased to have Mr. Hull's preliminary results on the rate of nucleation and growth for what may be considered a fairly representative steel. His results are in agreement with those of Scheil with respect to the manner in which the rate of nucleation changes during reaction, and we believe are more trustworthy (see discussion of Scheil's work, ref. 25). It is obvious that reaction curves calculated on the assumption of constant nucleation must not be applied to such cases, but that curves calculated with provision for variation in the rate of nucleation must be used, as stated in the paper; the method of treating such cases is given in Appendix B. Such studies as Mr. Hull reports are in our opinion of utmost importance in making progress in this field, and have been selected as an important part of a comprehensive study of such reactions in this laboratory. As experimental data accumulate, mathematical treatment will assume a greater degree of reality. Much simple metallographic work remains to be done; for example, under what conditions do growing pearlite nodules trespass grain boundaries, what are the metallurgical conditions that favor general nucleation, what circumstances favor edgewise growth of pearlite (ref. 25)? Perhaps Mr. Hull may procure some of this badly needed information.

It seems quite possible that Mr. Hull's suggestion that he is dealing with what *approximates* general nucleation is correct. We have used his data to calculate a reaction curve according to the method given in Appendix B, by fitting an equation to his nucleation curve [the equation for rate of nucleation was $N_v = 11(1 + 0.04545t^2 + 0.0002636t^4)$] and using his value of G; following the procedure given in Appendix B, we obtained a reaction equation

$$\ln u(t) = -9.275 \times 10^{-7}[t^4 + 0.003030t^6 + 0.000003766t^8]$$

where $f(t) = 1 - u(t)$ and time is expressed in seconds. According to this equation, about 17.5 sec. is required for 20 per cent transformation, which agrees very well with Mr. Hull's value of "about 16 seconds."

The discussion by Messrs. Dorn and De Garmo reveals an appreciation for the mathematical difficulties involved in the derivations given in the appendixes. In answering this and Mr. Avrami's discussion it will be necessary to discuss in detail several aspects of the derivations.

Several years ago one of us (W. A. J.) derived a reaction equation for general nucleation employing what appears to be a method identical to that used by Messrs. Dorn and De Garmo. The result was

$$f(t) = \frac{\pi G^3 N_v}{3}t^4 - 0.51428\left(\frac{\pi G^3 N_v}{3}\right)^2 t^8 + 0.18199\left(\frac{\pi G^3 N_v}{3}\right)^3 t^{12} - \cdots$$

If this result is rewritten in the exponential form used by the discussers, it is identical with their equation as given. However, we believe that this expression is less accurate than the one given in this paper, because of the less accurate method of treating impingement. Let us consider the derivation of the reaction equation in detail. It may be stated immediately that provision for the decrease in rate of nucleation in proportion to the amount of reaction has been made. (This is in reply also to Mr. Avrami.)

The determination of the impingement factor is the most difficult step in the analysis. Following Appendix A, the elementary increase in volume of a sphere nucleated at time T is, at some later time t

$$d\phi = 4\pi G^3(t - T)^2 dt;$$

this volume is a thin spherical shell surrounding a completely transformed sphere. Let the fraction of untransformed matrix be $u(t)$ at time t. If an entirely random region of the specimen as a whole is considered, the fraction of it that lies in untrans-

formed matrix is $u(t)$. Let us examine the conditions under which the volume $d\phi$ may be considered as random. If we write that the number of nuclei per unit volume formed in a short time dT is proportional to the fraction of untransformed matrix; i.e.,

$$dn = N_v u(T)dT$$

we have confined the small shell under consideration to certain restricted locations, since, at the time of nucleation, the center could not lie within already transformed material. Since for randomness in the position of the shell $d\phi$ we should allow its center to lie anywhere in the specimen, we do not have, under these circumstances, a randomly placed volume. It is easily seen that the average fraction of the shell lying in untransformed matrix is not, correspondingly, $u(t)$, as Messrs. Dorn and De Garmo assume. An approximation to the correct impingement factor under these conditions can be made. Consider the possible positions of a randomly placed shell: (1) entirely within transformed material, (2) entirely outside of transformed material, (3) partly within and partly outside of transformed material. For position 1 the fraction of shell lying outside of transformed material is 0; for position 2, the fraction is 1; for position 3, the fraction is between 0 and 1. The required fraction for a randomly placed shell is obtained by weighting the fractions for the three positions properly, and is $u(t)$. If the shell is constrained to lie in only positions 2 and 3, however, the fraction is made larger than $u(t)$, since we have neglected all positions for which the fraction is 0. It can be shown that under these circumstances the factor to allow for impingement is not $u(t)$ but rather $u(t)/u(T)$. Consequently, the equation given by Messrs. Dorn and De Garmo and that at the beginning of this discussion are incorrect.

Let us consider how the derivation given in Appendix A avoids this error. We shall now write for the number of nuclei formed

$$dn = N_v dT$$

which seemingly contradicts the assumption that nuclei form at a constant rate per unit *untransformed* volume. The nuclei are considered to grow as interpenetrating spheres; in calculating the rate of reaction, however, only that portion of the increase in volume of a sphere that lies in untransformed matrix is considered, and that portion of the increase in volume of a sphere that lies in transformed matrix is neglected. Thus, physically, any nuclei that lie in transformed material add nothing whatsoever to the reaction rate, since they never grow outside of the sphere in which they form. The word "nucleus" as we are using it at the moment refers to the assumed randomly distributed centers; these are nuclei in the true sense of the word only when they fall within untransformed material. The number of effective nuclei which actually grow and contribute to the reaction is then

$$dn = N_v u(T)dT$$

and thus allowance is made for a decrease in the rate of nucleation in proportion to the amount of reaction. Now let us consider the impingement factor. A consideration of what has been said will show that since the distribution of the "nuclei" is now entirely random, the fraction of the spherical shell to be added, the impingement factor, is just $u(t)$ as employed in Appendix A.

An entirely similar situation obtains in calculating the impingement factor for the case of grain-boundary nucleation, although the factor developed is somewhat more complicated. As has been shown above, it is necessary to write for the number of nuclei formed

$$dn = 4\pi a^2 N_s dT$$

That is, the rate of nucleation must be written as independent of the amount of grain surface transformed in order that in the consideration of impingement the increments of area may be considered as random; as is easily shown by an argument analogous to that previously used, no error is introduced, since only that portion of the increment in area lying in untransformed matrix is counted—thus, "nuclei" forming in already transformed material add nothing whatsoever to the reaction and the effective rate of nucleation varies with the amount of grain-boundary area transformed.

With regard to the suggestion of Dorn and De Garmo that the impingement factor should be

$$\frac{4\pi x^2 p(t,x)}{4\pi x^2 - S_1} \qquad \text{rather than} \qquad \frac{4\pi x^2 p(t,x)}{4\pi x^2 - S}$$

we can only explain in detail our choice of impingement factor, since we are unable to infer any reason for their substitution of S_1 for S.   Fig. 19 is a schematic diagram of the surface of the shell, the overlapping circles representing the intersections with the shell of the spheres growing from nuclei on the surface of the grain.   The rings represent the increase in area—transformation—in time dt.
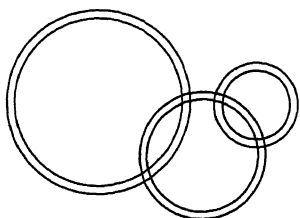
Let us fix our attention on any one of the rings. We wish to calculate the fraction of this ring that lies in material not transformed; i.e., lies in area not occupied by any circle.   If we designate the fraction of the surface untransformed as $p(t,x)$, it might be supposed that the fraction of the ring in untransformed area is also $p(t,x)$, since the center of the ring is randomly placed, but this is not true for even though the center of the ring is placed at random, the ring cannot be considered as equivalent to a random ring.   If a ring of this size were placed at random on the configuration shown in Fig. 19, the fraction of it lying in untransformed material would be $p(t,x)$, and the fraction of the circle enclosed by the ring lying in untransformed material would also be $p(t,x)$.   Since the whole area within the ring is entirely transformed, it is clear that we cannot treat the problem as one of a random ring.   In any such problem of probability, we may write that the probability of an event happening is the ratio of the number of ways it may occur favorably to the total number of ways it may occur.   Thus, if $q(t,x)$ is the probable fraction of the ring lying in untransformed material—impingement factor—then, since the ring must lie outside the circle it surrounds,

$$q(t,x) = \frac{\text{untransformed area outside the growing circle considered}}{\text{total area outside the growing circle considered}}$$

or

$$q(t,x) = \frac{4\pi x^2 p(t,x)}{4\pi x^2 - S}$$

which was used.   If S_1 is substituted for S in this expression, we should apparently require that the ring lie partly within itself.

Unfortunately, the correctness of this method of calculating $q(t,x)$ is not obvious; it will perhaps be wise to describe another method yielding the same result.   We shall find it convenient to refer to Fig. 20, which represents the same situation as Fig. 19, but in which for simplicity the rings are omitted.   We shall again consider any particular circle, randomly placed, and for convenience shall consider the one with double crosshatching.   As was explained above, we cannot consider the ring surrounding this circle as equivalent to a random ring; we can, however, modify the configuration shown in Fig. 20 so that the ring may be treated as a random ring:

Fig. 19.

we need only to suppose that the transforming circle within the ring does not exist and calculate the fraction of the surface transformed by all other circles; in removing the circle about which the ring lies, however, we do not remove those portions of it which lie in other circles. The new situation is shown in Fig. 21, in which we may now consider the ring as entirely random; the impingement factor sought is clearly the fraction of the surface in Fig. 21 that is untransformed. Let $\bar{q}(t,x)$ be this fraction. The fraction of the area within the ring lying in area not covered by other circles is $\bar{q}(t,x)$. Since the area within the ring is S, the area within the ring not covered by any other circle is $S \cdot \bar{q}(t,x)$, the area not crosshatched in Fig. 21. If we
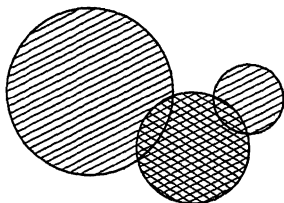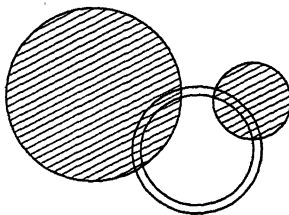
FIG. 20.   FIG. 21.

now subtract this area from the total transformed area in Fig. 20, we obtain the total transformed area of Fig. 21, which is thus

$$4\pi x^2[1 - p(t,x)] - S \cdot \bar{q}(t,x)$$

The fraction of the surface transformed is

$$\frac{4\pi x^2[1 - p(t,x)] - S \cdot \bar{q}(t,x)}{4\pi x^2}$$

which is, by definition $1 - \bar{q}(t,x)$. Equating the expressions we obtain

$$\bar{q}(t,x) = \frac{4\pi x^2}{4\pi x^2 - S}p(t,x)$$

as before. Messrs. Dorn and De Garmo's statement, "The divisor in the impingement factor is the total area of the shell of radius x outside the *nodule* considered," is incorrect; the divisor is rather the total area of the shell of radius x outside the *circle* considered. Thus the denominator they suggest is too large and the impingement factor too small; i.e., they calculate the effective rate of growth as less than it actually is.

It can now be shown why it is necessary to consider the most probable time of formation of the first nucleus. We shall first examine the result to which we are led if we treat the whole sample as a single *average* grain. Quoting Dorn and De Garmo, "Because of the application of differential methods the time of formation of the first nucleus is spread over a small time-range such that at times less than the most probable time of formation only a fraction of a nucleus is nucleated. From a statistical point of view this means that at a time less than the most probable only a fraction of the grains considered have nucleated." Let us see whether we are led to the same result by considering a fraction of a nucleus in a single grain as by considering complete nuclei in a fraction of all the grains; we are not. The complete mathematical analysis for what follows is too lengthy to include here, but the necessary steps can be determined by following the general method given in Appendix D. If we neglect the specific effect of the first nucleus and calculate a reaction equation in the manner employed by Dorn and De Garmo—but with the proper impingement factor as developed above —we find that for any finite rate of nucleation, no matter how small, the grain is completely transformed in a time not longer than corresponding to $z = 2$. This is

brought about by the fact that the impingement factor becomes infinite for $z = 1 + y$. In the other case, the grains having nuclei will have transformed completely within time $z = 2$ but the remaining grains, in which nuclei formed later, will not have completely transformed; i.e., the sample as a whole has not completely transformed. Thus it is not permissible to treat the aggregate of grains as a single average grain. This fact has necessitated the treatment given in Appendix D, in which the time of formation of the first nucleus in each grain has been considered. It should be pointed out that while this refinement is not necessary for large value of λ—i.e., cases in which no grain transforms very much before all grains have nucleated—it is essential for small values of λ when some grains will have completely transformed before others have nucleated.

It now becomes apparent why the contribution of the nucleus formed at time $T = 0$ was added to the equation for rate of growth, for time is measured from the instant this complete nucleus forms. A slight error is introduced in thus measuring the time scale for nucleation, and we might better consider it as beginning at a time after the formation of the first nucleus by half the average time to form a nucleus in a given grain. This introduces considerable difficulties, however, which more than offset any possible gain in accuracy. It is easily shown that to neglect entirely the contribution of this first nucleus leads to a much greater error than to include it.

Thus we feel that the criticisms offered by Messrs. Dorn and De Garmo to the derivation of either reaction equation are not valid and we believe that the equations given in this paper are more accurate than the ones they propose.

We agree with Messrs. Dorn and De Garmo that the coincidence between calculated and experimental reaction curves is "rather fortuitous." We do not wish to imply that such agreement is to be expected in general. We would consider agreement within 10 or 20 per cent or more as good agreement. We are somewhat puzzled, however, by a statement of the discussers which seems to imply that the percentage transformation as measured on a plane is not the same as that measured in the volume. We cannot understand how this is possible if the plane is large enough to give true sampling.

We are happy to have the remarks on the microscopic determination of rates of nucleation, and should point out that these probably do not apply to the discussion by Mr. Hull, who apparently is dealing with a case of quasi-general nucleation.

It is probably well to reply in some detail to Mr. Avrami at the risk of repeating a good deal of the paper, for he has misapprehended much of its content and does not appear to understand its purpose. The purpose of the paper is not to provide any information whatever on the rate of nucleation or the rate of growth; its purpose is only to provide derivations of reaction curves in terms of these rates, not only for the case where these rates remain constant during the reaction, which is the simplest case, but also for the case where they vary. It must be obvious that an analytical expression cannot be applied to a process in which the assumptions used in deriving the expression are invalid; for such a case another expression must be developed using assumptions which are valid for the process to which the analysis is to be applied. The treatment is wholly general, providing methods for the introduction of any variation in the rates of nucleation and of growth that experiment might discover.

Actual data on rates of nucleation and growth are very scant; they are of first importance and are now being obtained for the austenite-pearlite reaction in this laboratory—see discussion by Mr. Hull. Hammer's data refer only to organic substances; Scheil's data on the austenite-pearlite reaction are not entirely satisfactory (ref. 25) though they show an increasing rate of nucleation as the reaction proceeds, as do those of Mr. Hull. Such variations in the rate of nucleation during reaction may be introduced into the analytical expressions provided in the paper. It should be noted in passing that Volmer's methods of calculating the rate of nucleation are purely

formal in application to solid-solid reactions, and cannot be used to give actual values (see ref. 25, and reply to Dr. Madigan above).

The factors that favor nucleation, which Mr. Avrami bulks under the term germ nuclei, have been recognized for many years. As pointed out earlier (ref. 25), inhomogeneities of the inclusion type favor nucleation. The consumption of such special points within the system, however, does not assist in the explanation of nucleation-time curves such as were obtained by Scheil or Hull, for such a process would provide a rapid initial rate of nucleation and a decrease of this with time, whereas the reverse is found (see Hull's curve). Ideas on other possible points of favorable nucleation are, apart from grain boundaries, at present too elusive to deserve much consideration. It is somewhat dangerous to impute all variations in N to what Mr. Avrami calls germ-nuclei; other factors may in time prove important. Hammer's data for N_v in freezing show an initial maximum value and are thus different from those in the austenite-pearlite reaction.

The comments of von Göler and Sachs and of Huber concerning the observed deficiency of small grains are of somewhat doubtful significance, for they are based on grain-size distribution calculations made from the incomplete von Göler and Sachs equation, which call for many more small grains than required by Fig. 9. Scheil's distribution curves for pearlite approximate the curve of Fig. 9, but are of doubtful accuracy; Tammann and Crone's experimental method probably prevented truly general nucleation, at least in some measure—moreover, the absence of small grains in recrystallization is probably often caused by coalescence. The point need not be stressed, however; it is quite possible that a deficiency of small crystals, if it is real, may mean a decreasing value of N. In any event, no "conceptual change" is required.

Mr. Avrami apparently has misinterpreted our statements concerning the relative importance of the rate of nucleation and the rate of growth. In general nucleation, a given fractional change in G exerts a greater effect upon the time of reaction than the same fractional change in N_v; in grain-boundary nucleation the circumstance is even more extreme. It is to be noted that this is all based on equal fractional changes. In systems, for example, where G is always constant and N_v alone varies, obviously variations in N_v alone are important. The relative importance of N (N_v and N_s) in a general sense is thus purely a matter of possible ranges of variation in these quantities, upon which the mathematical analysis presented can furnish no comment. Thus the statement by Scheil, that the rate of nucleation is the more important variable, whether correct or not, has nothing to do with the mathematical analysis.

It is probably unnecessary to point out that we are not "compelled to resort to a surface-nucleation theory" in order to explain the diversity of shapes of reaction curves in the austenite-pearlite reaction. Surface or grain-boundary nucleation in this reaction is not a theory but a fact, as metallurgists well know (see references given in ref. 25); further, even in reactions exhibiting only general nucleation, a wide variety of shapes of the reaction curve is possible, as shown in the discussion of the effect of varying N_v and G, in the text and in Appendix B. Since nucleation of pearlite is in large part at austenite grain boundaries, it is of importance to attempt a mathematical treatment on this basis. This process has little similarity to general nucleation, differing fundamentally both with respect to locations available for nucleation and to the factors that restrict the growth of nodules. Two departures from this simple process may be recognized: (1) when nucleation occurs at grain boundaries but the nodules grow to spheres across the grain boundaries, and (2) when general nucleation in addition to grain-boundary nucleation occurs. We need experimental studies on both these points, but with information once available such data can be treated by the methods proposed.

It seems to us very inadvisable and highly dangerous to consider such processes as approximating general nucleation, for such a treatment would lump grain-boundary

nucleation with general nucleation and prevent their differentiation, an unfortunate circumstance in attempting to understand each of the factors controlling the rates. The factors controlling impingement are quite different in grain-boundary nucleation from those in general nucleation (see ref. 25); some grain-size factor is necessary, otherwise the effect of grain size on rate of reaction is lost; since in grain-boundary nucleation the rate of nucleation will decrease with the amount of grain-boundary area transformed, experimental studies based on the assumption that the rate should vary with the volume transformed will lead to incorrect values of the rate of nucleation, and would give data on the rate of nucleation showing high values in the first part of the reaction (when there is much untransformed boundary area available), and low, in some cases zero values, in the latter part (when most or all of the boundary area has been consumed)—and would therefore also give wholly incorrect information on the variation of the rate of nucleation during the course of the reaction.   Concepts concerning a "saturation value" in the number of nuclei may rest on this error.   Finally, we should point out that in the special case 1 above, the reaction curve would be of the same shape as that for general nucleation when the grain size is small and when the rate of nucleation is small, but with larger grain sizes and in the case in which grain boundaries restrict growth, the reaction curve definitely has neither the same shape nor time scale.

Much of the latter part of Mr. Avrami's discussion, dealing with the selection of a factor for impingement, has been answered in reply to Messrs. Dorn and De Garmo and this discussion need not be repeated here.

The argument advanced to justify our treatment of the rate of nucleation is by no means in error.   Mr. Avrami has apparently misunderstood the argument.   It is, of course, quite true that the contribution to the transformed volume of those spheres which appear inside the already transformed regions, is not a fraction of their extended volume "but definitely zero."   We do not imply that the contribution of every shell is the product of its volume by the fraction of the matrix untransformed; only when the average contribution of all the shells is considered may the factor $u(t)$ be used to calculate the average contribution.   Thus for each shell that contributes nothing there are others that contribute a fraction greater than $u(t)$—the *average* fractional contribution only is $u(t)$.

The early work of Karnop and Sachs mentioned by Mr. Avrami deserves comment. These authors obtained a reaction equation identical with that given here though they made different assumptions; most important, they made no correction for impingement.   Our assumptions are quite different physically and are, as a matter of fact, not equivalent mathematically.   Mr. Avrami has been perhaps misled into believing the assumptions to be equivalent mathematically by the fact that Karnop and Sachs obtained the same final equation we did; however, the mathematics employed in obtaining their reaction equation is in error and the reaction equation resulting from their assumptions differs very considerably from ours.   It is clear that if no correction is made for impingement, the fractional transformation must eventually exceed *unity*, but the Karnop and Sachs equation never reaches *unity*. Von Göler and Sachs recognized this error and corrected it; in the von Göler and Sachs equation, the fraction of transformation increases without bound.   For purpose of record we would point out that in their intermediate equation

$$dV = (V_0 - V) \cdot c \cdot dt \cdot w^3 \cdot (t_1 - t)^3$$

dV is not the differential of V and hence it is not permissible to separate variables and integrate as Karnop and Sachs did.   Von Göler and Sachs's later procedure of writing (changing the symbols so as to be consistent) is correct; i.e.,

$$V_1 = cw^3 \int_0^{t_1} (V_0 - V)(t_1 - t)^3 dt$$

Phase Changes in 3.5 Per Cent Nickel Steel in the Ac₁ Region

By I. N. Zavarine,* Associate Member A.I.M.E.

THE observations presented in this paper were recorded during a study of the spheroidizing process.

Spheroidization of cementite in steel is either brought about to develop a set of desirable mechanical properties or is an incidental result of mechanical and heat-treating manipulations. Physical properties of steel are materially influenced by the state of the cementite. Conversion of cementite from the lamellar to the spheroidal state is usually accompanied by a decrease of hardness and of strength and by an increase in ductility. The spheroidized structure is usually considered as an ultimate step in the process of the softening of steel.

The unorthodox hardening of a 3.5 per cent Ni steel (SAE No. 2330) after a heat-treatment that previously proved entirely suitable for a complete spheroidization of cementite in carbon steels led to the observations that constitute the subject of the present paper.

EXPERIMENTAL PROCEDURE

The steels used for the experiments described were bought on the market. All were in the form of ¾-in. round bars. Their chemical compositions are given in Table 1.

TABLE 1.—*Chemical Compositions of Steels*

Mark	Material	Composition, Per Cent						
		C	Mn	S	S	P	Ni	Cr
A	Carbon steel	0.46	0.72	0.08	0.072	0.11		
B	Nickel steel	0.32	0.70	0.10	0.045	0.011	3.29	0.21
C	Nickel steel	0.31	0.71	0.22	0.020	0.009	3.44	0.05

The spheroidization of cementite in steels can be obtained in several ways. The method used in the present work is, perhaps, the least known. It consists of cyclic heating and cooling of steel, the temperature being

varied about the A_1 point of the steel. This method of spheroidizing the cementite is mentioned in the earlier work of Portevin and Bernard,[*] and also in the Metals Handbook. The literature on the subject is notably vague. Data are lacking, particularly with respect to the essential details such as the temperature, the amplitude of the oscillations, time of the cycles, etc.

Preliminary experiments showed that the cyclic heating and cooling illustrated in Fig. 1 is the most advantageous method of spheroidizing the carbide in steels. In this method the metal is heated to the Ac_1 point exactly and is immediately cooled in the furnace below the Ar_1 point of steel. The procedure is then repeated as long as desired. This method of spheroidization of the carbide proved to be very successful with the hypoeutectoid and hypereutectoid carbon steels, and also with many low alloy steels.

The experimental arrangement for obtaining the cyclic heating and cooling is very simple. A thermocouple connected with an automatic temperature recorder is placed in a hole drilled in the specimen of the steel under investigation. The specimen and the thermocouple are then placed in an electric furnace. The furnace is provided with a second thermocouple, which is placed near the roof or near the heating elements of the furnace and is connected with an automatic temperature controller. The furnace is then started and the controller attached to the second thermocouple is adjusted[†] so as to give a record of temperature inside the sample which agrees with the record reproduced in Fig. 1. It should be noted that this method is independent of the thermocouple calibration, because the cycles of heating and cooling are adjusted in accordance with the actual position of the critical points of the steel on heating and on cooling. The critical points are automatically recorded by the instrument connected with a thermocouple embedded in the steel. More than one specimen can be spheroidized at the same time by this method if the furnace is large enough to insure the uniform heating and cooling of all specimens. The recording thermocouple in this case is placed in the hole drilled in a dummy specimen having the same dimensions and made of the same material as the rest of the specimens.

The time required for one complete cycle depends upon the heating and cooling rate and upon the load of the furnace. In experiments described here the time amounted to about 45 minutes in a certain electric furnace with four 5-in. specimens each $\frac{3}{4}$ in. round.

---

[*] Portevin and Bernard: *Jnl.* Iron and Steel Inst. (1921) **104**, 145.

[†] A Leeds and Northrup recording controller was used for this purpose. The instrument has two cams, which operate two contacts for closing and opening of the heating circuit. Adjustments of the cams in a proper position allows the cyclic operation of the furnace. The temperatures at which the heating circuit is closed or opened are different from the maxima and minima of the cycles shown in Fig. 1.

The carbon steel requires only a few cycles of heating and cooling to start the spheroidization of the carbide. The proeutectoid as well as
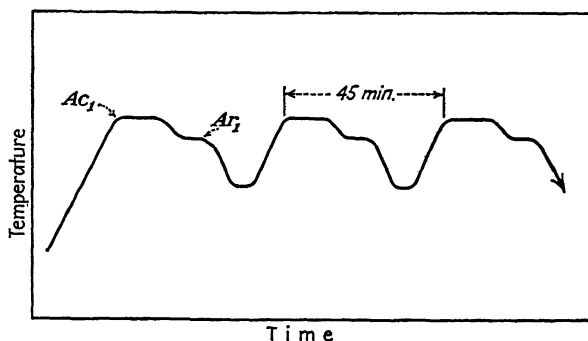
Fig. 1.—Cyclic spheroidizing heat-treatment.
Part of an actual temperature recorder chart. Thermocouple placed in the hole drilled in the specimen. The temperature controller of the furnace is adjusted to give this type of variation of temperature with time.
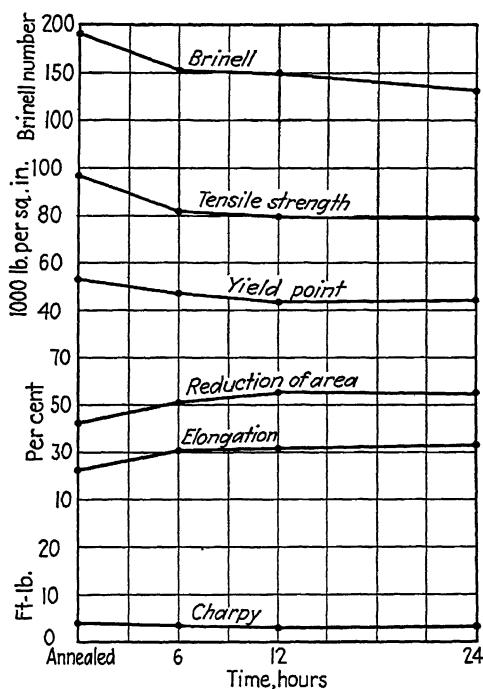
Fig. 2.—Changes in mechanical properties of a 0.45 per cent C steel A with length of spheroidizing heat-treatment.

the eutectoid carbide of carbon steels is completely spheroidized in 6 hr. of the cyclic heat-treatment.

Spheroidization of the carbide in carbon steels by this method is accompanied by softening, an observation that is in agreement with

other investigators. In Fig. 2 are presented the results of the tensile tests, hardness measurements and Charpy tests for the carbon steel A (Table 1). Standard 0.505 by 2-in. tensile specimens and 5 by 10-mm. Charpy notched specimens were used in these tests. All tests were made in duplicate and the points plotted in Fig. 2 represent an average of the two tests. The values of the physical properties plotted near the origin of Fig. 2 are those of annealed steel having the cementite in lamellar form. The time plotted on the abcissa of Fig. 2 represents the approximate
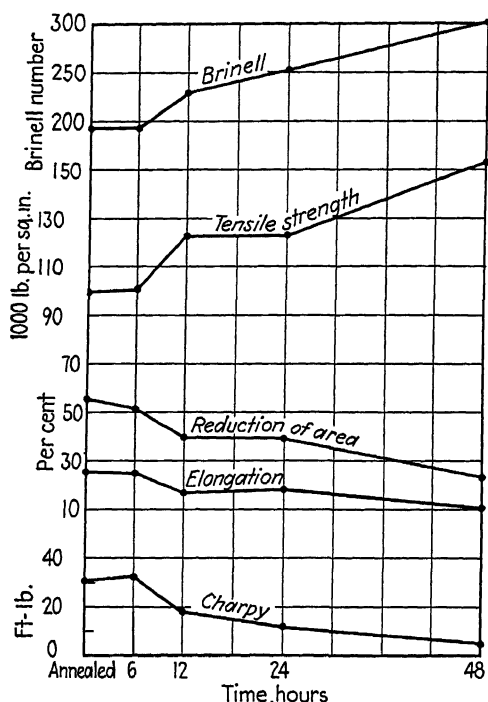
FIG. 3.—CHANGES IN MECHANICAL PROPERTIES OF A 3.5 PER CENT NI STEEL B WITH LENGTH OF CYCLIC HEAT-TREATMENT.

length of cyclic heat-treatment. The time was noted from the moment the steel reached the Ac_1 temperature of the first cycle until the furnace was turned off at the maximum temperature of the last cycle. All specimens were then furnace-cooled to room temperature.

Fig. 2 indicates that the medium carbon steel A is gradually softened by the cyclic spheroidizing heat-treatment. The yield strength, tensile strength and Brinell hardness decrease with heat-treatment, while the ductility increases. The impact strength is low and not materially changed by the treatment. The cyclic heat-treatment of this steel changes the mechanical properties in the same direction as any other method of spheroidizing.

Steels containing 3.5 per cent Ni responded to the cyclic heat-treat-
ment in unexpected ways.   In Fig. 3 are reproduced the results of the
mechanical test of steel B (Table 1), after a series of cyclic heat-treat-
ments.   The experimental conditions were identical with those described
for the carbon steel A.   The range of cyclic temperature variations
was, of course, modified to compensate for the difference in the position
of the critical temperatures on the temperature scale, as compared with
carbon steel.   The specimens were furnace-cooled to room temperature.
Fig. 3 shows that the tensile strength and hardness increase and the
ductility and impact strength decrease with the cyclic heat-treatment of
this steel.   The yield point was conspicuous by its absence from all heat-
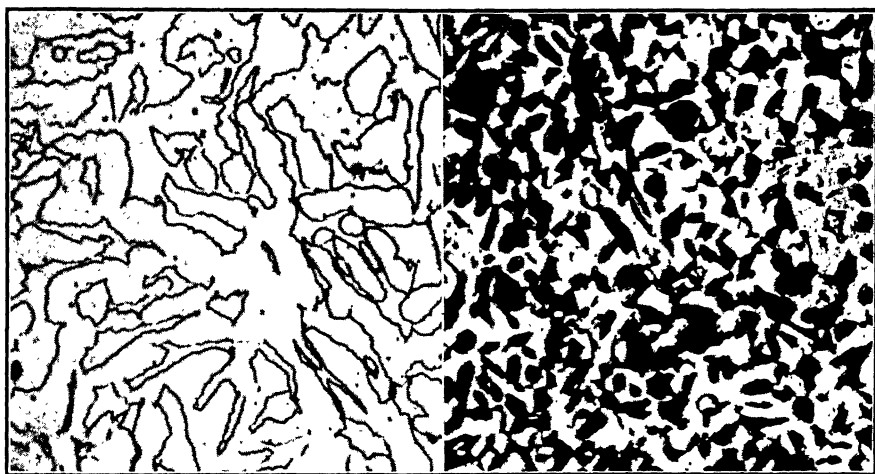
FIG. 4.   FIG. 5.
FIGS. 4 AND 5.—STEEL B.   MICROSTRUCTURE OF TENSILE-TEST SPECIMEN SUBJECTED
TO 48 HOURS OF CYCLIC HEAT-TREATMENT AND FURNACE-COOLED.
Fig. 4, nitric acid etch.   × 2000.   Fig. 5, sodium picrate etch.   × 1000.

treated specimens.   The limit of proportionality was not recorded with
sufficient accuracy but was very low with all samples subjected to the
cyclic heat-treatment.   The hardening observed with 3.5 per cent Ni
steel subjected to the cyclic heat-treatment called for an explanation, and
the rest of this paper is devoted to an attempt to find it.
The microstructure of a tensile specimen of steel B subjected to the
cyclic heat-treatment is shown in Figs. 4 and 5.   The structure is charac-
terized by the presence of two constituents, which etch white with nitric
or picric acid.   Longer etching with acids colors one of the constituents
slightly.   The second constituent is colored dark by the sodium picrate
etch, as shown in Fig. 5.   The microstructure is characterized by a
complete absence of carbide, the constituent etching dark with sodium
picrate cannot be a carbide in steel containing only 0.32 per cent C.   The

highest available magnification failed to show any secondary structure in the dark-etching constituent. The structure of 3.5 per cent Ni steel after the cyclic heat-treatment and furnace-cooling consists of ferrite and a constituent quite different from the usual products of austenite decomposition on slow cooling or even quenching. It was assumed at this time that a form of solid solution was produced during the cyclic spheroidizing heat-treatment, and that the solid solution was partly or completely preserved at room temperature by furnace-cooling. It was apparent from this that the solid solution existing in the 3.5 per cent Ni steel at the time when the furnace-cooling started was appreciably different from austenite. The hardening effect observed in the 3.5 per cent Ni steel after the cyclic heat-treatment was evidently associated
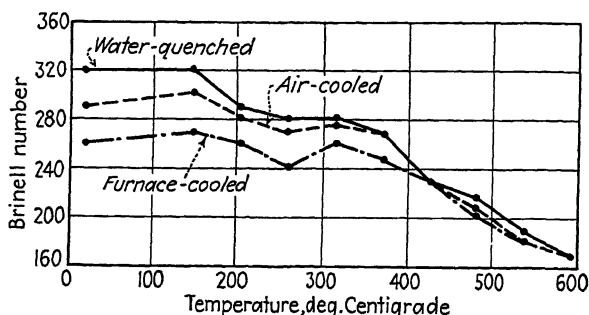
FIG. 6.—STEEL C. CHANGE IN HARDNESS OF SPECIMENS REHEATED TO INDICATED TEMPERATURE.
   Preliminary heat-treatment consisted of heating samples at constant temperature 25° C. below the Ac₁ point for 48 hours followed by water-quenching, air-cooling and furnace-cooling.

with the formation of a solid solution at the temperatures of heat-treatment. The cyclic heat-treatment of 3.5 per cent Ni steel caused the cementite to dissolve in the solid solution instead of causing it to spheroidize.

The formation of austenite during the cyclic heat-treatment was considered at first as the cause of the peculiar microstructure. Austenite was presumably formed at the Ac₁ temperature during the cyclic treatment. However, it was not clear why the austenite so formed should fail to break down into an agglomerate of ferrite and cementite at the Ar₁ temperature on slow furnace-cooling.

The following experiments demonstrated that the formation of a solid solution, first observed in the specimens subjected to the cyclic heat-treatment, is also possible at temperatures considerably below the Ac₁ point. Three specimens, 6 in. long, of steel C (C, 0.31 per cent; Ni, 3.44) were heated at a constant temperature 25° C. below the Ac₁ point for 48 hr. The first specimen was water-quenched after the heat-treatment, the second air-cooled and the third was furnace-cooled. Their micro-structures were identical and are represented by Fig. 7. Their hardness

numbers after the treatment were as follows: water-quenched, 321 Brinell; air-cooled, 293; furnace-cooled, 262. The same steel furnace-cooled from 850° C. showed a hardness of 187 Brinell.
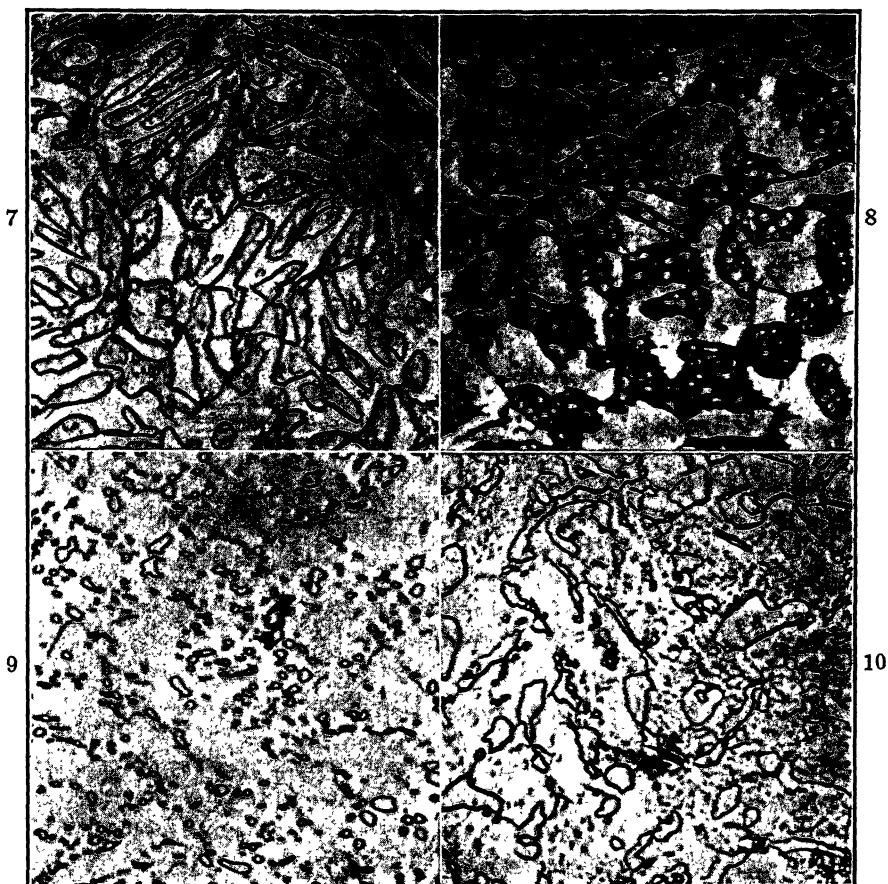
FIG. 7.—STEEL C.   STRUCTURE OF SAMPLE HEATED 48 HOURS AT TEMPERATURE 25° C.
BELOW Ac_1 POINT AND WATER-QUENCHED.
FIG. 8.—PRELIMINARY HEAT-TREATMENT AS IN FIG. 7.   HEATED 24 HOURS AT 370° C.
AND WATER-QUENCHED.
FIG. 9.—PRELIMINARY HEAT-TREATMENT AS IN FIG. 7.   HEATED 24 HOURS AT 540° C.
AND WATER-QUENCHED.
Spheroidized carbide in 3.5 per cent Ni steel.
FIG. 10.—PRELIMINARY HEAT-TREATMENT AS IN FIG. 7.   HEATED TO 595° C. AND
WATER-QUENCHED.
All picric acid etch.   × 2000.

This shows that the solid solution formed in the 3.5 per cent Ni steel at a temperature considerably below the Ac_1 is affected by the rate of cooling. However, the hardness of a specimen that was furnace-cooled from such a temperature was considerably higher than the hardness of a specimen furnace-cooled from a temperature above the Ac_3 point.

The three samples heat-treated as just described were cut into speci-
mens ¾ in. long. The short pieces thus obtained were reheated at a
series of subcritical temperatures for 24 hr. and then water-quenched.
Their hardness was measured and their microstructure was examined.
The results of hardness measurement are presented in Fig. 6, which
shows that a gradual softening is induced in the samples irrespective of
the preliminary heat-treatment.

The microstructure of specimens before reheating is shown in Fig. 7.
There was no detectable difference in structure between the water-
quenched, air-cooled and furnace-cooled specimens. There was also no
difference between the specimens reheated to a given temperature. The
microstructure of all specimens changed with reheating. The parts of
the structure described originally as a solid solution began to etch darker
and darker as the reheating temperature was increased. A definite
precipitate could be detected at a magnification of 2000× in a specimen
reheated to 370° C. (700° F.) as shown in Fig. 8. Spheroidized carbide
was observed in specimens reheated to 540° C. (1000° F.) as shown in
Fig. 9. This structure is interesting because it shows a truly spheroidized
carbide in 3.5 per cent Ni steel. The spheroidal particles of carbide
began to go back into solution (Fig. 10) after heating for 24 hr. at 595° C.
(1100° F.).

The process of softening shown by these experiments is apparently
similar to the tempering process in carbon steels.

This series of experiments showed that the formation of a solid solution
of carbide (or carbon) is possible in 3.5 per cent Ni steel at temperatures
considerably below the Ac₁ point, and that the solid solution thus formed
is more stable than the austenite formed above the Ac₁ point. The solid
solution thus formed is not hardened by quenching to the same extent
as austenite. Furthermore, it differs from austenite in that it does not
precipitate on slow cooling the carbide that is detectable under the
microscope. Precipitation of carbide does take place on the reheating of
the product of the solid solution. This process continues up to about
540° C. Reheating to this temperature results in the formation of ferrite
and spheroidized carbide. The carbide starts to go back into solution at
a temperature of about 600° C.

The phenomena just described can be conveniently studied by heating
suitable specimens in a temperature-gradient furnace. Specimens heated
in such a furnace show clearly the steps described above. Specimens
originally annealed and then heated in the temperature-gradient furnace
show first the spheroidization of cementite at intermediate temperatures,
then the gradual formation of a solid solution at a range of subcritical
temperatures, and finally the transformation of the subcritical solid
solution into austenite. The austenite areas are preserved at room
temperature in the form of martensite if the specimen is quenched. The

austenite decomposes into ferrite and carbide by furnace-cooling. The microstructure of the subcritical solid solution is not materially affected by the rate of cooling.

The formation of the subcritical solid solution was also observed in other nickel steels. Figs. 11 and 12 show the microstructures of SAE steels 2320 and 2515 subjected to the cyclic heat-treatment and furnace-cooled.
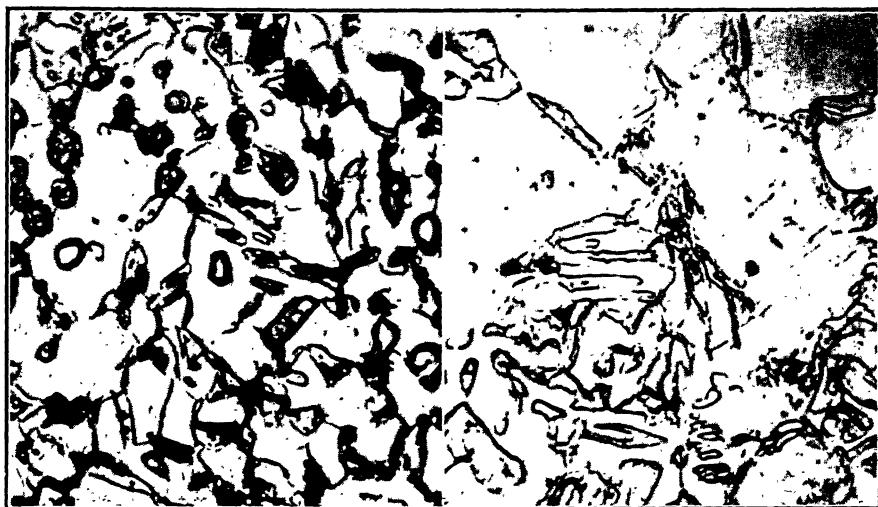
FIG. 11.   FIG. 12.

FIG. 11.—STRUCTURE OF SAE. No. 2320 STEEL SUBJECTED TO CYCLIC HEAT-TREAT-MENT FOR 48 HOURS AND FURNACE-COOLED.

FIG. 12.—STRUCTURE OF SAE. No. 2515 STEEL SUBJECTED TO CYCLIC HEAT-TREAT-MENT FOR 48 HOURS AND FURNACE-COOLED.

Both picric acid etch. × 2000.

DISCUSSION OF RESULTS

It is shown in this work that the hardening of 3.5 per cent Ni steels subjected to cyclic heating and cooling was due to the formation of a solid solution. It is shown also that the carbide in nickel steels is dissolved partly or completely at temperatures considerably below the critical point on heating. The lowest temperature of the beginning of solid solubility of the carbide in these steels was observed in the neighborhood of 600° C. The subcritical solid solution is different from austenite. It is not hardened by quenching to the same extent as austenite and it does not transform into ferrite and microscopically visible carbide as austenite does on slow cooling.

The nature of the subcritical solid solution must remain obscure until a reliable constitutional diagram is evolved for the iron-nickel-carbon alloys. Limited experience with 3.5 per cent Ni steel allows the consideration of two possibilities:

1. The solid solution formed at subcritical temperatures is a distinct phase, intermediate between the ferrite-carbide agglomerate and austenite;

2. The subcritical solid solution is a mixture of alpha and gamma phases. Possibility of existence of the two phases in iron-nickel alloys was indicated by the other investigators.* Solubility of carbide in the mixture of two phases and unusual behavior of such solution on cooling present an interesting problem.

A study of the mechanism of the formation of the subcritical solid solution in nickel steels and the future study of its properties should prove interesting and profitable.

SUMMARY

1. It is shown that the cyclic heat-treatment applied to the medium-carbon steel results in spheroidization of carbide. Spheroidization of carbide is accompanied by softening of this steel.

2. The cyclic heat-treatment resulted in hardening of 3.5 per cent Ni, medium-carbon steel.

3. Metallographic investigation indicated a possibility of the formation of a solid solution in this steel at subcritical temperatures. The product of decomposition of this solid solution accounted for the hardening of the 3.5 per cent Ni steel.

4. Experimental work shows that the subcritical solid solution is different in many respects from the austenite of this steel.

DISCUSSION

(E. S. Davenport presiding)

B. R. QUENEAU,[†] New York, N. Y.—Considering our present knowledge of low-alloy steels, it is of considerable interest that Professor Zavarine should report the occurrence of a new phase in a 3.5 per cent Ni steel in the region of 600° to 700° C. Dr. Bain discussed[1] in considerable detail the decomposition of austenite of a similar nickel steel in this same temperature range. He showed that it required approximately one minute for the first rejection of proeutectoid ferrite and more than one hour before the transformation of austenite to ferrite and carbide occurred. After holding at 635° C. for several days the cementite itself decomposed into iron and graphite and the final equilibrium products were a 3.5 per cent Ni ferrite and graphite.

* Metals Handbook (1936) 271.
† Instructor, School of Mines, Columbia University.
[1] E. C. Bain: Rates of Reactions in Solid Steel. *Trans.* A.I.M.E. (1932) **100,** 13.

With this in mind, it is indeed strange that the new phase reported by Professor Zavarine should be formed by heating the nickel steel above the Ac_1 and slow cooling. It would appear more likely that the austenite of eutectoid composition formed just above the Ac_1 had not had sufficient time to transform to ferrite and carbide in the 45-min. cycles described and on final cooling to room temperature the austenite had transformed to martensite. This would explain satisfactorily most of the facts recorded by Professor Zavarine.

First the increase in hardness of the nickel-steel samples can readily be accounted for by the presence of martensite. The decrease of hardness by tempering is as would be expected. Figs. 7, 8 and 9 then represent ferrite and martensite, ferrite and tempered martensite and ferrite and spheroidized carbides, respectively.

There is one statement for which I see no explanation: Why should the carbide go into solution at 600° C. upon heating? To what extent did the carbides dissolve at this temperature, since if this solution was slight it could be accounted for by the small increase in solubility of carbon in ferrite with increase in temperature?

Also, what temperature was considered as the Ac_1 temperature of the nickel steels, what temperatures were actually used in the cyclic heat-treatment, and to how low a temperature were the samples allowed to furnace-cool below the Ac_1 temperature before being removed from the furnace. Finally, was there no X-ray study made of the new phase?

A. R. Kommel,[*] Pittsburgh, Pa.—Professor Zavarine's interesting observations of "unorthodox hardening of a 3.5 per cent Ni steel" are apparently a clear demonstration of the presence of a three-phase equilibrium, alpha plus gamma plus carbide, in the section of the constitutional diagram containing these steels.

Fig. 10 shows that at a temperature of about 600° C. ferrite, austenite and carbide are evidently in equilibrium in these steels. If the temperature of heat-treatment is raised, more carbide is dissolved in the austenite, until at the upper limit of the alpha plus gamma plus carbide range all the carbide is dissolved in the austenite, which is then of a relatively high carbon content and in equilibrium with ferrite. If the heat-treating temperature is raised beyond this limit into the alpha plus gamma range, more austenite is formed at the expense of the ferrite and diffusion depletes the original austenite of carbon until, at a temperature above A_3, the austenite is of the same carbon content as indicated by the analysis of the steel.

Inasmuch as the A_1 transformation in these steels occurs over a range of temperatures, rather than at constant temperature as in the pure iron-carbon alloys, the Ac_1 temperature as determined by the author's method represents only that temperature at which the alpha plus carbide $\rightarrow$ austenite transformation takes place rapidly with the particular heating rates employed. It can have no relationship to any equilibrium transformation temperature. The results of the author's experiments indicate that his "Ac_1" temperature is probably near the boundary of the three-phase, alpha plus gamma plus carbide, and the two-phase, alpha plus gamma, fields.

This being the case, the austenite in the specimens treated at just below the "Ac_1" temperature would be of a considerably greater carbon content than in those cooled from above A_3. As a result of the greater hardenability of the higher-carbon-content austenite, a specimen, air or furnace-cooled, from the lower temperature would probably be harder than one cooled from above A_3. However, if quenched, the one cooled from above A_3 should be harder, as it would be completely martensitic, whereas considerable free ferrite would be present in the specimen quenched from the three-phase or two-phase field.

Such an explanation of the observed phenomena based on known principles should certainly be investigated before claims for "anomalous hardening" are advanced.

A. B. WILDER,* Urbana, Ill.—The formation of a new constituent in nickel steel under the conditions described by Professor Zavarine may be associated with a phase change during the alpha-gamma transformation. Although the constituent is formed at temperatures below the observed Ac₁ critical point, it is true that a phase change has occurred and the constitutional diagram should provide for the conditions observed.

In a study of ingot iron, carburized bars of ingot iron heated in a temperature-gradient furnace and, recently, low-carbon weld metal, a constituent not unlike that described in this paper has been observed. The gamma-alpha transformation represents a group of reactions that have received extensive consideration. The alpha-gamma transformation has received limited consideration. The factors that contribute toward the stability of the intermediate constituents that may form during the alpha-gamma transformation are unknown, and it would seem that the constituents may be observed only in certain types of steel.

This discussion is only an attempt to emphasize the importance of the observations recorded in this paper and the explanation offered is to be considered of a speculative nature.

H. H. BLEAKNEY † AND A. W. GROSVENOR, † Philadelphia, Pa.—The author has done a service of great practical significance in this valuable paper. The vexatious and puzzling impairment of elastic ratio and ductility observed in nickel steels after treatment at temperatures slightly below the accepted Ac₁ range has presented a problem which for many years has failed to command the attention warranted by its importance. The assertion is here ventured that much nickel steel, particularly in large forgings, is being mistreated today because this characteristic has not heretofore been advertised.

The full measure of commendation earned by the publication of the existence of this phenomenon cannot, unfortunately, be bestowed upon the author's explanation for it. The conclusion that "the nature of the subcritical solid solution must remain obscure until a reliable constitutional diagram is evolved for the iron-carbon-nickel alloys" is regrettable. This "subcritical" solid solution behaves strikingly like martensite. Two characteristics that appear to deviate from those of martensite the author postulates as follows:

1. "That the formation of a solid solution is possible at temperatures considerably below the Ac₁ point."

2. "That the solid solution was partly or completely preserved at room temperature by furnace cooling."

The inadvertent use of the expression, "Ac₁ point," is unfortunate, as its implication may be misleading to younger readers. The author is unquestionably aware of the fact that the eutectoid transformation in a ternary steel occurs over a range of temperature. The point most open to question, however, is the assumption that the Ac₁ range of 3.5 per cent Ni steel begins at such a high temperature. The present writers are especially interested in this feature, as they were investigating the anomalous behavior of this steel at the time the author's paper appeared. The present writers, however, found it much easier to suspect an error in the commonly published temperature of Ac₁ inception, rather than to credit the occurrence of an entirely new constituent in the steel. As a consequence, the curve illustrated in Fig. 13 was obtained. Fig. 14 illustrates the curve for a carbon steel, included for comparison. A dilatometer was used, rather than the thermal method, in order that the slow heating rate of ½° F. per minute might be employed, thus ensuring more accurate determination of the first stages of transformation. From the curve, it is apparent that a

---

* Assistant Professor of Metallurgical Engineering, University of Illinois.

† School of Engineering, Drexel Institute of Technology.

decrease in the amount of expansion per degree, entirely consistent with the formation of gamma iron, occurs at a temperature between 1000° and 1050° F.
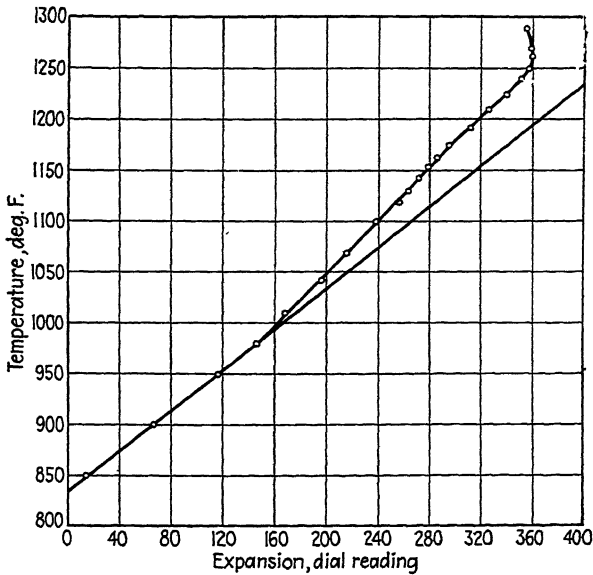
FIG. 13.
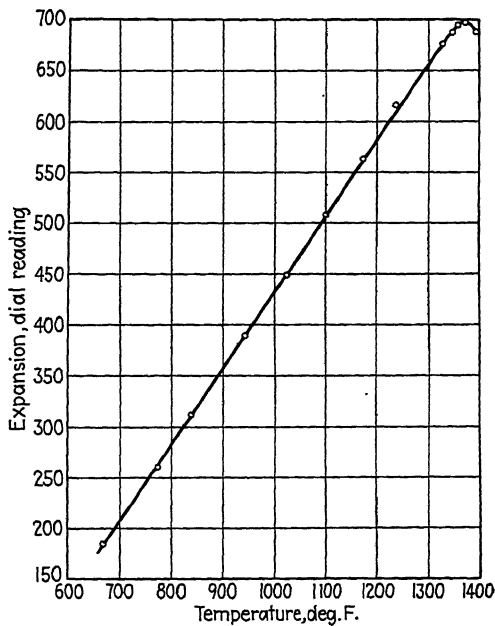
FIG. 14.

That the austenite formed in the range just above these temperatures decomposes on furnace cooling to martensite rather than pearlite is not hard to believe.   McMullan

has observed[2] that "Martensite or martensite in an austenite matrix may occur in air-cooled low-carbon steels of fairly low alloy content," after treatment within the critical range, and substantiated his contention with indubitable evidence. Since air cooling can produce such a structure in low-alloy steel, it is an entirely reasonable concept that furnace cooling from within the critical range will produce a similar effect in SAE 2330.

The writers hope to present a theory of the mechanism by which the structures under discussion are obtained, in a later paper.

F. B. FOLEY,[*] Philadelphia, Pa.—When a 3.5 per cent Ni steel containing 0.30 per cent C is heated to just into the Ac₁ transformation temperature and held there a length of time, the eutectoid of the composition undergoes transformation to austenite and the carbide dissolves in the austenite, so that the two phases, ferrite and austenite, form. This eutectoid austenite has strong air-hardening properties. Probably the ferrite at this temperature also takes some carbon into solution. The presence of nickel lowers the transformation temperature upon heating and produces considerable hysteresis upon cooling. It is therefore as likely as not that no transformation of the eutectoid austenite occurred during the first coolings applied in the cyclic treatment and that reheating and holding at what was assumed to be just below the Ac₁ transformation actually was within the bottom end of it, so that no metallographic change occurred. During the final cooling to room temperature the eutectoid austenite, being of high carbon, has transformed to martensite at a low temperature and a structure consisting of ferrite and martensite has resulted. The softer result attained by furnace cooling from 850° C. (well above the Ac₁) is due to the fact that the austenite formed at this temperature is of carbon 0.30 per cent and consequently requires a faster rate of cooling to suppress the formation of pearlite than does the eutectoid austenite produced by heating to just within the Ac, range.

A very low proportional limit and the absence of a definite yield point are characteristic of the physical properties resulting from heating to just within the lower end of the temperature range of transformation. In the treatment of large pieces that require long holding times during drawing such results sometimes are produced when the drawing temperature, assumed, as in this case, to be under the Ac, actually proves to be within the lower end of it. In practice this is sometimes referred to in the shop as "scratching the critical." Tensile strength goes up, elastic limit falls, ductility is lowered and we say we have dropped the bottom out of the physical properties.

I. N. ZAVARINE (author's reply).—The principal point of the discussion of the author's paper is an objection to his suggestion of existence of an intermediate solid solution in 3.5 per cent Ni steel on heating to temperatures below the critical point and before formation of austenite. It is suggested instead that the austenite is formed at subcritical temperatures in this steel. The possibility of the gamma-phase formation at subcritical temperatures is not excluded from the author's discussion of his experimental work. Limited amount of experimental work does not permit a definite answer to the questions raised in the discussion. The author believes that the answer will be possible only after an extensive study of the iron-nickel-carbon system. Argument by analogy with other systems is of questionable value.

Importance of a study of the subcritical changes in nickel steel from the point of view of practical heat-treatment is pointed out in the discussion by Messrs. Bleakney and Grosvenor and by Mr. Foley.

---

[2] McMullan: *Trans.* Amer. Soc. Steel Treat. (1933) **21**, 1035–1060.
[*] The Midvale Company.

Chromium in Structural Steel

By Walter Crafts,* Member A.I.M.E.

Structural steels containing chromium have become widely used in the last 20 years. In the earlier part of this period the major applications were in chromium-molybdenum aircraft tubing and similar special high-strength steels. During the past 10 years there has been a notable expansion in the use of chromium-bearing steel for structural purposes when welding was utilized for fabrication. The chromium-bearing steels introduced by Saklatwalla[1] (chromium-copper), Kinzel[2] (chromium-manganese-silicon), and Schultz[3] (chromium-copper) are being extensively used at the present time.

General Effects of Chromium

Chromium is so widely known for its carbide-forming tendency that its capacity to stabilize oxygen, nitrogen, and phosphorus is often overlooked. In low-carbon steels of the structural type these so-called secondary characteristics become more prominent. For this reason also, chromium in structural steel is definitely a toughening agent. As the carbon content is increased, the more widely known hardening effect becomes more evident.

In low-carbon steels chromium increases the notched-bar impact strength substantially. This property persists at subzero temperatures and is utilized for low-temperature service in chromium-copper steel.[4] Chromium also reduces any tendency to strain-aging embrittlement. In addition to improving the toughness of steels with the usual impurities, chromium has the specific property of counteracting the brittleness induced by high phosphorus.[5,6] In steels low in carbon and alloys, chromium has an almost negligible effect on tensile strength, and a hardening influence is noticeable only in the stronger steels. The ductility of welds adjacent to the base plate is also improved by chromium, both in the range of foolproof welding steels having strengths of less than 80,000 lb. per sq. in. as well as in the higher strength steels.

As the distribution of chromium between ferrite, carbide, phosphide, etc., changes with the other elements present in the steel, similar changes are reflected in the mechanical properties. The differences are so marked that discussion of the effects of chromium has been divided into three parts dealing respectively with steels having tensile strengths of approximately 60,000, 75,000 and 90,000 lb. per sq. inch.

The degree of corrosion resistance imparted by chromium to steel is also determined largely by the other components of the composition. In general, the small amounts of chromium present in structural steels tend to improve the resistance to oxidizing media. In atmospheric oxidation, chromium tends to change the character of the rust. It has been stated[7] that chromium doubles the atmospheric corrosion resistance of copper-bearing steels. Although the corrosion loss is important, the fine grain and abrasion-resistant character of the scale may be even more significant with regard to service life. In Fig. 1 are shown specimens of low-alloy copper-bearing steels that were exposed for a year to an industrial atmosphere with vigorous scrubbing by a wire brush weekly. The rust on the carbon steel is coarse and loose. The alloy steel without chromium has oxidized to form tubercles, and the low-phosphorus chromium steel has a relatively fine-grained rust with few tubercles. The chromium-phosphorus steel has a closely adherent, fine-grained, abrasion-resistant rust. Continuation of the test for a second year has shown practically no change in the relative appearance of the samples and indicates that accelerated corrosion caused by lifting of paint by rust would be minimized in the chrome-copper-phosphorus steel.

CHROMIUM IN STEEL HAVING TENSILE STRENGTH OF 60,000 POUNDS PER SQUARE INCH

Steel of this grade is usually rimmed or semikilled and contains 0.15 to 0.25 per cent C with only sufficient manganese to avoid hot-shortness. Unless unusual precautions are taken, the steel has an Izod impact strength of less than 50 ft-lb. and is subject to strain-aging embrittlement. Although strain-aging in structural steel is usually associated with failure at rivet holes or similarly highly strained locations, a similar embrittlement, due to straining at temperatures between 200° and 450° C. and immediate aging, is produced along the edges of welds. This type of embrittlement is particularly severe and is more harmful when the section is thick or the weld is restrained so that high stresses are developed. In arc welding, the Izod impact strength of the hot-strained plate may drop to values in the range of 5 to 10 ft-lb.

A survey of elements, except grain-refining deoxidizers, that are effective in reducing strain-aging embrittlement of semikilled structural
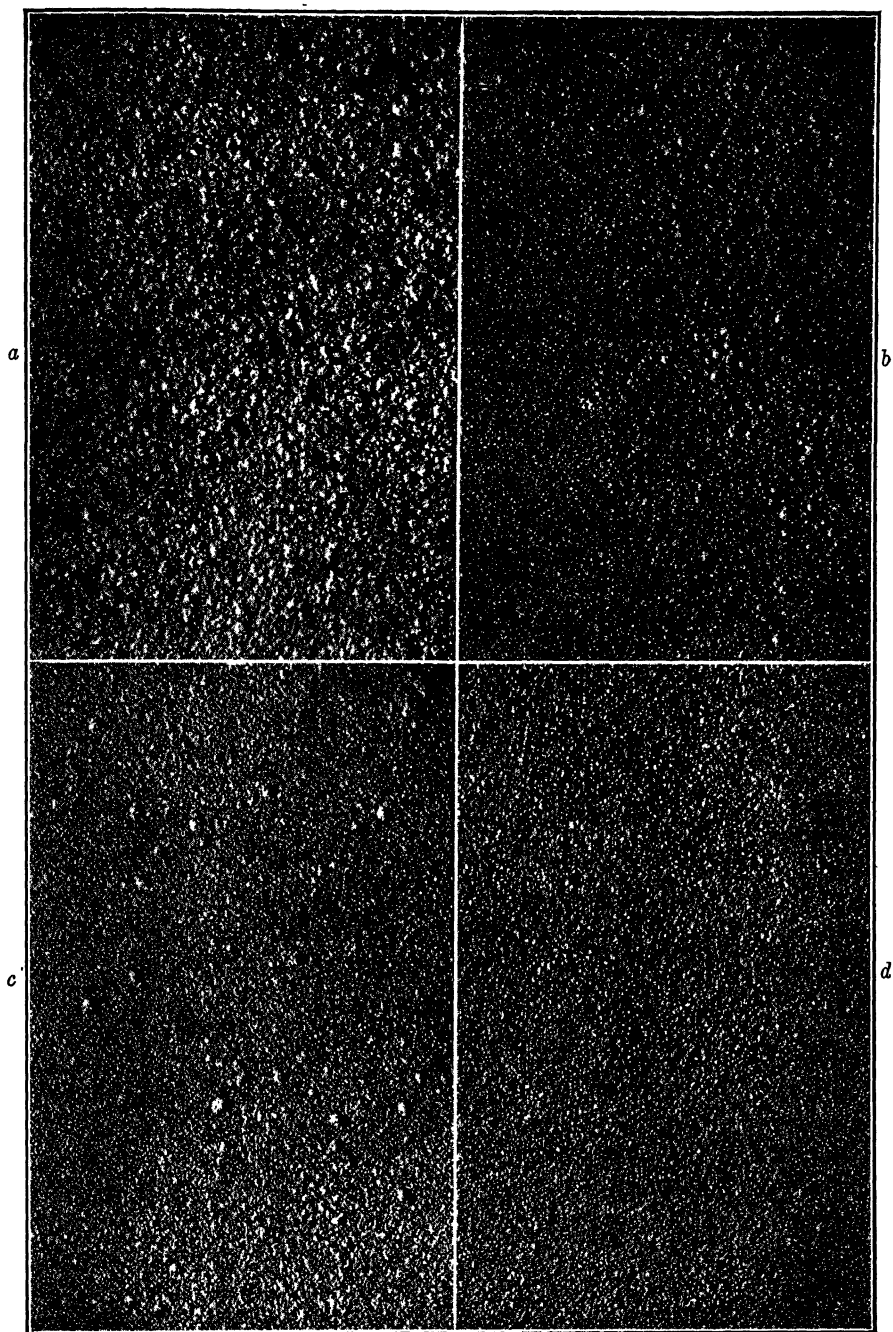
FIG. 1.—EFFECT OF CHROMIUM ON CHARACTER OF RUST.
a, plain carbon steel; *b*, alloy steel, without chromium; *c*, chromium steel without phosphorus; *d*, chromium-phosphorus steel.

steel was carried out on steels produced at the Union Carbide and Carbon Research Laboratories. The steels were hot-rolled carefully to give even the plain carbon steel a high initial impact strength, and were strained at room temperature and aged at 200° C. for 24 hr., with the results shown in Fig. 2. The chromium and manganese steels were not harmed, while the nickel and molybdenum produced only a relatively minor improvement. The other mechanical properties of the chromium and high-manganese steels are indicated in Table 1. It is notable that chromium changes the tensile properties very little but, in addition to the toughening action, improves the welding properties. The increase of manganese, on the other hand, confers an appreciable increase of strength, permitting
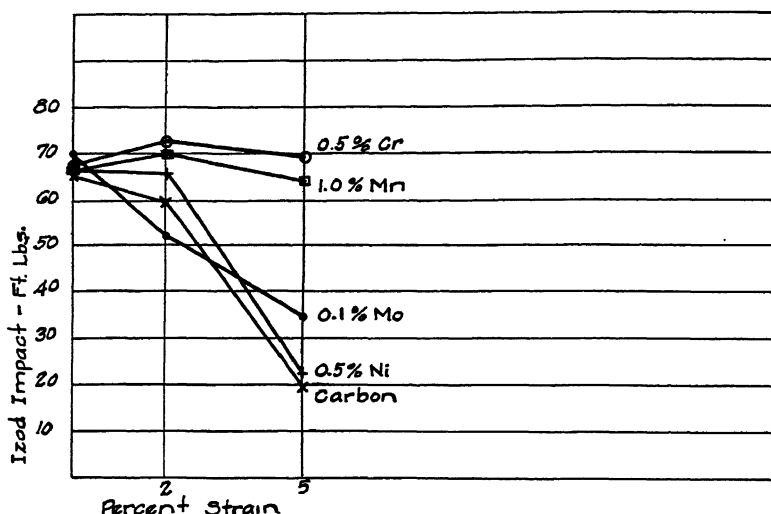
FIG. 2.—IMPACT STRENGTH OF STRAINED AND AGED SEMIKILLED STEELS.

a lower carbon content as well as improving the welding properties and toughness.

In connection with the use of alloys such as manganese and chromium in amounts that are not normal for rimmed and semikilled steel, it has been observed that such steel can be successfully rimmed with manganese up to slightly above 0.75 per cent. When the manganese is normal, say 0.30 to 0.50 per cent, rimming has been obtained experimentally with additions of up to 0.75 per cent Cr. It is evident that chromium is not as effective in "killing" power as manganese, and for that reason rimmed steels may be toughened more readily with chromium than with manganese. Both chromium and manganese additions may be made in effective amounts and used to obtain toughening in semikilled steel. In killed steels the type of improvement conferred by chromium and manganese can also be obtained from the use of silicon and a grain-refining deoxidizer.

Chromium in Steels Having Tensile Strength of 75,000 Pounds per Square Inch

Although structural steels in this range of tensile strength have been made with more than 0.13 per cent C, such steels generally are not capable of being welded safely without a subsequent stress-relieving anneal. Chromium is not usually employed in these higher carbon steels, and the discussion will be restricted to steels containing about 0.10 per cent C.

TABLE 1.—*Analysis and Properties of Three Steels*

Type	Chemical Analysis, Per Cent		
	C	Mn	Cr
C	0.15	0.50	
Cr	0.15	0.51	0.54
Mn	0.09	1.06	

Tensile Properties

	Yield Point, Lb. per Sq. In.	Tensile Strength, Lb. per Sq. In.	Elongation, in 2 In., Per Cent	Reduction of Area, Per Cent
C	37,100	56,150	38.0	67.7
Cr	38,500	59,750	42.0	70.9
Mn	41,700	57,100	42.0	74.0

Welding Properties

	Oxyacetylene Butt Bend, Per Cent	Arc Butt Bend, Per Cent	Arc Tee Bend, Degrees	
			As Rolled	Normalized
C	32	44	32	33
Cr	38	50	31	32
Mn	40	52	35	38

As publications[8-10] describing the low-carbon, high-strength steels have almost without exception described particular compositions, it has been difficult to evaluate the effect of any single element. In order to show the effects of each element under comparable conditions, a series of steels containing many combinations of alloys has been tested. In order to obtain as reproducible conditions as possible, the tensile properties were determined in the normalized condition on bars approximately 1 in. in diameter. Welding tests were made on ½-in. plate in the as-rolled condition. Except where noted the steels were made without grain-size control and had an intermediate grain size.

In order to demonstrate the effect of chromium on mechanical properties, it has been necessary to restrict the investigation to no more than two amounts of the elements other than chromium. An effort has been
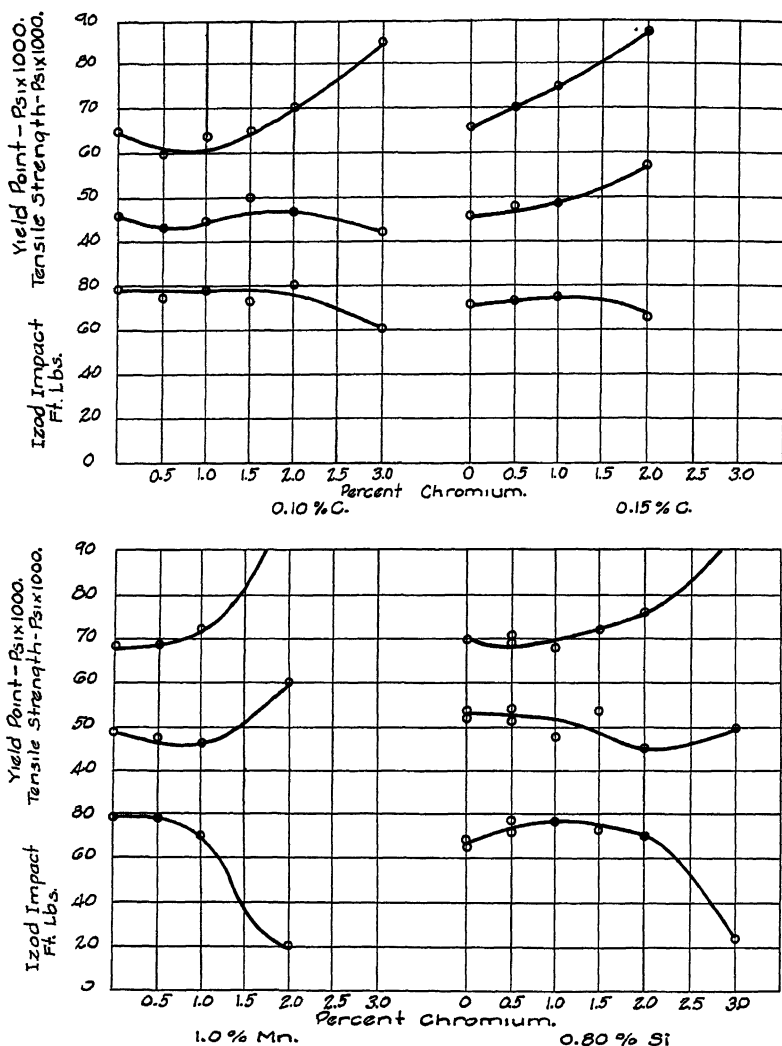
FIG. 3.—EFFECT OF CHROMIUM ON STEELS CONTAINING 0.10 PER CENT CARBON, 0.50 PER CENT MANGANESE, 0.01 PER CENT PHOSPHORUS, 0.20 PER CENT SILICON, 0.20 TO 0.50 PER CENT COPPER EXCEPT WHEN OTHERWISE SPECIFIED.

made to make these amounts the most generally practical or effective quantity, and no effort has been made to include some types of composition even though they have commercial application, as with the precipitation-hardening copper steels. The base composition was nominally as follows: C, 0.10 per cent; Mn, 0.50; P, 0.01; Si, 0.20; Cu, 0.20 to 0.50.

Unless otherwise indicated, the addition or increase of an element was to the following amounts: C, 0.15 per cent; Mn, 1.00; P, 0.09; Si, 0.80; Ni, 0.50; Mo, 0.25.
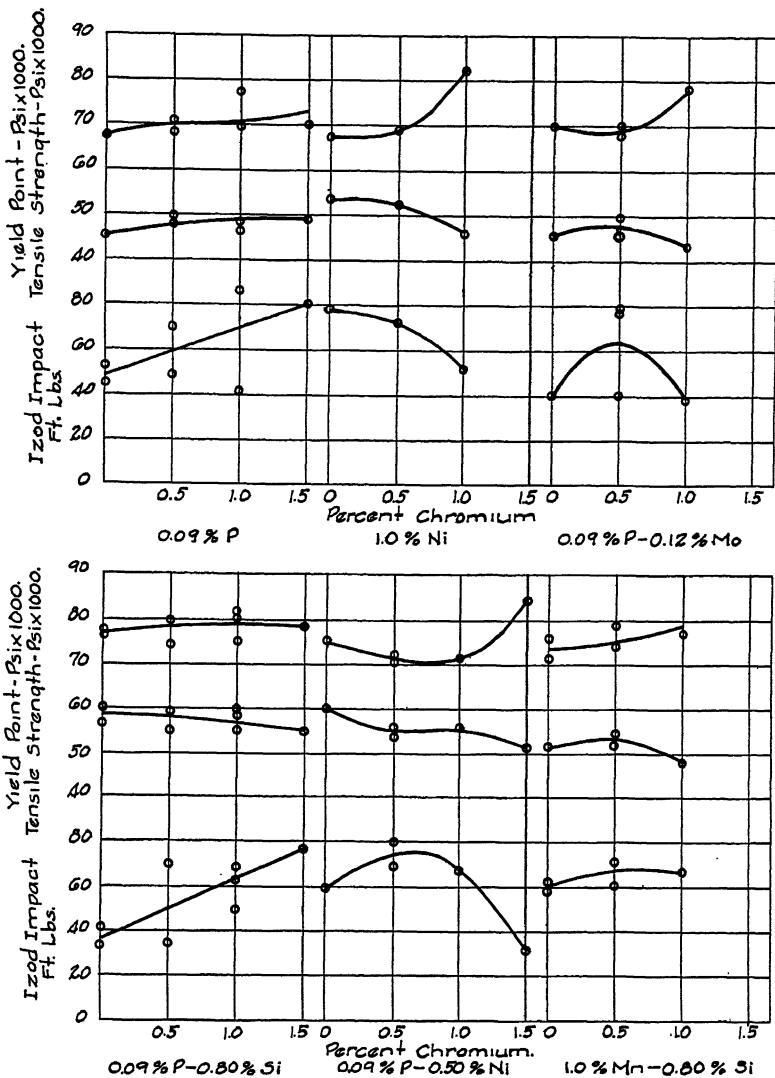
FIG. 4.—EFFECT OF CHROMIUM ON STEELS CONTAINING 0.10 PER CENT CARBON. 0.50 PER CENT MANGANESE, 0.01 PER CENT PHOSPHORUS, 0.20 PER CENT SILICON, 0.20 TO 0.50 PER CENT COPPER EXCEPT WHEN OTHERWISE SPECIFIED.

The tensile strength, yield point and Izod impact strength are shown in Figs. 3 to 5. The properties indicated by the points on the curves in Figs. 3 and 4 were derived mainly from steels that approached the nominal composition very closely, while the points of Fig. 5 were derived

in part from interpolation with respect to carbon.   The carbon contents
of the steels were largely within the range of 0.09 to 0.12 per cent in the
0.10 per cent C group and 0.15 to 0.19 per cent in the higher carbon group.
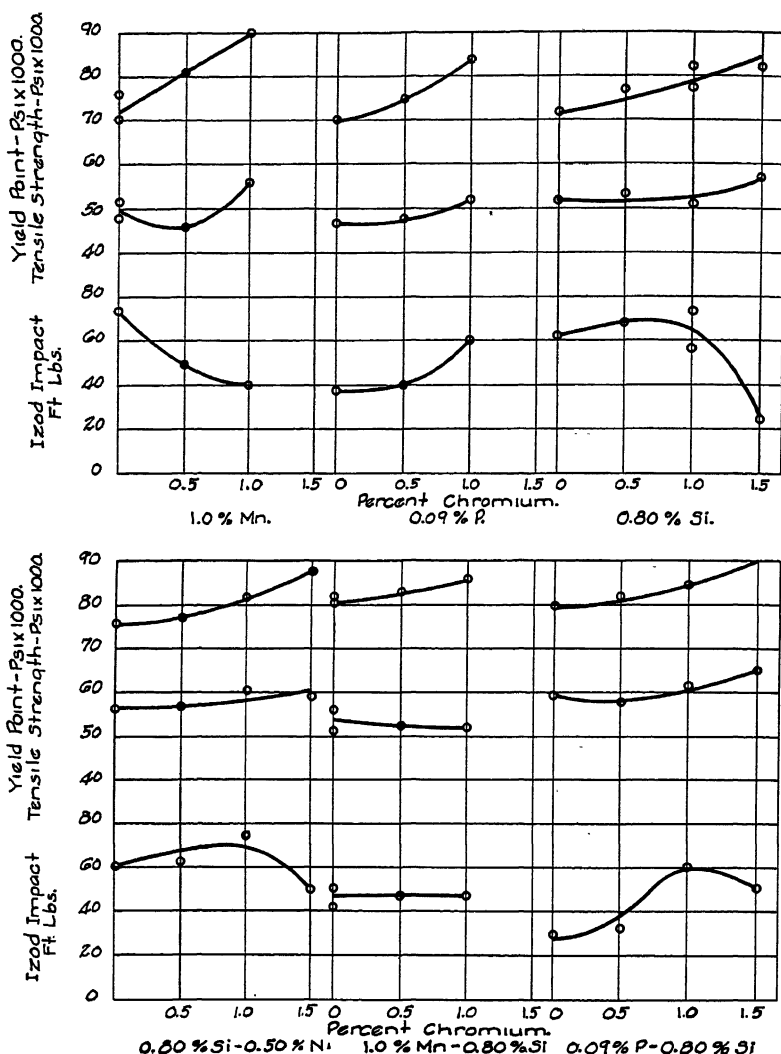
FIG. 5.—EFFECT OF CHROMIUM ON STEELS CONTAINING 0.15 PER CENT CARBON,
0.50 PER CENT MANGANESE, 0.01 PER CENT PHOSPHORUS, 0.20 PER CENT SILICON, 0.20
TO 0.50 PER CENT COPPER EXCEPT WHEN OTHERWISE SPECIFIED.

The effect of chromium on the base composition at 0.10 per cent C,
Fig. 3, is to initially depress both yield point and tensile strength.   Larger
amounts cause a reversal in this tendency, an increase of strength being
developed at intermediate amounts of chromium and an increase of yield
point at higher chromium contents.   The amount of chromium producing

a decrease in strength becomes less as the carbon content increases, and an initial decrease is not observed at 0.15 per cent C. Manganese has an effect comparable to that produced by carbon although the increase of strength and loss of toughness above 1 per cent Cr is very abrupt.

Silicon raises both yield point and tensile strength without appreciable loss of impact strength. The "tolerance" for chromium is reduced by silicon only a little, in spite of the increase of tensile strength. Phosphorus, as shown in Fig. 4, has an effect similar to silicon in raising the the tensile strength and yield point and making them insensitive to chromium additions. The addition of 1 to 1.5 per cent Cr improves the impact strength of steel containing phosphorus. Nickel, like silicon, raises the yield point and tensile strength without affecting the impact strength. Molybdenum has relatively small effects until the content of other alloys is fairly high. It then produces a marked loss of yield point, some increase of tensile strength, and moderate reduction of impact strength.

The properties of some complex 0.10 per cent C steels are also illustrated in Fig. 4. The most striking effect of chromium is that almost invariably it produces an increase of impact strength. This is particularly evident in the high-phosphorus steels but is usual even in the low-phosphorus steels. The impact strength tends to be lowered by chromium only when the strength is increased sharply. This occurs only in critical alloy ranges, and it is apparent that chromium up to 1.5 per cent has little hardening effect in these low-carbon steels.

The effects of chromium on the properties of the 0.15 per cent C steels are illustrated in Fig. 5. It is particularly notable that in almost every case, even though chromium produces an increase of tensile strength, there is a maximum impact strength at 0.5 to 1.0 per cent Cr. In these steels chromium consistently produces an increase of tensile strength but leaves the yield point unchanged.

The ratio of yield point to tensile strength tends to be maintained at a constant value or raised somewhat by the alloys that dissolve in the ferrite, such as silicon, nickel and phosphorus. Carbon and the carbide-forming elements, manganese, chromium and molybdenum, in small amounts have little influence on the yield ratio but when the effective amount is appreciable they tend to lower it either by producing a lower yield point or by raising the tensile strength more than in proportion to the rise of the yield point. The shift to a lower yield ratio is critical with respect to the amount of the alloy and is most abrupt with molybdenum, somewhat less so with manganese, and least critical with chromium. The critical amount of carbide-forming alloy that produces a lower yield ratio also becomes smaller as the carbon content is raised. In 0.10 per cent C steels containing a significant amount of only one carbide-forming alloy, the critical amount is between 1.0 and 1.5

per cent Mn., 1.5 and 2.0 per cent Cr., and 0.12 and 0.25 per cent Mo. When the carbon is raised or more than one carbide-forming alloy is present the critical amounts are appreciably lower, as indicated on the curves.

TABLE 2.—*Mechanical Properties of Fine-grained Steels*

Composition, Per Cent							Deoxidizer	Yield Ratio, Per Cent	Yield Point, Lb. per Sq. In.	Tensile Strength, Lb. per Sq. In.	Elongation in 2 In., Per Cent	Reduction of Area, Per Cent	Izod Ft-lb
C	Mn	P	Si	Cu	Cr	Mo							
0.10	0.50	0.088	0.24	0.30			None	67.5	45,500	67,500	33.0	59.8	53.2
0.11	0.50	0.090	0.32	0.34			Al	78.9	54,000	68,500	33.0	59.7	77.7
0.13	0.48	0.090	0.29	0.34			Cb 0.12	77.8	61,200	78,600	30.0	53.4	70.4
0.10	0.53	0.059	0.29	0.34			V 0.13	78.3	54,000	69,000	33.0	57.8	80.8
0.09	0.92	0.093	0.77	0.33			None	67.1	52,000	77,500	35.0	63.0	30.0
0.09	1.00	0.086	0.80	0.35			Al	76.6	59,000	77,000	33.5	59.6	85.7
0.10	0.90	0.084	0.78	0.33			Cb 0.12	77.0	60,100	78,200	34.0	64.1	84.7
0.08	0.96	0.077	0.83	0.36			V 0.12	76.4	58,000	76,000	24.0	54.7	81.8
0.11	0.95	0.090	0.28	0.34		0.12	None	53.8	40,000	74,500	32.0	58.6	38.1
0.13	1.01	0.090	0.35	0.33		0.13	Al	75.4	61,000	81,000	29.0	50.8	78.8
0.09	0.84	0.087	0.26	0.37		0.18	Cb 0.12	78.0	57,150	73,200	33.0	62.0	64.0
0.09	0.92	0.088	0 22	0.36		0.14	V 0.14	78.5	58,000	74,000	33.5	61.6	84.5
0.11	0.99	0.088	0 82	0.37	0.53		None	68.5	56,500	82,500	29.0	51.1	37.5
0.11	0.98	0.084	0.84	0.32	0.55		Al	74.0	60,000	81,000	30.5	59.8	90.8
0.10	0.98	0.086	0.80	0.34	0.55		Cb 0.12	77.5	63,500	82,000	27.0	56.2	57.3
0.11	1.01	0.074	0.81	0.38	0.55		V 0.15	65.0	53,000	81,500	23.0	48.6	76.0
0.12	0.46	0.090	0.25	0.33		1.00	None	68.0	52,000	76,500	30.0	69.7	57.4
0.10	0.50	0.088	0.30	0.32		1.00	Al	71.6	52,500	73,300	35.0	64.7	86.2
0.08	0.45	0.084	0.23	0.35		0.99	Cb 0.11	77.5	56,500	73,000	27.0	55.7	71.8
0.09	0.48	0.075	0.24	0.34		1.01	V 0.12	74.0	54,000	73,000	33.0	62.1	83.7

The critical amount of carbide-forming alloy can be raised by the use of a grain-refining deoxidizer. As shown in Table 2, the yield ratio is increased by raising the yield point rather than by lowering the tensile strength. The impact strength is also substantially improved. In the main there are relatively small differences between comparable steels treated with different deoxidizers, and choice of the grain-refining agent depends on other factors, such as cost and desired welding characteristics.

A survey of the data in Figs. 3, 4 and 5 reveals that in order to meet a yield point of 50,000 lb. per sq. in. at least two elements of the group, manganese, phosphorus, silicon and nickel should be present in the following effective amounts: Mn, 1.00 per cent; P, 0.09; Si, 0.80; Ni, 0.50; and only one of the carbide-forming elements should be present in appreciable amount, accompanied by a grain-refining deoxidizer if the following maximum values are approached: C, 0.15 per cent; Mn, 1.5; Cr, 1.5; Mo, 0.25. Obviously the formula expresses the minimum of the alloy requirements and is not meant to imply that other compositions

are not practical or that the "effective" amounts are the maximum that can be utilized to advantage.

In order that steels of this type have good toughness and good manufacturing and fabricating properties, certain limitations must be observed. For example, it is a matter of general experience, although difficult of rigorous proof, that the tensile strength should not exceed 80,000 lb. per sq. in. for "foolproof" welding properties. Similarly, it is considered that the carbon content should not exceed 0.15 per cent—preferably 0.13 per cent—for the same reason. The presence of carbide formers such as molybdenum, chromium and vanadium is also desirable to retard grain growth during welding. Chromium should be present with high

TABLE 3.—*Ductility of Butt Welds*
Steels Containing 0.10 Per Cent C, 0.09 P, 0.20 to 0.50 Cu

Type	Oxyacetylene Weld				Arc Weld			
	0 Cr	0.5 Cr	1.0 Cr	1.5 Cr	0 Cr	0.5 Cr	1.0 Cr	1.5 Cr
	Bend Elongation, Per Cent							
Plain...................		21	17			37	35	
Mn.....................		33				50		
Si.....................		20	23	31		46	49	66
Mo....................	15	18			40	43		
Ni.....................		42	29			52	32	
Mn-Si.................	22	43			60	40		
Mn-Ni.................	33	43			59	64		
Ni-Si..................	24	42	32		46	52	48	
Ni-Mo.................	34	24	24		52	48	56	

phosphorus to insure toughness. Copper should not exceed 0.50 per cent unless precipitation-hardening or a special property such as corrosion resistance is desired. Nickel should be associated with high copper to insure good rolling characteristics. Many other factors bear on the problem of selecting a suitable composition for high-strength, "foolproof" welding steel, and it is evident that chromium in steel of this type has chiefly a toughening action that is effective in the plate as well as in welded joints.

The ductility of welds as indicated by the bend test on butt welds of ½-in. thick plate are shown in Table 3 for high-phosphorus steels. Chromium is generally beneficial and, as the values are all rather high, the minor variations are probably due in large part to differences in welding technique. Because of limited material, the welds were made under adverse conditions, and the generally high order of the ductility is a tribute to the facility with which the steels may be welded.

It is evident that in well balanced steels in the 75,000-lb. per sq. in. tensile strength range, chromium adds to the toughness and has little influence on the yield point or tensile strength. When the carbon, alloy, or chromium content is high enough for chromium to increase the strength appreciably, the toughening influence becomes less strong. The optimum chromium content therefore depends on the degree of toughening that is required.

CHROMIUM IN STEEL HAVING TENSILE STRENGTH OF 90,000 POUNDS PER SQUARE INCH

Steels having a higher tensile strength than about 80,000 lb. per sq. in. are generally stress-relieved after welding, so that, aside from special purpose steels, the principal metallurgical requirement is a high order of toughness in the base metal. The higher strength also implies more difficulty in production and fabrication, and in order to take advantage of the higher strength the surface must be practically perfect, especially if repetitive loading is involved.

The property of chromium in reducing segregation and ingotism, as indicated by reduction of brittleness[11] and improvement of welds,[12] becomes of more obvious advantage in these harder steels. Likewise, the decarburization at the surface is reduced by the oxidizable alloys like chromium, manganese and silicon. While the presence of these alloys will not guarantee a high fatigue life of structures having oxidized surfaces, they at least facilitate the development of a more favorable surface condition. More obvious surface defects such as seams, laps and scabs are also minimized.

As the advantages of alloys have become better known, the average carbon content of steel in this strength range has dropped until most of the widely used steels are in the range of 0.15 to 0.20 per cent C. As indicated in Fig. 5, chromium produces higher strength in this carbon range. A survey of the graphs will also reveal that chromium at the same time often causes an actual increase of impact strength and a relative increase in toughness even in the high strength ranges. A similar tendency to greater toughness is produced by silicon and nickel, while phosphorus and manganese have an adverse influence. It is apparent that the toughening property of chromium in the lower strength steels is maintained, and that at higher strengths chromium is both a toughening and a hardening agent. This is also true in the welded steel,[12] in which chromium, like molybdenum, tends to prevent the formation of a brittle martensite in the metal adjacent to the weld.

SUMMARY

Some of the more significant properties contributed by chromium to structural steels have been outlined, and the field of utility of chromium

and its interrelation with other alloys have been described. The outstanding property of chromium is its toughening influence, especially in conjunction with a high phosphorous content. This is manifested by added resistance to strain embrittlement in unkilled steel, by increased impact strength in steel of the high-strength structural types, and by improved ductility in welds. Chromium also has a material influence on the atmospheric corrosion resistance of high-phosphorus copper-bearing steel.

The influence of alloys other than chromium on the properties of structural steel has been outlined, and the effective amounts and interrelation of alloys necessary to obtain suitable high-strength steel have been indicated. From these relationships it may be concluded that although chromium is essential only in some types, as in high-phosphorus steels, it is eminently desirable and advantageous in almost all combinations of alloys.

ACKNOWLEDGMENTS

APPENDIX

Tables on the Physical Properties of Low-alloy Structural Steels may be obtained in the form of microfilm or photoprints, from the American Documentation Institute, 2101 Constitution Avenue, Washington, D. C. Prices are: 41 cents for microfilm; $2.30 for photoprint.

REFERENCES

1. B. D. Saklatwalla: U. S. Patent No. 1599435 (Sept. 14, 1926).
2. A. B. Kinzel: *Trans.* Amer. Soc. Steel Treat. (1928) 14, 866.
3. E. H. Schulz: *Stahl und Eisen* (1928) 48, 849.
4. A. B. Kinzel, W. Crafts and J. J. Egan: *Trans.* A.I.M.E. (1937) 125, 560.
5. C. H. Lorig and D. E. Krause: *Metals and Alloys* (1936) 7, 9, 51, 69.
6. J. A. Jones: *Jnl.* Iron and Steel Inst. (1937) 135, 113.
7. F. N. Speller: *Trans.* A.I.M.E. (1934) 113, 13.
8. G. N. Schramm, E. S. Taylerson and A. F. Stuebing:*Iron Age* (Dec. 6,1934)134,33.
9. H. L. Miller: *Metal Progress* (July 1935) 28, 28.
10. S. Epstein, J. H. Nead and J. W. Halley: *Trans.* A.I.M.E. (1936) 120, 309.
11. A. B. Kinzel and W. B. Miller: *Trans.* Amer. Soc. Steel Treat. (1930) 18, 908.
12. K. L. Zeyen: *Krupp. Monatschefte* (1931) 12, 214.

Surface Allotropic Transformation in Stainless Steel Induced by Polishing

By J. T. Burwell* and J. Wulff,† Member A.I.M.E.

As is well known, the alloys of iron containing $18 \pm$ per cent chromium, $8 \pm$ per cent nickel and less than 1.2 per cent carbon exhibit the same allotropic modifications as iron. The face-centered cubic or gamma phase is stable at high temperatures and the body-centered cubic or alpha ferrite is presumably stable at room temperature. The transformation from the gamma phase to the alpha phase in alloys of the above composition (18-8 or stainless steel) is sluggish; even moderately rapid cooling permits the retention of the gamma phase. Cold-work, however, causes the transformation from gamma to alpha to occur at room temperatures. It is difficult, nevertheless, to induce complete transformation regardless of the method of cold-working. Since metallographic polishing is very effective in transforming the surface austenite to ferrite, as indicated by the magnetic studies of Buehl and Wulff,[1] it was decided to investigate the phenomenon by electron diffraction methods.

Apparatus

The apparatus used (Fig. 1) was a hot-filament type employing movable slits, similar to that described by Germer.[2] The sample-to-photographic plate distance was 69 cm. and the accelerating voltage 30 kv. Since electrons do not in general follow geometrical paths, it is necessary that either the electron source or the sample be movable in a plane normal to the beam. In this case the sample is fixed and the electron source is movable. The source is adjusted until the shadow of the sample appears in the brightest part of the beam as viewed on the fluorescent screen, then the slits composing the two pinholes are moved into position one by one. The system is evacuated by means of a mercury diffusion pump backed up with a Cenco Hypervac oil pump. Pressures lower than 10^{-4} mm. of Hg are read on a calibrated ionization gauge.

A potential of 30,000 volts supplied by a transformer and kenetron set is used to accelerate the electrons.

EXPERIMENTAL RESULTS

The stainless steel alloy used had a composition of 18.13 per cent Cr, 8.94 per cent Ni, 0.08 per cent C and the remainder iron. It was cold-rolled and annealed to bring it wholly to the austenitic state. Three samples, $\frac{1}{2}$ by $\frac{1}{2}$ by $\frac{1}{8}$ in., were carefully prepared for polishing. On one the polishing operation was carried out through 0000 emery paper and
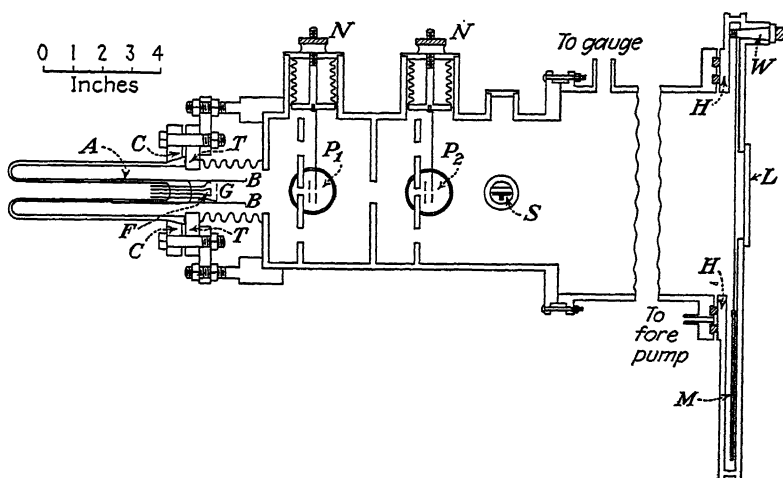
FIG. 1.—DIFFRACTION APPARATUS.

A, flanged Pyrex tubing.   H, rubber gasket. P_1, P_2, pinholes.
B, focusing sleeve.   L, fluorescent screen.   S, sample.
C, collar.   M, photographic plate.   T, steel base plate.
F, hot filament.   N, knurled nut.   W, winch.
G, slit.

in the last step light pressure only and unused portions of the paper were employed. This left the surface in a finely abraded condition. The other two samples were carried through the usual procedure of metallographic polishing, the last step including a polish with levigated alumina on velvet.

In order to determine the depth of the transformed layer, small amounts of metal were removed from the surface by electrolytic etching with oxalic acid and diffraction pictures were taken after each etch. From subsidiary experiments on the same material a correlation between the amount of metal removed from the surface by electrolytic etching and the time of etching was obtained. The sample was weighed before and after etching and from the loss in weight the decrease in thickness from one face was computed. The bath was a 10 per cent oxalic acid solution and the current density was one ampere per square inch. All

the sides of the sample save the polished surface were freshly painted with shellac before immersion. The current density was chosen as a compromise, since at high densities it is hard to remove a small thickness of material in a controllable length of time and at low current densities there is a pronounced tendency to pit, which means that a given weight of metal has not been removed uniformly from the surface. The current density employed corresponded to a rate of removal of a thickness of 1.52×10^{-6} cm. per second.

Using these data, the actual test samples were then etched to remove known thicknesses, and pictures were taken at successive stages. Diffraction patterns of the samples before etching (Fig. 2a) showed the two diffuse rings that are always typical of polished metal surfaces. (An exception to this was the abraded sample, which initially showed a pattern of body-centered cubic ferrite with an intense background.) These two features, (1) patterns showing only two diffuse rings and (2) patterns with very intense backgrounds on otherwise crystalline rings, always appear when a metal surface has been polished or burnished and are not indicative of the material or phase present, but it is found on etching that these patterns give way to purely crystalline ones typical of the substance under examination. This was found to be true in these experiments and in every case the first crystalline pattern to appear after metal was gradually removed by etching was a pattern of alpha ferrite with no trace of the face-centered austenite rings. Such a pattern is shown in Fig. 2b. At a depth of about 2.5×10^{-5} cm. in the polished samples and at about 1×10^{-4} cm. in the abraded sample, the face-centered cubic pattern began to appear superimposed on the body-centered one and for a small range of depths the two appeared together. Fig. 2c shows a picture containing both patterns. Below about 4×10^{-5} cm. in the polished samples and 2.1×10^{-4} in the abraded sample the body-centered rings disappeared entirely, leaving only the face-centered pattern typical of the bulk metal, such as is shown in Fig. 2d. To check our calibration of the rate of etching, one of these samples was weighed both before and after the experiment and the loss in weight agreed within 10 per cent of that calculated from the time of etching.

DISCUSSION AND CONCLUSIONS

It should be noted that there is considerable difference in the depths of the transformed layer on the abraded and on the polished sample. Now the thickness removed can only be calculated from the weight of removed metal, on the assumption that the surface is flat and that the metal on etching is removed uniformly. These conditions are much more nearly fulfilled by the polished sample than by the abraded one, whose surface is covered with sharp ridges which are probably etched away
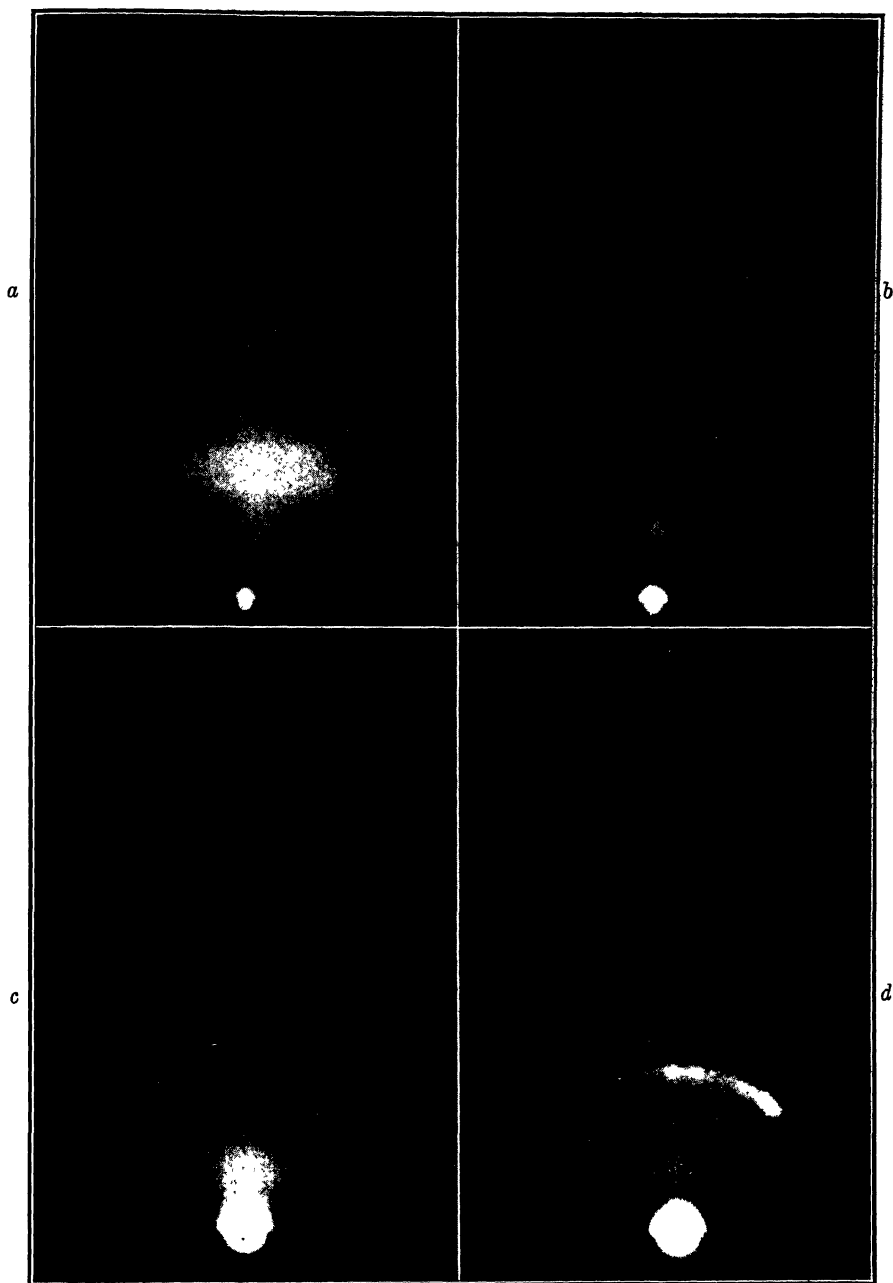
FIG. 2.—DIFFRACTION PATTERNS.
a. Diffuse ring.   Polished austenitic stainless steel.
b. Same surface as in a, slightly etched.   Rings represent body-centered structure.
c. More deeply etched surface.   Body-centered and face-centered rings present.
d. Deeply etched surface.   Only rings of face-centered lattice are present.

first, and so the figure of 4×10^{-5} cm. as the approximate depth of the transformed layer should be taken as the most valid one. Even in this case, however, one should only consider the figure an order of magnitude, since such an operation as manual metallographic polishing is reproducible only with difficulty.

The relation between the percentage of transformed ferrite and the cold-work necessary to produce it has been investigated by Aborn[3] and by Wosdwijensky and Sergeev[4] using X-rays, and by Wulff and Buehl[5] using magnetic susceptibility measurements. This relation depends on the composition of the alloy but in general it may be said that 50 per cent cold reduction will produce about 10 to 15 per cent transformed ferrite. Machined surfaces may show as much as 65 per cent ferrite, as stated by Aborn. Patterns such as Fig. 2b show no trace of austenite, which if present in this layer could not have been more than 10 per cent by volume of the total. This means that there was over 90 per cent transformed ferrite and the figures given above indicate the very severe work that is necessary to produce such an amount. It bears out the fact that the local stresses met in polishing are extremely high.

In this connection Bowden and Hughes[6] observed that during polishing the temperature of the contact surface may reach the melting point of the metal. If this is so, one would expect the uppermost surface layer of the samples to possess the face-centered structure, such a phase resulting from the change of initial austenite to ferrite by cold-working and the transformation of the surface layers of this ferrite back to austenite during the latter stages of polishing, where the temperature is locally very high. Unfortunately, this austenite if present could not be detected by electron diffraction because the surfaces of polished metals always yield diffraction patterns consisting of two diffuse rings, regardless of the metal under consideration, and from this pattern it is impossible to determine the phase present in the surface. These diffuse rings have been the subject of considerable discussion,[7] being attributed either to very small grain size approaching the amorphous state or to the physical contour of the surface, and are dealt with by one of the authors elsewhere. Regardless of their origin, it is found in the present work that when enough of the polished surface has been etched away to give a diffraction pattern typical of the sample itself the first phase to appear is alpha ferrite.

In conclusion, it may be said that the observable effects of metallographic polishing of austenitic stainless steel extend to a depth of about 4×10^{-5} cm. below the polished surface. In the first 2.5×10^{-5} cm. of this depth the metal is 90 per cent ferritic (body-centered) and beyond 4×10^{-5} cm. it is wholly austenitic (face-centered). The working of the metal may well extend to depths lower than this but its magnitude is not sufficient to effect the transformation.

REFERENCES

1. J. Wulff and R. Buehl: private communication.
2. L. H. Germer: *Rev. Sci. Instr.* (1935) **6,** 138.
3. R. H. Aborn: U. S. Patent No. 1918731.
   R. H. Aborn and E. C. Bain: Nature of the Nickel-chromium Rustless Steels. *Trans.* Amer. Soc. Steel Treat. (1930); also private communication from R. H. Aborn.
4. Wosdwijensky and Sergeev: *Tech. Phys.* U. S. S. R. (1935) **2,** 257.
5. J. Wulff and R. Buehl: Private communication.
6. F. P. Bowden and T. P. Hughes: *Nature* (1937) **139,** 152.
7. G. I. Finch and S. Fordham: *Chem. and Ind.* (1937) **56,** 632.

DISCUSSION

(F. T. Sisco presiding)

N. P. Goss,* Youngstown, Ohio.—The electron diffraction patterns presented in this paper justify the authors' conclusions that the surface of the stainless steel is substantially transformed ferrite.

I should like to ask the authors how many specimens were examined in this manner and were the results duplicated? In presenting the paper the authors drew a curve on the blackboard (not given in their paper) which shows the relation between the amount of ferrite transformed from the austenite as the cold-working is increased. The following experiment can be easily performed to see whether this relationship is approximately correct over a considerable range of cold-working.

Stainless steel can be easily rolled on a Steckel mill, and reductions in excess of 90 per cent can be made without intermediate heat-treatments.

The authors, Aborn and others, have shown by X-ray methods that 10 to 15 per cent of transformed ferrite results when stainless steel is cold-rolled 50 per cent. How much is transformed when the cold reduction is about 90 per cent? If a narrow band of stainless is cold-rolled from a strip 0.020 in. thick to 0.002 in., the reduction will be 90 per cent, and if the curve the authors presented is correct, more ferrite should be transformed.

Might it not be possible that the diffuseness in the rings of Fig. 2a is caused by the abrasive or polishing materials used during the preparation of the specimen? This seems to be a plausible explanation, since only a very light etching removed this condition.

L. THOMASSEN,† Ann Arbor, Mich.—Some time ago, Mr. McCutcheon and I[8] published an investigation on the depth of cold-working by machining. Carefully annealed 70-30 brass was used, which reflected well resolved $\alpha_1\alpha_2$ Mo doublets. The work was carried out by etching off the machined surface in steps and taking X-ray pictures of the etched surface after each etching. As long as the $\alpha_1\alpha_2$ doublets appeared blurred, it was considered that the region of undeformed metal was not yet reached. The angle between the beam of X-rays and the surface of the metal was kept at 14° so as to keep down the penetration of the rays. The order of magnitude of the depth of cold-work produced with a milling cutter, using a feed of 0.007 in., was 0.005 in. (12.5 × 10⁻³ cm.), which is considerably larger than the results obtained by the authors of this paper.

---

* Cold Metal Process Co.
† Associate Professor of Metallurgical Engineering, University of Michigan.
⁸ *Mech. Eng.* (1934) **56,** 155, 306.

In the preliminary work on our investigation, it was observed that in order to get sharp reflections from metallographically polished specimens it was necessary to give them a metallographic etch, repolish them and etch five or six times, in order to get away from the effects produced by the preparation of the specimen. Such a treatment removes 6 to 7/10.000 in. (1.7 × 10⁻³ cm.). Subsequent experiments by Mr. McCutcheon showed that as much as 12/10.000 in. (3 × 10⁻³ cm.) must be removed in order to get down to undisturbed metal, after the sample had been given a preliminary metallographic polish.

Let us assume that brass and 18-8 behave similarly with regard to working except for transformation of the latter. On that basis, cold-work given specimens goes 10 to 100 times deeper observed by X-rays than by the transformation effect. This is not astonishing, however, in view of the fact that a high degree of cold-working is necessary to bring about the transformation. A combined study of the transformation effect and the depth of cold-working according to our method might bring interesting results regarding the way that the cold-working tapers off in mechanically deformed specimens.

R. Schnurmann,[*] Derby, England.—The statement by Dr. Burwell and Professor Wulff that polished samples of stainless steel finished on levigated alumina on velvet show as electron diffraction pattern the two diffuse rings which are typical of metal surfaces polished in air, while a sample finished on 0000 emery shows body-centered cubic ferrite with an intense background, is in good agreement with Dobinski's[9] results. He pointed out that metal surfaces polished in air are readily oxidized and that this oxidation process is accentuated when different oxides in the presence of water are used as polishing media.

It is interesting that removal of the surface layers of the polished samples by etching reveals a thicker cold-worked layer with the 0000-emery finish than with the levigated alumina finish.

Mechanical polishing must be considered as a process of sliding friction. Whatever the true mechanism of sliding friction may be, abrasion undoubtedly plays a part, although, maybe, a secondary part, and its effect is more pronounced for oxidized surfaces than for surfaces free from oxides. Since Dobinski's result suggests higher rate of oxidation when levigated alumina is used in the last step of polishing, it appears plausible that abrasion during polishing was larger than when the 0000-emery finish was used and that, therefore, the thickness of the remaining cold-worked layer, which is measured by controlled etching, is thinner in the former than in the latter case.

J. T. Burwell (author's reply).—Since the publication of this work another experiment has been performed, which should be of some interest. A sample of 18-8 stainless steel was cold-reduced 40 per cent and was found by means of X-rays to contain about 5 per cent ferrite by volume. This, of course, was an average throughout the whole volume. An electron diffraction picture was taken but it showed little owing to the poor condition of the cold-rolled surface. Consequently a thickness of about 300 Å. was removed by electrolytic etching and a second picture was taken. It showed a pure alpha ferrite pattern like that of Fig. 2b. Thus the surface layers of a cold-rolled sample were composed entirely of ferrite even though the bulk of the sample contained less than 5 per cent. This may be a means of demonstrating the extreme nonuniformity of deformation in the cold-rolling process, although other explanations of the observed phenomenon are possible, such as chilling of the surface layers by the rolls or the development of high temperatures in the interior of the sample.

---

[*] London Midland and Scottish Railway Co., Research Laboratory.
[9] S. Dobinski: *Phil. Mag.* (1937) **23**, 397.

Akimow and Pevsner[10] have observed the same thing using X-rays instead of electrons. They show a curve of percentage of ferrite versus depth below the surface in a sample of stainless steel which had been cold-reduced 46 per cent. The curve runs from about 55 per cent ferrite at the surface to about 5 per cent ferrite at a depth of 0.6 mm. Had they used electrons instead of the more penetrating X-rays their curve would undoubtedly have risen to nearly 100 per cent ferrite at the surface also. This is a striking illustration of the superiority of electrons over X-rays for certain kinds of work.

In reply to Mr. Goss's first question, three samples were studied and the agreement was fairly good. Since the metal was removed in discrete steps, generally about 500 Å. at a time, we could not fix the depths given any more closely than that, and, in fact, such accuracy would be meaningless, since the alpha phase shades gradually into the gamma phase. However, the depths at which the gamma phase first appeared and at which the alpha phase finally disappeared did not vary by more than 500 Å among the three samples.

In reply to Mr. Goss's second question, although we have done no work on the variation of ferrite with depth in cold-rolled samples, still, judging by Akimow and Pevsner's curve, one would guess that in very thin material the percentage of ferrite would be rather high. Their curve shows somewhat more than 20 per cent ferrite at a depth of 0.2 mm. below the surface.

Mr. Goss's and Dr. Schnurmann's suggestions that the diffuse rings of Fig. 2a might be caused by the presence of polishing materials are interesting, but such diffuse rings may be produced in the absence of any polishing material. For instance, Plessing[11] polished gold, silver, nickel, copper and alpha iron under benzene without any polishing material and obtained the diffuse rings, and I have obtained such rings[12] from a surface of 18-8 from which metal had been evaporated in a vacuum.

While I agree with Professor Thomassen that the effects of cold-work probably extend to a much greater depth than is evidenced by a phase change if it occurs, I wonder how definite the point is at which the $K\alpha$ doublet ceases to be "blurred," as he calls it.

It has been noted by Hopkins[13] and Lees[14] that a layer of more or less oriented crystals may immediately underlie the so-called polished layer on metals. (Lees measured the depth of this layer in copper and obtained a figure considerably less than that given in the present paper for 18-8, but his method is open to criticism.) Hopkins,[15] studying polished cleavage faces of calcite, observed a layer of twinned crystals at a depth of 6000 Å. Such effects—preferred crystal orientation and twinning—might be studied as a measure of the depth of mechanical deformation in a worked surface in metals where no phase change takes place, although even here lattice distortion resulting from cold-work will undoubtedly extend below the above-mentioned layers.

---

10 G. Akimow and L. Pevsner: *Tech. Phys. U. S. S. R.* (1938) **3**, 142.

11 E. Plessing: *Phys. Ztsch.* (1938) **39**, 618.

12 J. T. Burwell: *Jnl. Chem. Phys.* (1938) **6**, 749.

13 H. G. Hopkins: *Trans.* Faraday Soc. (1935) **31**, 1095.

14 C. S. Lees: *Trans.* Faraday Soc. (1935) **31**, 1102.

15 H. G. Hopkins: *Phil. Mag.* (1936) **21**, 820.

The Nature of Passivity in Stainless Steels and Other Alloys, I and II

By H. H. Uhlig* and John Wulff,† Member A.I.M.E.

PART I. EXPERIMENTS ON PASSIVITY

Since its first mention in the literature in the eighteenth century[1,2] the phenomenon of passivity in metals has stimulated much speculation and attendant controversy as to its nature and cause. No one of the numerous theories so far proposed has been generally accepted.‡ Faraday,[7] in 1836, associated the passivity of iron with a protective film over the surface of the metal, which materially prevents or slows down reaction with corrosive environments. His theory was that oxidizing acids like nitric acid form an unstable oxygen or oxide layer over the iron surface, which protects the underlying metal from further attack. This concept was simple yet plausible, and without alteration has frequently been assigned in present-day discussions as explanation of the passivity of many metals. With the advent in recent times of stainless steels, it is not surprising that this oxide film theory of passivity proposed by Faraday has been used to explain the phenomenal corrosion resistance of stainless steels and other passive alloys. The passive alloys, such as the chrome-iron alloys, are supposedly covered with a protective oxide film, which forms on exposure of the alloy to air, is extremely stable and self-healing, and accounts for the remarkable resistance of these alloys to corrosion.

Within the past few years, several investigators, following the theory of film protection, have attempted to gauge the resistance of the supposed film on steels. Brennert[8] and Donker and Dengg[9] determined the potential at which a negative ion (e.g., Cl⁻) moving in an electric field reacted with the metal anode, as detected by increased current flow or change in potential of the steel electrode in an electrolytic cell. The potential corresponding to reaction Brennert called the film break-through potential.

Fenwick[10] added chloride salts, all of which are efficient in breaking down passivity, to a cell made up of steel and calomel electrodes and determined the concentration of Cl$^-$ which corresponded to suddenly appearing activity of the metal electrode, indicated by a potential change. This was called the chloride concentration corresponding to film breakdown of the steel electrode. Although some information of a practical nature was obtained in tests of the kind mentioned above, the necessity, implied, for a protective film as source of corrosion resistance is not proved.

On the whole, the oxide film theory of passivity offers a practical explanation for the experiments mentioned above and many of the phenomena associated with the passivity of pure metals like iron, which become passive under special conditions. It has, in addition, been able to account in large measure for the properties of passive alloys. The recent isolation of visible films from iron and low-chromium iron alloys by Evans[11] and Evans and Stockdale[12] is considered by many an ultimate argument for the film concept of passivity.

Despite the simplicity and plausible character of the oxide film theory, many conflicting theories based on significant experiments have appeared from time to time in the literature. Hittorf[13] found that he could anodically passivate chromium in iodide solutions. He found no ready explanation for this in the oxide film theory, hence ascribed the passive state of chromium not to a protective oxide film but to a *zwangszustand* (strained state) of the atoms. This admittedly vague term he used to describe atoms of chromium that by some means or other were restricted in their ability to react, and therefore were passive.

The hydrogen solution theory of passivity was proposed and developed in papers, notably by Grave,[14] Adler,[15] Rathert[16] and Schmidt.[17] According to this picture of passivity, if hydrogen gas enters the surface layer of atoms, through dipping the metal, for example, in hydrochloric acid, the metal lattice is altered, possibly loosened by dissolved hydrogen, and metal atoms readily dissolve. This is then the active state. If hydrogen is removed—as, for example, by dipping the metal in nitric acid—the catalytic effect of hydrogen is lost, and the metal becomes less reactive. This is the passive state. On the film theory, hydrochloric acid would be assumed to dissolve the oxide film, exposing underlying metal, whereas nitric acid would build the protective film by oxidizing surface layers of metal atoms.

A series of experiments was devised by the proponents of the hydrogen solution theory which was consistent with their viewpoint, and difficultly reconcilable with the oxide or protective film theory. Iron, for example, was made passive by heating in nitrogen or vacuum. An iron electrode was made active by diffusing hydrogen through the metal from a face not in contact with the electrolyte of the cell used to measure the electro-chemical potential of the iron.

Smits[4] proposed the theory that passivity of various elements like iron, nickel and chromium was accounted for by relative concentration of passive and active atom species in the metal. The proportions of each could be disturbed by changes in electron concentration, and also by so-called catalytic agents, like hydrogen and oxygen.

Russell[18] ascribed to passive metals, not a passive film protection, but an electronic change within the metal possible especially in the transition group of elements in the periodic system. In a series of experiments he showed that passivity could exist in some metals even when they were dissolved to form dilute solutions in mercury.

The work carried on in this laboratory on the pit corrosion of stainless steels has frequently brought to the fore the question of passivity. Many of the experiments carried out can be reasonably interpreted on the basis of the oxide film theory from a practical standpoint; several experiments, however, cast doubt on the necessary relation of such a film to passive properties of the metal. These experiments included:

1. Electrochemical potential measurements, which show that chromium alloys can transform from the active to the passive state in the complete absence of molecular oxygen at a rate dependent on the presence of electrolyte solutions (NaCl) in contact with the alloy. The rate of transformation was found to increase with molybdenum additions to the alloy. These results will be published separately.

2. Analysis of stainless-steel anode corrosion products in sodium halide solutions, which showed that the passivity of chromium-nickel-molybdenum (Mo 18-8) steel was more stable in chloride solutions than the similar alloy not containing molybdenum. The stability was not greatly different, however, in bromide or iodide solutions.

3. Measurement of threshold potentials of halide ions discharging on stainless-steel anodes, which disclosed their identity with the commonly measured decomposition potentials. An explanation of the threshold potentials of stainless steel is possible, therefore, without the assumption of a protective film. The data indicate that the difference in tendency for chlorides to react with 18-8 compared with Mo 18-8 is pronounced; only a slight difference in tendency appears for bromides, and no difference for iodides. The tendency for pure molybdenum to anodically corrode is the same in the three solutions.

Another series of experiments included electron diffraction studies of various metals and alloys with 30-kv. electrons. On stainless steels exposed to air or treated with nitric acid, oxide films of 10 Å. thickness, as predicted by others, were not found. Only on iron exposed to air for 24 hr. after immersion in concentrated nitric acid or on exposure for 24 hr. after vacuum annealing was a true oxide film noted.

These experiments combined with those of other investigators have induced us to seek another explanation for passivity in alloys. The

explanation arrived at is given in preliminary form in part II. Its utility, we believe, lies in the possibility of quantitatively describing the composition of alloys that are passive, its correlation of data on passivity of metals and alloys, and its inherent explanation of passive phenomena in general, combining features of many previously proposed theories.

RESULTS

Electron Diffraction Studies

The pioneer work of G. P. Thomson[19] on electron diffraction studies of passive iron did not indicate the presence of a measurable oxide film. If present, according to Thomson, it was probably beyond the resolving power of his apparatus. Very pure evaporated iron films, according to Nelson,[20] show an oxide pattern on exposure to air, but it is not mentioned whether these exhibit passivity. According to Iitaki et al.,[21] films may be stripped from passive iron and proved to be of oxide nature. Others[22] have pointed out that the stripped film is not necessarily the same film that causes passivity. Tronstad's[23] optical measurements of films on the metal suggest that the passive film on iron is of the order of 10 to 40 Å. in thickness and on austenitic stainless steel in dry air 10 to 20 Å., in ozone 20 to 30 Å. and in nitric acid of the order of 20 Å.

With a 30-kv. electron diffraction apparatus of the Germer type, studies of the surface of passive metals and alloys were made in this laboratory with the assistance of Dr. Burwell.[24] Measurements included stainless steels of the 18 Cr, 18-8 and Mo 18-8 types that had been treated with hot concentrated nitric acid, or exposed to air after vacuum annealing (in vacuo of 5×10^{-6} mm. pressure of mercury at temperatures of 1050° to 1200° C. for ½ to 1 hr. by induction methods). Films of 10 Å. are detectable with the diffraction apparatus, yet more often not as crystalline patterns by reflection measurements but as diffuse rings.

Of the pure metals, iron, nickel, chromium and molybdenum, thoroughly outgassed in vacuo at high temperatures (1000° C. ±) for long periods, only iron exhibited an oxide film and then only after a 24-hr. exposure to laboratory air. The latter film was either γ Fe_2O_3 or Fe_3O_4. Armco iron freshly passivated in hot nitric acid and inserted in the diffraction apparatus did not show an observable film until it was exposed to air for a period of 24 hours.

On stainless steels treated with concentrated nitric acid or air exposed after vacuum annealing, no film was detected. Exposure of the samples to air for various periods up to three months likewise did not indicate the formation of an oxide film observable by diffraction methods.

It can be inferred but not proved from Tronstad's measurements on stainless steels that the film he reports is an oxide. For films less than 10 Å., however, the source of error in optical measurements may be large,

as Tronstad himself pointed out.[25]   It appears from the electron diffraction results that if any film exists on stainless steel it would be an adsorbed gas film less than 10 Å.   Apparently from known lattice dimensions of oxides a film less than approximately 7 Å. thick would probably simulate an adsorbed gas film.   Films of this order of thickness can be studied only by use of extremely soft electron beams, and the interpretation of such results is fraught with difficulty.   Although the electron diffraction work contributes no positive information on the probability of a film of some kind on the surface of stainless steels, the results indicate that a true oxide film of the order of 10 Å. in thickness is not observable in air-exposed or nitric acid-treated specimens.

Corrosion Products

In order to examine the nature of stainless-steel surfaces from another angle, corrosion products were studied.   Work in this direction was stimulated by the high resistance offered by molybdenum-containing austenitic stainless steels to pit corrosion in saline solutions.   The corrosion products of ordinary austenitic stainless steels in salt solution were uniformly found to be mixtures of ferric, chromic and nickel hydrated oxides.   The proportion of the metals in the corrosion products for long exposures as well as short exposures was that of the alloy, within the limits of accuracy of chemical analyses in the former and spectroscopic analyses in the latter.*   Analyses of oxide films, by way of comparison, produced by heating stainless steels, analyze appreciably higher in chromium than would be expected from the chromium content of the alloy.[27]   It would appear from this that: (1) contrary to the results obtained from thermally produced films, the supposed surface oxide film has the same composition as the alloy, or (2) no oxide film exists.

Analyses of anodic corrosion products were also made as distinct from analyses of gross corrosion products, in a manner to reduce the influence of contamination by atmospheric gases or cathodic reactions.   This is extremely difficult to do for the pits (anodic areas) as ordinarily formed, hence electrolytic methods were employed.   Since there is little doubt that pitting of stainless steel is electrochemical in nature,† production of anodic corrosion products in an electrolytic cell seemed to be justified. In such a cell the conditions approximating those of the pit were reproduced and the valence of the corrosion products easily determined contrary to experience with anode-cathode reaction products obtained in aerated salt solutions.

The cell used contained a 4 per cent NaCl solution, a platinum cathode (6 by 6 cm.) and an alloy-steel anode (8 by 8 cm.) separated from the

---

* The same conclusion was reached for acid solutions and tap water by S. A. Burke.[26]

† This is the subject of a separate publication.

cathode by a permeable membrane. After passage of about 1 amp. for 30 min., the anode compartment solution was analyzed. The qualitative analyses are given in Table 1. The quantitative analyses of the anolyte

TABLE 1.—*Qualitative Analyses*

Anode	Electrolyte, 4 Per Cent	Anode Corrosion Product		
		Cr	Fe	Ni
18-8.............................	NaCl	Cr^{+++}	Fe^{++}	Ni^{++}
18-8.............................	NaBr	Cr^{+++}	Fe^{++}	Ni^{++}
Mo 18-8[a].......................	NaCl	CrO_4^{--}	Fe^{+++}	Ni^{++}
Mo 18-8.........................	NaBr	Cr^{+++}	Fe^{++}	Ni^{++}

[a] Actual analysis: Mo, 3 per cent; Cr, 21 per cent; Ni, 10 per cent.

for 18-8 disclosed corrosion products in amount closely representative of the weight loss of the anode. The ratio of metal content of corrosion products approximated those of the alloy electrode (Table 2).

TABLE 2.—*Ratios of Metal Contents*
ANODE 18-8, ELECTROLYTE 4 PER CENT NaCl

Current, ½ Amp., 2 Hr. Anode Current Density, 0.0108 Amp. per Sq. Cm.

Analysis of Steel		Analysis of Anode Corrosion Product	
Cr 18.17	Cr/Ni 2.04	Cr^{+++}	Cr/Ni 1.94
Ni 8.94		Ni^{++}	
Fe 72.07	Fe/Ni 8.07	Fe^{++}	Fe/Ni 8.09

Current efficiency of cell, calculated, 99 per cent.

In all of the 18-8 or Mo 18-8 anodes, numerous pits were formed over the faces and edges of the electrode. According to Table 1, it is evident that for Mo 18-8 in sodium chloride the corrosion products are in the higher oxidized state; for example, they contain chromates. (Chromate solutions are often recommended for passivating treatment.) This fact is probably connected with the unusual resistance of this alloy to attack by chloride ion. In contrast, the 18-8 corrosion products are all in lower valence states. In bromide solutions, however, the corrosion products of Mo 18-8 and ordinary 18-8 are the same and all in lower valence states.

Using smaller anodes and higher current densities with the presence of KSCN as an indicator for Fe^{+++} in the NaCl solution, it was noticed that iron dissolved initially from 18-8 as Fe^{+++} but that the initial red due to Fe (SCN)$_3$ was rapidly replaced by green $FeCl_2$. Interruption of the current for a number of seconds, depending on the rapidity with

which the corrosion products diffused away from the anode, followed by closing the switch initiated again the temporary formation of Fe^{+++} ions which was followed by Fe^{++} ions. The temporary Fe^{+++} ions formed in oxygen-free as well as air-saturated solutions. The change in valence seems therefore to be one that involves an electrode surface reaction and not a subsequent oxidation of Fe^{++}. In contrast to this, Mo 18-8 electrodes did not show a valence transition—the corrosion product remained Fe^{+++} throughout the duration of the experiment. When NaBr was substituted for NaCl, the Mo 18-8 behaved exactly like 18-8 in the NaCl solution, Fe^{+++} formed initially followed by Fe^{++}. The 18-8 electrodes did not show any different behavior in NaBr as compared with NaCl. In NaI solutions, I_2 was liberated at the anode, and attack of the anode was, in the time of experiment, negligible.

Pure iron anodes always corroded as Fe^{++}, and only at current densities considerably higher than those usually used did Fe^{+++} appear. At higher magnitudes of current density, the iron of 18-8 electrodes in NaCl and NaBr and Mo 18-8 in NaBr always dissolved, after a few minutes elapsed, as Fe^{++}.

Pure molybdenum anodes corroded electrolytically as molybdenum oxide, some of which adhered to the anode and some of which went into colloidal solution as a blue or green sol, whether the electrolyte used was a chloride, bromide or iodide. For the Mo 18-8 electrodes, however, molybdenum dissolves either as molybdate or molybdenum salt.

The distinct and unique valences of anodic corrosion products of Mo 18-8 as compared with 18-8 are difficult to reconcile on the film hypothesis. The identity of valences for the two alloys using sodium bromide as electrolyte makes any tentative film explanation even more difficult.

Threshold Potentials

Another series of experiments analogous to the measurements of film breakdown potential by Brennert[8] and Donker and Dengg[9] shed additional light on the nature of the electrode reactions. The measurements consist essentially in determining the voltage-current curves of a cell made up of a reversible cathode and a steel anode. Using iron or stainless-steel anodes, the presence of an oxide film and its role in an electrode reaction may be uncertain. The use of a platinum anode removes any uncertainty in interpretation from this source. The measurements were begun, therefore, using a bright platinum anode in $\frac{1}{2}$ M NaCl solution and a reversible cathode of Ag-AgCl. This cell was connected to a source of variable potential as illustrated in Fig. 1.

R and R' are slide wire resistances measuring 96 ohms and 5.8 ohms, respectively, connected to a storage battery B. R' is for vernier adjustment. A is a milliammeter of two ranges 0 to 10 and 0 to 100, calibrated

in 0.05 and 0.1 ma., respectively.   A voltmeter, V, range 0 to 1.5 volts, is calibrated in 0.01 volts.   The solution of cell C measuring 3 liters was kept stirred and thermostated at 25.0° C.   The platinum electrode measured 6 by 6 cm.   The Ag-AgCl electrode was made by using 24 in. of 1.75-mm. silver wire anodized in pure 0.1 N HCl for 1 hr. at ¼ amp. S is a switch used to open or close the electric circuit through the cell. Measurements were taken by closing S long enough to read A and. V.
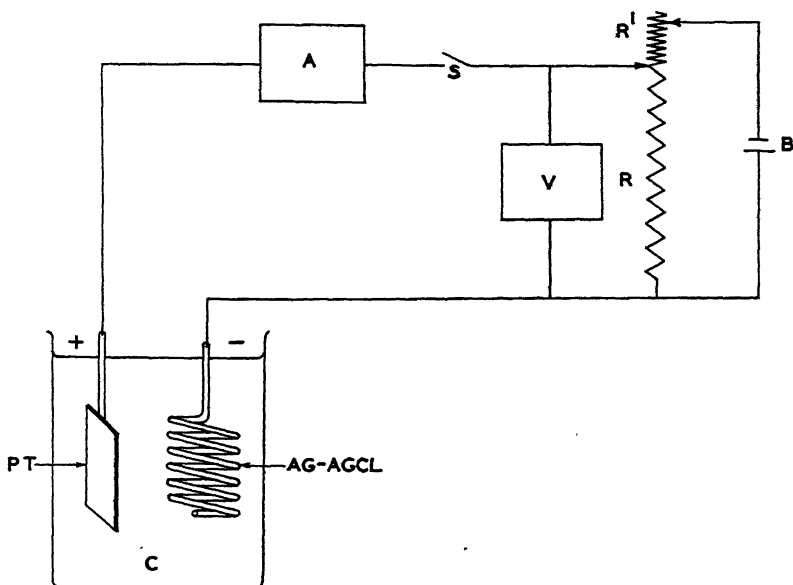
FIG. 1.—APPARATUS FOR MEASUREMENT OF THRESHOLD POTENTIALS.
A, milliammeter.
B, storage battery.
C, cell.
R, R' slide wire resistances.
S, switch.
V, voltmeter.

S was then opened for approximately one or two minutes, to allow the system to come to equilibrium before a second reading at a higher potential was taken.   If the ammeter A showed a drift on closing S, a reading was taken only after the major surge of current had disappeared.

As the potential is increased a value is reached at which the current through the cell markedly increases.   This we call the threshold potential analogous to the decomposition potential.   At this value of the potential, chlorine gas appears at the anode surface (allowing sufficient time) and at this potential or higher, electrolysis can proceed rapidly.   Threshold potentials are also obtained if ½ M NaBr and ½ M NaI solutions are substituted for ½ M NaCl, and Ag-AgBr and Ag-AgI reversible electrodes respectively for Ag-AgCl.   Plotting values of the current I

with voltage V, curves are obtained as shown in Fig. 2 for platinum in $\frac{1}{2}$M NaCl, NaBr and NaI solutions.

Because the reversible silver electrodes impress only a constant electromotive force on the circuit, and their current-voltage plots as electrodes show no discontinuities, the current discontinuity at the threshold potential is an idex of the anode reaction only. Corrected for the constant impressed electromotive force, the threshold potential corresponds to the potential at which Cl_2 gas, for example, is produced from Cl^-. Except for overvoltage effects, this potential should be a measure of the free energy attending this reaction. The free energy of
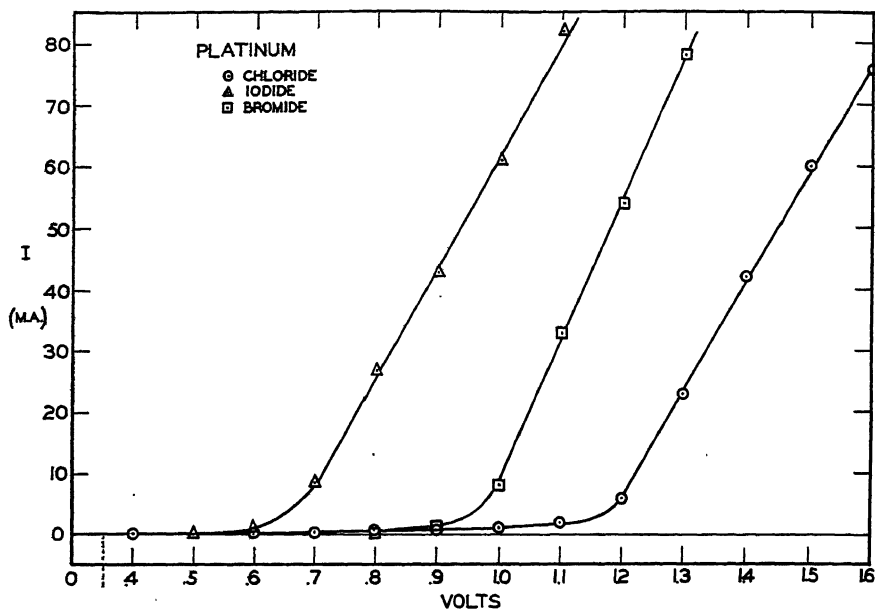
FIG. 2.—CURRENT-VOLTAGE CHARACTERISTICS OF PLATINUM IN 0.5 M SODIUM HALIDE SOLUTIONS.

halogen formation from its ions has already been reported in the literature through electromotive force measurements of cells in which chlorine gas, as an example, is in equilibrium with a platinum electrode immersed in a chloride solution. It is reasonable that the threshold potentials should be related to these molal electrode potentials obtained from electromotive force determinations, and is found to be true. The electromotive force of a halogen-platinum electrode is calculated from the well-known relation $E = E_0 - \dfrac{RT}{nF} \ln \dfrac{(Hal)^{\frac{1}{2}}}{(Hal\ ion)}$ where the activity of halogen ion in a $\frac{1}{2}$ M solution is considered to be 0.5. E_0 is the molal electrode potential recorded in the literature and R, T, n, F have their usual significance. The activities of Cl_2, Br_2 and I_2 are considered unity.

TABLE 3.—*Threshold Potentials*

Halide	Threshold Potential, Volts	Ag-Ag Halide Potential, 0.5 N Halide-ion Solution, Volts	Threshold Potentials, Corrected, Volts	Potential of Halogen → 0.5 N Halogen Ion − e Observed Measurements of Electromotive Force, Volts
Cl.....................	1.1	−0.240	1.34	1.38
Br.....................	0.95	−0.091	1.04	1.08
I......................	0.6	+0.133	0.47	0.55

Even if the activities of the dissolved halogens at the electrode surface differed appreciably from their molal saturation values in water, the effect on the calculated electromotive force would be small. (A tenfold change in activity would produce a change in potential of 0.03 volt.) From the observed threshold potential is subtracted the constant electromotive force of the reversible silver-silver halide electrode, which is calculated from the relation $E = E_0 - \dfrac{RT}{nF} \ln \dfrac{1}{0.5}$. Threshold potentials so corrected are listed in Table 3 for Cl⁻, Br⁻ and I⁻ on platinum. The second column reproduces the potential obtained from the points of discontinuity of the curves of Fig. 2. The third column is a list of the normal electrode potentials of silver-silver halide electrodes corrected for immersion in 0.5 N halide-ion solution. Column 4 lists the threshold potentials corrected for the silver-silver halide electrodes. Column 5 is a list of the normal electrode potentials given in the literature for the reac-

TABLE 4.—*Threshold Potentials*
VOLTS

Anode	Cl⁻	Anodic Reaction Product	Br⁻	Anodic Reaction Product	I⁻	Anodic Reaction Product
Pt.....................	1.1	Cl_2	0.95	Br_2	0.6	I_2
18-8...................	0.35	Fe^{++}	0.5	Fe^{++}	0.7	I_2
Mo 18-8...............	1.15	Fe^{+++}	0.7	Fe^{++}	0.7	I_2
Mo....................	−0.05	MoO_2	0.1	MoO_2	0.35	MoO_2

CORRECTED FOR SILVER-SILVER HALIDE POTENTIALS

	Cl⁻	Br⁻	I⁻
Pt.....................	1.34 (1.38)	1.04 (1.08)	0.47 (0.55)
18-8...................	0.59	0.59	0.57
Mo 18-8...............	1.39	0.79	0.57
Mo....................	0.2	0.2	0.2

tion Halogen → Halogen ion $-e$, corrected for the activities of 0.5 N halogen ion in our experiment. The fair agreement of the fourth and fifth columns within the limits of the experiment indicates that the threshold potentials are related to the equilibrium potentials. Whatever the nature of the electrode reaction at the anode using different types of anodes or electrolyte solutions, this analysis of the threshold potential lends confidence to interpretation.

Similar curves are obtained for 18-8 (by actual analysis 19 per cent Cr, 9 per cent Ni) and Mo 18-8 (by actual analysis 3 per cent Mo, 21 per cent Cr, 10 per cent Ni) anodes shown in Figs. 3 and 4 and for molybdenum in Fig. 5. The experimental arrangement was the same as for
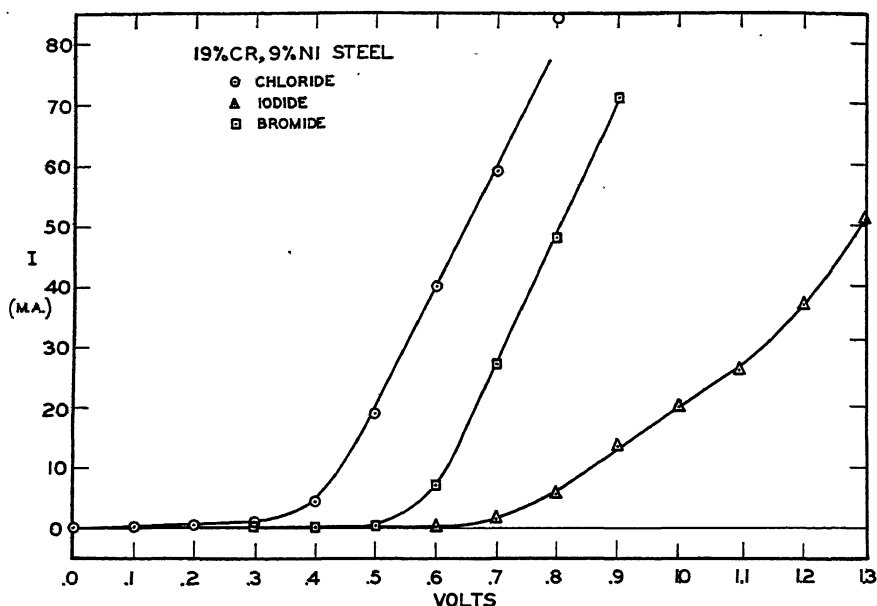
Fig. 3.—Current-voltage characteristics of 18-8 in 0.5 M sodium halide solutions.

platinum except that an air stream was circulated over the anodes to keep the steels in a uniformly passive state. The steels were allowed to remain in the solution approximately 1 hr. before measurements were begun, to insure temperature and oxygen equilibrium. The threshold potentials are listed in Table 4. In the first column are given the anode materials, the threshold potentials from Figs. 3, 4 and 5 are listed under the halide ion, followed by a column indicating the main anodic reaction product for a particular halide solution and anode. In the second part of the table, the threshold potentials have been corrected for the constant potentials of the reversible silver-silver halide electrodes. The figures in brackets following the potentials for platinum anodes

are those calculated for Halogen → Halogen ion −e from molal elec-
trode potentials, reproducing values given in Table 3.

Outstanding in Table 4 is the high threshold potential for Mo 18-8 in
NaCl accompanied by Fe^{+++}, whereas in NaBr the threshold potential is
nearer that of 18-8 and the corrosion products are the same.   The high
potential for Cl$^-$ on Mo 18-8 agrees with the behavior of this alloy in
resisting corrosion in chloride solutions, and the lower potential for Br$^-$
indicates that resistance to bromide solutions is probably not as good.
The resistance of Mo 18-8 in presence of bromide ion is greater than for
18-8, however.   The same potentials for Br$^-$ and Cl$^-$ in contact with 18-8
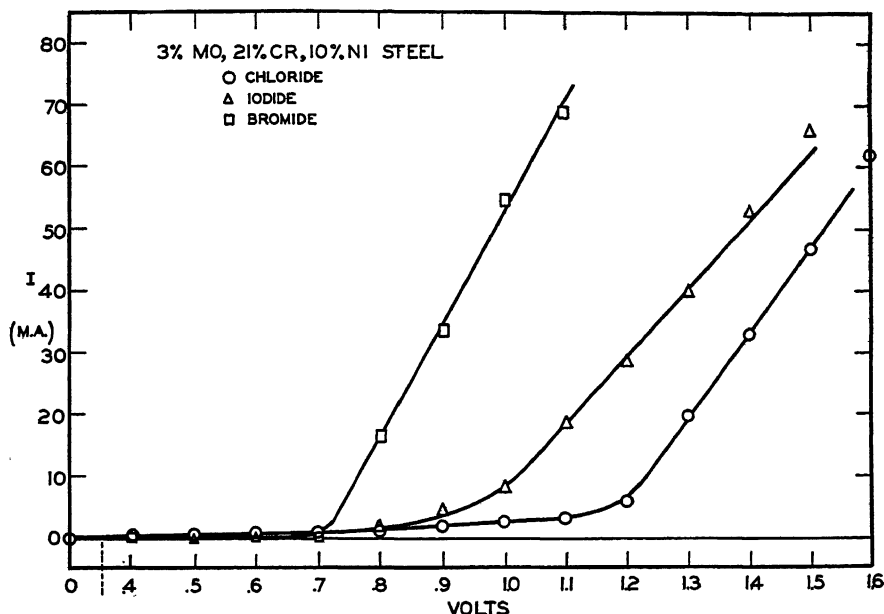
FIG. 4.—CURRENT-VOLTAGE CHARACTERISTICS OF Mo 18-8 IN 0.5 M SODIUM HALIDE
SOLUTIONS.

point to similar tendencies of the alloy to corrode in either solution, the
difference in rate of reaction presumably accounting for greater weight
losses when corroded with chlorides as compared with bromides.

Molybdenum is uniformly oxidized to MoO_2 or an analogous oxide
regardless of the halogen ion in solution.   Correspondingly the threshold
potentials are the same for all solutions, dependent apparently on con-
centration of OH$^-$ rather than halogen ion.

Corrosion weight losses substantiate the general predictions obtained
from Table 4 relating to the susceptibility of 18-8 and Mo 18-8 to bro-
mides and chlorides.   The steels were corroded in a standard 4-hr.
accelerated test using the so-called Drop-tester described in detail else-

where.[*]   The Drop-tester has previously been used in this laboratory to grade several kinds of stainless steels.   For corroding solution, 10 per cent $FeCl_3.6H_2O$ in 0.05 N HCl was used.   Ferric bromide, not readily available in pure form, was made approximately 10 per cent in concentration.   For sake of comparison and to elucidate the effect of the two kinds of ions, corrosion tests were also carried out using mixtures of bromides and chlorides.   One sheet of rolled 18-8 or Mo 18-8, tested as such, after cleaning in organic solvents, was used for all the tests. The weight losses, averaged for two or more determinations, are recorded in Table 5.
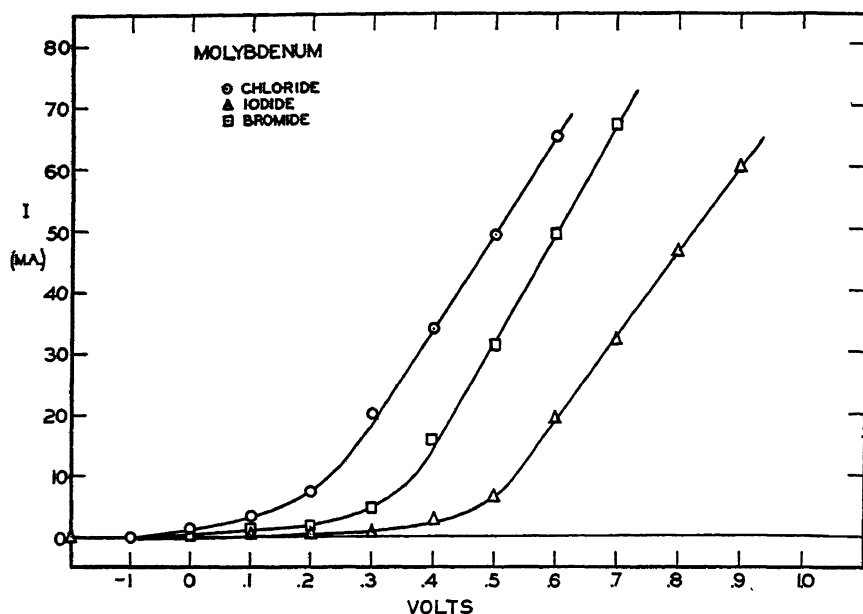
FIG. 5.—CURRENT-VOLTAGE CHARACTERISTICS OF MOLYBDENUM IN 0.5 M SODIUM HALIDE SOLUTIONS.

It is observed that $FeCl_3$ has no large effect on Mo 18-8 steel; in fact, the attack is so small that the test can be continued for many hours with no pitting and no significant change in weight loss.   The loss of 18-8 is 35 times larger, using $FeCl_3$, and the alloy pits.   In $FeBr_3$, however, 18-8 and Mo 18-8 lose the same weight and both steels pit. Bromide ion in presence of Mo 18-8, therefore, as the threshold potentials lead us to expect, specifically accounts for increased attack of greater magnitude.

In mixtures of ions, the situation is more complex.   Again bromide ion in $FeCl_3$ solution succeeds in breaking down Mo 18-8, and the cor-

rosion weight loss is 49 times that in FeCl$_3$ alone. The corrosion of 18-8 is also stimulated by addition of bromide ion, although the increase is 6.5 times as compared to 49 times. The increase in corrosion of 18-8 in FeCl$_3$-FeBr$_3$ mixtures would seem to be related to the decrease in pH of ferric salts on addition of a neutral salt. In further experiments, however, where the pH of all solutions was adjusted by acid additions, the weight losses were still a major function of the NaCl concentration. It appears, therefore, that the pH of ferric salt solutions is not the critical factor.

TABLE 5.—*Weight Losses*

Solution	Weight Loss, Grams per Sq. Dm.			Pits per Test Area, (5.74 Sq. Cm.)	
	pH of Solution	19 Per Cent Cr, 9 Per Cent Ni	3 Per Cent Mo, 21 Per Cent Cr, 10 Per Cent Ni	19 Per Cent Cr, 9 Per Cent Ni	3 Per Cent Mo, 21 Per Cent Cr, 10 Per Cent Ni
1. 10 per cent FeCl$_3$.6H$_2$O in 0.05 N HCl......................	1.10	0.122	0.0035	4	0
2. FeBr$_3$, approximately 10 per cent.	1.02	0.042	0.042	2	2
3. Same as solution 1 plus 100 grams NaBr per liter................	0.75	0.798	0.171	43	8
4. Same as solution 1 plus 42.1 grams NaCl per liter.................	1.03	0.530	0.0096	17	0

The effect of NaCl addition is indicated in the results of the fourth row of Table 5 in which NaCl has been added to FeCl$_3$ in similar manner to the addition of NaBr in the results of the row above. The addition of NaCl is accompanied by a 4.4 increase in corrosion rate of 18-8. The attack of Mo 18-8 is not appreciably increased, considering the experimental error of corrosion weight losses.

It has been customary to consider curves depicted in Figs. 3 and 4, using stainless-steel anodes instead of platinum, as evidence of film resistance to breakdown and to consider that the threshold potential is a measure of the external force necessary to drive negative ions through a supposed nonconducting film. Such a view, while possibly presenting a plausible explanation of the situation for stainless steel, is not necessary for platinum, as oxide films are not possible in the ordinary sense. But for stainless steels, too, the film concept is difficult to reconcile with observation. Table 4 shows bromide ion more easily reacting with the anode than the smaller chloride ion, contrary to the ability of smaller ions to more easily penetrate a supposed protective film. The explanation is more difficult in view of the behavior of chloride and bromide ions on 18-8, which show no differential in reaction tendency. Sup-

posedly, the reason for the resistance of Mo 18-8 to Cl^- cannot logically be attributed to the film-forming properties of molybdenum. Molybdenum, as Table 5 shows, has a low threshold potential in all halogen solutions despite the fact that it forms an oxide layer over the surface when used as anode in electrolysis. It shows no peculiar behavior in chloride solutions as compared with bromide solutions.

It appears that bromide ions impelled by an electric field succeed in breaking down passivity of a Mo 18-8 anode, thereby forming Fe^{++}, whereas chloride ions show no pronounced tendency to destroy passivity and the anode corrodes as Fe^{+++}. Ferrous ion, Fe^{++}, is characteristically the corrosion product of active iron or nonpassive iron alloys, whereas if solution of passive iron or passive steel alloys is accomplished, ferric ion, Fe^{+++}, is the usual corrosion product. This fact was early pointed out by Finklestein[28] in his valence theory of passivity.

One important conclusion of our study of corrosion products has been that appreciable corrosion of passive alloys without the influence of an electric field is almost always preceded by breakdown of passivity. Hence, when Mo 18-8 is pickled in acid, the corrosion products are the lower valence salts, such as ferrous salts, indicating that passivity is broken down by the pickling agent. Electrochemical potential measurements of the same steels previously in contact with strong pickling solutions have also proved to us that the alloy is made active by such contact. When the same steel is corroded by electrolysis as anode in NaCl, higher valence salts result, indicating that the steel is dissolving as a passive alloy. Normally, however, potentials operating to produce corrosion are less than the external potentials used to electrolytically corrode Mo 18-8.* Hence one is led to the conclusion that Mo 18-8 corrodes less in salt water or ferric chloride, because the rate at which it transforms from passive to active state is low. Bromide ions, according to this concept, are considerably more active than chloride ion in breaking down the passivity of the alloy, and hence corrode Mo 18-8 more actively than chloride ion.

Further evidence that Mo 18-8 can corrode electrolytically in two different states of passivity in NaCl solution, depending on the external potential, is contained in the current-voltage plot for Mo 18-8 in Fig. 4. Although the threshold potential for Mo 18-8 in NaCl in Table 4 is given as 1.15 volts, the curve, unlike the others of the series, actually shows an initial threshold potential at 0.7 volt. This corresponds with the threshold potential of Mo 18-8 in NaBr (which electrolytically

---

* The potential between active and passive Mo 18-8 is about 0.5 volt. This represents the magnitude of potential available for corrosion. In these electrochemical experiments, 4 volts was used.

corrodes as Fe^{++}) and indicates that some corrosion of Mo 18-8 begins at this point, presumably forming Fe^{++}. This was checked experimentally in a cell using 4 per cent NaCl, oxygen free, with Mo 18-8 as anode and Ag-AgCl as cathode. One volt was impressed on the cell. After a period of about one hour dilute green corrosion products of the anode were in evidence. Analysis of the electrolyte showed ferrous ion, whereas ferric ion is found when electrolysis is speeded up, using about 4 volts. Corrosion, although taking place at these low values of the potential, is very small, as indicated by the small values of the current at potentials below 1.15 volts. It appears that corrosion below 1.15 volts depends upon conversion of passive to active alloy which, in Mo 18-8, is a slow process, whereas corrosion above 1.15 volts is more rapid because the alloy can at this high external potential dissolve in the passive state.

The conclusions from these experiments are that Mo 18-8 is more passive or more stably passive than 18-8. Furthermore, transformation of passive Mo 18-8 to the nonpassive state takes place less readily compared with 18-8. Bromide ion is more effective than chloride ion in breaking down the passivity of Mo 18-8.

SUMMARY OF PART I

The electron diffraction work reported in this paper for stainless steels does not indicate the presence of an oxide film of the order of 10 Å. or greater, whether crytalline or amorphous. In accordance with the work of G. P. Thomson[19] on passivated iron, it can only be said that the film if present on the alloys must be less than 10 Å. and probably less than 7 Å. In such case the films are probably more like those of an adsorbed nature than a true oxide. It must be pointed out, however, that even the presence of a thin adsorbed film (regardless of what it is composed) as a fundamental cause for passivity is speculative and cannot logically be inferred from electron diffraction experiments.

It has been shown, through a study of corrosion products of stainless steels, that the surfaces of the alloys are of essentially the same composition as the alloy. This can be interpreted either that contrary to conclusions based on analysis of thermally produced films, the surface film is of the same composition as the alloy, or that no oxide film exists.

Analyses of anodic corrosion products show that an 18-8 containing 3 per cent Mo, which is very resistant to chlorides, corrodes electrolytically in NaCl solution as higher valence salts, including chromates and ferric salts. The latter corrosion products, useful as passivating agents, are apparently associated with the alloy resistance to chloride ions. Mo 18-8 corrodes electrolytically in NaBr to form lower valence salts

like Cr^{+++} and Fe^{++}. Anodic corrosion products of 18-8 either in NaCl or NaBr are Cr^{+++} and Fe^{++}. Iodine is discharged as the element on either 18-8 or Mo 18-8 anodes, using iodides as electrolyte. Molybdenum as anode in chlorides, bromides or iodides, forms the oxide.

By impressing an increasing electromotive force on a cell made up of a steel anode and silver-silver halide reversible cathode, the potential has been determined at which a halogen ion begins to react with the steel anode. This is called the threshold potential. It is shown that the threshold potentials for platinum correspond to the decomposition potentials of halide ions and agree satisfactorily with electromotive force equilibrium potentials reported in the literature. It is shown that threshold potentials for stainless steels, contrary to indications in the literature, can be explained without reference to a hypothesized protective film. The threshold potential is not necessarily a film break-down or film breakthrough potential, but analogous to the decomposition potential.

It is shown through threshold potential data that the tendency for 18-8 to react with chloride and bromide ions is the same. For Mo 18-8, the tendency to react with bromide ion is somewhat less than that for 18-8, but with chloride ion, Mo 18-8 shows extreme resistance. In accordance with these results, it was found that 18-8 corrodes by pitting in either ferric chloride or bromide. Mo 18-8 resists the action of ferric chloride, but corrodes by pitting in ferric bromide. Bromide ion more effectively than chloride ion breaks down passivity of the Mo 18-8 alloy, which is contrary to expectations according to the porous film theory. It is concluded that 1.5 mole per cent Mo in 18-8 stabilizes the passivity of the alloy by another mechanism.

It is proposed that passivity of stainless alloys is not due primarily to a protective oxide or oxygen film, for the following reasons:

1. Electrochemical potential measurements of stainless alloys in oxygen-free electrolytes are inconsistent with an oxide or oxygen film theory.

2. Analyses of anodic corrosion products, the specific effect of bromides in corrosion of Mo 18-8 and the effect of 1.5 mole per cent Mo added to 18-8 are not readily explained by a protective oxide film.

3. Threshold potential measurements mentioned in the literature as gauge for film resistance are readily explained as decomposition potentials not involving film concepts. The considerably greater tendency of bromide ion to react with Mo 18-8 than the smaller chloride ion and the equal tendency of both ions to react with 18-8 does not readily fit into the porous film picture of passivity.

4. A theory of passivity based on electron sharing within the metal lattice accounts quantitatively for the composition of several passive iron alloys, and plausibly explains the experimental results described without resorting to a protective film. This is discussed in Part II.

PART II. THE NATURE OF PASSIVITY

The experiments described in part I require more, it would seem, than a single picture of passivity based on a multiproperty oxide film of one kind or another, which protects the metal from attack. The experiments do not exclude the possibility of a film under certain conditions on the surface of stainless steels, but rather emphasize the necessity for investigating the properties of the surface metal atoms to account for all the phenomena observed. Any general picture of passivity based on a protective veneer afforded by a layer of atoms either adsorbed or in chemical combination with the surface metal is inadequate to explain all the results of experiment.

The theory of the surface of a metal is particularly complex. Great strides have been made in explaining some of the bulk properties of metals and alloys, such as conductivity, magnetism, cohesion and the like. In doing so, the quantum theory of atoms has been applied to lattice aggregates whereby the atomic energy levels lose their identity in energy levels for the whole metal. In this manner individual atomic energy levels are considered to contribute corresponding levels in the lattice. In dealing with the surface, however, no complete theory of correspondence has been worked out. So far the employment of potential barriers has proved useful in describing thermionic emission[29] and kindred effects including electrochemical action.[30]

In this paper, in an attempt to explain the experiments on passivity, is outlined a theory based on atomic energies and interaction, without the complication of an approach involving the more complex concepts of the metal lattice. In this sense the theory represents only a beginning, pointing the direction in which a more general and exact theory of passive alloys will needs follow. We consider passivity of metals as well as alloys describable in terms of electron rearrangement within the metal and sharing of electrons of the atoms. This has suggested some interesting and useful relations in alloys and has correlated much of the information on passivity of metals contained in the literature. The theory relating to alloys is outlined in the following sections. The general treatment of passivity is more properly the subject of another paper.

ELECTRON SHARING IN ALLOYS

When two metals are brought into intimate contact, as by melting, some kind of bonding is expected between the two species of atoms. Sometimes a definite compound is formed. This is detected by typical behavior of composition-temperature lines of the phase diagram or by changes in lattice parameter as revealed by X-ray photograms. Bonding characterized by stability at melting temperatures of the alloy, or of such a nature as to change the lattice parameters, would be detected with

no difficulty by these means; other types would not be evident.   Every reason exists, however, that electron sharing between two metal atom species can and does take place.   Hardness and high tensile strengths of alloys indicate that there is considerable atomic interaction and bond formation.   Contact potentials indicate that transfer of electrons does take place between two metals, although the energies involved are much smaller than for the usual bond formation.   Furthermore, an analogy exists, which is afforded by the theory of chemical combination, as in NaCl. When sodium reacts with chlorine, the one electron of the outer shell of Na tends to fill the one vacancy of the outer shell of the Cl atom to take on a noble gas structure.   This is typical of ionic bond formation. Although the bonding may differ, a similar transfer of electrons may take place in an alloy, especially if one of the metal constituents has an incomplete inner shell requiring one or more electrons to saturate the shell. For example, chromium has the configuration $3d^54s$, which leaves five electron vacancies in the third shell.   The tendency is for the third shell to fill up to form a saturated electronic configuration of $10d$ electrons, even though this may not be revealed in compound formation as ordinarily detected.   Iron has the configuration $3d^64s^2$, which leaves four vacancies in the third shell.   When an iron atom comes in contact with a chromium atom, it would be expected that electrons from iron would be displaced in the direction of the chromium atom to fill the vacant levels of the chromium shell.   Although no experimental data are available to prove that this is so, one can reason from the difference in energy for chromium in the ground state $3d^54s$ and the excited state $3d^44s^2$.   The value from spectroscopic data is given as 0.96 electron volts.   For iron, on the other hand, the difference between the ground state $3d^64s^2$ and the excited state $3d^74s$ is 0.86 electron volts.   The chromium excitation represents an electron jump from third to fourth shell; for iron, a jump from fourth to third shell, each with positive energy change.

Chromium would therefore be expected to have the greater electron affinity.   This is inferred from a comparison of the electron affinities and energies of excitation of the halogens given in Table 6.[30]

TABLE 6.—*Electron Affinity and Energy*

Halogen	Electron Affinity, Electron Volts	Ionization Potential, Electron Volts
F	4.1	18.6
Cl	3.8	12.96
Br	3.6	11.30
I	3.2	10.44

If chromium has the greater electron affinity, it is expected that electrons from iron would tend to transfer to chromium to occupy vacant

energy levels (Fig. 6). This process would take place despite the setting up of differences in electrical potential by the electron transfer. Experimentally the potential difference is observed for metal atom aggregates as the so-called contact potential. This would probably apply not only to pairs of iron and chromium atoms but also to the general state of atoms in the metal lattice. Although spectroscopic data used in this reasoning is solely information of electron energies applied to the atom and not to atomic aggregates, from present theory of the solid state we know the energies are related. The energy levels in Fig. 6 are considered to exist for the metal as well as for the atom even though the absolute energies and relative displacements of each level are probably altered. Again, energies for the metallic state may not coincide with those operating at the surface, but correlation is expected and experiments on adsorption indicate that this is so.[31]

The sharing of electrons of iron by chromium atoms we denote as the mechanism whereby iron is made passive when alloyed with chromium. When one electron of an iron atom is so shared, it is considered to be in the passive state. Lacking such sharing, it is active. Although this mechanism involves an assumption as to the configuration of passive iron as compared with active iron, the assumption is reasonable in that it is known empirically that active iron is normally in equilibrium with Fe^{++}, whereas passive iron is in equilibrium with an ion containing one less electron; namely, Fe^{+++}. This can be interpreted that one electron of each

FIG. 6.—ENERGY LEVELS OF CHROMIUM AND IRON ATOMS.

passive iron atom is not free, presumably by the electron sharing process, to enter solution with the iron ion.

The number of iron atoms that are passivated by a chromium atom, we can judge by the properties of iron-chrome alloys. When chromium is alloyed with iron, the alloy, at low chromium concentrations, dissolves in dilute nitric acid, has an electrochemical potential of the order of zinc, and, by and large, behaves as an active metal. At approximately $\frac{1}{7}$ to $\frac{1}{6}$ mole fraction of chromium, however (13.4 to 15.7 weight per cent) the alloy markedly changes in properties. It no longer dissolves in nitric acid, its electrochemical potential is of the same order as silver and its properties are best summed up in describing it as a passive alloy. It behaves in similar manner to passive iron in resisting almost all corroding solutions; oxidizing solutions best, chloride solutions least. As the chromium concentration is increased, the chemical properties of the

alloy undergo no further marked change.   Only above the critical con-centration of the order $\frac{1}{6}$ mole fraction chromium does the alloy undergo a radical change in chemical properties, which makes it so useful as a corrosion-resistant alloy.   Hence, approximately five iron atoms are passivated by one chromium atom, which is exactly the number one would predict from the number of electron vacancies in the chromium electron configuration.   Chromium lacking $5d$ electrons in the third shell can fill these levels with five electrons from five iron atoms, thereby making each iron atom passive.   The particular electron of iron that is shared to produce passive iron is not evident from its configuration.   Although it is plausible from energy considerations that one of the $3d$ electrons is available, one of the $4s$ electrons might also serve the purpose.

The range of composition between active and passive chromium-iron alloy varies with conditions of the metal surface and the nature of the medium in which passivity is measured.   Apart from the relative homo-geneity of the alloy, which is a factor, the explanation is contained in the relative electron-absorbing tendencies of the solution itself, which influences the measured passivity of the metal.   Thus, nitric acid, which has a large electron-absorbing capacity (oxidizing agent), would supple-ment the action of chromium in keeping the iron in the passive state. The same is true for oxygen-containing solutions, for oxygen adsorbed on the surface would tend to share two electrons per atom.   One would expect, therefore, the experimentally known result that the potential of stainless steel is more noble in oxidizing solutions than in salt solutions. The opposite situation would hold for nonoxidizing solutions, which readily give up their electrons (reducing agent) and hence would counteract the effect of chromium.

When a passive alloy steel normally noble in potential is dipped into hydrochloric acid, potential measurements show that the steel assumes the properties of an active metal like iron or zinc.   This condi-tion still holds if the steel is transferred to an oxygen-free solution, as our potential measurements show.   If oxygen is admitted to the electrode, the noble potential of the steel rapidly, although not instantly, is regained. This has usually been explained as solution of the protective oxide coating of the steel by acid and rebuilding of the film by oxygen.   On the elec-tronic concept, which excludes the film as the primary cause of passivity, the acid reaction with the steel destroys passivity by an entirely different mechanism.   Hydrogen is usually evolved when acids react with stainless steels.   This hydrogen presumably discharged atomically has the ability to adsorb on the surface and, without doubt, dissolve at least in the upper layers of the metal atoms.   The solution tendency of hydrogen in iron, for example, is very pronounced, as is illustrated by a simple laboratory experiment designed to collect hydrogen gas on one side of an iron plate, although generated by acid reaction on the other.   When hydrogen

dissolves in steel there is evidence[32,33] that the gas dissolves not atomically, but as the proton and electron. Electrons from hydrogen in a passive alloy would immediately be available to fill unoccupied energy levels characteristic of such alloys, as illustrated in Fig. 6, or levels occupied by virtue of electron sharing with iron atoms. Once the levels were so filled, the bond between iron and chromium would be displaced, and the iron immediately lose its passivity. The electrons entering the unfilled levels of chromium would also destroy its passivity, so that all the constituents would take on the potential of active metals.

It is presumably by the mechanism of adding electrons to unfilled energy levels in passive elements like chromium, nickel and cobalt that these metals are made increasingly active or decreasingly passive. Hydrogen-free chromium, such as is produced by aluminum reduction, is therefore expected to be considerably more passive than electrolytically deposited chromium, which always contains hydrogen. This is found to be true.[34]

As soon as the active alloy is exposed to oxygen or an oxidizing agent like nitric acid, the hydrogen is oxidized to water and withdrawn from the alloy surface. The alloy thereupon becomes passive again. In this manner, the destruction of passivity by acids or cathodic treatment in which hydrogen is discharged at the surface of the metal, or the process of passivation, is explained without necessity for the passive film.

PASSIVE ALLOY COMPOSITIONS

The relative merit of the electronic theory of passivity just described depends upon its harmony with the facts regarding other passive alloys and elements.* The electronic configuration of molybdenum is given as $4d^5 5s$, which is very similar to that of chromium $3d^5 4s$. One would expect the chemical properties of the two metal atoms also to be similar. The difference in energy between the ground state of molybdenum given above and the state $4d^4 5s^2$ is 1.36 electron volts. This energy is 1.4 times the energy for the corresponding transition in chromium. Reasoning as before, one would expect the electron affinity of molybdenum to be pronounced, as probably it is for chromium, and, from energy considerations, that it would exceed the value for chromium. Molybdenum alloyed with iron should, therefore, produce a passive alloy, more stably

---

* It is interesting that the passive elements are mostly those of the transition and pre-transition elements of the periodic table. This was early pointed out by Bohr and later emphasized by Russell[18] in his theory of passivity of metals. Russell assumed that iron was passive when one electron of the fourth shell fell into the third shell. This differs from the electronic changes we propose for the metallic state. Though novel and suggestive, Russell's scheme does not lead to as fruitful an explanation of passivity.

passive, at the same critical quantitative mole fraction as in the chromium alloys. This would be true if other properties of molybdenum and chromium coincided. Molybdenum, contrary to chromium, does not form a solid solution throughout the range of concentration; hence, although the theory applies as for the chromium system, the mutually insoluble phases of the iron-molybdenum system must be taken into
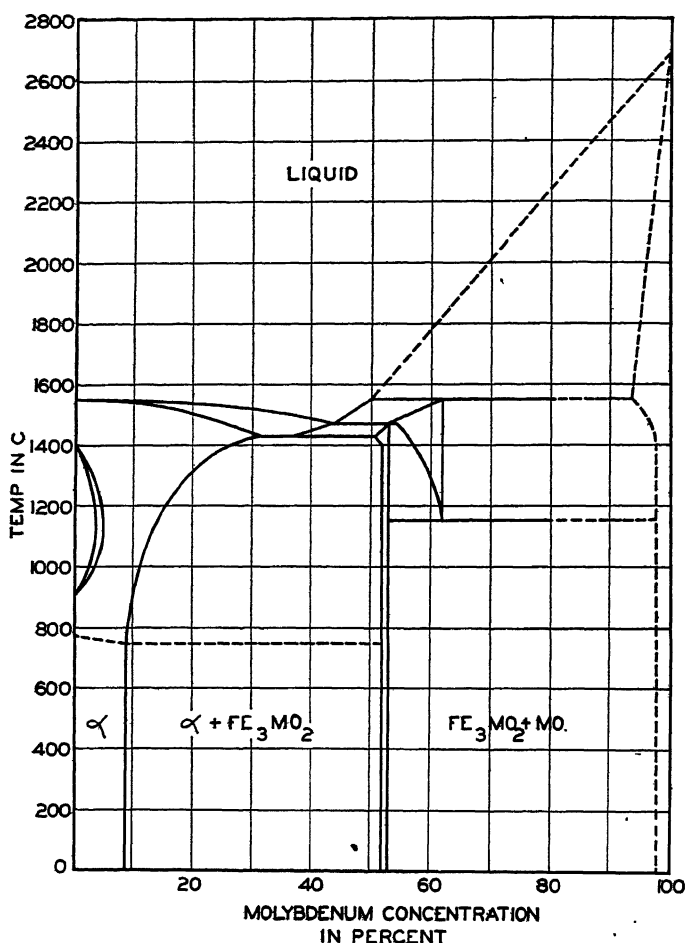
FIG. 7.—PHASE DIAGRAM OF IRON-MOLYBDENUM.

account. The phase diagram is reproduced in Fig. 7. Solid solution exists up to 9 per cent Mo (5.5 mole per cent), a mixture of solid solution and Fe_3Mo_2 to about 55 per cent Mo, and above 55 per cent Mo a mixture of Fe_3Mo_2 and Mo.

According to our predictions, a solid solution of molybdenum and iron should be active below 16 mole per cent Mo and passive above this concentration. Hence the solid solution of Mo-Fe should be active,

Above 9 per cent Mo and below 55 per cent, the solid solution of Mo-Fe should still be active, although the compound with which it exists contains 40 mole per cent Mo and therefore should be passive. Galvanic action between active and passive crystals in this region generating hydrogen would tend to destroy the passivity of the compound, therefore this region should likewise be active. Above 55 per cent Mo the passive compound exists with pure Mo, which in itself is passive, so that this region should according to theory be passive. Tammann and Sotter[35] measured the electrochemical potentials of the molybdenum-iron system and found that the alloy was noble or passive above approximately 60 to 70 per cent Mo; active below. The agreement between predicted and observed regions of passivity is satisfactory.

The theory is further strengthened through the experiments of Schmidt and Wetternick,[36] who determined the weight losses of nickel-iron-molybdenum solid solutions in boiling dilute hydrochloric acid and also in 1:4 sulphuric acid. Measurement of passivity is not best conducted in acids because of their passivity-destroying properties, but sulphuric acid is much less active in that respect than hydrochloric. The weight losses of nickel-iron-molybdenum alloys in 1:4 sulphuric acid recorded by Schmidt and Wetternick are given in Table 7, where mole ratio of Mo to Fe has been substituted for weight per cent listed in the

TABLE 7.—*Corrosion Weight Losses of Nickel-iron-molybdenum Alloys*

MOL RATIO $\frac{Mo}{Fe}$	WEIGHT LOSS, MG. PER SQ. CM. PER 24 HR.
60 PER CENT NICKEL	
0	18.5
0.029	809.0
0.088	1166.0
0.189	13.6
0.266	6.7
0.487	3.4
0.618	1.2
35 PER CENT NICKEL	
0.0018	44.2
0.017	1023.
0.047	1535.
0.083	1383.
0.144	20.4
0.183	29.8
0.240	21.5
28 PER CENT NICKEL	
0.0038	129
0.0166	977
0.039	1299
0.088	all diss.
0.121	all diss.
0.194	301
0.209	35.8

original paper. The theory predicts that maximum passivity, or in this case minimum solution rate, would begin at about $\frac{1}{7}$ (0.14) to $\frac{1}{6}$ (0.17) mole ratio Mo to Fe. For all the data reproduced in Table 7 the break occurs at approximately the predicted value.

The theory is further confirmed by a consideration of corrosion data of iron-nickel alloys. Nickel has the configuration $3d^8 4s^2$, which leaves two unfilled d levels, which would tend to absorb two electrons just as chromium tends to fill its five unfilled levels. This means that one nickel atom should passivate a maximum of two iron atoms, and nickel-iron alloys should be passive beginning at $33\frac{1}{3}$ mole per cent Ni (34.4 weight per cent). Schmidt and Wetternick,[36] from corrosion weight losses in sulphuric acid, found that nickel-iron alloys were best in corrosion resistance beginning at 34 per cent nickel.

Lack of experimental data has delayed at this time extension of the theory to general alloy systems, although it appears that eventually this will be possible. For example, copper behaves in alloy structures and sometimes chemically as a passive element. It is known that for copper-nickel alloys containing more than approximately 30 per cent Ni, corrosion in saline solutions takes place predominantly by pitting, typical of a passive alloy. Below 30 per cent, corrosion is predominantly by general solution, typical of a nonpassive alloy. This information indicates that, like iron, one copper atom in solid solution can be passivated by sharing one electron with another atom like nickel.

Promising as the theory appears in treating alloy systems, its utility also extends to the older and more controversial subject of passivity in pure metals. It is not possible to treat the subject adequately in a paper of this kind, other than to mention the phenomena for which it offers explanation. The theory based on a mechanism similar to that presented for alloys explains variable degrees of passivity in metals. It also makes clear that the role of adsorbed oxygen in passivating metals is similar to the action of chromium on iron; i.e., an electron-sharing process takes place. It thereby lends support to the views of Langmuir[37] on passivity and adsorption, and of Bennett and Burnham,[3] on the nature of the passive film on iron. It offers explanation for the effect of temperature on passivity based on occupancy of higher energy levels at a critical higher temperature, a concept that does not involve assumption of a critical solution temperature for oxides. By a similar mechanism, it explains plausibly the action of the magnetic field in destroying passivity of iron.

DISCUSSION OF EXPERIMENTAL DATA

This reasoning, when applied to the experimental work of part I, suggests why molybdenum added to chrome-nickel steels shows increased corrosion resistance. The pronounced capacity of molybdenum to absorb

and share electrons increases the stability of the passive alloy. When Mo 18-8 is made the anode in sodium chloride solution the conversion of passive to active alloy is so retarded by the presence of molybdenum that the corrosion products, Fe^{+++} and CrO_4^{--}, are those typical of the passive state. An 18-8 anode whose passive-active conversion rate is higher dissolves more readily as active alloy and only at higher current densities does ferric ion appear, and then only temporarily.

The first appearance of passive alloy-corrosion products (i.e., Fe^{+++}) is probably the result of normal electrode reaction uninfluenced by external factors, but as corrosion products concentrate in the neighborhood of the surface, their acid hydrolysis products succeed in charging the surface with hydrogen and breaking down passivity. The marked ability of stainless-steel corrosion products to destroy passivity of the alloy we proved by electrochemical potential measurements and corrosion tests. Once passivity is destroyed, the corrosion products are the same as those for active metals (i.e., Fe^{++}).

The reason that bromide ion readily attacks Mo 18-8 steels whereas chloride ion has less effect is presumably related to the more intense electric field surrounding the smaller chloride ion, the greater resistance to distortion in any electric field and its higher electron affinity. When a chloride ion approaches a Mo 18-8 steel anode, the field of the ion repels electrons from the surface; so that when the anode atoms go into solution they do so minus more electrons than for bromide attack, hence the iron-corrosion product tends to be Fe^{+++}. Bromide ion approaching the same anode has a less intense field of its own and its greater tendency to distort under the influence of the external field, or temporarily give up an electron to the unfilled energy levels of the metal surface, insure conditions favorable to lapse of passivity. The anode-corrosion products in this case are partly, at least, those of lower valence salts. Once electrolysis is under way, the corrosion products further convert passive to active alloy; so that eventually only lower valence salts are produced. This is not true for Cl^- attack on Mo 18-8 by electrolysis, because the oxidizing capacity of the higher valence corrosion products prevents breakdown of passivity. Chloride attack of 18-8, as contrasted with Mo 18-8, is not different in nature from that of bromide, probably because passivity of the alloy is not as stable as that for the molybdenum-containing alloy. The metal ions enter solution at low potentials (Table 4); too low for Cl^- to approach sufficiently near the 18-8 anode so that its field could induce all iron atoms to dissolve as Fe^{+++} rather than Fe^{++}. Iodine discharges at a lower potential than that necessary for metal ions to enter solution; so that it does not destroy passivity of stainless steels. The ability of iodine to absorb electrons is sufficiently pronounced, on the other hand, to passivate chromium in an electrolytic cell according to Hittorf's experiments.[13]

The unfilled ˚electronic levels in chromium steels probably account for high surface fields, sometimes called secondary valence forces. Iodine atoms discharging on such electrodes are more firmly bound to the surface by these secondary valence forces, hence the threshold potentials for iodine on 18-8 exceed the value for iodine on platinum. This gives explanation to results of Table 4, showing that iodine molecules have less tendency to form on stainless-steel electrodes than on platinum.

DISCUSSION AND CONCLUSION, PART II

We have attempted to show that the passivity of metals and alloys can be ascribed to electron sharing of metal atoms. This concept explains the effect on passivity of alloy constituents like chromium and molybdenum in stainless steels as well as the effect of the normally considered passivating agents like nitric acid or a layer of adsorbed oxygen atoms.

It has been shown that where the proper sharing ratios occur in the metal, we have experimental proof that the surfaces exhibit the properties of passive metals. In evolving such a theory for alloys, we have limited ourselves to the transition and pre-transition elements, which, indeed, show a striking tendency, as pointed out by others, to exhibit passive characteristics. These same elements may have exactly the surfaces most suited for chemosorption, particularly of oxygen, and in certain media chemosorption may always be a concomitant of passivity. The indication remains, however, that these chemosorbed films are not always the cause of passivity, particularly for the passive alloys. The same may be said for normal oxide films; that any part they play in protecting the metal surface of passive alloys or transition elements as would a paint film is secondary to the actual change that takes place in the reactivity of the metal itself when becoming passive. The situation for elements like aluminum and magnesium may be another case. Here we are dealing with a closed-shell atom with the chemical oxide coating playing a role in protection and the effects of adsorption not as apparent.

Our concept of passivity is that in the pure state the passive alloys and the transition and pre-transition elements like chromium and nickel are passive. They are more passive if in contact with an oxidizing or electron-absorbing agent like nitric acid or an adsorbed layer of oxygen atoms (not the oxide). They lose passivity if charged in some way with hydrogen, which tends to dissolve in the metal lattice as protons and electrons. Dissolved hydrogen is considered to fill in electronic energy levels of the lattice normally responsible when unoccupied for passivity. By removing hydrogen through exposure of the metal to air or an oxidizing medium, the metal changes from an active state to one that is passive.

It will be observed that the present theory of passivity based on electronic sharing combines and makes a consistent unity of many of the previously proposed theories; particularly the hydrogen solution theory of Grave[14] and others, the oxide film theory of Faraday[7] and more recently U. Evans[38] and W. J. Müller,[39] the allotropic change theory of Smits,[4] the valence theory of Finkelstein[28] and the adsorption theory of Bennett and Burnham[3] and Langmuir.[37] Russell's scheme[18] of passivity based on electronic configuration of the atom also finds its counterpart in the present paper, although in the use of spectroscopic data we have followed another path.

The utility of the present viewpoint rests on its greater breadth of applicability to passive phenomena in general and the treatment of passive alloys in particular. The theory is shown to be in agreement with known compositions of passive iron-chromium, iron-molybdenum, iron-nickel and iron-nickel-molybdenum alloys. Furthermore, it permits an interpretation of anodic corrosion products of stainless steels as well as threshold potential measurements in halide solutions, which an oxide film theory can account for only with difficulty.

REFERENCES

1. C. F. Wenzel: Lehre von der Verwandschaft der Korper, 108.   Dresden, 1782.
2. T. Bergmann: Opuscula Physica et Chemica, **3**, 84, 140.   Upsala, 1783.
3. C. Bennett and W. Burnham: *Trans.* Electrochem. Soc. (1916) **29**, 217.
4. A. Smits: Theory of Allotropy.   1922.   Longmans Green & Co.
5. S. Glasstone: The Electrochemistry of Solutions.   London, 1930.
6. Gmelins.Handbuch der Anorg. Chem., Ed. 8, No. 59, pt. A, issue 3, 313.
7. M. Faraday: *Phil. Mag.* (1836) [3] **9**, 122.
8. S. Brennert: *Jnl.* Iron and Steel Inst. (1937) **135**, 101.
9. H. Donker and R. Dengg: *Korr. und Metallschutz* (1927) **3**, 217, 241.
10. F. Fenwick: *Ind. and Eng. Chem.* (1935) **27**, 1095.
11. U. Evans: *Jnl.* Chem. Soc. (1927) 1020.
12. U. Evans and J. Stockdale: *Jnl.* Chem. Soc. (1929) 2651.
13. W. Hittorf: *Ztsch. physik Chem.* (1899) **30**, 481.
14. Grave: *Ztsch. physik. Chem.* (1911) **77**, 513.
15. Adler: *Ztsch. physik. Chem.* (1912) **80**, 835.
16. Rathert: *Ztsch. physik. Chem.* (1914) **86**, 567.
17. Schmidt: *Trans.* Faraday Soc. (1914) **9**, 257.
18. A. S. Russell: *Nature* (1925) **115**, 455; (1926) **117**, 47.
    A. S. Russell, D. Evans and S. Rowell: *Jnl.* Chem. Soc. (1926) 1872.

19. G. P. Thomson: *Proc.* Royal Soc. (1930) **128-A**, 649.
20. H. R. Nelson: *Jnl. Chem. Phys.* (1937) **5**, 252.
21. I. Iitaki, S. Miyake and T. Iimori: *Nature* (1937) **139**, 156.
22. A. G. Quarrell: *Proc.* Phys. Soc. (1938) **50**, 962.
23. L. Tronstad: *Trans.* Faraday Soc. (1933) **29**, 502.
24. J. Burwell: Ph. D. thesis, Mass. Inst. of Tech., 1938.   See page 486, this volume.
25. L. Tronstad: *Trans.* Faraday Soc. (1935) **31**, 1151.
26. S. A. Burke: *Trans.* Faraday Soc. (1937) **33**, 309.
27. F. Fenwick and J. Johnston: *Ind. and Eng. Chem.* (1936) **28**, 1374.
28. Finklestein: *Ztsch. physik. Chem.* (1902) **39**, 91.
29. A. Hughes and L. DuBridge: Photoelectric Phenomena.   New York, 1932. McGraw-Hill Book Co.
30. R. W. Gurney: Ions in Solution.   New York, 1937.   Macmillan Co.
31. I. Langmuir: *Ind. and Eng. Chem.* (1930) **22**, 390.
32. R. Fowler and C. Smithels: *Proc.* Royal Soc. (1937) **160-A**, 37.
33. C. B. Post and W. Ham: *Jnl. Chem. Phys.* (1937) **5**, 913.
34. E. Müller and K. Schwabe: *Ztsch. Elektrochem.* (1931) **37**, 185.
35. G. Tammann and E. Sotter: *Ztsch. anorg. Chem.* (1923) **127**, 257.
36. M. Schmidt and L. Wetternick: *Korr. und Metallschutz* (1937) **13**, 184.
37. I. Langmuir: *Trans.* Electrochem. Soc. (1916) **29**, 260.
38. U. Evans: Metallic Corrosion, Passivity and Protection.   London, 1937.
39. W. J. Müller: Die Bedeckungs Theorie der Passivität der Metalle.   Berlin, 1933.

DISCUSSION

(Anson Hayes presiding)

R. M. Burns,* New York, N. Y.—The authors are to be complimented upon their ingenious experiments, which throw light upon the basis of passivity of stainless steels.   Emphasis upon the chemical nature of the phenomenon should lead to a better understanding of the mechanism involved.   There can be little doubt that more or less solid films of corrosion products do retard or prevent corrosion, but it seems unnecessary to assume that a physical barrier several molecules thick is essential to the passive state.   Even where an oxide film of appreciable thickness is associated with passivity, there is reason to believe that the effective part of the film is the "two-dimensional" region of monomolecular thickness at the metal-metal oxide interface.   The fact that electron diffraction studies do not disclose the existence of a surface film on stainless steel is not inconsistent with the concept that passivity is the result of a chemical reaction, which occurs within a layer of approximately monomolecular dimensions.

J. B. Austin,† Kearny, N. J.—There is an unfortunate tendency in scientific work to regard any concept that has proved useful and convenient over many years as established beyond question, and we are prone to forget or disregard uncertainties in the foundation of such concepts.   It is very desirable, therefore, to have a complacent attitude of this kind challenged every now and then and to be forced into a review of the evidence upon which the concept is based; for if this evidence is faulty or inconclusive, the concept can then be appropriately altered, whereas if the concept seems to continue to fit the facts brought to light by the most recent investigations, it becomes more firmly established than ever.   The so-called oxide-film theory of passivity is just such a concept, which must now be reviewed in the light of the

---

weaknesses upon which Messrs. Uhlig and Wulff have focused attention. Whether these weaknesses necessitate the scrapping of the theory is still a matter of opinon; I do not believe that they do, but at the same time the questions that have been raised cannot be dismissed lightly. They call rather for a complete and critical reexamination of our present views together with those advanced as substitutes by the authors.

The first step in this direction might well be a clarification of certain views expressed on the paper. In some portions, much is made of the fact that "a true oxide film" is not present on passive metal. This, I take it, means that no massive oxide exists, neither is there any material that possesses the ordered lattice structure of an oxide. Although there are some who hold that passivity requires the presence of a film of massive oxide, I believe the great body of opinion holds that adsorbed oxygen may be just as effective as "true oxide." It is further stated that "electrochemical potential measurements . . . are inconsistent with an oxide or oxygen-film theory." Yet in the section labeled "Discussion and Conclusion, Part II" it is admitted that oxygen or oxide films are often present; indeed, may always be present in some cases. This apparent straddle is confusing and I hope the authors will clarify their views in this respect.

The contention that no oxide film is present on 18-8 stainless steel raises certain other questions. We know that at high temperature this material scales to give a visible oxide film, indicating that it is not passive to oxygen under these conditions. There should therefore be some temperature at which passivity disappears. This fact is admitted by the authors when they say that higher energy levels are occupied "at a critical higher temperature." If such a critical temperature exists, it must be charac- teristic of the whole mass of metal and it should certainly be indicated on the specific- heat curve of the alloy, yet so far as I am aware, no such critical phenomena have been observed.

Much significance is attached to certain electron diffraction experiments, which are described but briefly. It is alleged that the results show that any film, if present, must be less than 7 Å. thick, and it is implied that no film is formed. This result and the implication are, it seems to me, hardly justified on the basis of these observations. In the first place, the conditions of the experiment—high vacuum and bombardment of the surface with electrons, even soft electrons—are just those under which an adsorbed film initially present would be removed. It is not safe to judge from such measurements what the condition of the surface is when exposed to the atmosphere. Moreover, one wonders by what method the limiting thickness of 7 Å. was calculated, and whether the electron beam was transmitted or reflected at grazing incidence.

In any event, there are positive indications that an iron surface is covered with an adsorbed layer of oxygen when exposed to air or oxygen. One indication is the classic experiment by Bridgman that iron broken under mercury amalgamates, whereas it is not wet by mercury after the briefest exposure to air. Furthermore, recent measurements by Dr. Armbruster of the adsorption of oxygen on iron and on stainless steel show that two or three molecular layers are taken up instantaneously on exposure of a clean surface to the gas. It is difficult to escape the conclusion, therefore, that these metals are covered by an adsorbed layer of oxygen.

The effect of hydrogen in destroying passivity, which is emphasized by the authors, suggests an interesting experiment. If a piece of 18-8 stainless steel is exposed on one side to a nonoxidizing acid, the hydrogen should penetrate the metal and cause the other surface to become active, which could be indicated by a simple test such as displacement of copper from a solution of a copper salt.

In several places the authors refer to a metal as being "more passive" or "less passive." This use seems to be very vague and I should like to suggest that they are confusing passivity in a given environment with reaction in different environments.

The term "passive" means inert or not active. In any given environment the metal is either active or inert; if inert it cannot be "more" or "less" inert. In another environment the metal may be active, but one is hardly justified in saying that it is "less passive"—it is not passive at all. The difficulty appears to have arisen from judging passivity from the potential in different solutions, but the mere fact that a potential changes with change of electrolyte is hardly justification for saying that the metal is "more" or "less" passive.

In this connection, particular attention should be called to the unorthodox use of the term "electrochemical potential" of any alloy and to the very questionable inclusion of passive alloys in the electromotive series. This is not a specific criticism of Messrs. Uhlig and Wulff, although they do speak of 18-8 as having an electrochemical potential of the order of that of silver, but is rather a protest against a careless usage, which is growing daily more common. The electrode potential of an element, upon which the position of the element in the electromotive series is based, is defined as the potential of the metal against a solution which is 1N in the ion of the metal. This definition has no meaning when applied to an alloy and one cannot compare the potential of the alloy in one solution with that of any element under the standard conditions specified. In any case, the composition of the solution should always be specified in discussing potentials. It is, of course, possible to make a series of elements and alloys in which they are listed in the order of potential against one given solution, but this is not the ordinary electromotive series.

In conclusion, attention should be called to the fact that the authors suggest that we may have to have one explanation, and not that based on an oxygen or oxide film, for the transition elements, and yet another for metals such as aluminum and magnesium. Is not this a good place to apply "Occam's razor"? Are we yet ready to discard the oxygen film concept, which is quite simple yet fairly general, for a set of speculations that appears to be rather specific and that must be altered for different groups of metals? These questions deserve widespread consideration and it is to be hoped that this paper will stimulate new investigations, so that we may have satisfactory answers in the near future.

J. T. BURWELL,[*] Kearny, N. J.—Since Dr. Uhlig and Professor Wulff have referred briefly in their paper to some electron diffraction investigations of the passive layer on stainless steel, a more complete description of these experiments might be of interest.

The apparatus was similar to that described by Germer,[40] the sample-to-photographic plate distance being 69 cm. and the potential 30 kv. Preliminary reflection diffraction patterns of flat surfaces of chromium, 17 per cent Cr steel and 18-8, which had been polished and etched to various depths to remove the disturbed surface layer and then allowed to stand in air for times ranging up to three months, yielded only the crystalline patterns of the metals themselves. (On 18-8 this pattern turned out to be the body-centered cubic one of ferrite and is discussed elsewhere.[41]) The absence of the pattern of any foreign substance indicated that if a film was present it was much thinner than the oxide films generally present on metals, and that if it was to be detected by means of electron diffraction some special procedure would have to be employed.

As first pointed out by G. P. Thomson[42] diffraction by reflection from a polycrystalline surface is probably produced by transmission of the electron beam through the sharp ridges that are present on abraded or etched surfaces. The beam enters

* Research Laboratory, U. S. Steel Corporation.
[40] L. H. Germer: *Rev. Sci. Instr.* (1935) 6, 138.
[41] J. T. Burwell and J. Wulff: Page 486, this volume.
[42] G. P. Thomson: Wave Mechanics of Free Electrons. 1930.

the local surface almost vertically, refraction effects are absent, and a thin film that might overlay the surface of the more massive substrate is relatively least effective in producing a pattern of its own. The obvious way to improve this condition is to flatten the surface out locally, as by polishing or evaporating in a vacuum, so as to remove these peaks, and then the beam by entering the surface at a more grazing angle will have a longer path through the film and a shorter path through the underlying metal. However, if this is done it is common experience that the diffraction patterns obtained consist merely of two diffuse rings regardless of the chemical composition or crystallographic structure of the surface. By analogy with the X-ray diffraction patterns of liquids and glasses, it was at first thought that this proved that the polished layer on metals was amorphous, but it has since been shown by Kirchner,[43] Germer,[44] and Burwell[45] that such patterns may arise from polycrystalline films or from surfaces composed of relatively large crystals. The origin of this effect has been ascribed both to refraction at the surface and to the fact that very little of each crystal in the surface may be exposed to the beam, but whatever the true explanation may be it can certainly be concluded that when such a diffuse pattern is obtained nothing can be said about the nature of the surface producing it except that it is very flat locally.

When diffraction patterns were taken of polished surfaces of the samples that had been exposed to air, only the usual two diffuse rings appeared. This then meant that positive identification of an oxide film by means of electron diffraction was impossible since on the roughened surface the film would have to be relatively thick to produce an observable pattern and on a flat surface the method can tell us nothing about the material on the surface. No more than this can be said positively.

In certain cases relatively thin films may be detected by reflection methods. For instance, Finch[46] reports that on forming unimolecular paraffin layers of different chain lengths on a smooth single-crystal surface he finds that if the chain length is greater than 43 Å. the paraffin pattern completely obscures that of the single crystal beneath, while if the chain length is less the single-crystal pattern will appear. This then gives an order of magnitude of the thickness of a film that may be detected in this, a favorable case. On the other hand, Germer[44] reports that he obtained a diffuse pattern by reflection from a vaporized ZnS film about 800 Å. thick, which proved to be crystalline when examined by transmission. The only conclusion to be drawn from these results is that, as has been pointed out by others,[47] great caution must be exercised in the interpretation of electron diffraction data, particularly when negative results are involved.

As Dr. Austin has pointed out, a beam of fast electrons would probably remove any adsorbed gas film from the surface being examined, hence it would not be observed. It may be added that even if the adsorbed gas film were not cleaned off but remained intact under the electron beam it is extremely doubtful whether such a film would give any observable pattern with fast electrons. Likewise, a massive oxide film if in an amorphous state probably could not be detected either.

P. R. KOSTING,* Watertown, Mass.—With reference to the role of oxygen in inducing passivity, it appears from what has been said that only chemiadsorbed oxygen and not oxide induces passivity. What role does the oxide play in passivity? From the work of U. R. Evans and others, there is no doubt that oxide does exist

[43] F. Kirchner: *Erg. exakt. Naturwiss.* (1932) **112**.

[44] L. H. Germer: *Phys. Rev.* (1933) **43**, 724; (1936) **49**, 163.

[45] J. T. Burwell: *Jnl. Chem. Phys.* (1938) **6**, 749.

[46] G. I. Finch: *Jnl.* Chem. Soc. (Aug. 1938) 1137.

[47] W. H. J. Vernon: *Proc.* Phys. Soc. (1938) **50**, 961; R. Beeching: *Ibid.*

* Chemical Engineer, Watertown Arsenal.

in some cases. In this new theory, does the oxide film have a part or is it to be regarded as the same as a point film?

Further questions might be brought up. Table 7 shows that the mol ratio of Mo-Fe is evidently not affected by the presence of 60, 35 or 28 per cent Ni, yet 34 per cent Ni makes iron passive. This seems to indicate that one atom does not affect the required mol ratio of another atom, but if both atoms are each present to the required extent, the degree of passivity is enhanced. Yet 1.3 mol per cent Mo in 18-8 induces passivity under conditions that 18-8 is active.

On page 513, it is indicated that 13.4 to 15.7 per cent Cr is required to bring about passivity. The work of many others has shown that lower percentages of chromium, as 10 to 12 per cent, are very effective indeed. How are these two ranges in percentage to be reconciled?

S. P. ODAR* AND H. A. SMITH,* Massillon, Ohio.—It is always refreshing to have new theories for consideration. It is also fortunate if these newer ideas can include older ones as special cases. Of course, each one will attempt to fit his own experience into new theories in an attempt to simplify a complex situation. This process of constructive criticism is the natural way in which new theories are tested.

In what follows we shall offer constructive suggestions and discussion of our experience as applied to the theory and the material which the authors use for its support.

Our corporation, together with its forerunner in this district, has had a wide experience in the application and investigation of stainless steels containing molybdenum. With but few exceptions, to be mentioned later, we have consistently found that the addition of molybdenum to an 18-8 type of analysis markedly improves the corrosion resistance. This improvement in corrosion resistance is considerably greater than that for which account can be given by the replacement of an amount of iron by an equivalent amount of molybdenum. The authors' results as given in Table 4 are, in this respect, in satisfactory agreement with our observations. The pit corrosion data of item 2, Table 5, are not in agreement with either the authors' potential measurements as given in Table 4 or our experience. Account can reasonably be made for this by the observation that the molybdenum-bearing steel of the composition given must be of a two-phase structure with reasonably large quantities of delta iron present while the 19-9 is undoubtedly a single-phase structure. To be able to validly compare results both alloys should have the same structure. Also, the alloys should have more nearly comparable chromium contents. A 2 per cent difference in chromium in this range of analysis may make an appreciable difference in corrosion resistance. We find consistently that two-phase stainless alloy structures of delta and gamma iron pit more profusely than single-phase structures, due consideration being given to other factors. Thus, the data (weight loss and number of pits) in item 2, Table 5, for the molybdenum-bearing steel we feel are too high. Taking this into account, if a single-phase steel had been used, the authors' data in Tables 4 and 5 would probably be found to be consistent.

Mention is made in several places by the authors of 1.5 atomic per cent Mo in the 18-8 alloys, as if this were a significant figure. Our experience indicates that about one-half of this amount (say 0.75 atomic per cent) confers upon stainless alloys a corrosion resistance very nearly the same as that conferred by 1.5 atomic per cent Mo. Interesting results would be obtained by working with a series of wrought stainless alloys whose composition is similar except as to the molybdenum content. Care should be taken to see that all alloys of such a series are single-phase in structure.

With respect to oxidizing conditions, both at high temperatures and in water solutions, we know that molybdenum in stainless steels is the most readily oxidized metallic component in the steel. If sheet slabs preheated for rolling are allowed to

* Central Alloy District, Republic Steel Corporation.

get too hot, clouds of white molybdenum oxide can be seen coming from slab as it is withdrawn from the furnace and after the first pass in the breakdown. If molybdenum-bearing steel is heated for long periods at high temperatures, detectable amounts of molybdenum may be lost from the alloy. Tests in highly oxidizing inorganic acids such as nitric and chromic acids indicate clearly that in such solutions molybdenum-bearing steels are inferior to similar analyses not containing molybdenum.

Electrochemical potential measurements, as previously reported by one of us,[48] were made under identical conditions in a saturated potassium chloride solution also saturated with air on three types of stainless steel—a 12 per cent Cr, an 18-8 and an 18-12 Mo type. These measurements made from the instant that the solution came into contact with the steel indicate that the molybdenum-bearing steel has initially the lowest corrosion resistance. However, surface reactions between the steel and the solution cause the corrosion resistance to increase to the most noble of the three steels. The 18-8 has initially a higher resistance to corrosion than the steel just mentioned, but the final state of its surface is at a less noble potential than that of the final state of the molybdenum-bearing steel. This indicates that there is some sort of reaction between the steels and the chloride solution and further that the molybdenum-bearing steels build up from initially the most reactive surface a surface finally the least reactive. If we suppose that oxygen of some sort here plays a role, it may again be seen that the molybdenum-bearing steels are more reactive to oxidizing conditions than is the usual 18-8.

This background of experience indicates that oxygen in some form held in some way on the surface of molybdenum-bearing steels may reasonably be expected to account for superior corrosion resistance on the basis of a passive surface layer.

It seems to us that the authors are taking an unnecessarily narrow viewpoint when they intimate that from their electrochemical potential measurements *molecular* oxygen is the only type of oxygen that need be considered in the formation of passive films on stainless. Within any water solution besides dissolved molecular oxygen there are hydroxyl ions always present. For metals as reactive toward oxygen as are chromium and molybdenum, it is not at all unreasonable to assume that some reaction takes place between the metals and hydroxyl ions or their products of decomposition that may take place on the metallic surface.

May we commend to the authors' attention electrochemical potential measurements in nonionized organic solvents, preferably such solvents as contain no oxygen in their molecules. From the result of such measurements one should be able to say something quite definite about the role played by oxygen in the passivity of stainless steels.

It does not seem to be the only alternative to suppose that halide ions are discharged on the stainless steel when a positive electric charge with accompanying current flow is imposed upon the steel in a halide solution. The solutions here dealt with contain, at least, the following simple ions Na^+, H^+, OH^- and Cl^-, or Br^- or I^-. Just what reactions may occur at the anode in such solutions may be determined by the temperature, current density, imposed potential, relative concentrations of H^+ and OH^- and upon the anode metal together with its previous history.

From a number of considerations, it may reasonably be supposed, for instance, that in neutral chloride solutions hypochlorites are formed at the stainless anode and that bromates are formed at the stainless anode in neutral sodium bromide solutions. Of these two compounds the hypochlorites are definitely the most active oxidizing agents. According to these concepts, we should expect the molybdenum-bearing steels to be definitely better in chloride solutions than in bromide solutions, as such steels are especially sensitive to oxidizing conditions and the building up of a highly

[48] H. A. Smith: *Metal Progress* (1938) **33**, 596–600.

protective layer is possible. Any attempt of chloride ions to penetrate this layer may result in the formation of further hypochlorites with resultant passivation and we have under some conditions a self-healing film.

In the 18-8, where the sensitivity to oxidizing conditions is not so marked, the difference in the oxidizing characteristics of the hypochlorites and the bromates is not so evident, and the superior effectiveness of the Cl^- in penetrating a protective film becomes the dominating factor and the 18-8 is less resistant to chloride than to bromide solutions.

According to our concept of a more highly oxidizing condition existing at the steel solution interface in chloride than in bromide solutions the character of the corrosion products of 18-8 and a similar molybdenum-bearing alloy finds a ready explanation. For instance, the authors find iron in the Fe^{+++} state to be dissolved initially from both steels in both types of solution. The existence of some sort of a protective film of an oxidizing nature would give rise to this condition. It is further found that as corrosion proceeds the only instance where Fe^{+++} continues to be found is with the molybdenum steel in chloride solutions. It is also noticeable that the chromium dissolved under this condition is in the oxidized state. This situation is consistent also with our views that under the influence of electric current the chloride solutions are more highly oxidizing than the bromide solutions, especially so on the surface of a molybdenum-bearing steel.

R. B. MEARS* AND R. H. BROWN,* New Kensington, Pa.—We wish to congratulate Dr. Uhlig and Professor Wulff on their new and interesting theory of passivity. Although the new theory has much to commend it, we do not believe that all of the criticisms leveled by the authors on the older oxide theory are justified. Apparently, the authors' criticisms of the oxide theory are based on three types of measurements; therefore, we will discuss these briefly in turn below.

Electron Diffraction Studies.—Electron diffraction results require considerable care in interpretation. For example, a recent paper by J. T. Burwell (ref. 45) discusses electron diffraction patterns obtained from stainless steel after various treatments. Dr. Burwell found that the electron diffraction pattern for specimens of this material after polishing, etching, and vacuum annealing at 1000° C. was diffuse, although it was obtained by reflection from large-grained crystalline material; therefore, we cannot see how even a crystalline oxide layer could be always expected to give a definite pattern. Evidently surface contour is of considerable importance in electron diffraction work and, in fact, can often conceal the true atomic arrangement of the surfaces.

In addition, we believe that one point in the preparation of specimens may have been overlooked. It should be possible to obtain oxide films on certain metals exposed to air pressures as low as 10^{-5} mm. Hg. For example, the dissociation pressure of FeO is only about 10^{-12} mm. Hg. at 1000° C. Therefore oxidation of iron could occur at pressures as low as 10^{-5} mm. This means that there is a possibility that the surface will react with oxygen unless the partial pressure of oxygen is about 10^{-12} mm. or less. It also means that possibly the diffuse pattern obtained by Dr. Burwell after heating the stainless steel at a low pressure (Fig. 3 of ref. 45) may have been caused by an amorphous oxide layer.

It should also be pointed out that many metals, such as iron, chromium, and aluminum, can react directly with oxygen-free water to form the metallic oxide and free hydrogen. This attack is usually self-stopping, since as soon as a protective layer of the oxide or hydroxide is formed, further action ceases. The free energies for many of these reactions have been calculated. For example, that for the reaction of iron with air-free water to form magnetite results in a decrease in free energy of

---

* Aluminum Research Laboratories, Aluminum Company of America.

4430 cal. per gram atom of iron. The decrease in free energy for the oxidation of Cr to Cr_2O_3 by air-free water is even greater. It is to be expected that on immersion in air-free water (or an aqueous solution), stainless steel too would form a thin oxide film, which would be generally protective.

Corrosion Products.—We do not believe that the composition of the anodic corrosion products has any close relationship to the composition of the oxide films formed on the surface of the metal. Corrosion products are formed only if the film breaks down and ceases to be protective at some point. Although from such points of breakdown some of the film may be removed mechanically and subsequently be mixed with the corrosion product, still the film is so thin that the proportion of the corrosion products made up of the film will be negligible. Naturally, if corrosion is not self-stopping, or if there is no redeposition of some of the constituents, the corrosion products must have the same composition as the alloy from which they are formed. Therefore, an analysis of corrosion products cannot throw any light on the composition of protective or passive films.

Threshold Potentials.—In the authors' work on threshold potentials, we note that "an air stream was circulated over the anodes to keep the steels in a uniformly passive state." If oxide films do not produce passivity, why was it necessary to bubble air around the stainless-steel anodes in this work? It is difficult to see what function the oxygen performed besides maintaining the protective film in good repair.

On page 496, the authors make the statement that "Measurement of threshold potentials of halide ions discharging on stainless-steel anodes . . . disclosed their identity with commonly measured decomposition potentials." Apparently this statement is based on the data in Table 4, yet inspection of these data reveals that agreement between threshold potentials for platinum and 18-8 anodes is reasonably good only with the I^-; between threshold potentials for platinum and molybdenum 18-8 with the Cl^- and I^-. Thus, there is an agreement in only about 50 per cent of the cases studied. With this low proportion of agreements, we do not believe that an inclusive statement such as that quoted above is justified. Furthermore, even if agreement had been good, we do not see why it would have established that there was no oxide on the stainless steel. If the stainless-steel anode yielded the same "threshold potentials" as a platinum anode, it would only mean that the stainless steel was inert under those conditions. It does not necessarily prove the presence or absence of oxide films. In fact, massive oxides of some metals can serve as inert electrodes in certain solutions.

Fe_3O_4 anodes have been used in the Griesheim alkali-chlorine cell, since they are more inert than carbon. Sacerdote[49] has found that the chlorine overvoltage is almost exactly the same on magnetite anodes as on smooth platinum anodes. PbO_2 forms inert anodes in the production of HIO_4 or CrO_3. The list could be much extended. Undoubtedly, if a continuous oxide film were formed on a metal electrode it would function as a massive oxide electrode. It is also interesting to note that Foerster[50] showed that platinum oxide was formed on platinum anodes and that Grube identified this oxide as PtO_3.

We would also like to ask the authors whether or not they actually observed the evolution of Cl, Br, or I at the threshold potentials.

Further Evidence for Oxide Films.—It would appear difficult to explain by the electron sharing theory why passive anodes can become activated at scratches, abrasions, or cut edges. Also Bryan and Morris[51] have found that stainless steel

[49] Sacerdote: Die Elektrochemischem, **2**, 140. Uerfahren, 1917.

[50] F. Foerster: *Ztsch. phys. Chem.* (1909) **69**, 236; *Ztsch. Elektrochem.* (1910) **16**, 353.

[51] J. M. Bryan and T. N. Morris: Report Director Food Investigations (British) (1932) 174, 177.

or nickel-chromium alloys were much more severely attacked in the absence of oxygen than in its presence. Bengough and Wormwell[52] found that at high oxygen pressures passivity could be induced on ordinary steel specimens if they were first exposed to the gas phase, but that the specimens remained active if exposed to the chloride solution first at low oxygen pressure and then subsequently the oxygen pressure was raised to the high value. Presumably, in the first case, on exposure to oxygen at the high pressure a passive film was formed, which did not break down on exposure to the liquid. Many other observations of this type have been made, which appear to explain without assuming that a passive oxide, or other, film is formed.

To sum up, we believe the authors have outlined a very ingenious theory to account for the passivity of stainless steel. However, we do not believe that they have brought forth any definite experimental evidence that cannot be satisfactorily explained by the older oxide theory.

J. S. MACKAY, Stamford, Conn.—There is a connection between the last two papers in that both show that decreased free energy of the surface leads to less corrosion, in the first by decreasing the mechanical strains and in the second by decreasing the molecular or atomic energy. The difference between molecular oxide and adsorbed oxygen in the creation of corrosion resistance was stressed. It is true that adsorbed oxygen would have a larger sphere of influence so far as iron atoms are concerned, but will not the effect differ in degree rather than in kind? Under oxidizing conditions sufficient for oxide formation one would have both states, and though the oxygen in molecular combination has a more limited sphere it still influences more than the iron atoms whose electrons it shares. Thus an oxide film could only be considered in the same light as a paint film when it is applied as a paint film.

The technique used in eliminating passivity of iron in nitric acid by decreasing the gas pressure above it could be used to show how much of the passivity of the steel is due to oxygen and how much to the alloying under varying conditions.

H. H. UHLIG and J. WULFF (authors' reply).—It is a pleasure to have received such fundamental and detailed discussion of our paper. Dr. Burns' succinct remarks are especially gratifying and we agree with and appreciate Dr. Austin's comments that certain aspects of our paper permit of further discussion.

There is a fundamental difference between the passivity of a surface due to adsorbed oxygen and the protective action of a massive oxide film (of the order of 30 Å.). A protective oxide film covering the metal surface appears to act like a paint or lacquer film, offering physical protection to metal underneath. Once the oxide coating is scratched or penetrated, the film is no longer protective and the metal can be attacked. In oxides all valences of metal and oxygen have been satisfied, so that the extremely short-range molecular forces operating at the oxide surface have no significant effect on the metal atoms in contact. For the sake of clarity, we have arbitrarily separated instances of this kind where chemical inertness is due to physical protection from other instances where protection appears to be due to alteration in the metal atoms composing the surface.

Chromium, by its ability to share electrons, can bring about this latter change in atoms of iron. Likewise, adsorbed oxygen can share electrons with metal atoms, but in such a manner that valences remain largely unsatisfied, the metal atoms remain in their typical metal lattice, and true chemical reaction has not taken place. The electron sharing accompanying adsorption as well as electron sharing accompanying alloying we propose as cause of passivity. Hence, iron, according to these concepts of passivity, can be made passive by an adsorbed film of oxygen, but not by a film

---

[52] G. D. Bengough and F. Wormwell, quoted by U. R. Evans: Metallic Corrosion Passivity and Protection, 293.

composed of normal oxide. If the oxide should, however, be a higher unstable oxide, such as Bennett and Burnham[53] proposed for passive iron, or should contain entrained or dissolved oxygen, the valence forces operating might well suffice to produce the electronic changes in metal atoms necessary for passivity.

An iron-chromium alloy, however, containing approximately 15 per cent Cr or more, does not require either an oxide or adsorbed oxygen film to account for its passivity. The electron-sharing process between iron and chromium makes the alloy permanently passive, regardless of oxygen concentration exterior to the alloy. Oxygen may, of course, adsorb on stainless steel, in which case passivity may to some degree increase. The electrochemical potential of stainless steel already noble may be made more noble by contact with oxygen. Likewise, permanently passive metals like chromium and nickel, whose electron configurations are naturally those of the passive state, need no adsorbed films to account for their passivity. Like stainless steels, they lose passivity whenever hydrogen is charged into the surface.

Critical temperatures for the passivity of iron have frequently been mentioned in the literature.[54-56] This can be accounted for by the fact that the adsorption bonds between iron and oxygen are temperature dependent. For iron-chromium alloys the energy states may be different for higher temperatures than for lower ones; quantum statistics employs this concept in the treatment of the thermionic emission of all metals. Yet, in this case, as in that of passivity, the surface-energy levels are probably different from those for a continuous metal and hence bulk measurements of the kind Dr. Austin suggests may mask surface effects. Nevertheless, there is some indication that our viewpoint gleaned from free atom considerations plays some role in bulk lattice considerations. The electrical,[57] the thermal,[58] and the magnetic[58] properties of Fe-Cr alloy compositions do show inflections at about 15 per cent Cr content.

In regard to the electron diffraction work, we trust Dr. Burwell's discussion elucidates most of the points brought up. From further work we should like to add to this discussion. If an oxide film amorphous or crystalline of the order of 30 Å. resides on an etched surface of stainless steel, it does affect the intensity background and distribution of the pattern of alpha-ferrite as obtained when such a massive film is not present. When it is not present the resolving power of our apparatus, 7 to 10 Å., does not permit us to detect adsorbed films. We doubt Burwell and Austin's view that slow or fast electrons of the kind used in electron diffraction in vacua of 1×10^{-4} to 1×10^{-6} are capable of removing chemosorbed oxygen. Electronics experiments initiated by Langmuir all show that the bonding of adsorbed layers on tungsten, molybdenum and presumably on transition elements of like electronic structure is extremely tight. We do not wish to overemphasize, however, the electron diffraction work, but only to point out that the massive films detected by others on stainless steel cannot be achieved by "air passivation." To be sure, we have been able to put oxide films on stainless steel by oxygen-ion bombardment and in thicknesses of from 20 to 100 Å. In such cases the surface pitted at a rate that was greater than ever experienced before.

The interesting experiment suggested by Dr. Austin, showing effect of hydrogen on passivity, has fortunately already been tried. We took a piece of thin iron sheet

[53] *Trans.* Electrochem. Soc. (1916) **29**, 217.
[54] Bancroft and Porter: *Jnl. Phys. Chem.* (1936) **45**, 37.
[55] C. Desch: Chemistry of Solids, Cornell Univ. Press, 1934.
[56] E. Hedges: Protective Films on Metals, D. Van Nostrand Co., 1937.
[57] Boudouard: *Rev. de Mét.* (1912) **9**, 294.
[58] Stäblein: *Archiv Eisenhüttenwesen* (1929) **3**, 302.

(0.004 in.), pickled, allowed hydrochloric acid to react with one face and measured the potential of the opposite side not in contact with acid. When the acid came in contact with the iron sheet, the potential of the opposite side immediately became more active by several hundredths of a volt. The potential assumed its original value again when the acid was replaced with water or nitric acid. This experiment proved that hydrogen diffusing through the iron, some bubbles of which collected on the side not in contact with acid, could alter iron to make it more active, and that removing the source of hydrogen restored the original activity. The same experiment with stainless steel has not yet been made successful, probably because the diffusion rate of hydrogen through stainless steel is so low compared with the rate through iron.

Regarding the use of terms "less" or "more passive," the very nature of the phenomenon suggests that this usage is justified. The above experiment, for example, illustrates differing activity of iron in the same environment. Other experiments also show that metals can be made successively passive or active without discontinuity. W. Kistakowsky[59] published a list of varying states of passivity of iron and how such states could be produced. Finally, inertness as criterion of passivity is not in itself an absolute term. All metals, despite their possibility of being passive, corrode to some extent in corrosive media, the rate varying with the medium and the state and nature of the metal.

The justification for placing stainless steels in the electromotive series with the noble metals is that immersed in various media they resemble in behavior the noble metals. The potential difference between silver and 18-8 in salt water is, for example, very nearly zero, indicating that 18-8 immersed in silver nitrate (or salts of metals below silver in the electromotive series) will not replace metal ions in solution. Dr. Austin is correct in pointing out that one cannot ordinarily speak of a molal electrode potential for an alloy. This particular potential for a metal is calculated for the metal in an aqueous solution of its ions 1N in activity. The electromotive series can be set up using these potentials to establish relative order of the metals. The concentration of metal ions corresponding to unit activity is, however, frequently outside the concentration encountered practically, so that setting up a series based on potentials obtained in media actually responsible for corrosion seems not only justified but desirable.

The points that Dr. Kosting raises have fundamental significance. The role of adsorbed oxygen and oxide which he brought up was treated in the answer to discussion by Dr. Austin.

Regarding the mutual effects of molybdenum and nickel on iron, any ternary alloy is a naturally complex system, yet the passive properties of the binary solid solutions seem approximately additive in the molybdenum-nickel-iron system. Differences in energy accompanying electron sharing presumably account for the greater passivating effect of molybdenum as compared with nickel. The effect of nickel, nevertheless, is evident in corrosion properties of its alloys with iron and molybdenum immersed in sulphuric acid, even though its effect is less marked than molybdenum. In Table 7, comparative weight losses for the alloys containing 28 per cent Ni are in most cases higher than those for either composition above the critical concentration for passivity; namely, 34.4 per cent Ni. This is as one would predict from corrosion properties of the binary nickel-iron system.

The exact percentage of chromium necessary to bring about passivity in iron is a function of the solution in which passivity is measured. In well-aerated solutions the percentage of chromium required for passivity is less and may be in the neighborhood of 10 to 12 per cent. In oxidizing solutions like chromates or nitrates, the percentage required may be still less. For neutral salt solutions free of oxygen, the

---

[59] *Ztsch. Electrochem.* (1925) **31**, 628.

critical concentration is the theoretical, approximately 13 to 15 per cent. In acids that generate hydrogen by reaction with the steel, the amount of chromium necessary for passivity will exceed 15 per cent until, if the acid is sufficiently reactive, the chromium alloys in all ranges of concentration are active and never passive.

It is not quite clear what discrepancy between Table 4 and Table 5 Mr. Odar and Dr. Smith have in mind. In our discussion of the results presented by these two tables of data, we have attempted to emphasize the consistency of the information obtained by two entirely independent means and to show that predictions on the basis of Table 4 are realized in actual corrosion tests. For example, in Table 4, the threshold potential for Cl⁻ on molybdenum 18-8 is very high, showing resistance of the alloy to Cl⁻ attack, but for Br⁻ the potential and resistance are less. Table 5 shows that ferric chloride in the time of the test does not pit molybdenum 18-8, but ferric bromide does so consistently.

The threshold potentials for 18-8 in chlorides and bromides are identical. We would predict, therefore, that pitting would take place in presence of either ion, which is verified by Table 5. Threshold potential data, of course, indicate pitting tendency only and not rate of pitting. With equal pitting tendency the weight losses by pitting in ferric bromide, for one reason because of the lower conductivity of bromides, would not be expected to be as high as for chlorides.

We do not feel that a two-phase structure for molybdenum 18-8 would in any manner account for pitting of the alloy in ferric bromide as compared with lack of pitting in ferric chloride. It is our experience that the presence of delta iron is not a major factor in formation of pit foci in alloys of this type. If the pit susceptibility has been unusually high, the alloy would probably have pitted in ferric chloride, which, however, was not the case. Likewise, a small variation in chromium content of 2 per cent would in no case with which we are familiar account for the difference in an 18-8 that invariably pits and one that invariably does not.

The adsorption of OH⁻ and its relation to passivity has been mentioned before by Langmuir[60] but its applicability to passive alloys is still in question. We have found that a high concentration of OH⁻ (20 per cent NaOH) activates 18-8 in a manner similar to HCl and further that the same OH⁻ concentration with KMnO₄ passivates 18-8.

Dr. Mears comments on electron diffraction are well taken, especially since the paper by Burwell, which he quotes, was carried out under the supervision of one of the authors. Dr. Burwell's discussion of the present paper and our answer to Dr. Austin's probably cover the questions brought up. We may add that samples finely abraded or etched in air show a ferritic lattice without indication of diffuse or crystalline oxide diffraction patterns. If they were of appreciable thickness some indication should be observable. We are, furthermore, in accord with the possibility of oxidation in low vacua as well as in air-free water, yet films if formed under such conditions would be of such a slight thickness, 1 to 3 atoms or molecules, that they would not be distinguishable from an adsorbed film.

The commentators do not distinguish between adsorbed and true oxide films. Our comments on Dr. Austin's query undoubtedly covers our viewpoint in this matter. We are not trying to straddle in this connection by also emphasizing adsorption (chemosorption), but we care only to emphasize that the nature of the basis metal (e.g., its electronic structure) is responsible for such adsorption, which in turn affects the chemical reactivity of the metal.

Oxygen in contact with stainless steel immersed in an aqueous solution may be considered to increase passivity either by the mechanism of reaction with or adsorption on the surface or by oxidizing and thereby removing hydrogen from the metal

---

[60] T. A. Langmuir: *Phys. Rev.* (1915) **6**, 79.

surface. It is the latter viewpoint that experiment leads us to prefer, hence circulating air over the anodes in the threshold potential measurements can be assumed to maintain passivity by other than oxide formation.

In answer to the question concerning observation of the evolution of chlorine, bromine or iodine during threshold potential measurements on platinum, we actually observed accumulation of halogens in the electrolyte if the trial runs were repeated several times using the same electrolyte. Data later recorded were obtained before such accumulation became significant.

Scratches in metals usually introduce strains. These strains set up galvanic currents with normal metal, which result in accumulation of corrosion products at the strain or scratch. Corrosion products, as potential measurements show, can destroy passivity of alloys, accomplishing this, according to our viewpoint, by charging hydrogen into the metal surface, causing further accentuation of corrosion at the scratch. Explanation by rupture of an oxide film, although plausible, in this case, is therefore not necessary.

Our work is but a start on one of the problems relating to metallic surfaces and especially passivity; but by an interchange of critical ideas on the subject, supported by experiment, a general and consistent picture should eventually ensue.

Thermal Expansion of Nickel-iron Alloys (Nickel from 30 to 70 Per Cent)

By J. M. Lohr* and Charles H. Hopkins†

(Detroit Meeting, October, 1938)

A COMMERCIAL development requiring a suitable alloy or alloys for sealing into various grades of glass made it desirable to have a more exact knowledge of the expansion characteristics of the nickel-iron alloys than appeared in the published literature. The expansion of the more common
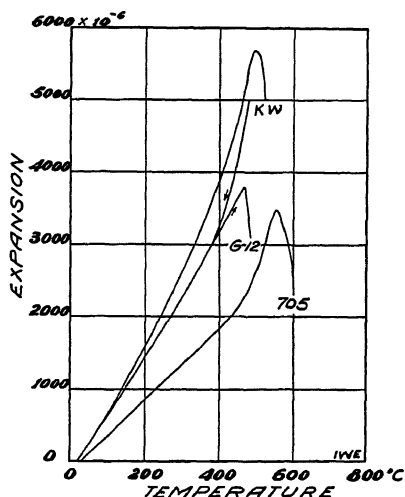
FIG. 1.—EXPANSION CURVES OF SEVERAL TYPES OF GLASS. (*Courtesy of R. C. A.*)
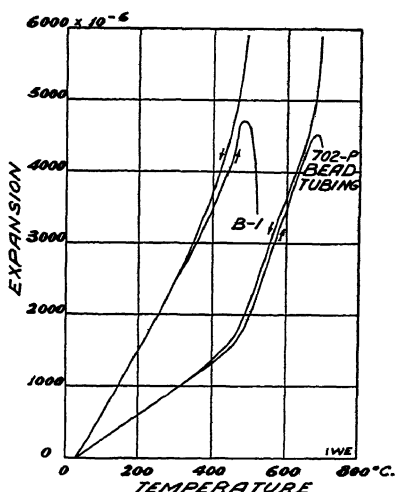
FIG. 2.—EXPANSION CURVES OF TWO TYPES OF GLASS. (*Courtesy of R. C. A.*)

types of glass under consideration varies from 2.7 to 10.4 × 10⁻⁶ per degree Centigrade, over the range 20° to 400° C. For reference, the thermal expansion curves of several types of glass used for sealing by the lamp and tube industries are given (Figs. 1 and 2).

This paper covers a detailed investigation of the thermal expansion of a series of nickel-iron alloys in which the nickel content varies from 30 to 70 per cent. Particular stress is laid on the alloys that contain between 40 and 55 per cent Ni.

Alloys of iron and nickel possess many anomalous properties depending on the relative proportions of the two constituents in the alloy. Guillaume,[4] in an early intensive investigation of a series of varying composition, found coefficients of linear expansion ranging from a small negative value (-0.5×10^{-6}) to a large positive value (20×10^{-6}). More recently, Scott[17] has studied the expansion characteristics of nickel steels over the range 31 to 50 per cent Ni from minus 200 to plus 600° C.
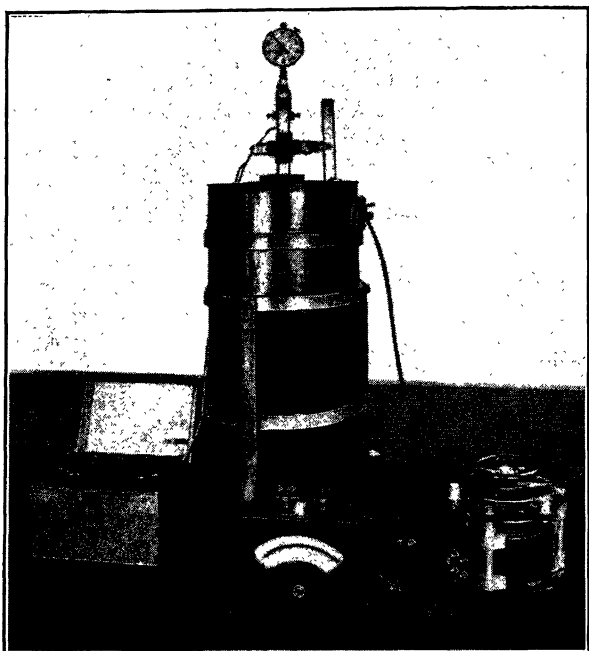
FIG. 3.—FUSED SILICA TUBE EXPANSION APPARATUS WITH AUXILIARY EQUIPMENT.

In applying the low-expansion nickel steels to individual applications it must be recognized that the low-expansion characteristics of these alloys are available only over a limited temperature range.

METHOD

Fourteen-pound heats were melted in a 35-kva. Ajax furnace, using Armco iron and electrolytic nickel. The heats were cast into 2½ by 2½-in. ingots, which were forged to 1 in. square. These were hot-rolled to ¼-in. rod.

The determinations of thermal expansion were made on 4-in. lengths. The apparatus (Fig. 3) makes use of the differential expansion between the test specimen and fused silica. The method described by Hidnert[7] was followed, in all essentials except that in these determinations the

specimen is held in position by a loosely fitting fused silica sleeve slightly shorter than the specimen.

All samples were preheated to 800° C, held for one hour and then slowly cooled to room temperature before any readings were taken.

TABLE 1.—*Composition of Alloys*

Heat No.	Composition, Per Cent		
	Mn	Si	Ni
14836	0.11	0.02	30.14
3632	0.15	0.33	35.65
23735	0.12	0.07	38.70
14436	0 24	0.03	41.88
5934			42.31
173C[a]			43.01
173D[a]			45.16
173A[a]	0.35		45.22
23535	0.24	0.11	46.00
173E[a]			47.37
23635	0.09	0.03	48.10
23933	0.75	None added	49.90
173F[a]			50.00
1074	0.25	0.20	50.05
6385	0.01	0.18	51.70
23235	0.03	0.16	52.10
26032	0.35	0.04	52.25
23335	0.05	0.03	53.40
23835	0.12	0.07	55.20
10936	0.25	0.05	57.81
11036	0.22	0.07	60.60
11136	0.18	0.04	64.87
5418	0.00	0.05	67.98

[a] Data and corresponding curves furnished by Stanton Umbreit, Radio Corporation of America, Harrison, N. J.

RESULTS

The compositions of the alloys used are given in Table 1. In the method used for determining the nickel content, the nickel and cobalt were separated. Consequently, the values given represent nickel only. The cobalt content probably does not exceed 0.15 per cent. Carbon was not determined, but in every case should be under 0.05 per cent. In Table 2 are listed the inflection temperatures, increase in length at the inflection temperature and the average coefficient of expansion from room temperature to the temperature of inflection, of the different alloys.

Expansion curves for the 23 nickel-iron alloys covered by this paper (nickel varying from 30.14 to 67.98 per cent over the temperature range

TABLE 2.—*Expansivity Characteristics*

Heat No.	Nickel Content, Per Cent	Inflection Temperature, Deg. C.	Increase in Length at Inflection Temperature	Average Coefficient to Inflection Temperature × 10⁻⁶
14836	30.14	155	0.0012	9.2
3632	35.65	215	0.0003	1.54
23735	38.70	340	0.0008	2.50
14436	41.88	375	0.0017	4.85
5934	42.31	380	0.0018	5.07
173C	43.01	410	0.0022	5.71
173D	45.16	425	0.0029	7.25
173A	45.22	425	0.0027	6.75
23535	46.00	465	0.00335	7.61
173E	47.37	465	0.00354	8.04
23635	48.10	497	0.00415	8.79
23933	49.90	500	0.0042	8.84
173F	50.00	515	0.0045	9.18
1074	50.05	527	0.00475	9.46
6385	51.70	545	0.0050	9.61
23235	52.10	550	0.00535	10.28
26032	52.25	550	0.0053	10.09
23335	53.40	580	0.0059	10.63
23835	55.20	595	0.0065	11.40
10936	57.81			14.46[a]
11036	60.60			14.72[a]
11136	64.87			15.07[a]
5418	67.98			15.38[a]

[a] Average coefficient of expansion to 1000° C.   No inflection point observable.

20° to 1000° C.) are shown in Figs. 4, 5, 6 and 7.   Observations taken on both heating and cooling are plotted.   The effect of the nickel content on the inflection temperature is shown in Fig. 8, and in Fig. 9 the average coefficient of expansion up to the inflection temperature is plotted against the nickel content.

SUMMARY

Expansion curves of 23 nickel-iron alloys resulting from an effort to find a satisfactory alloy or alloys for sealing into various types of glass, and covering from 30 to 70 per cent Ni were obtained.   Special attention was given to alloys containing between 40 and 55 per cent Ni.   Over this range observations were made on alloys of which the variations in nickel content were exceedingly small.

Heating and cooling curves are shown for most of the alloys, and curves showing the effect of the nickel content on both the inflection temperature and on the expansion up to the inflection temperature are given.
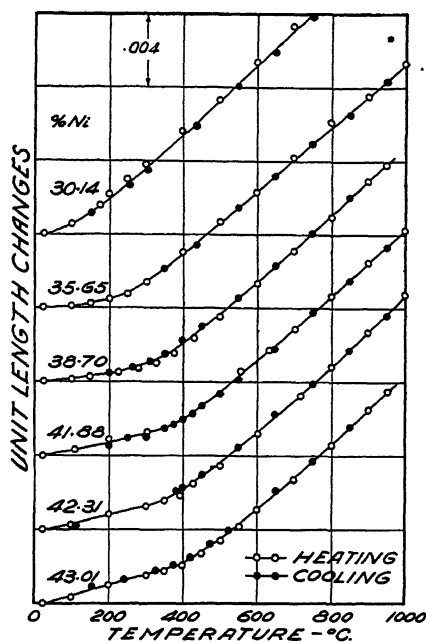
FIG. 4.—NICKEL CONTENTS FROM 30 TO
43 PER CENT.
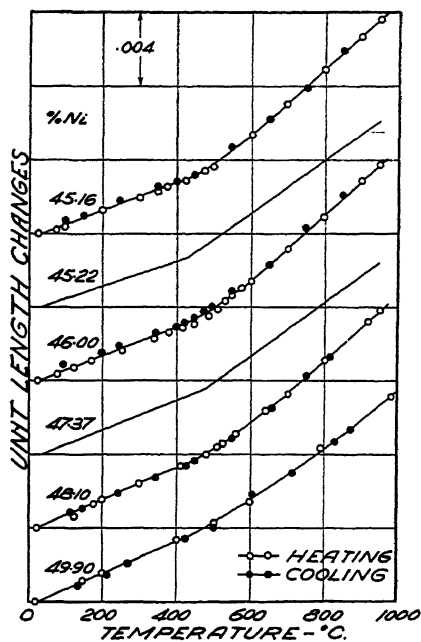
FIG. 5.—NICKEL CONTENTS FROM 45 TO
50 PER CENT.
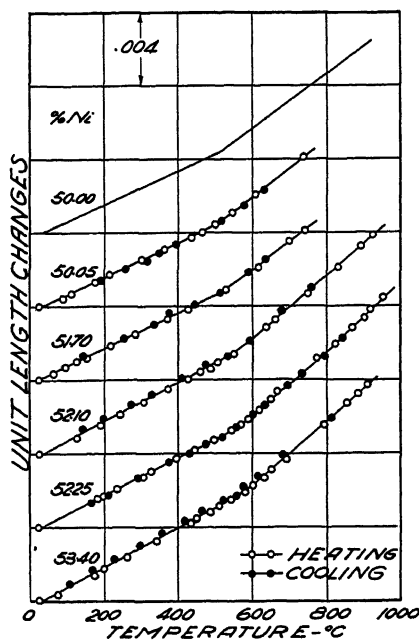
FIG. 6.—NICKEL CONTENTS FROM 50 TO
53 PER CENT.
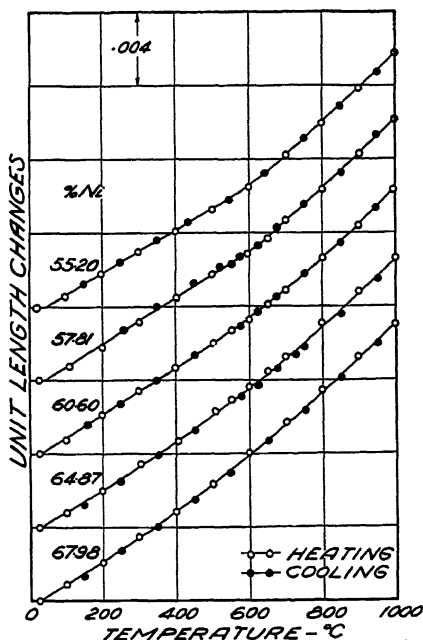
FIG. 7.—NICKEL CONTENTS FROM 55 TO
68 PER CENT.

FIGS. 4–7.—EXPANSION CURVES OF REVERSIBLE NICKEL-IRON ALLOYS.

The results obtained here on alloys previously investigated are in substantial agreement with the published data.
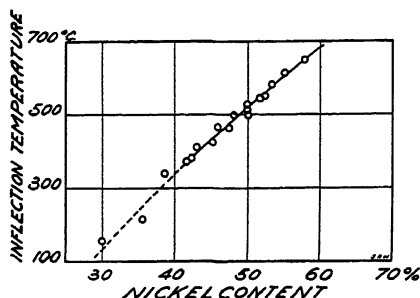
FIG. 8.—EFFECT OF NICKEL CONTENT ON INFLECTION TEMPERATURE OF NICKEL-IRON ALLOYS.
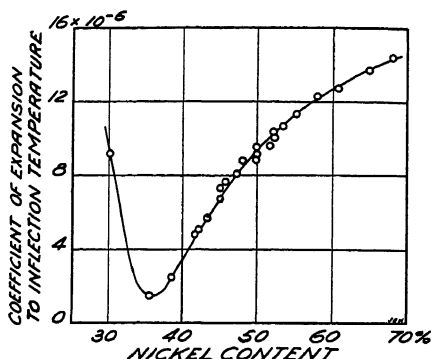
FIG. 9.—EFFECT OF NICKEL CONTENT ON AVERAGE COEFFICIENT OF EXPANSION UP TO INFLECTION TEMPERATURE OF NICKEL-IRON ALLOYS.

REFERENCES

1. Burgess and Aston: Magnetic and Electrical Properties of Iron-nickel Alloys. *Met. and Chem. Eng.* (1910) **8**, 23.
2. Chevenard: *Rev. de Mét.* (1914) **11**, 841.
3. Chevenard: *Rev. de Mét.* (1922) **19**, 209.
4. Guillaume: *Rev. de l'Ind. Min.* (Oct. 15, 1922).
5. Guillet and Cournot: *Rev. de Mét.* (1922) **19**, 215.
6. Hanson and Hanson: *Jnl.* Iron and Steel Inst. (1920) **102**, 39.
7. Hidnert and Sweeney: Nat. Bur. Stds. *Jnl. of Research* (1928) **1**, 771.
8. Hull and Berger: Glass to Metal Seals. *Physics* (Dec. 1934) **5**.
9. Invar and Related Nickel Steels. Nat. Bur. Stds. *Circ.* No. 58 (1923). Contains a bibliography.
10. Masumoto: On the Thermal Expansion of the Alloys of Iron Nickel and Cobalt and the Cause of the Small Expansibility of Alloys of the Invar Type. *Sci. Repts.* Tôhoku Imp. Univ. (1931) **20**.
11. Masumoto: Thermal Expansion of Alloys of Cobalt Iron and Chromium. *Sci. Repts.* Tôhoku Imp. Univ. (1934).
12. Portevin: *Rev. de Mét.* (1909) **6**, 1264.
13. Ritter: U. S. Patent 1794983.

14. Roush: *Met. and Chem. Eng.* (1910) **8**, 468.
15. Sands: Invar, Elinvar and Related Iron-nickel Alloys. *Metals and Alloys* (June and July 1932).
16. Scott: Nat. Bur. Stds. *Sci. Paper* No. 376 (1920).
17. Scott: Expansion Characteristics of Low-expansion Nickel Steels. *Trans. Amer. Soc. Steel Treat.* (1928) **13**, 829.
18. Scott: Expansion Properties of Low-expansion Fe-Ni-Co Alloys. *Trans.* A.I.M.E. (1930) **89**, 506.
19. Souder and Hidnert: Nat. Bur. Stds. *Sci. Paper* No. 433.
20. Souder and Hidnert: Nat. Bur. Stds. *Sci. Paper* No. 524.
21. Williams: Invar, Elinvar and Other Nickel Steels. *Raw Material* (Oct., Nov., Dec., 1922) **5**.
22. Yensen: *Jnl.* Amer. Inst. Elec. Engrs. (1920) **39**, 396.

DISCUSSION

(H. J. French presiding)

H. SCOTT,* Pittsburgh, Pa.—It is gratifying to know that the authors confirm the writer's early work in this field. There was some question in my mind at that time as to whether or not values for the inflection temperature could be duplicated by different observers. Now there is no doubt that they can be. Such carefully determined data are a welcome addition to the literature on low-expansion nickel steels.

---

* Westinghouse Electric and Manufacturing Co.

Low-temperature Transformation in Iron-nickel-cobalt Alloys

By L. L. Wyman,* Member A.I.M.E.

The exact nature of the changes that take place in the iron-nickel alloys, giving rise to the interesting and useful expansion alloys in the Invar range, has yet to be fully understood. Similarly, the ternary iron-nickel-cobalt alloys, which also possess such commercially useful expansion characteristics,[1,2] are concerned with transformations that appear to be identical with those found in the parent iron-nickel alloys.

The investigations on iron-nickel alloys in the range 26 to 29 per cent Ni have been reported by several authors[3-9] wherein it is shown that there are factors other than temperature, such as stress and grain size, which play an important part in determining the temperature at which the low-temperature transformation takes place.

It will be shown in this paper that the ternary iron-nickel-cobalt alloys having nickel contents comparable to the alloys mentioned above behave in a parallel manner.

The alloys in the range of 26 to 31 per cent Ni and 16 to 21 per cent Co have a coefficient of expansion of about 4.0×10^{-6} per degree Centigrade, and the alloys in this range of composition find considerable application in making glass-to-metal seals, because these expansion properties so well match commercial glasses.

The behavior of these alloys is not a simple matter, for it has been observed in alloys of 28.5 per cent Ni and 18.5 Co that severe working can cause the appearance of a second phase having a needlelike structure similar to the martensite structure in carbon steels. Fig. 1 shows the change brought about in an alloy of this composition when a strip of this material was cut with tin shears. This second phase has been identified as the body-centered cubic alpha phase, and it is the purpose of this paper to describe the results of some of the preliminary investigations in the study of the changes involved in these alloys.

Materials

The past work on these alloys has concerned itself primarily with materials made by the usual casting procedure and involving the use

of such additional materials as carbon, manganese and silicon, some of the effects of which have been previously described.[2]

In order to eliminate these variables, alloys were prepared by F. C. Kelley, of the General Electric Research Laboratory, by the powder method, utilizing the purest chemically prepared hydrogen-reduced metals, and fabricating the alloys in hydrogen atmosphere.

One of the greatest advantages of this method is the ease with which the compositions of the alloys can be accurately controlled by the initial mixtures used, as there are no losses encountered and no contamination involved.

Analyses on the finished materials show that there are but traces of manganese (0.006 per cent) and silicon (0.028 per cent) present, and that the carbon content of the alloys so prepared is of the order of 0.02 per cent or less.

The pressed bars of these alloys were sintered for 32 hr. at 1350° C. in hydrogen, hot-worked to 0.200 in. dia., annealed in hydrogen for 1 hr. at 1100° C. and then subjected to the expansion tests.

INVESTIGATIONS

Dilatometer samples of 0.1500-in. diameter and 1.914 in. long were carefully machined from the rods prepared as described above, and these were tested for expansion in a precision differential dilatometer in an atmosphere of dry hydrogen. This dilatometer is of the Chevenard type, with photographic recording, has jeweled bearings, and is fully automatic except for periodic checking to insure uniformity of temperature along the samples. Temperatures are determined by: (1) a base-metal couple inside the metal-lined furnace and almost touching the fused quartz sample tubes. This couple is connected with a photoelectric controller driven at a rate of $2\frac{1}{4}$° C. per min. by a telechron motor; (2) a noble-metal couple in the test sample, which registers on a precision potentiometer indicator and must coincide with experiment 1 above as to temperature; (3) a "dummy" sample, in a fused quartz tube similar to those holding the sample and chronin standard, consists of pure iron of the same size as the sample with chromel wires spot-welded to its ends. These, in turn, are connected to a mirror galvanometer sufficiently sensitive to have a fairly wide deflection for a temperature difference of 0.25° C. between the two ends of the dummy sample, thus acting as a null point couple.

Any tendency for a gradient to exist can be corrected by balancing the resistors in line with the split windings on the furnace.

The expansion characteristics at low temperatures were determined by means of a simple dilatometer consisting of an enclosed tube of fused quartz in which were placed the samples as described above, and the

FIG. 1.—STRIP CUT WITH TIN SHEARS.   × 250.
   28.5 per cent Ni, 18.5 per cent C.   Etched with HCl, HNO₃, CuCl₂.
FIG. 2. —PRECIPITATION OF BODY-CENTERED CUBIC PHASE ALONG POROUS SEAM.   × 500.
   28.5 per cent Ni, 18.5 per cent Co.   Etched with HCl, HNO₃, CuCl₂.

quartz push rod, which actuates a dial indicator, graduated to 0.0001 in. and easily readable to 0.00002 inch.

In order to obtain more uniform temperature distribution, the sample tube is enclosed by alternate pairs of heavy copper jackets and fused quartz tubes.

The low temperatures are obtained by scheduled additions of liquid air to a vacuum bottle with which the outer tube is enclosed. Check tests on this apparatus show that the temperature gradients are of the order of 5° C. between the sample ends. Empirical methods of operation have led to a schedule of additions of liquid air that will give a cooling rate of 3½° C. per min. over nearly the entire range from room temperature to that of liquid air.

After reducing the temperature to minus 192° C., the entire flask is filled with liquid air and allowed to remain overnight—that is, about 17 hr. at liquid-air temperature—before "heating up" to room temperature. This heating is accomplished by introducing an air stream into the flask and "blowing out" the liquid air. The heating rate is very close to the cooling rate up to about minus 25° C., where the rate becomes much slower.

All samples subjected to expansion tests were measured on a special fixture, utilizing a dial gauge similar to that described above, in order to give an additional check on the expansion results wherein any permanent change resulted.

The alloys were examined microscopically also, and by X-ray diffraction at room temperature.

OBSERVATIONS

Previous mention was made of the fact that this second phase having a body-centered cubic structure could be formed by merely shearing the sample, indicating that high stress can cause this change. Furthermore, wherever high stresses might be expected, as at rod surfaces, along seams, at notches, etc., in the rod, this observation has been verified repeatedly. An interesting example of this is shown in Fig. 2, where the separation has occurred along a porous seam in a particularly large-grained sample.

Turning to the expansion characteristics of these alloys, it may be observed in Fig. 3 that when the metal has been returned to room temperature after running to about 1000° C. the curves are not very far from reversibility. When this same sample is cooled to liquid-air temperature and then back up to room temperature a definite elongation has taken place.

This low-temperature change nearly always takes place as a gradual change, there being but three exceptions in nearly 150 tests.

The re-running of this cold-tested sample to 1000° C. in the dilatometer reveals a change taking place at about 450° C. on heating, and

that following this change the expansion characteristics are comparable to those obtained initially except for a shifting of the inflection point.

The change at 450° C. is the alpha-gamma transformation on heating, and remains at this temperature for all of the compositions studied when run at the 2¼° C. per min. heating and cooling rate. A change in the
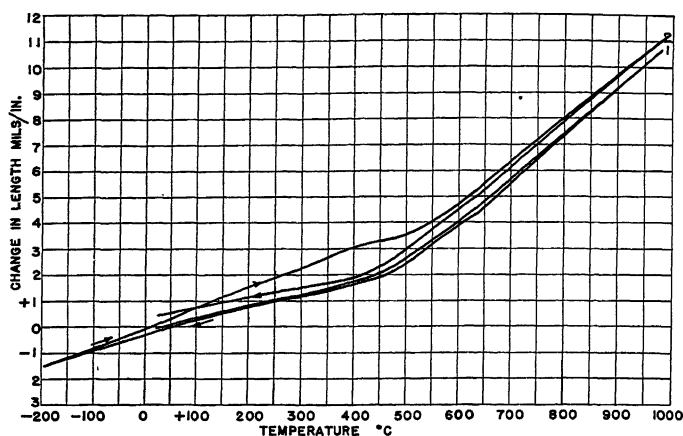
FIG. 3.—EXPANSION TESTS ON AS-RECEIVED MATERIAL.
28.5 per cent Ni, 18.5 per cent Co.
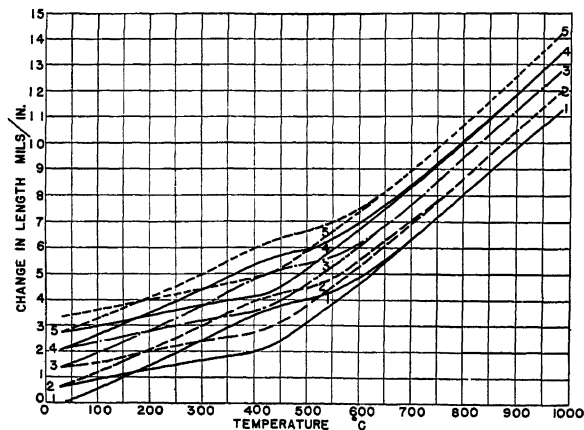
FIG. 4.—EXPANSION TESTS ON AS-RECEIVED MATERIAL. FIVE CONSECUTIVE RUNS.
26.5 per cent Ni, 18.5 per cent Co.

rate of heating and cooling to 11° C. per min. caused the transformation to take place at 525° C.

When the alloys are tested in the as-received condition there is no material difference in expansion characteristics between runs made at the two rates.

The alpha-gamma transformation at 450° C. apparently does not go to completion on the second dilatometer run, for when additional

runs are made there is a gradual decrease in the elongation acquired on each run, as five repeated runs have shown, indicating that when once formed, this alpha phase is not readily re-transformed.

With compositions between 26.5 and 30.5 per cent Ni with 20.5 to 16.5 per cent Co, balance Fe, the expansion determinations show that with decreasing nickel contents there is an increase in permanent elongation after the cold test. This holds true to somewhere between 28.0 and 26.5 per cent Ni, where a marked decrease is noted, but only because most of the transformation occurs above room temperature.

The occurrence of part of the transformation above room temperature in the alloy containing 26.5 Ni and 20.5 per cent Co gave further oppor-
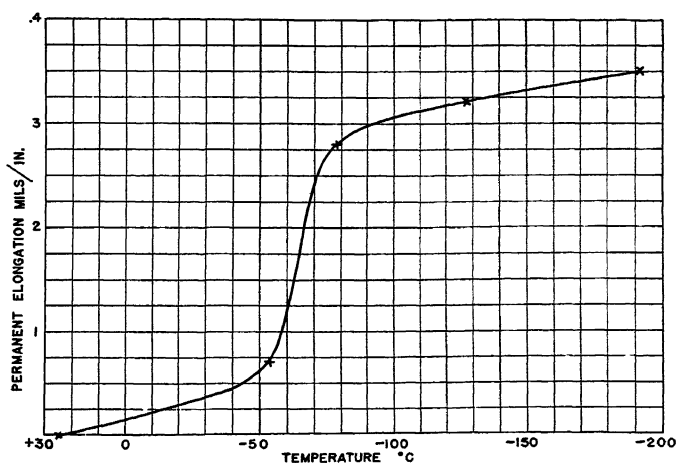
FIG. 5.—PERMANENT ELONGATION AFTER COLD TEST AT DIFFERENT TEMPERATURES. 28.5 per cent Ni, 18.5 per cent Co.

tunity to verify the completeness of the alpha-gamma transformation, thus this alloy was given five succeeding runs without removal from the dilatometer, as was the previously mentioned sample, the results being shown in Fig. 4.

The absence of any marked change in expansion characteristics between room temperature and that of liquid air could only be interpreted as meaning that the change was gradual. However, much better information could be obtained by cooling to different temperatures and observing the change after heating to room temperature.

By means of various freezing mixtures, a series of cold tests was run wherein the lowest temperatures were minus 53.8, minus 78.0, minus 127.2 and minus 192.0° C., the rates, time at temperature, etc., being the same as the regular cold-test schedule. The results of these tests are plotted in Fig. 5 and indicate that between minus 53.8° C. and minus 78.0° C. there is a much greater change than in any other range.

TABLE 1.—*Summary of Results*

Composition of Alloys, Per Cent			First Dilatometer Run		Cold Test, Length Change, Mils per In.	$\alpha \rightarrow \gamma$ Transformation on Heating, Deg. C.	Second Dilatometer Run		Structure after Cold Test		Structure after Second Dilatometer Run		Inflection Temperature Calculated on[a]	
Ni	Co	Fe	Average Inflection Temperature, Deg. C.	Average Length Change, Mils per In.			Inflection Temperature, Deg. C.	Length Change, Mils per In.	γ	α	γ	α	Ni	Co
26.5	20.5	53.0	452	+0.88	+0.28	437	438	−0.98	tr.	bal.	bal.	some	533	480
28.0	19.0	53.0	445	−0.06	+0.78	450	437	−0.12	some	bal.	bal.	some	480	466
28.5	18.5	53.0	448	+0.18	+0.28	433	437	+0.16	about	equal	bal.	some	462	455
28.5	18.5	53.0[a]	441	0.00	+0.12	425	450	−0.03	bal.	some	bal.	some	462	455
29.5	16.5	54.0	414	−0.10	+0.28	450	422	+0.43	about	equal	bal.	tr.	415	430
29.5	17.0	53.5	442	+0.10	+0.23	450	437	+0.28	about	equal	all	none	415	436
29.5	17.5	53.0	426	−0.12	+0.21	425?	430	−0.12	about	equal	bal.	tr.	415	442
29.5	18.5	52.0	441	−0.09	+0.01	none	437	−0.11	bal.	some	bal.	sl. tr.	415	455
30.0	17.0	53.0	437	−0.09	0.00	none	427	−0.26	bal.	tr.	bal.	sl. tr.	408	436
30.5	16.0	53.5	439	−0.08	−0.05	none	435	−0.05	bal.	tr.	bal.	sl. tr.	390	430
30.5	16.5	53.0	447	±0.15	0.00	none	442	0.00	all	none	all	none	390	430
34.0	10.0	56.0	395	−0.09	−0.01	none	392	−0.08	all	none	all	none	266	348

[a] Restricted grain size.

FIG. 6.—TYPICAL STRUCTURES WHEN ALPHA PHASE SEPARATES OUT. × 250. 29.5 per cent Ni, 16.5 per cent Co.

a. As received. Etched with HCl, HNO₃, CuCl₂. *b.* After cold test. No additional etching. *c.* Same area as *b* after light polishing and etching.

FIGS. 7 AND 8.—EFFECT OF EXPANSION. × 250.
28.5 per cent Ni, 18.5 per cent Co.
Fig. 7.   As received.   Fig. 8.   After first dilatometer test (five runs).
Etched with HCl, HNO₃, CuCl₂

FIGS. 9 AND 10.—SAME ALLOY AS FIG. 7.   × 250.
Fig. 9.   After dilatometer plus cold test.
Fig. 10.   After dilatometer plus cold test plus dilatometer.
Etched with HCl, HNO₃, CuCl₂.
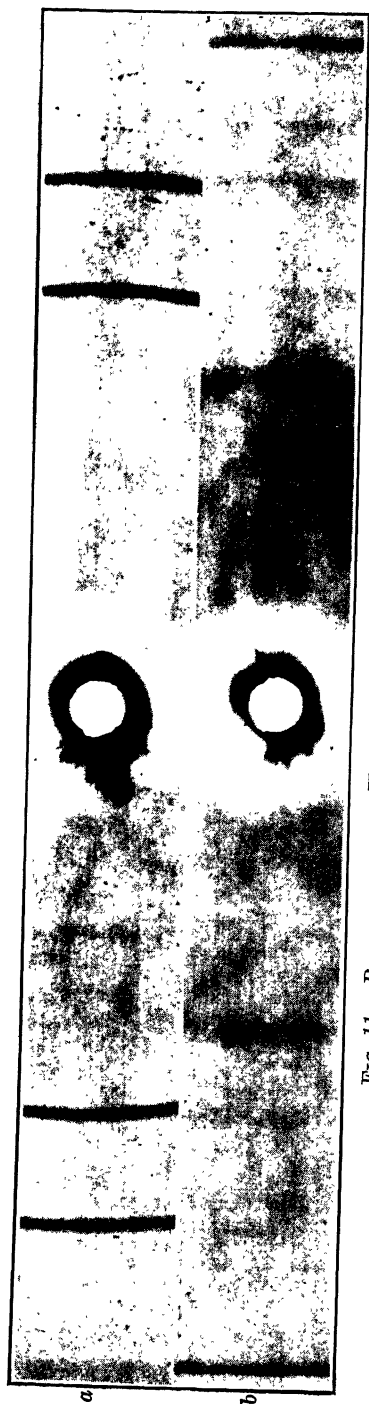
FIG. 11.—BACK-REFLECTION X-RAY DIFFRACTION PATTERN, FE RADIATION. 28.5 per cent Ni, 18.5 per cent Co: (a) as received; (b), after cold test.

Of the range of compositions covered in this investigation, only those having at least 30 per cent Ni with 16 per cent Co show no transformation when subjected to the cold test.

As it is impracticable to present expansion curves, structures, etc., on the numerous samples studied, the results are summarized in Table 1, giving the average results obtained by the standard treatments.

Scheil and Forster[4] made acoustic tests on iron-nickel alloys by attaching the sample to a microphone armature and amplifying the impulses arising from the formation of the alpha needles, their results indicating that the change is gradual beginning at minus 31° C., the individual needles being formed in 0.002 seconds.

Similar tests were made on the present alloys, with comparable results, the impulses coming gradually at first then building up to a maximum, then gradually diminishing, the entire cycle requiring about 10 min. for a sample 0.200-in. dia. and 0.750 in. long.

Microscopic examinations were made on each sample: (1) as received, (2) after the first dilatometer run, (3) after cold test, and (4) after final dilatometer tests following the cold test. Typical structures encountered when the alpha phase separates out may be seen in Fig. 6, where the section is shown in the as-received condition and after cold test. Fig. 6b represents a polished and etched microsection, which was run through the cold-test schedule, causing the transformation and making the needles stand in relief on the sample.

FIG. 12.—STREAK OF BODY-CENTERED CUBIC PHASE.   ✕ 250.
28.5 per cent Ni, 18.5 per cent Co.
FIG. 13.—FINE GRAIN AFTER COLD TEST.   ✕ 250.
28.5 per cent Ni, 18.5 per cent Co.
Both etched with HCl, HNO₃, CuCl₂.

Inasmuch as some doubt has existed regarding the ability to microscopically differentiate these phases, the sample represented in Fig. 6b was very lightly polished to remove the relief and obtain a plane unetched surface, then etched (Fig. 6c). A detailed examination will disclose that Figs. 6b and 6c represent the same area on the sample.

Figs. 7 to 10, inclusive, represent the correlation of the microstructures with the expansion curves, there being a small amount of alpha present after the dilatometer run, the structure consisting mainly of needles after the cold test, and remanents still remaining visible after the second dilatometer run.

It was noted also that this gamma-alpha transformation was more pronounced in large-grained samples than in small-grained ones. In fact, a number of instances were noted (Fig. 11) wherein the alpha separation in large-grained areas died out in the small-grained areas of a duplex structure. This observation was further substantiated when samples were intentionally made fine-grained, and gave very little transformation (Fig. 12).

To date, X-ray diffraction studies have been made only at room temperature, in order to corroborate the microscopic and expansion tests. Fig. 13 shows the patterns obtained on an alloy of 28.5 per cent Ni and 18.5 per cent Co, which are typical of the alloys undergoing a change on cold test.

Conclusions

It is somewhat misleading to conclude that the transformation taking place below room temperature is actually a gradual one, for when it is considered that stress, grain size, temperature and time all have a bearing on the transformation, any one or more of these may be exerting an influence that would tend to cause the transformation sooner than it should under truly equilibrium conditions. This is substantiated by the graded cold tests, Fig. 5, which show that the change is not gradual.

Because of these factors it would seem rather hazardous to attempt to calculate expansions and inflection points on the basis of the composition alone. A comparison of the pure alloys concerned in this paper with the cast alloys upon which Scott[2] based his calculations shows that (Table 1) there is considerable discrepancy between the calculated and observed values. Such calculations on these pure alloys would require 28.8 per cent Ni, 18.1 per cent Co to keep the transformation near minus 100° C. That this does not hold true is shown in the behavior of the 28.5 per cent Ni, 18.5 per cent Co alloys, like that shown in Fig. 5.

It may also be observed from Table 1 that inflection temperatures of 450° C. can be obtained from a variety of alloy compositions. Thus it must be concluded that such calculations must be restricted to the particular group of alloys described by Scott.

The work of investigators[3,5,7,8,9] concerned with the $\gamma \rightleftarrows \alpha$ transformation in iron-nickel alloys shows that:

1. The transformation takes place by a "slip" mechanism and occurs in the same way whether caused by thermal or by mechanical methods.[5,7]

2. Both strain and grain size influence the transformation.[3,9]

3. The amount of low-temperature transformation is dependent on the composition.[5,8]

The experiments on pure ternary iron-nickel-cobalt alloys described above show that:

1. The low-temperature transformation in the ternary alloys is the same as that in the binary iron-nickel alloys, the behavior of the alloys directly paralleling the binary alloys.

2. These ternary alloys directly parallel the behavior of the iron-nickel alloys.

3. The low-temperature transformation occurs over a range of temperature because of lack of equilibrium conditions and is influenced by time, temperature, stress and grain size.

4. The $\alpha \rightarrow \gamma$ transformation occurs at or below 450° C.

5. The transformations do not go to completion within the experimental conditions used.

6. The behavior of the alloys should not be calculated.

It is obvious that previous treatment is of vast importance in determining the behavior of these alloys. This is of particular significance because it is known (has been for some time) that these alloys are further complicated by high-temperature changes, as recently mentioned by Hessenbruch.[10] These changes not only influence the expansion characteristics but the low-temperature transformations as well. These relationships are the objectives of investigations now in progress and, it is hoped, will find future presentation.

REFERENCES

1. Hull and Burger: *Physics* (1934) [12] **5**, 384.
2. Scott: *Jnl.* Franklin Inst. (1935) **220**, 733; *Trans.* A.I.M.E. (1930) 506.
3. Scheil: *Ztsch. anorg. Chem.* (1932) **207**, 21.
4. Scheil and Forster: *Ztsch. Metallk.* (1936) **29**, 245.
5. Bumm and Dehlinger: *Ztsch. Metallk.* (1934) **26**, (5) 112; (1937) **29**, (1) 29.
6. Wever-Lange: *Mitt.* K.W.I. Eisenforch. (1936) **18**, 217.
7. Nishiyama: *Sci. Repts.* Tohoku Imp. Univ. (1935) [1] **25**, 94.
8. Ruer and Kuneko: *Ferrum* (1913) **2**, 34.
9. Wassermann: *Arch. Eis.* (1937) **10**, 321.
10. Hessenbruch: *Ztsch. Metallk.* (1937) **29**, 193.

DISCUSSION

(H. J. French presiding)

E. S. DAVENPORT,* Kearny, N. J.—Can the acoustic method of detecting the transformation of austenite be applied at moderately elevated temperatures (for

---

example, in the range 400° to 800°F.) for following the isothermal transformation of carbon and low-alloy steels, as in the development of S-curve data?

H. Scott,[*] Pittsburgh, Pa.—The low-expansion iron-nickel-cobalt alloys discussed in this paper, now widely used in applications where low expansion coupled with ease of fabrication and low cost is essential, have best expansion properties when the Ar_3 transformation starts just below room temperature and the content of other elements is low. For practical reasons, however, the start of the Ar_3 transformation must be kept below approximately −80° C.

In my original paper,[11] and in U. S. Patent No. 1942260, the composition relations that must be fulfilled to meet the requirement that Ar_3 start at about −100° C. are given as follows:

$$\frac{\%\ Ni + 2.5(\%\ Mn) + 18(\%\ C)}{\%\ Fe} = 0.55$$

This relation is derived from observations made on a large number of alloys of different compositions all annealed at 800° C. After publication, we found, as does Mr. Wyman, that the start of the transformation occurs at a somewhat higher temperature when the specimen is annealed at a considerably higher temperature than 800° C., say 1100° C. An explanation of the surprising fact that the higher temperature, presumably conducive to homogeneity, should raise the transformation temperature would be most welcome. This fact was recognized, however, early in the commercial production of our glass-sealing alloy, Kovar, by a slight increase in the value of the ratio.

Mr. Wyman does not make a clear-cut issue, but apparently insinuates that the composition-transformation relation just mentioned is not accurate and that any iron-nickel-cobalt alloy is likely to be unstable as regards transformation. I am, however, unable to find any evidence in support of either suggestion, either in Mr. Wyman's paper or elsewhere. It is difficult to compare results directly because Mr. Wyman does not give values for the start of the transformation, but a few qualitative comparisons can be made, which indicate that Mr. Wyman's data are in close accord with mine.

One particular alloy that he mentions is 28.5 per cent Ni, 18.5 per cent Co, which he reports as transforming above −80° C., but below room temperature presumably after annealing at 1100° C. or higher. Manganese and carbon are supposed to be nil, so the ratio of equivalent nickel content to iron content is:

$$\frac{28.5}{100 - 18.5 - 28.5} = \frac{28.5}{53.0} = 0.538$$

Being lower than 0.55 and coarse-grained, the alloy should transform above −80° C. just as he observed. If a manganese and carbon-free alloy is desired that will meet the requirements set up, it should contain 29.5 per cent Ni and 17.5 per cent Co. This is a large change in composition from that previously noted relative to the accuracy of compounding required in this alloy field.

It is only by the highest grade of analytical work that we were able to establish the relations under consideration. Mr. Wyman indicates by his reporting of compositions to the nearest half per cent that no analysis was made, composition being determined only by the weight of components in the mixture. Such an estimation might be quite accurate with careful compounding were the composition of the components accurately known. He fails, however, to report cobalt in the nickel,

nickel in the cobalt and copper in the iron, all of which are major impurities, the contents of which range from 0.10 to 1.0 per cent.

Mr. Wyman apparently uses the degree of permanent expansion on cooling to some subzero temperature as a measure of instability of an alloy at atmospheric temperatures rather than the temperature at which the Ar_3 transformation starts. This is, of course, an easy test to make and we once tried it for routine inspection, but found the results to be inconsistent. Investigating further we found that degree of transformation cannot be measured accurately because of surface effects. A surface grain assumes a ruffled surface after transformation as Mr. Wyman has shown in his admirable pictures. The dilatometer, however, measures from the top of the highest projection, so that the observed length increment is much larger than for normal expansion and is also a function of the shape of the specimen ends relative to its supports.

Taking advantage of the surface ruffling, we have used it to detect the actual start of transformation. Our specimens have flat ends, as do the contacting dilatometer parts, so that there is maximum-surface area of the specimen available to influence the gauge. In this experimental condition the first surface crystal that transforms registers this fact strongly on the dial gauge as well as by a click, and we have a perfectly clear-cut and very sensitive observation of the start of transformation. All production heats are so tested.

Reverting back to Mr. Wyman's doubts about the accuracy of my original data and composition relations, it is clear that he has made no case against them. As a matter of fact, what substantial information I have been able to glean from his oral presentation fully supports my composition-transformation relations, even though extrapolation of my data to zero manganese and carbon content is involved.

As regards stability of the alloys made in accordance with the rules given here, he fails to give a single example of transformation near atmospheric temperature in a legitimate alloy. The examples given were all off compositions, which would not pass our routine inspection tests for production metal. Practically all of the metal is cold-rolled and if that induced transformation the cold-rolling mill would forcefully make it known. High-temperature heating is of no concern because the composition is so adjusted as to be stable with considerable latitude after such treatment; inspection tests, in fact, being made only under conditions most unfavorable to the alloy.

Mr. Wyman also disagrees with my values for inflection temperature. In this connection there is some gross misconception because he indicates values for a given composition calculated on the basis of nickel content to be different from those based on cobalt content. Actually the effects of nickel and cobalt are additive and indistinguishable, as repeatedly noted in my previous publications. The value for the inflection temperature over the temperature range concerned is:

$$19.5(\% \text{ Ni} + \text{Co}) - 22(\% \text{ Mn}) - 465° \text{ C.}$$

The ratio of nickel to cobalt is immaterial as long as the alloy is in the gamma state.

For a specific comparison we may take Ni + Co = 47.0 per cent, a value used in several of his specimens, for which the inflection temperature with zero manganese is:

$$19.5 \times 47.0 - 465 = 451° \text{ C.}$$

It would indeed be surprising if no errors could be found in so comprehensive an undertaking as reported in my 1930 paper, particularly in view of the improvements in apparatus and increase in knowledge since that time. As the case stands now, however, no serious error or discrepancy has yet been called to my attention. It is one of the few attempts that have been made to relate physical properties to chemical composition in an exact, compact and comprehensive manner. If the basis of the structure is unsound, let that be clearly and forcefully demonstrated. Otherwise, let us build on the foundation that has already been laid.

L. L. WYMAN (author's reply).—As to the possible use of the acoustic method at temperatures up to 800° C., I frankly do not know, and only direct experiment could give the answer. At first thought, it might seem that the plasticity of the metal itself at elevated temperatures would materially reduce the "shock" encountered at the instant of transformation—cushion it, so to speak, and thus detract from the value of the method.

This entire region was studied by means of a series of alloys, differing in composition by steps of 0.5 per cent, on checked analyses for impurities, the steps being statements of compositions rather than indications of variation. Mr. Scott's quoted range of 0.10 to 1.0 per cent impurity range is one, upon which I heartily agree with him, is applicable to cast alloys. However, to one familiar with powder methods, even the 0.10 per cent variation is a wide latitude with known starting materials such as are used in the present paper.

As to the accuracy of the expansion measurements, I believe that careful perusal of the description of the dilatometer used should dispel any doubts, particularly when it is considered that the temperature scale is such that 1° C. is slightly less than 0.5 mm. and consequently quite easily readable.

Having used the dial-gauge type of instrument, of accuracy corresponding to that used in all of Mr. Scott's work, for the lower temperatures, I fully realize the limitations on such equipment and the element of personal error involved. The high precision, automatic photographic recording, and elimination of the personal element in the operation of the large dilatometer produce results hardly to be criticized.

I feel that Mr. Scott has answered the many points that he raises concerning the calculation of the transformation point by one of his earlier statements to the effect that after the publication of his original article he found, in agreement with the findings presented in the present paper, that the transformation occurred at a higher temperature than he calculated.

The explanation Mr. Scott asks for is one of the principal findings of this series of experiments; to wit, that factors other than composition have the controlling influence in the placement of this transformation, as has been clearly shown in Fig. 1.

Concerning the commercial alloy cited in the discussion, I am sure Mr. Scott can see his way clear to agree with me that the experiences of a number of metallurgists with the practical applications fully substantiate the present findings.

I am in somewhat of a quandary concerning the term "legitimate alloy" as used by Mr. Scott, but I do believe that definition, or even common usage, will qualify all the alloys used in these experiments, even as to color.

Mr. Scott's citation of cold-rolling experiences further substantiates such factors as are brought forth in this paper, and clearly shown in the figures. As to the high-temperature heating, the transformation troubles encountered there have already been shown by Hessenbruck, among others, and with which I am in complete agreement.

The expansion characteristics under discussion are inherent characteristics of the iron-nickel system, as slightly modified by cobalt additions. We are, therefore, going back to see whether the same peculiarities of transformation particularly applicable to the binary iron-nickel alloys actually do hold true within the ranges of ternary compositions under discussion.

The similarity is established, and with it, a number of the factors that will cause transformation at other than the calculated temperatures—factors which in themselves cannot be set to figures.

The preparation of a series of alloys strictly in accordance with a rigid procedure may apparently be formulated, but when variations in treatment, cold-work, stress, grain size, etc., all are known to influence a type of transformation that has become understood only within the past few years, it is obvious that rigid formulation can have but little if any part in the behavior prediction of alloys of this kind.

Fracture of Steels at Elevated Temperatures after Prolonged Loading

By R. H. Thielemann* and E. R. Parker,* Junior Member A.I.M.E.

(Detroit Meeting, October, 1938)

The conventional short-time tensile test provides a reliable means of predicting the sustained load-carrying capacity of steels only when the temperature is such that continuous plastic flow does not occur. At elevated temperatures, stresses considerably less than the short-time rupture value may produce continuous flow, with fracture occurring only after long periods of time. The amount of flow or creep accompanying failure varies for different steels, and depends, to a large extent, on the temperature and the duration of the test. Service records of cracking stills, steam superheaters and high-temperature boilers have shown that brittle fractures sometimes occur with little or no warning. In installations of this type, localized stresses are often encountered, and steels must be capable of withstanding a certain amount of deformation without fracture. The sustained-load rupture test determines the expected life and corresponding ductility of steels at various stresses and temperatures. It also yields additional information regarding the effect of microstructure and metallurgical stability on the high-temperature properties.

Present Status of Sustained-load Rupture Test

The sustained-load rupture test conducted at elevated temperatures is not entirely new. Dr. Zay Jeffries[1] presented in 1919 the results of a large number of rupture tests made on copper, iron and tungsten. These tests were made with various strain rates and at temperatures ranging from the boiling point of liquid air to 1000° C. At that time he observed the interesting phenomenon characteristic of metals, that a temperature exists below which a metal is ductile and breaks with a transcrystalline fracture (through the grain) and above which the metal is brittle and breaks with an intergranular fracture (through the grain boundaries). He observed that this temperature varied with the testing speed, and that a minimum temperature, slightly above the recrystallization temperature, existed at which the cohesion of the grains themselves was

equal to the cohesion between the grains. Jeffries termed this point the temperature of equal cohesion, or equicohesive temperature. At the same time he discussed the effect of grain size on the properties of metals, basing his deductions on Beilby's amorphous cement theory. Jeffries found that a larger grain size promoted higher strength, reduced ductility, and increased resistance to deformation at elevated temperatures.

Recently, Messrs. Clark, White, and Wilson[2,3,4] have contributed further information regarding the rupture test and have obtained some very pertinent information on many materials now in common use. Also important was their discovery of the straight-line relationship resulting from a log-log plot of the stress against the time required for failure for a given steel at a particular temperature.

APPARATUS AND TECHNIQUE

The apparatus developed in the Research Laboratory of the General Electric Co. for conducting high-temperature sustained-load rupture
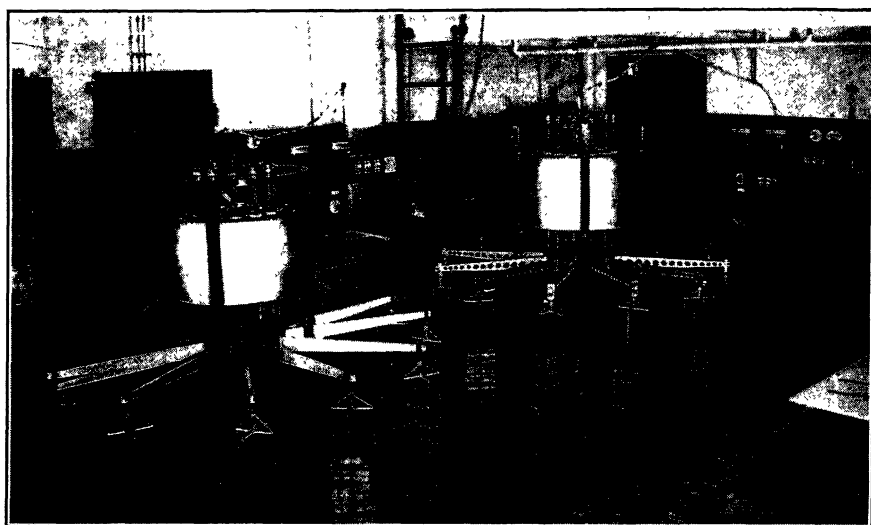
FIG. 1.—TESTING EQUIPMENT FOR SUSTAINED LOAD FRACTURE.

tests is shown in Fig. 1. There are, at present, two furnaces, each capable of testing simultaneously 12 test bars at the same temperature. The specimens are symmetrically arranged in the cylindrical furnaces and are tested under constant load applied by means of a simple lever and weights. The temperature variation between specimens is less than 2° F., and the temperature of each specimen is uniform over a 6-in. gauge length. The furnace temperature is controlled within ±3° F. Various shapes and sizes of test bars have been used, including the standard 0.505-in. tensile bar, 0.253-in. centerless ground rods, 0.250-in. inside diameter

seamless tubing and 0.150 by 0.250-in. strips machined from larger tube sections. The machines are designed to allow test bars to be quickly changed. Spherically seated washers under the loading nuts assure alignment of the test bars. Included in the equipment is a system of time meters for recording the time under load.

DISCUSSION OF TEST RESULTS

Typical results from time to failure tests are shown in Fig. 2. For a given material at a constant temperature, a logarithmic plot of the stress against the corresponding time for fracture results in a straight line. As indicated in Fig. 2 and as shown in comparing Figs. 4 and 6, two distinct
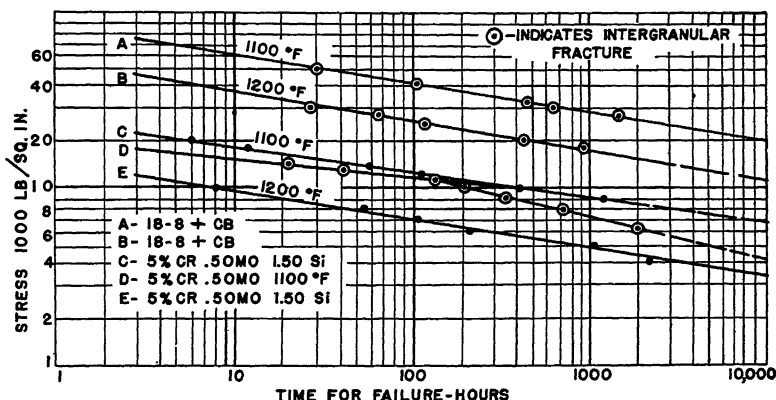
FIG. 2.—STRESS TIME FOR FAILURE AT 1100° AND 1200° F. Diameter of test bars 0.253 in.; area, 0.05 sq. in.; 6-in. gauge length.

fracture types are found from sustained-load rupture tests on various steels at elevated temperatures. With the transcrystalline type of fracture the break occurs through the grains, and for ductile materials the grains are elongated in the direction of the load, as shown in Fig. 6. The intergranular failure, however, takes place through the grain boundaries, and, as shown in Figs. 4 and 8, occurs with very little deformation of the grains. Materials exhibiting this type of fracture behave as brittle materials and often fail with little or no warning.

The 5 per cent Cr, 0.50 per cent Mo steel, as indicated in Fig. 2 and shown by the microstructure in Fig. 4, fails with an intergranular fracture. Even with testing times as short as 20 hr., the same type of fracture was found. For this material the straight-line relationship on the log-log plot incurs a change of slope after 150 hr., indicating its susceptibility to intergranular oxidation.

At 1200° F., a 5 per cent Cr, 0.50 per cent Mo steel containing 1.5 per cent Si failed with a ductile transcrystalline fracture after 2500 hr. Although the oxidation resistance of this material is superior to that of the 5 per cent Cr, 0.50 per cent Mo steel without silicon, surface oxidation
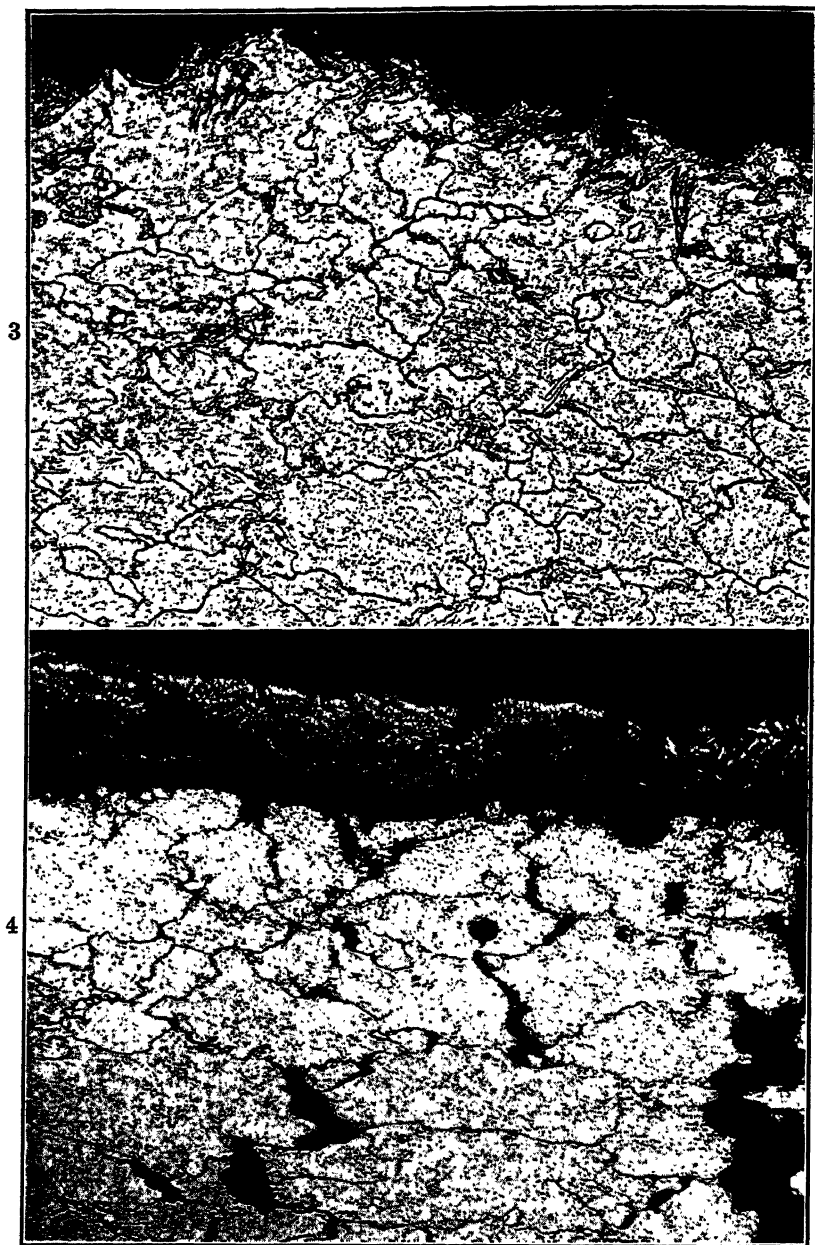
FIG. 3.—STRUCTURE BEFORE TESTING OF STEEL CONTAINING 5.0 PER CENT CHROMIUM
AND 0.5 PER CENT MOLYBDENUM.   ✕ 250.

FIG. 4.—SECTION NEAR FRACTURE OF STEEL CONTAINING 5.0 PER CENT CHROMIUM AND
0.5 PER CENT MOLYBDENUM.   ✕ 250.

Stressed at 10,000 lb. per sq. in. for 265 hr. at 1100° F.   Elongation 8.5 per cent in
6 in.; reduction of area, 12 per cent.
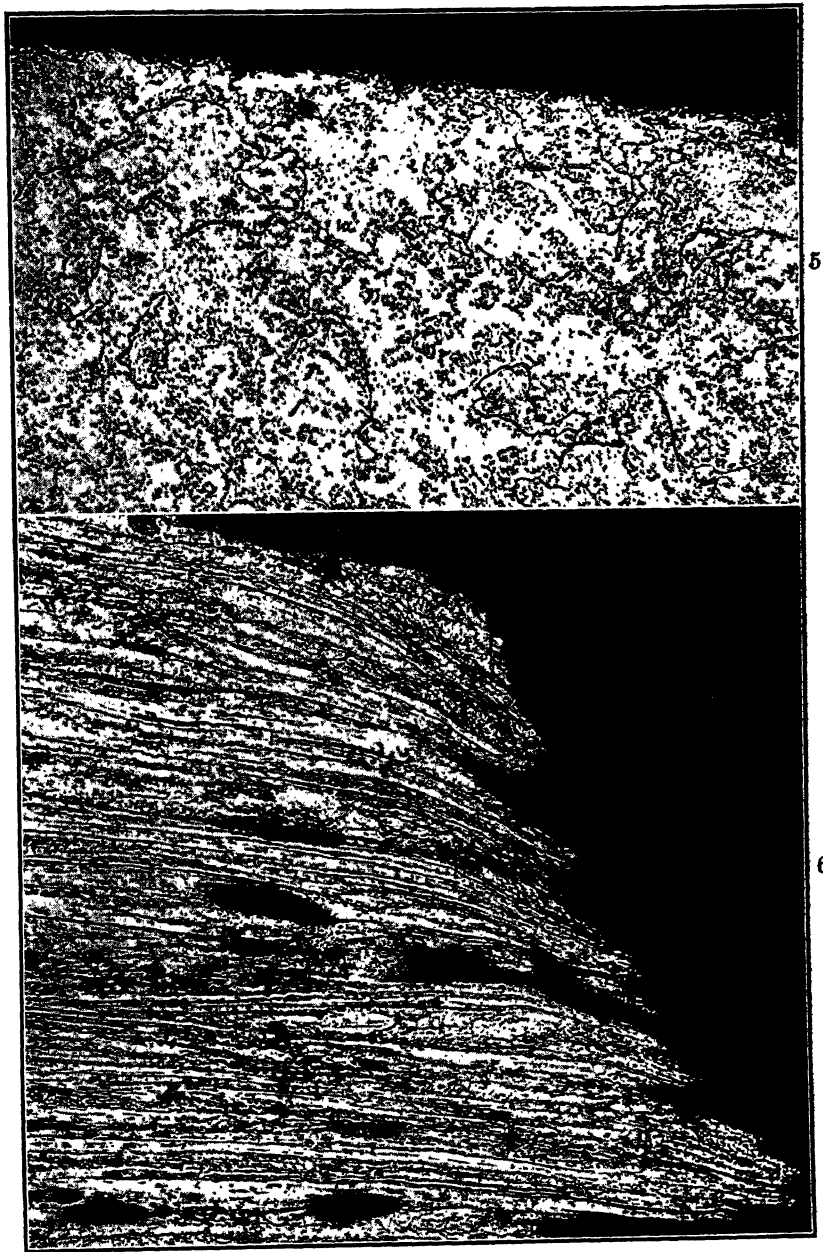
FIG. 5.—STRUCTURE BEFORE TESTING OF STEEL CONTAINING 5.0 PER CENT CHROMIUM, 0.5 PER CENT MOLYBDENUM AND 1.5 PER CENT SILICON.   × 250.

FIG. 6.—FRACTURE OF STEEL CONTAINING 5.0 PER CENT CHROMIUM, 0.5 PER CENT MOLYBDENUM AND 1.5 PER CENT SILICON.   × 250.

Stressed at 10,000 lb. per sq. in. for 330 hr. at 1100° F.   Elongation 40 per cent in 6 in.; reduction of area, 75 per cent.
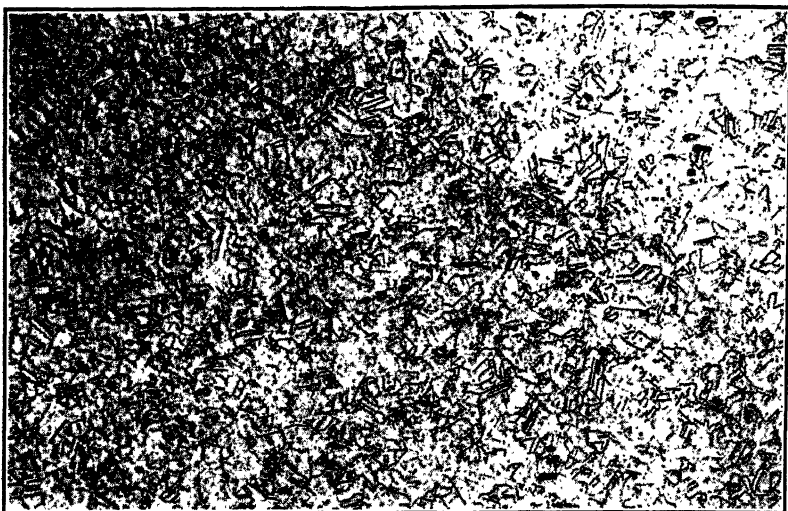
FIG. 7.—STRUCTURE OF COLUMBIUM STABILIZED 18-8 BEFORE TESTING.   × 250.
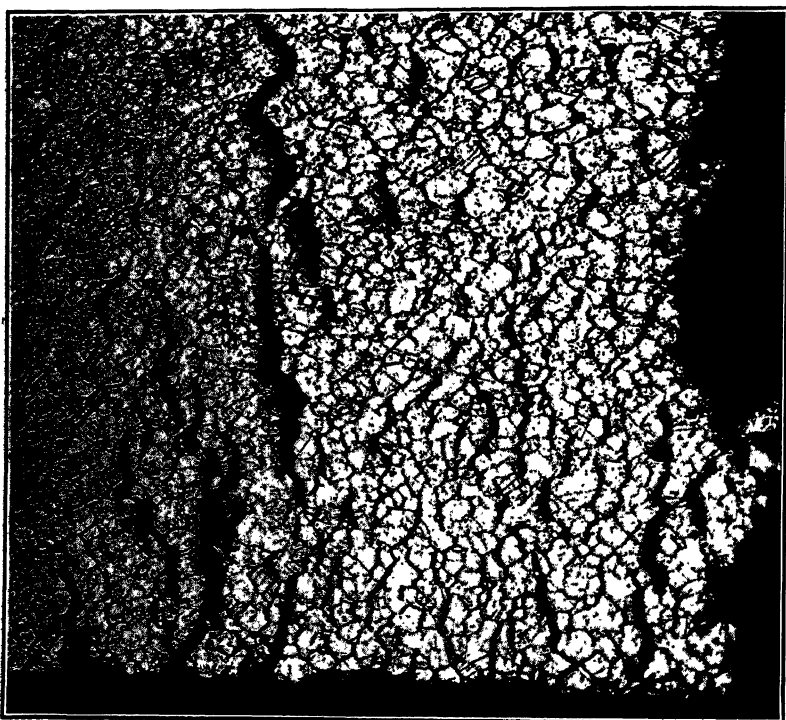
FIG. 8.—INTERGRANULAR FRACTURE AT EDGE OF 18-8 BAR.   × 250.
Stressed at 32,500 lb. per sq. in. for 376 hr. at 1100° F.   Elongation 8.3 per cent in 6 in.; reduction of area, 10 per cent.

TABLE 1.—*Materials Tested*

Materia	Chemical Analysis, Per Cent									Heat-treatment
	C	Mn	P	S	Cr	Mo	Si	Ni	Cb	
18-8.........	0.07	0.53	0.004	0.025	19.0		0.27	9.14	0.76	1000° C, 2hr. a.c.
Cr-Mo-Si....	0.12	0.30	0.013	0.010	5.20	0.50	1.42			Annealed
Cr-Mo......	0.096	0.50	0.018	0.014	4.88	0.65	0.3386			Annealed
Armco iron..	0.03	0.005	0.002	0.037			0.005			Annealed
C-Mo.......	0.10	0.08				0.51	0.25			Annealed

was noticeable. It appears that as long as the fracture is of the trans-crystalline type, intergranular oxidation has not occurred, and the slope of the rupture curve remains constant.
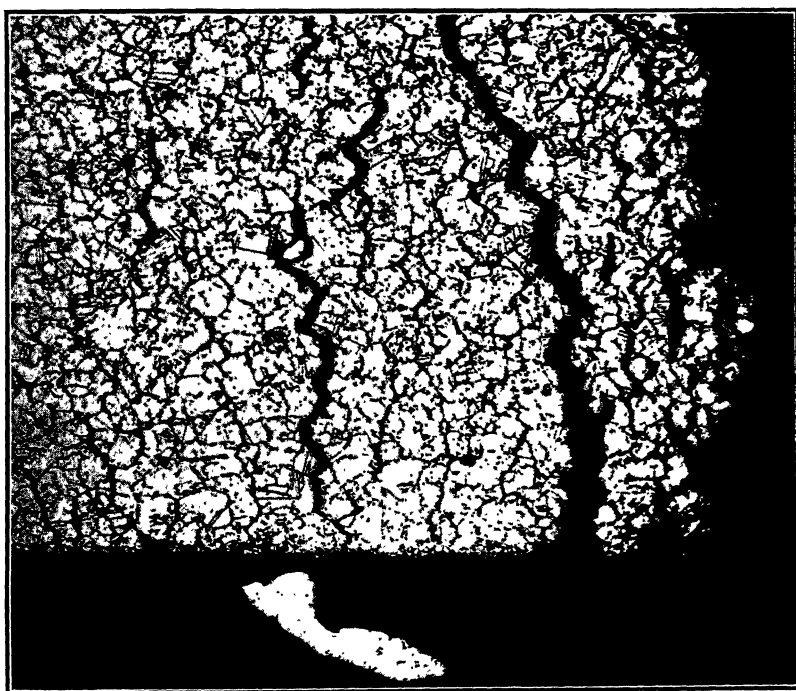
FIG. 9.—INTERGRANULAR FRACTURE AT EDGE OF 18-8 BAR. × 250.
Stressed at 18,000 lb. per sq. in. for 914 hr. at 1200° F. Elongation 2.86 per cent in 6 in.; reduction of area, 3 per cent.

The results from tests on columbium stabilized 18 and 8 at 1100° F. and 1200° F. are interesting in that all of the fractures were of the inter-granular type with no change in slope of the rupture curve within 1000 hr. of testing. Microscopic examinations of the fractured specimens showed excessive carbide precipitation at the grain boundaries, but there was no

evidence of intergranular oxidation. Figs. 8 and 9 show that the intergranular cracking takes place over the entire cross section.

The results from the tests on these three materials indicate that intergranular failures are inherent to certain steels and cannot be attributed
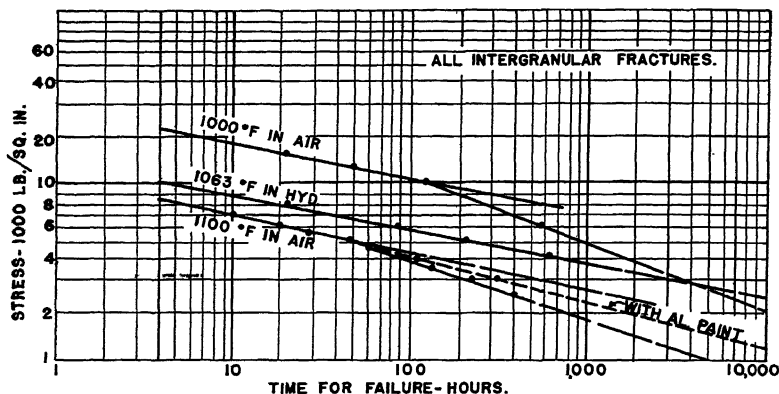
FIG. 10.—STRESS TIME FOR FAILURE OF ARMCO IRON IN AIR AND IN HYDROGEN ATMOSPHERES.
Diameter of test bars, 0.253 in.; area, 0.05 sq. in.; 6-in. gauge length.
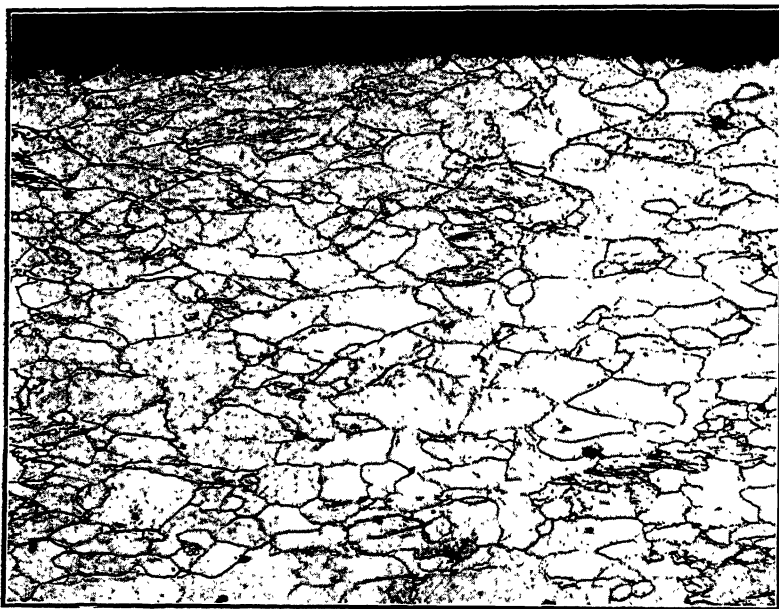
FIG. 11.—STRUCTURE OF ARMCO IRON BEFORE TESTING. × 250.

to intergranular oxidation. Also, it is apparent that intergranular cracking may or may not be accompanied by intergranular oxidation. It seems that transcrystalline fractures can be accompanied by surface oxidation only.

RUPTURE TESTS IN HYDROGEN ATMOSPHERE

The effect of oxidation on the rupture strength and fracture of steels at elevated temperatures is further demonstrated by tests made on Armco iron in a pure dry hydrogen atmosphere. For these tests it was necessary to install a thin-walled steel tube through one section of the 1100° F. furnace, so that a continuous flow of hydrogen could be main-
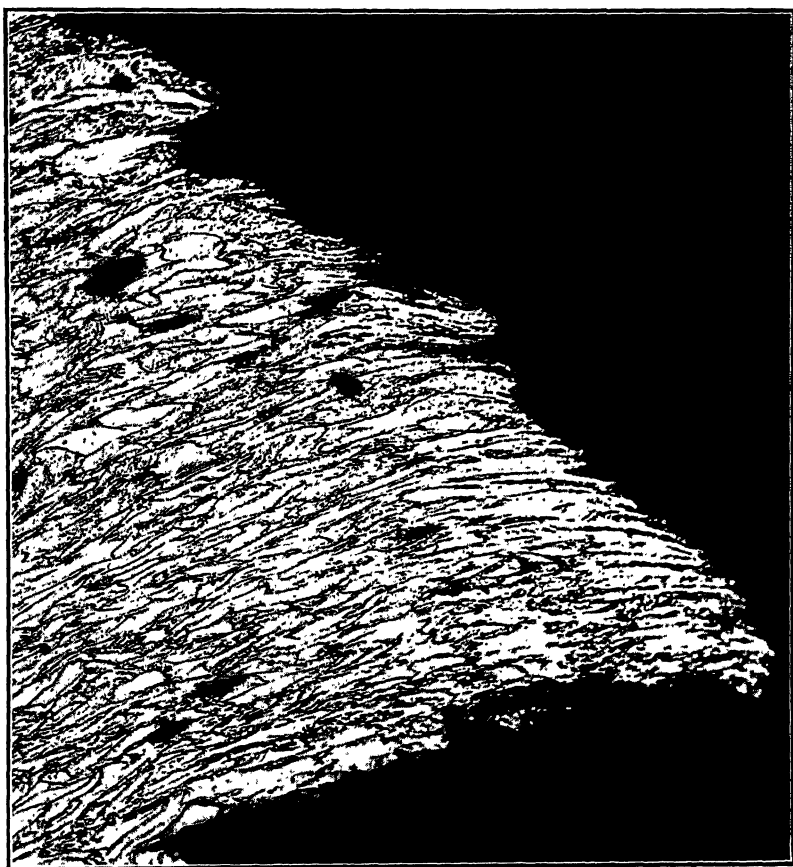
FIG. 12.—ROOM-TEMPERATURE TENSILE FRACTURE OF ARMCO IRON. × 250.

tained around the test bar. Suitable packing arrangements were provided at each end of the tube to insure a gastight test chamber. The hydrogen gas, after passing through a purifier train to remove all moisture and oxygen, was admitted at the top of the tube and exhausted at the bottom, a slight pressure being maintained in the tube at all times. The cooling effect of the conducting steel tube and the circulating hydrogen gas lowered the temperature of the enclosed test bar to 1063° F.
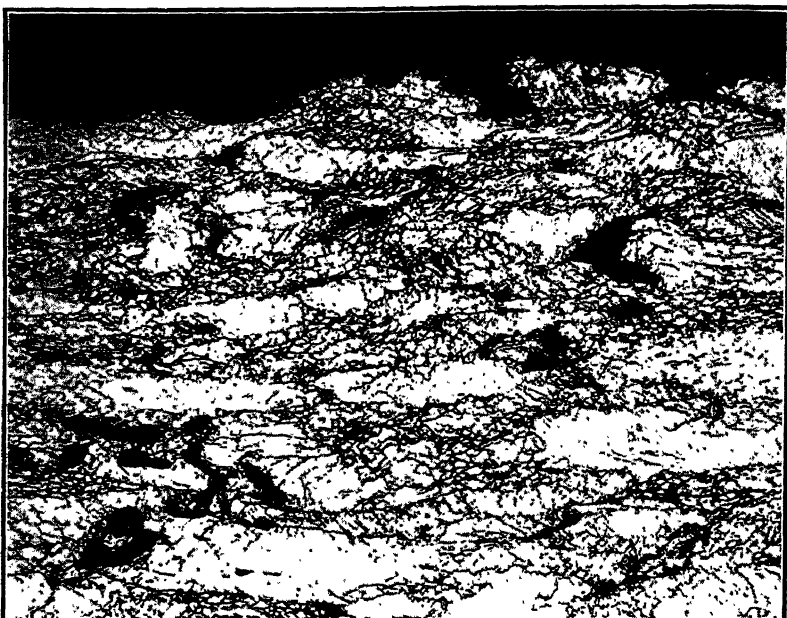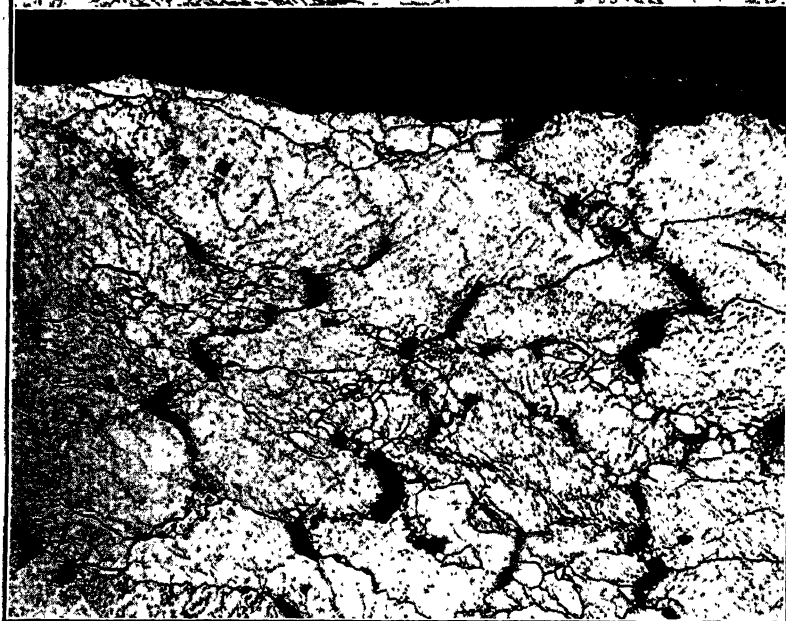
FIG. 13.—SECTION NEAR FRACTURE OE ARMCO BAR.   × 250.
   Stressed at 15,000 lb. per sq. in. for 19 min. at 1100° F.   Elongation 15.2 per cent in 6 in.; reduction of area, 78 per cent.

FIG. 14.—SECTION NEAR FRACTURE OF ARMCO BAR.   × 250.
   Stressed at 5500 lb. per sq. in. for 28 hr. at 1100° F.   Elongation 5.7 per cent in 6 in.; reduction of area, 6 per cent.
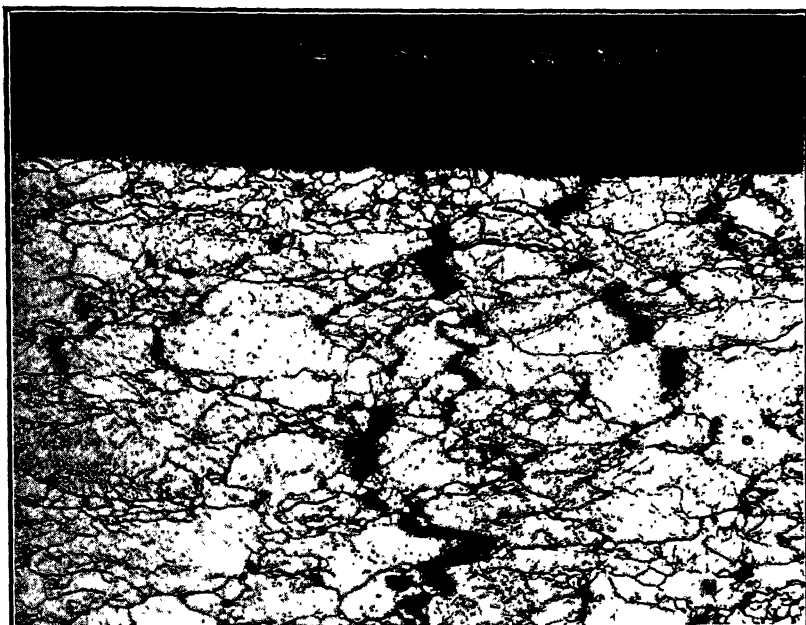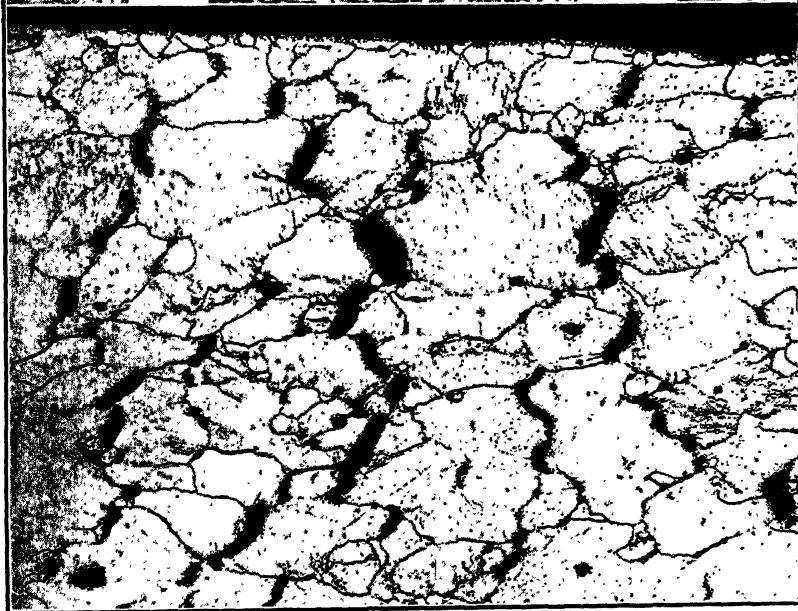
FIG. 15.—SECTION NEAR FRACTURE OF ARMCO BAR.   × 250.
Stressed at 2500 lb. per sq. in. for 409 hr. at 1100° F.   Elongation 2.6 per cent in 6 in.; reduction of area, 3 per cent.
FIG. 16.—SECTION NEAR FRACTURE OF ARMCO BAR.   × 250.
Stressed at 4000 lb. per sq. in. for 608 hr. in hydrogen at 1063° F.   Elongation 3 per cent in 6 in.; reduction of area, 3 per cent.

Previous tests on Armco iron in air at 1000° F. and 1100° F. all showed pronounced intergranular failures.   Also, the oxidation resistance in this temperature range was comparatively poor.   The log-log rupture curves for Armco iron at 1000° and 1100° F. in air and at 1063° F. in hydrogen are shown in Fig. 10.   At both temperatures in air a change of slope of the log-log plot occurs after a comparatively short period of time, and all of the fractures are of the intergranular type.   A careful microscopic examination of the fractures at various points along the curves revealed that intergranular oxidation occurred only on the second slope of the log-log plot.   The photomicrographs of Figs. 13, 14 and 15 indicate the nature of the intergranular cracking inherent to this material. For Fig. 13, the stress was sufficient to produce fracture in 19 min., and considerable deformation occurred within the grains.
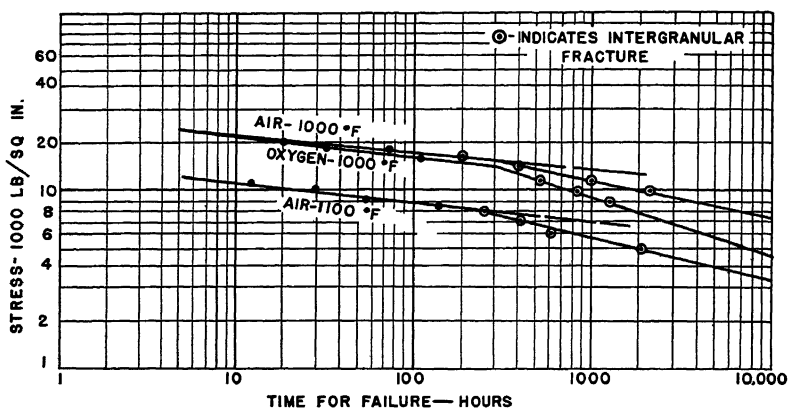
FIG. 17.—STRESS TIME FOR FAILURE FOR S.A.E. 1015 STEEL, SHOWING EFFECT OF OXIDATION ON FRACTURE TIME.
Diameter of test bars, 0.253 in.; area, 0.05 sq. in.; 6-in. gauge length.

The results from the tests in hydrogen are interesting in that fractures are still intergranular but no change of slope occurs in the log-log plot. By interpolating between the 1000° F. curve and the 1100° F. curve, it will be found that the curve at 1063° F. is approximately linearly located by its temperature ratio with respect to the other two.   Consequently, the first part of the curve is the same as would be obtained from tests on the same material in air at 1063° F.   Fig. 16 shows the microstructure and intergranular cracking near the fracture after 608 hr. at 1063° F. in hydrogen.

EFFECT OF PROTECTIVE COATINGS

An attempt to reproduce the straight-line log-log plot in air at 1100° F. by applying a protective coating of special aluminum paint was not entirely successful.   As shown in Fig. 10, these test points fall between the log-log plots in air and the extrapolated straight-line plot that would

result from tests in hydrogen at the same temperature. The inability of the aluminum paint to withstand deformation without cracking made it possible to obtain only partial protection. Similar results could be expected from other forms of protective coatings, the effectiveness depending, of course, on the degree of protection established.

ACCELERATED TESTS IN OXYGEN

Rupture tests at 1000° F. in oxygen clearly illustrate the accelerating effect of intergranular oxidation on the fracture time of a 0.10 per cent carbon steel. As shown in Fig. 17, a change in slope of the log-log rupture curve is found at about 350 hr. for the tests in both air and oxygen. This change of slope is more pronounced for the tests in oxygen, indicating the increased severity of the intergranular attack. Similar results at elevated temperatures might be expected from other corrosive gases.

All of the tests on the 0.10 per cent carbon steel at 1000° F. of less than 350 hr. duration resulted in transcrystalline fractures. As evidenced by microscopic examination, intergranular cracking occurred with fracture times in excess of 350 hr. Equally important is the fact that surface oxidation only could be found for tests of less than 350 hr., whereas surface and intergranular oxidation were detected with tests of longer duration. It appears, then, that intergranular cracking must precede intergranular oxidation. With Armco iron at 1000° F., intergranular cracking occurred without intergranular oxidation for tests of less than 120 hr. It is quite possible that for different steels a critical adjustment of temperature and stress is necessary before the intergranular cracking will be sufficient to allow the oxygen to enter the grain boundaries.

EFFECT OF ALLOYING ELEMENTS ON TYPE OF FRACTURE

Previously, it was shown that a 5 per cent Cr steel containing 0.5 per cent Mo and 1.5 per cent Si exhibits ductile transcrystalline fractures at 1100° F. and 1200° F. for long periods of time. The 5 per cent Cr, 0.50 per cent Mo steel without silicon exhibited brittle intergranular fractures at 1100° F. for tests of short duration. Numerous rupture tests at elevated temperatures on straight 5 per cent Cr steels of various carbon contents have also shown intergranular fractures. It would, then, seem that silicon markedly increases the ductility of metals at elevated temperatures. Fig. 18 shows the annealed structure of a 1 per cent Si steel before testing. Fig. 19 shows a section near the fracture of a bar stressed at 8000 lb. per sq. in. for 54 hr. at 1100° F. The elongation of this bar at fracture was 5 per cent and the fracture was mostly intergranular. Similar results were obtained from tests at 1100° F. on a 0.10 per cent C, 0.50 per cent Mo steel. The structure before test is shown in Fig. 20 and Fig. 21 shows a section near the fracture after 964
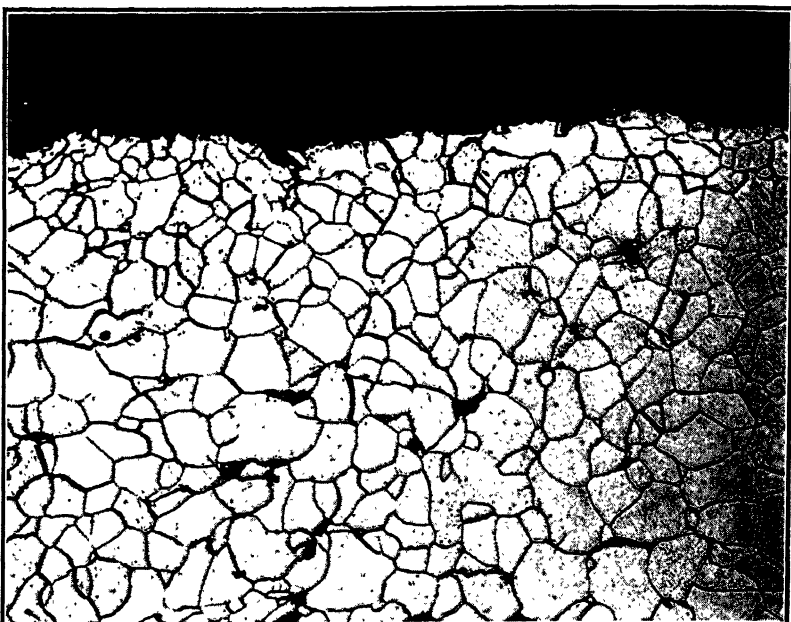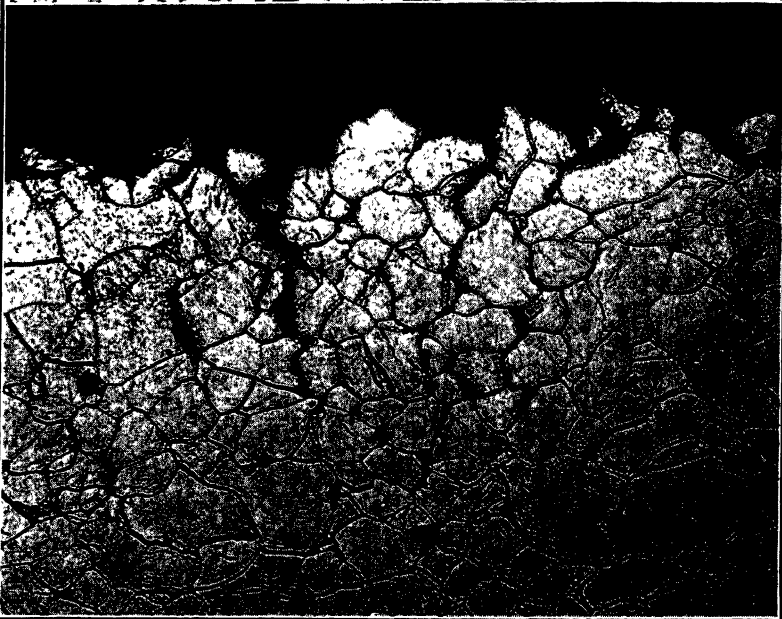
FIG. 18.—STRUCTURE BEFORE TESTING OF STEEL CONTAINING ONE PER CENT SILICON.
× 250.

FIG. 19.—SECTION NEAR FRACTURE OF STEEL BAR CONTAINING ONE PER CENT SILICON.
× 250.

Stressed at 8000 lb. per sq. in. for 54 hr. at 1100° F.   Elongation 5 per cent in 4 in.; reduction of area, 10 per cent.
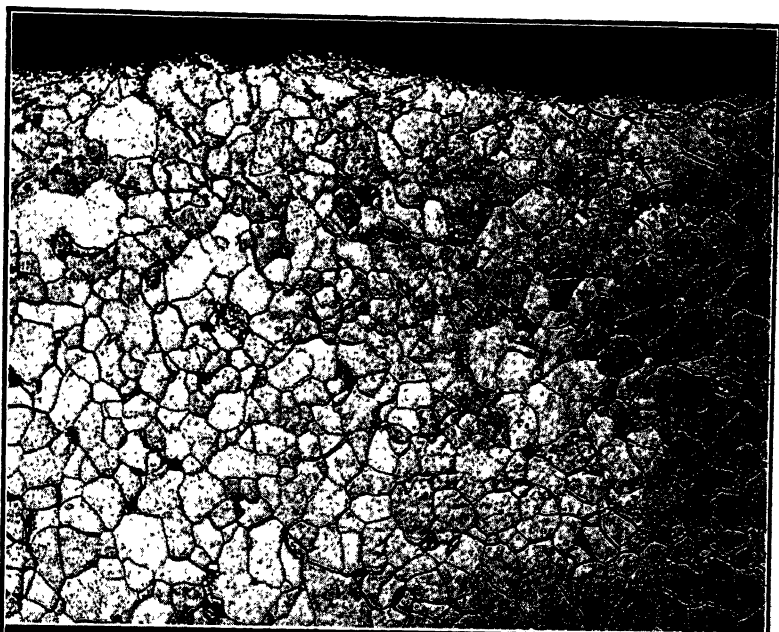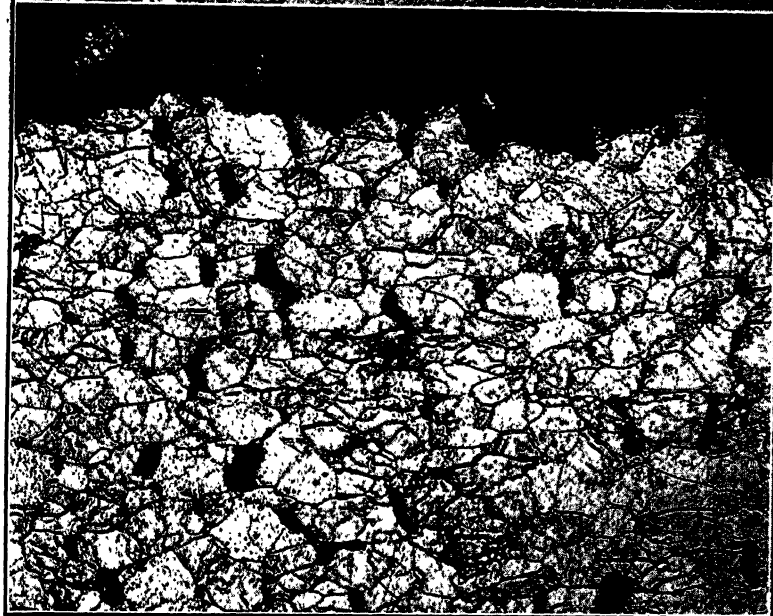
FIG. 20.—STRUCTURE BEFORE TESTING OF STEEL CONTAINING 0.10 PER CENT CARBON
AND 0.50 PER CENT MOLYBDENUM. × 250.

FIG. 21.—SECTION NEAR FRACTURE OF STEEL BAR CONTAINING 0.10 PER CENT CARBON
AND 0.50 PER CENT MOLYBDENUM. × 250

Stressed at 10,000 lb. per sq. in. for 964 hr. at 1100° F. Elongation 7.5 per cent in
4 in.; reduction of area, 22 per cent (mostly due to oxidation).

hr. under a stress of 10,000 lb. per sq. in.   This fracture was of the brittle intergranular type and occurred with 7.5 per cent elongation.

It is evident, then, that separate additions of silicon, molybdenum or chromium in the proportions mentioned above will not enhance the ductile properties of steel at elevated temperatures.   When present together in proper amounts, a suitably ductile material for elevated temperature service is obtained.   Rupture tests on a large number of alloys indicate that additions of certain elements to steel promote transcrystalline fractures, whereas additions of other elements enhance brittle intergranular fractures.   Increased creep and rupture strengths can be expected from the presence of molybdenum and tungsten.   Addi-
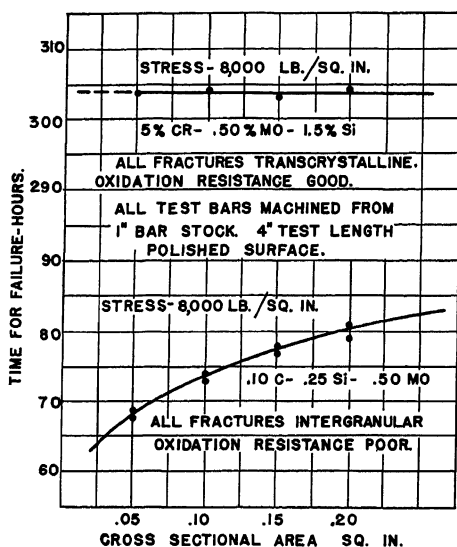
FIG. 22.—EFFECT OF SIZE OF TEST BAR ON TIME REQUIRED FOR FAILURE AT 1200° F. FOR CR-MO-SI AND C-MO STEELS.

tions of chromium, silicon and aluminum in certain combinations increase the resistance to oxidation.   In selecting a steel for service at elevated temperatures, each of the desired properties must be carefully considered before adoption of the final analysis.

EFFECT OF TEST-BAR SIZE

The data shown in Fig. 22 were obtained to determine the effect of specimen size on the fracture time at elevated temperatures in air. Here, the time for failure is plotted against the cross-sectional area. The 5 per cent Cr, 0.5 per cent Mo, 1.5 per cent Si steel, which is not appreciably affected by oxidation and breaks with a transcrystalline fracture, shows no size effect.   The 0.10 per cent C, 0.50 per cent Mo

steel, which is very susceptible to oxidation and intergranular cracking, shows a marked size effect. Apparently this steel should be used only in the presence of nonoxidizing atmospheres.

CONCLUSIONS

Sustained-load rupture tests of this nature are of direct interest as a means of evaluating steels for high-temperature service. Aside from the practical point of view, much information of a scientific nature pertaining to the mechanism by which steels deform and fracture at elevated temperatures is obtained. The fragmented grains resulting from ductile transcrystalline fractures lends support to the theory that crystalline deformation must result from a shearing action along the slip planes of the crystal lattice. The more nearly equiaxed structure accompanying intergranular fractures indicates that considerable deformation has occurred in the grain boundaries.

Higher temperatures and lower strain rates apparently favor the intergranular cracking of steels. The temperature at which intergranular cracking first occurs seems to be closely related to the recrystallization temperature of the steel and, for tests of comparatively long duration, can reasonably be termed the equicohesive temperature. Intergranular failures do not occur when high rates of deformation are employed. It seems likely that the precipitation of carbides or of impurities to the grain boundaries should materially influence the high-temperature tensile fracture.

The log-log plot of the stress against the corresponding fracture time results in a straight line, which, it seems, may reasonably be extrapolated to longer periods of time. The degree of accuracy of such extrapolations increases with tests of longer duration and might easily be influenced by the long-time metallurgical stability of the steel. The effect of oxidation is to accelerate the fracture time. Transcrystalline fractures are accompanied by surface oxidation only. Intergranular fractures may or may not be accompanied by intergranular oxidation. The occurrence of intergranular oxidation will be indicated by a change of slope in the log-log plot. Tests in hydrogen show that intergranular fractures are not always caused by intergranular oxidation.

ACKNOWLEDGMENT

REFERENCES

1. Z. Jeffries: Effect of Temperature, Deformation, and Grain Size on the Mechanical Properties of Metals. *Trans.* A.I.M.E. (1919) **60**, 474.
2. A. E. White, C. L. Clark and R. L. Wilson: Fracture of Carbon Steels at Elevated Temperatures. *Trans.* Amer. Soc. Metals (1937) **25**, 863.
3. A. E. White, C. L. Clark and R. L. Wilson: Rupture Strength of Steels at Elevated Temperatures. *Trans.* Amer. Soc. Metals (1938) **26**, 52.
4. A. E. White, C. L. Clark and R. L. Wilson: High Temperature Characteristics of Steels as Revealed by the Stress-Rupture Test. Western Metals Congress, March, 1938.
5. M. Fleischmann: Selection of Steel for High-temperature Service. *Oil and Gas Jnl.* (Oct. 21, 1937).
6. M. Fleischmann: Influence of Silicon Additions on High-temperature Characteristics of 4 to 6 per cent Chromium-molybdenum Steels. *Nat. Petr. News* (Nov. 3, 1937).
7. A. E. White, C. L. Clark and W. G. Hildorf: High-temperature Characteristics of Steels as Revealed by the Stress-rupture Test. Western Metals Congress, March, 1935. Extracted: Stress Rupture Test for Heated Metal. *Metal Progress* (March 1938) 266.
8. R. L. Wilson: High-temperature Strength of Steels. *Metal Progress* (May 1938) 499.
9. S. Dushman: Cohesion and Atomic Structure. *Proc.* Amer. Soc. Test. Mat. (1929) **29**, pt. II.
10. C. H. M. Jenkins, H. J. Tapsell, C. R. Austin and W. P. Rees: Some Alloys for Use at High Temperatures, Nickel-Chromium and Iron-Nickel-Chromium Alloys. *Jnl.* Iron and Steel Inst. (1930) **121**, 237.

DISCUSSION

(R. H. Aborn presiding)

C. L. Clark* and W. G. Hildorf,* Ann Arbor, Mich.—This paper is especially gratifying to us, for it not only substantiates our findings with respect to the logarithmic relationship that exists between stress and fracture time but likewise certain of the steels considered were of the same type previously used by us and the results from the two laboratories are in good agreement.

As the authors point out, the results from the fracture test are of considerable importance, not only as a basis of design but also in indicating the combined influence of time, temperature and stress on the resulting surface and structural stability and on the total hot ductility up to fracture. It is believed that the value of this paper would be greatly increased if the authors would include the ductility characteristics of at least the most prolonged fracture specimens for each steel at each temperature. When this is not done, one of the chief merits of the test is lost.

A casual review of this paper might lead to the conclusion that intergranular fractures always result in low ductility or brittleness. That is not correct. Tests on a large number of steels over a wide temperature range show that a temperature exists for each analysis above which the fracture is intercrystalline with the grains in the vicinity of the fracture not appreciably deformed. This critical temperature is believed to be the equicohesive or lowest possible temperature of recrystallization. Many steels show a very high degree of ductility at these higher temperatures under prolonged testing periods. In fact, if we conclude that an intergranular fracture always results in brittleness, it would have to follow that all steels show low ductility

* Department of Engineering Research, University of Michigan.

at the higher temperatures, a condition not subtantiated by either laboratory or commercial experience.

As an illustration of this, we may consider the 4 to 6 Cr + Mo + 1.5 Si steel used by the authors. We have likewise found a transcrystalline fracture at 1100° and 1200° F. with the total elongation after a fracture time of 1000 hr. being 63.5 and 75.0 per cent, respectively. Intercrystalline fractures were, however, obtained with this steel at 1300° and 1500° F. and the elongation values after approximately 2500 hr. for fracture were 44.0 and 74.0 per cent, respectively. In other words, this steel could not be classified as brittle at either 1300° or 1500° F., even though the fractures were intercrystalline.

H. SCOTT,* Pittsburgh, Pa.—The authors carefully distinguish between inter-granular and transcrystalline fractures in their test specimens. This distinction is significant because the mechanism of separation is as different as the appearance of the fractures. An intergranular fracture implies failure of cohesion rather than parting on shearing planes, which is indicated by a transcrystalline fracture and is typical of ductile metals. The cohesive strength of iron is calculated by Dushman[11] to be about 9 million lb. per sq. in., and there is much experimental evidence to support a value of this magnitude. Intergranular fractures, however, are observed at loads less than 9000 lb. per sq. in. Even when allowance is made for stress concentration effects assuming a factor of 15, the technical cohesive strength is still 600,000 lb. per sq. in., a value obtainable experimentally. How, then, can the cohesive strength of iron or iron-base alloys be lowered to less than $\frac{1}{60}$ of its attainable room temperature value simply by heating to, say, 500° C?

Apparently the authors believe that the bonding between grains becomes weaker with increasing temperature, until at some characteristic temperature the cohesion between grains is less than twice their resistance to shear. In accordance with this criterion of type of rupture set up by Heindlhofer,[12] the metal will then fail with an intergranular fracture under the applied tensile stress when it exceeds this value. Perhaps the inherent cohesive strength drops with increasing temperature, but that it drops so rapidly is highly doubtful. It is more probable that some other factor enters to reduce the cohesive strength—a factor that is a function of time. There are at least two familiar phenomena that can influence grain-boundary cohesion, both of which are probably active in these tests; namely, (1) intergranular oxidation or chemical attack, and (2) grain-boundary precipitation. An important consideration in this work, therefore, is to determine which if either of these factors is responsible for the low values of cohesive strength observed.

The authors' experiment of testing iron in a hydrogen atmosphere eliminates intergranular oxidation and suggests that either grain-boundary precipitation is the weakening agent or that it is an inherent property of the pure metal in a chemically inactive environment. The latter conclusion is very difficult to accept without further tests on highly purified metals that are demonstrated to be free of any precipitable constituent. Another possible criterion is a short-time test before and after a precipitation heat-treatment.

As regards the other metals, no definite relation between intergranular oxidation and intergranular fracture was found. It should be realized, however, that extremely thin films of oxide at the grain boundaries, which cannot be revealed by ordinary metallographic technique, can easily ruin the cohesion between grains. This is a very important field for experimental work and one from which many interesting developments may be expected in the future.

* Westinghouse Electric and Manufacturing Co.
[11] Dushman: *Proc.* Amer. Soc. Test. Mat. (1929) **29**, 7.
[12] K. Heindlhofer: *Trans.* A.I.M.E. (1935) **116**, 232.

R. F. MILLER,* Kearny, N. J.—It is unfortunate that in the present paper, as in other recent publications on the subject of sustained-load rupture tests, the words "ductility" and "brittleness" have been used with two different meanings. "Ductility" has been used to signify either a large *amount of elongation* before fracture, or the *transcrystalline type of fracture.* "Brittleness" has been used to mean either a small *amount of elongation* before fracture, or an *intergranular type of fracture.*

In their introduction, the authors state that the purpose of their tests is to determine the relative amounts of elongation that various steel alloys will withstand before fracture, in order to avoid using materials in service that might fail with little or no warning. According to the authors, "The sustained-load rupture test determines the expected life and corresponding ductility of steels at various stresses and temperatures." Yet the subject of "ductility" in the sense of amount of elongation is not discussed in their paper—their criterion of ductility is a transgranular as contrasted with an intergranular (brittle) type of fracture.

The difficulty is that both transgranular and intergranular fractures can be found in any given type of steel, depending on the rate of straining. As the authors themselves state in their conclusion, "Intergranular failures do not occur when high rates of deformation are employed—lower strain rates apparently favor intergranular cracking of steels." I therefore disagree with their statement that intergranular fracture is inherent to certain steels. This ambiguity was discussed by Dr. Walter Rosenhain in a Letter to the Editor in *Metal Progress*, February 1932. He said: " . . . intercrystalline rupture occurs in all metals when slowly stretched at relatively high temperatures. Modern investigation on the behavior of engineering materials at high temperature has shown that these conclusions apply in every case, provided that either the temperature is high enough or the rate of elongation sufficiently slow . . . This kind of behavior is sometimes interpreted as 'intercrystalline cracking,' as if it resulted from an embrittlement of the material. Nothing is further from the facts, since the material, if rapidly tested just before rupture, would show practically its original ductility."

Tests run at the Research Laboratory of the United States Steel Corporation, at Kearny, N. J., tend to confirm this viewpoint, and to emphasize the fact that the appearance of intergranular fracture under certain strain rates need not discourage the use of any particular material. A specimen of 0.10 C, 0.50 Mo steel was subjected to a stress of 5000 lb. per sq. in. for 4000 hr. at 1100° F. During this time, the specimen elongated 4 per cent. The stress was then raised to 7500 lb. per sq. in. and the specimen then extended 99 per cent more, finally failing 700 hr. later with 103 per cent total elongation and a transgranular fracture. Yet this is the same type of steel that the present authors describe as being very susceptible to intergranular cracking, and which Bailey in England claims should not be subjected to more than 0.5 per cent extension without danger of intergranular cracking. Metallographic examination of many specimens of carbon-molybdenum steel that have been tested in creep at 1000° or 1100° F. for 3000 hr. or more, with up to 3 or 4 per cent extension, has never disclosed any signs of intergranular cracking or oxidation.

Since the rate of straining of a steel at elevated temperature greatly affects the amount of elongation and the mode of fracture, it seems to be fundamentally incorrect to subject a series of specimens of a given steel alloy to several constant loads, causing different strain rates in each specimen, and then to state that such a series of tests shows the effect of stress and time at temperature on the ductility (amount of elongation) of the material. Quite different results might be expected if the series of specimens had all been held under the same stress (approximating operating stresses) for different time periods, and then tested to fracture at the same strain rate. This

---

* Research Laboratory, U. S. Steel Corporation.

type of test would give information of more use from a service standpoint, since the relative effects of time, temperature, and operating stress could be evaluated in terms of the ability of the material to withstand an overload at a high temperature.

It is a curious coincidence that the steel—namely, 5 Cr, ½ Mo, 1¼ Si—indicated in this paper as having a transcrystalline fracture at the longest time period is the steel with the lowest creep strength (fastest creep rate). Similar trends have been shown by other creep-to-fracture tests. Rapid strain (or creep) rates are known to favor transcrystalline fracture, while low strain (creep) rates are known to favor intergranular fracture. It may be that the present creep-to-fracture tests are simply indicating the relative strengths of the materials.

What we need is: first, knowledge of the relative creep strength of the various alloys, and second, information on the effect of stress and time at temperature on ductility (amount of elongation), rather than the effect of stress on time for failure.

T. M. JASPER,* Milwaukee, Wis.—This paper deals with a fundamental method of testing that was started by H. J. French[13] prior to 1925, for in that year he showed three curves for a steel tested at 560° F., 810° F. and 1100° F., in which load and time for fracture were the variables. Since 1926 the writer has tested by this method a considerable number of steels and suitable welds at temperatures up to 950° F. for the purpose of evaluating them for the building of pressure vessels to operate at elevated temperatures.

It is very gratifying, therefore, to see more interest being taken in long-time ultimate-strength tests because it is the writer's belief that this method offers promise to the designing engineer of a fixed point below which at elevated temperatures fracture is not likely to occur in steels. At lower temperatures than that used by the authors, it is believed that the relation between stress and time for fracture is not a straight-line log-log relation if oxidation during the tests is eliminated. The writer has been able to get material back from elevated-temperature service after about 13 years operation at 900° F. and has found that there is no deterioration in the steel quality when retested at 900° F. in the laboratory by the same method that the authors have employed, although at a lower temperature than their tests were made. I am citing this fact to help me suggest that it is possible that it is not the oxidation of grain boundaries that is inclined to accelerate the fraction time, because if this were so it might be expected that the steel from such a long elevated-temperature service should have oxidized the boundaries to a considerable depth and therefore given considerably lower results upon retesting.

May I suggest a substitute thought. We all know that in the solidifying of metal the grain boundaries are the last to become solid. The grain boundaries in steel, because they contain more carbon, are likely to be stronger at ordinary temperatures than the grains. This presents a reason why fracture usually occurs across the grains at ordinary temperatures. When the grain boundaries solidified, the grains were at that time much stronger than the boundaries. Therefore, there must be a temperature at which the boundaries and the grains are equally strong. Above this temperature the grain boundaries are weaker than the grains and below this point they are stronger. To follow through with this thought and understanding, the relative volume between grains and their boundaries in a piece of steel, there can result an explanation for the so-called brittle fracture in one case and a ductile fracture in the other without resorting to the idea of attack on the grain boundaries.

R. H. THIELEMANN AND E. R. PARKER (authors' reply).—As Dr. Clark and Mr. Hildorf have stated, the importance of knowing something about the hot ductility

---

* A. O. Smith Corporation.

[13] H. J. French: *Proc. Amer. Soc. Test. Mat.* (1925) **25**, 38.

that can be expected for a given steel at fracture cannot be overemphasized in view of the engineering demands required of materials in certain high-temperature applications. The sustained-load rupture test, conducted at elevated temperatures, provides an excellent means of obtaining this information.

In presenting this paper, it was not the intention of the authors to imply that intergranular fractures always result in low ductility or brittleness. In many instances we also have noted rather large values of elongation when the fracture was predominantly intergranular in nature. It does seem, however, that the materials that are most susceptible to intergranular cracking are apt to show less elongation at fracture, such as the austenitic 18 Cr, 8 Ni alloy reported in this paper. Materials of this nature are usually strong, and very little, if any, deformation takes place within the grains themselves. In other words, practically all of the deformation appears to take place in the grain boundaries, and the fracture is entirely intergranular.

Many of the steels that do show intergranular cracking behave more or less like "in between" alloys, and, although the fracture appears brittle in nature, it will be found on close examination that a large amount of the deformation has taken place in the grains themselves. An example of this type of deformation is shown by the drawn-out grains of the 5 per cent Cr, 0.5 per cent Mo steel in Fig. 4. When this occurs, elongations accompanying fracture have been found between 10 and 50 per cent in a 6-in. gauge length and there is little local "necking down" in the vicinity of the fracture. It seems evident that various alloys possess various degrees of intergranular susceptibility when stressed for various periods of time at elevated temperatures. The criterion of ductility of any steel, whether at room temperature or elevated temperatures, is determined by the ability of the grains to be deformed by shear along the many slip systems without fracture.

The 4-6 Cr + Mo + 1.5 Si steel when in the annealed or hot-rolled condition does, as shown in this paper and also by the results of Dr. Clark, show good hot ductility values over a wide temperature range. If, however, with this same material, the stiffness of the grains is increased by a heat-treatment that will produce a martensitic structure (the steel is air-hardening) the hot ductility will be greatly reduced. For instance, a bar of the same material as reported was held for 2 hr. at 1000° C. and air cooled. At 1200° F. with 9000 lb. per sq. in. of stress, fracture occurred after 347 hr. with only 9.35 per cent elongation in 6 in. and 9 per cent reduction of area, the fracture being predominantly intergranular, with very little local ductility or necking down at the break.

Mr. Scott's question as to the large discrepancy between the experimentally obtainable value of 600,000 lb. per sq. in. for the cohesive strength of iron and the low value of 9000 lb. per sq. in. required to produce fracture at, say, 500° C. is indeed worthy of consideration. It should be kept in mind, however, that to obtain a value of 600,000 lb. per sq. in. as a tensile strength for iron, the iron must first be in an extremely cold-worked condition. On the basis of the original cross-sectional area, this same iron in the annealed condition might show a tensile strength of, say, 60,000 lb. per sq. in., or a value only one-tenth of the experimental value. By comparison, then, the discrepancy between the two room-temperature values is really larger than between the annealed room-temperature value and the 9000 lb. per sq. in. value for 500° C.

Except for tests of extremely short duration, it is hard to see how, at elevated temperatures, the stress that will produce fracture in a prolonged period of time can be a direct measure of the cohesive strength of the metal. In the plastic range, metals are prone to creep and deform under stresses that are many times less than the short-time tensile value. Thus, high-temperature fractures result from the progressive weakening of the material under load and it is difficult to picture just what part of the crystal structure is in play at the time fracture occurs. Whether

the deformation occurs in the grains or in the boundaries is apparently totally dependent on the inherent properties of the metal. If the stress is high enough to cause slip along glide plane, transcrystalline fractures will result—and conversely, if the stress is too low to cause slip, grain-boundary deformation will occur.

As Dr. Miller suggests, and as explained above, the relegation of the word "ductility" to the transcrystalline type of fracture and the word "brittleness" to the intergranular type of fracture may be misleading. Without exception, however, from the long-time elevated-temperature fracture tests with constant load, the authors are unaware of any case in which the elongation for a given material is not less when the intergranular fracture occurs. Dr. Miller's statement, "The difficulty is that both transgranular and intergranular fractures can be found in any given type of steel, depending on the rate of straining," would be more enlightening had the words "and on the temperature" been added. As far as we can determine certain alloys, such as the low-carbon 18 per cent Cr type, continue to show transcrystalline fractures with large elongation values at 1100° and 1200° F., even after tests of 12,000 hr. duration. There is no evidence whatsoever of intergranular cracking, and the elongations at 1200° F. are even higher than for 1100° F. Possibly, with very low stresses, which would produce fracture in, say, a million hours, intergranular fracture might result, but for the time being we will conclude that certain alloys will remain ductile when subjected to prolonged constant stressing at elevated temperatures up to, say, 1200° F. for periods as long as the useful life of many of our engineering structures. We agree with Dr. Rosenhain that the phenomenon of intergranular cracking is nothing more than mechanism of deformation and failure, rather than an actual embrittlement of the material.

We note with interest that Dr. Miller has secured a long-time ductile fracture with carbon-molybdenum steel at 1100° F. With constant stress tests of more than a few hundred hours duration on this material at 900°, 1000° and 1100° F., we have found only intergranular fractures with elongation values ranging from 1 or 2 per cent to a maximum value of around 20 per cent. It should be pointed out that this difference in results might be attributed to the technique of testing. Whereas the authors have employed a constant value of stress for the duration of the tests, Dr. Miller's test was made using increased values of load. Had his test been continued for another four or five thousand hours at the original stress of 5000 lb. per sq. in., we feel that he would have obtained an intergranular fracture with around 10 to 15 per cent elongation. Also, had the higher load of 7500 lb. per sq. in. been applied from the start, intergranular fracture would have resulted after one or two thousand hours.

We heartily agree with Dr. Miller's suggestion that tests in which constant loads are applied for several thousand hours and then increased to approximate overloading to determine hot ductility would be valuable. We undertook these tests because we encountered brittle intergranular fractures in some of our commercial engineering work, and these we have reproduced by our present rupture test procedure. We have also observed fractures of a more ductile nature that have occurred in a variety of services due to sudden excess temperatures and stresses. Fractures of this type are probably what Dr. Miller referred to.

It seems quite likely, as Mr. Jasper suggests, that at the lower temperatures (800° to 950° F.), a stress value can be arrived at from the rupture curve from which fracture will never occur. From our tests, we have found that at 900° F. the log-log rupture curve of stress versus time for certain alloys is very flat and the magnitude of the difference in stress that will produce fracture in a short time is only a few thousand pounds per square inch greater than the stress that will produce fracture after many thousands of hours. There is, however, reason to believe that any steel that continues to exhibit creep when subjected to stress and temperature must ultimately fracture if stressed for long enough periods of time.

Mr. Jasper presents an interesting thought regarding the difference in carbon content of the grains and the grain boundaries. Where there is the tendency for the grain boundaries to fail rather than the grains, it seems altogether possible that the phenomenon can be attributed to the random orientation of atoms or possibly crystallites that compose the grain boundaries, as well as to variations in carbon content. However, it is difficult to attribute the phenomenon to variations in carbon when it is considered that the pure carbon-free metals such as iron, aluminum, copper, and nickel behave in the same way as do commercial steels.

Tests are under way, which, when completed, should throw more light on the problem of intergranular cracking and its relation to the long-time hot ductility that can be expected. It is obvious that a large amount of information is needed before many of the questions pertaining to high-temperature performance of metals under stress can be answered.

INDEX

583

CONTENTS OF VOLUME 133

TRANSACTIONS A.I.M.E., 1939, Institute of Metals Division

Papers

ɪ